

---

D/B/F 98: Final Report  
Of the AIAA Student Aircraft  
Design, Build & Fly  
Competition

Grant: N00014-98-1-0493

**DISTRIBUTION STATEMENT A**  
**Approved for Public Release**  
**Distribution Unlimited**

**REPORT DOCUMENTATION PAGE**Form Approved  
OMB No. 0704-0188

Public reporting burden for this collection of information is estimated to average 1 hour per response, including the time for reviewing instructions, searching existing data sources, gathering and maintaining the data needed, and completing and reviewing the collection of information. Send comments regarding this burden estimate or any other aspect of this collection of information, including suggestions for reducing this burden, to Washington Headquarters Services, Directorate for Information Operations and Reports, 1215 Jefferson Davis Highway, Suite 1204, Arlington, VA 22202-4302, and to the Office of Management and Budget, Paperwork Reduction Project (0704-0188), Washington, DC 20503.

1. AGENCY USE ONLY (Leave blank)		2. REPORT DATE 17 January 1998	3. REPORT TYPE AND DATES COVERED Final Report, 1 April - 31 December 1998
4. TITLE AND SUBTITLE D/B/F 98: FINAL REPORT OF THE AIAA STUDENT AIRCRAFT DESIGN, BUILD & FLY COMPETITION			5. FUNDING NUMBERS G: N00014-98-1-0493 PR: 97PR04749-00
6. AUTHORS By Gregory Page, Chris Bovias, Michael Selig and the student participants of D/B/F 1998. Compiled by Robert Paczula, AIAA			
7. PERFORMING ORGANIZATION NAME(S) AND ADDRESS(ES)  American Institute of Aeronautics and Astronautics ATTN: AIAA Foundation 1801 Alexander Bell Dr., Ste 500 Reston, VA 20191-4344			8. PERFORMING ORGANIZATION REPORT NUMBER  98DBF7630
9. SPONSORING/MONITORING AGENCY NAME(S) AND ADDRESS(ES)  Office of Naval Research 800 North Quincy St (ONR 351) Arlington, VA 22217-5660			10. SPONSORING/MONITORING AGENCY REPORT NUMBER
11. SUPPLEMENTARY NOTES			
12a. DISTRIBUTION/AVAILABILITY STATEMENT  APPROVED FOR PUBLIC RELEASE			12b. DISTRIBUTION CODE
13. ABSTRACT (Maximum 200 words)  This report is made up of the combined reports of 17 separate teams of students who entered the 1998 Design, Build & Fly Competition. The objectives of the Design, Build & Fly Competition were to have students teams design, build and fly unmanned remote control electric aircraft designed for maximum range on a limited battery. A "fly-off" took place on the Westport Airport near Wichita, KS, in April 1998. Winners of the contest: 1st place, University of Southern California; 2nd, Texas A&M University; 3rd, Syracuse University. The Design, Build & Fly Competition was supported by Cessna, the Office of Naval Research and the AIAA Foundation.			
14. SUBJECT TERMS  Unmanned / Remote / Control / RC / Student / Design / Build / Fly / AIAA			15. NUMBER OF PAGES  791
			16. PRICE CODE
17. SECURITY CLASSIFICATION OF REPORT	18. SECURITY CLASSIFICATION OF THIS PAGE	19. SECURITY CLASSIFICATION OF ABSTRACT	20. LIMITATION OF ABSTRACT  SAR

NSN 7540-01-280-5500

Computer Generated

STANDARD FORM 298 (Rev 2-89)  
Prescribed by ANSI Std Z39-18  
298-102

DTIC QUALITY INSPECTED 2

# TABLE OF CONTENTS

<u>Tab Number</u>	<u>School</u>
1	University of Alabama
2	University of Arizona
3	University of California at Los Angeles
4	University of Central Florida
5	University of Illinois at Urbana-Champaign
6	Massachusetts Institute of Technology
7	Oklahoma State University
8	San Diego State University
9	Queen's University at Kingston
10	University of Southern California
11	Syracuse University
12	Texas A&M University
13	University of Texas at Austin
14	Utah State University
15	Virginia Polytechnic Institute & State University
16	Washington State University
17	West Virginia University

# **Wings**

AIAA/Cessna/ONR Student Design/Build/Fly Competition  
Wichita, Kansas

Department of Aerospace Engineering  
University of Alabama

16 March, 1998



## Table of Contents

Executive Summary.....	1
Management Summary.....	3
Conceptual Design.....	6
Preliminary Design.....	9
Detail Design.....	14
Manufacturing Plan.....	19
Appendix A – References.....	23
Appendix B – Acknowledgements.....	24
Appendix C – Sponsors.....	25

## Executive Summary

The design of the aircraft was broken into three major phases. These phases were the conceptual, preliminary, and detailed design phases. During the first stage of design, the conceptual phase, the mission parameters were considered, while choosing the overall configuration of the airplane. A traditional airplane was chosen. In the next phase, the preliminary phase, major components were sized for a given flight mission profile, payload, and maximum battery weight. The final stage, the detailed design phase, included a detailed analysis of the aircraft. This analysis was used to size the internal structures. Once all internal and external structures had been sized, the necessary materials were ordered and plans for construction began.

The types of aircraft considered during the conceptual phase were the three-surface, canard, and conventional aircraft. After these configurations were selected each type was rated on its flight characteristics, controllability, and ease of construction. Other features of the aircraft investigated included fixed versus retractable landing gear, tricycle versus taildragger landing gear, high wing versus low wing, and t-tail versus conventional tail. The flight characteristics weighed most heavily in determining aircraft configurations were trim drag reduction, stall behavior, and general stability. The type of motor that would be used and the capacity and voltage of the battery were also topics investigated during this phase. Design tools used to determine which features were most efficient included advice from faculty and Raymer's text, *Aircraft Design, A Conceptual Approach*.

The preliminary design phase was greatly influenced by a desire to achieve the greatest efficiency. The characteristics given the most attention were the cruise velocity and lift coefficient of the airplane. The fuselage length and cross section was also given much attention during this phase. The wing's aspect ratio, taper ratio, twist, and sweepback angle were also important characteristics examined at this time. The horizontal and vertical tail airfoils were also investigated during this stage. The characteristics scrutinized for the horizontal and vertical tails as well as the wing were aspect ratio, taper ratio, and sweepback angle. MathCAD and MATLAB were used to predict the trim and performance of the airplane.

Obtaining a final wing configuration was the primary objective of the detailed design phase. Numerous airfoils were closely examined in order to find the airfoil that would perform as needed to meet the mission parameters. The rate of climb and take off performance for the aircraft were also predicted during this phase. Another important element of the airplane investigated during the detailed design phase was the position of the centers of gravity for the wing and horizontal and vertical tail. The centers of gravity for all the other major components were also calculated at this time. After the placements of the vertical and horizontal tail were determined, wing and horizontal tail incidences were calculated. All of the aforementioned characteristics were decided by using approximations from Raymer, knowledge gained in previous classes, and advice from faculty members. Once the airplane's major attributes were agreed upon, the materials and components were ordered and construction plans were begun.

The three phases of the design as well as the design parameters considered in each phase and their relative importance to the design are illustrated in the table below:

Phase of Design:		Relative Importance:
Conceptual:		
	1. Aircraft type	10%
	2. Gear Type/Placement	6%
	3. Wing Position	3%
	4. Motor type and Battery capacity and voltage	10%
Preliminary:		
	1. Cruise Velocity and Lift Coefficient	10%
	2. Aspect Ratio of Wing	4.5%
	3. Wing Taper Ratio, Twist, and Sweepback Angle	2.5%
	4. Fuselage Length and Cross Section	5%
	5. Horizontal and Vertical Tail Airfoils	3.5%
	6. Horizontal and Vertical Tail Sizes, Aspect Ratios, Taper Ratios, and Sweepback Angles	5%
	7. Sizes of Ailerons, Elevators, and Rudder	4%
Detailed:		
	1. Wing Airfoil	12%
	2. Position of Aerodynamic Centers of Wing and Horizontal and Vertical Tails	6%
	3. Centers of Gravity of Components	5%
	4. Vertical Placement of Horizontal Tail	2.5%
	5. Wing and Horizontal Tail Incidence	3%
	6. Rate of Climb Required and Take Off Performance	8%

**Table 1.1**

## Management Summary

The University of Alabama's Design/Build/Fly (DBF) Team is composed of the following people, with the following duties: Tara O'Neill, Team Leader and Communications Specialist; Brian Isaac, President of AIAA and Co-Team Leader; Calvin Kalbach, Head of Design; Michael Knight, AMA Pilot and Assistant in Design and Construction; Norman Antonio, Raymond Lenski, Tryshanda Moton, Anne-Michelle Reif, and Chad Woodard, Assistants in Design and Construction.

The original team concept was that Tara was our Team Leader and Communications Specialist, and the other team members were Assistants. As time went on, however, this structure gradually changed to what is stated above. The final team structure, as well as the communication and command structure is illustrated in Figure 2.1, with the arrows showing the appropriate directions of communication and authority.

As Team Leader, Tara's responsibilities included scheduling meetings and informing the team of design developments, sponsor contacts, and financial status. As Communications Specialist, she also served as the contact person for our sponsors. Due to his status as AIAA president and his previous involvement in DBF, Brian served as Co-Team Leader, assisting Tara in scheduling team meetings and in communicating with the AIAA faculty advisor regarding monetary funds specifically for DBF. As a graduate student, Brian also assisted Calvin in designing the aircraft. Calvin served as Head of Design, due to his status as a senior and his design experience. In this capacity, he delegated duties to the Assistants, such as finding the prices of components and formatting and analyzing information leading to the choice of the wing airfoil, construction materials, radio, propulsion system, and landing gear. He also scheduled meetings to design and build the aircraft, as well as reporting design progress to Brian and Tara during general meetings. Michael Knight is our Pilot, as he is the only member of our team with an AMA License and remote piloting experience. The remainder of the team served as Assistants in Design and Construction of the aircraft, as well as preparing the final report.

Figure 2.2 is a chart showing planned and actual execution of each step in the design project.

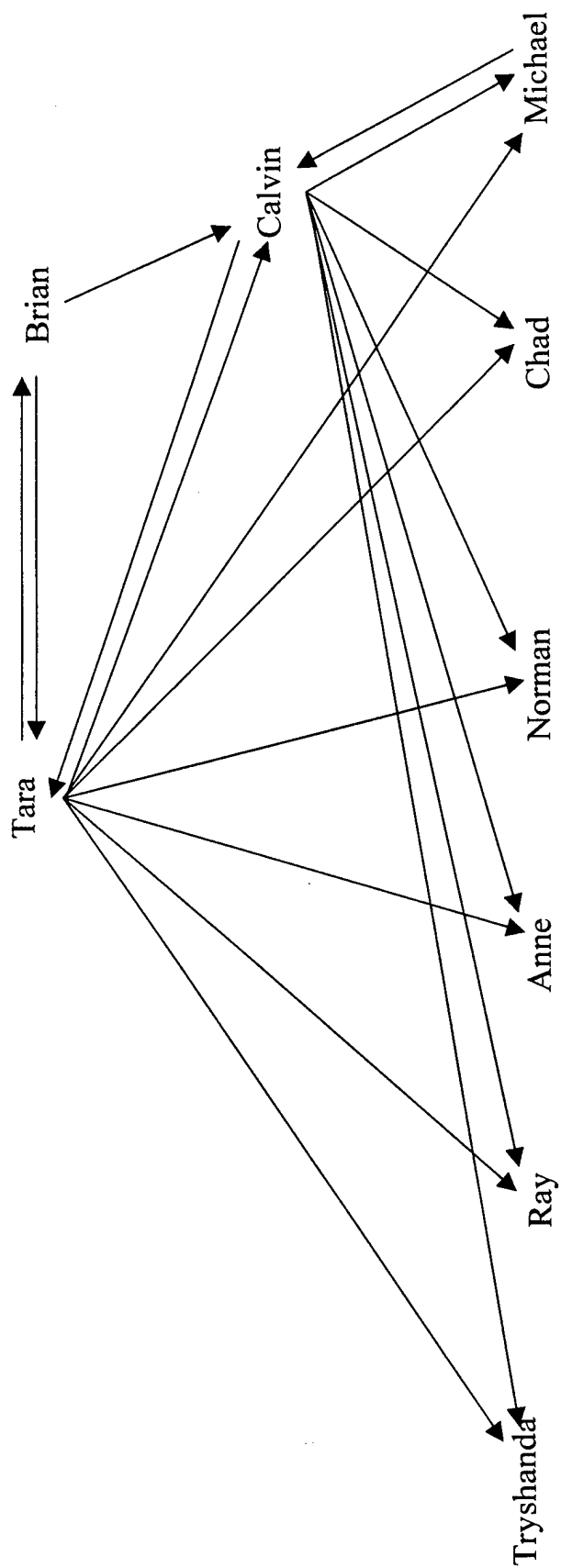


Figure 2.1 Chain of Command

Project	August	September	October	November	December	January	February	March	April
Recruitment of team members		(August 20 - September 1)							
Mailing Sponsorship Proposals/ Contacting interested sponsors					(September 20 - November 7) (September 2 - November 15)				
Conceptual Design				(September 2 - September 29) (September 2 - October 1)					
Preliminary Design/ Contact Suppliers about Materials					(October 1 - November 3) (September 25 - December 5)				
Detail Design/ Order Materials for Structural Testing					(November 3 - December 5) (January 12 - January 25)				
Order Materials/ Construction on Aircraft				(January 12 - March 30) (January 12 - March 30)					
Proposal Phase Paper				(February 19 - March 10) (March 3 - March 10)					
Flight Testing/ Optimization						(April 1 - April 15)			Proposed
Addendum Phase						(April 1 - April 7)			Proposed

Proposed Timing

Actual Timing

Figure 2.2 Milestone Chart

## Conceptual Design

There were four major parameters considered during the conceptual design phase. These parameters, as well as their relative importance to the design were as follows:

- |  |     |
|--|-----|
| 1. Aircraft Type                               | 10% |
| 2. Gear Type and Placement                     | 6%  |
| 3. Wing Position                               | 3%  |
| 4. Motor Type and Battery Capacity and Voltage | 10% |

These four parameters were important because they heavily influenced the aerodynamic efficiency of the design and affected many of the later decisions made regarding the design.

There were three types of aircraft considered in the conceptual design stage: three-surface aircraft, canard aircraft, and traditional aircraft. The factors which were considered in choosing a specific aircraft type were lift efficiency, handling characteristics, design complexity and availability of data, structural complexity, and, finally, control complexity.

The primary advantage of a three-surface aircraft was its increased lift efficiency due to the fact that the two control surfaces can be trimmed so that the main lifting surface operates at a lower lift coefficient. By balancing the downward component of lift produced by the control surface behind the wing with the upward component of lift produced by the surface ahead of the wing, the main wing can be used solely to lift the weight of the aircraft. As a result, the main lifting surface operates at a reduced lift coefficient reducing induced drag. With the reduction of induced drag, trim drag is also reduced. However, with three surfaces comes an increase in pressure drag and skin friction drag. The three-surface design also suffered from design complexity and a lack of availability of aerodynamic data, as well as structural and control complexity.

Another type of aircraft considered was the canard. The main advantage of the canard design is the increased lift efficiency due the fact that both the canard and the main lifting surface are lifting the weight of the airplane. With a canard design, induced drag and trim drag are reduced while skin friction drag and pressure drag remain comparable to that of a traditional design. The canard design also suffered from a slight stability problem. Historical information has shown that the canard design has a tendency to become unstable at extremely high or extremely low speeds. Another problem with the canard design was the lack of available design data. Design complexity, structural complexity, and control complexity are all comparable to that of a traditionally configured aircraft.

The final type of aircraft considered was the traditional design. The main advantages of the traditional configuration were the availability of design data and overall stability at varying speeds. These factors outweighed the decrease in lift efficiency and reduction of induced drag found in the three-surface and canard designs. Along with the above listed factors, the design, structure, and control for a traditional design is less complex than that

of a three-surface design and is comparable to that of a canard design. All of these factors led to the decision that a traditional design would be used.

Along with considering different aircraft types, several landing gear types and configurations were considered. The two types of gear considered were fixed landing gear and retractable landing gear. The main advantages of retractable gear were reduced drag and power required to cruise. However, complexity of design and structure and the problems with increased weight associated with retractable gear led to the decision to use fixed landing gear.

Once the type of landing gear was decided upon, gear configuration needed to be considered. The two configurations that were considered were the tricycle landing gear and the taildragger. The main advantages of the taildragger configuration were reduced drag and simplicity of control. However, with a taildragger configuration, the volume of the extreme aft fuselage section became extremely full, leading to structure and control interference problems. Also there are ground control problems with the tail dragger configuration. A tricycle design was chosen over the tail dragger design because of the structure and ground control problems. Those factors were judged to outweigh the increased drag associated with the tricycle configuration.

For the propulsion part of the conceptual design, two types of electric motors were considered, brushed and brush-less. When considering the type of motor, efficiency was the primary factor considered. At their highest efficiencies, brushed and brush-less motors of the same quality are very similar. The power setting at which the maximum efficiency occurs is different between the two types of motors. For a brushed motor, the highest efficiency typically occurs at about 75% power. The highest efficiency for a brush-less motor typically occurs at significantly lower power settings (35%-50%) and remains high for a wider power range than the typical brushed motor. The brush-less motor's high efficiency at low power was its most appealing attribute since most of the flight will be at cruise speed which is predicted to require a power setting of about 35% - 50%. Along with using a brush-less motor, it was determined from early power requirement calculations that one motor in the tractor position would be sufficient in powering the plane. The tractor position was chosen for balance of the aircraft and to increase propeller ground clearance.

The range calculations indicated that the battery should be composed of the maximum number of cells possible of a given capacity subject to the design weight restrictions. For a given capacity, the higher the voltage, the lower the amperage required to produce the power required and the longer the battery pack will last. Higher voltages and lower amperages are also desirable in order to minimize the power losses encountered due to resistance.

Various wing configurations were also considered during the conceptual design. The main factors considered for each configuration were aerodynamic efficiency, structural complexity, weight, and stability. A high wing configuration was considered for its stability, but was disqualified due to its lower aerodynamic efficiency and the fact that



longer landing gear struts would be required to give adequate propeller clearance. Upon deciding against the high wing configuration, a low wing configuration was considered. The advantages of a low wing configuration were the greater aerodynamic efficiency and the shorter landing gear struts required to give adequate propeller clearance. The shorter landing gear struts produce less drag. It was further decided to use an aspect ratio that was as high as possible, limited by the point at which pressure drag and structural weight begin to govern the design. The low wing design suffers from a stability disadvantage that was offset by the incorporation of sufficient dihedral.

## Preliminary Design

Several design parameters were investigated during the preliminary design stage. The design parameters are listed below along with their relative importance to the overall design.

- |  |      |
|--|------|
| 1. Cruise Velocity and Lift Coefficient  | 10%  |
| 2. Aspect Ratio of Wing  | 4.5% |
| 3. Wing Taper Ratio, Twist, and Sweepback Angle  | 2.5% |
| 4. Fuselage Length and Cross Section   | 5%   |
| 5. Horizontal and Vertical Tail Airfoils   | 3.5% |
| 6. Horizontal and Vertical Tail Sizes, Aspect Ratios, Taper Ratios, and Sweepback Angles | 5%   |
| 7. Sizes of Ailerons, Elevators, and Rudder  | 4%   |

Each of these design parameters may be varied to control different aspects of the aircraft's performance, control characteristics, or construction costs. The design parameters considered in the preliminary design and their effects are discussed below.

The choices of cruise velocity and cruise lift coefficient are closely related to each other and are governed by three factors. The first factor was that the airplane must comply with American Model Association's (AMA) rules. The AMA rules state that the contest will not be suspended unless winds exceed 40-mph (58.67 ft/sec). This velocity was considered to be unreasonable for this design and a lower velocity was eventually chosen.

The second factor influencing the choice of cruise velocity and lift coefficient is the dependence of wing area on cruise lift coefficient and velocity. For a given wing area, as velocity increases, lift coefficient decreases. The cruise velocity is then chosen so as to produce a cruise lift coefficient near the maximum aerodynamic efficiency value. Alternately, holding cruise velocity and cruise lift coefficient constant results in a required wing area to support the aircraft's weight. As the cruise velocity decreases for a given lift coefficient, the wing area must increase which, in turn, increases the structural weight of the wing and the drag produced by the wing. The cruise velocity, therefore, was chosen to produce a reasonable wing area at a lift coefficient near the lift coefficient for maximum efficiency (calculated in detailed design). The choices of cruise velocity and lift coefficient are illustrated in Table 4.1 on page 12.

The third factor influencing the choice of cruise velocity and lift coefficient are the capabilities and configurations of the motor, battery, speed controller, and propeller combination. The choice of cruise lift coefficient and velocity heavily influences the drag at cruise and the power required from the motor to cruise. In general the greater the cruise lift coefficient, the greater the cruise drag coefficient and power required to cruise. The greater the power required, the shorter the battery pack will last and the fewer laps the aircraft will complete. The prop must also be matched to the motor and cruise speed. If the propeller pitch is too small, the aircraft will not reach cruise speed. If the propeller pitch is too large, the motor will draw too many amps which may burn up the motor or speed controller.

The aspect ratio of the wing is an important design parameter as it directly affects the lift efficiency of the aircraft, the length and weight of the wing, and the power required to cruise. The higher the aspect ratio of a wing, the more aerodynamically efficient the aircraft becomes until the pressure, drag, and weight of the wing begin to counter these benefits. For a given wing area, as aspect ratio increases, wing length also increases. This increase in wing length tends to increase the structural weight of the wing and the pressure drag produced by the wing. As weight and drag increase, the power required increases, decreasing the range available from the battery and motor combination. The aspect ratio was chosen to produce a reasonable wing length and still maintain a high aerodynamic efficiency. This design trade study is illustrated in Table 4.2 on page 12.

The choice of taper ratio, twist distribution, and sweepback angle were also investigated due to their effect on wing length, weight, and aerodynamic efficiency. Prandtl is credited with discovering that an elliptic lift distribution along a wing produces a minimum of induced drag. The taper ratio and twist of a wing can be used to control the shape of the lift distribution of a wing and therefore, the induced drag. The taper ratio also affects the length and therefore the weight of the wing. As the taper ratio decreases, the length of the wing increases and the structural weight of the wing increases. By using a comparison of Shrenk's approximation of lift distribution with the approximate lift distribution produced by the wing, and also comparing the length of the wing generated by various taper ratios, a taper ratio of about 0.5 was determined to be a good compromise between aerodynamic efficiency and wing length. Twisting the wing is also used to generate an elliptical lift distribution. Twist, however, was deemed too costly in terms of construction time and complexity to be justified in this design. The wings were not swept as there was no chance of shocks forming on the wings at the low speeds at which the aircraft will fly. Sweepback can also be detrimental to aerodynamic efficiency as the flow over the wings may not flow straight over the airfoil shapes resulting in a loss of lift or increased drag.

The fuselage length and cross section were designed to be as aerodynamically efficient as possible so as to minimize the power required to pull the aircraft through the air. The fuselage is long and slender to minimize pressure drag. The forward cross sections are elliptical to allow more room for mounting internal components and yet maintain a small surface area and therefore lower friction drag. The taper behind the elliptical wing root section gently narrows to a small circular cross section to reduce friction drag and avoid separation from the surface and unnecessary pressure drag. The fuselage length is chosen to produce a reasonably small horizontal and vertical tail so as to reduce skin friction and pressure drag and yet still give good control authority to the pilot. The effect of fuselage length on the horizontal and vertical tail sizes is illustrated in Table 4.3 on page 13. The horizontal and vertical tail surfaces are sized by the method of tail volumes described in Raymer's book *Aircraft Design: A Conceptual Approach*<sup>1</sup>.

The airfoils for the horizontal and vertical tails were chosen to minimize the pressure drag of the tail, yet still produce good structural rigidity. The NACA 0009 airfoil was chosen for the horizontal tail because it will produce a low pressure drag and yet is thick enough to allow a light structure to be used to resist bending moments about the roots of

the horizontal and vertical tails. The NACA 0009 airfoil also has a very high airfoil efficiency of about 90% which means that it will be very effective for its size, i.e. it will produce a large change in aerodynamic force due to a small change in angle of attack.

The taper ratios, aspect ratios, and sweepback angles of the horizontal and vertical tails were designed to reduce drag, structural weight, and structural complexity. The horizontal and vertical tails were tapered slightly to produce a more elliptical lift distribution over the horizontal and vertical tails and therefore, reduce the induced drag of the tails. The taper ratios of 0.75 are not as significant as for the wing so as to keep the horizontal and vertical tail spans relatively short, reducing structural weight and pressure drag. The aspect ratios of the horizontal and vertical tails are also modest at 6.0 and 1.5 respectively. The dependence of the spans of the horizontal and vertical tails on aspect ratio is illustrated in Table 4.4 on page 13. Both the horizontal and vertical tails are swept back slightly so as to place the trailing edges at right angles to the fuselage centerline. This was done so that the hinge line of a constant chord rudder and elevators would also be oriented at right angles to the fuselage centerline simplifying the mechanism required to actuate these control surfaces.

Flaps, ailerons, elevators, and rudder surfaces are sized in order to give excess control authority to the pilot. If, in flight testing, the pilot finds that the control surfaces are too large, causing the aircraft to be difficult to fly, the rigging of the control surfaces will be modified in order to produce smaller control deflections for a given displacement of the pilot's controls. The control surfaces are integrated into the wing, horizontal tail and vertical tail airfoils so as to be effective yet produce minimal drag. The control surface gaps are tightly toleranced to minimize control surface gap losses.

		Cruise Velocity (ft/sec)								50
		10	15	20	25					
Cruise Lift Coefficient	0.1	1514.58	673.15	378.64	242.33				60.58	
	0.2	757.29	336.57	189.32	121.17				30.29	
	0.3	504.86	224.38	126.21	80.78				20.19	
	0.4	378.64	168.29	94.66	60.58				15.15	
	0.5	302.92	134.63	75.73	48.47	33.66	24.73	18.93	12.12	
	0.6	252.43	112.19	63.11	40.39	28.05	20.61		10.10	
	0.7	216.37	96.16	54.09	34.62	24.04	17.66		8.65	
	0.8	189.32	84.14	47.33	30.29	21.04			7.57	
	0.9	168.29	74.79	42.07	26.93	18.70			6.73	
	1	151.46	67.31	37.86	24.23	16.83			6.06	
	1.1	137.69	61.20	34.42	22.03				5.51	
	1.2	126.21	56.10	31.55	20.19				5.05	
	1.3	116.51	51.78	29.13	18.64				4.66	
	1.4	108.18	48.08	27.05	17.31				4.33	
	1.5	100.97	44.88	25.24	16.16				4.04	
		Wing Area (ft^2)								

Yellow indicates range of desirable lift coefficients for aerodynamic efficiency.

Gray indicates intersection of acceptable lift coefficients and cruise velocities.

Border indicates cruise velocity, lift coefficient, and wing area chosen for design.

Table 4.1

Wing Area (ft <sup>2</sup> )							
13.523		Wing Span (ft)	Mean Aerodynamic Chord (ft)	Best Lift to Drag Ratio of Aircraft	Lift Coefficient for Best Lift to Drag Ratio		
Aspect Ratio	6	9.008	1.501	19.976	0.368		
	7	9.729	1.390	21.028	0.394		
	8	10.401	1.300	21.028	0.418		
	9	11.032	1.226	22.725	0.44		
	10	11.629	1.163	23.422	0.459		
	11	12.196	1.109	24.04	0.478		
	12	12.739	1.062	24.594	0.495		
	13	13.259	1.020	25.091	0.51		
	14	13.759	0.983	25.541	0.525		
	15	14.242	0.949	25.949	0.539		
	16	14.709	0.919	26.32	0.552		
						Aspect Ratio Chosen	

Table 4.2

		Area of Horizontal Tail (ft <sup>2</sup> )	Area of Vertical Tail (ft <sup>2</sup> )
Fuselage Length (ft)	4	2.659	2.706
	5	2.127	2.165
	6	1.772	1.804
	7	1.519	1.546
	8	1.329	1.353
	9	1.182	1.203

Table 4.3

Area of Horizontal Tail (ft <sup>2</sup> ): 1.519				Area of Vertical Tail (ft <sup>2</sup> ): 1.546		
Aspect Ratio of Horizontal Tail:	Span of Horizontal Tail (ft):		Mean Aerodynamic Chord of Horizontal Tail (ft):	Span of Vertical Tail (ft):		Mean Aerodynamic Chord of Vertical Tail (ft):
	3	2.135	0.712	0.75	1.077	1.411
	4	2.465	0.616	1	1.243	1.222
	5	2.756	0.551	1.25	1.390	1.093
	6	3.019	0.503	1.5	1.523	0.997
	7	3.261	0.466	1.75	1.645	0.923
Aspect Ratio of Vertical Tail:	8	3.486	0.436	2	1.758	0.864
	9	3.697	0.411	2.25	1.865	0.814

Table 4.4

## Detailed Design

The detailed design involved more in-depth studies of some of the concepts touched on in the preliminary design as well as several new concepts which had not been considered before. The parameters principally investigated in the detailed design were as follows:

- |  |      |
|--|------|
| 1. Wing Airfoil  | 12%  |
| 2. Position of Aerodynamic Centers of Wing and Horizontal and Vertical Tails | 6%   |
| 3. Centers of Gravity of Components  | 5%   |
| 4. Vertical Placement of Horizontal Tail                                     | 2.5% |
| 5. Wing and Horizontal Tail Incidence  | 3%   |
| 6. Power Required to Produce Rate of Climb Required and Take Off Performance | 8%   |

The final configuration of the aircraft is illustrated in Figures 5.1 and 5.2 on pages 17 and 18.

The choice of an airfoil for the wing is an important design parameter due to its influence on lift efficiency, structural weight of the wing, stall characteristics, and sizing of the horizontal tail and elevator for trim. The University of Illinois at Urbana-Champaign (UIUC) maintains a website on which lift, drag, and moment data are displayed for several airfoils that have been tested in their wind tunnel at low speeds. The design team ranked these airfoils by lift to drag (L/D) ratios, lift coefficient at which the best L/D occurs, and L/D and stall characteristics. It is desirable for the airfoil to operate at its lift coefficient for best L/D when the aircraft is cruising at the aircraft's lift coefficient for best L/D. It is also beneficial for the L/D ratio to remain high at lift coefficients that are higher and lower than the lift coefficient for best L/D to maintain high aerodynamic efficiency at off-design flight conditions. The airfoil's stall characteristics are also important to the pilot's ability to recognize and respond to an impending stall. It was deemed desirable for the stall to be somewhat "soft", that is for flow separation to happen over a range of angles of attack prior to full stall rather than all at once. The airfoil list was first narrowed down to about 6 airfoils using UIUC's data and these airfoil cross-sections were further compared by entering the airfoil cross-sections into a commercially available computational fluid dynamics code known as SUB-2D. SUB-2D is able to generate lift, drag, and moment predictions of two-dimensional objects in both inviscid and viscous flow. Again, lift to drag ratios, lift coefficients for best L/D, and stall characteristics were compared and the WASP airfoil shape was chosen. Several of the better airfoil options, their characteristics, and their figures of merit are illustrated on page 16 in Table 5.1.

The positions of the aerodynamic centers of the wing and horizontal tail as well as the center of gravity of the aircraft determine the static longitudinal stability of the aircraft. As the aircraft pitches up about the aircraft's c.g., the horizontal tail acts as a weathervane and counters the up attitude pitch. If the aerodynamic center of the wing is too far ahead of the c.g., the horizontal tail will not be effective enough to overcome the wing's contribution to moment about the c.g. and the aircraft will be unstable. If the aerodynamic center of the wing is too far behind the c.g., the horizontal tail will not be

able to overcome the aircraft's tendency to nose down and no matter how much elevator deflection the pilot commands the aircraft will not pull out of its dive. The optimum point is a point that gives the aircraft good stability and yet maintains the pilot's control authority. The position of each of the centers of gravity of the components also contributes to the static longitudinal stability as they determine the c.g. of the aircraft. The centers of gravity of the wing, fuselage, horizontal tail, and vertical tail were initially estimated to be at 35% chord of each component. That is, the c.g. of the wing airfoil was assumed to be located at 35% of the wing airfoil chord at each cross section. The c.g.s of each of the other components was assumed to be nearly in their centers as most of the other components are rectangular in shape. Table 5.2 on page 16 shows the weight and estimated center of gravity of each component with respect to the nose of the aircraft as well as the c.g. of the aircraft. The configuration and layout chosen produces an aircraft with a static margin of stability of about 12% which is considered to be quite stable. The payload is placed slightly behind the aircraft c.g. so as to produce nearly the same static margin with and without the payload.

The placement of the vertical tail is an important design parameter as it affects the strength of the effects of the wing downwash on the horizontal tail. The closer the horizontal tail is to the wing both horizontally and vertically the greater the effect of the wing's downwash on the horizontal tail. These downwash effects can be adverse to longitudinal stability if they are strong enough. By placing the horizontal tail at the tip of the vertical tail in a T-tail configuration, the designers have minimized the downwash effects of the wing on the tail.

The wing and horizontal tail incidence angles with respect to the fuselage centerline are calculated so as to result in the fuselage being at zero angle of attack when the aircraft is cruising at design conditions. Holding the fuselage at zero angle of attack during cruise, minimizes the cross sectional area of the fuselage relative to the flow which will minimize the pressure drag produced by the fuselage provided there are no separation effects from the fuselage that are corrected by having the fuselage at an angle of attack other than zero.

The final parameter considered was the power required to take off and climb. The pilot requested at least 100 feet per minute of climb capability. To determine the power required to operate at climb flight conditions, the designers assumed the aircraft to be operating at 75% of cruise aerodynamic efficiency and at cruise velocity. The power required was determined by summing the power required to change the aircraft's potential energy with the power required to overcome aerodynamic drag. By multiplying the gross weight of the aircraft by the vertical velocity (100 ft/min) the designers determined the power required to raise the aircraft weight in altitude. The power required to overcome the aerodynamic drag was found by dividing the gross weight by the expected lift to drag ratio and multiplying by the cruise velocity. The power required to climb was compared with the power required to provide adequate take-off performance. Take-off performance was estimated by integration of the second order differential equation resulting from  $\Sigma F = ma$ . Aerodynamic drag, ground roll friction drag, and thrust vs. velocity estimates are used to estimate the sum of forces term of the motion equation.



Rotation speed for take-off was assumed to be 25% greater than stall speed and ground effects were neglected. Position and velocity approximations are predicted by using a Taylor Series expansion and a modified Euler integration routine in one variable up to the rotation point. Energy balance is then used to estimate the climb path angle after rotation based on the power required for flight and the power available from the motor. The lift coefficient and drag coefficient are assumed to be constant along the runway as the angle of attack of the wing is unchanged prior to rotation. The lift produced by the wing affects the ground roll rolling resistance and is accounted for in the program. A motor with a maximum power output of 300 watts was chosen to fulfill performance requirements.

<b>Airfoil Selection:</b>					
Percent Importance to Design:		12%			
<b>Airfoil:</b>	<b>High L/D:</b>	<b>High L/D Near Desired Lift Coefficient:</b>	<b>Structural Weight:</b>	<b>Stall Characteristics:</b>	<b>Figure of Merit:</b>
Percent Importance to Decision:	20%	35%	20%	25%	
A 18	8	8	5	6	6.9
BE 50	8	7.5	5	5	6.475
K 3311	8	7.5	5	5	6.475
S 7055	8	7.5	5	7	6.975
WASP	8	7.5	5	8	7.225
1 = Poor      5 = Average      10 = Excellent					

Table 5.1

<b>Calculation of C.G. of Aircraft:</b>			
<b>Component:</b>	<b>Weight of Component:</b>	<b>Position of Component:</b>	<b>Moment of Component About Nose:</b>
	(lb.)	(ft from nose)	(ft lb.)
Battery	2.5	1.167	2.917
Payload	7.5	1.742	13.063
Motor/Prop	1	0.125	0.125
Wing	2.5	0.75	1.875
Fuselage	2.5	2.1	5.25
Horizontal tail	0.25	6.665	1.666
Vertical tail	0.25	6.423	1.606
Radio Receiver	0.0625	0.75	0.047
Receiver Battery	0.2225	0.75	0.167
Aileron Servo	0.125	2.333	0.292
Rudder/Nosegear Servo	0.125	0.75	0.094
Elevator Servo	0.098	2.563	0.251
Speed Controller	0.111	0.75	0.083
Nosegear	0.25	0.458	0.115
Maingear	0.375	2.333	0.875
Gross Weight:	<b>17.87</b>		<b>1.591</b>
			C.G. of Aircraft (ft from nose)

Table 5.2

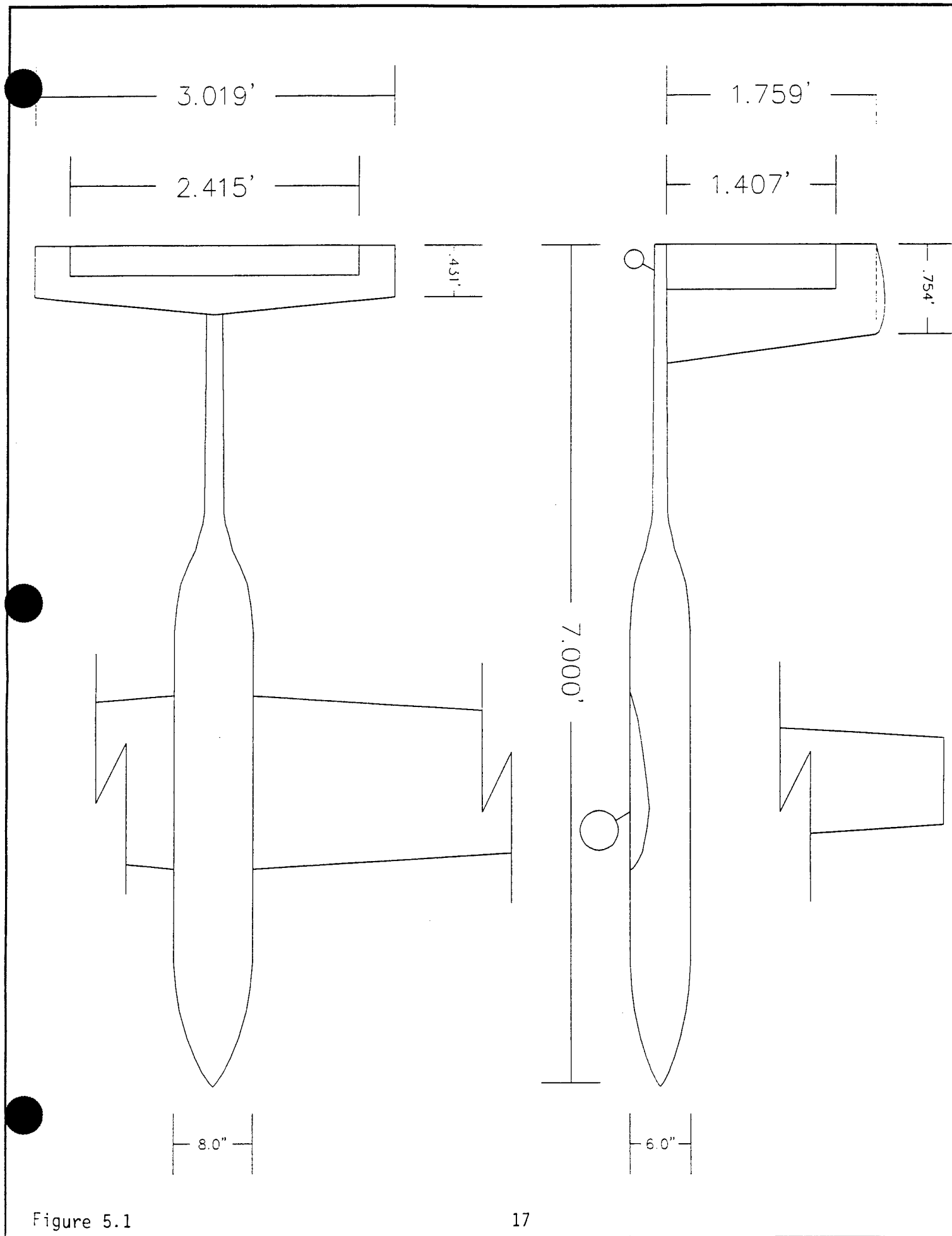


Figure 5.1

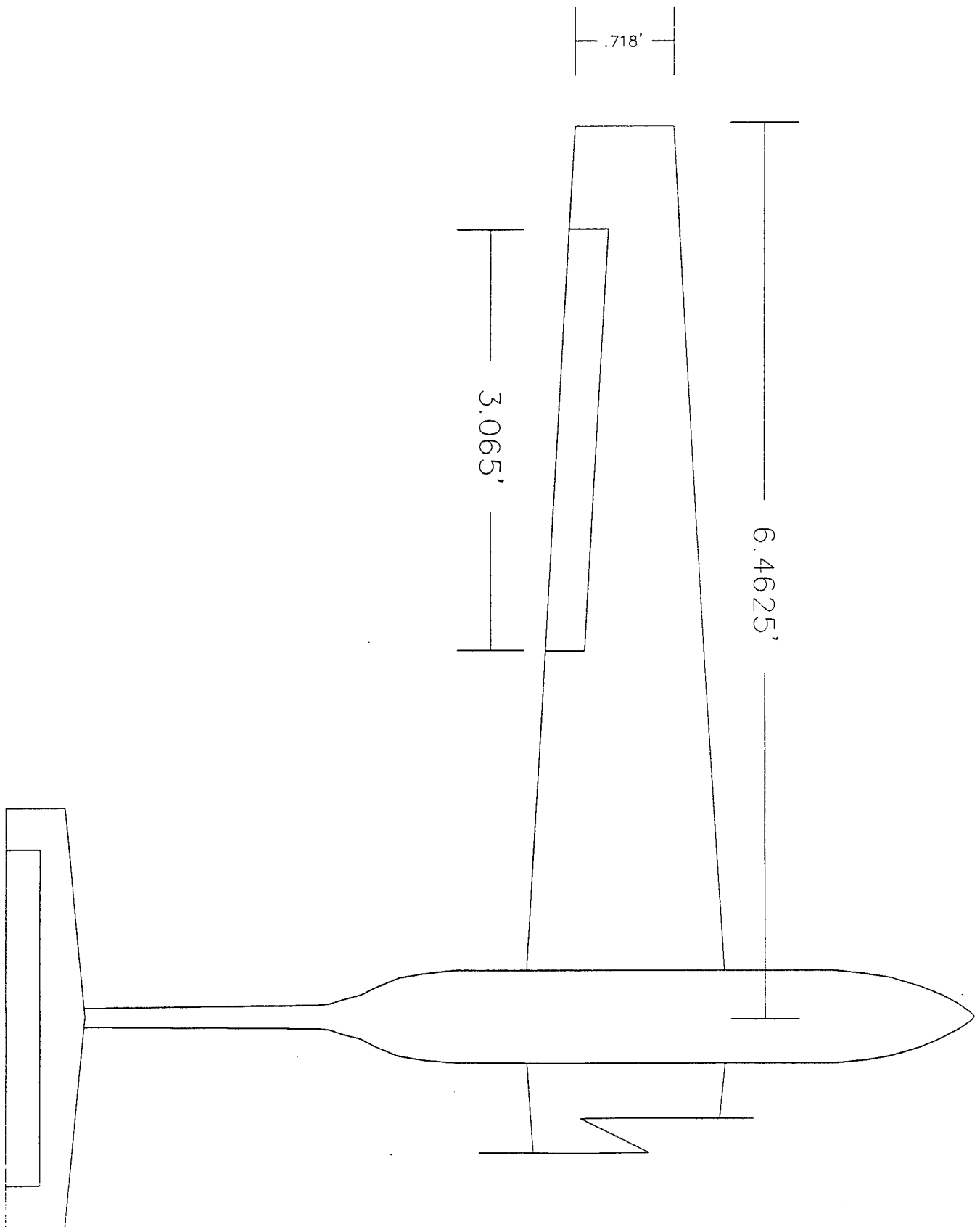


Figure 5.2

## Manufacturing Plan

The choice of materials used to manufacture the aircraft was largely governed by the stiffness to weight characteristics of the available materials. Many of the large airframe components such as the wing, fuselage, horizontal tail, and vertical tail are subject to large bending or torsion loads during flight. The aircraft was designed to withstand a 10g acceleration load factor on the wing and appropriate loads on all aerodynamic surfaces. Such a large load factor was chosen because the pilot receives no motion cues from the aircraft to assist him in limiting the loads encountered by the aircraft. Instead, he is solely dependent on his visual assessment of how the aircraft is behaving for control, and loads can quickly become excessive due to violent maneuvers.

Building the large aerodynamic components by such methods as covering frameworks composed of spars and ribs or formers with sheeting was rejected due to the weight required to produce a sufficiently stiff structure. Fiberglass reinforcement of foam cores was also considered. This technique was rejected for building the wing and fuselage due to the excessive weight of the foam cores. The horizontal and vertical tails, however, were built using this method due to the fact that their cross sections were too narrow for the same techniques to be used as were used in the fuselage and wing as described below. The root and tip airfoils for the horizontal and vertical tails were machined out of aluminum sheets on a CNC machine by University of Alabama technicians and glued on blocks of foam of appropriate lengths. A hot wire cutter was used to cut the horizontal and vertical tail shapes out of the foam blocks. The horizontal and vertical tails were then covered with a thin layer of fiberglass reinforced epoxy in a process known as vacuum bagging.

Vacuum bagging the horizontal and vertical tails was accomplished through the following process. First, the cores were cut as described above. A piece of thin fiberglass cloth was cut to fit the shape of the core. The fiberglass cloth was draped over the leading edge of the wing cores so that the seams were located at the trailing edges (see Figure 6.1, page 21). A high quality epoxy resin and hardener were applied to the fiberglass cloths impregnating the cloths and adhering the cloths to the surface. A layer of release film was draped over the wetted fiberglass cloths and allowed to soak up any excess epoxy on the surfaces. The release film served two purposes. It both soaked up excess epoxy and also made it possible to remove the final two layers of the vacuum bagging lay-up from the fiberglass cloths themselves. Another benefit of the release film was that it left the surfaces of the fiberglass coarse and made extra layers easier to apply. This was a disadvantage for the horizontal and vertical tails since extra layers were not applied. Instead, the outer surfaces were sanded after the release film was removed. The next step in the vacuum bagging process was the application of the breather film. This film allowed the vacuum pump to evenly extract the air from between the release films and the outer vacuum bag layers. Atmospheric pressure then pressed all of the layers evenly onto the cores facilitating a strong bond between the fiberglass and the foam cores. The final step is to add an airtight vacuum bag around the entire lay-up and apply a vacuum of about 20 inches of mercury for 24 hours.

The wings used a slightly different vacuum bagging procedure from that of the horizontal and vertical tails due to the difference in the wings' construction. The wings were constructed using a "sandwich" construction method that resulted in their being hollow (see Figure 6.2, page 22). First, a wood core for the wings was machined using a CNC machine by the University of Alabama technicians. The wing core cross section was calculated from the desired wing airfoil cross section with a thickness of 0.25 inches removed from the surfaces. A plastic release film was applied to the core. This was a different type of release film from the release film used earlier in that the epoxy could not soak through the plastic film to stick to the core. The plastic film made it possible to remove the core after vacuum bagging was complete. Fiberglass reinforced epoxy was applied over the layer of release film in much the same way that was described for the horizontal and vertical tails. A sheet of 0.25 inch thick, heat formable foam was then wrapped over the core and fiberglass and placed inside a vacuum bag. Again, a vacuum was applied for 24 hours to hold the foam, fiberglass, and epoxy in place around the core and form them to the shape of the core. After the 24 hour bagging process, the bag was removed and a layer of fiberglass reinforced epoxy was vacuum bagged around the core/fiberglass/foam assembly in a similar manner to the way in which the horizontal and vertical tails were covered. The outer layer of fiberglass served as the aerodynamic surface of the wing and was sanded smooth to reduce drag. The wooden core was removed leaving a hollow wing that was light and stiff.

The fuselage was constructed in a similar way to the wing. A core was generated with a thickness of 0.25 inches removed from the outer surfaces. The core was then cut in half down the centerline of the fuselage so that the fuselage could be vacuum bagged in two halves and the two halves joined together. The 0.25 inch thickness foam was again heat formed around the fuselage shapes and vacuum bagged over an inner layer of fiberglass. A second layer of fiberglass was vacuum bagged over the foam. The two halves of the fuselage were joined by using a narrow strip of thin fiberglass tape and epoxy on the inner and outer surfaces.

The elevators, ailerons, and rudder were cut from the completed wing, horizontal tail, and vertical tail using a scroll saw with a wire blade. This procedure allowed the control surfaces to be cut with square corners instead of rounded corners. Since the wing was hollow and the horizontal and vertical tails were filled with foam, fiberglass tape and epoxy was used to close the open areas. These were also used as mounts for the hinges of the different control surfaces. The control push-rods were mounted inside the wing with small control horns on the control surfaces to which the push-rods attached to control the surfaces.

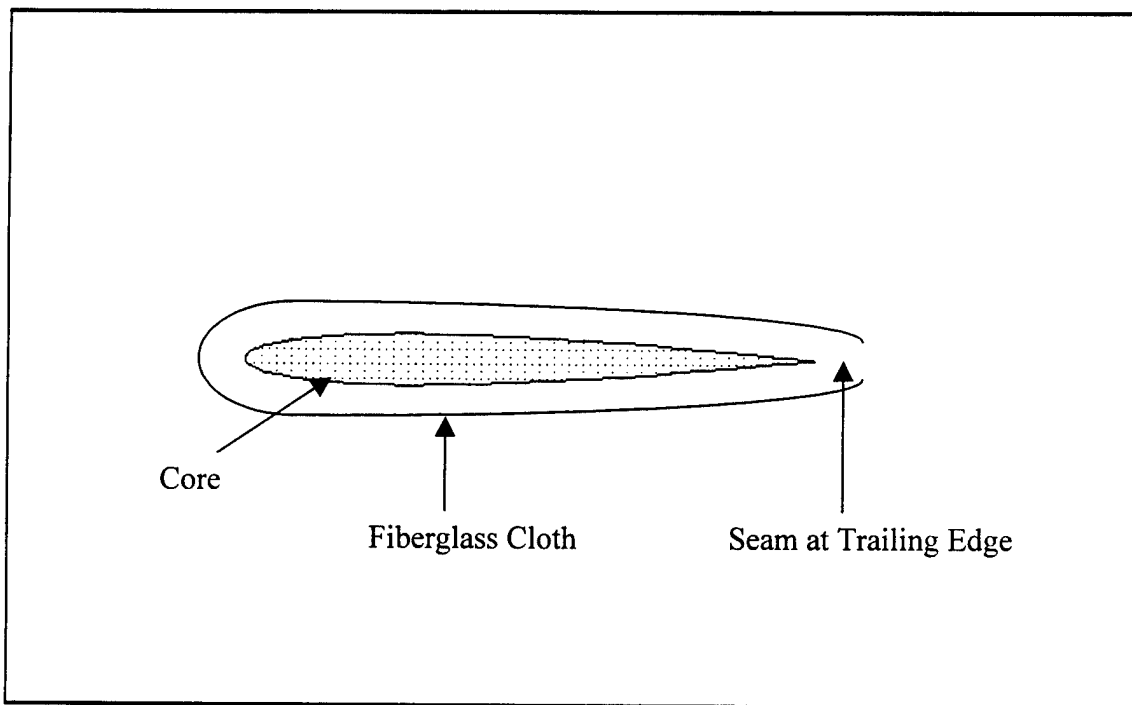
The nose gear was mounted in the nose of the fuselage prior to the fuselage being closed by use of a mounting box glued to the lower surface of the fuselage. The nose gear was linked by a control cable to the servo that controls the rudder and operates in the same direction. The main gear were mounted in mounting boxes in the wing roots and are removed with the wings from the fuselage. The nose and main gear were given appropriate lengths to allow the wing to generate some lift during the take off roll, but not to allow the aircraft to lift off until the pilot commands the takeoff rotation. This was

done to allow the pilot to find the aircraft's flight trim condition prior to full rotation for takeoff. This resulted in the fuselage being slightly nose down when sitting on the gear and effectively increased the tail clearance and tipback angle allowed for takeoff rotation and landing.

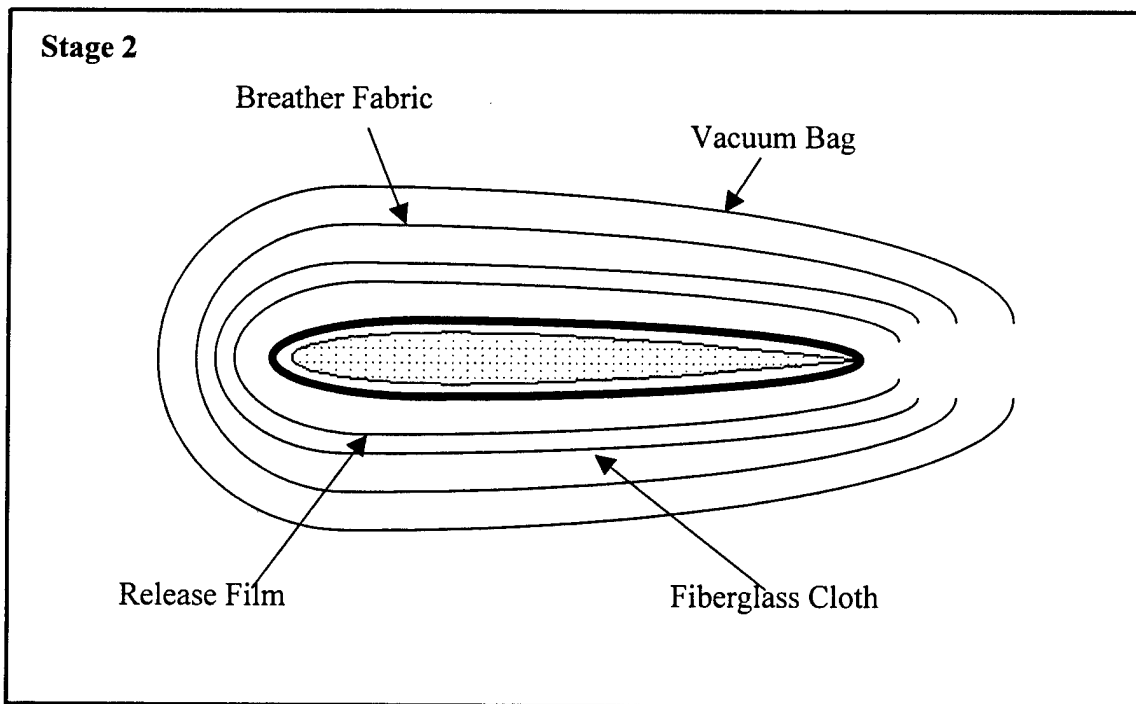
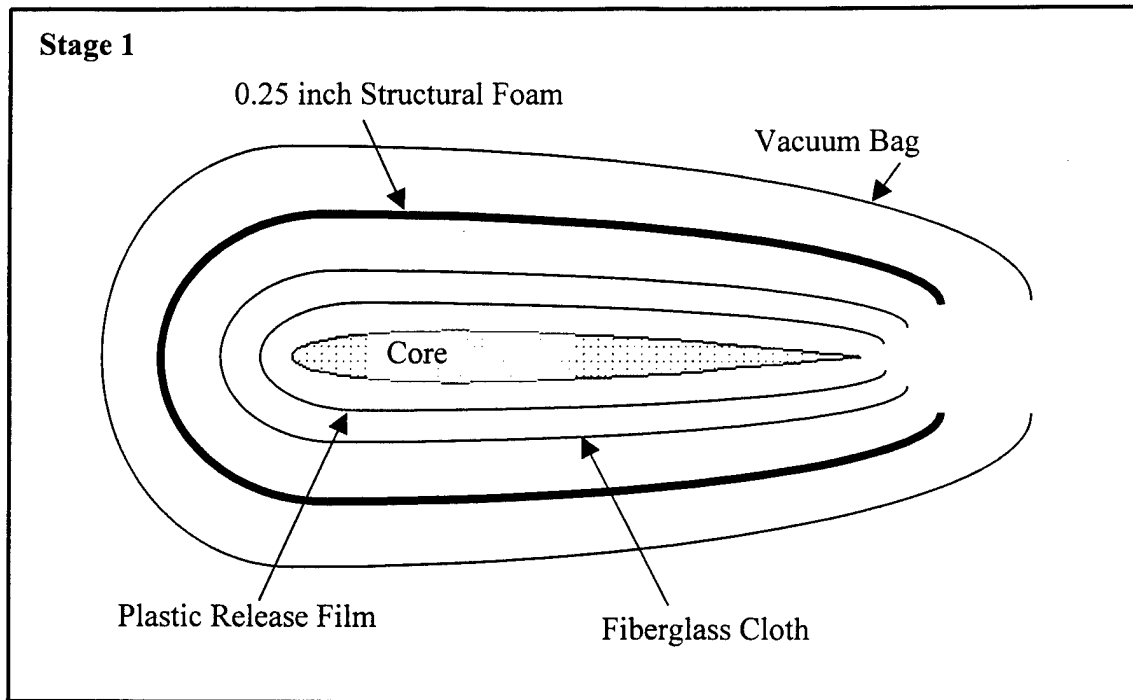
The motor was mounted in the nose in the tractor position via a bulkhead behind the motor. A mounting ring also served to stiffen the motor mount against vibration and to blend the motor aerodynamically into the fuselage.

The payload and battery were mounted above the wings in the fuselage. The payload was placed in a specific position so as to allow it to be easily removed and to keep the longitudinal stability of the aircraft from changing when removed. A hatch in the top of the fuselage gives access to both the battery and payload for easy removal or replacement.

The radio, speed control, and control servos were mounted in trays glued inside the fuselage. A single servo controls the ailerons. A smaller servo controls the elevator and a single servo controls the rudder and nose wheel.



**Figure 6.1**



**Figure 6.2**

## **Appendix A**

### **References**

Raymer, Daniel P., *Aircraft Design: A Conceptual Approach*, American Institute of Aeronautics and Astronautics, Inc., Washington, D.C., 1992.



## **Appendix B**

### **Acknowledgements**

We would like to thank our advisors, Dr. Charles Haynes and Ms. Diane Brown. We would also like to thank Dr. Jackson, Dr. Beth Todd, Dr. Tom Zeiler, and the rest of the Aerospace Engineering and Mechanics Staff.

## Appendix C Sponsors

We would like to thank our sponsors:

### Top Gun – For a donation of \$100 or more:

DB Technologies  
Geno Brett  
Glass Doctor  
Hare Brained Ideas  
Jimmy Hartley Muffler  
McAbee Construction  
McBiffert and Assoc., Inc.  
McFarland Mall  
Mary Anne O'Neill  
Omar Baker  
Park Plaza Motor Inn  
Roland Pugh Construction  
The Track/Gulf Shores  
Tuscaloosa Chevrolet  
Wings Sports Grill

### Memphis Belle – For a donation of \$50 - \$99:

Karen Bryan  
Mr. And Mrs. Chris Kyle  
New Light Video Productions  
Precision Petroleum Supply  
Sentell Engineering

### Wright Flyer – For a donation of \$1 - \$49:

Barton and Associates  
Major General George F. Hamner  
Swain Optical Service Company

# **Wings**

AIAA/Cessna/ONR Student Design/Build/Fly Competition  
Wichita, Kansas

Department of Aerospace Engineering  
University of Alabama

Addendum Phase  
4 April, 1998

## Lessons Learned

The completed competition aircraft differs significantly from the original design in only two areas. These areas are: Anticipated cruise velocity, range and flight duration; and control surface sizes and gaps.

Due to the availability of a battery with more cells (higher voltage) than originally anticipated, the range expected from the aircraft has increased as well as the duration of the flight. Preliminary predictions put the range at approximately 11 miles and the duration at 25 minutes. Since the time limit in competition is only 7 minutes, the pilot will most likely be instructed to fly the aircraft at a cruise velocity that is significantly higher than the design cruise velocity. This will allow the aircraft to fly farther in the same time than was originally anticipated. An additional benefit is realized by increasing the cruise velocity. As the cruise velocity increases, the aircraft's cruise lift coefficient decreases and approaches the theoretical lift coefficient of maximum aerodynamic efficiency.

The size of the control surfaces, and the hinge gaps between the control surfaces and flight surfaces are the final ways in which the competition aircraft differs from the original design. The control surface sizes are slightly reduced to simplify the methods used to actuate the control surfaces. The original design required hinge lines in the horizontal tail that would have necessitated two control linkages to actuate both elevators. The elevators were instead cut in such a way that both elevators share a common hinge line and a single linkage can be used to actuate both sides of the elevators. During control surface construction, the hinge gaps required to provide adequate control deflections for the rudder and elevator were found to be larger than originally anticipated. In order that the enlarged gaps not interfere with smooth flow over the control surfaces and in order to reduce drag, the control surface gaps are covered with an adhesive gap seal that keeps air from leaking through the gaps and streamlines the control surface hinge lines.

At this time there are several areas which can be improved in the design phase of the project. Sufficient wind tunnel testing is needed to better predict required control surface sizes and deflections. Wind tunnel evaluation of the drag and moment contributions of the fuselage should also be done to assist in predicting stability and performance characteristics of the aircraft. Finally, wind tunnel testing of the drag contribution due to landing gear should be done to more adequately determine the figures of merit for fixed vs. retractable gear as well as to better predict aircraft performance. These design changes may be expected to require approximately 6 weeks of labor (about 240 man-hours) as well as the additional costs of running the wind tunnel and materials for fabrication of test articles.

The manufacturers list price of many of the components used in the design are as follows:

<b>Manufacturer</b>	<b>Component</b>	<b>Price</b>
1. SR Batteries, Inc.	Battery	\$188.00
2. Airtronics	Radio/Servos	\$598.97
3. Wicks Aircraft Supply	Fiberglass Cloth	\$308.00
	¼ inch Foam	\$145.08
	Vacuum Bag	\$ 7.05
	Breather Material	\$ 19.50
	Release Cloth	\$ 36.60
	Epoxy	\$ 48.53
	Wax Mold Release	\$ 18.59
4. Sig Manufacturing Co., Inc.	Fiberglass Cloth	\$ 22.70
5. AVEOX	Motor	\$200.00
	Speed Controller	\$250.00
6. Black Warrior Custom Counters	Particle Board	\$ 40.00
7. Excel Foam, Inc.	Structural Foam	\$ 12.44
8. NSP	Battery Charger	\$150.00
	Volt-Amp Meter	\$ 68.00
9. Various Manufacturers	Misc. Hardware	<u>\$100.00</u>

**Total Cost:**

**\$2213.46**

The majority of the estimates of component costs used during the design phase were within 10% of the actual costs encountered with the exception of the cost of fiberglass cloth and the cost of the speed controller. Both of these items cost significantly more than was originally expected. In retrospect, however, no part of the design would have been changed solely due to these cost overruns. At this time there appears to be no viable alternative which will reduce the cost of the actual materials or the manufacturing processes in any future design.

The Electric Boogaloo

Submitted by:

University of Arizona chapter of AIAA

To the AIAA Design, Build and Fly Competition;  
in accordance with the Applied Aerodynamics, Aircraft Design,  
and Flight Test Technical Committees of the AIAA.

## Executive Summary

Our design began with a general layout of the major components that were to be part of the aircraft. The layout included the battery packs, motor, radio transmitter, servos, and the placement of the payload. This proved to be a tricky proposition, since a slight change of the payload could drastically alter the center of gravity (cg) location, and hence affect the stability of the entire aircraft. Once we agreed upon a layout we began to design the aircraft around the components. This led to several more alternatives, ranging from high wing designs to low wing setups, sailplane designs, and more traditional aircraft layouts. Hoping to minimize excessive drag elements, we opted for a combination sailplane/low wing design. This configuration gives a high lift to drag ratio, which will help conserve battery power during level flight. This would help to assure that the maximum flight time could be attained. Choosing this configuration meant that a substantial wingspan would be required, which created its own area of concern: how to design a wing that would be lightweight but strong enough to withstand the necessary 2.5 g test?

A wood constructed wing was chosen rather than a foam structure due to the substantial weight savings. Starting at an approximate weight of twelve pounds, due to the weight of necessary components, we set out to create an aircraft that would weigh less than seven pounds. At this point is where the team began to divide up and devise solutions to the task at hand. The aerodynamics group started researching high lift, low Reynold's number airfoils. The configuration group started analysis on wing designs that would be able to support the expected loading. When the groups met at a later date to discuss results an airfoil shape was selected as well as the design of the main wing spar. At this point Matlab was utilized to plot out points of the airfoil cross-section. From this plot a template was created by which the wing would be designed.

Construction of a prototype wing was initiated at this point. Once complete, the wing was subjected to a wing loading test. At a weight of ten and a half pounds the wing failed at the wing box. The failure occurred at a bolt location, where the wood split apart on the main spar. This problem was corrected by the use of stronger wood at the mounting location of the spar. Once this was done the test was repeated. During this test at a weight of fourteen and a half pounds

the wing once again failed. This time the failure occurred at about ten inches from the root chord, where the balsa wood being used for the top and bottom spar split lengthwise along the span. The failure was initiated in a location where a reinforced web was used and proceeded down the span to the next location of the web. At this time it was decided to use a stronger wood for the entire spar instead of the balsa wood that was originally used.

Once the wing passed the loading test, construction on the fuselage was started. During the testing of the wing, the configuration group had been using AutoCAD to create the fuselage for the aircraft. The final design was essentially two cylinders connected together, the larger of which would house all major components; the smaller one would hold the vertical and horizontal stabilizers. Components were packed as tightly as could be managed in order to avoid excessive building materials and keep weight to a minimum. AutoCAD provided a good approximation of the weight of the aircraft by entering the type of materials used and their densities. This allowed the team to keep track of weights as they added up during the early stages of the design. This kept construction time to a minimum, as there was no wasted time in constructing an airframe that was heavier than need be.



## Management Summary

The design team of the Electric Boogaloo consisted of eight students:

Gary Newson .....	Project Manager, Pilot, and Propulsion Systems
Paul Sieck.....	Controls (Leader)
Jason Nichol.....	Configuration, Materials (Leader)
Greg Mondeau.....	Aerodynamics (Leader)
April Register.....	Configuration
Sung-Lieh Lin.....	Aerodynamics
Jefferson Chen.....	Propulsion
Brian Ibbotson.....	Materials

Each team leader was responsible for setting schedules regarding material within their respective areas and assuring that project deadlines were met. The groups met as a whole generally every other Thursday to discuss progress, problems that had arose, and participate in construction. Singularly each group met on regular basis, particular to that group's time constraints from course loads, work, etc.

Design meetings were conducted by the project manager and progress or delays noted. Deadlines were created in order to keep the project moving forward in a timely manner. These deadlines often were set around tests and other class related projects, so that member's grades would not suffer.

	<b>Milestone Chart</b>	
	<u>Projected Deadline</u>	<u>Achieved</u>
<b>Conceptual Design</b>	Nov. 20, 1997	Nov. 20, 1997
<b>Conceptual Report</b>	Dec. 15, 1997	Dec. 15, 1997
<b>Preliminary Design</b>	Jan. 20, 1998	Jan. 28, 1998
<b>Preliminary Report</b>	Jan. 30, 1998	Feb. 6, 1998
<b>Flight Testing</b>	Feb. 20, 1998	Feb. 28, 1998
<b>Detailed Design</b>	Mar. 5, 1998	Mar. 10, 1998
<b>Final Report</b>	Mar. 10, 1998	Mar. 12, 1998

## Conceptual Design

From the original layout of the components, three possible configurations were investigated. These platforms included a powered sailplane design, a high wing design, and a low wing design. Each of these designs brought forth their own positive and negative attributes. In order to choose one, each had to be evaluated by the parameters dictated by the mission requirements. The mission required a lightweight aircraft that could complete as many laps as possible in a specific time. In order to meet these requirements the winning platform would have to be as efficient as possible, by means of maximizing the lift to drag ratio ( $L/D$ ), strength to weight ratio ( $Str/Wght$ ), acceleration during take off, rate of climb ( $R/C$ ), cruise speed  $V_c$ , controllability, manufacturability. Also, the winning design would minimize weight, cost, and wing loading ( $W/S$ ). These parameters could be met by properly matching the wing span, wing design, configuration, materials, and the propeller.

Lift-to-drag ratio is important in that the higher the value, the more battery power that can be conserved while in level flight. It is necessary to have an aerodynamically clean aircraft that reduces drag as much as possible while producing lift, since increased lift increases induced drag. It then became necessary to choose an airfoil to meet these requirements while operating in a low Reynold's number environment.

Strength-to-Weight ratio is also a deciding factor in that an extremely lightweight airframe is needed; yet that airframe must still be able to support the loads encountered during flight. Choosing the right materials to accomplish this goal is a key factor in the overall choice of a platform, the bigger the aircraft the more materials needed and therefore the higher the weight required to adequately carry the load.

Acceleration in takeoff is a crucial factor in choosing a design. The design of choice has to be able to attain its takeoff velocity ( $V_{TO}$ ) and clear the obstacle in the required distance.

The rate of climb is essential in that it would be beneficial to reach altitude quickly and avoid excessive use of available power. A platform choice that climbs quickly while suffering little drag might be the platform that wins the competition.

Cruise velocity at altitude is important in that more laps could be completed in the given time. This is a very important parameter; a tradeoff must be made between speed and the power used to maintain that speed.

Controllability is important in that the chosen platform must be stable and easy to control. If a design is hard to control then staying on course might be a problem at best, or at worse a catastrophic crash could result.

Being able to manufacture the aircraft is also essential to the design, in that complicated structures increased manufacture time and cost, while possibly increasing weight. With both limited resources and limited manufacturing knowledge, ease of construction played a major role in choosing a configuration.

Weight is by far the most important criteria. With a limited weight for the propulsion system and a required payload, minimizing the design is essential for a working model. If a heavy model were able to meet the takeoff requirements it would likely be sluggish while in the air, thus affecting the number of laps that could be successfully completed. An ultralight model would likely fail the loading test, or worse, fail in flight.

Keeping costs low is also an important factor in the design. Cost constraints affect the selection of materials and the means by which production is achieved. It also gives the team members incentive to not waste materials.

A low wing loading is desired in order to keep structure weight to a minimum. This also helps in maneuverability of the aircraft.

Many of these parameters can be evaluated by means of the basic laws of aerodynamics and general formulas such as:

- |    |                                      |                         |                   |
|----|--------------------------------------|-------------------------|-------------------|
| 1) | $W = L = \frac{1}{2} \rho S V^2 C_L$ | for steady level flight | $S = \text{area}$ |
| 2) | $D = \frac{1}{2} \rho S V^2 C_D$     | for steady level flight |                   |
| 3) | $A = b^2/S$                          | Aspect Ratio            |                   |

These are utilized for a general sense of how a particular design performs against the others. These are just basic observations but they give an idea of how a particular design may perform before exploring a more in depth analysis.

To help narrow down the three choices, each was ranked in a number of categories on a 1 to 10 scale. The rank was dependent upon how it would perform in general and relative to the other choices as well. The results are posted in the table below

<b>FOM Ranking Chart</b>			
	Sailplane	High Wing	Low Wing
<b>L/D</b>	10	7	6
<b>Str/Wght</b>	4	6	8
<b>Acceleration</b>	4	9	7
<b>R/C</b>	9	8	8
<b>Cruise Vel.</b>	5	8	8
<b>Controllability</b>	7	8	7
<b>Manufact.</b>	8	7	9
<b>Weight</b>	8	6	8
<b>Cost</b>	7	7	9
<b>W/S</b>	8	7	7
<b>Avg</b>	7	7.3	7.7
<b>Scale 1 - 10</b>			

As a result of the study, a merger of sorts was chosen between the low wing design and a sailplane. This combination is felt to give both a high L/D ratio, and good takeoff capabilities. This also seems to offer a low drag solution. Construction would be simplified and the payload would be more stable in flight while maneuvering. This configuration allows the payload to "rest" on the wing and be supported during a turn, whereas in the high wing option, the wing and payload would tend to pull apart while maneuvering.

## Preliminary Design

This stage of design is where the initial sizing began, early performance estimates made, and the confirmation of whether or not the right configuration was chosen. In sizing the aircraft the wing area was calculated first. This was done by taking our projected weight of seventeen pounds and multiplying it by a factor of safety of 1.5. This gave us a weight of 25.5 pounds. The aerodynamics group at this point chose a spica airfoil of 11.3 % maximum thickness. This choice was made from data acquired through the program "Sailplane Design" (version 3). This program provides essentially a collection of common airfoils, and data on how they perform under low Reynolds number conditions. This chosen airfoil is said to provide a  $C_{Lmax}$  of 1.4, although it was decided to use a lower value of 1.2 for calculations. Using Equation 1) from the Conceptual Design section yielded the following results for the required wing area, assuming a cruise velocity of 51.3 ft/s.

$$25.5 = (1.2)(.5) (.00238)(51.3)^2 \cdot A$$

$$A = 6.78 \text{ ft}^2$$

Using a chord length of 11 inches results in a wing span of 7 ft 5 in. Now it was known how much room was needed for components within the fuselage and the required span.

The next step was to size the tail. This was accomplished by calculating the neutral point of the aircraft, with a ten- percent margin of stability. The equation for this calculation is

$$X_n := \frac{X_1 \cdot S_1 \cdot a_1 + X_2 \cdot S_2 \cdot a_2 - 2 \cdot V_f}{(S_1 \cdot a_1 + S_2 \cdot a_2)}$$

$X_n$  – location of neutral point  
measured from the  
nose

$X_1$  = location of main wing

$X_2$  = location of tail

$S_1$  = area of main wing

$S_2$  = area of tail

$a_1 = 2\pi / 1 + (2/A)$   $A$  – Aspect Ratio

$a_2 = (1 - (a_1/\pi A))$

$V_f$  = virtual fuselage volume

This resulted in a tail area of 1.3 ft<sup>2</sup>. To allow for enough pitching authority it was decided to make the tailboom three feet in length.

The vertical tail was sized according to the convention of the AIAA Aerospace Design Engineers Guide, where the vertical tail is about ten percent of the main wing. This resulted in an area of just over a half a square foot.

With the major components of the airframe sized it was necessary to look into the expected performance of the aircraft. An Astroflight 25G motor was selected for use and data acquired from the manufacturer helped to predict the output power of the motor. These values, when used with conservative estimates regarding losses, helped to predict more detailed estimates of the performance. When used with eighteen cells the motor could produce over 500 watts of power. This however would put an extremely high load on the motor, reaching close to fifty amps. This would severely damage the motor and had to be avoided. A more conservative estimate of the output was in the neighborhood of 400-480 watts. At full power this could theoretically produce speeds of sixty to eighty miles per hour. These numbers are found by taking the rpm of the motor multiplying the pitch of the propeller and a conversion factor.

$$V = \text{RPM} * \text{Pitch} * (.00095)$$

For various combinations of propeller sizes, and number of cells an estimate of performance could be found. For example using an 11X7 propeller with eighteen cells (1700 mA-H) a speed of sixty-five mph should be attained. This number reflects propeller theory and does not take into account a fully loaded propeller attached to an airframe, but it is a good start.

Using these numbers and adding in some extra losses the Electric Boogaloo is projected to attain a takeoff velocity of thirty-three mph and have a stall speed of just over twenty-five mph. A projected ground roll of 270 ft is required to reach  $V_{TO}$  and clear the six-foot obstacle. This estimate also predicts a minimum  $V_C$  of thirty-eight mph.

## Detail Design

Entering this phase of design dealt with compiling the data gathered and comparing actual performance with that estimated. The final configuration had a total length of five and a half feet, a wing span of eight feet, and weighed 16.8 pounds. The final design also passed the wing tip loading test, but was not tested to failure. The total g load capability is roughly estimated at 2.7-2.8. This also yields a payload fraction of 45%.

In order to remain stable while in flight the wings are set in a dihedral. A standard four percent angle was used. For the given wing span of eight feet this is equivalent to a one and a half-inch height difference in the wing from root to tip. This is essential, as the final configuration does not use ailerons. Like many trainer RC aircraft the model uses only the rudder and elevator to negotiate turns. This method of control was chosen for a few reasons the partial weight savings from the lack of an additional servo and the associated hardware. Additionally, this choice helped in the manufacturing process as the wing could be assembled without having to make room for control rods, hinges, or having to incorporate the added moving surface that would have been attached to the wing.

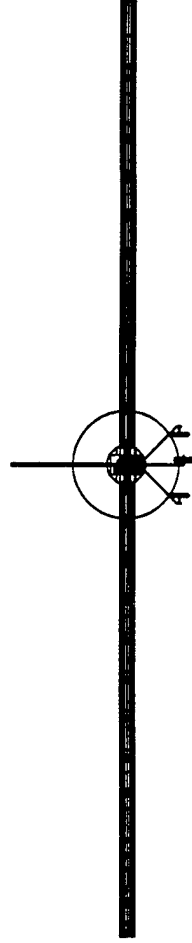
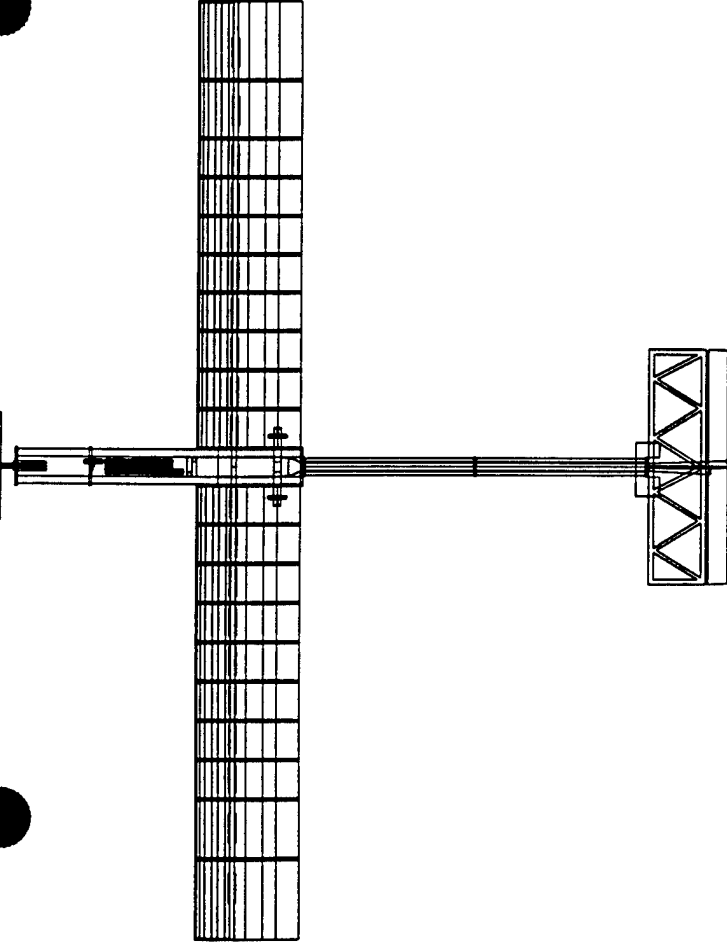
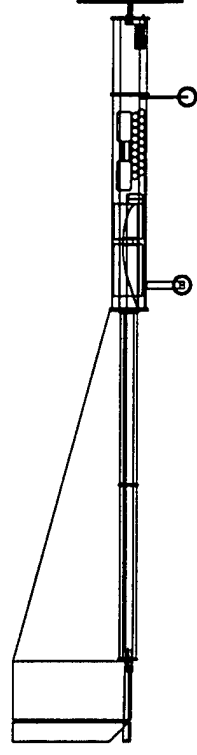
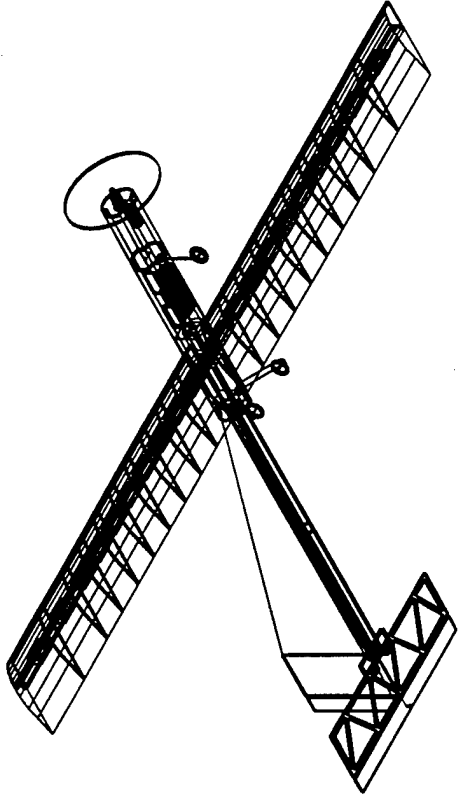
The control mechanisms are a push-pull type that uses a flexible plastic control rod that slides inside of a hollow rod that is bent around the sides of the fuselage and down the center of the tailboom. This setup was chosen over other options as there were fewer parts, the system is lightweight, and does not rely on piano wire that could break in flight. The nose wheel is attached to the same servo as the rudder to allow for steering while on the ground. This gives a total of only three channels for operation, including the throttle. This system is both simple and user friendly allowing the pilot to concentrate on maintaining a tight flight path around the course.

The propulsion system is controlled through a standard electric speed control, made by Astroflight, connected to an Astroflight FAI-25G motor. Eighteen SANYO RC-2000 batteries power the system and provide approximately thirty amperes at eighteen volts at full throttle. These values can be altered depending upon the type of propeller used, which can alter the performance of the system by as much as forty percent. A larger prop diameter with a lower pitch yields good acceleration qualities but only yields modest cruise speeds. Moving in the opposite

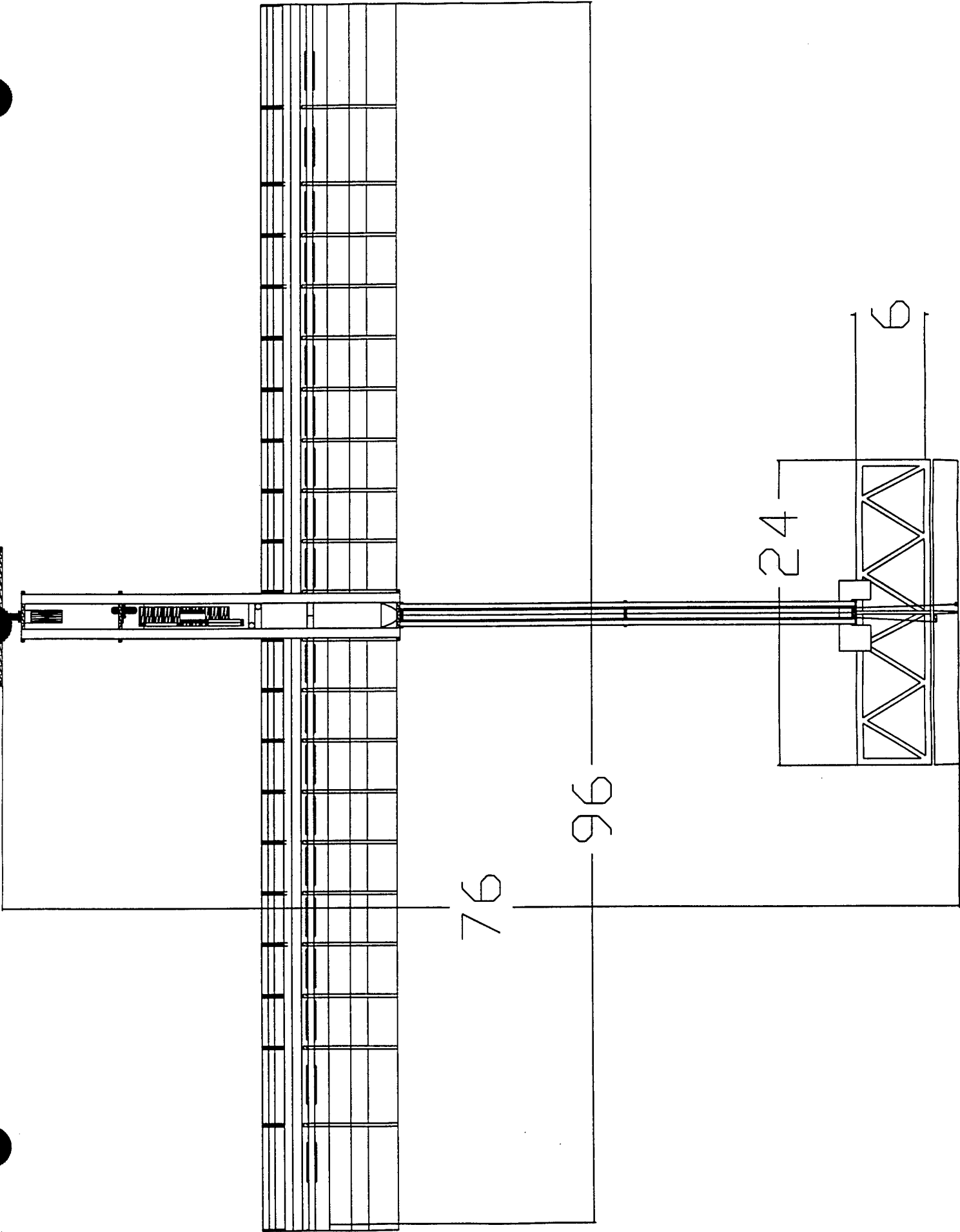
direction, a high pitch prop that is shorter in diameter will reach high cruise speeds but needs a longer ground roll. This has led to the full testing of two separate propellers an 11X7 and a 12X6. Depending upon conditions the shorter propeller often pushes the limits allowed for takeoff; while the larger diameter propeller has never come close to not meeting the requirements for takeoff. There is a noticeable difference in velocity during level flight but turns are negotiated easily for either choice. As of yet a very tight turn radius has not been attempted due to the desire to keep the aircraft safe until the competition.

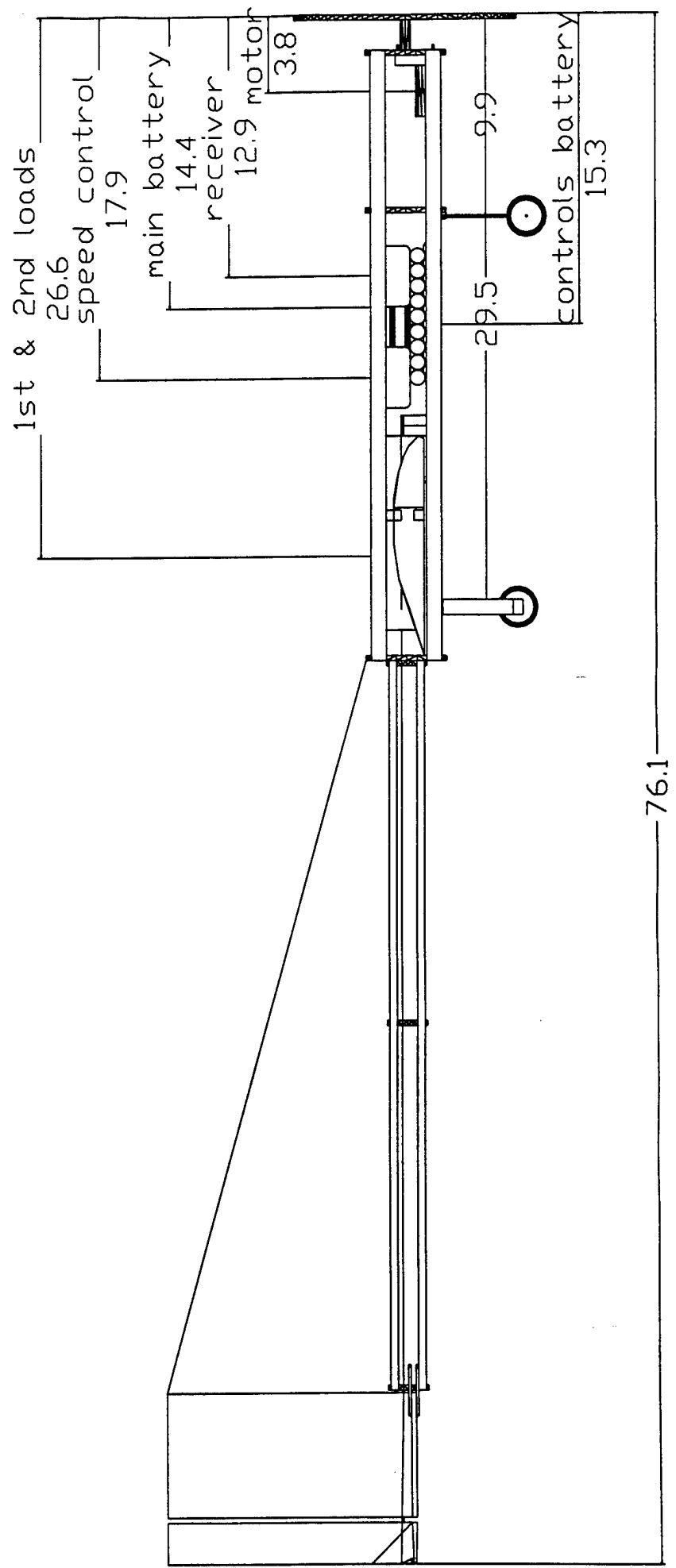
Careful attention must be paid to throttle control as pushing for more speed drastically reduces the flight duration. This is known by testing the charge left in the battery pack once the flight is completed. To date the longest flight attempted has only been four minutes although it appears as though reaching a window of seven minutes can be reached. Currently only basic flight have been attempted, mostly takeoffs, touch and goes, and landings. There has been little damage outside of a broken bulkhead where the front wheel is attached due to a hard landing.



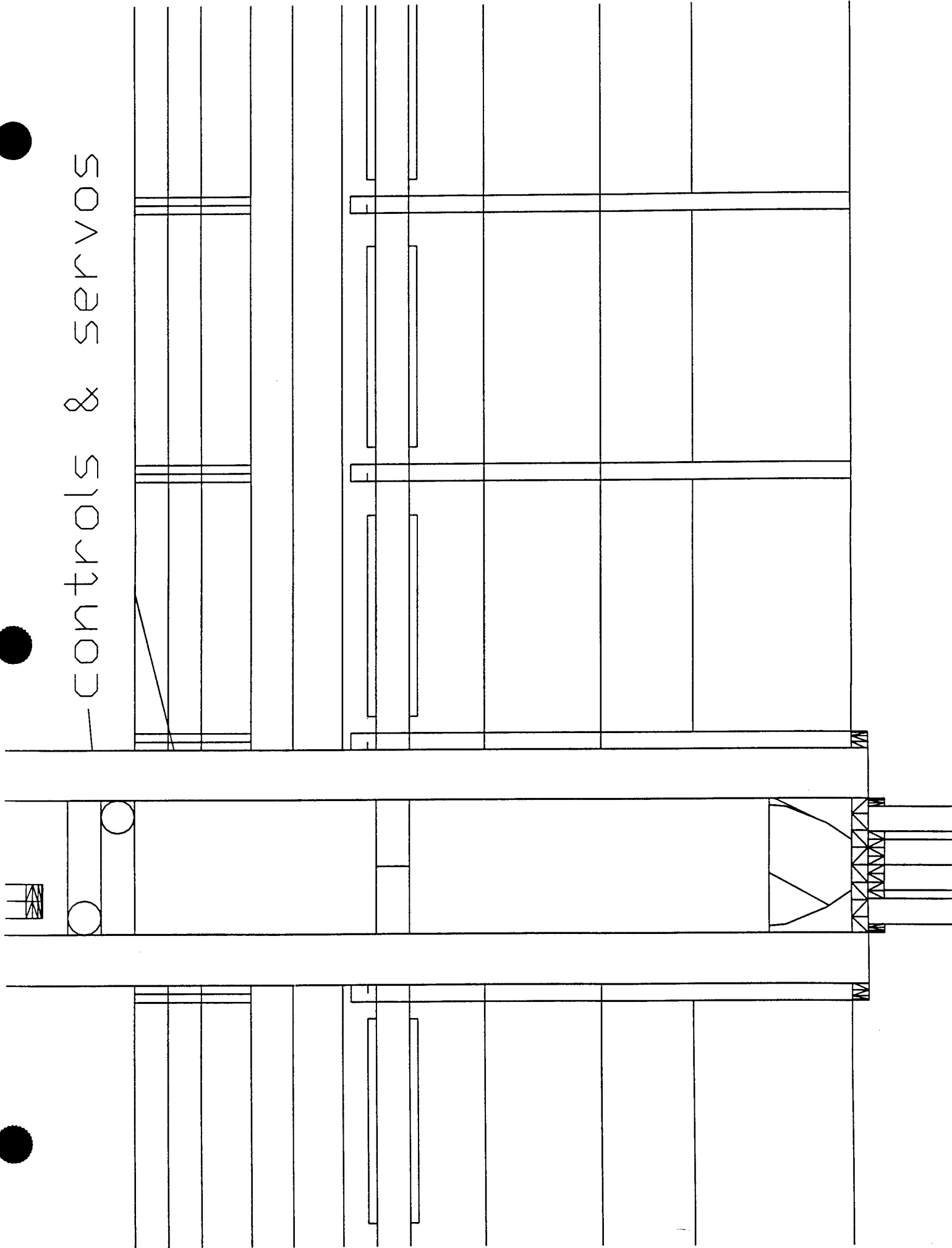


SCALE 1"=20"



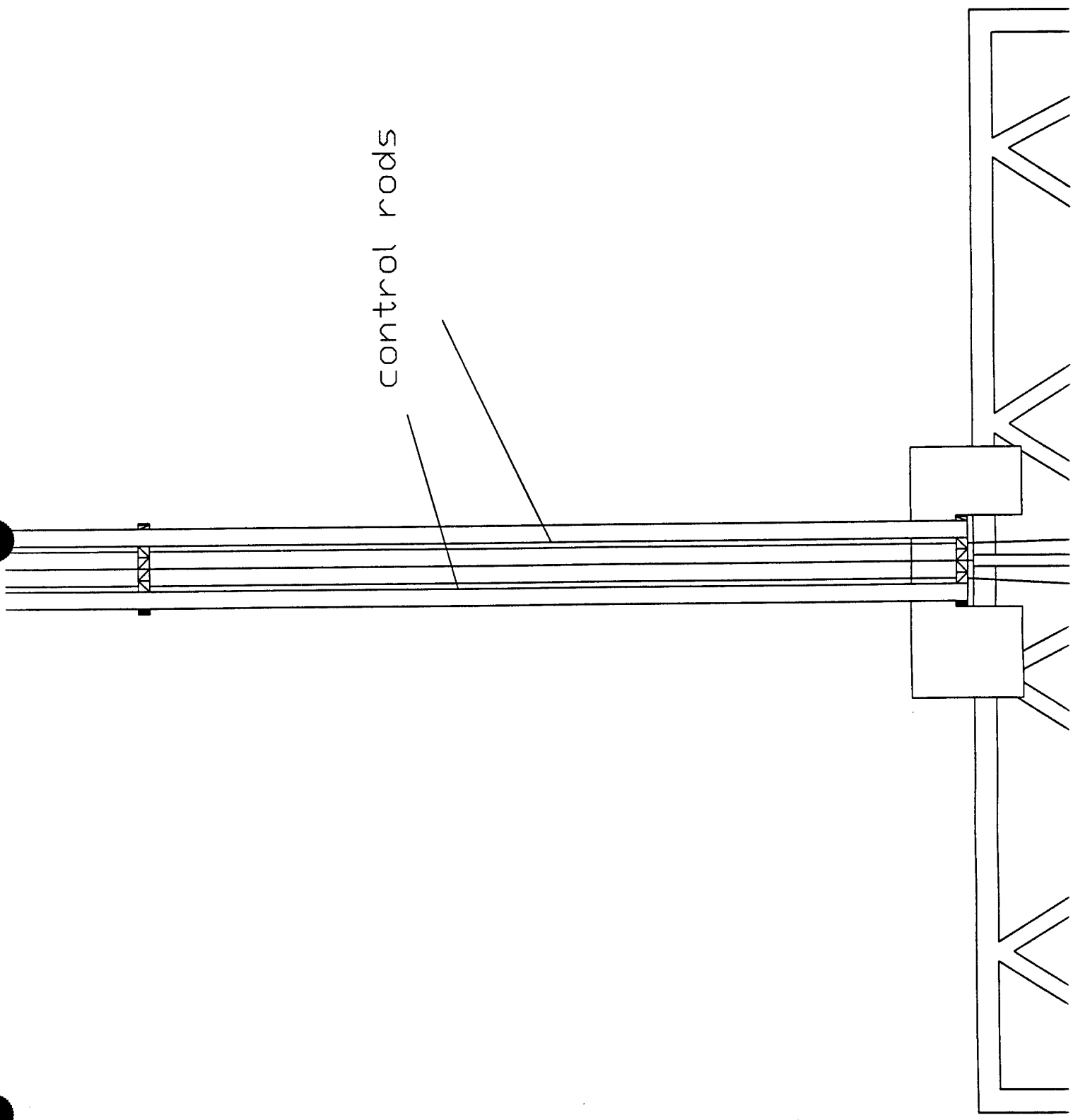
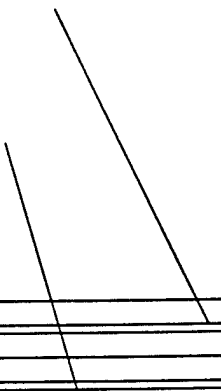


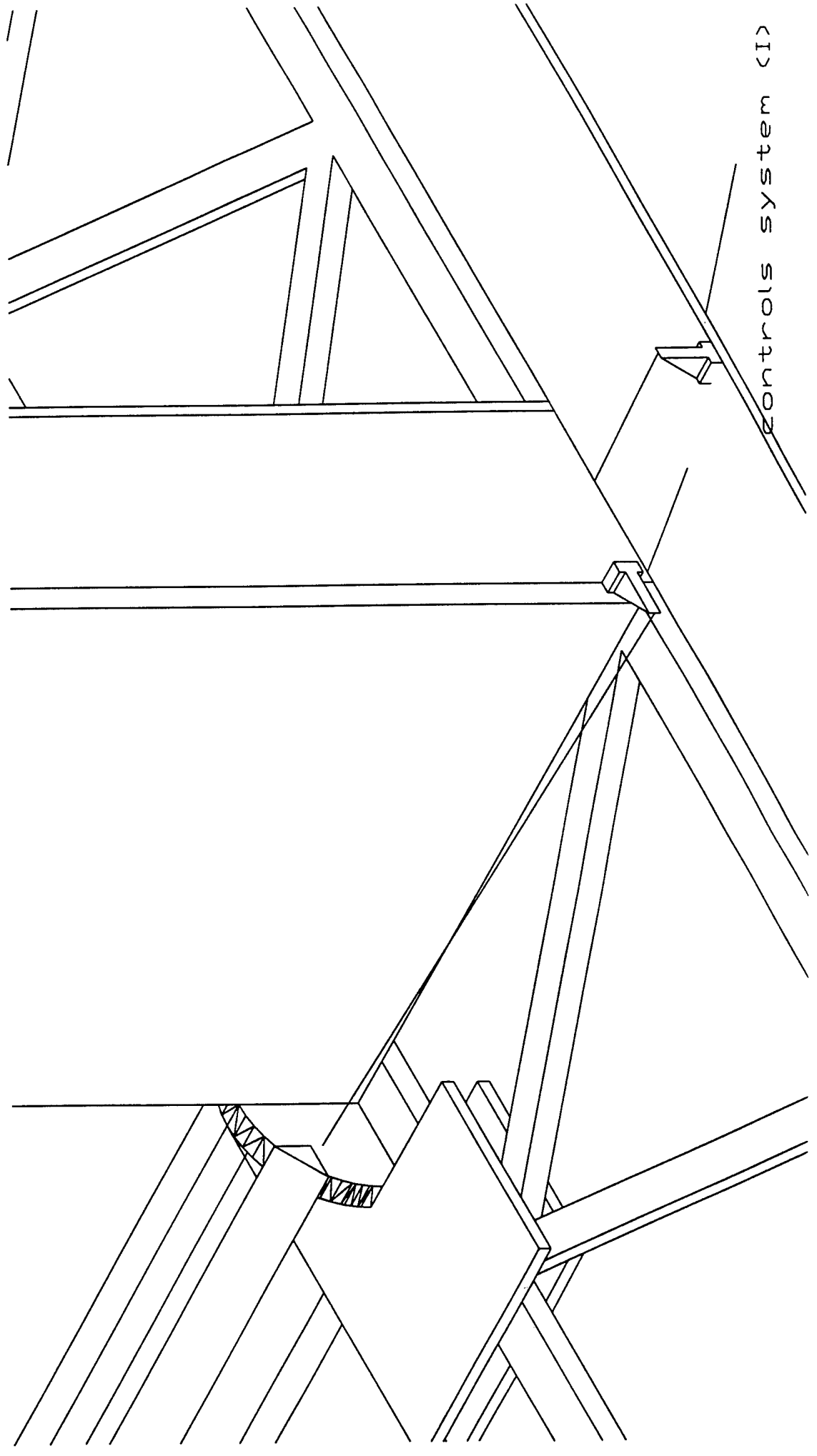
controls & servos





control rods

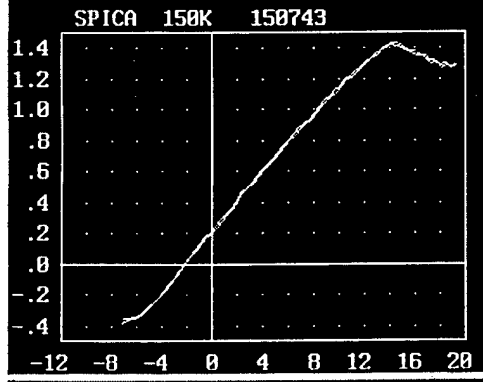
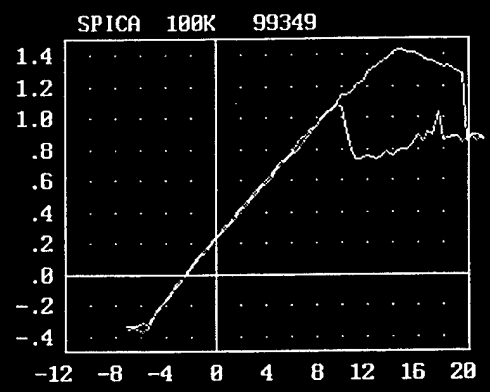
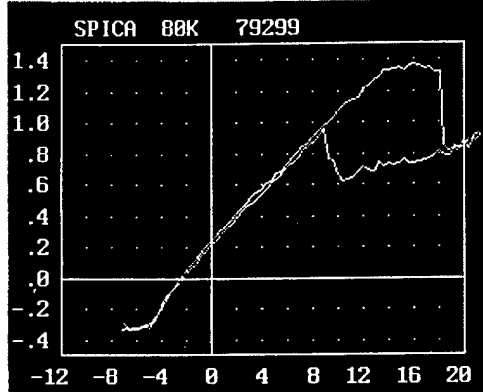




controls system (I)

SD - SAIL

Auto



## Manufacturing Plan

The primary mission of the manufacturing process was to create as lightweight airframe as possible and yet maintain the structural integrity needed to fulfill the mission. Initially, the use of composite materials was investigated for use in the fabrication of the aircraft, but this idea was put aside due the complexities that arose. These problems consisted of: acquiring materials, cost, and the facilities needed to work the materials. Lightweight woods were then chosen as they were easily accessible, cost effective, and relatively easy to fabricate with little more than the normal array of shop materials.

The construction process consisted of both traditional methods and a few innovative means of weight reduction. It was decided that in order to save on weight the traditional method of constructing a wing would be altered. This was done by means of avoiding the use of solid wing ribs.

### *Wings*

The wing is made up of two separate wings joined at the fuselage in a wing box. The wing spar followed a traditional means of fabrication, as this was to be the major load bearing structure of the entire aircraft. There is both an upper and lower spar, with a web along the span for reinforcement from bending. The upper spar is smaller than the lower one, as its loading would be compressive in addition to the expected bending. It was hard to locate birch sticks that were over four feet in length so two sticks had to be spliced together. Each was cut at a forty-five degree angle and then glued together with cyanoacrylate. The ribs were then spaced every eight inches along the span.

For this design, the major manufacturing hurdle was the formation of the ribs. The lightweight balsa stringer-style rib was difficult to bend around the tight curvature of the airfoil's leading edge. Three main solutions to this problem were investigated: stress-relief cracks, steaming, and abrasive thinning.

The stress-relief cracks were basically notches cut into the wood on the outside of the curve, so that fibers in tension were regularly broken rather than split from the rest of the wood.



This method met with only marginal success, as the cracks supplied a starting point for the wood to split. After several experiments varying notch spacing and depth, this process was ruled out as a viable solution.

Steaming the wood met with more success. The wood was placed in a steam bath for 30-45 minutes, then removed and promptly fitted about an airfoil form, then allowed to set overnight. Noticeable increases in flexibility were observed, but wood splitting and buckling still occurred at the tightest curve of the leading edge.

The final option was sanding the wood at the high-curvature sections. This method dramatically reduced the buckling and splitting at the leading edge. While the results varied widely with wood quality, the best flexibility resulted from a 60% or greater reduction in thickness. This method appeared to be the solution for the leading edge buckling problem, but it offered no assurance of the airfoil shape accuracy away from the leading edge.

A combination of sanding and steaming was ultimately chosen to shape the ribs. The distance to the leading edge was measured from the trailing edge along the bottom of the airfoil, and then this region was sanded down to approximately 1/32 in. The wood was placed in a steam bath for 45 min., and then wrapped around the airfoil form to cure overnight. This created a rib that was true to the design airfoil, while still maintaining rigidity over the lifting surface. Once the rib was in place, a double layer of heavy-bond drawing paper was applied to the structure to add tensile strength and to prevent the Monokote from "bowing in" between the ribs along the high-curvature leading edge. Several glues were tested to adhere the paper to the wing structure; among them were cyanoacrylate, carpenter's glue, and ordinary white paste. The cyanoacrylate and carpenter's glue held the best, but the cyanoacrylate absorbed into the paper, strengthening the material further than the bonding surface, so cyanoacrylate was chosen for the purpose. The second paper layer was expected to adhere to the first over the entire surface of the wing, so an aerosol contact cement was chosen for its ease of application and commercial availability.

### *Fuselage and Tailboom*

In this design the fuselage and tailboom are essentially the same structure, with the fuselage being twice the diameter of the boom. Each consists of four birch longerones set at every ninety degrees beginning at forty-five degrees, with balsa wood spacers running between them. The longerones provide the main support for the structure with the spacers being utilized to hold the shape of the fuselage once Monokoted. This configuration was chosen so that the wings could be mounted slightly below the centerline of the fuselage thus enabling the wings to essentially carry the payload.

The structures were formed by cutting circular bulkheads to the necessary diameter and then notching where the longerones would be located. Once finished the created product was a cylindrical volume that was both torsionally strong and resistant to bending. The main fuselage was then reinforced with birch ply where heavy components are located. The two cylinders are attached to each other by four 10-32 bolts run through the main bulkhead of each component.

The wing box is a built up structure of half-inch balsa block and four-ply birch secured into rear of the fuselage by both cyanoacrylate and bolts. The wings are slid into the box from the sides and secured to the box by four nylon bolts in each wing.

Under the entire length along of the fuselage along the lower longeron there is a support for the payload, battery pack, and a point for attaching the rear landing gear. The support is a three sixteenth piece of four-ply birch, secured to the fuselage by cyanoacrylate. At the point where the landing gear is attached a balsa block is sandwiched between two pieces of ply. This is due to the rear wheels being located under the majority of the payload, which is divided into two pieces. The plate that the weight rests on is a little less than half an inch above the rest of the bottom of the fuselage.

	<u>Manufacturing Milestone Chart</u>	
	<u>Projected Deadline</u>	<u>Achieved</u>
<b>Wing (prototype)</b>	Jan. 10, 1998	Jan 10, 1998
<b>Wing (final)</b>	Feb. 1, 1998	Feb. 11, 1998
<b>Fuselage</b>	Feb. 15, 1998	Feb. 22, 1998
<b>Tailboom</b>	Feb. 15, 1998	Feb. 22, 1998
<b>Assembly</b>	Feb. 19, 1998	Feb. 26, 1998
<b>Flight Testing</b>	Feb. 20, 1998	Feb. 28, 1998

The manufacturing process was initially set to a strict schedule but due to classroom requirements, funding, and unforeseen delays, there was some difficulty in meeting each of the set deadlines.

The Electric Boogaloo

Addendum to Design Report

Submitted by:

University of Arizona chapter of AIAA

To the AIAA Design, Build and Fly Competition;  
in accordance with the Applied Aerodynamics, Aircraft Design,  
and Flight Test Technical Committees of the AIAA.

## Lessons Learned

The final design to be used in the competition has been slightly altered from the original design submitted. The obvious differences can be seen in the placement of the rear wheels, moved from the fuselage to the wings and slightly back. The front wheel was also altered in order to provide more ground clearance. This change is merely the result of a longer nose wheel assembly. These alterations resulted in nearly three more inches of clearance, allowing for the use of a larger propeller. This was needed as once the aircraft was fully loaded takeoff performance was greatly diminished and the design requirements were not met.

There is also a more subtle change in the current design, in the wing structure itself. This is a secondary result of the original rear wheel placement. The narrow gap between the rear wheels caused a wing to be fatally damaged during a landing attempt. It is possible that the wing was already weakened from the loading test, much like the original wings with the all-wood spar. Because of the lengthy process to construct the original wings it was decided to follow a more traditional route and use a material that would pass the loading test without concern.

The new wings are a single spar structure made from the Metalite floorboard material currently being removed from many commercial aircraft. (Newer airline floorboards use a Kevlar/Nomex composite sandwich, with a much higher cost.) The new wings also use a solid rib versus the original open-rib style. The solid ribs resulted in slight weight increase that was offset by the ease of manufacture. The spar material is made from 0.25-in. balsa wood sandwiched between two 0.03-in. sheets of aluminum. This material was tested by the same means as our original loading tests. The new wings not only passed at our prescribed weight of 18.2 pounds, but also passed at a weight of nearly thirty pounds. This gives a very large critical load factor of 4.1. This was not the intended result, as the material was cut to match the size of our original wing spars. This new structure only added to our original weight by about 1.7%.

The major area where improvements can be made is in the experience of those involved. As typical RC applications do not necessarily hold for this contest many areas had to be investigated for the first time. These include wing assembly, wing loading, stress analysis, proper matching of propeller and motor, and weight reduction from non-load bearing parts. Weight

reduction is another area where another large set of improvements could be made, as time constraints did not allow for some pieces of the aircraft to be altered following the redesign of the wing. An example of this is the original location of the rear wheels. Once the wheels were moved out on the wings, there was no longer a need to have a reinforced area for attachment below the fuselage.

A second-generation version of this aircraft would have a redesigned fuselage structure. The current fuselage is overdesigned to be sure the steel payload is properly supported, and to withstand small impacts. A better fuselage would be lighter and easier to replace, rather than the current damage tolerance. Also, fuselage aerodynamics would be improved to reduce skin friction and base drag.

The main cost-reduction emphasis would lie on more efficient use of materials. The current manufacturing process produced a large amount of scrap paper, wood, and Monocote. Resource management and planning in the early manufacturing stages will be effective in reducing waste material, thereby lowering costs. Actual costs for the construction of the current aircraft were higher than predicted, due to the wing failure and the aforementioned material waste problems. Effective use of materials could result in cost savings up to 10% in the manufacture of the fuselage.

	<u>Manufacturers List Price</u>		
<u>Component or System</u>			<u>Cost (\$)</u>
Propulsion	Motor & Speed Control		235
	Battery Pack & Charger		251
	Propellers and Acc.		30
Radio	On Loan		0
Controls			16
Fuselage	Main Fuselage & Boom		35
	Landing Gear		24
Wings			18
Misc			51
		Total	660

# **UCLA AIAA Student Chapter**

Proposal For the Design/Build/Fly  
Student Competition  
1997/98

*The airplane stays up because it doesn't have time to fall.*  
-Orville Wright

## **Part I: Executive Summary**

### **I. Summary:**

This year's design is an all-wing, or "flying wing" aircraft. We reached this design by analyzing the benefits and costs associated with particular configuration. The aircraft is constructed with a hybridized method utilizing foam cores, fiberglass, and balsa sheeting and spars. The engine is arranged as a pusher, in order to provide greater stability. The aircraft has fixed landing gear, since the flight speeds for maximizing the number of laps completed do not justify the extra weight and complexity of retractable gear. For the first series of tests with the full size aircraft, the nose gear was unsteerable. This is both to reduce weight and complexity, and because of the faith we have in our pilot.

The engine-propeller combination is the same as that used last year, and is ungeared just as last year. The plane is equipped with fast charge batteries instead of the high capacity cells used last year because the high capacity cells were incapable of handling the high current demanded, and therefore were subject to excessive heating and the associated losses.

Our configuration offers the simplicity of a two control surface arrangement, with "elevon" mixing. This limits the number of cross-couplings to be considered and lightens the weight of the aircraft by a few ounces. In our configuration, the location of the center of gravity must be located precisely relative to the aerodynamic center. The lack of a tail for trimming forces requires the wing to be tailored for one center of gravity condition only. We are able to save approximately two times the weight of an item in the rear by eliminating it, so every ounce "counts double".

The only vertical surfaces are winglets at the wingtips, and these act to both counter induced drag and provide a restoring moment to limit sideslip, especially on the approach.

We predict that the aircraft will be able to complete 13 to 14 laps with the power at our disposal, and this measures up favorably with the results from last year's competition, where the winning team completed 12 laps in an untimed contest.

Our team consisted of a design leader and an otherwise unstructured group of other members. This particular arrangement is due to the fact that our team size is limited this year to only 4 truly active members, and perhaps 4 more occasional members.



## **Part II: Management Summary**

### **I. Members:**

#### Full time team:

Design leader: Christopher Silva (Sr, AE)  
Pilot: Gary Fogel (almost PhD, biology) AMA: 50601  
Team member: John Moreland (So, AE)  
Team member: Jeff Sinsay (Fr, AE)  
Team member, AIAA  
President: Po-Hao (Adam) Huang (Sr, AE)

#### Part time team members:

Team member: Ching-yi Wang (So, EE/CS)  
Team member: Brian Leung (So, Mat Sci & E)  
Team member: Hwa Heng (Sr, ME)  
Team member: Franklin Meng (Jr, EE)  
Team member: Wayne Lu (Sr, AE)

### **II. Structure and philosophy:**

The division of the assignments was based upon the needs we had and the skills people possessed. Since most people were new to this process of construction and certainly flying wing aerodynamics, we all had to learn as we went along.

The design leader was in charge of designing the wing aerodynamically, and at the weekly design review meetings, the current design would be presented along with the predictions of performance, so that the progress could be seen. Components and subsystems were presented, such as the wing divisions, landing gear, and control surfaces.

All of the members of the team were invited to research aerodynamics and flying wings, and a good many new sources of information were discovered and studied. The design leader was in charge of accumulating the research of the other members, along with his own findings, and providing a concise overall picture for analysis and to present to the team members.

The members would then discuss the advantages and drawbacks of a particular system, and calculations would be presented if necessary. The timeline impact was always mentioned, and an updated timeline was generated at the conclusion of each meeting, along with goals for the week and schedule availability of the members.

Due to this method, it is exceptionally difficult to define a single timeline. However, some milestones were placed along the calendar (see next page).

Milestone:  
48" span prototype  
flown

Anticipated date:  
End of November

True date:  
End of December

Full size aircraft  
construction begun

Mid January

Mid February

First Flight of full size  
aircraft

End February/  
early March

Mid March  
(March 15?)

All other details were in constant change, and only defined in relative times to those above.

For example: The cutting of the cores and spar placements are planned to take half a weekend, and the covering with balsa and vacuum bagging require a whole weekend and the week surrounding it. (This estimate was accurate)

### **Part III: Conceptual Design**

#### **I. Specifying the Design:**

A proper starting point for the discussion of this year's design choice is to make an assessment of last year's competition. The rules for the competition are the same with regards to propulsion, payload and structural strength. However, there has been an important shift in the mission that the plane must carry out. This change in the project goal necessitated a different type of design than that applied last year.

The rule change which most effected the design strategy is the incorporation of a time limit, which shifts the goal from maximum range to maximum speed over the course. Last year's competition witnessed many planes with high aspect ratio wings to maximize the aerodynamic efficiency ( $L/D$ ). This led to aircraft that seemed a great deal like sailplanes. This result is as expected, judging by calculations that maximizing the aerodynamic efficiency maximizes the range for electric powered propeller aircraft (See part 4, Section I). This year, however, the optimization problem is more complex, and it appears that high aspect ratio wings might introduce structural and maneuvering complications.

Due to some nagging problems that our team had, we were unable to fly at the last competition. However, if the aircraft had been able to become airborne, our testing indicated that we could fly for 12 minutes on the battery power at our disposal. This is almost twice the limit imposed by the current competition rules. Thus the optimization employed in last year's design is in all likelihood inappropriate for the current competition.

As early as last year, we had discussed configurations for the 1998 DBF competition. Without knowledge of the rules changes, these suggestions could only be considered as preliminary at best. However, the designs of this period were of great significance, because the problems encountered in the *Grand Master B* were fresh in our minds. The analysis of the shortcomings of our design and construction indicated that special attention should be paid to: (1) structures, including wing and landing gear strength; (2) control surfaces; (3) flight testing; (4) transportation to the contest site; (5) potential electromagnetic interference.

After our difficulties in constructing an aircraft with a balsa structure to meet the mission requirements of last year's competition, we decided to look into new construction methods and materials. The team had considered manufacturing components such as the wing from composite materials last year, but the startup problems associated with it proved too complex. The team members in general had little, if any, experience in the construction of radio controlled aircraft, and certainly nobody in the group had any experience with composite construction. This year, however, the team had the experience of the *Grand Master B* construction under its belt, and had developed a good deal of practical experience. This allowed the members to make better judgments about the availability of components, and could also evaluate the feasibility of manufacturing and installing certain subsystems.

The difficulties associated with composites as the primary building materials mirrored those faced last year, but to a lesser extent. Team members would require training in the application of composites, and would have to research procedures for composite fabrication. In order to make the most informed decision possible on the issue of materials selection. Dave Hall and Gary Fogel, two people who had a great deal of sailplane experience, were able to give valuable advice. Dave Hall in particular had a wealth of knowledge about composite construction of sailplane wings. He offered us a one day tutorial at his workshop, where we were given the

opportunity to create a sample section of wing. The construction method demonstrated (see Part 6, section II ) proved that composite construction could indeed offer an accurate result with less manufacturing time than a balsa construction would.

Another issue which we sought to address in our preliminary design configuration selection was that of maintaining structural integrity while allowing for transportation across the country to the contest site. The wing is usually the most critical member in this regard, because it is typically the largest member. The wing also suffers the most from structural stresses, which necessitates great care in planning of joints between sections. The team decided to impose the constraint that the joints be placed somewhere other than the middle of the wing, where the bending stresses would be highest. This is especially true if the plane carries the payload in the center of the wing, either in a fuselage or integrated into the wing.

Rapid prototyping of concept demonstrators was also stressed. If the configuration selected required too great an investment of resources, we might be left with a fatal flaw in the design which would be very difficult to rectify in time. A simpler design would allow for accurate testbeds to be built quickly and cheaply, increasing the potential for ultimate success.

The *Grand Master B* had never achieved a successful test flight with the payload and receiver combination, and therefore we were caught off guard by the interference that plagued our aircraft. Both the motor and speed control were equipped with noise canceling devices, but glitches kept the aircraft from making a successful flight at the contest. The first priority was to evaluate potential sources for the interference. The most likely cause was the routing of the power cables over the payload. This was speculated to be the cause of the problems, but in our testing after the competition we were unable to recreate the phenomenon. In order to reduce the likelihood of a similar occurrence, the designs evaluated would have to allow for the segregation of the payload and engine power lines.

The landing gear issue that had plagued us last year was exacerbated by the lack of adequate flight testing with the payload. The admirable attempt to swap landing gear at the contest site failed because of inadequate planning for that situation. The team members therefore opted for fixed landing gear this year, trading an increment of drag for a savings in weight and higher reliability. Last year's landing gear was not retractable, but inadequate nonetheless.

As was the case with last year's competition, we asked our membership for ideas regarding the configuration of the aircraft. During the first meeting of the 1997-1998 school year, the situation was reviewed, in light of the latest design specifications. The two configurations which found the most support at the end of the 1997 competition also seemed to be the best suited for the new contest rules. These two designs were an all-wing aircraft and a canard aircraft. The design goals that were stressed to the membership were performance and innovative configurations. The membership was then given the opportunity to evaluate the potential benefits of the designs, along with the drawbacks.

The first of the two designs presented was the all-wing, or "flying wing" option. It was noted that our particular design competition requires heavy load lifting capability, with the additional requirements of high speed, range, and maintaining adequate maneuverability. A similarity then became evident between our criteria and those demanded of a bomber or attack aircraft. Both of the most recent designs (that is, those made public) proposed for such missions, the B-2 and A-12, were all-wing designs. Mention was also made that the xb-49 of the Northrop corporation, which stemmed from the early jet age, was a craft that made a serious challenge for the speed record, despite its large size. In principle, the elimination of vertical surfaces, fuselage,

and empennage should produce a minimum profile drag, where all surfaces are providing lift in addition to their inescapable drag increment. This of course is a simplistic approach, but in essence the conclusion should be a good indicator of the potential for performance. Certainly a sailplane would have comparable if not superior lift to drag properties, but high aspect ratio wings pose structural problems at high speed due to the increase in the risk of flutter, aileron reversal, and tortuous bending stress in the high speed turns required to complete the most laps in seven minutes.

Another advantage inherent in an all wing approach is a smaller wingspan. This benefit arises because of the large root chord required to store the payload and mechanisms internally, which in turn increases wing area for a given span. Also, this thicker wing would have greater load handling abilities, and would offer the potential for "span loading" of the aircraft to distribute the weights, thus reducing the root bending moment (see part 6, section III). If the weight was distributed away from the aircraft centerline, the routing for power lines to a pusher motor would be well separated from the payload, reducing our fears of electromagnetic interference from that source.

The most obvious drawback inherent in the design was the potential for low stability in yaw, due to the lack of vertical surfaces. This issue caused great concern due to fears about sideslip during the landing approach. Such sideslipping would be catastrophic for the landing gear, and might cause a severe tumbling when the aircraft touched down. Suggestions for possible corrections to the sideslip issue were presented, including the addition of vertical winglets with rudders installed on the wing tips, drag rudders, and differentially actuated spoilers.

The winglets, if employed, would provide a restoring moment as sideslip began, but might be placed too far apart in the spanwise direction to have effective rudders installed inside of them. Another proposal to provide the pilot with control over the yawing of the aircraft on approach was the implementation of "drag rudders". These devices may be found on the Northrop flying wings and on the Lockheed Martin Darkstar tailless UAV. These had the advantage of precedence in their practical application, but were perhaps too complicated mechanically, and might be ineffective at low speeds typical of the approach phase. For these reasons, a "proof of concept" demonstrator would have to be manufactured before the design would be frozen with drag rudders as the sole means for yaw control. The drag rudder concept did also offer a lower drag due to their much smaller profile drag when not deployed. A control system which used yaw feedback for drag rudder actuation was also suggested, if the oscillations about the vertical axis proved too fast for a pilot to handle. Another benefit of manually operated drag rudders is that perhaps crosswinds at landing could be counteracted by the lack of a restoring tendency in an all wing design. This might allow the pilot to land normally despite the crosswind. The use of spoilers to take advantage of roll-yaw coupling and differential drag to straighten out the aircraft seemed an exceptionally dangerous method to use on approach, where lowering a wingtip might lead to ground contact.

The second design considered in the final configuration selection was a canard approach. Canards offer perhaps high agility, and the potential for high speed and load lifting with two lifting surfaces. The agility of an aircraft that doesn't use a downward force to increase its angle of attack and therefore its lift is immediately apparent. By careful choice of a lift distribution between main wing and canard, the spans and loadings can be tailored to provide a substantial benefit in bending stresses at the wing and canard roots. However, parasite drag was higher, requiring more battery power, and therefore was not selected.

## Part IV: Preliminary Design

### I. Initial Optimization:

The 1997-1998 competition rules include an important deviation from the previous specifications. This change, seemingly subtle, causes an important adjustment in the requirements for victory. The change is the imposition of a seven minute time limit for the completion of the laps around the course.

From a simplified approach to the problem, a rough estimate of the relevant aerodynamic concerns may be made. For our first try at optimizing, it will be assumed that the course is level flight at a constant cruise velocity. This should provide an upper bound to the number of laps if we divide the maximum range by 1400 feet (the distance of the straight-aways).

Some definitions and assumptions:

$$P = T v$$

$$P = (\eta_{\text{motor}} * P_{\text{batt}}) \eta_{\text{prop}}$$

$$\eta_o = \eta_{\text{motor}} * \eta_{\text{prop}}$$

We will assume that these efficiencies,  $\eta_i$ , are approximately constant for each phase of non-accelerating flight.

$$C_D = \frac{D}{\rho S_w} = C_{D0} + k C_l^2$$

$$k = \frac{1}{\pi A e}$$

$$e = \frac{1}{1 + \delta + k'' \pi A}$$

During cruise:

$$L = W \quad T = D$$

$$\dot{E}_{\text{batt}} = P_{\text{batt}} = \frac{P}{\eta_o} = \frac{T v}{\eta_o} = \frac{D v}{\eta_o} = \frac{1}{2 \eta_o} \left( \rho S_w C_{D0} v^3 + \frac{1}{\pi A e} \frac{4 W^2}{\rho S_w} \frac{1}{v} \right) \quad (1)$$

By the chain rule,

$$\frac{\dot{E}_{\text{batt}}}{v} = \frac{dE_{\text{batt}}}{dx} = \frac{1}{2 \eta_o} \left( \rho S_w C_{D0} v^2 + k \frac{4 W^2}{\rho v^2 S_w} \right) \quad (2)$$

For optimization purposes, define a "range factor", RF, such that

$$RF = \left( \rho S_w C_{D0} v^2 + k \frac{4 W^2}{\rho v^2 S_w} \right)$$

$$\frac{d(RF)}{dv} = 2 \rho v S_w C_{D0} - 2 k \frac{4 W^2}{\rho v^3 S_w} = 0$$

$$v^4 = \frac{4W^2}{\rho^2 S_w^2 \left( \frac{C_{DO}}{k} \right)}$$

$$v = \sqrt{\frac{2W}{\rho S_w \sqrt{\frac{C_{DO}}{k}}}} = v_{E_{max}} \quad \text{Which explains last year's configurations.} \quad (3)$$

The maximum range for an aircraft such as our flying wing, which has a weight of approximately 20 lbs, a wing area of 13 ft<sup>2</sup>, a C<sub>DO</sub> of approximately 0.01, with an η<sub>O</sub> of perhaps 60%, and a k of approximately 0.07, using 2.4Ah at 14.4V, would be 51,750 feet. This corresponds to 36 straight line laps, and a flight lasting almost 15 minutes at 40 miles per hour.

Now, if the battery power available while flying at E<sub>max</sub> (maximum lift to drag ratio) were just sufficient to power a plane around the course for seven minutes, the optimization is nearly finished. The takeoff, first lap maneuvers, and turning are all that remain. However, in our case, we ran the motor for 12 minutes at approximately 80% power last year, which indicates that if the aircraft is at maximum efficiency at this power setting, we would exceed the contest specifications, even if the takeoff and first lap are taken into account.

It is therefore necessary to consider the time limit and the speed issue that it poses. A simplifying assumption made for these calculations is that the course consists of three phases. the first phase is takeoff and climb. This phase requires the aircraft to accelerate from rest and reach flight altitude. The analysis of this phase is complex because of the widely varying speeds, and the accompanying variations in thrust and efficiency.

The other two phases of interest are level flight at approximately constant speed and level turning flight, also at approximately constant speed. The approximation of constant speed is included to both simplify the calculations, and to provide a more efficient flight. It might be more accurate to state that we wish to keep the power setting constant. The constant power setting should eliminate transient loading on the propulsion system, which is difficult to accurately model, and which also increases the losses incurred.

Since the goal is the maximum number of laps in seven minutes, not necessarily the greatest range, we must provide additional constraints to the previous analysis. Defining N=number of timed laps,

$$N = \text{int} \left( \frac{7 \text{ min}}{t_{lap}} \right)$$

This N is the value that we truly wish to maximize.

$$t_{lap} = \sum_{portions} \frac{\text{portions}}{\text{lap}} \cdot \frac{d_{portion}}{v_{portion}}$$

Using the steady, level flight approximations for the timed sections, we can begin building our optimum flight trajectory.

In order to determine the requirements for the takeoff segment, the optimization of the timed portion should be completed first. This is done in order to demonstrate that if more energy is available for the timed portion, more laps will be completed. This is of course an obvious result, but for completeness, it should always be recalled that we are optimizing timed laps. This method insures that all phases of the optimization will be prepared with the proper goal in mind.

A spreadsheet was created, and an approximate optimization was found that varied speed in the turns, load factor in the turns, and straight-away speed. The results obtained in this way were surprising. Our analysis indicates that the optimal speed division between straight-away and turning is nearly unity. This means that a constant speed approximation may provide quite accurate predictions for the optimum speed. For such an approximation, the length of a lap is easily determined as:

$$D_{lap} = 1400 + 2\pi \left( \frac{v^2}{\sqrt{n^2 - 1}} \right)$$

The speed division that provided the greatest number of laps was such that the turning speed was 0.9 times the straight-away speed. Another interesting result observed was that the load factor in the turns which provided the greatest number of laps was only 1.5. This means that the turns should be fairly gradual, and therefore the structural concerns may be overstated. It was found that increasing the load factor to 2.0 causes the power requirements to nearly double during the turns, and only adds approximately 1-2 laps overall.

From knowledge about batteries and motors, it is recalled that if the power used is kept approximately constant, such that the throttle is not varied by much, this should result in the most efficient use of the battery power. This prediction coincides with the prediction made based on aerodynamic calculations in the spreadsheet. Taking these two results together, the conclusion may be made that the greatest number of laps achieved will be at a more or less constant throttle setting that maximizes the drain from the batteries in the time limit allowed. The basis of the conclusion is found by examining the data, which shows that for an aircraft similar to ours, little is gained by draining the batteries by a quick exhaustion, perhaps even the greater losses encountered in the powerplant would further limit the laps completed.

Another way to reach this conclusion is to refer to the time unlimited analysis, which indicates that if time were not an issue, one would try to fly at a speed that would maximize aerodynamic efficiency. By plotting the power requirements as a function of aspect ratio and as a function of airspeed. The power required as a function of airspeed is a stronger function of parasite drag than aspect ratio. This is obvious by noting that battery power required goes as the parasite drag multiplied by the velocity cubed, and the induced drag factor is divided by the velocity (equation (1)).

The maximum efficiency speed for aircraft with high aerodynamic efficiencies ( $L/D$ ) is typically quite slow. Using intuitive reasoning, it is clear that the contest time limit requires flight speeds faster than this maximum efficiency speed, indicating that a high maximum efficiency speed is preferred if drag may be maintained at low levels (verified by the spreadsheet). By examining the equation for  $V_{Emax}$  one sees that to increase this speed without changing the wing area or weight (keep wing loading constant for takeoff and landing) we can either reduce  $C_{DO}$ , or increase  $k$ . Since only reducing  $C_{DO}$  results in a drag decrease and therefore a power savings, it is the solution. Hence the flying wing. Aspect ratio is somewhat sacrificed in our design, but hopefully by offsetting the gain in  $k$  by the reduction of  $C_{DO}$ , we can make a winning airplane. Also, a lightly loaded plane might save some overall drag due to having a lower flight  $C_L$ .

The first portion, takeoff and climb should be planned such that it consumes the minimum power, since it will be untimed, and the more power available the greater the performance. The takeoff constraint of a takeoff in 300 feet over a 6 foot obstacle should be the limiting factor. Also, the first lap, which is also untimed, should most likely be completed near  $E_{max}$ , so that the maneuvers leave the maximum battery power for the timed section. This is of course a



simplification since there are turns during this phase as well, but the analysis of the timed section indicated that the laps, which are similar to the first lap maneuvering, are the most efficient when carried out gently. This means that  $V_{E_{max}}$  should be the target velocity. Fortunately, we have as our pilot a very accomplished glider pilot, who is more than capable of operating a radio controlled aircraft near its maximum efficiency.

A calculation of the required takeoff distance, including clearing a six foot obstacle was performed. The calculation is based on our results from last year to provide estimates of takeoff performance. We determined that this year we would require in the neighborhood of 250 feet to accomplish the takeoff. This is close to the limit, therefore it is not possible to risk failure of this crucial test by trying to squeeze a few more amp hours into our timed section.

The portion of the rated battery energy left over after the takeoff, climb, and first lap is approximately 73%. This value is inserted into the equations for the timed section, and a value of 13-14 laps is the result. The turns should be completed at a bank angle of approximately 45 degrees, and the flight speed in the straight-aways should be about 50 miles per hour. Of course, this result is based on a flight path that is the minimum distance required, where in reality we need to make sure that we pass the straight-aways wing-level, meaning that some distance is gained each lap.

figure 4-1

			Velocity division ( $v_{turn}/v_{straight}$ ):		0.9		
C <sub>Do</sub> :	0.011		Battery cap (mAh):		1.9		
A:	6		Flight time (FT, min):		7		
winglet "k":	0.84375		Voltage:		19.2		
A <sub>effective</sub> :	7.111111		Battery portion usable:		0.73		
e:	0.75		Current for FT min (A):		11.88857		
Sw (ft <sup>2</sup> ):	13.5		Cont. batt pwr (W):		228.2606		
$\rho$ (slug/ft <sup>3</sup> ):	0.002377		$\eta_o$ (motor/prop):		0.6		
W (lb):	20						
k:	0.059683		straightaway length (ft):		700		
max load (n):	1.5		accel of gravity (ft/s <sup>2</sup> )		32.2		
V <sub>E</sub> max (fps):	53.88442						
			straight	turn			
			batt	batt			
straight			ft*lb/s	ft*lb/s		approx	
v (fps):	D (straight	D (turn) (lb):	power reqd:	power reqd:	dist/lap	laps:	
20	3.790387	11.544371	126.34624	346.33113	1456.548	5.767062	
25	2.490973	7.4470106	103.79056	279.2629	1488.356	7.054766	
30	1.812083	5.2455516	90.604155	236.04982	1527.232	8.25022	
35	1.430828	3.9434264	83.464989	207.02989	1573.177	9.344149	
40	1.212335	3.1243573	80.822343	187.46144	1626.19	10.33089	
45	1.09217	2.5894762	81.912763	174.78964	1686.272	11.20816	
50	1.036397	2.234041	86.366421	167.55307	1753.422	11.97658	
55	1.025762	1.998627	94.028196	164.88672	1827.641	12.63924	
60	1.048682	1.8474831	104.86821	166.27348	1908.928	13.20113	
65	1.097849	1.7580546	118.93367	171.41033	1997.284	13.66856	
70	1.168468	1.7155418	136.32131	180.13188	2092.708	14.04878	approx
75	1.257287	1.7099069	157.16091	192.36452	2195.2	14.34949	Const pwr
80	1.362037	1.7341475	181.60497	208.0977	2304.761	14.57852	Too much
85	1.481096	1.783258	209.822	227.36539	2421.391	14.74359	power in
90	1.613281	1.8535833	241.99209	250.23374	2545.088	14.85214	the turns
95	1.757709	1.9424041	278.30386	276.79259	2675.855	14.91112	
100	1.913714	2.0476636	318.95235	307.14954	2813.689	14.92702	
105	2.080785	2.1677825	364.13745	341.42575	2958.593	14.90574	
110	2.258524	2.3015323	414.06282	379.75283	3110.564	14.85261	
115	2.446618	2.4479454	468.93509	422.27058	3269.604	14.77243	
120	2.644816	2.6062516	528.96318	469.12529	3435.713	14.66945	
125	2.852918	2.7758316	594.35792	520.46843	3608.89	14.54741	
130	3.070761	2.9561828	665.33164	576.45565	3789.135	14.40962	
135	3.298213	3.146894	742.09787	637.24604	3976.449	14.25895	
140	3.535162	3.347626	824.87118	703.00146	4170.831	14.09791	
145	3.781518	3.5580971	913.86696	773.88612	4372.282	13.92865	
150	4.037205	3.7780718	1009.3013	850.06615	4580.801	13.75305	

## **Part V: Detail Design**

### **I. Design Constraints:**

Once the configuration was selected, many of the freedoms enjoyed by the designer were removed. For instance, the trailing edge sweep was limited by the specification for a pusher powerplant. Also, the root chord had to be long enough so that an airfoil with suitable thickness could accommodate the payload and components. The wingspan and taper also had to be determined so that enough wing area would be made available. Winglet sizing was based on calculations and test flights with the prototype. Propeller sizing was dictated by the length of the landing gear.

### **II. Testing:**

The design team decided to do a good deal of the aerodynamic evaluation based on flight testing of scale models and wind tunnel results. In order to obtain the tunnel results, a model with a 24" wingspan was constructed for us by Dave Hall. The specifications for this model were made to meet the original design, which would have an 8 foot wingspan, 24" root chord, 23 degree quarter-chord sweep, 3 degrees of linear washout, and 0.333 taper ratio. The airfoil used for this model was the EH2012, an airfoil designed specifically for flying wings. This airfoil is also intended for use at the low Reynolds numbers typical of model flight. We discovered that the wingspan of the model caused interactions between the tip vortices and the end walls, creating data that was hard to compare to the full size aircraft.

Simultaneously, work was underway on a balsa model with a 48 inch wingspan, and would be essentially a mid point between the wind tunnel model and the full scale version. The flying prototype was a glider, since we wished to avoid the complications involved with propulsion and create a model as soon as possible. This version included 6 degrees of washout, this time starting from 2/3 of the way out to the tip. This aircraft also had an EH2012 airfoil, but included vertical fins for stability. The fins were located as vertical winglets, and had a chord of 3 inches and a span of 4 inches. In addition, drag rudders were placed at the trailing edge near the wingtips, and these were coupled into the aileron deflections. These drag rudders were planned to evaluate the effectiveness of the devices in our aircraft, and to study the mechanisms required to actuate them.

During the first series of test flights, performed in a grassy field, the center of gravity position was studied and the neutral point was located. The flight testing indicated the very reassuring result that the neutral point lies approximately at the quarter chord of the mean aerodynamic chord. This demonstration was another hurdle that we sought to cross in our design of a flying wing. We were not at all certain what the center of gravity limits were for such a craft, and defining the aerodynamic center would allow much better analysis of the flight characteristics.

The aircraft was later flown in another grassy field, this time on campus. the static margin was calculated to be 5% for these test flights, and we sought to evaluate the washout and trim elevon positions. Another primary goal was the study of the aircraft's yawing characteristics, and its response to drag rudder deployment. The elevons and drag rudders constituted the only control surfaces, and were still linked to the same control inputs for roll. During these tests, several stalls were initiated, both planned and

unplanned. It became evident that the drag rudders, as installed, were largely ineffective at low speeds and high angles of attack near stall. This was also coupled with the observation that the aircraft was less stable than had been hoped. However, it should be noted that these tests were conducted by pilots who were unfamiliar with the particular aircraft, and were not nearly as experienced as our official pilot.

From these tests, a few relatively long flights were made, allowing us to determine that both the washout and center of gravity facilitated smooth flight if the plane was allowed to fly at an approximately level flight path angle. This indicated that the formulas we had found in references [1], [2] and [3] were more or less valid.

The next flight tests were conducted without the drag rudders, and with 6 inch tall vertical winglets. This time, the official pilot was at the controls.

On February 26th, 1998, our small prototype UCLA flying wing was flight tested as a sailplane at Point Dume, near Malibu, California. Point Dume is a 100 foot high coastal slope and open space preserve facing a prevailing westerly sea breeze. Gary Fogel has flown radio controlled sailplanes at this location for 5 years without incident on a variety of models, including some flying wings. When we arrived at the slope, balance and elevon throw were checked by Silva and Fogel. Two test glides were made from a nearby hill to verify correct positioning of the center of gravity and suitable control. Both of these flights were very successful and landings were made without incident. Our prototype was originally designed to include drag brakes at the outer tips of the wing just inboard of the winglets. These were taped together in the closed configuration for our first set of soaring flights. This was done on the assumption that the ailerons would induce the necessary turning ability and that the prevailing wind would aid in slowing the sailplane down for landing.

Silva launched the flying wing into the prevailing 15-17 knot northwesterly breeze while Fogel piloted the aircraft. After launch, it was clear that this was a very fast and maneuverable sailplane. By flying back and forth along the ridge, we maintained an altitude of about 50 feet above the launching point. The glider appeared to have a slight pull to the left, perhaps as a result of our hasty taping of the drag brakes. Trim correction was added to keep the plane flying straight and true. Fogel slowly experimented with slower and slower flight speeds in an attempt to find the best speed to fly and correct setting of the elevator. He found that the initial setting was nearly correct, but that the plane would rise in the slope lift much better with a slight addition of up elevator trim. After gaining several hundred feet over the slope, Gary initiated a "dive test" to estimate the position of the center of gravity. At a 45° dive into the wind, the flying wing pulled out nicely over an extended distance without the addition of up elevator. This indicated to Gary that the center gravity was within acceptable limits for soaring flight. Had the glider pulled out very quickly, there would have been too much nose weight. Had the glider not pulled out of the dive without elevator command, there would have been too little nose weight. The "dive test" is a standard testing aid used by many radio controlled model sailplane enthusiasts around the country. After a succession of high speed low altitude soaring passes of the cliff, Fogel successfully landed the glider behind on the top of the slope within short walking distance from the point of takeoff.

Silva and Fogel attempted to re-trim the aircraft based on our first flight. Once again, Silva launched the glider and another 15-20 minute flight ensued. This flight

included loops, a test of tip-stalling characteristics, and straight-ahead stalling characteristics. Each of these gave a convincing testimony that the configuration we had chosen for would be successful. Tip stalls, although somewhat severe, were difficult to initiate. Straight-ahead stalls made directly into the prevailing wind were shallow and true. Loops required a good amount of speed to accomplish, but suggested that the balsa airframe was quite strong. With the prevailing wind ebbing in the afternoon, we decided to land. Landing was made in nearly the identical spot to the first landing.

Our first test flights indicated that the addition of drag brakes for turning was an unnecessary complication. However, it was agreed that some form of air brakes (either spoilers or flaps) was necessary for the full scale version to aid in landing at a high wing loading. Our tests also indicated that the glider flew straight and true around turns, without the expected yaw for a flying wing. This was perhaps entirely due to the addition of high winglets to the wing tips. It was recommended by Fogel that the full-size prototype be flown fast around turns to avoid any possibility of tip-stall at low altitudes, even though it appeared that our prototype had difficulty making a tip-stall.

From these tests it was concluded that our larger design should be successful and foam core cutting began on the first full-size prototype soon thereafter.

### **III. Final Design Specifications:**

Having developed a great deal of flight data on the initial design, several areas for improvement were found. The first of these was an increase in wing area. The increased wing area was sought as a means to provide a better performance in the approach phase, because our initial glider seemed like it might be too fast if weighed down by the payload in the full size version. The second change was to eliminate all control surfaces except the elevons, yet maintain the ability to add spoilers or other features later if the need presented itself in the test program. The last major change was reducing the taper ratio and sweep. This change was initiated as a response to the tip stalling issue, which was feared to endanger the aircraft if it were pushed to the limits.

The wingspan is now 9 feet, the root chord is still 2 feet, and the tip chord is now 1 foot. The leading edge sweep is 23 degrees, and the trailing edge sweep is defined by the other parameters. The trailing edge sweep is now approximately 12 degrees, which allows a pusher installation to be maintained as an option. The airfoil section for the final flight version is also different from the previous two prototypes. It is a MH60, an airfoil that has been successfully employed in FAI F3B glider flying wings. This airfoil has a good deal of documentation available, and it is capable of superb all around performance, as witnessed by it's implementation in the varying requirements of F3B.

There are two major spar structures. The first one consists of two separate pieces of material, each made of 1/4" balsa and 1/2" deep into the foam, coming from both the top and bottom. This material is located so that at the root (wing center) it's midpoint is 6" back from the nose (at the quarter chord), and it follows the locus of the quarter chords to the tip. The plane is divided into three sections in the spanwise direction. The center section extends left and right 1.5 feet (18", for a total width of 3 feet), and the outer wings extend 3 feet further each. The separation point is along an airfoil 20" long, and this

means that the spar mentioned earlier at the quarter chord passes through this airfoil at 5" from its leading edge. At the tip the airfoil is 12 inches long, and the spar goes from the break along the same line to 3 inches from the leading edge of this airfoil. These outer portions of the spar go from 1/2" deep at the 20" long airfoil on its side of the cut, to 1/4" deep at the wingtips.

The angle of attack, and therefore washout, is defined with respect to the root airfoil's chord line. For the definitions used in this project, washout of  $x$  degrees means that at that station the airfoil is rotated by  $x$  degrees with respect to the root airfoil's chord line. Washout is defined so that twisting the airfoil such that its nose moves downward relative to the trailing edge is positive. We have a linear washout in our aircraft for simplicity. The washout at the separation point (18" out spanwise from center, airfoil length = 20") is 2 degrees, and at the tips it is 6 degrees.

The other main spar is much more complicated. It also continues its line after the separation of sections, but it is transverse with no sweep. It crosses the root chord at 17.1 inches from the nose, is also 1/4" balsa, and comes down from the top of the airfoil 3/4". It is a single spar cut from the top. At the separation of sections, the spar is 1" thick, and the continuation is only 1/2" thick. It crosses the 20" separation airfoil at 9.45 inches from the leading edge. Where the two spars meet in the outer panels, the transverse spar is cut at an angle to mate with the upper portion of the quarter chord spar. None of the spars are twisted, despite the washout. This means that all of the spars (and servo channels, see below) are aligned with the vertical. This method is the only feasible way to install the spar/stringers, and it results in a very quick (on the order of 1 hour for two workers) installation time for all of the spars.

There are two motor placements planned for along the centerline. One is the pusher configuration, the other is the tractor configuration. The pusher uses the motor mounted semi-recessed just forward of the transverse spar, with a shaft out the rear to the bearing, which is located about 2" from the trailing edge. The motor is about 1.75 inches in diameter, 3 inches long, and the shaft is about 13/64" in diameter. The propeller is 12" in diameter. In order for the propeller to clear the trailing edge with the pusher, the propeller should be no closer than approximately 1.5 inches to the trailing edge of the root airfoil.

The batteries (2 separate packages, about two inches tall by 1 inch wide by 8 inches long) are located ahead of the main spar, lying on their sides, with their power cables coming through the center of the two portions of the main spar. The batteries are approximately 3" forward of the main spar, and the long axis follows the general sweep of the quarter chord spar. After the wires pass through the center spar, they plug into the speed control, which is about 2" wide by 3" long by 1/2" high. The receiver and its batteries are mounted beside the speed control (which is on the centerline). They start about 2" back from the quarter chord spar. This battery and speed control arrangement allows the use of both pusher and tractor motors, and also keeps the battery wires far from the payload, lessening our fears about interference.

There is a channel dug out to rout the wiring from the receiver out to the servos, which are located in the outer panels. The channel is located such that it is 1.5" behind the quarter chord spar. This channel is cut from the top, 1/4" wide, and 3/4" deep throughout. At the outer section, this channel is no longer cut from the top (in order to

avoid the transverse spar which is still cut from the top). Instead, it is cut from the bottom and is 1/2" deep throughout.

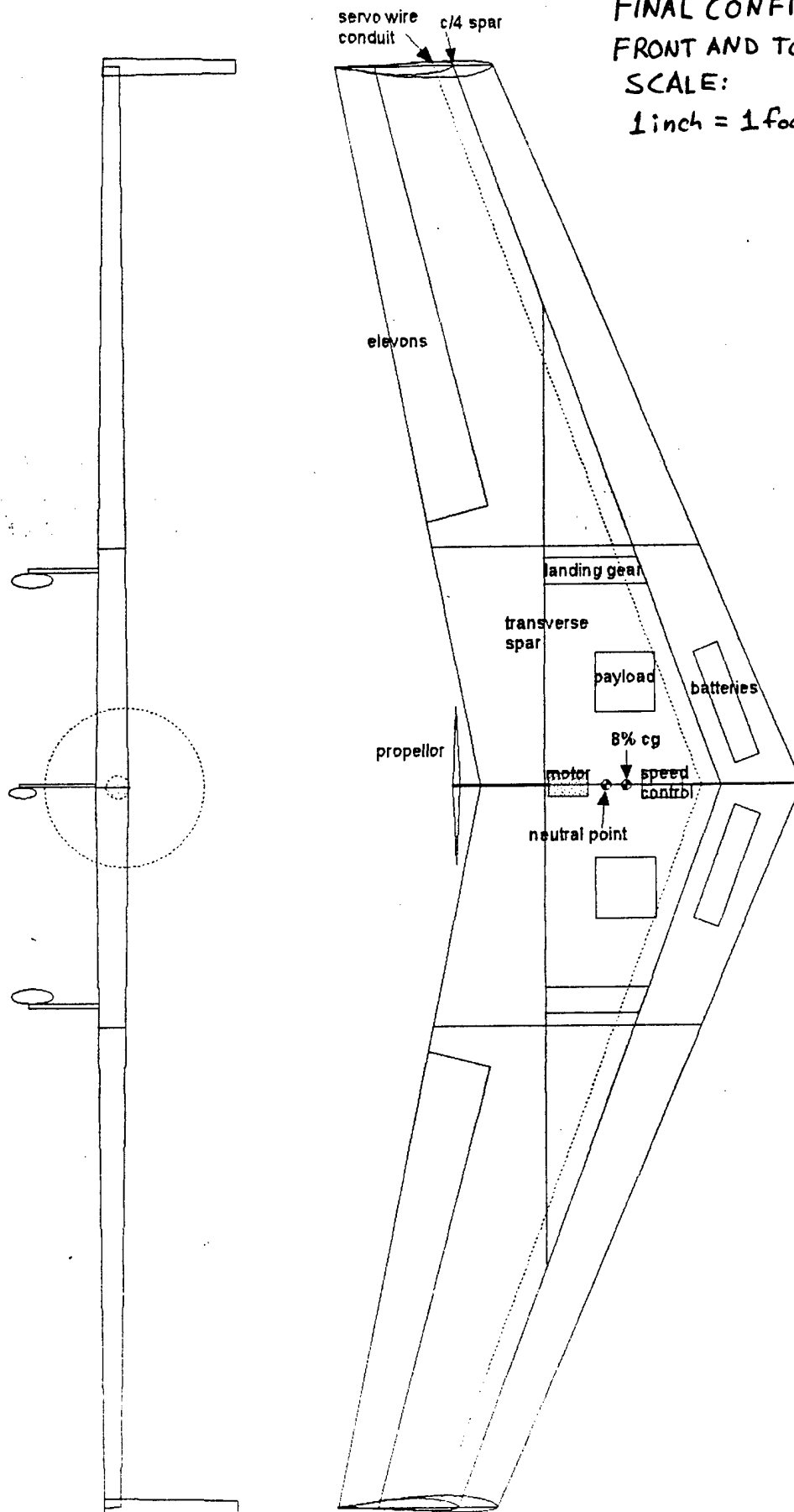
The elevons are located on the outer panels, and start at 3 inches from the separation point. They are about 20-25% of the chord length in the longitudinal (front-back) direction, and go from the point where they start (again 3" from the separation, the airfoil at that point is 19.333 inches long) to 1" from the wingtip. These control surfaces were sized based on our success with the 48" wingspan prototype. Since the center of gravity was moved a little more forward in this version, the sweep was increased slightly along the trailing edge, and the elevons were extended further aft, this should provide the same high level of control despite the greater weight and loading of the final version.

The winglets are located at the wingtips. They stick up vertically from the wingtip by 10". The winglets are sized based on an approximation given in reference [1]. The airfoil cross section employed on the winglets is the same as that on the wing, a MH60 profile. Their chord where they meet the wingtip is 12", the same as the wingtip, and they have an 8" chord at their tips.

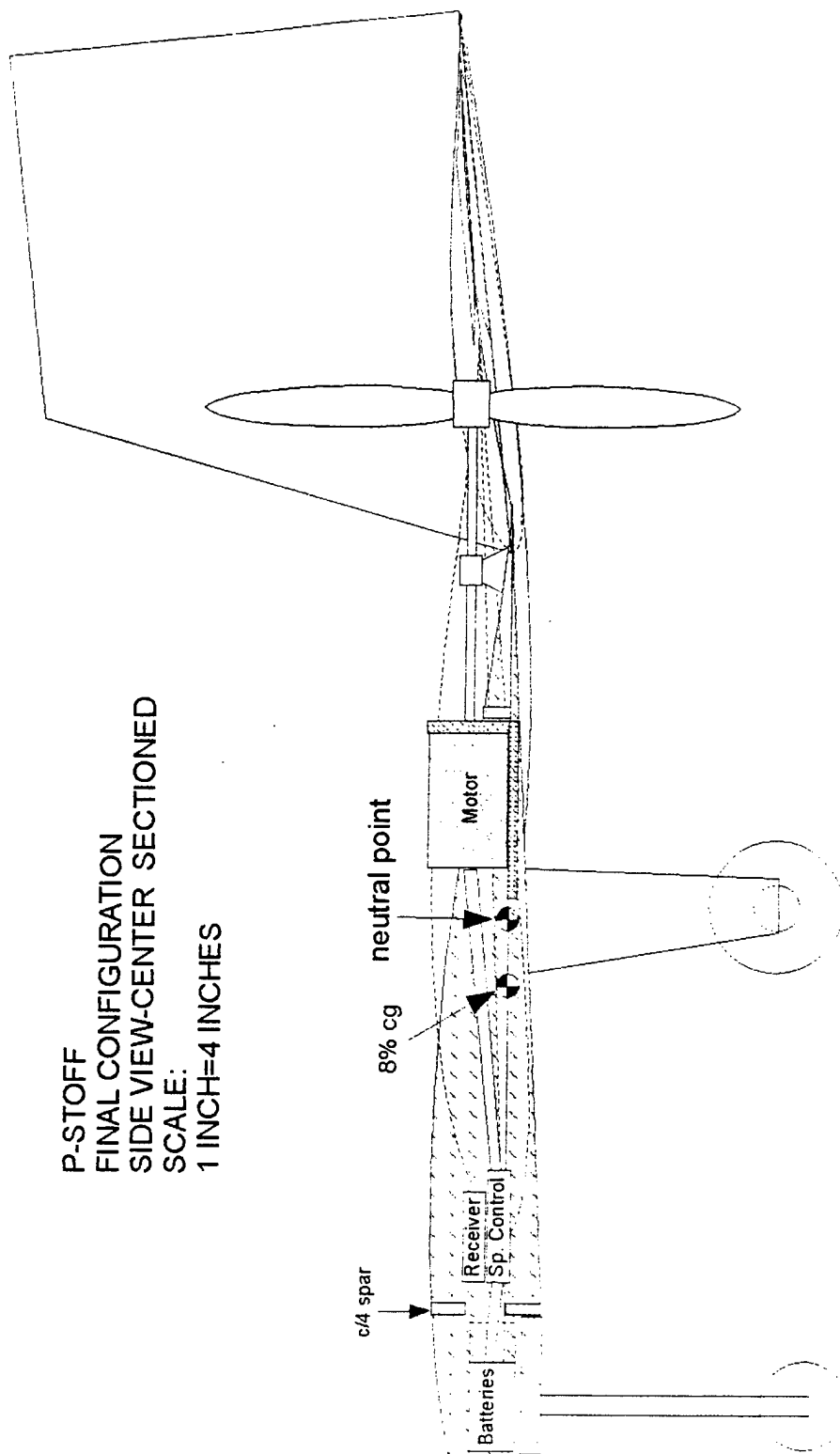
Item:	Weight	distance from	moment	
	(oz):	nose (in):	(oz*in):	
batteries	32	3.5	112	
nose gear	3	4	12	
speed control	2.2	88	193.6	
receiver	1	10	10	
receiver batteries	2	10	20	
servos (2)	3	20	60	
main gear	16	14.5	232	
motor	16.4	15.2	249.28	
motor shaft	2	20	40	
shaft bearing	2	23	46	
propeller	1	25.5	25.5	
foam cores	39	16	624	
balsa sheet	18	16	288	
fiberglass	13.5	16	216	
epoxy	16	16	256	
winglets	5	29	145	
payload	120	13.8	1656	
Nose weight	12	2	24	
totals:	304.1 oz		4209.38 oz-in	
	19.00625 lb			
cg at:	13.842091			



P-STOFF  
FINAL CONFIGURATION  
FRONT AND TOP VIEWS  
SCALE:  
1 inch = 1 foot



P-STOFF  
FINAL CONFIGURATION  
SIDE VIEW-CENTER SECTIONED  
SCALE:  
1 INCH=4 INCHES



## **Part VI: Manufacturing Plan**

### **I. Materials Selection:**

The materials employed for the construction must provide strength, ease of construction, light weight, and cost effectiveness. The two different methods which were considered were foam core/composite construction, and built up balsa construction.

Construction from balsa has several advantages. The first of these is that our team was already quite experienced in implementing balsa as a construction material. This meant that little if any time would need to be spent training the members to work with the materials and methods. This time could then be spent early in the project building the sections of the aircraft.

Foam core/composite construction was largely a new art to our members, and it would take a longer time before the nuances of the method would be second nature. We were unaware of many details about the process, including how pushrods and wiring should be run through the structure.

The weight issue also favors balsa construction over composites. A balsa structure may be tailored from the inside to provide the best load carrying structure with the minimum weight. If the balsa structure is properly planned and built, with tight fittings between the balsa members, a very strong, yet exceptionally lightweight structure is the result.

Composites require a foam core or a mold. If a mold is used, the manufacturing is a bit more complicated, but the structure is lighter than if foam is used as a core. On the other hand, skin buckling is an important concern as a failure mode, and with a stiff foam core the skin is less prone to this type of failure, allowing thinner skins to be used. Foam core has the disadvantage that it places too much weight in places that do not need it structurally, therefore resulting in a heavier plane.

The inevitable damage that might occur during the testing and early life of an experimental aircraft require that repairs be made easily, and in the field if need be. Here again, balsa construction has the advantage. A plane constructed from balsa, spruce and plywood is easy to patch and repair, often with a little cyanoacrylate glue and maybe epoxy or tape. This is evidenced by the quick repair work done on the *Grand Master B* last year, after its traumatic first flight. Another point to mention while discussing repairs is that the flying wing has very few protruding features, unlike the *Grand Master B*, and this should make repair and realignment less troublesome.

Foam core construction is not very forgiving, in that it usually requires more than just tape or glue. It might require cutting a section, sanding the surface for preparation, and placing the article in the vacuum bag for a few days to cure. Certainly, cyanoacrylate glue is not an option in this case, since it does not bond to foam, but attacks it. It is possible to use short set time epoxy for the repairs, but this might only partially restore the structural integrity at the expense of weight. In the case of a hollow composite structure, repair is even more troublesome, and in many cases an adequate repair is prohibitively difficult.

Balsa is cheap. A comparable aircraft made from foam core and graphite might cost more than twice as much. Fiberglass is less expensive, but it is also less effective. Kevlar and Spectra are incredibly tough and resistant to damage, but they are also expensive and difficult to work with. A concern with composite construction is the tooling costs associated with it. Hot wire and its associated tools must be purchased, the

epoxy and fabrics require bagging and a vacuum pump, and a device to ensure proper taper of the planform must also be acquired.

In planning out the routing for wires and pushrods or tubes, one must consider what the requirements are. If a plane suffers a component failure, it must be accessible for repair or replacement. Again, balsa construction is superior in this regard. Not only can a built up balsa plane have the routing taken care of as the structure takes shape, it can be made with prefabricated bays to house servos and other components, with blind nuts and other important features already installed. Also, servo wires can be accessed easily either by leaving a conduit tube in the aircraft as it is built, or by cutting some of the skin if need be and supplying a patch.

Composite construction with molds or foam cores are more difficult to plan bays for, and the penalty for cutting through the skin is a major loss in strength. All wiring must have suitable conduits pre-installed, and there must be adequate planning to ensure that contingencies are possible to repair or replace failed components.

The major drawback inherent in balsa construction is the time that must be invested. A good deal of sanding must take place to ensure adequate fits, and there are many small pieces that are difficult to hold in place. In a swept tapered wing, such as that employed on *P-Staff*, there are at most two ribs that match. In last year's *Grand Master B*, the wing was straight and untapered, which meant that each rib had perpendicular joints and could be sanded together with many other ribs to ensure that the ribs were consistent and that the fit would be secure.

Time is a critical issue on any project, and on a project with limited resources, time saved translates into flight time and potential repair time. Also, the availability of our pilot is severely limited by his work towards his doctorate, so the earlier the aircraft is completed, the more chances we have to complete test flights around his schedule. On the issue of time, the built up balsa structure would require a sizable investment of resources, and would perhaps take too long to complete. On the other hand, making a plane from foam cores can be accomplished in a much shorter time frame once the supplies and tooling are gathered together.

An additional set of concerns arises from the sweep, washout, and dihedral. The sweep requires that the proper angle must be maintained relative to the spar while cutting, and that the width of the cuts is not the same as the spar width, but rather the projected length. The addition of washout and possibly dihedral add complexity in lining up the airfoils correctly, and maintaining the correct angle when cutting. It is exceptionally difficult to assure accuracy to within a few degrees when fitting a balsa rib with sweep, dihedral and washout. It is also difficult to shape the leading edge to match these features and sit well on the airfoils. The 48 inch wingspan prototype verified all of these concerns. It became clear from the experience with the prototype that a full size version made from balsa would require a Herculean effort.

One of the great concerns that we had from last year's competition was the wingtip to wingtip test. This particularly brutal test should in principle simulate a load factor of about 2.5. However, the principle reason why such a test is so rigorous is that the test is conducted by placing a point load at each wingtip. If one were free to design an aircraft without this specification, it would be natural to provide a lighter structure at the outer wings, where the flight loading is less intense than at the root, and a significant savings in weight and rolling inertia could be gained. To provide structural strength, balsa is inferior to composite construction, at least for the skin. The failure mode we

encountered last year when stressing the Grand Master B was skin buckling, and our experience indicated that a stronger material should therefore be investigated.

From some research into composites, it was found that many different materials could fit the need. The team consulted model sailplane enthusiasts, who routinely deal with high aspect ratio thin wings. Sailplanes also have strict weight tolerances that must be met by the building materials. We discovered that it was possible to apply fiberglass over the top of a balsa-sheathed foam core, thus producing a light, inexpensive, easy to build, and yet quite strong wing structure. Since it is evident that such a structure might provide a benefit if repairs are required, we decided to build the plane in such a manner.

The repair issue proved a significant motivator, since the experimental nature of the airplane might lead to unforeseen failure in flight testing. Also, the possibility of field repairs due to damage sustained by a contest day mishap would be more likely with the balsa surface, which allows greater surface area to apply a patch with epoxy. The fear that the aircraft might also become damaged while shipping it to the contest site also indicated that the balsa-fiberglass method was superior to the others examined.

## **II. The Construction Techniques:**

With foam core and balsa-fiberglass sheeting selected as the building materials, it was time to prepare the tooling for the assembly. The foam core selected was 2 pound per cubic foot density "blue" foam, with an open cell structure. The balsa thickness was originally planned as 1/32", but the limited availability of the material and its high cost made 1/16" thickness stock was used. Two sheets of fiberglass, the first 3.5 oz/yd<sup>2</sup>, and the second type 1 oz/yd<sup>2</sup>, were selected as the outer materials. The epoxy used to bind balsa to wood and to other balsa was 5 minute quick set, and that chosen for the fiberglass was 30 minute set EZ-LAM, a product prepared for this purpose.

The blue foam provided certain advantages over standard closed cell white foam. The first of these is that the airfoils that are generated by the hot wire are smoother, due to the more uniform nature of the open cells. The blue foam is also more rigid than white foam, which adds more structural integrity to our wing. Our particular type of blue foam is also much more tolerant of handling than the white foam. Blue foam has less of a tendency to develop "finger dents" from handling, allowing the airfoil to remain true to specifications.

The foam technique employed requires a hot wire to be run over the foam, melting a path through the foam in the shape of the end templates. The technique involves placing the templates on either side of a foam block that has been cut to the correct spanwise length and the correct sweep, along with only enough excess to allow the hot wire to rest on the templates before the cutting has begun. The end templates are of great importance to this process. The templates must be manufactured from a material resistant to the hot wire and must be precisely shaped. The material selected for this purpose was common Formica. Template plans are generated by computer to meet the airfoil specifications, printed, and these are glued to the Formica. The Formica is then rough cut with a band saw or scroll saw, sanded with a belt sander, and finally hand sanded to remove burrs. It is critical that the templates be as smooth as possible, since any burrs would catch the wire and cause one side to stick while the other side remained free to move. This would result in an inaccurate airfoil. If the templates are of different lengths, then tapered wing sections may be cut without effecting the intermediate airfoil shapes. Another advantage

over rib cutting for balsa is that linear washouts may be generated easily by printing an airfoil template plan that incorporates the desired twist and offsetting heights for dihedral.

The typical balsa used for sheeting these projects is 1/32" thickness stock, which is very thin, but has impressive strength characteristics when used in this type of manner. However, our primary supplier of balsa did not carry such balsa. When suppliers were found, their balsa was too expensive to compete with the 1/16" thickness balsa from our primary supplier, which cost less than half as much to cover the same area. If the 1/32" thick balsa had been purchased, there would have been essentially no cost savings over carbon fiber for our project. Over the center section, the balsa sheeting was oriented such that its grains were aligned spanwise, and there were few joints at the wing root. This would provide the greatest resistance to the root bending moment during flight, and it would also resist the moment on landing.

Over the balsa, the layer of 3.5 oz/yd<sup>2</sup> weight fiberglass was placed, with the 1 oz/yd<sup>2</sup> fiberglass forming the outermost layer. Both layers had a bi-directional weave, unlike the unidirectional carbon fiber which we had at one point discussed using. The heavier layer of this fiberglass provides much of the strength of the aircraft skin, and the outer layer contributes to making a smooth outer surface as well as increasing the strength.

A balsa wood structure was included to both provide attachment points for section joints and to distribute point loads over the skin. Two of the major structural concerns that were raised about composite construction were point loading and skin buckling. Once it was determined that spars and stringers could be placed in the cores and bonded to the skin, many fears about composite construction were alleviated. In an all wing design, the loading forces are placed directly on the wing instead of on a fuselage structure. The most severe of these point loads is due to the landing gear. A spar structure could be planned to spread the landing loads over the skin, while at the same time this structure would be able to transmit and resist flight loads. The spars could be placed in such a way that the couplings between sections would use the spars as anchors for rigidity and load transmission. Also, a transverse spar could be placed in such a way that it would counteract the landing loads of two wheels outside of a central payload, and resist the formidable wing root bending moment. Spar geometry was therefore selected to create a triangular structure in the center, which would transmit tricycle gear landing loads, and provide some greater strength for flight.

The spars could not be made as single pieces connecting the top skins to the bottom skins, because this would require cutting the foam cores, and might cause misalignment. Therefore, the spars might be better classified as stringers because of their role in helping to prevent buckling. The wing sections are joined by aluminum rods inserted in brass tubes. The tubes are bonded with epoxy to the quarter chord spars, following the spar sweep angle. There are also smaller brass tubes with steel wire inside at the trailing edges. After this, the joints are taped in place.

### **III. Anticipated failure load:**

The use of balsa as skins and spar/stringers makes it quite difficult to analytically predict the strength of the structure, and also its weight. A small variation in skin thickness may vary the weight and to a lesser extent the strength, of a member dramatically. If an average weight of the skin is determined, then this weight may be used

with only some certainty to project the total weight of another section. Variations of an ounce are not at all uncommon between parts such as the outer wing panels. Since these panels each weigh approximately 2 pounds, this corresponds to about 3% of error from the predicted weight in balsa alone. This seems rather trivial, but because this weight in the outer panels is significantly far away spanwise and longitudinally from the planned center of gravity, this might prove a significant factor when the plane is balanced.

In order to predict the ultimate failure stress, one needs to assume the flight loading, and the failure stress of the structure. The flight loading may be more or less approximated by assuming that the lift is distributed linearly with the chord length. This approximation is invalid at the wing root and at the tips, but since there are winglets at the tips and the wing root effect is limited to a small area, it is a fair enough approximation, given the other uncertainties. Using a cantilever beam to model each side of the wing, and assuming for simplicity that the weight is concentrated at the center, we may obtain a pessimistic value for the bending at the root.

Using the above approximation, the wing root bending moment is found to be:

$$M_R = \frac{bnW}{4(1+\lambda)} \left[ \frac{1+\lambda}{3} + \lambda \right], \text{ where } M_R \text{ is the root bending moment, } b \text{ is the total}$$

wingspan,  $n$  is the load factor,  $W$  is the weight, and  $\lambda$  is the taper ratio, tip chord/root chord.

If the plane has the payload, batteries, and landing gear located away from the center, as it does, then the value of the moment is the previously calculated moment, subtracting the component moments from this simplified arrangement. Mention should be made that a typical aircraft with the components situated in the fuselage would be subjected to the loading predicted from the concentrated weight in the center. In our case, placing components spanwise reduces the value of the bending moment by approximately 15%. This means that since the moment is linearly related to the load factor, a 15% higher load factor may be expected compared to a fuselage and wing airplane.

Since the moment of inertia for a spar or other rectangular cross section object is related to the cube of its height and proportional to the width, a large root chord such as that necessary for internal component storage in our flying wing is very advantageous in relieving stress. The extra drag of a larger wing is traded for a resistance to bending that is much greater than a high aspect ratio wing such as those seen last year. The large surface area created by the substantial chord size allows for a smaller wingspan, which also reduces the bending moment substantially.

In conclusion, while the final failure stress is difficult to determine analytically due to the nature of the materials selected, it can be stated that the final load will be substantially (perhaps 50%) higher than a comparable conventional aircraft, allowing tighter turns, and therefore shorter laps, if the aerodynamics dictate this result.

**Cost Summary:**

(manufacturer's or supplier's list prices)

*Propulsion:*

Motor:	\$198.23
Speed control:	\$89.99
Batteries:	\$94.87

*Airframe:*

Foam Cores:	\$40.00
Balsa sheeting/spars	\$30
EZ-LAM Epoxy	\$38.00
Fiberglass (3.5oz/yd <sup>2</sup> ):	\$18.00
Fiberglass (1 oz/yd <sup>2</sup> ):	\$13.00
Epoxy (5 minute):	\$11.00

*Vacuum bagging supplies:*

Mylar	\$36.00
Mold release wax	\$8.00
Vacuum bag	\$24.00
Vacuum bag connector	\$8.00
Hot wire	\$3.00
Thermal power supply	<a variac may be used>
Vacuum pump	\$69.00

*Radio and Controls:*

Servos (2)	\$16.98
Servo extension wires (2)	\$9.00
Receiver (1)	cost unknown, based on radio we go with
Receiver batteries (4.8V)	\$11.99



**References:**

1. Nickel, Karl and Wohlfahrt, Michael, *Tailless Aircraft in Theory and Practice*, AIAA Education Series, 1994
2. Panknin twist formula, <http://www.halcyon.com/bsquared/Panknin.html>
3. Martin Hepperle's web page, <http://beadec1.ae.bs.dlr.de/Airfoils>

# UCLA AIAA Student Chapter

## Design Report - Addendum Phase

AIAA Student Design/Build/Fly Competition  
1997-1998

## Part VII: Lessons Learned

There are several minor changes to the aircraft layout, which only moderately affect the aerodynamic predictions, and do not change the planform or wing dimensions in any way.

The design has undergone air trials, during which some design flaws were discovered. The landing gear strength is once again an issue. The weight of the aircraft also proved to be a significant concern, and several measures were undertaken to resolve that issue. In order to provide a more stable airplane without increasing the weight, a tractor configuration was selected. Otherwise, the overall design remains essentially quite similar to that listed in the proposal phase, and a test model has been built and tested.

The landing gear issue arose during the initial trials of the first full size model, and while the plane seemed eager to accelerate to takeoff speed, the landing gear suffered failures prior to some takeoffs. This was in part due to our test facility, which was a dry lake. In reality, the lake was just drying out from recent rains when we tested there, and the surface was a bit uneven in places, with large cracks covering the lake bed.

The landing gear failed at the nose gear, largely due to the spring section incorporated in the "music wire" strut. This type of landing gear is typically robust enough to accommodate model aircraft, and a similar wire handled the *Grand Master B*, without incident. The length of the landing gear in the first version was approximately 8 inches, which contributed to the flexibility problem. However, propeller clearance requires about this length, and little could be done to shorten it. The main gear also differs in that it uses a single assembly instead of two separate assemblies located further outboard. This reduces complexity and building time. However, it introduces more bending moments on the center section when landing. Fortunately, the landing gear fairly evenly distributes the loading via a block of oak wood buried under the skin.

Our second set of trials consisted of high speed taxi tests and short takeoffs. These trials were accomplished in an empty parking lot near campus. The landing gear had been changed to a wire without a spring section in it. The test surface was much smoother, and trials proceeded to short hops. On one of the hops, the nose gear gave way on the landing phase, indicating that a new configuration would be required. The solution decided upon was to introduce a triangular brace for the nose gear wire to prevent bending and shorten the effective length of the rod without requiring a major redesign.

Throughout these misfortunes, however, the airframe remained undamaged, indicating that our construction was rugged enough to perform well once the landing gear issues were resolved.

The foam used in the second model was "white foam" as opposed to the "blue foam" used for the first incarnation. The white foam has a measured density of 1.6 to 1.7 pounds per cubic foot as opposed to the measured 1.8 pounds per cubic foot for the blue foam. The cells in the white foam are closed, and it is not as rigid or strong as the blue foam. These drawbacks are considered as minor, since the weight savings will allow a more stable aircraft with the center of gravity further forward. Additionally, the outer panels have holes in the cores to save some weight behind the center of gravity. The structural strength that was lost is once again considered negligible, since the skin is the primary load carrying structure in our semi-monocoque arrangement.

The outer spar/stringers were also rearranged, such that the spar that would be the continuation of the longitudinal spar is now swept back. This allows for easier routing of the wiring for the elevon servos, and for easier placement of the spar, with only a mild weight penalty. This weight penalty is not as high as that saved by the holes in the outer section, and the new spar is predicted to increase the overall strength of the outer sections despite the lost material of the holes.

An additional weight savings was achieved by using thinner 1/20" thickness balsa sheeting and using a different bonding agent to attach it to the foam. Some strength is definitely lost in the process, but the reduction of thickness saves approximately 4 ounces, and most of that is behind the intended center of gravity.

The end result of these changes is a plane that is almost 2 pounds lighter, with an empty weight to maximum gross weight fraction of 37%, instead of 44%. The plane will have a wing loading of 21 oz/ft<sup>2</sup> instead of the previous 23 oz/ft<sup>2</sup>.

The tractor configuration was selected since the aircraft was approximately neutrally stable without the payload and with an aft mounted motor. The solution to this dilemma is to either add approximately 1.5 pounds of nose weight, or move the motor to the nose. If enough weight could otherwise be removed from behind the center of gravity, then this would not be an issue. However, the best that the other changes could accomplish was to provide 2-3% of static margin, where our testing indicated that a minimum of 5-8% was required for well behaved flight.

Inherent in flying wing designs is the fact that design modifications to the wing to accommodate different sized payloads can result in a complete redesign. If a fuselage section was incorporated, perhaps this modification would be more easily accomplished. However, as we discovered in our first full size model, if the designers plan ahead for several eventualities, then a quite modular design can still be built.

Examples of the design features incorporated to enhance modularity include the servo wire conduits in the outer panels, the speed control placement, the nose gear placement, and the wire routing.

The servo wire conduits were placed such that the outer panels could include additional control surfaces, such as spoilers or drag rudders, or rudders mounted on the winglets. The speed control is centrally located so that wires from the battery may be easily routed aft to a pusher or forward to a tractor. The nose gear is mounted slightly aft of its ideal location, such that nose weight or a motor can occupy the furthest forward location in the nose.

After building two different versions of the full size aircraft and one small version built of balsa, we have come to the conclusion that from the standpoint of production time, foam core construction is easier than expected and provides quite satisfactory results. Balsa construction, while slightly lighter for similar strength, is much too complicated to produce large quantities without investing in precision tooling to cut patterns quickly and accurately.

For prototyping purposes, there is no doubt that foam core construction has the advantage. For a fraction of the tooling costs, a highly accurate prototype may be constructed from scratch in a matter of weeks. We estimate that a two man crew could produce a full scale version of our aircraft in no more than two weeks. If four people worked on the project, then the production time could be one week, limited only by the

curing time for the epoxy laminating resin employed for the fiberglass. Therefore, the production rate could be increased further by preparing other foam cores while the first set is curing.

Once the tooling is purchased, the cost per aircraft quickly approaches the cost of materials and labor only, since the tooling required is reusable and constitutes only a small fraction of the total aircraft cost.

#### Manufacturer's list prices

Motor		\$198.23
Batteries		\$112.00
Speed Control		\$89.99
Propellers		\$14.40
Prototype supplies		approx. \$110
* Composite materials		\$183.67
* Balsa for full size		approx. \$50
* Paint		\$26.97
* Radio equipment		approx. \$450
* Tools	56.54+3	59.54
* Alignment rods and tubes	2*(2*1+2*.8)	\$7.20
* Linkages	2*2.60	\$5.20
* Adhesives	2*11.00	\$22.00
* Miscellaneous equipment (landing gear, etc.)		approx. \$100
Total:		\$1400

\* supplies for 2 separate full size airplanes



# PEGASUS



## Team Members:

**Aruni Athuada**  
**Lashan Athuada**  
**Jason Bachelor**  
**Sebastian Echinique**  
**Shelly Ellis**

**Wayne Fulford**  
**Benjamin Goff**  
**Jennifer Huddle**  
**Cheree Kiernan**  
**Anabel Marcos**

**Arthur Morse**  
**James Richards**  
**Louis Turek**  
**Kiet Van**  
**Phil Wadsworth**

## Table of Contents

1.0 Executive Summary.....	3
2.0 Management Summary.....	5
3.0 Conceptual Design.....	6
4.0 Preliminary Design.....	9
5.0 Manufacturing Plan.....	13
Appendix A.....	19
Appendix B.....	26
Appendix C.....	27
Appendix D.....	29
Reference.....	30

## 1.0 Executive Summary

### 1.1 Overview

The goals and constraints of a particular project dictate the design of an airplane. The primary objective for the aircraft designed to compete in the annual 1998 AIAA Cessna/ONR Design/Build/Fly Competition is to fly the maximum number of complete laps over a specified flight course in a specified time period. UCF's *Pegasus* Aircraft is designed to comply with the following competition design restrictions and constraints:

- . Complete a takeoff over a 6ft obstacle.
- . Must execute one left hand and one right hand level 360° turn.
- . Specified time limit: 7 minutes
- . Specified track length: An oval course with 700 ft. legs.
- . Land in 300ft (does not have to come to a complete stop)
- . Max battery weight: 2.5 lbs.
- . Payload: 7.5 lbs.
- . Max gross weight: 55 lbs.

### 1.2 Design Development

The design of the aircraft began with a rush of brainstorming and research. First, the UCF team wanted to learn about the previous year's competition and the schools that had placed among the top competitors. In finding this information and determining what initial parameters we might be dealing with, the team divided the design into three major areas that would have to be optimized and harmonically pieced together to compile the best design: power, flight stability & control, and design & construction.

The main goal of the design is to fly the most laps around the given course in a specified amount of time. We must complete the course while also maintaining the set design criteria for developing a plane that could fly the legs of the oval shaped course relatively fast and make level turns at the edges with a small turning radius and a minimum decrease in cruising velocity. For the stability and control group, this dictated the problem of a design compromise between a plane with the stability criteria for speed and maneuverability and a plane stable enough to lift the aircraft and its payload.

The construction & structural design group set the goals of creating a strong plane that could endure the wear and tear suffered by the flight of model aircraft, lift the required payload, be moderately easy to manufacture, and most importantly, be lightweight. Both materials and construction methods used by airplane modelers were researched and noted for future use. This group was also responsible for the research of airfoils appropriate for this design, including but not limited to, symmetrical, cambered, and low speed.

The power team's goal was to maximize the cruise velocity for the greatest amount of time with the power that would be available from 2.5lbs of Nickel Cadmium batteries. Research on the motors (gear driven and direct drive), turbfans, propellers, and their corresponding efficiencies was collected and mapped out on spreadsheets for ease in final selection of the components.

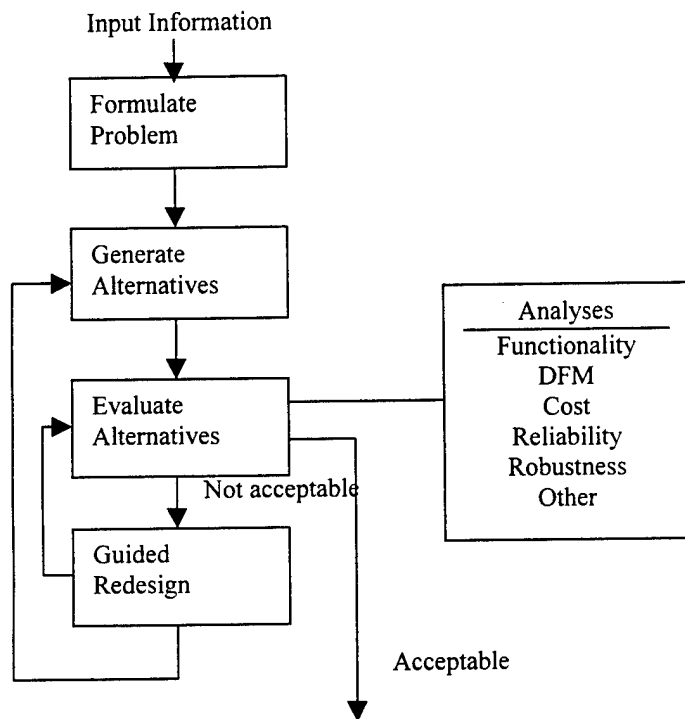
To complete the initial stage of the design, "back of the envelope" calculations were performed by all of the groups to determine the best parameters: maximum power available, power required, cruise velocity, weight of the design and components, lift and drag coefficients, lift to



drag ratio, and so on. Consequently, the advent of each phase of design brought about a more detailed and elaborate investigation of the parameters and components researched (Figure 1.1) until the design was complete enough to initiate the procurement of materials and components.

### 1.3 Guided Iteration Methodology

The guided iteration methodology involves five major steps that were utilized by the design team throughout all phases of the design. The steps as followed from Engineering Design and Manufacturing by John Dixon, are as follows:

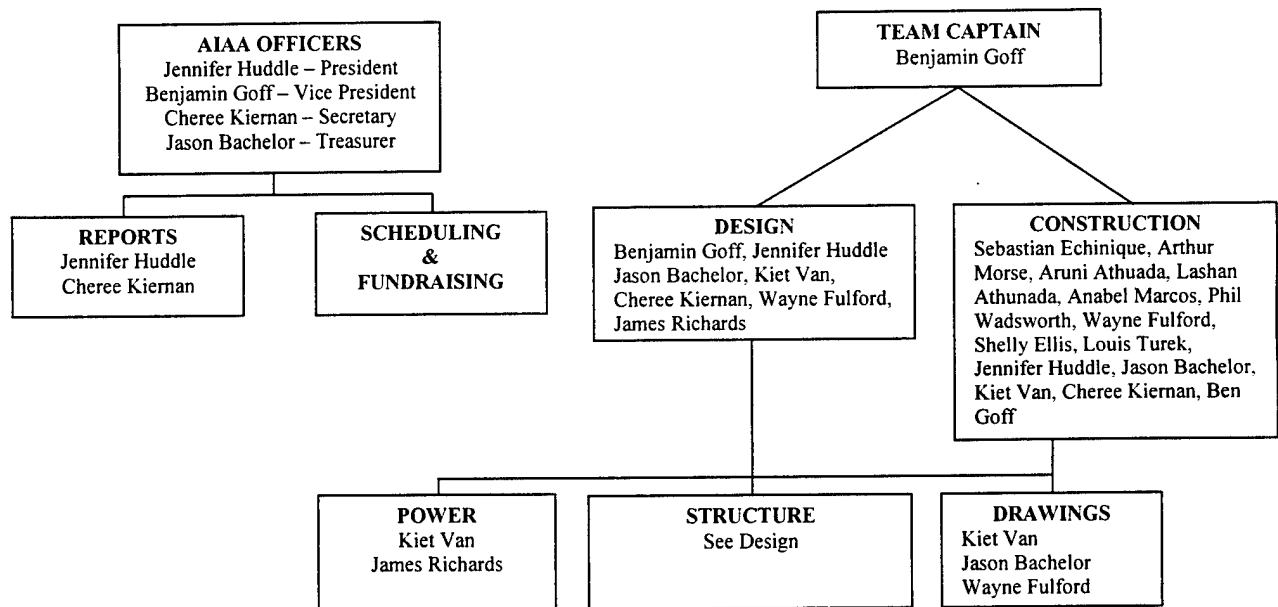


**Figure 1.1**  
**The Guided Iteration Method**

“In guided iteration, the path to a solution is effectively pointed out by the results of previous evaluations, by qualitative physical reasoning, and by knowledge of manufacturing process” (Dixon p. 1-13).

## 2.0 Management Summary

The University of Central Florida's student branch of the AIAA focuses on both the education of students through hands-on workshops and activities such as the Design/Build/Fly Competition and on the use of teamwork and concurrent engineering techniques. Student participation at all stages of the aircraft design and construction, both preliminary and detailed, is highly encouraged by the branch officers and the design team captains. The following chart graphically represents the hierarchy of our design team:



The design of the *Pegasus* Aircraft has been divided up into conceptual design, detailed design and construction phases. The project timeline for the aforementioned phases of development are as follows:

Design Process	Anticipated Time of Completion	Actual Time of Completion
<b>Conceptual Design</b> Evaluation of Constraints Evaluation of Competitors Statement of Goals Research & Development (i.e. model aircraft, building methods & materials, batteries & motors, airfoils)	December 1	January 1
<b>Preliminary Design</b> Selection of batteries, motor, airfoil, and materials Stability Criteria	January 10	February 15
<b>Detailed Design</b> Confirmation of above info. Purchase of materials Construction	February 28	March 30
<b>Report Preparation</b>	March 10	March 13
<b>Testing</b> Motors, batteries, aircraft in flight	April 15	TBA

### 3.0 Conceptual Design

*"The beginning is the most important part of the work"*

Plato, *The Republic*

Using a combination of the method of guided iteration and direct decomposition; the first necessity of the conceptual design process is to define the problem. To determine the various problems that would be arise as a result of the competition constraints and requirements, the following mission statement was produced:

*Mission Statement:* Design a remote controlled model plane powered by Nickel Cadmium batteries (2.5lbs. max), takeoff over a six foot obstacle at the end of the given runway, fly the maximum number of laps around a predetermined oval course in the allotted time of seven minutes and obtain a flat roll landing within a designates 300ft. landing strip.

Analyzing the diverse design criteria, direct decomposition was utilized and the design team divided into three different groups: power, stability & control, structural design & construction. Each of the three teams then defined specific functions for each with the goal of optimizing each design feature.

#### 3.1 Power

After reviewing the competition requirements and the goals established by the design team, the power team had to distinguish what areas they needed to research and optimize. The combination of battery and motor would determine the length of flight thus determining the number of laps that could be completed in the allotted seven minutes.

##### 3.1.1 Batteries

The battery requirements established by AIAA specifies that they be "off the shelf" Nickel Cadmium (NiCd) batteries cumulatively weighing no more than 2.5lbs. This immediately establishes a limit of the maximum power available with which to operate the motor. Many NiCd battery types were researched. The properties of the batteries that we were concerned with included the storage capacity, operating voltage, weight, size, and price. The two main types of batteries looked at were C and AA's. Then it was determined that a high capacity battery complying with our weight and size restrictions would increase the flight time. Figure 3.1 shows the Dominic Matrix used to determine the best battery choices to carry forward to the next phase of design.

The priorities for the battery (B) selection were as follows:

**High:** low weight, **WB**  
small size parameters, **SB**  
**Moderate:** high capacity, **CB**  
**Low:** Cost, **SB**

The battery types were: Sanyo Cadnica (KR Series) Standard C, **1B**  
Sanyo Cadnica (E Series) AA KR-1200AAE, **2B**  
Sanyo Cadnica (H Series) SUB C KR-SCH, **3B**

**Figure 3.1: Dominic Decision Matrix**

RATING	PRIORITY		
	HIGH (WB, SB,	MODERATE (CB	LOW (\$B,
EXCELLENT	3B 1B 2B	3B	
GOOD	2B 3B	1B 2B	2B 3B
FAIR	1B		
POOR			1B
UNACCEPTABLE			

### 3.1.2 Motor Selection

Research on motors was done mainly over the Internet. The initial research on model aircraft yielded two common alternatives; direct drive or gear driven motors. The gear driven motors are typically for low speed heavy-lift model aircraft while the direct drive motor is for racing. Noting the goal of lifting a payload, but also at a decent speed, the team decided to utilize the planetary gearbox with a ratio of 3.7:1. This enables the motor to turn a larger diameter prop at a greater speed, with minimal efficiency loss of the motor. Determining the capabilities of the batteries, however, narrowed our search for an appropriate motor. At the time of conceptual design, the parameters were not solid enough to select the best combination of batteries with a motor.

### 3.1.3 Ducted Fans/ Propellers

The information collected on the propellers and ducted fans present two alternatives. The fans showed a lot of promise initially for their higher efficiencies and capability to obtain higher velocities. They did, however, present a problem for the design of the aircraft. Utilizing ducted fans would increase the complexity of the manufacturing process and also would pose heating problems that made the propeller driven alternative much more appealing.

## 3.2 Stability & Control

Designing a plane so that it will have both stability and moderate maneuverability presents the use of a design compromise. It is known that as the stability of an aircraft increases the maneuverability of the plane decreases. The reasoning behind the desire to design a plane to have increased maneuverability is to minimize the turning radius at the edges of the course. This theoretically would allow more time to complete full laps, the underlying goal of this competition. Determining exactly what the compromise in stability will be is a question to be determined through future calculations. These calculations include the placement of the center of gravity, mean aerodynamic chord, etc. This type of design parameters will also be utilized by the structural design group for the proper placement of components in the airframe.

## 3.3 Structural Design & Construction

It is very easy to find information of the latest building trends of modelers. Numerous publications, Internet websites, and videos carefully explore the various alternatives that can be used when building a plane. It is usually a common goal to build a lightweight yet durable aircraft for flight. The most common materials currently used for construction are balsa wood, foam, and carbon fiber. All of these products are lightweight and strong and when placed together properly.

At this stage of the design ideas about the materials and the structural aspect of the vehicle were being invented by several team members. It was now time to gather the best ideas and start working toward one realistic design. The determination of the actual size of the plane; the wingspan, aspect ratio, weight and size of the fuselage, was beginning to converge into one design. A vast array of ideas were initially discussed. Since the majority of the team members have minimal experience in construction and design techniques, the team settled on a plan to combine the simplistic designs with those that were the most efficient, and relatively easy to construct. By utilizing classical construction techniques, the team was able to use a majority of the ideas discussed previously.

Until the team members are more experienced with the building process, the decision was made unanimously to try and combine the more simplistic wing sections and tail surfaces. The wings for this project would be solid foam wings rather than the more complicated and time consuming built-up wing configurations. The major driving force for this decision was the uncomplicated procedure with which the wings would be manufactured, and the time that would be saved by utilizing this design technique. Several options were examined to determine that a more conservative or traditional design was the optimum decision for such a young team. Perhaps in the future design competitions more challenging and innovative designs will emerge. Figure 3.3 shows the decision matrix for various components of the vehicle. The number scale utilizes a 1 for simplistic designs or level skill and 5 for complex designs or more challenging construction techniques.

**Figure 3.3**

<b>Design Options</b>	<b>Complexity of Design</b>	<b>Level of Construction</b>	<b>Required Skill Level</b>	<b>Time Input Required</b>	<b>Design Ranking</b>
Box Style Fuselage	Utilizes series of rectangular sections	2	1-2	2	2
Streamlined Fuselage	Creates more curved and aerodynamic surfaces	4	3-4	4-5	4
Solid Foam Wings	Requires hot-wire to cut foam	2-3	2	1-2	2
Built-Up Wings	Requires multiple rib and spars	4-5	4-5	4-5	4-5
In-Ducted Fan	Runs faster, but creates heating problems	3-4	2-3	3-4	4
Prop-Driven	Works Ideally with Gear Driven System	2-3	2-3	2-3	2-3

## 4.0 Preliminary Design

In this phase of the design, specific components are narrowed from the conceptual design phase. The choices for airfoils are narrowed to a specific curve, and the final design with the maximum lift characteristics that are desired for the application. Final power requirements and motor selection are discussed in this phase of the design. After parts are configured, the parts and the assemblies to which they belong are given dimensions, tolerance, and exact material specifications. The preliminary design consists of three major parts: aerodynamic forces, performance data, and stability and control calculations.

### 4.1 Aerodynamic Forces

The aerodynamic forces that act on the body include lift forces due to the pressure differences between the upper and lower surfaces of the wing. The weight of the plane effects the overall lift-drag characteristics of the design. The Drag Force of the plane counters the Thrust provided by the motor. The lift and drag characteristics of the aircraft will be derived mainly from the NACA 4412 airfoil. This information is extrapolated from airfoil data compiled from the National Advisory Committee of Aeronautics (NACA). Lift, drag and moment coefficients were systematically measured for the shape of the airfoil in a low-speed wind tunnel. This data enabled the team to select the airfoil without having to re-create the airfoil testing process normally associated with the selection of an airfoil.

#### 4.1.1 Lift

The total lift of a body is given by the equation:

$$L = \frac{1}{2} \rho V^2 S_w C_L \quad 4-1$$

The 2 Dimensional lift slope angle from appendix A was used in the 3 dimensional conversion equation to obtain a 3-D lift slope. Using the lift slope equation in Appendix B, we set the Lift Coefficient ( $C_L$ ) as a function of the angle of attack ( $\alpha$ ).  $C_{L_{max}}$  can be found easily by substituting ( $\alpha_{max}$ ) into the equation, and found to be  $C_{L_{max}} = 1.32$ . Utilizing equation 4-1, the maximum Lift developed is found to be  $L = 13.722$  lbs.

#### 4.1.2 Drag

Total drag on an aircraft is denoted by the following equation:

$$C_D = C_{D_0} + C_{D_i} \quad 4-2$$

Where  $C_{D_0}$  is the Parasite drag or the drag due to the shape of the aircraft, and  $C_{D_i}$  is the drag induced by the lift of the aircraft. The induced drag can be calculated using equation 4-3.

$$C_{D_i} = C_L / \pi e_i AR \quad 4-3$$

Using  $C_{L_{max}}$  and an assumed Oswald Efficiency Factor,  $e_i$  of .75, in conjunction with the Aspect Ratio AR calculated in appendix B, the induced drag  $C_{D_i}$  was found to be  $C_{D_i} = .0607$ . The parasite drag coefficient is representative for all surfaces of the aircraft. The assumed parasite drag coefficient for the "Pegasus" aircraft is  $C_{D_0} = .025$ . From equation 4-2, the total drag on the aircraft can be found as a function of the angle of attack assuming the maximum drag will occur at the maximum angle of attack,  $\alpha_{max}$ . The total drag force on the aircraft is found by:

$$F_D = 1/2 \rho V^2 S_w C_{Dmax}$$

4-4

Using the Lift off Velocity,  $V_{LO}$  the total drag force was found to be  $F_D = 1.28 \text{ lb}$ .

## 4.2 Performance

The performance of the aircraft will determine the overall parameters that maintain the flight of the aircraft. The thrust that is required to maintain flight, the maximum available velocity and power dictated by design parameters of the aircraft will effect the overall flight limitations and boundaries of the vehicle. The section will outline the major operating limitations of the aircraft with respect to power, achievable and maintainable speeds, and overall take-off performance of the vehicle.

### 4.2.1 Power Curves

The maximum lift-to drag ratio ( $L/D$ ) for the aircraft can be obtained from the power Required ( $P_R$ ) versus Velocity Relation. Ranging the free stream velocity from 10 ft/s to 195 ft/s. The Thrust required is dependent on the Weight and the Lift to Drag Ratio of the airfoil.

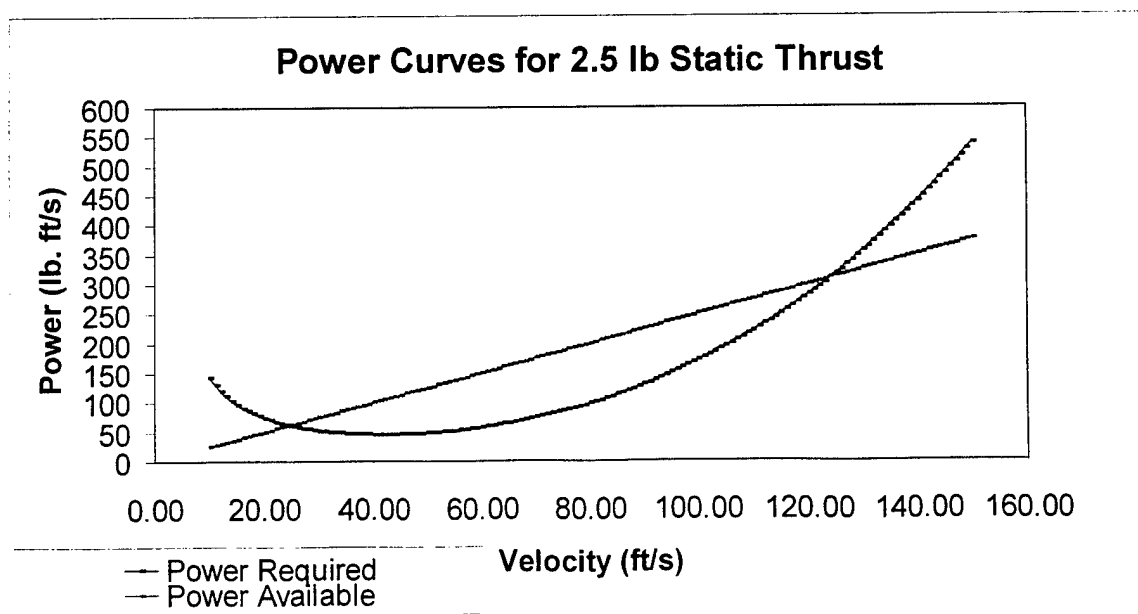
$$T_R = W / (L/D) \quad 4-5$$

$$P_R = T_R * V_{LO} \quad 4-6$$

The Power Available is limited to the motor that is selected. The motor that the team picked is the Aveox 1406/4Y with a 3.7:1 planetary gear ratio. Since the power available is limited, we narrowed the available static thrust to be 2.5 lbs. This is a conservative estimate of the thrust of this electric motor. The Power Available will be a linear relationship. The area between the Power Available and Power Required Curves will give a graphical representation of the maximum velocity achievable with the wing configuration and motor selection. Subsequently the maximum Lift to Drag ratio can be calculated from the noting the minimum thrust location and substituting it in the following relationship:

$$(L/D)_{max} = P_R / T_{Rmin} \quad 4-7$$

The Power Curve for the NACA 4412 and Aveox 1406-4Y with planetary gear ratio 3.7:1 is shown below:



#### 4.2.2 Stall Speed and Take-Off Performance

The stall velocity of the aircraft can be calculated by  $V_s = \sqrt{\frac{2W}{\rho C_L \max S_w}}$  4-8

From equation 4-7 the stall velocity was found in appendix B to be 42.04 ft/s. The Take-Off Velocity is simply the stall velocity multiplied by a safety factor (SF) as suggested by Anderson<sup>6</sup>. Using a Safety Factor of 20 percent (1.2),  $V_{L.O.}$  is found to be  $V_{L.O.} = 50$  ft/s. The suggested lift-off distance neglecting drag and friction is characterized by:  $S_{L.O.} = SF^2 * \frac{W^2}{g \rho S_w C_L T}$  4-9

This equation neglects drag, friction and is assuming there is no wind for the take-off distance.  $S_{L.O.} = 246.49$ . This is the distance that is required for the aircraft to lift off the ground safely.

#### 4.2.2 Rate of Climb

The rate of climb is given as the excess power available to lift a specified weight:

$R/C = (P_A - P_R) / (W)$  4-10. The rate of climb for the maximum L/D supplied by equation 4-7 was calculated to be  $R/C = 8.18$  ft/sec.

#### 4.2.3 Load Factor, Wing Loading and Turning Radius

The load factor  $n$ , is defined as  $n = L/W$  4-11. The load factor is usually quoted in terms of 'g's'. The load factor of the aircraft was found to be  $n = 88$  g's. Since the competition is mainly endurance race in terms of laps the minimum turn radius. The minimum turning radius  $R$  will be a minimum and angular velocity,  $\omega$ , will be maximum when both  $C_L$  and  $n$  are maximum. The relationships are shown in Equations 4-12 and 4-13 below:

$$R_{\min} = (2/\rho g C_{L \max}) * (W/S) \quad 4-12 \quad \omega_{\max} = g \sqrt{\frac{\rho C_L \max n \max}{2(W/S)}} \quad 4-13$$

The minimum turning radius will be at  $R_{\min} = 63.36$  ft and the maximum angular velocity,  $\omega = .953$ .

#### 4.3 Stability and Control

A major contribution to stability and control is that of the tail. The tail volume ( $V_H$ ) is defined as the ratio of the size and location of the tail to the volume characteristics of the wing. The tail volume is defined as  $V_H = S_{t_l} / S_w MAC$  4-14. Equation 4-14 yielded a tail volume ratio of  $V_H = .7524$ .

In order to satisfy longitudinal static stability, the zero lift coefficient of moment,  $C_{M_0}$ , must be greater than zero. From Perkins and Hage<sup>7</sup>,  $C_{M_0}$  can be represented by:

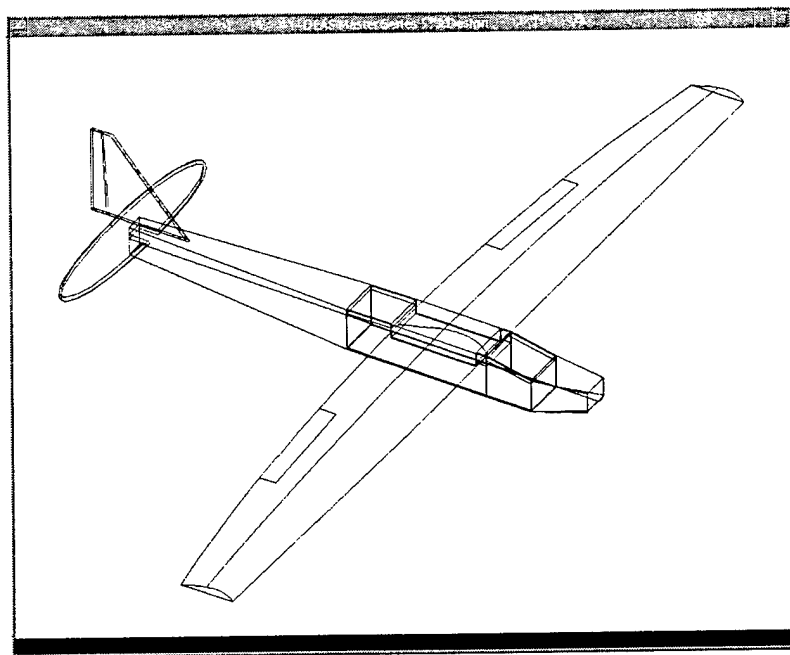
$C_{M_0} = [C_{MAC} - V_H \eta_t a_t (i_t - i_w + \alpha_0)]$  4-15. Where  $i_t$  is the incidence of horizontal tail,  $i_w$  is the incidence of the wing,  $\alpha_0$  is the zero-lift angle of attack, and  $\eta_t$  is the horizontal tail efficiency. Solving equation 4-15, we find that the zero lift moment coefficient,  $C_{M_0} = .2550$ . These results show that for this configuration, the tail volume is sufficient to overcome the  $C_{MAC}$ , therefore, the longitudinal static stability criterion is satisfied.

The other criterion to meet the longitudinal stability is that the coefficient of the moment slope must be less than zero. This is shown by the formula in appendix B. As shown by Perkins and Hage<sup>7</sup> the downwash rate and partial of the moment with respect to the lift coefficient has been calculated in Appendix B. By setting the partial of  $C_M$  with respect to the lift coefficient equal to zero (the neutral point) and the neutral point is found to be  $h_n = .44\%$ . The static margin ( $h_n - h_{ac}$ ) must be positive and found to be equal to  $(h_n - h_{ac}) = .196\%$ .



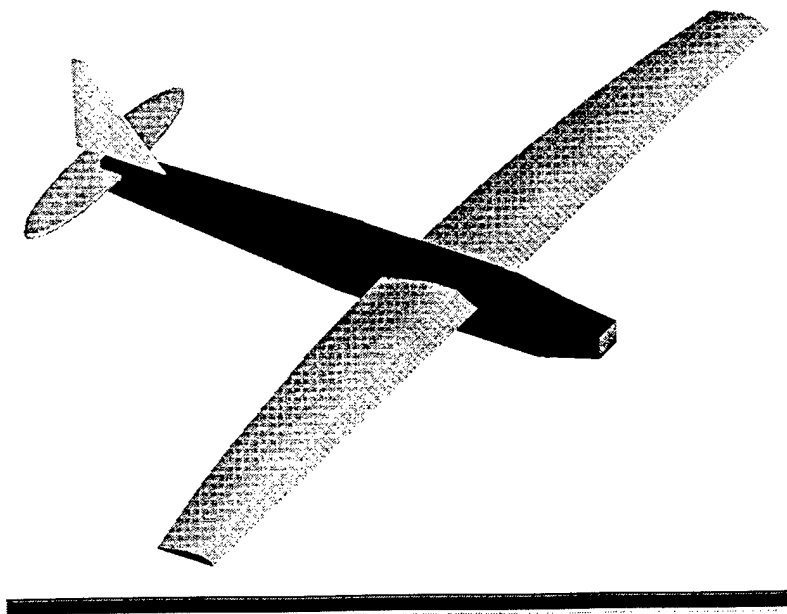
## PEGASUS

Wire-Frame View



Solid View

I-DEAS Master Series 5: Design



Refer to Appendix D for the Drawing Package of Aircraft

## 5.0 Manufacturing Plan

### 5.1 Overview

The Manufacturing Process of the aircraft was one of the most integral points of this competition. The first stage of the process was the overall design of the various components of the plane. The fuselage design was implemented around the general dimensions of various sections such as avionics, payload and structural support pieces. Once the overall design was established the building process was started. Integration of key components such as power, avionics, and payload placement dramatically effected the overall stability of the aircraft and were also a critical part of the manufacturing process.

Scheduling and Cost Analysis played a vital part in the Manufacturing Plan of this project. In addition the ease of construction of a classic design aircraft would enable the younger members to be more actively involved during the construction phase of the project. Thursday evenings and Saturday afternoons were scheduled days for the construction of the aircraft. Multiple days were schedule to adhere to the varying schedules of team members. This provided the flexibility need for all team members without jeopardizing the schedule of construction for the aircraft.

### 5.2 Construction Process

The construction process was delegated to the team members based on individual skill level. Also, the teams were based on the required component being built and the time management of student schedules. The tasks were divided between both upper and lower classmen. One objective of this project was to involve underclassmen. For each section of the plane construction, a mentorship situation was initiated between an experienced upper classmen and lower classmen. This enabled the construction techniques to be demonstrated while the actual building process was in progress. The building process included the construction of different sections of the aircraft. These sections focused mainly on construction of the fuselage, wings, tail and boom section.

#### 5.2.1 Fuselage Construction

The type of construction used on the fuselage is known as classic construction. It is by far the easiest construction method for the lesser experienced modelers. A classic construction offers a wide verity of knowledge to the beginner in modeling. By using basic joints, woods, glues and common sense, the student has a moderately easy time of building the aircraft. The fuselage utilizes simplistic construction technique such as the elimination of doublers in the construction, but does require reinforcement at strategic locations. The fuselage was also designed and built in a modular fashion. Each component or module of the aircraft was designed separately from all others sections. They were then "virtually integrated" by computers and formulas to determine if they would work well in a cohesive unit. By obtaining the optimum characteristics of all components separately, we ensure a tightly integrated, high performance aircraft.

Several new and interesting techniques were developed during the construction process. For example, Volume Density Trade, is a unique solution to a weight trade-off. Rather than use a heavy wood like balsa, a thinner, denser, stronger material is utilized. This is one of many exciting construction techniques that members of our team are developing. This was used in the construction of the tail eponage section.

The reinforcement of strategic locations in the fuselage is necessary to ensure that the payload and avionics are protected throughout flight. Bulkheads provide most of the reinforcement for the fuselage and carbon fiber reinforces the rest.

Bulkheads were the first order of business in the building of our aircraft. The design calls for three main bulkheads; the firewall, and two on both side of the payload section to ensure

strength. This design allows several secondary bulkheads. The three bulkheads were constructed out of several pieces of balsa wood using a technique of woodworking called tongue and groove. The construction the bulkheads were then reinforced by carbon-fiber laminate.

The airframe of our aircraft is made of a material called lite aircraft ply. This material yielded the highest strength to weight ratio of the materials that we tested. The airframe was cut out of the ply and attached to bulkheads by 12-minute epoxy. After cured the bottom of the airframe is cut and shimmed to provide a best fit. Because of the classic construction a completely composite fuselage was discounted to due to the inexperience of the team in working with composites.

### 5.2.2 Empennage-Tail Section

The back of the airplane or the empennage, is structured around a carbon fiber rod. The nose and tail bulkhead were small secondary bulkhead. Their dimensions allow it to be a square and aid in the ease of construction. The carbon-fiber rod is the main load-bearing structure. The aft section is constructed by using four  $\frac{1}{4} \times \frac{1}{4}$  balsa wood sticks and poster-board. It is completely covered by poster-board (tough skin) utilized as an aerodynamic surface. The carbon-fiber rod acts much like a tail boom supporting the empennage and the stabilizers. The tail boom runs directly through center of the empennage, connecting the tail with the fuselage. The two secondary bulkheads support the carbon-fiber rod. The sticks of balsa provide little structural value to the aircraft, but they allow a clean aerodynamic surface. The stabilizers are constructed separately from the fuselage and then integrated to ensure the best alignment configuration. The fully embodied enponage minimizes drag, and deflection of the tail under the aerodynamic loads associated with stabilizer deflection.

### 5.2.3 Horizontal Stabilizer

The horizontal stabilizer is located on the tail section and separated from the fuselage by the enpanage. The distance between the wings and the stabilizers creates a moment arm for the tail to counter the wing moments. The horizontal stabilizer is an elliptical flying stabilizer utilizing a NACA 0009 airfoil section. These symmetric airfoils are often used in tail surfaces. The traditional elevator was discounted due to the amount of tail lift required to counter the high wing moments developed by the NACA 4412 airfoil. The flying horizontal stabilizer functions as one large elevator and increases the CG range to a wide variation in stability and control characteristics. The horizontal stabilizer is rather difficult to construct. First, the mounting hardware was acquired and a built-up construction was begun. The winglet is formed out of 12 cross-member beams, a leading and trailing edge, and two balsa wood blanks to sand the elliptical shape. After the winglet had been "framed," it was covered with thin balsa wood. Finally the elliptical shape was sanded into the shape and it was monokoted.

### 5.2.4 Vertical Stabilizer

The vertical stabilizer is a more traditional design. It is designed and constructed for appearance to aid in the quickness and agility of the aircraft. It also serves its purpose of stabilization . The larger area of the rudder created with a swept back look allows excellent handling characteristics at low speeds as well as high speeds. The construction is straightforward, Three pieces of balsa wood are formed together in a triangle arrangement. The rudder is connected to the Vertical stabilizer by a hingeless joint, to minimize friction.

Concurrently, while the stabilizers are being constructed, the fuselage is undergoing a series of structure tests, optimum CG location tests, and payload section reinforcement. The reinforcement is done by adding a carbon fiber weave to the bottom of the fuselage. Also during this time the fuselage is being modified to accept a wing socket. This is done by cutting out a

section of the side. After the successful completion of the tests, and the modifications are complete, the components of the fuselage are integrated becoming a fully optimized fuselage.

The final stage of fuselage construction is the fine-tuning. This includes the final sanding and surfacing. We choose a film covering or Monokote. This rugged and durable material can offer our plane many hours of flight before resurfacing.

#### 5.2.5 Wing Construction

The wings are one of the most difficult parts of the aircraft to manufacture. The incorporation of washout, taper, dihedral and generation of a three dimensional wing must be symmetric for the left and right wings to ensure proper lift distribution and good stall characteristics

Wing construction involved many steps and several different techniques. First was the fabrication of templates. Then came the cutting of the foam. Reinforcing the wing with carbon fiber lamination followed, and finally the construction ended with the monokoting of the surface of the wings.

Looking on the Internet we found many airfoils that we could use for our wings. We decided on NACA 4412 and printed a template for the of the root and tip sections. Then we cut the plotted point out and glued them onto a piece of hard wood. After that we cut the hard wood template out We sanded the template to more closely match the printed plot points. We then at regular intervals marked the template to make the hot wire-cutting process smooth.

We used the hot wire foam cutting technique to cut the wings from the Polyurethane R3 insulating foam. To cut and shape the foam we use a bow to "hot-wire" the foam. The bow consists of two fiber glass rods anchored in a large wood rod. The fiberglass rods are span by a piece of Nichrome wire. The wire is connected to a small electrical source, thus creating heat and cutting the foam when dragged across. The wire actually cuts the foam by sending an electric current through the wire making it hot and thereby melting the foam.

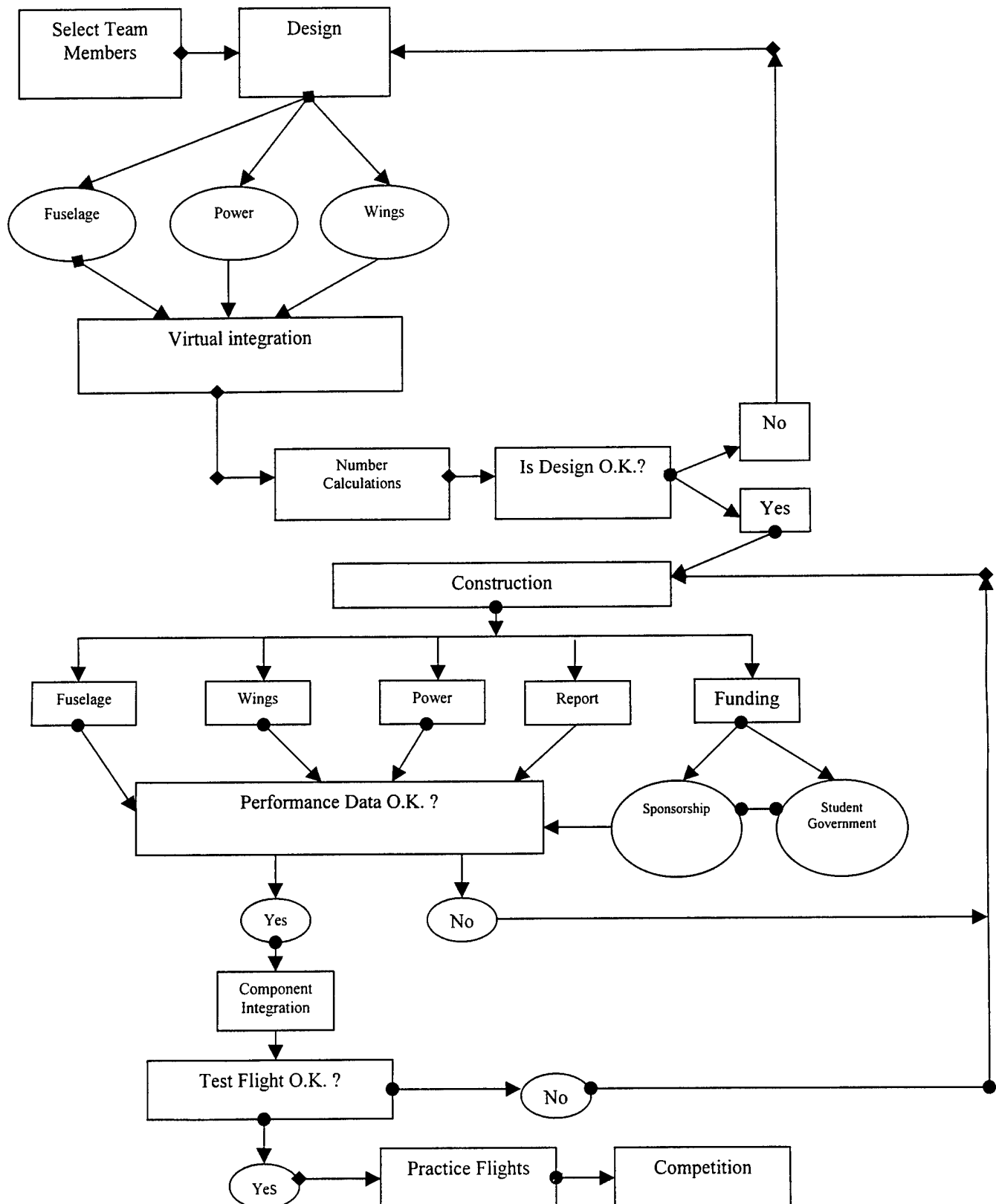
To construct the wings, we attached the templates of the wing's root and tip to the ends of the blue foam. Then two team members cut along the templates on each side. Several sets of wings were cut allowing the involvement of younger team members with more experienced senior members of the team. While cutting, the intervals were called out in unison to ensure the wing's overall surface smoothness. Both the top and bottom surfaces of the wing were cut using this technique. The section of the foam that is cut away from the actual airfoil section, making a perfect protective casing around the shaped foil is referred to as the saddle. When a set of wings have been cut they are stored in the saddle as a way of protection from the environment. They also serve as reverse molds for the curing process.

In order to prep the wings for carbon fiber process, we used a spray adhesive to glue left and right wings together. After the glue has set, the wing is then cut along the quarter chord and the spar is inserted. Twelve-minute epoxy is used to adhere the two halves of the wing to the spar. The leading and trailing edges of the wing are not always uniform. To alleviate this problem both the leading and trailing edges were removed and replaced them with balsa stock. The leading edge was made from prefabricated balsa and sanded to match the airfoil. However, the trailing edge was made from a block of balsa sanded to meet the airfoil's shape.

To reinforce the wings we used carbon fiber, and we laminated the surfaces of the wings. However, before the weave is applied the ailerons and servos are added. Epoxy is brushed onto the wing surface and massaged the carbon fiber into the wing. After the carbon fiber was massaged into the wing we then brushed in a thin second layer of epoxy in order to smooth out any imperfection. The bottom half of the saddle was covered with non-adhesive sheet to prevent the adhering of the wing to the saddle. Next the wing was placed into the bottom half of the saddle

and covered with a non-adhesive sheets. The top half of the saddle was placed on the wing, in addition 20lbs of force is applied to the entire saddle. The saddle and wing assembly is then allowed to cure. After the curing is complete final sanding is done to leading and trailing edges of the wing. To complete the wing, end caps are placed on the ends of the wings, and then final integration into the fuselage is done. The placement of the wing socket is located at one quarter of the length of the aircraft. This allows excellent flight characteristics as well as a virtually seamless integration

## Design and Manufacturing Flow-Chart



## Terminology

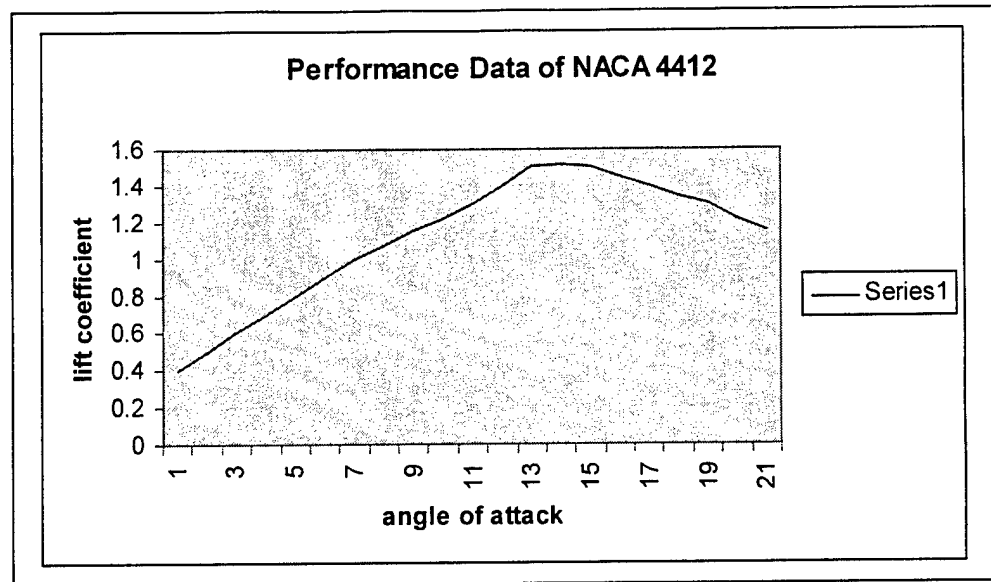
$a_w$	= Lift curve slope of the wing
$a_t$	= Lift curve slope of the horizontal tail
$A_f$	= Fuselage area (in <sup>2</sup> )
$A_t$	= Tail area (in <sup>2</sup> )
$A_b$	= Tail boom area (in <sup>2</sup> )
$A_{plane}$	= Total planform area (ft <sup>2</sup> )
$AR$	= Wing aspect ratio
$\alpha$	= Angle of attack
$\alpha_0$	= Zero lift angle of attack
$C_L$	= Wing lift coefficient
$C_{Di}$	= Induced drag coefficient
$C_{D0}$	= Parasite drag coefficient
$C_{mac}$	= Moment coefficient about MAC
$C_{mo}$	= Zero lift moment coefficient
$C_M/ C_L$	= Moment curve slope w.r.t. lift coefficient
$E_i$	= Total aircraft aerodynamic efficiency
$F_D$	= Force due to drag
$g$	= Gravity
$h$	= Center of gravity
$h_{ac}$	= Aerodynamic center
$h_n$	= Neutral point
$i_w$	= Incidence of the wing
$i_t$	= Incidence of the tail
$L$	= Lift
$m.a.c.$	= Mean aerodynamic center
$P_R$	= Power required
$R/C$	= Rate of climb
$S_{L0}$	= Lift-off distance
$S_w$	= Wing planform area
$T_S$	= Static thrust
$T_R$	= Thrust required
$\tau$	= Tailform factor
$V$	= Flight velocity
$V_H$	= Tail volume
$V_{LO}$	= Lift-off velocity
$V_S$	= Stall velocity
$W_t$	= Total aircraft weight
$W_p$	= Payload weight
$W_a$	= Aircraft weight (empty)

**APPENDIX A**  
**AIRFOIL DATA**



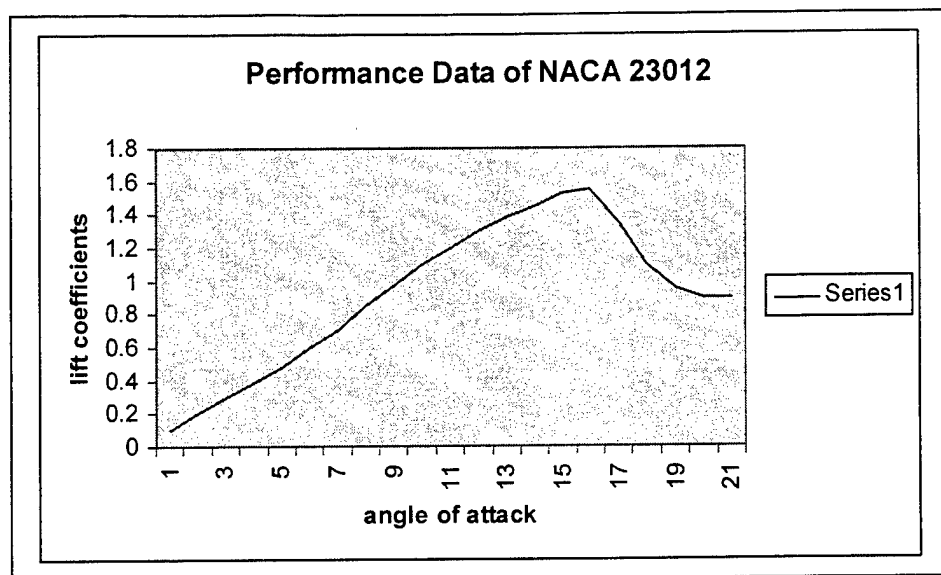
## NACA 4412

$\alpha$	$c_l$
0	0.4
1	0.5
2	0.6
3	0.7
4	0.8
5	0.9
6	1
	1.07
8	1.15
	1.22
10	1.3
	1.4
12	1.5
	1.52
14	1.5
	1.45
16	1.4
	1.35
18	1.3
	1.22
20	1.15



NACA 4412 is the airfoil chosen for this specific airplane. The above are experimental results for the lift and moment coefficients. Here, the quarter-chord point is used to take the moment coefficient. The maximum value of the lift coefficient was a major aspect in choosing this airfoil, and so was the performance data of the airfoil. A process of elimination took place where all of the parameters were compared and the airfoil chosen.

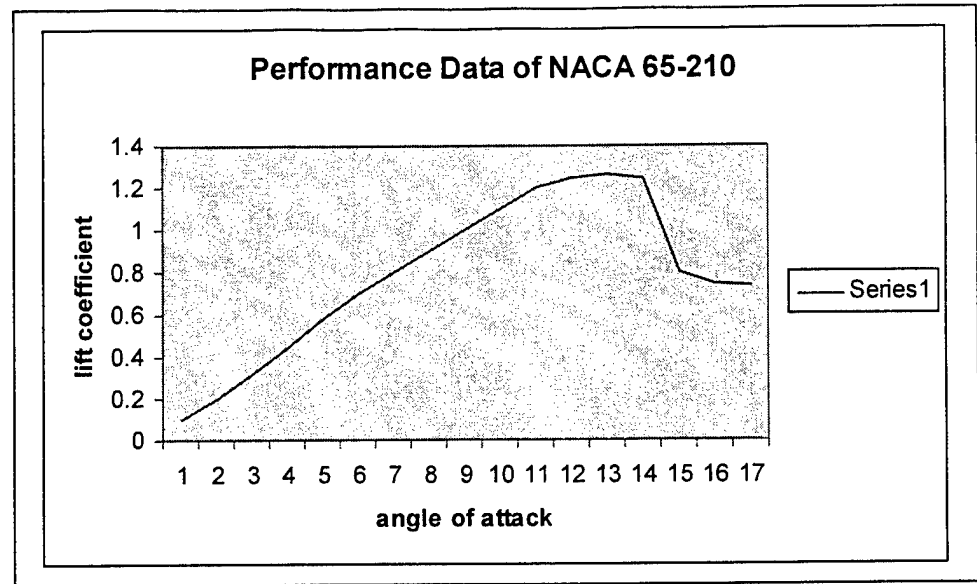
$\alpha$	$c_l$
0	0.1
1	0.2
2	0.3
	0.38
4	0.48
	0.6
6	0.7
	0.85
8	0.97
	1.1
10	1.2
	1.3
12	1.38
	1.45
14	1.53
	1.55
16	1.35
	1.1
18	0.95
	0.9
20	0.9



This is the NACA 23012 airfoil. The above are experimental results for the lift and moment coefficients. Here, the quarter-chord point is not used to take the moment coefficient, rather the aerodynamic center. The NACA 23012 is a high performance airfoil, not used in this specific case due to its fairly unstable take-off and cruising speed.

## NACA 65-210

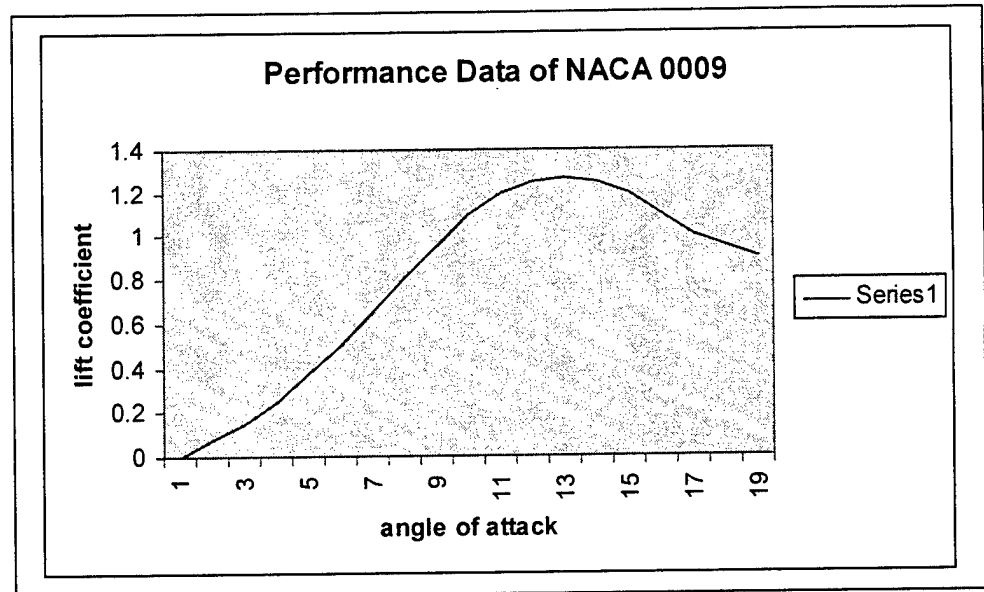
$\alpha$	$c_l$
0	0.1
1	0.2
2	0.32
3	0.45
4	0.58
5	0.7
6	0.8
7	0.9
8	1
9	1.1
10	1.2
11	1.25
12	1.26
13	1.25
14	0.8
15	0.75
16	0.74



This is the NACA 65-210 airfoil. The above are experimental results for the lift and moment coefficients. This is a high performance airfoil. The aerodynamic center is used to take the moment coefficient. The NACA 65-210 is an airfoil with increasing thickness, which tends to decrease the coefficient of lift, and is therefore, not a suitable airfoil for this airplane.

## NACA 0009

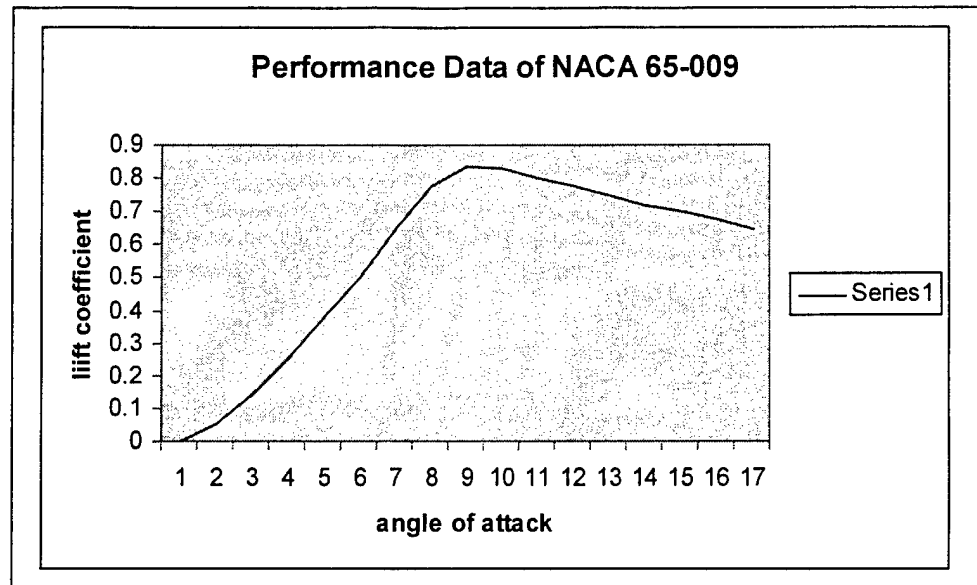
$\alpha$	$c_l$
0	0
1	0.075
2	0.15
3	0.25
4	0.38
5	0.5
6	0.65
7	0.81
8	0.95
9	1.1
10	1.2
11	1.25
12	1.27
13	1.25
14	1.2
15	1.1
16	1
17	0.95
18	0.9



This airfoil is the NACA 0009. The above are experimental results for the lift and moment coefficients. This airfoil is a symmetric airfoil with a maximum thickness of 9 percent. The moment coefficient is taken about the quarter-chord point. This point for a symmetric airfoil is both the center of pressure and the aerodynamic center. The lift coefficient is linearly proportional to the angle of attack.

## NACA 65-009

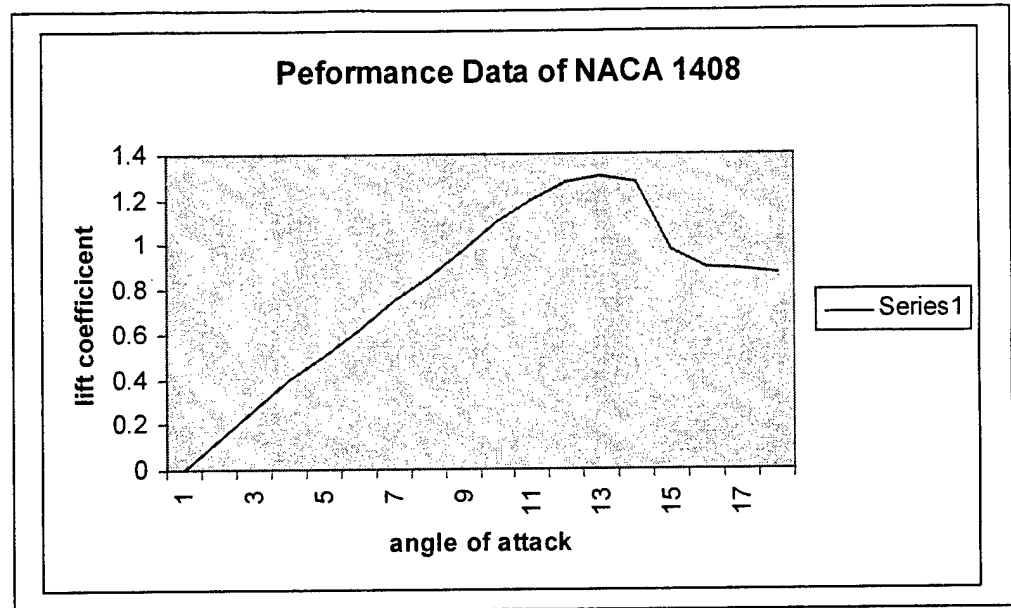
$\alpha$	$c_l$
0	0
1	0.05
2	0.14
3	0.25
4	0.38
5	0.5
6	0.65
7	0.78
8	0.835
9	0.83
10	0.8
11	0.78
12	0.75
13	0.72
14	0.7
15	0.68
16	0.65



This is the airfoil NACA 65-009. The above are experimental results for the lift and moment coefficients. This series of airfoils tend to increase in thickness and influence the value of the coefficient of lift. The aerodynamic center is used to take the moment coefficient. This is also a high performance airfoil.

## NACA 1408

$\alpha$	$c_l$
0	0
1	0.13
2	0.26
3	0.4
4	0.5
5	0.62
6	0.75
7	0.85
8	0.98
9	1.1
10	1.2
11	1.28
12	1.3
13	1.28
14	0.98
15	0.9
16	0.89
17	0.87



The last airfoil considered is the NACA 1408. The above are experimental results for the lift and moment coefficients. The maximum camber is .01c or 1 percent camber at 40 percent chord, with 8 percent thickness. The moment coefficient is taken about the quarter-chord point, this point for a symmetric airfoil is both the center of pressure and the aerodynamic center.

**APPENDIX B**  
**CALCULATIONS SHEET**

<u>Variable</u>	<u>Meaning</u>	<u>Equation</u>	<u>Value</u>
W	(Weight aircraft w/ 7.5 lb. Payload 'lb')		15.59375
AR <sub>w</sub>	(Aspect Ratio)	$AR_w = b_w^2 / S_w$	12.19047619
b <sub>w</sub>	(Wing Span 'in.')		96
S <sub>w</sub>	(Wing Area 'in. <sup>2</sup> )	$S_w = [c_r + c_t] * 1/2 * b_w$	756
c	(Mean Chord Length 'in.')	$c = (c_r + c_t) / 2$	7.875
c <sub>r</sub>	(Root Chord Length 'in.')		10
c <sub>t</sub>	(Tip Chord Length 'in.')		5.75
c/4	(Quarter Chord 'in.')		1.96875
X <sub>ac</sub>	(Aerodynamic Center 'in.')	From leading edge	1.929375
X <sub>cg</sub>	(Center of Gravity 'in.')		1.96
M <sub>ac</sub>	(Mean Aerodynamic Center 'in.')		-0.087
S <sub>f</sub>	(Fuselage Plan Area 'in. <sup>2</sup> )		244.5
S <sub>t</sub>	(Tail Plan Area 'in. <sup>2</sup> )		140
S <sub>tb</sub>	(Tail Boom Area 'in. <sup>2</sup> )		81.25
A <sub>p</sub>	(Total plan View Area 'ft <sup>2</sup> )	$A_p = [S_w + S_f + S_t + S_{tb}] * 1/144$	8.484375
α	(Angle of Attack 'degrees')		0
V <sub>4</sub>	(Average Freestream Velocity 'ft/s')		70
ρ	(Standard Density 2000ft 'slugs/ft <sup>3</sup> )		0.00224
T	(Standard Temperature 2000ft °R)		511.56000
P	(Standard Pressure 2000ft 'lb/ft <sup>2</sup> )		1967.70000
μ <sub>4</sub>	(Dynamic Viscosity of Air 'slug/ft <sup>3</sup> )		0.00000
M <sub>4</sub>	(Freestream Mach Number)	$M_4 = V_4 / (r(1.4 * 1716 * T))$	0.06314
T <sub>s</sub>	(Static Engine Thrust 'lb-f')	= 9 oz. (? Lbs)	2.50000
g <sub>c</sub>	(Gravitational Constant)		32.2
η <sub>p</sub>	(Propeller Efficiency)		0.7
C <sub>mac</sub>	(Coefficient about MAC)		-0.087
S.F.	(Safety Factor)		1.2
δ	(Empirically determined quantity relating to span efficiency)		0.1
a <sub>t</sub>	(Lift curve slope of horizontal tail NACA 0009)		0.1
α <sub>t</sub>	(Incidence Angle of for Tail 'Degrees')		-1
α <sub>o</sub>	(Zero Lift Angle of Attack-degrees)	(taken from NACA lift-slope graph)	-4
<u>Variable</u>	<u>Meaning</u>	<u>Equation</u>	<u>Value</u>
a <sub>o</sub>	(2-D Lift slope for wing)		0.233333333
Re	(Reynolds Number)	$Re = (\rho * V_4 * c) / \mu_4$	3.31E+06
q	(Dynamic Pressure)	$q_4 = (1/2) * \rho * V_4^2$	5.49E+00
AR <sub>w</sub>	(Aspect Ratio-wing)	$AR = b^2 / S_w$	12.19047619
	(Taper Ratio)	$c_t / c_r$	0.575
e	(Oswald span efficiency )	$e = (1 + \delta)^{-1}$	0.909090909
a	(3-D lift slope)	$a = (a_o) / (1 + (a_o / \pi AR e))$	0.231779964
<u>Wing Efficiency</u>			
c <sub>l</sub> (α)	(lift coefficient as a function of angle of attack)	$c_l(\alpha) = a_o[\alpha - \alpha_o]$	0.933333333
c <sub>l</sub> (α <sub>max</sub> )	(maximum lift coefficient-2D)	$c_l(\alpha_{max}) = \text{from chart}$	1.5
C <sub>L</sub> (α)	(3-D lift coefficient as a function of AOA)	$C_L(\alpha) = a[\alpha - \alpha_o]$	0.927119855
C <sub>L</sub> (α <sub>max</sub> )	(maximum lift coefficient-3D)	$C_L(\alpha_{max}) = a[a - a]$	1.32



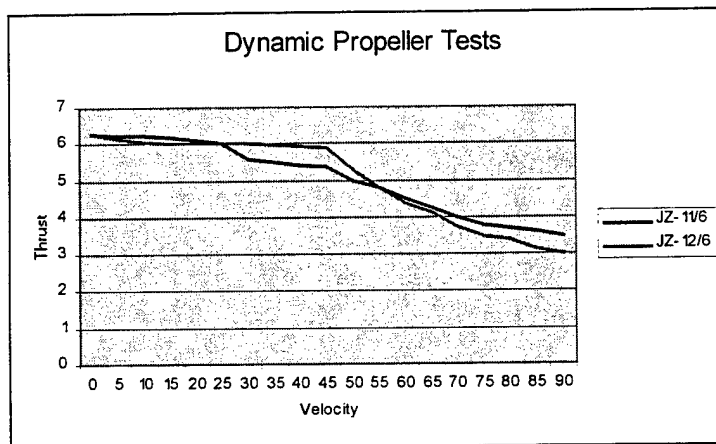
<b>Velocity as a function of <math>\alpha</math></b>			
$V(\alpha)$	Stall Velocity	$V(\alpha)=[(2*W)/(\rho C_L(\alpha)S_w)]^{1/2}$	42.03913409
$V(\alpha_{max})$	ft/s	$V(\alpha_{max})=??$	42.039134
$V_{L.O.}$	(Lift Off Velocity[ft/s])	$V_{L.O.}=SF*V(\alpha_{max})$	50.4469608
$S(\alpha)=S_{L.O.}$	(Lift off Distance [ft])	$SF^2*(W^2) / (g*\rho_a*S_w*C_L(\alpha)*T_S)$	246.4873906
<b>Drag</b>			
$e_i$	(Total aircraft aerodynamic efficiency)	assumed	0.75
$C_{Di}(\alpha)$	(Induced Drag Coefficient)	$C_{Di}(\alpha)=[C_L(\alpha)^2 / (\pi*e_i*AR)]$	0.0299254
$C_{Di}(\alpha_{max})$	Maximum Induced Drag Coefficient	$C_{Di}(\alpha)=[C_L(\alpha_{max})^2 / (\pi*e_i*AR)]$	0.060661907
$C_{Do}$	Parasite Drag Coefficient	conservative assumption	0.025
$C_D(\alpha)$	(Total Drag Coefficient)	$C_D(\alpha)=C_{Di}(\alpha)+C_{Do}$	0.0549254
$C_D(\alpha_{max})$	(Maximum Total Drag Coefficient)	$C_D(\alpha_{max})=C_{Di}(\alpha_{max})+C_{Do}$	0.085661907
$F_D$	(Force due to drag -lbs)	$F_D=1/2*\rho_a*V_{L.O.}^2*S_w*C_D(\alpha_{max})$	1.282358736
<b>Performance</b>			
$L(\alpha)$	Lift Developed (lb-f)	$L(\alpha)=1/2*\rho_a*(V(\alpha))^2*S_w*C_L(\alpha)$	9.638
$L(\alpha_{max})$	Maximum Lift Developed (lb-f)	$L(\alpha)=1/2*\rho_a*(V(\alpha_{max}))^2*S_w*C_L(\alpha_{max})$	13.722
$V(\alpha)=10,11 \dots 195$ for several different cases			
$C_{L_{firstm}}[V_{firstm}]$		$C_{L_{firstm}}[V_{firstm}]=W / (1/2*\rho_a V_{freestream}^2*S_w)$	0.541006774
$C_{D_{freestream}}[V_{freestream}]$		$C_{D_{freestream}}[V_{freestream}]=C_{Do} + ((C_{l_{freestream}}*(V_{freestream}))^2)/(\pi*$	0.035189986
$C_{L_{firstm}}[V_{L.O.}]$		$C_{L_{firstm}}[V_{firstm}]=W / (1/2*\rho_a V_{L.O.}^2*S_w)$	1.041666671
$C_{D_{freestream}}[V_{L.O.}]$		$C_{D_{freestream}}[V_{L.O.}]=C_{Do} + ((C_{l_{freestream}}*(V_{L.O.}))^2)/(\pi*e_i*AR)$	0.062776849
$L/D$	(Lift to Drag Ratio)	$L/D=C_L/C_D$	15.3738842
$L/D$	(Lift to Drag Ratio at L.O. Velocity)		16.5931659
$T_R$	(Thrust required lb-f)	$T_R=W/(L/D)$	0.975680564
$P_R$	(Power required lb-f)	$P_R=T_R*V_{freestream}$	39.02722255
$T_A$	(Thrust Available lb-f)	$T_A$	2.5
$P_A$	(Power Available lb-f)	$P_A=T_A*V$	175
$R/C$	(Rate of Climb ft/s)	$R/C=(P_A-P_R)/W$ (ft/s)	8.719697151
$T_{R \text{ at L.O.}}$	(Thrust required lb-f at L.O.)	$T_{R \text{ at L.O.}}=W/(L/D)$	0.939769426
$P_{R \text{ at L.O.}}$	(Power required lb-f at L.O.)	$P_{R \text{ at L.O.}}=T_R*V_{L.O.}$	47.40851142
$R/C \text{ at L.O.}$	(Rate of Climb ft/s at L.O.)	$R/C \text{ at L.O.}=(P_A-P_R)/W$ ft/s	8.182219709
$n$	(Load Factor "gees")	$n=L/W$	0.879999996
$R_{min}$	(Minimum Turning Radius)	$R_{min}=(2/\rho*g*Cl_{max})*(W/S)$ ft	62.36902861
$\omega_{max}$	(maximum Angular velocity)	$\omega_{max}=g*((\rho*Cl_{max}*n)/((W/S)^{1/2})$	0.953234558
<b>Static Stability and Control</b>			
$c_i(\alpha)$	Tail Lift Coefficient	$c_i(\alpha)=a_i*\alpha_i$	-0.1
$V_4$	Ffix Freestream Velocity at $V_{L.O.}$		50.4469608
$l_t$	Length of Tail Boom 'inches' / 'feet'		32
$l_t(\alpha)$	Tail Lift	$l_t(\alpha)=1/2*\rho_a*V_4^2*S_t*c_i(\alpha)$	-0.277222221
$V_H$	Horizontal Tail Volume	$V_H=(S_t*l_t)/(S_w*c)$	0.75249853
$i_t$	Incidence angle of tail to centerline	(degrees)	-1
$i_w$	Wing incidence	(degrees)	0
$\eta_t$	Tail efficiency	$\eta_t=e$	0.909090909
$C_{Mo}(\alpha)$	Zero Lift moment coefficient	$C_{Mo}(\alpha)=(C_{mac}-V_H*\eta_t*a_i*(l_t-i_w+\alpha_o))$	0.255044786
$h_{ac}$	Aerodynamic center	(%chord)	0.245
DWR	Downwash Rate		0.33
$h$	Center of gravity	(%chord)	0.25

MCS	Moment Curve slope	$MCS = ((h - h_{ac}) - V_H * ((\eta_t * (a_t/a_0) * (1 - DWR))))$	-0.191431435
<i>Setting the moment curve slope equal to zero and solving for h yeilds the percent chord location of the neutral point.</i>			
$h_n$	Neutral point	$h_n = h_{ac} + (V_H * (\eta_t * (a_t/a_0) * (1 - DWR)))$ % chord	0.441431435
$h_n - h_{ac}$	Static Margin	$h_n - h_{ac}$ (% chord)	0.196431435
$\tau$	Tail Form Factor	(assumed)	0.55
$C_{M\delta}$	Trim Moment Coefficient	$C_{M\delta} = -V_H * a_t * \tau$	-0.041387419
$\delta_{trim}$	Elevator Trim Angle (degrees)	$\delta_{trim} = (C_{mo}(\alpha) + MCS * C_{L}(\alpha_{max})) / (C_{M\delta})$	-0.056908427

**APPENDIX C**  
**DYNAMIC PROPELLER TESTS**

### Propeller Dynamic Testing:

The powerplant selected was Aveox 1406/4Y and cannot be modified in any way. The propeller chosen depends on temperature and wind conditions. From dynamic thrust testing, the propeller of choice is a JZ-11/6 (Figure 1). The propeller produces excellent static thrust measurements. It unloads less drastically than lower pitch propellers and generates better thrust at takeoff and cruise velocities. The JZ-11/6 yields the best power available just above stall velocity where the maximum rate of climb is essential to power out of ground effect.

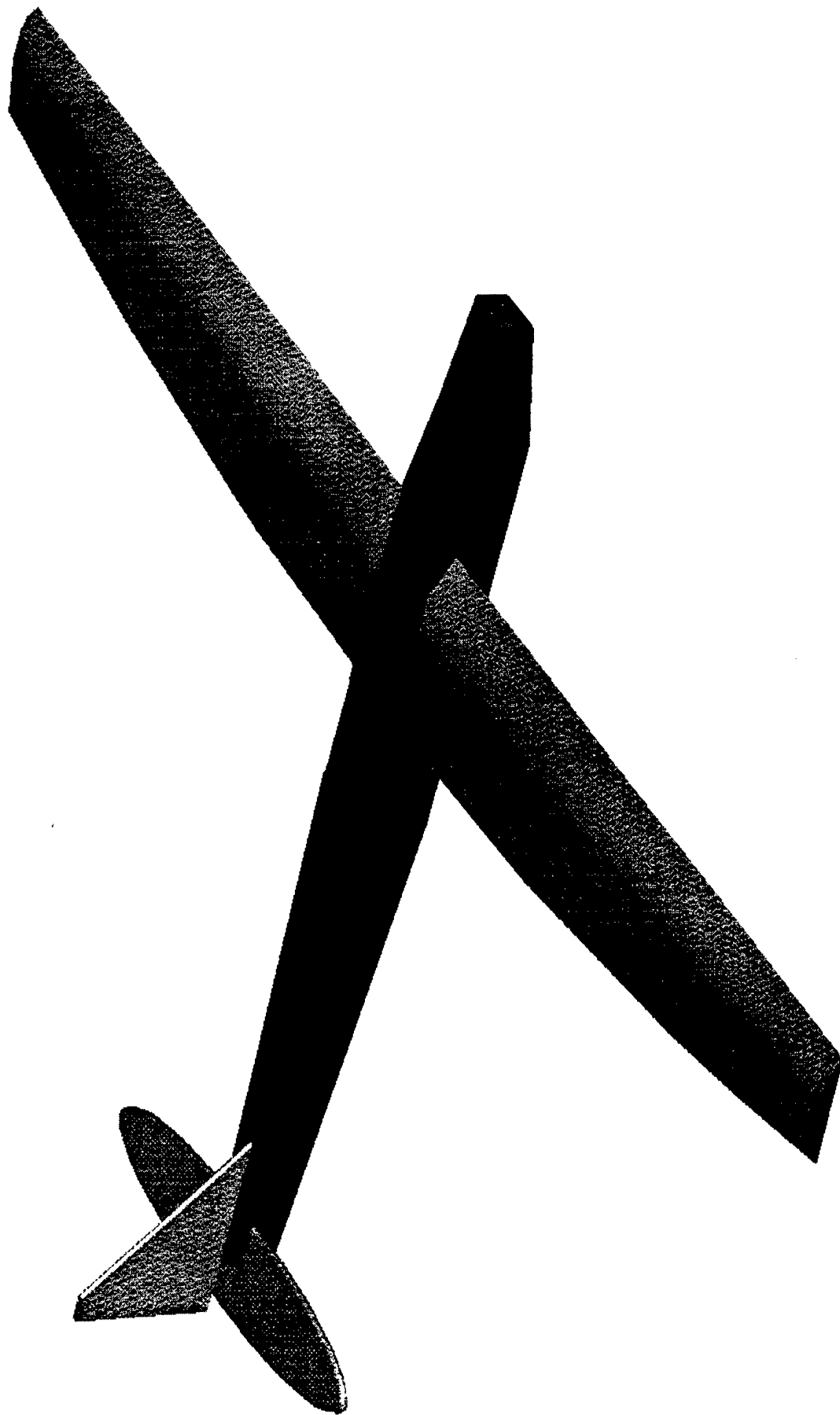


**Figure 1:** Dynamic Propeller Tests

**APPENDIX D**  
**DRAWING PACKAGE**

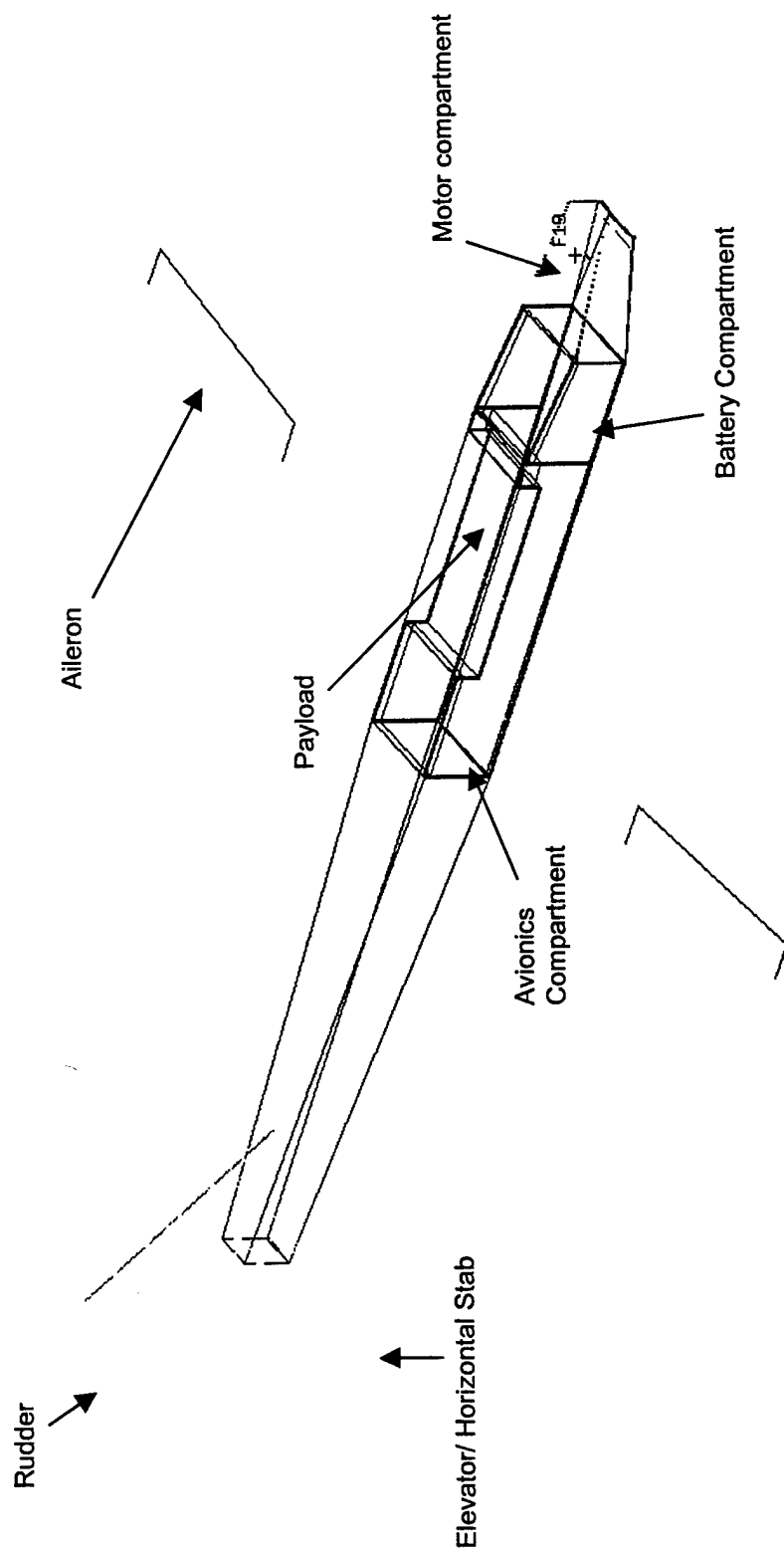
## Aircraft Overview

I-DEAS Master Series 5: Design



# Internal Compartment Structure

I-DEAS Master Series 5: Design



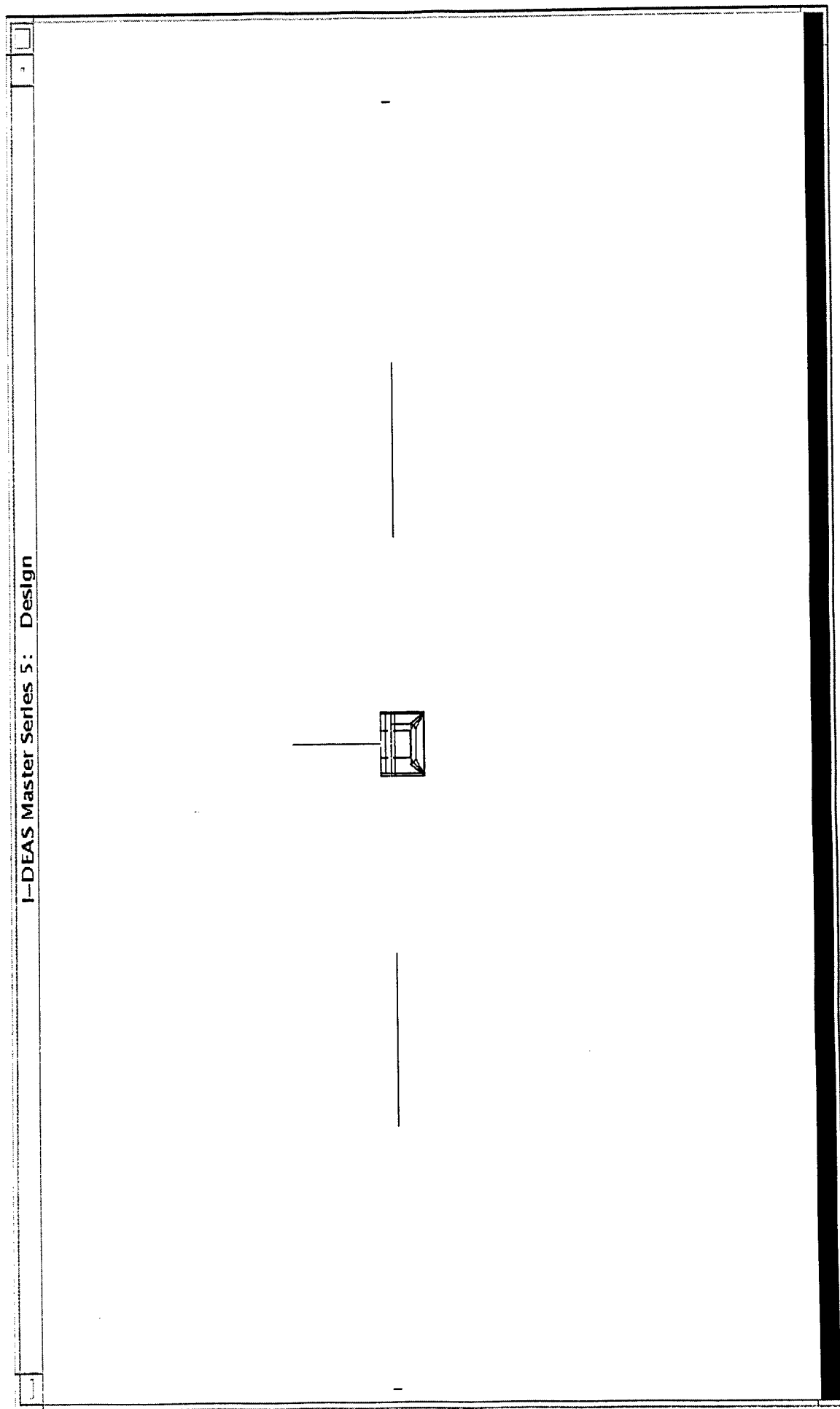
## Front View

I-DEAS Master Series 5: Design





## Forward build-up view



## Side View

I-DEAS Master Series 5: Design

rudder

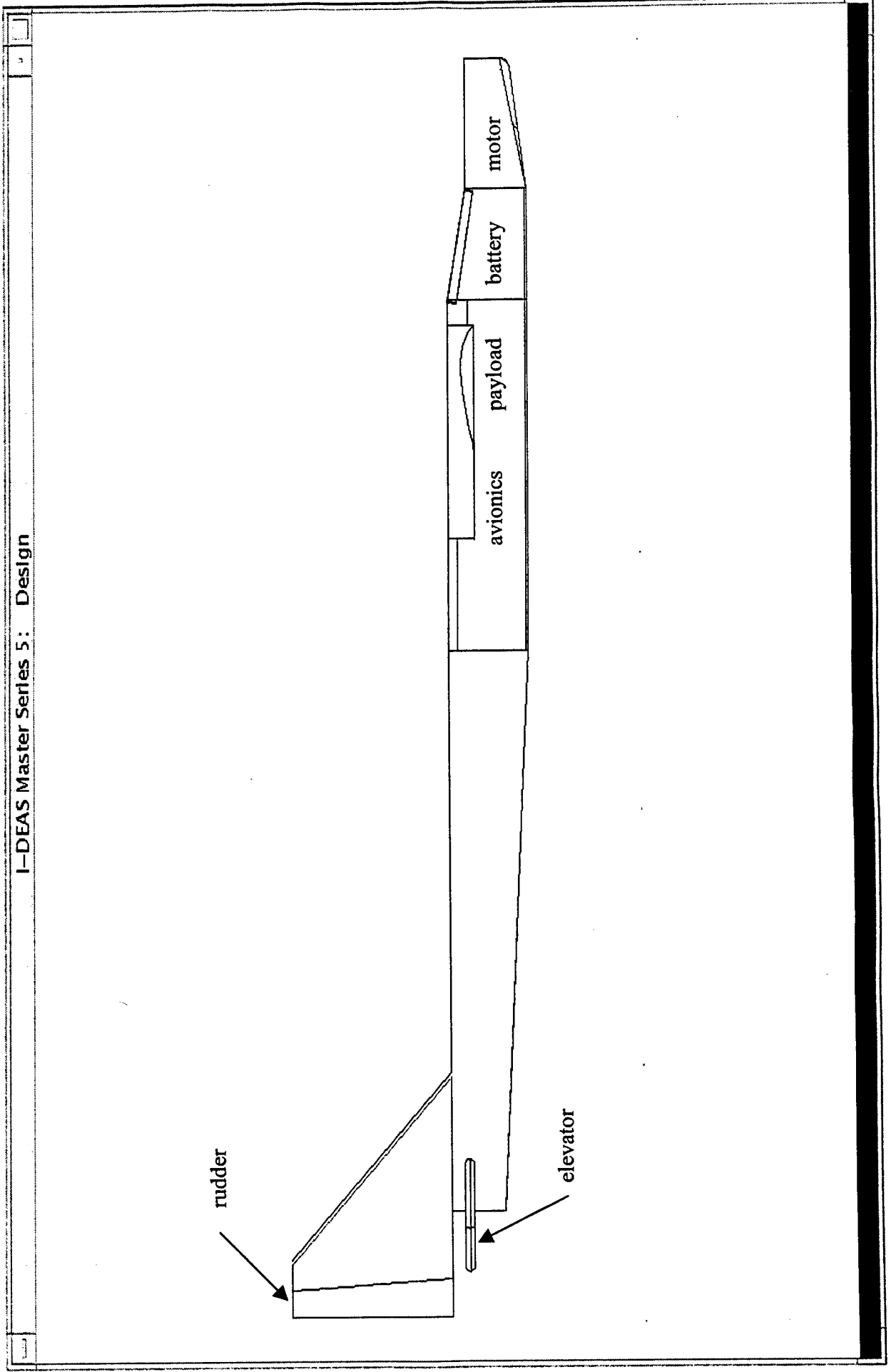
elevator

motor

battery

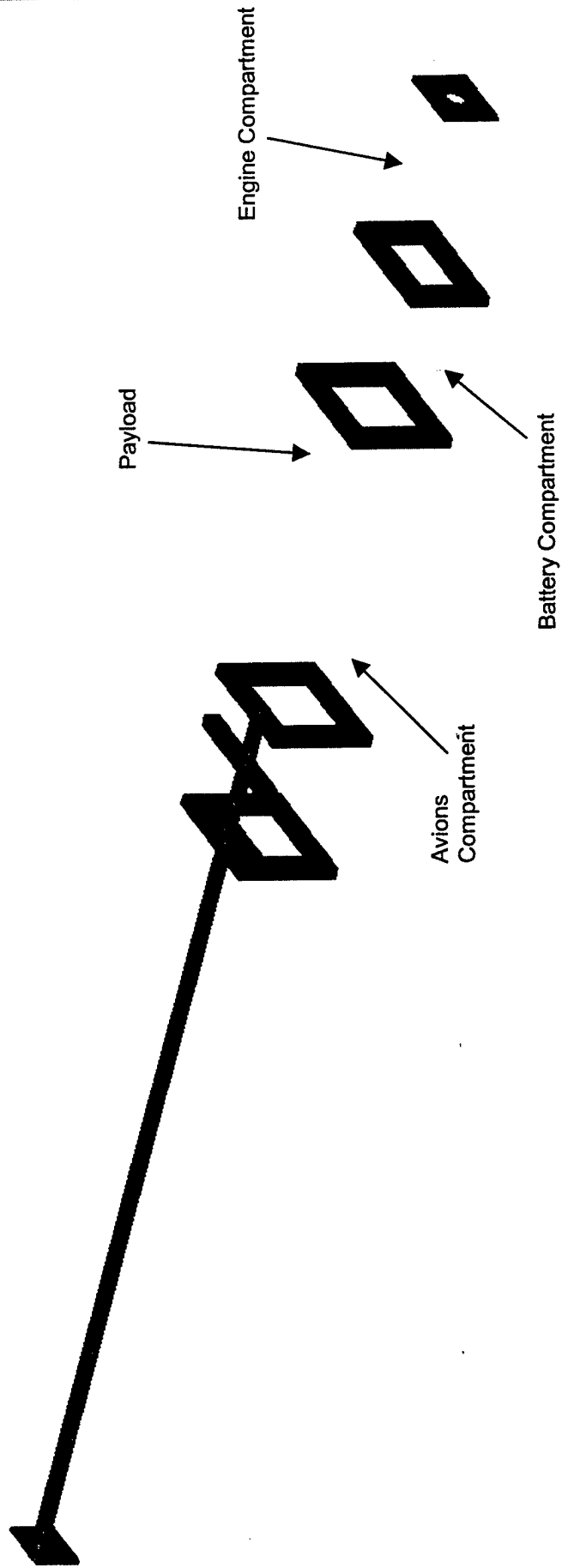
payload

avionics



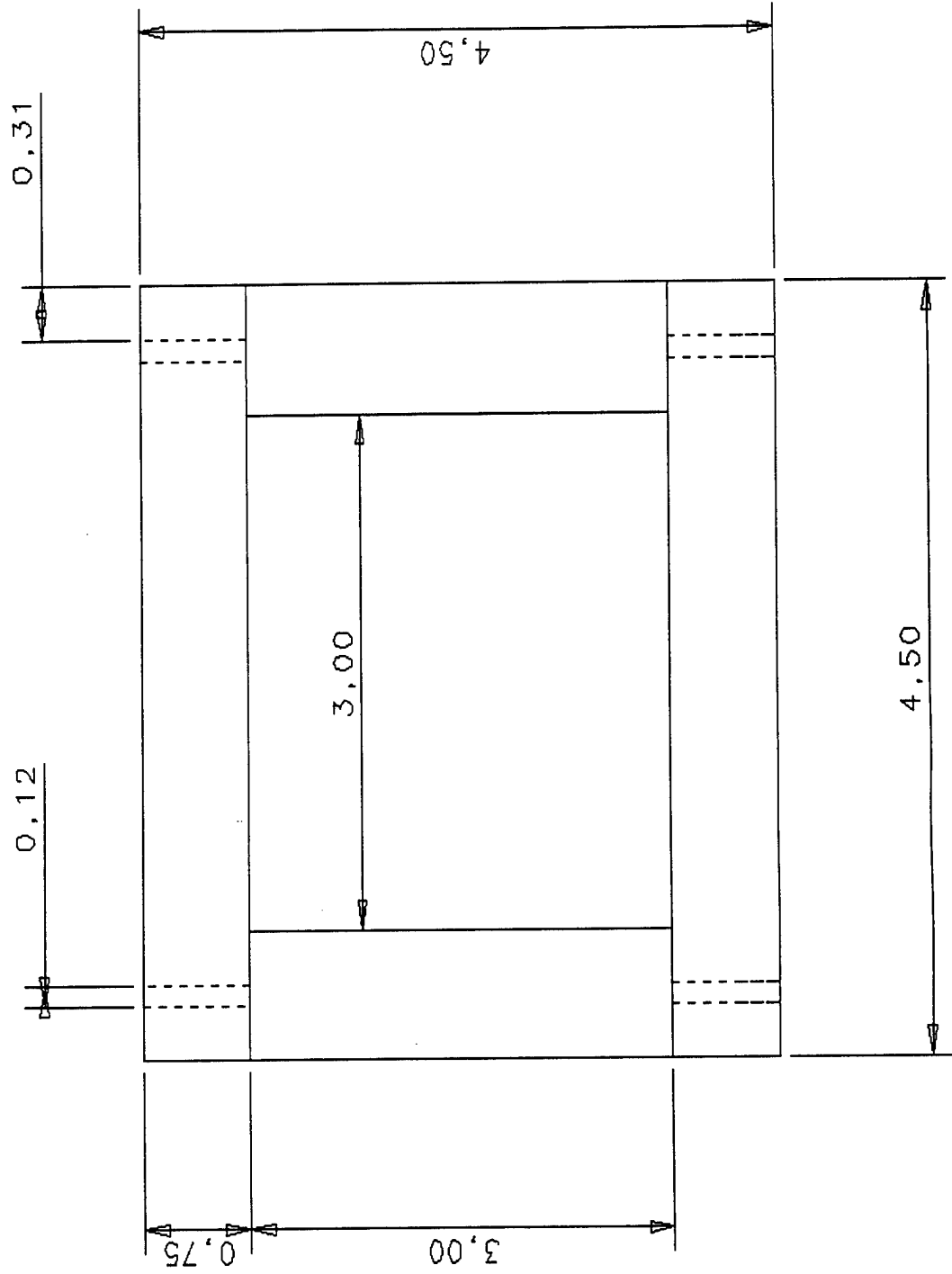
# Internal Support Structure

I-DEAS Master Series 5: Design



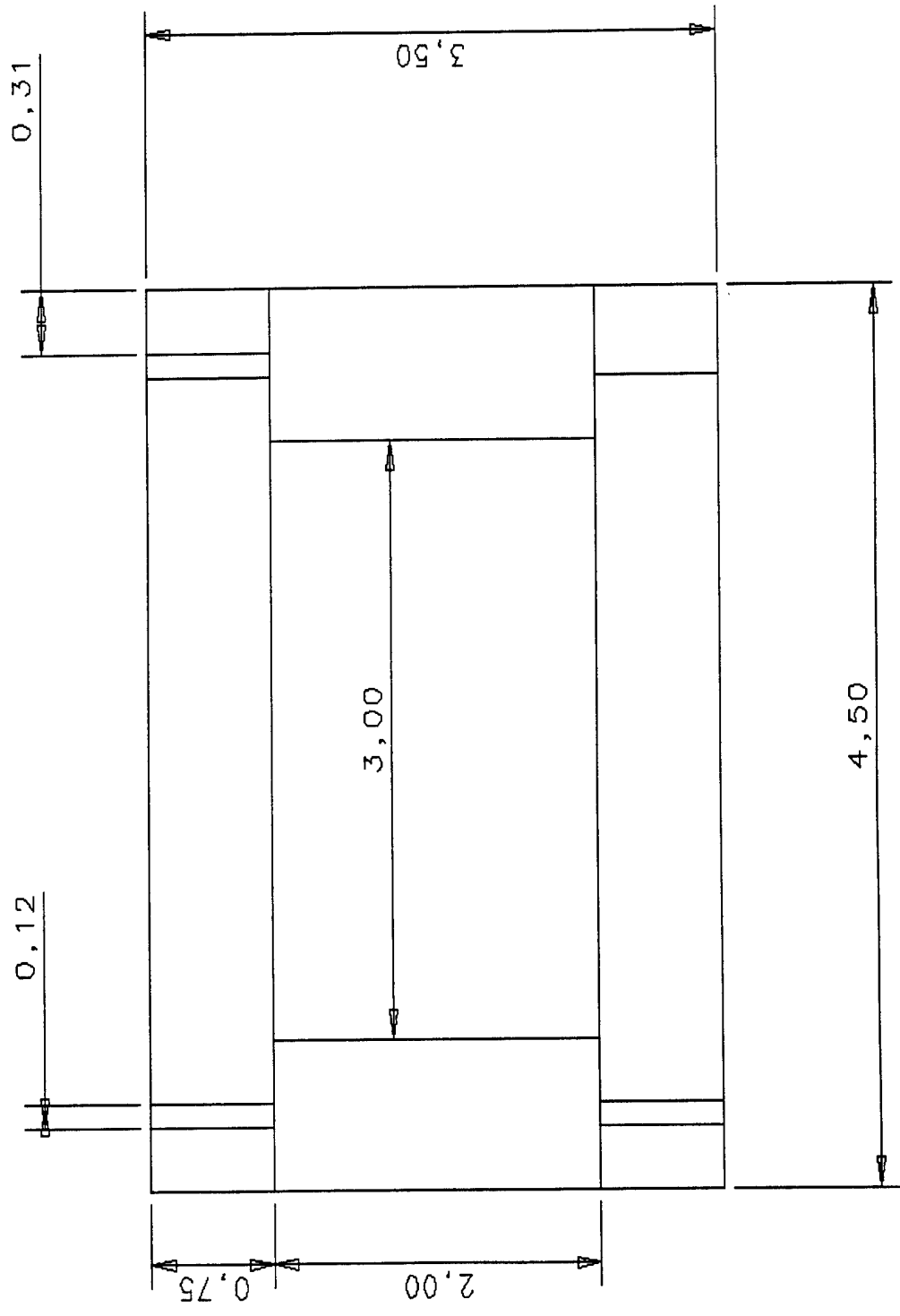
# Motor Mount

I-DEAS Master Series 5: Design



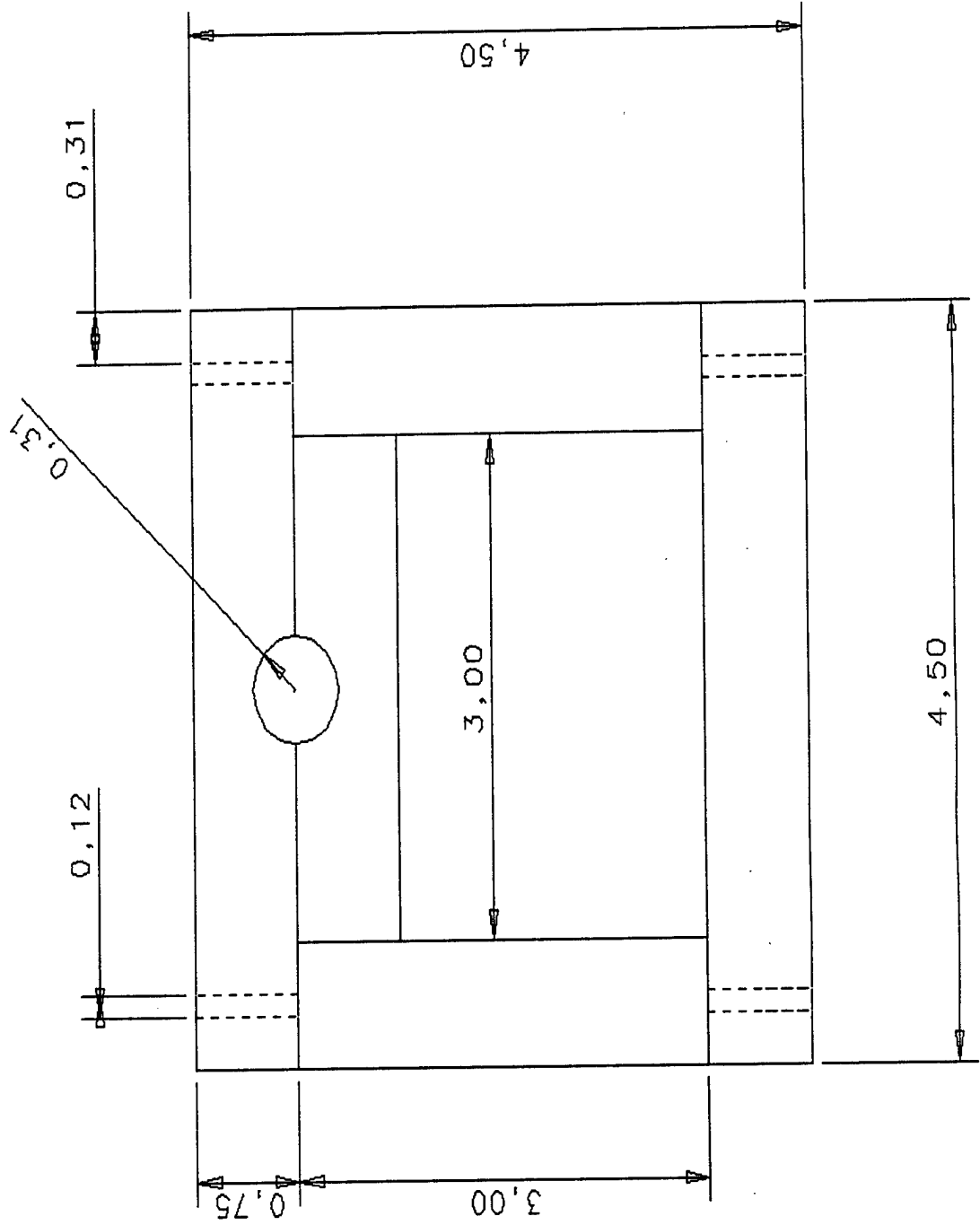
# Bulkhead Design

I-DEAS Master Series 5: Design



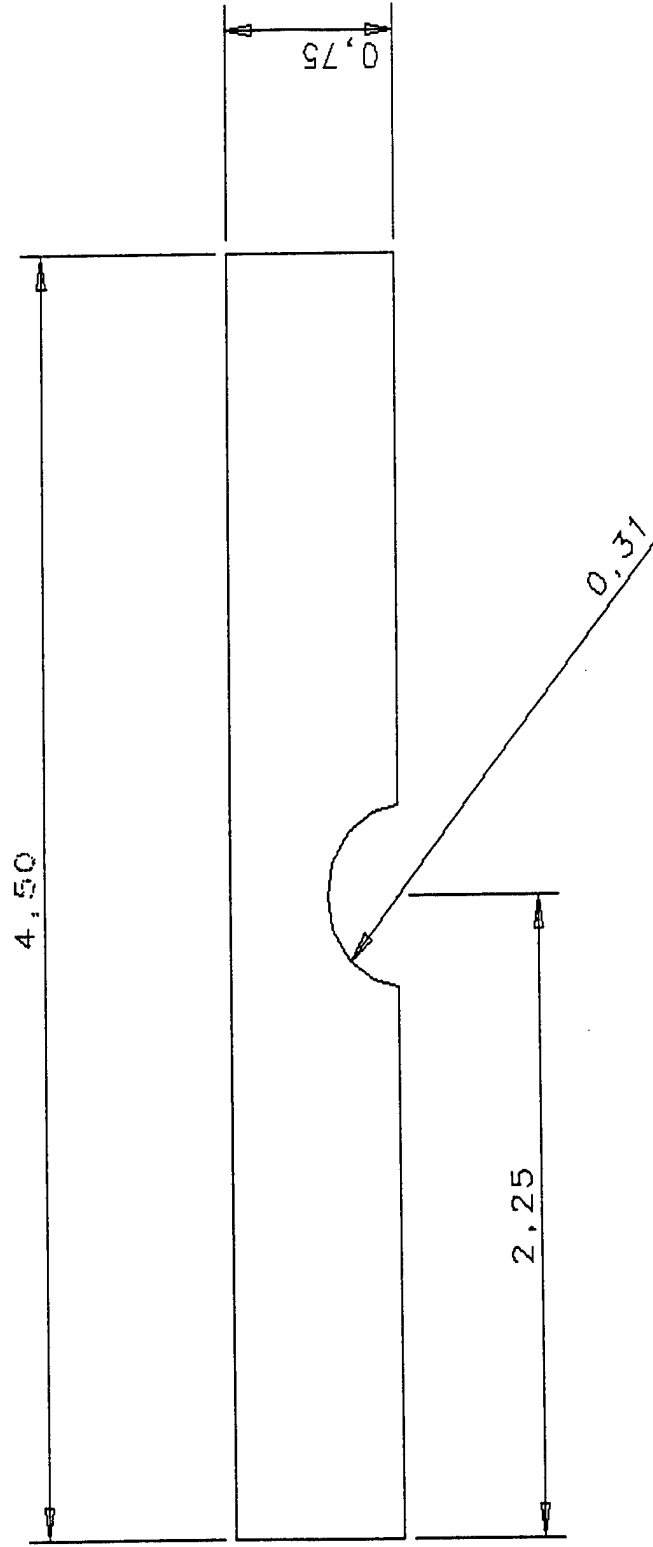
# Bulkhead 3

I-DEAS Master Series 5: Design



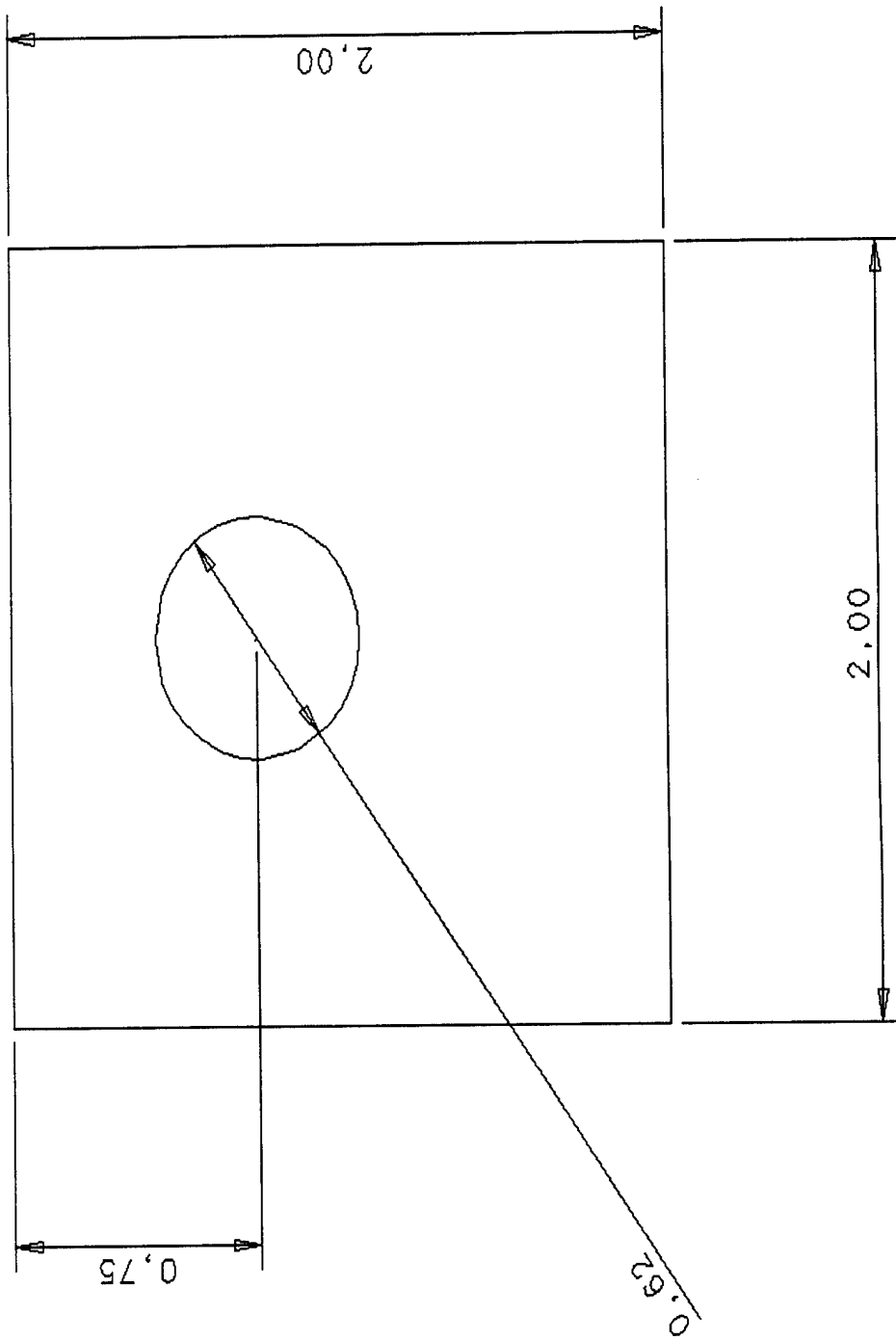
## Upper support Bulkhead

I-DEAS Master Series 5: Design



# Aft Bulkhead Design

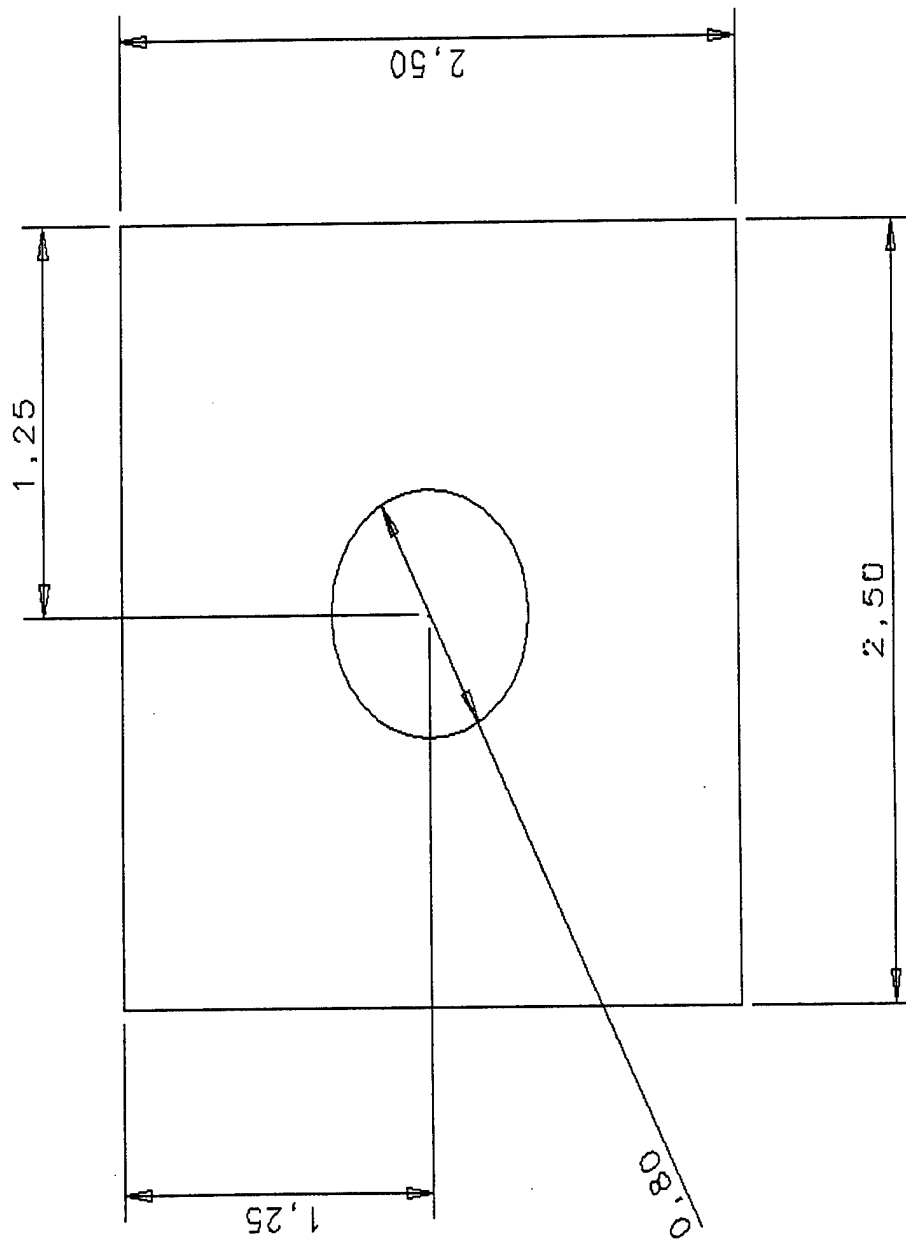
I-DEAS Master Series 5: Design





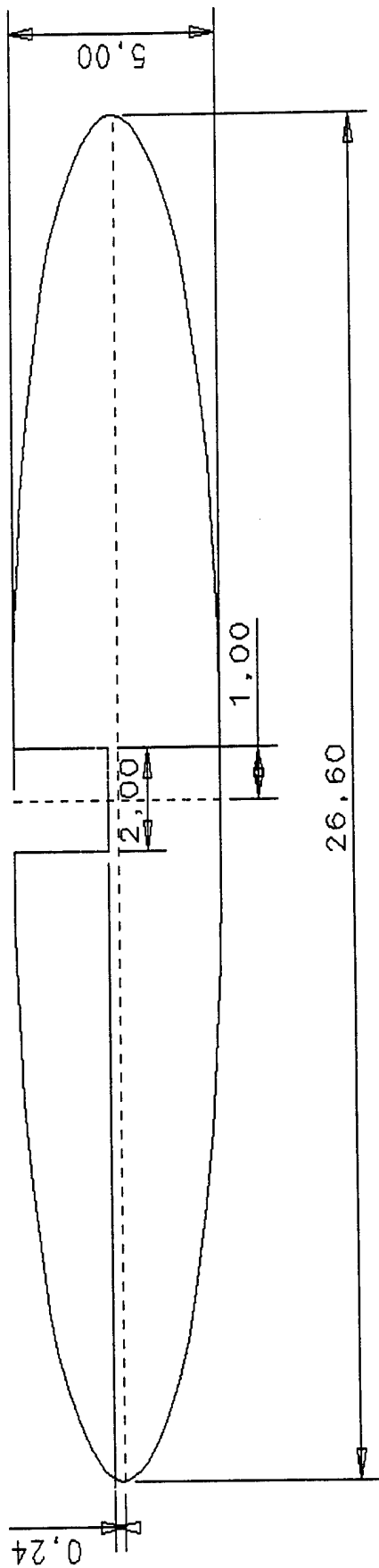
## Rear Bulkhead

I-DEAS Master Series 5: Design



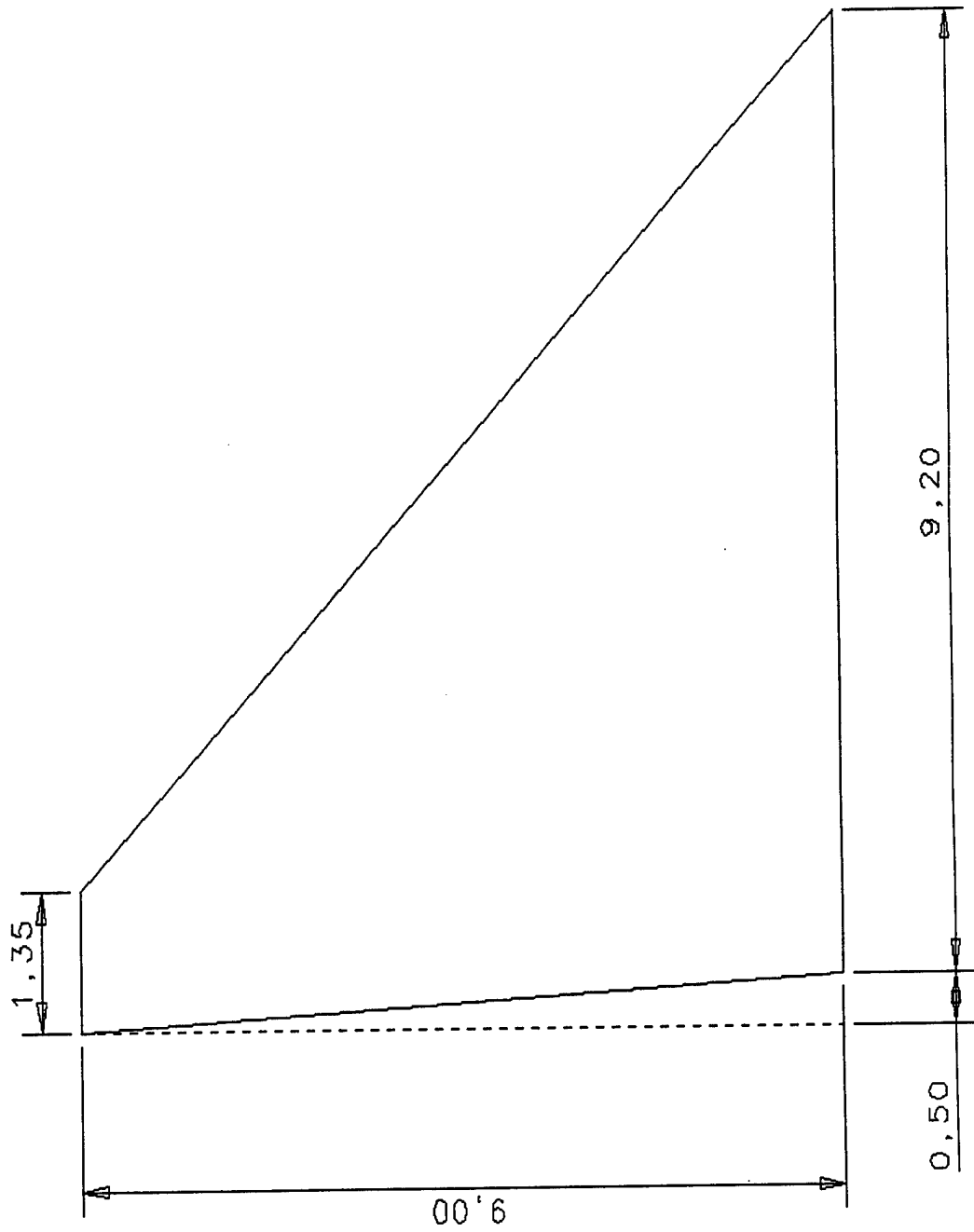
# Horizontal Stabilizer

I-DEAS Master Series 5: Design



# Vertical Stabilizer

I-DEAS Master Series 5: Design



### REFERENCES

1. AIAA Cessna/ONR Design/Build Fly 1998 Competition Rules
2. McCormick, B.W. "Aerodynamics, Aeronautics, and Flight Mechanics", John Wiley & Sons Inc., New York, 1979.
3. Nelson, Robert C "Flight Stability and Automatic Control", McGraw-Hill, Inc., New York, 1989.
4. Shevell, R.S., "Fundamentals of Flight", Prentice-Hall, Englewood Cliffs, NJ 1983.
5. Anderson, J.D., "Fundamentals of Aerodynamics", McGraw-Hill, Inc, New York, 1984.
6. Anderson, J.D. "Introduction to Flight", McGraw-Hill, Inc., 1985.
7. Hage, R.E., Perkins, C.D., "Stability and Control", John Wiley & Sons, Inc., New York, 1965.



# *PEGASUS*

*Design Report  
Addendum Phase*

## **Team Members:**

**Aruni Athuada  
Lashan Athuada  
Jason Bachelor  
Sebastian Echinique  
Shelly Ellis**

**Wayne Fulford  
Benjamin Goff  
Jennifer Huddle  
Cheree Kiernan  
Anabel Marcos**

**Arthur Morse  
James Richards  
Louis Turek  
Kiet Van  
Phil Wadsworth**

## Table of Contents

1.0 Final Design .....	1
2.0 Cost Evaluation.....	2
3.0 Future Considerations.....	4
References.....	5

## 1.0 Final Design

The lessons learned throughout the design and construction of the Pegasus aircraft were instrumental in the final design process. The driving force for selection of the final components and subsystems were determined by the *mission statement*:

*Design a remote controlled model plane powered by Nickel Cadmium batteries (2.5 lbs. max), take-off over a six foot obstacle at the end of the given runway, fly the maximum number of laps around a predetermined oval course in the allotted time of seven minutes and obtain a flat roll landing within a designated 300 ft. landing strip.*

The three areas that determine the final design of an aircraft capable of achieving the goals established in the mission statement were broken into three groups; Power, Stability and Control, and Structural Design.

### 1.1 Power

The power design of the aircraft was the most crucial part of the final design process. The power available and needed to sustain the seven minute flight was analyzed by evaluating three important areas; battery, motor, and propeller optimization.

The battery selection involved evaluating the Dominic Matrix outlined in the proposal section. This analysis led to the final selection of the Sanyo Cadnica (H series) Sub C 2000 mAh, batteries. These batteries held an obvious advantage due to their relatively low weight, which allowed for more cells to be used. The final configuration of the batteries involved splitting the battery pack into two groups. The first group with 11 cells and the second with 8 cells. Two diodes aided in the voltage regulation between the two packs.

The motor selection was determined in conjunction with the battery selection. The motor that was selected was the Aveox 1406/4Y brushless motor, with a 3.7:1 planetary gear box. The speed controller that was chosen is the M60 60 amp controller. This motor was able to deliver high power at efficiencies between 80-85%. The motor resistance is relatively low, so the motor is able to produce more torque. The output torque is increased due to the fact that the output torque is multiplied by the gear ratio. The major advantage to this brushless motor is the increased climb rate, however the major disadvantage is that it is more costly. This is a perfect example of a trade-off that was made in the design process.

### 1.2 Stability and Control

The stability and control of the aircraft is determined by the physical parameters and performance calculations that are a direct result of the geometry of the aircraft. The preliminary design is essentially the same as the proposal report, with the exception of the wing size.

It was determined that the wing loading that the aircraft would experience needed to be reduced to ensure the integrity of the aircraft. The wing loading is the ratio of the weight of the plane to the planform area. The desired wing loading was  $W/A=0.20$ , to accomplish this goal the planform area was increased to 1125 in<sup>2</sup>. The wing span was increased to be

128 in, with a root chord of 10in and a tip chord of 7.6 in. This increased the Aspect Ratio to 14.55.

### 1.3 Structural Design & Construction

In addition to the area added to the wing configuration, a construction difference was added to ensure structural integrity to the wing. The wing would have a carbon fiber reinforced spar running the length of the wing. The foam previously being considered was the high density blue foam. White foam is being used to reduce the overall weight of the wing. This is another trade-offs that was established in the final design process. The skin of the wing is going to be carbon fiber that has been vacuum-bagged to ensure a smooth aerodynamic surface. This will also help add strength to the wings. One solid wing will be used instead of two wings, and is connected by a reinforced joiner. The two halves will be glued together and re-enforced by carbon fiber.

The empennage is aligned around a carbon fiber rod and is the main load-bearing structure. This section is supporting the empennage, horizontal and vertical stabilizers. The horizontal stabilizer is an elliptical flying stabilizer using the NACA 0009 airfoil section. This is structurally the same design introduced in the proposal phase of the report. The vertical stabilizer is also the same traditional design. The large area of the rudder was designed to assist the stability of the aircraft.

The Design matrix in the proposal stage outlined the skill levels of construction, complexity of design, and required construction time. This led to a direct decision to stay with a more classic, box style fuselage. The primary reason for the classic design was the simplicity of construction. The ease of construction and straight forward applications could enable even the more inexperienced team members in the construction of the frame.

The landing gear is comprised of an aluminum alloy piece. The Pegasus aircraft will use a tricycle landing gear configuration. The main gear will be placed directly under the center of gravity, where the main load of the aircraft will be carried. The forward landing gear keeps the propeller from striking the ground when the plane lands. This design was chosen over a tail-dragging system, mainly because of the box shaped fuselage.

## 2.0 Cost and Time Evaluation

The local student chapter of AIAA sponsored two major plane projects this year. This required a budget for the Cessna/ONR competition. Student Government (SG) funded the two projects so a preliminary budget was prepared in order to adhere to SG policies. In the conceptual and preliminary design stages cost for components and systems were a major consideration with design advantages. This directly affected the selection of the electric motor and battery sources. Since power is the main system in the electric powered vehicle, buffers were added to ensure the expenditures did not exceed the allotted budget. It was crucial to the electric plane team that we stay within the limitations of the initial budget. The costs of every order were monitored to the money allotted to the project.



### 1998 AIAA Cessna Electric Budget

<u>Flight Equipment</u>	<u>Fuselage</u>	<u>Wing</u>	<u>Radio/Nose Gear</u>	<u>General</u>	<u>Power Supply</u>
Motor \$200.00	Liteply \$15.00	Carbon \$30.00	Hardware \$20.00	Glue \$ 15.00	Propellers \$ 30.00
Receiver \$150.00	Tail \$20.00	Tubes \$80.00	Axles \$10.00	Ultra \$ 78.00	NiCad pk. \$300.00
Battery \$ 20.00	Balsa \$30.00	Liteply \$15.00	Rods \$15.00	Graphics \$100.00	Charger \$200.00
Servos \$300.00	Spinner \$15.00	Cutting \$50.00	Nose \$20.00	Payload \$ 10.00	Controller \$150.00
	Mount \$ 5.00	Kevlar \$10.00	Collars \$ 2.00	Sheet(Al.) \$ 2.00	
	Boom \$25.00	Ailerons \$10.00			
	Carbon \$25.00	Misc. \$50.00			
<b>Subtotal \$ 670.00</b>	<b>\$195.00</b>	<b>\$245.00</b>	<b>\$67.00</b>	<b>\$223.00</b>	<b>\$780.00</b>
<b>Estimated Total Cost</b>					<b>\$2,180.00</b>
<b>Allotted Budget</b>					<b>\$2,737.33</b>

The overall allotted budget of \$2737.33 was the underlying goal of the cost analysis of the Pegasus project. This budget was made prior to any conceptual or preliminary design stages of the aircraft. The actual budget, shown below, was taken directly from purchasing vouchers and arranged so that a comparison could be made between the initial budget and the actual budget. For next year this will be an effective tool in the initial planning stages.

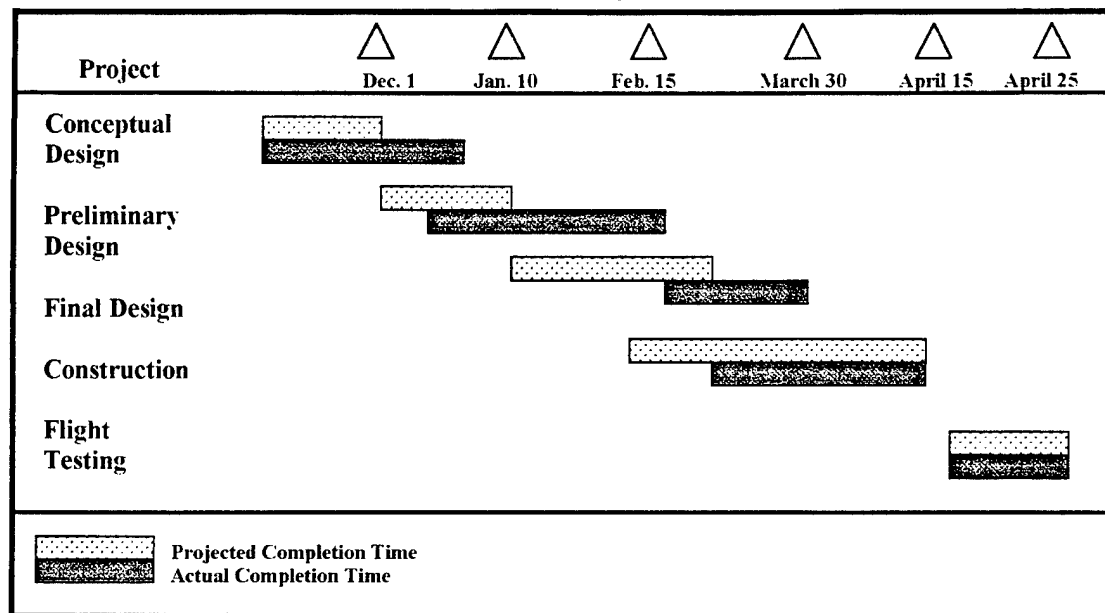
### Actual Expenditures for Electric Plane

Motor \$285.00	Woods \$150.00	Carbon \$285.00	Hardware \$ 50.00	Glues \$60.00	propellers \$ 30.00
Receiver \$120.00	Misc. \$ 85.00		Landing \$ 15.00	Kotes \$70.00	NiCad pk \$380.00
Battery \$ 42.00	Spinner \$ 10.00		Odd Ends \$150.00	Payload free	charger \$220.00
Servos \$390.00					Controller \$250.00
<b>Subtotal \$ 837.00</b>	<b>\$245.00</b>	<b>\$285.00</b>	<b>\$215.00</b>	<b>\$130.00</b>	<b>\$880.00</b>
<b>Allotted Budget</b>					<b>\$2,737.33</b>
<b>Actual Cost</b>					<b>\$2,592.00</b>

The actual budget reflects the expenditures that were incurred by the team from the conceptual and preliminary design stages to the construction process of the aircraft. Although the actual expenses exceed the estimated cost, the project costs are within the allotted budget. This will help the future electric design teams in the planning, design, and building stages.

The schedule for the Pegasus team started with Conceptual Design and proceeded through Preliminary Design, Final Design, Construction and Flight Testing. The Conceptual Design involved analysis of constraints, mission goals, research and development on competitors and various construction methods. The Preliminary design was involved more detailed study of airfoils, power plants, batteries, and some performance and stability calculations. The Final Design stage combined the previous design phases to the final system components. Flight Testing is the ultimate proof that the numbers and design are sound. The projected and completed time events are shown in the figure below.

### 1997/1998 Electric Project Timetable



### 3.0 Future Considerations

This is the second year of this competition. This will be UCF's inaugural year at the Cessna/ONR Design/Build/Fly Competition. The lessons that were learned are invaluable for all the members of the team. There are no graduating seniors on the Pegasus team this year. This will enable the group to move forward into next years competition with a more experienced team. In the future the cost and time management skills will undoubtedly improve upon this years goals and accomplishments.

The most challenging and limiting factor in this contest was the power supplied by the batteries. Battery technology has many more complex factors when compared to the alternative option, the internal combustion engine. Research in this area will be the important with respect to this competition. This research must include different battery configurations and enable utilization of hardware such as transformers, capacitors and inductors to optimize the selection. The choice of the ideal motor is directly related to the energy supply.

In the next year a more experienced team with improved construction and design techniques will look towards the second generation Pegasus. This will undoubtedly include a lighter more aerodynamic fuselage, which will in turn improve the performance characteristics of the aircraft. The basic applications taught to all members of the team this year could lead to more challenging design and construction tasks such as a built up wings.

The future goals of the Pegasus team should include involvement from new freshman and sophomore members. This ensures that the learning cycle will continue with the next generation. This is vital to coordinate theory learned in the classroom with practical applications provided by these student design competitions.

### REFERENCES

1. AIAA Cessna/ONR Design/Build Fly 1998 Competition Rules
2. McCormick, B.W. "Aerodynamics, Aeronautics, and Flight Mechanics", John Wiley & Sons Inc., New York, 1979.
3. Nelson, Robert C "Flight Stability and Automatic Control", McGraw-Hill, Inc., New York, 1989.
4. Shevell, R.S., "Fundamentals of Flight", Prentice-Hall, Englewood Cliffs, NJ 1983.
5. Anderson, J.D., "Fundamentals of Aerodynamics", McGraw-Hill, Inc, New York, 1984.
6. Anderson, J.D. "Introduction to Flight", McGraw-Hill, Inc., 1985.
7. Hage, R.E., Perkins, C.D., "Stability and Control", John Wiley & Sons, Inc., New York, 1965.

**RPR-2**  
**Final Design Report**

AIAA Student Design/Build/Fly Competition  
Wichita, Kansas

Department of Aeronautical and Astronautical Engineering  
University of Illinois at Urbana-Champaign

April 26, 1998

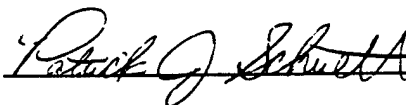
## Acknowledgements

The success of this team from the University of Illinois at Urbana-Champaign is due to the efforts of many wonderful people. We would like to take this opportunity to acknowledge the unparalleled support we have received from them. First of all, we would like to thank Jim Schmidt and Hobbico for their generous donations of building materials, tools and other components. Their willingness to work directly with us in the procurement of these items made the difference in meeting last minute construction deadlines. We also thank the Department of Aeronautical and Astronautical Engineering for providing the necessary space for a workshop as well as the use of a low-speed wind tunnel for propulsion testing. There were also several sources of monetary support used to purchase aircraft components and fund propulsion testing and travel. We thank the University of Illinois College of Engineering, the Illinois section of the AIAA, AIAA Region III and the Department of Aeronautical and Astronautical Engineering. We also thank Andy Broeren for his assistance with the take-off analysis. Finally, we thank Professor Kenneth Sivier for his outstanding guidance as faculty advisor. Professor Sivier set a high standard for success and took on the challenges necessary to ensure that this standard was achieved.

## RPR-2 Project Team



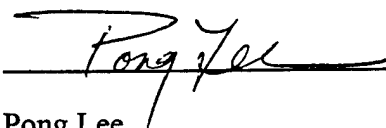
Ashok Gopalarathnam



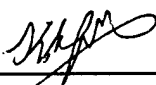
Patrick Schuett



Chris Lyon



Pong Lee



Chong Hin Koh



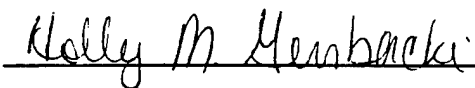
Sam Lee



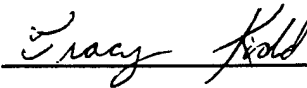
Darren Jackson



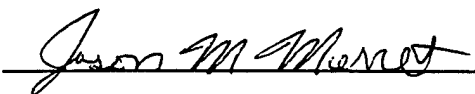
Shalin Mody



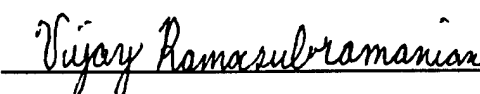
Holly Gurbacki



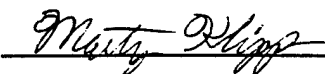
Tracy Kidd



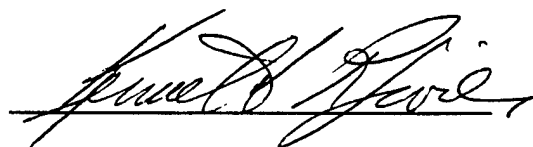
Jason Merret



Vijay Ramasubramanian



Marty Klipp



Dr. Kenneth R. Sivier

Faculty Advisor

## Table of Contents

1.0 Executive Summary .....	1
2.0 Management Summary.....	3
3.0 Conceptual Design .....	6
3.1 System Requirements and Design Drivers .....	6
3.2 Figures of Merit.....	6
3.3 Analysis Tools .....	7
3.4 Configurations Considered.....	7
3.5 Analysis Results .....	7
3.6 Conclusions .....	8
4.0 Preliminary Design.....	10
4.1 Design Parameter Investigation.....	10
4.2 Estimate of Aircraft Weight .....	10
4.3 Turn Analysis .....	10
4.4 Wing Optimization Analysis.....	11
4.5 Structural Analysis .....	12
4.6 Preliminary Stability Analyses.....	13
4.7 Preliminary Take-Off and Landing Analyses .....	14
4.8 Conclusion.....	14
5.0 Detail Design.....	21
5.1 Airfoil Selection .....	21
5.2 Wing Geometry .....	21
5.3 Propulsion System Selection.....	22
5.4 Fuselage, Internal Configuration, and Landing Gear .....	23
5.5 Stability and Control Analysis .....	24
5.6 G-Load Capability .....	25
5.8 Final Design and Performance Analysis .....	25
5.9 Conclusions .....	25

6.0 Manufacturing Plan .....	38
6.1 Component Requirements and Design Drivers .....	38
6.2 Manufacturing Processes Investigated .....	38
6.2.1 Wing .....	38
6.2.2 Fuselage .....	38
6.2.3 Winglets/Vertical Stabilizers .....	39
6.3 Figures of Merit .....	39
6.4 Methods of Analysis Used to Screen Manufacturing Processes .....	39
6.5 Results: Manufacturing Processes for Final Design .....	40
6.5.1 Wing .....	40
6.5.2 Fuselage .....	40
6.5.3 Winglets/Vertical Stabilizers .....	41
6.6 Construction Details .....	41
6.7 Cost Reduction Methods .....	41
References .....	45



## List of Tables

Table 3.1	Figures of Merit for Conceptual Design .....	9
Table 3.2	Final Ranking of Conceptual Designs.....	9
Table 5.1	Characteristics of S5010 and SD7003 Airfoils .....	26
Table 5.2	Wing Data for Final Design .....	26
Table 5.3	Propulsion System Data for Final Design .....	26
Table 5.4	Weight and Balance Data for Final Design.....	27
Table 5.5	Winglet Data for Final Design .....	27
Table 5.6	Comparison of Lateral and Longitudinal Stability Derivatives at Cruise Condition .....	28
Table 5.7	Various Stability and Control Results for Final Design.....	28
Table 5.8	Drag of Miscellaneous Components .....	28
Table 5.9	Miscellaneous Aircraft Components .....	29
Table 5.10	Distribution of Battery Energy Among Flight Mission Segments.....	29
Table 6.1	Figures of Merit Used in Manufacturing Plan Formulation.....	42
Table 6.2	Final Ranking of Figures of Merit for Wing .....	42
Table 6.3	Final Ranking of Figures of Merit for Fuselage.....	42
Table 6.4	Final Ranking of Figures of Merit for Winglets .....	43

## List of Figures

Figure 2.1 Project Milestone Chart .....	4
Figure 2.2 Subgroup Organization Diagram .....	5
Figure 3.1 Conceptual Sketch of Conventional Low-Wing and Flying Wing Designs .....	9
Figure 4.1 Effect of Turn Speed on Number of Laps Completed in 7 Minutes .....	15
Figure 4.2 CRUISE Program Flow Chart .....	16
Figure 4.3 MATLAB Wing Optimization Program Flow Chart.....	17
Figure 4.4 Aircraft Weight as a Function of Span and Area.....	18
Figure 4.5 Range Contours as a Function of Wing Span and Area.....	19
Figure 4.6 Range Contours as a Function of Wing Span and Area For 1996-1997 Rules.....	19
Figure 4.7 Bending Stiffness of Various Wing Test Specimens.....	20
Figure 4.8 Torsional Stiffness of Various Wing Test Specimens .....	20
Figure 5.1 Geometry and Performance Data of S5010 and SD7003 Airfoils .....	30
Figure 5.2 Geometry and Performance Data of S8025 Airfoil .....	31
Figure 5.3 Plot of Approximate Twist Distribution .....	31
Figure 5.4 Longitudinal Trim Plot at Cruise Using Elevon Deflection Only .....	32
Figure 5.5 Longitudinal Trim Plot at Cruise Using Flap Deflection Only.....	32
Figure 5.6 Rudder Trim Plot Demonstrating Ability to Trim in Sideslip .....	33
Figure 5.7 Elevon Trim Plot Demonstrating Ability to Keep Aircraft Level in Sideslip .....	33
Figure 5.8 V-n Diagram .....	34
Figure 5.9 Take-off Performance .....	34
Figure 5.10 Climb Performance .....	35
Figure 5.11 External Configuration 3-View.....	36
Figure 5.12 Internal Configuration 3-View.....	37
Figure 6.1 Placement of Fiber Spar Along Wingspan and Cross-Sectional View .....	43
Figure 6.2 Project Timeline for Construction of RPR-2 .....	44

## 1.0 Executive Summary

This report documents the design and construction of an unmanned aerial vehicle for entry in the second annual AIAA Student Design/Build/Fly Competition. Both the aircraft design and construction were performed over eight months by students from the University of Illinois at Urbana-Champaign. The final design, *RPR-2*, is the product of previous design experiences, detailed engineering analyses, and much enthusiasm.

Prior to the beginning of design development, a mission evaluation was performed to identify the critical maneuvers required by the aircraft. Owing to the seven-minute constraint placed on mission flight time, both a high cruise velocity and a high turning performance were seen to play pivotal roles in the successful completion of the mission. The tradeoffs, however, between efficient high-speed cruise and rapid turns were unclear. Therefore, several aircraft configurations were quickly designed and analyzed using computer simulations. The results showed cruise performance to be surprisingly insensitive to wing planform and mission performance to be very dependent on both turning radius and turning speed. Consequently, the decision was made to design an aircraft that would exhibit high turning performance.

Next in the design process was the identification of configurations with the potential to successfully completing the mission while maintaining acceptable turn performance. Three configurations were selected for further study: a conventional aircraft, a flying plank, and a swept and twisted flying wing. Drawing upon existing technology, the conventional aircraft was viewed as a clipped-wing derivative of UIUC's entry in the '96-'97 competition. By clipping the wings, it was hoped that both higher speeds during cruise as well as better turning performance would result. A further modification was performed to reduce the frontal area of the aircraft. The next configuration considered, the flying plank, immediately became attractive because of its low parasite drag, light weight, and its rugged construction (no empennage to damage). Despite these advantages, problems with center-of-gravity (CG) placement as well as obtaining adequate directional stability made this configuration a less viable solution. When considering the third configuration, the swept and twisted flying wing, a majority of the advantages afforded to the flying plank could be retained without the overwhelming CG or directional stability problems. It therefore became clear that the two leading contenders were the conventional aircraft and the swept-twisted flying wing.

The design process continued by modeling comparable planforms (i.e. the same aspect ratio) for these two configurations in a vortex lattice code (LinAir<sup>1</sup> or DIRECT<sup>2</sup>). The computational data were then used in combination with experimental airfoil data, an analytical propulsion model, and simple estimates for fuselage drag to determine mission performance over a wide range of velocities. Upon completion of the performance predictions, it became clear that neither design had an obvious advantage in flight performance. It was then decided to select the configuration based on more qualitative reasoning.

A list of advantages and disadvantages was compiled for each configuration. Based on this list, as well as the desire to be challenged, to construct a truly unique aircraft, and to learn from the experience, the swept-twisted flying wing was selected as the configuration for further development. With the configuration determined, time was spent identifying more specific design issues. Among these issues were the suitable placement of landing gear, location of the propulsion system (i.e. tractor or pusher), a wing planform allowing for a practical CG location, and the specific construction techniques that would be used to build the aircraft.

The landing gear configuration was largely determined by the desire for low frontal area. As a result, an inline configuration was selected which allowed for placement of the payload between the two wheels. Small wheels at the wing tips provide lateral balance during ground operations. Drawing from the team's experience at the '96-'97 competition, the need to protect the motor shaft from bending loads during rough landings was identified. Because the simplest method of protecting the motor shaft is to place the motor at the rear of the fuselage, a pusher configuration was chosen. Additionally, a pusher configuration would help make CG placement more manageable. Placement of the CG, along with directional stability considerations, also helped to determine acceptable wing sweeps. Finally, because flying wings are typically required to be extremely stiff in torsion, it was decided to construct the wing with foam, fiberglass and carbon fiber spars.

Thus, the final design of *RPR-2* was determined only after careful consideration of several design alternatives, extensive performance predictions, and the identification and solution of several design problems. Because of this thorough design methodology, the University of Illinois at Urbana-Champaign is proud to submit this design to the sponsors of the AIAA Design/Build/Fly Competition.

## 2.0 Management Summary

Following a very successful inaugural year, the project team had good momentum that carried through the summer of 1997 and into the fall of that same year. Upon team reorganization, which included the addition of several new members, a project milestone chart was created to keep the team focused and the new project on schedule. This chart is shown in Fig. 2.1 along with the actual time required to complete each milestone. Delays were typically two to four weeks, with the largest delay being one and a half months. The provision for delays within the schedule, however, made these deadlines fairly flexible, thereby making these lags acceptable.

To integrate and streamline operations, the team architecture was flexible and informal. The project coordinator assumed most of the administrative duties, including financial recording and meeting coordination. In an effort to eliminate unnecessary bureaucracy, a "just-in-time" purchasing system was utilized that allowed individuals to purchase materials on the spot and then receive reimbursement at a later date.

In an effort to quicken the aircraft design and construction process, most tasks were accomplished within small groups that were structured to allow individuals free reign over the issues being considered. Thus, their decisions were allowed to stand with only minimal oversight by the project team as a whole. Further enhancing the team's ability to stay on schedule was the involvement of most team members in both the design and fabrication efforts of the aircraft. As a result, difficulties in transferring technologies between the drawing board and the workbench were minimized. Manufacturing problems were further minimized as a result of advice provided by experienced team members. This allowed concepts to be evaluated with a knowledge of limitations in both the available materials and the building skills of the team.

A summary of team member responsibilities is provided in Fig. 2.2. Note that several members contributed to efforts in many areas critical to the success of the project. By doing so, team communication and project operation were also enhanced.

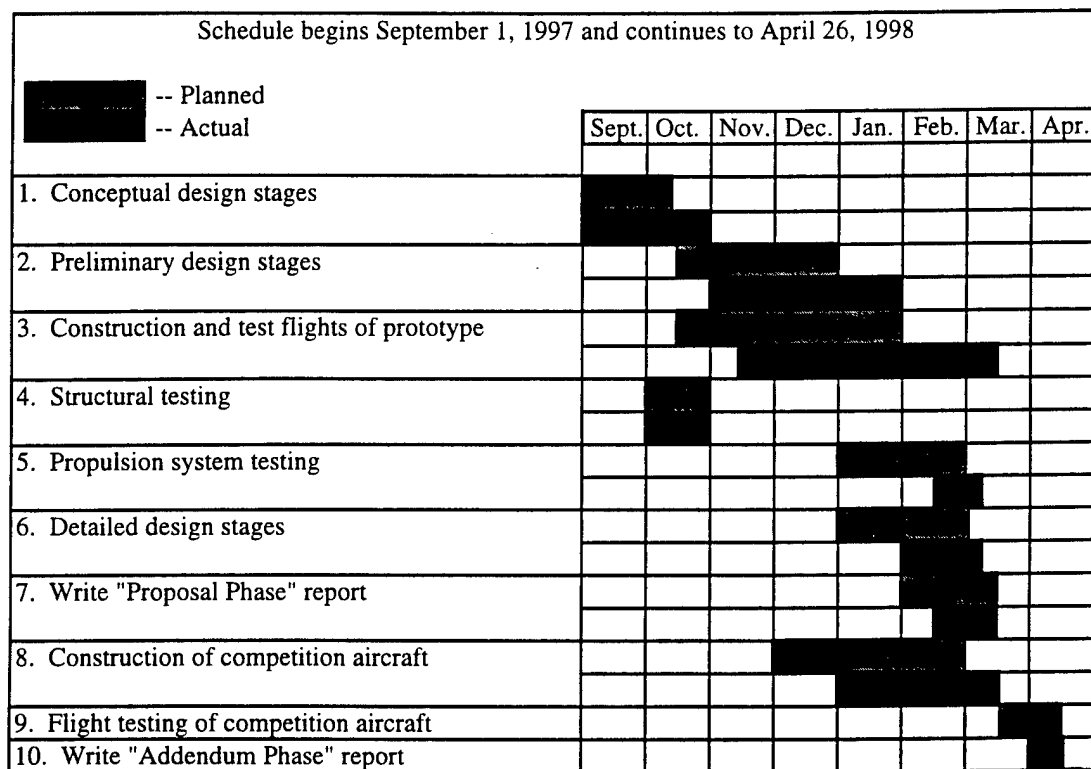


Figure 2.1 Project milestone chart showing the planned and actual timing of important activities.

**Project Coordinator**

- Chris Lyon

**Aerodynamics**

- Ashok Gopalarathnam
- Chris Lyon

**Performance, Flight Mechanics, and Stability and Control**

- Chris Lyon
- Darren Jackson
- Holly Gurbaki
- Tracy Kidd

**Propulsion System Research and Testing**

- Marty Klipp
- Sam Lee
- Vijay Ramasubramanian

**Fuselage Design**

- Ashok Gopalarathnam
- Chris Lyon
- Jason Merret
- Patrick Schuett
- Shalin Mody

**Wing Structural Design**

- Ashok Gopalarathnam
- Chong Hin Koh
- Chris Lyon

**Structural Testing**

- Ashok Gopalarathnam
- Chris Lyon
- Tracy Kidd

**Construction**

- Chong Hin Koh
- Chris Lyon
- Jason Merret
- Patrick Schuett
- Pong Lee

Figure 2.2 Subgroup organization diagram showing all team members and their area(s) of involvement.

### 3.0 Conceptual Design

#### 3.1 System Requirements and Design Drivers

The aircraft system requirements are stated in the 1997/1998 Contest Rules. Those identified as having the most significant influence on the design are:

- Achieve a maximum number of laps over the flight course while constrained to a maximum flight time of 7 minutes and a maximum battery weight of 2.5 lbf.
- Carry a 7.5-lbf payload, takeoff over a 6-ft obstacle within a 300-ft runway area, and successfully land within the same 300-ft runway area.
- The design must be balanced, offering high performance and good flight handling qualities, while implementing practical and affordable manufacturing processes.

From these principal system requirements, the following design drivers were identified:

- speed; i.e. maximum number of laps in a 7-minute time span
- fixed payload of 7.5 lbf and fixed battery weight of 2.5 lbf
- 300-ft take-off and landing field length
- good flying qualities for take-off, climb, cruise, turns, and landing
- good maintainability; quick payload removal
- practical and low cost manufacturing processes

The parameters of most importance to the success of the aircraft were determined to be both the time and energy constraints. A delicate balance between these two factors was deemed crucial to obtaining the maximum range from the aircraft within the allotted time. To elucidate this balance, a simple computer program was developed (CRUISE<sup>3</sup>) to study the effects of changing aircraft configurations and flight conditions. Because both takeoff and landing were considered to have secondary effects and would subsequently have little impact on the selection of the configuration, the computer program neglected these phases of the mission.

#### 3.2 Figures of Merit

With the preceding design drivers as guides, the following figures of merit (FOMs) were developed to aid in the comparison of various design concepts. Each FOM is described below and summarized in Table 3.1.

- Lap Rate: correlates to the potential number of laps flown by each configuration



- Robustness: represents the "good demonstrated flight handling qualities" requirement as well as the aircraft's performance at off-design flight conditions. Also represents the aircraft's ability to fly under varying weather or environmental conditions.
- Complexity: represents the level of difficulty in the design and construction of the vehicle. This includes the "margin for error" when constructing the aircraft.
- Innovation: represents the utilization of concepts unique to aircraft designed for mission requirements similar to the ones outlined in Section 3.1.

### 3.3 Analysis Tools

The primary tool used during the conceptual design process, as well as the tool used to assign values to the "Lap Rate" FOM, was an adaptation of the program CRUISE.<sup>3</sup> This program utilizes output from a vortex lattice code (LinAir<sup>1</sup> or DIRECT<sup>2</sup>) to predict the range and endurance of various configurations. This prediction is performed with the help of computational lift distributions, experimental airfoil data, simple drag predictions, and an analytical propulsion model derived from ElectriCalc.<sup>4</sup> Flight tests using last year's aircraft showed that the predicted cruise velocities from CRUISE were accurate to within 2 ft/s. More details on this program are given in Chapter 4.

### 3.4 Configurations Considered

During the conceptual design process, the configurations considered were (1) a conventional low-wing, (2) a flying plank, and (3) a swept-twisted flying wing. As a result of preliminary qualitative analyses, only the conventional low-wing and the swept-twisted flying wing were selected for further study. It was believed that by studying these two very different concepts, a final design would result which implemented elements of both concepts.

### 3.5 Analysis Results

Predictions from CRUISE were used to determine the impact of horizontal and vertical tail drag, fuselage drag, and cruise speed on mission performance for each configuration. While the effect of tail drag was minimal over a large range of cruise velocities, fuselage drag had a significant impact on the total drag of each aircraft, particularly at higher cruise velocities. CRUISE also predicted that maximum range would occur only for a cruise velocity that completely exhausted the propulsion system energy at the end of the 7-minute time constraint.

This velocity was typically between 75 and 85 ft/s for both the conventional and flying-wing configurations. It was therefore determined that smaller fuselages, and their subsequent lower drags, were highly desirable, and every effort would be made to reduce fuselage size.

Based on these insights gained from CRUISE, two more detailed aircraft were designed for both the conventional and flying wing configurations, with an emphasis placed on obtaining small fuselages and high cruise velocities. Conceptual sketches of these configurations are presented in Fig. 3.1. CRUISE was then used for a second time to help assign "Lap Rate" FOM values to each configuration. These values are presented in Table 3.2 along with values for the other FOMs discussed in Section 3.2.

For the conventional configuration, a maximum range of 15 laps per 7-minute time span (as predicted by CRUISE) received a value of 3 for the "Lap Rate" FOM, while the flying wing received a "Lap Rate" FOM value of 4 owing to its capability to fly 17 laps within the 7-minute time span. Values for the "Robustness" FOM were largely based on qualitative input from experienced team members. The team believed that the conventional configuration could be made robust with only moderate effort by drawing upon the large amount of technical data for such configurations. Therefore, it received a "Robustness" FOM value of 4. In contrast, uncertainty surrounded the potential robustness of the flying wing owing to the lack of easily obtainable data for such aircraft. Consequently, a "Robustness" FOM value of 2 was assigned. The "Complexity" FOM value for each configuration was roughly proportional to the perceived amount of specialized engineering needed (new technologies to the students) to complete the design. As the FOMs suggest, the team believed twice as much specialized engineering would be required for the flying wing. Finally, the innovative aspects of the flying wing were identified as more significant when compared to the typical conventional aircraft.

### 3.6 Conclusions

Based upon the FOM results presented in Table 3.2 and discussed in Section 3.5, the flying wing configuration was selected for the preliminary design. With the experience among the design engineers and manufacturing crew, the increased complexity of the flying wing was not foreseen as a hindrance to the completion of the aircraft. Additionally, the innovative aspects of such a design would add excitement to the work and provide a heightened sense of accomplishment when the project was completed.

Table 3.1 Figures of Merit for Conceptual Designs

Figure of Merit	Ranking		
	5	3	1
Lap Rate	fast	moderate	slow
Robustness	high	average	low
Complexity	simple	average	complex
Innovation	innovative	average	traditional

Table 3.2 Final Ranking of Conceptual Designs

Figure of Merit	Ranking	
	Conventional	Flying Wing
Lap Rate	3	4
Robustness	4	2
Complexity	4	2
Innovation	1	5
Total	12	13

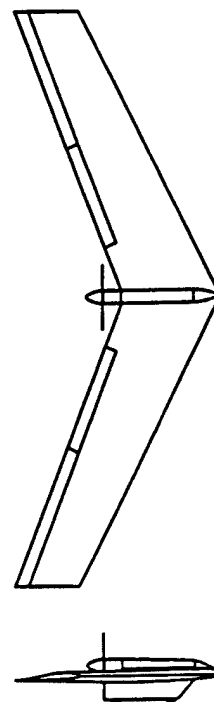
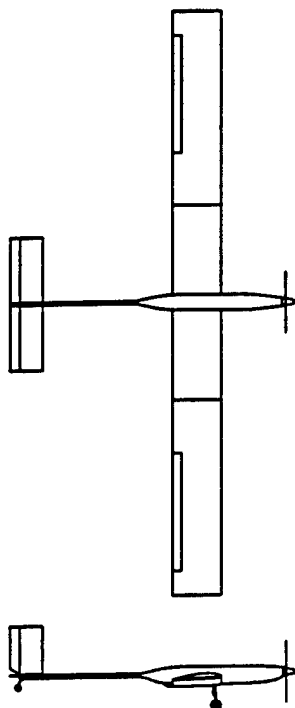


Figure 3.1 Conceptual drawings of the conventional and flying wing configurations.

## **4.0 Preliminary Design**

### **4.1 Design Parameter Investigation**

The information obtained during the conceptual design phase revealed the need to perform several more detailed studies in order to produce an optimized aircraft. These studies are listed below:

- Estimate the gross weight of the aircraft.
- Determine the effect of turn performance on range.
- Determine an optimum wing planform.
- Conduct wing structural testing to get reliable strength versus weight data.

In addition, two areas seen as unnecessary during the conceptual design phase, aircraft stability and take-off/landing performance, were also studied during the preliminary design phase of the aircraft.

### **4.2 Estimate of Aircraft Weight**

Based on the gross weight of last year's aircraft (18.5 lbf), aircraft weight was estimated to be no greater than 16 lbf. This 2.5-lbf weight reduction would be a result of three factors; (1) the aircraft would be smaller because of its higher cruise velocity and subsequent smaller wing area, (2) because a flying wing was selected, the weight would decrease owing to the removal of the empennage, and (3) a concerted effort would be made to use materials with higher strength to weight ratios.

### **4.3 Turn Analysis**

The need to maximize the number of laps within the seven-minute time constraint emphasizes the need to decrease the time and energy spent in turns. For an airplane turning at a specified bank angle (and therefore a specified g-load), the time spent in a 360 degree turn increases proportionally with flight speed. Figure 4.1 shows the effect of turn speed on the number of laps possible in 7 minutes given a fixed cruise velocity and bank angle. As turn speed is decreased from 80 ft/s (the cruise velocity) down to 30 ft/s, the number of possible laps increases by approximately 20%. While the discontinuities between a constant cruise velocity of 80 ft/s and constant turn speeds of less than 60 ft/s might be impractical, these results directly

show the importance of making tight turns. If a limitation were placed on the lowest allowable turn speed, tighter turns would then require higher bank angles and g-loads. As a result, this data indirectly emphasizes the need for strong wings capable of sustaining the highest g-loads possible.

#### 4.4 Wing Optimization Analysis

Optimization of the wing planform was performed to determine a wing area and span that would maximize the range of the aircraft over a 7-minute period during straight and level flight. By selecting wing span and wing area as the optimization parameters, insight into the effects of wing profile drag (area dependence) and wing induced drag (span dependence) would be provided.

The optimization routine used CRUISE in conjunction with a specialized MATLAB code that approximated the vortex lattice results required by CRUISE. A flowchart describing the methodology used by CRUISE to obtain aircraft performance is shown in Fig. 4.2. Figure 4.3 outlines the steps used by the MATLAB code. As suggested by step 2 of Fig. 4.3, the MATLAB code was also used to determine a more accurate weight prediction than that mentioned in Section 4.2. More precisely, the MATLAB code accounted for weight variations resulting from changes in wing planform by using the methods outlined in Fig. 4.4.

Results for the optimization study are presented in Fig. 4.5. The contours show maximum ranges possible within the 7-minute time constraint. As indicated by the fairly sparse nature of the plot, maximum range values are surprisingly independent of wing planform. Comparison of this data to similar results generated for last year's contest as shown in Fig. 4.6 (no constraint on flight time) makes this conclusion even more apparent. This insensitivity was a result of trade-offs between wing profile drag and wing induced drag as the wing planform varied. To be more specific, as the wing area increased for a given wing chord, the increased profile drag produced by the larger wing was offset through reductions in induced drag owing to an increase in aspect ratio. Due to the high Reynolds numbers experienced at cruise (near 500,000), drag changes due to chord variations were minimal.

The results shown in Fig. 4.5 suggest two conclusions. First, when the importance of turn performance as presented in Section 4.3 is considered, a wing planform more suitable for tight

turns (low aspect ratio) could be selected will little impact on the cruise performance of the aircraft. Second, the performance difference between the various aircraft at the competition is likely to be small since even the most haphazard selection of wing planform could result in a fairly high performance aircraft. Knowing this, the design team felt it important to stay inside the 6-mile curve in Fig. 4.5 where cruise ranges were the highest. This dictated a wing area of no greater than  $10 \text{ ft}^2$ . The desire for high turn performance further suggested the selection of a wing planform with a low aspect ratio (less than 10). This suggested spans of less than 10 ft given a minimum 1-ft wing chord. The 1-ft wing chord was selected as a minimum in order to avoid potential low Reynolds number effects encountered while taking off or landing. These constraints were met with the 9-ft span,  $9.5\text{-ft}^2$  area planform selected for further development.

#### 4.5 Structural Analysis

While the need for an elaborate wing construction technique was lessened after the selection of a fairly low aspect ratio wing, the desire to minimize aircraft weight still necessitated an investigation into the structural merits of various construction techniques. In particular, experimental values for both bending and torsional stiffness as well as ultimate strength were desired for various wing construction methods.

Five construction methods were investigated by fabricating and testing five wings: built-up, built-up with a thin mylar covering, built-up with balsa sheeting, foam core, and foam core with balsa sheeting. All test specimens had an 8" chord, 48" span, and top and bottom  $1/4$ " square spruce spars. The built-up wings additionally used  $1/16$ "-thick vertical-grain shear webs. The test specimens were cantilevered from a rigid structure while bending and torsional loads were applied at the wing tip. As the applied loads increased, measurements were recorded for both bending and torsional deflections until the specimen failed. Figures 4.7 and 4.8 show the bending and torsional stiffness of each specimen, with failure occurring at the maximum load plotted for each curve in Fig. 4.7. Unfortunately, the bracket used to mount the balsa-sheeted foam wing failed prematurely and no data could be collected for this construction method.

As expected, the sheeted test specimen demonstrated superior stiffness in both bending and torsion. An unexpected result, however, was the similar failure loads for the foam wing and the built-up wing with sheeting. Further analysis of the failed balsa-sheeted built-up specimen

indicated a premature failure as a result of sheeting buckling. Apparently, the sheeting was not sufficiently bonded to the wing ribs in order to prevent the upper surface from buckling. This type of failure was difficult to predict. Therefore, the built-up construction method that used sheeting was eliminated from further consideration.

Since flying wing configurations typically require extremely stiff wings in torsion in order to avoid flutter and other unwanted aeroelastic effects, all un-sheeted construction methods were also eliminated from further consideration. This leaves the untested balsa-sheeted foam-core wing as the final option from the original test matrix. Experience with this construction technique from last year's aircraft, however, suggested a difficulty in achieving thin trailing edges. Because the new aircraft would be operating at a higher cruise velocity than last year's aircraft, the drag penalty associated with a thick trailing edge was deemed unacceptable. The decision was then made to construct the wing using a fiberglass covered foam core. While this technique would require more skill from the manufacturing crew, the performance advantage was seen as being worth the extra effort.

#### 4.6 Preliminary Stability Analyses

For the preliminary design phase, the main goals of the stability analyses were to assure adequate longitudinal static stability and a positive lift coefficient at trim. Paramount in determining these parameters are the pitch-stiffness of the aircraft,  $C_{m\alpha}$ , and its zero-lift pitching moment,  $C_{m0}$ . While obtaining an appropriate value for pitch stiffness is largely a function of the center of gravity (CG) location in relation to the neutral point of the aircraft,  $C_{m0}$  is determined by several factors, among them being wing twist, wing sweep, and airfoil pitching moment.

Knowing this, the tasks at hand were two-fold. First, a reliable method of predicting the aircraft's neutral point would be required in order to accurately place the aircraft CG, thereby ensuring an acceptable pitch stiffness. This was accomplished by using both a vortex lattice code (either LinAir or DIRECT) as well as the simple techniques outlined in Raymer.<sup>11</sup> Second, a method was needed which could quickly estimate the effects of various wing twists, wing sweeps, and airfoil pitching moments on the aircraft's zero-lift pitching moment. The identification of the need for a code with such a capability was realized early in the design process and DIRECT was written in advance in order to fill such a niche.

While no concrete values for either pitch stiffness or zero-lift pitching moment were finalized at this time, several candidate flying-wing designs were analyzed using DIRECT in an effort to ensure that stable flying wings were possible given the wing span and area as outlined in Section 4.4. Several stable designs were achieved (10% static margin and a cruise lift coefficient of 0.2) for a wide range of wing sweeps (15-35 degrees).

#### **4.7 Preliminary Take-Off and Landing Analyses**

During the preliminary design phase, no complicated methods were used to predict the aircraft's take-off and landing performance. For take-off, it was assumed that 25% more power than that used for cruise would be required to take-off within the 300-ft runway length. Again, using predictions from CRUISE, it was found that a throttle setting of roughly 75% would be required to obtain the desired cruise velocity. This was seen as suitable evidence that the aircraft would take-off successfully.

Landing performance is heavily influenced by the aircraft's stall speed. As a result, an upper bound of 40 ft/s was placed on the stall velocity of the aircraft. Using the weight approximated in Section 4.2, the wing area selected in Section 4.4, and an approximate maximum lift coefficient of 1.0 (typical for flying wings), an approximate stall speed of 38 ft/s was achieved. Glide slope control during landing will be provided by flaps operated in conjunction with elevons in a "crow" type configuration.

#### **4.8 Conclusions**

As a result of these preliminary studies, several key design parameters were determined. The aircraft weight was expected to be near 16 lbf, the wing span was fixed at 9 ft, and the wing area was approximated to be 9.5 ft<sup>2</sup>. Also, after the structural testing of several wing test specimens, it was determined to construct the wing from foam and fiberglass. By doing so, thin trailing edges would easily be achievable thereby eliminating a source of unnecessary drag. Aircraft stability was addressed through the development of the code DIRECT, which will aid in the rapid analysis of the final aircraft's longitudinal static stability. Finally, the ability of the aircraft to take-off and land successfully was checked using simple assumptions. Among these checks was a stall speed of 38 ft/s.



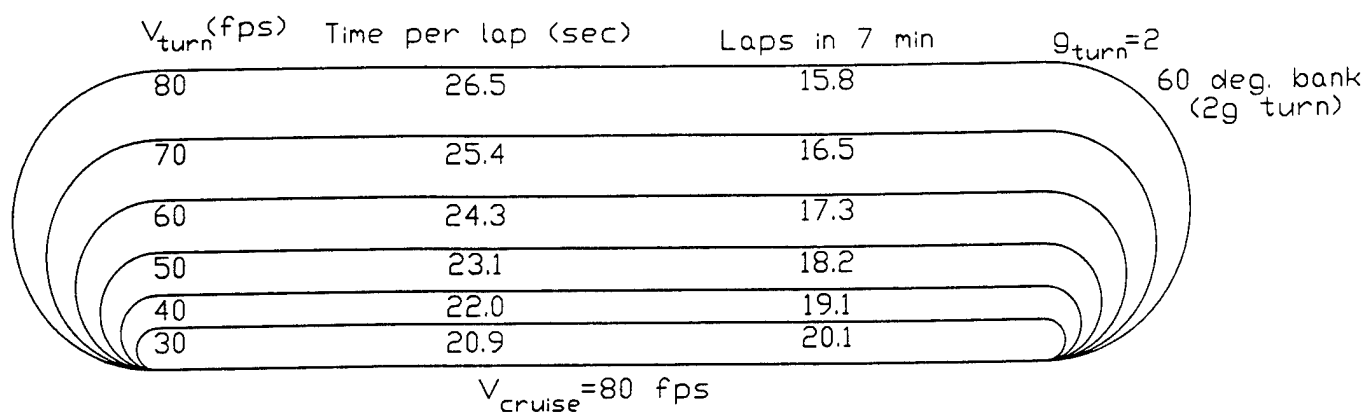


Figure 4.1 Effect of turn speed on the number of laps completed in 7 minutes.

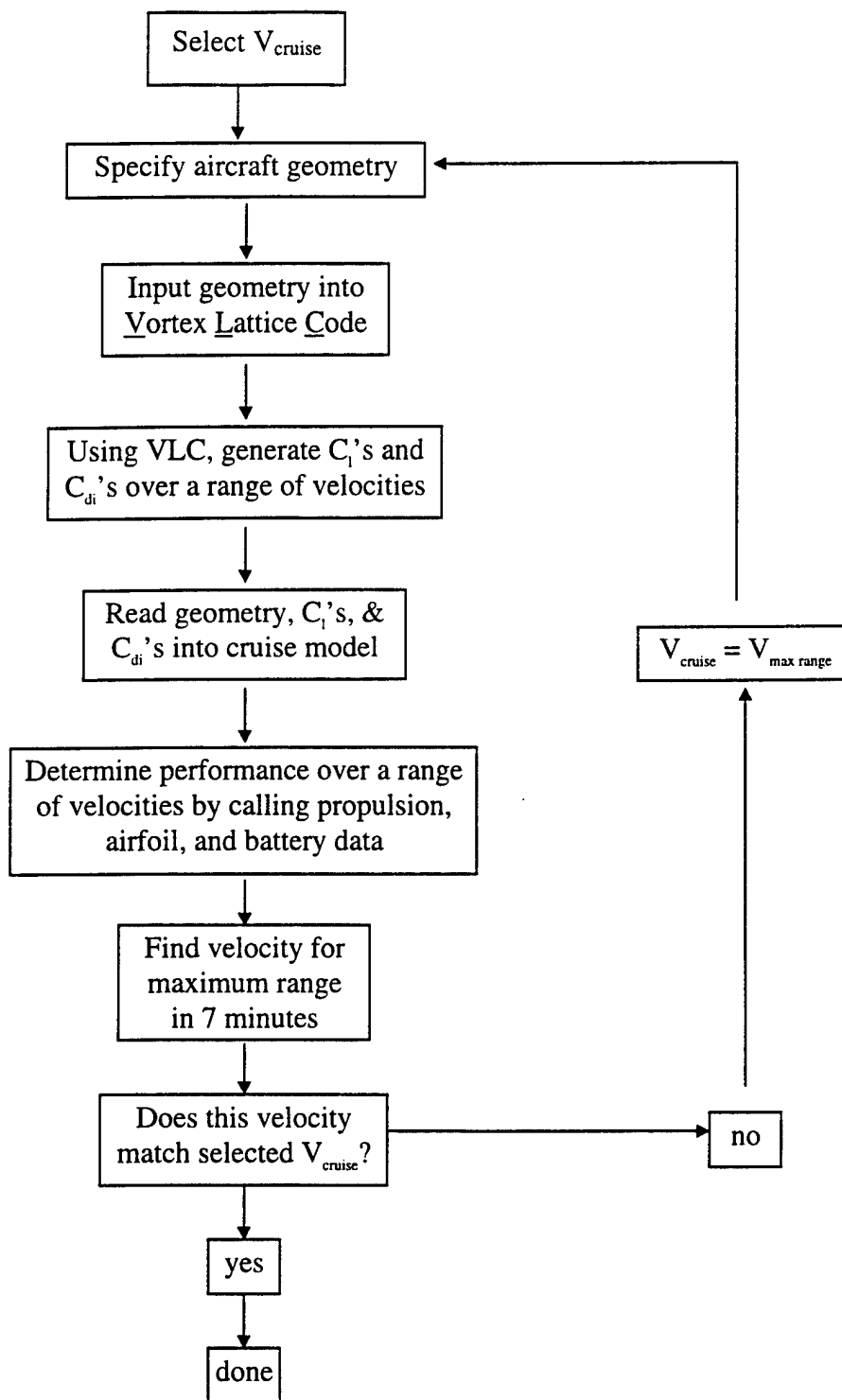


Figure 4.2 CRUISE program flow chart.

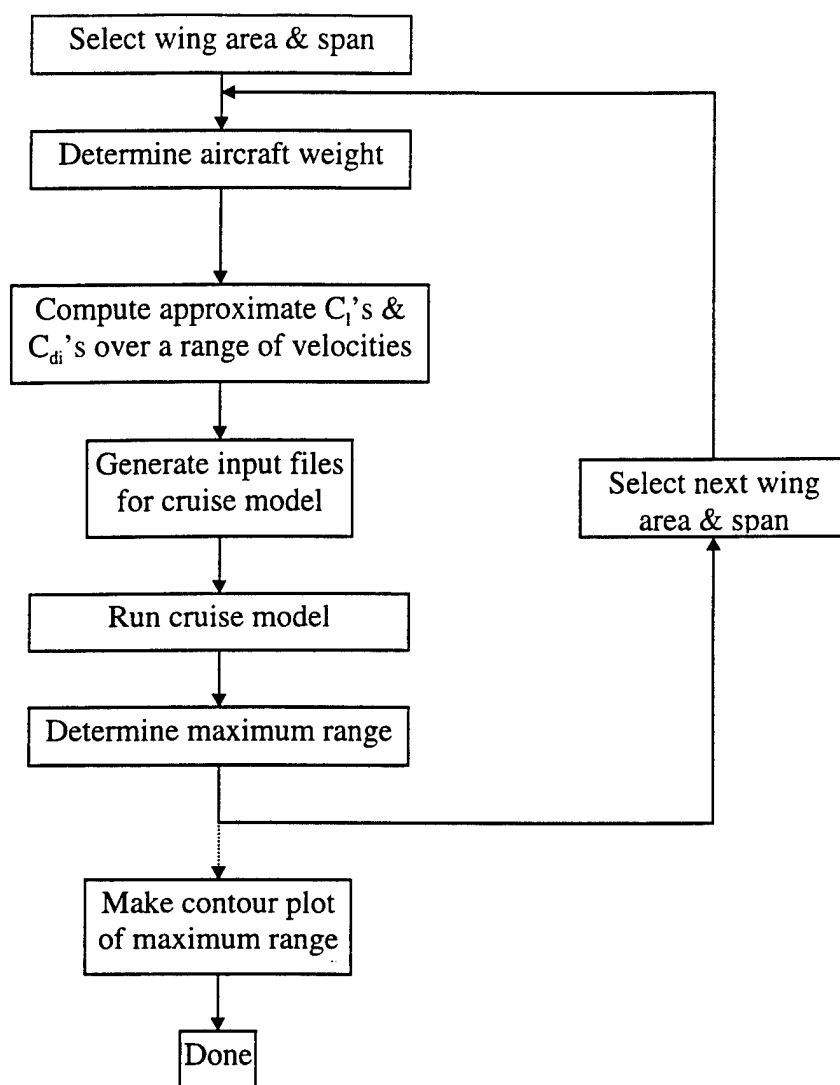


Figure 4.3 MATLAB wing optimization program flow chart.

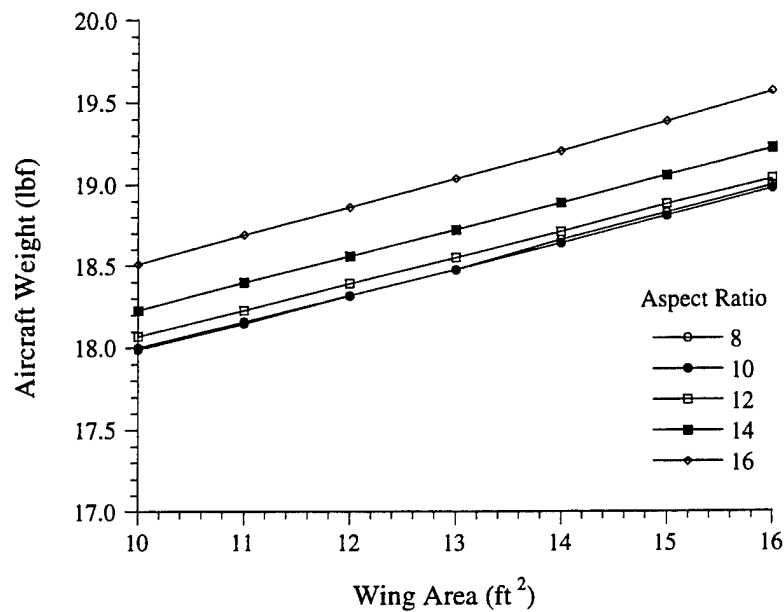


Figure 4.4 Aircraft weight as a function of aspect ratio and wing area.

### Modeling Equations

$S$  = Area (sq ft)

$b$  = Span (ft)

$AR$  = Aspect Ratio =  $b^2/S$

$W$  = Weight (lbf)

$$W_{\text{total}} = W_{\text{fixed}} + W_{\text{sheet}} + W_{\text{ribs}} + W_{\text{spar}}$$

$$W_{\text{fixed}} = \text{aircraft gross weight} - \text{wing weight}$$

$$W_{\text{sheet}} = 0.0793 \times S$$

$$W_{\text{ribs}} = 0.0420 \times S^2/b$$

$$W_{\text{spar}} = [0.0221 + 0.2085 \times 10^{-2} \times AR - 0.4796 \times 10^{-3} \times AR^2 + 0.3360 \times 10^{-4} \times AR^3] \times b$$

(Taken from Ref. 6)

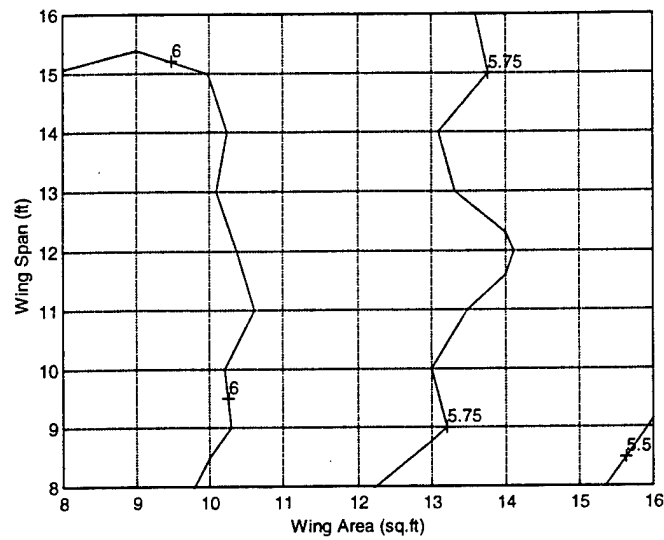


Figure 4.5 Flying wing range contours (in miles) as a function of wing span and area.

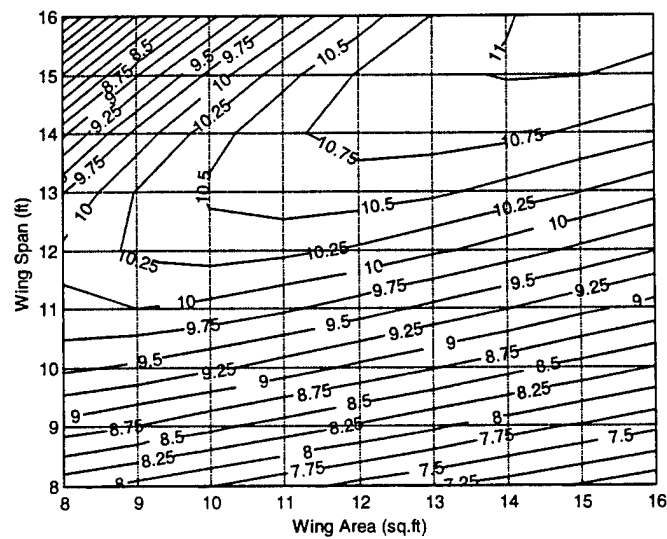


Figure 4.6 Conventional configuration range contours (in miles) as a function of wing span and area achievable using 1996-1997 rules.

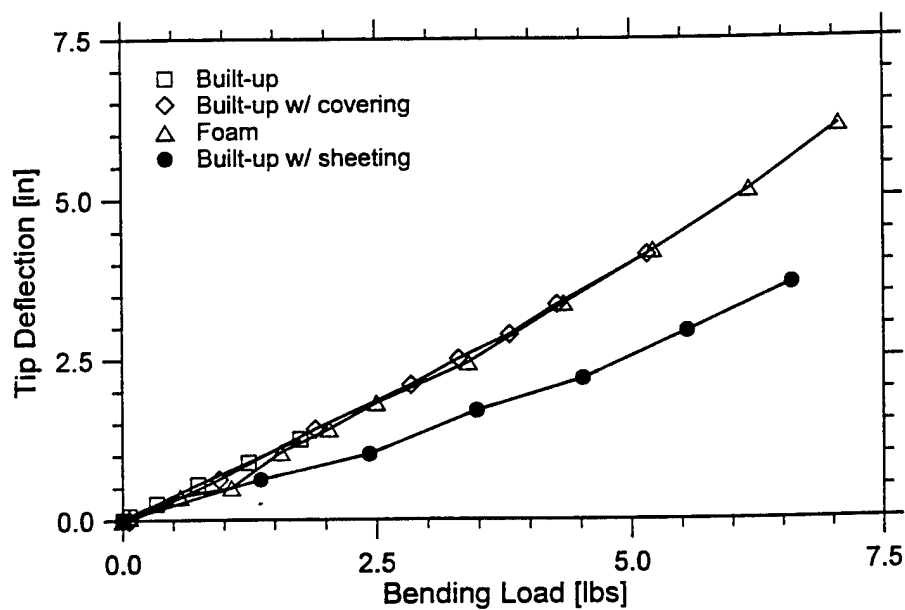


Figure 4.7 Bending stiffness of various wing test specimens.

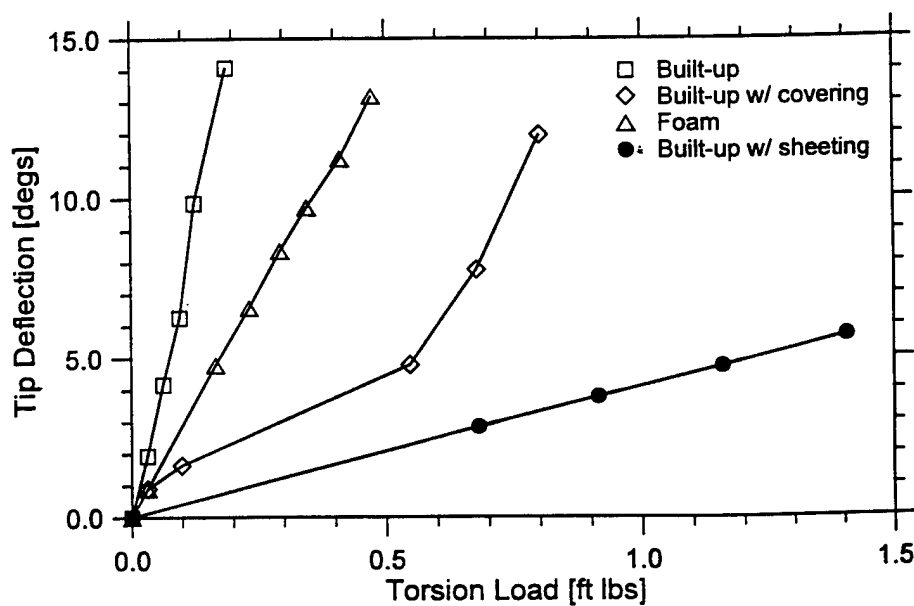


Figure 4.8 Torsional stiffness of various wing test specimens.

## 5.0 Detail Design

### 5.1 Airfoil Selection

As is typical for flying wings, airfoil selection was deemed critical in not only determining the performance of the aircraft, but also its longitudinal trim. Airfoils with large negative pitching moments were avoided owing to their negative impact on both of these parameters. To be more specific, trim for a given lift coefficient requires excessive wing twists when airfoils with large negative pitching moments are used. While such wing twists would not be detrimental at the design lift coefficient, unacceptable off-design performance would result. For acceptable performance, airfoils having near zero pitching moments should be selected

After the design of several candidate flying wings using INVERSE<sup>9</sup> (an inverse design code based on DIRECT), acceptable off-design performance characteristics were produced when airfoil blending occurred along the wing. In addition to the improved aerodynamic performance produced by this technique, it was deemed advantageous to use thick, structurally favorable sections near the wing root, and thinner, low-drag sections near the tips.

The airfoils selected for use were the S5010 and SD7003. The S5010 was used from the root to a location 60% out along the span blending into the SD7003 over the remaining 40%. Table 5.1 lists the major characteristics of each airfoil while Fig. 5.1 shows the geometry and performance data for each. As discussed in Section 5.5, winglets were deemed necessary to improve the directional stability of the aircraft. For these winglets, a nearly symmetrical airfoil, the S8025, was chosen. Its geometry and performance characteristics are shown in Fig. 5.2.

### 5.2 Wing Geometry

Using the values for wing span and area as detailed in Section 4.4, values for wing-sweep, wing-twist, and chord-distribution were finalized during this phase of the design. In contrast to most conventional aircraft, the wing of a pure flying wing must be capable of producing all of the aircraft's directional stability. As discussed in Nickle<sup>7</sup>, adequate directional stability without the use of vertical surfaces is produced for wings with sweep angles greater than 20 degrees. While directional stability further improves as wing sweep is increased, a maximum of 25 degrees is recommended owing to the occurrence of tip-stall problems at the higher sweep

angles. Following these recommendations, a quarter-chord sweep angle of 25 degrees was selected for increased directional stability.

Having finalized wing sweep, a rough estimate for the CG location was performed assuming a constant 1-ft chord wing as discussed in Section 4.4. Using a 10% static margin, the CG was located behind the wing-root trailing edge. The structures group saw this situation as undesirable. Since the payload needs to be located at the aircraft CG, a cantilever arrangement stemming from the wing trailing edge would be required. A solution was found by increasing the wing chord near the wing root. Starting from the 20% spanwise location, the wing chord was linearly increased to 19" at the root. Upon recalculation of the CG location, the payload could now be placed over the wing root, thereby eliminating the need for an elaborate cantilever arrangement. Note: this increase in wing chord near the root increased the wing area to 9.53 ft<sup>2</sup>.

Now that wing span, area, sweep, and chord distribution were finalized, the wing-twist could be determined. This was performed with the help of INVERSE which was written to calculate the wing twist required to produce an elliptic load distribution for a given wing planform, wing lift coefficient, and wing pitching moment. It is largely based on the methodology discussed in Jones.<sup>10</sup> Given the wing geometry outlined above, and an aircraft trim lift coefficient of 0.2 (the optimum as predicted by CRUISE), the required twist distribution is as plotted in Fig. 5.3. For manufacturing, this distribution is impractical. An approximation to this distribution was therefore made for construction purposes. This distribution is also plotted in Fig. 5.3. Finally, Table 5.2 lists all pertinent data for the wing geometry of *RPR-2*.

### 5.3 Propulsion System Selection

Investigations into battery technology revealed that little has changed during the past year in the realm of Nickel-Cadmium batteries. The Sanyo RC2000 cells the team used last year remain the best cells available in terms of energy density. Thus, the battery packs from last year are being used for *RPR-2*. The configuration of these packs are 19 Sanyo RC2000 cells in series, forming packs weighing 2.44 lbf each. The motor/speed controller combination selected this year was a MaxCim MaxNEO-13Y motor coupled with a MaxCim Maxμ 35A-25NB speed controller. There are two reasons for this choice: (1) the success with last year's older MaxCim motor indicated that such motors were capable of providing the required power, efficiency, and reliability that was sought and (2) while research of brushless motors originally suggested



possibility of increased efficiency with an Aveox motor, this was not the case when the new MaxCim Neodymium was considered. The new MaxCim Neodymium motor and corresponding speed controller specifications were compared with those of Aveox products. The calculations and results from ElectriCalc<sup>4</sup> indicated that the new MaxCim motor/speed controller combination could meet or exceed any advantages the Aveox products had over last year's propulsion system. Wind tunnel tests of the MaxCim combination will be performed to verify the ElectriCalc results. ElectriCalc was also used to determine that a gear ratio of 3.5:1 was best for providing both low current draw and suitable thrust production. All propulsion data is listed in Table 5.3.

The pusher configuration was selected for two reasons. First, because of CG constraints and the lack of a tail boom, the majority of the heavy items needed to be located near the CG. This dictated that the motor be located fairly near the trailing edge of the wing. Second, problems with bent motor shafts at last year's competition showed a need to better protect the motor. This could be accomplished by locating the motor at the rear of the fuselage. As a result, a pusher configuration was seen as the best solution to both of these problems.

#### **5.4 Fuselage, Internal Configuration, and Landing Gear**

Design of the fuselage and layout of the internal components of the aircraft were driven by several important considerations, some of which were learned from past experience. The following design drivers were recognized:

- A fuselage with low frontal area and, therefore, low drag.
- Easily removable internal components, particularly the battery and payload.
- Provisions for a simple cooling system.
- Sufficient ground clearance for the eleven-inch diameter propeller.

In order to achieve a low frontal area, the payload weights were sized to fit in the space between the fore and aft wheels while the wing was positioned at mid-fuselage to further reduce the frontal area. The internal components were positioned such that the battery and motor were inline near the top of the fuselage (see internal configuration drawings). Movement of the battery within the fuselage provided some control over the center of gravity, adding to the robustness of the design. The weight and balance data of the components are given in Table 5.4, with their

arrangement illustrated by the internal view included with the final aircraft drawings at the end of this chapter.

One innovative aspect of the design resulted from the aircraft's unique integration of landing gear and fuselage. As previously mentioned, the landing gear was a part of the fuselage design, rather than a required afterthought. The mono-wheel landing gear was positioned to set the wing incidence at four degrees angle of attack to allow take-off without rotation as the aircraft gained speed. The length of the payload was determined by the distance between the wheels. The selected wheel diameter insures ample ground clearance for the propeller. With the absence of typical landing-gear struts, wheels made from a shock absorbing material were chosen to dissipate the landing load. As opposed to conventional aircraft, *RPR-2* has no steering system and ground handling is accomplished by producing the required yawing moment to turn the aircraft using asymmetric elevon deflection. Wheels are located at each wing tip for lateral stability, which tolerates a maximum tip angle of six degrees.

## 5.5 Stability and Control Analysis

With the aid of INVERSE, the longitudinal static stability of the aircraft was finalized when the wing-twist distribution was finalized. Therefore, a study of the aircraft's directional stability was the final stability analysis to be performed. Initial calculations using methods detailed in Raymer<sup>11</sup> suggested that the sweep alone would not be sufficient to produce adequate directional stability. As a result, winglets were added to boost the yaw stiffness of the aircraft. The winglet dimensions are detailed in Table 5.5. As shown in Table 5.6, addition of winglets resulted in a yaw stiffness of only 23% less than that for a 4-place general aviation aircraft. The stability and control group saw this as adequate.

Control of *RPR-2* is provided by 3 sets of control surfaces: elevons, flaps, and rudders. Control surface sizes and locations, along with various other stability and control parameters, are detailed in Table 5.7. While rudder dimensions were chosen to "look right," the flap and elevon configurations were selected because of their beneficial effects on the pitching characteristics of the aircraft. In either case, the performance of each control surface was analyzed using the methods outlined in both Raymer<sup>11</sup> and Roskam.<sup>12</sup> Figure 5.4 shows longitudinal trim plots for various elevon deflections while Fig. 5.5 shows trim plots for various flap deflections. Figure 5.5 can be used in conjunction with Fig. 5.4 to determine the appropriate elevon deflections for

the "crow" mode used during landing. During "crow" mode, positive flap deflections are used in combination with negative elevon deflections to produce zero pitch change and high drag.

As part of the control analysis for the rudders, the ability to trim during a sideslip was investigated. Raymer<sup>11</sup> suggests that an aircraft be able to operate at an 11.5 degree sideslip angle while using less than 20 degrees of rudder deflection. Figure 5.6 shows that the final design will trim in this condition. The ability of the elevons to hold the aircraft level in this condition was also checked using a similar analysis. These results are shown in Fig. 5.7.

### 5.6 G-Load Capability

A V-n diagram for *RPR-2* is presented in Fig. 5.8. The aircraft was designed for a positive limit load factor of 6 and a negative limit load factor of 4. The stall speed was found to be 37 ft/s and the maneuver speed was 82 ft/s. The dive speed was estimated to be 95 ft/s. Because of the gust lines, the design limit load was decreased to 5.76.

### 5.8 Final Design and Performance Analysis

All of the final design parameters that have not already been explicitly stated appear in Tables 5.8 and 5.9. The payload fraction of the final configuration is 0.49 as listed in Table 5.4. The results for the take-off and climb analysis for the final design are shown in Figs. 5.9 and 5.10. These results were obtained by integrating the aircraft's equations of motion using a fourth-order Runge-Kutta algorithm. As the data suggests, *RPR-2* should easily satisfy the take-off requirement. The "energy budget" for the final design mission is given in Table 5.10. The data shows that the take-off and climb use minimal amounts of energy while turns use a significant amount. The number of complete laps predicted for *RPR-2* is 17, or 5.7 miles. These are completed at the expiration of the 7-minute time constraint. Uncertainties in system modeling, off-design flight conditions, and pilot handling may result in a slightly different number of actual laps flown.

### 5.9 Conclusions

This section described the analyses and results used to satisfy the design requirements established in the rules. In surpassing these requirements, the aircraft design has been optimized for the speed-competitive performance parameter. Advances in computer-programmed design and the propulsion system have improved predictions of the aircraft's performance.

Table 5.1 Characteristics of the S5010 and SD7003 Airfoils

Airfoil	$t/c$	$C_{m,c/4}$	$C_{l,max}$ @ $Re = 200,000$
S5010	9.83%	-0.007	1.12
SD7003	8.51%	-0.035	1.1

Table 5.2 Wing Data for Final Design

Wing Data	
span	108 inches
mean aerodynamic chord	12.92 inches
area	1371.6 square inches
aspect ratio	8.50
Inboard taper ratio	0.63
Outboard taper ratio	1
Sweep $\frac{1}{4}$ chord	25 degrees
Dihedral	0
Root airfoil	S5010
Tip airfoil	SD7003

Table 5.3 Propulsion System Data for Final Design

Component	Model
Motor	MaxCim MaxNEO-13Y Brushless
Gear Ratio	3.5 : 1
Propeller	Zinger 11-10 Pusher
Cells	Sanyo RC 2000 2200mAh
Battery Pack	19 Cells in Series
Speed Controller	MaxCim Maxμ 35A-25NB

Table 5.4 Weight and Balance Data for Final Design

Component	Weight (lbf)	Distance From Nose (in)	Weight*Distance (lb-in)
Propeller	0.04	22.45	0.98
Engine	0.61	20.64	12.64
Radio Receiver	0.15	6.39	0.96
Speed Controller	0.18	9.30	1.69
Main Battery	2.44	10.96	26.75
Servo Battery	0.20	3.27	0.65
Payload	7.50	14.90	111.73
Inboard Servos	0.10	17.37	1.74
Outboard Servos	0.10	26.62	2.66
Main Gear (Fore)	0.01	9.76	0.12
Main Gear (Aft)	0.01	20.28	0.25
Outrigger Gear	0.01	30.43	0.30
Fuselage	0.72	11.22	8.07
Spinner	0.08	23.45	1.88
Wing	3.06	20.15	61.70
Total	15.22		232.13
		C.G (in. from nose)	14.90
		Payload Fraction	0.49

Table 5.5 Winglet Data for Final Design

Winglet Data	
Span	8.13 inches
Mean Aerodynamic Chord	7.00 inches
Area	56.88 square inches
Aspect Ratio	1.16
Taper Ratio	0.75
Sweep $\frac{1}{4}$ Chord	25 degrees
Airfoil	S8025

Table 5.6 Comparison of Lateral and Longitudinal Stability Derivatives at Cruise Condition

Stability Derivative	RPR-2	RPR-1 Jack*	4-place General Aviation**
$C_{l\alpha}$ (rad <sup>-1</sup> )	4.395	5.498	4.600
$C_{m\alpha}$ (rad <sup>-1</sup> )	-0.435	-0.492	-0.890
$C_{mq}$ (rad <sup>-1</sup> )	-1.621	NA	-12.400
$C_{l\beta}$ (rad <sup>-1</sup> )	-0.043	-0.148	-0.089
$C_{lp}$ (rad <sup>-1</sup> )	-0.440	NA	-0.470
$C_{lr}$ (rad <sup>-1</sup> )	0.064	NA	0.096
$C_{n\beta}$ (rad <sup>-1</sup> )	0.050	0.245	0.065
$C_{np}$ (rad <sup>-1</sup> )	-0.051	NA	-0.030
$C_{nr}$ (rad <sup>-1</sup> )	0.010	NA	-0.099

\*Data from Ref. 6

\*\*Data from Ref. 12

Table 5.7 Various Stability and Control Results for Final Design

Control Surfaces	
Flap	25% chord, 37% span
Elevon	25% chord, 43% span
Rudder	29% chord, 74% span
Locations: (measured from a/c nose)	
Wing MAC	16.95 in.
Winglet MAC	24.14 in.
Center of Gravity	14.96 in.
Neutral Point	15.08 in.
Miscellaneous	
static margin	9.90%

Table 5.8 Drag of Miscellaneous Components

Component	Estimated Drag Coefficient
Fuselage	0.01047
Wing	0.003145
Induced	0.001981
Total	0.0156

Table 5.9 Miscellaneous Aircraft Components

Component	Brand	Model	Comments
Radio	Airtronics	IN660	6 channels
Micro Servos	Airtronics	94555	Metal gear
Wheels	Sullivan	Sky Lite	2.0" diameter

Table 5.10 Distribution of Battery Energy Among Flight Mission Segments

Mission Segment	Energy Consumed	Percent of Total Energy
Take-off and Climb	5602 J	3.10%
360 deg Turns x 2	2530 J	1.40%
Cruise: straight flight	127,394 J	70.50%
Cruise: turning flight	45,175 J	25.00%
Totals	180,700 J	100%

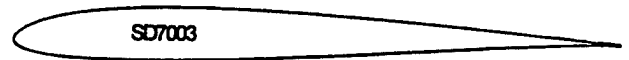
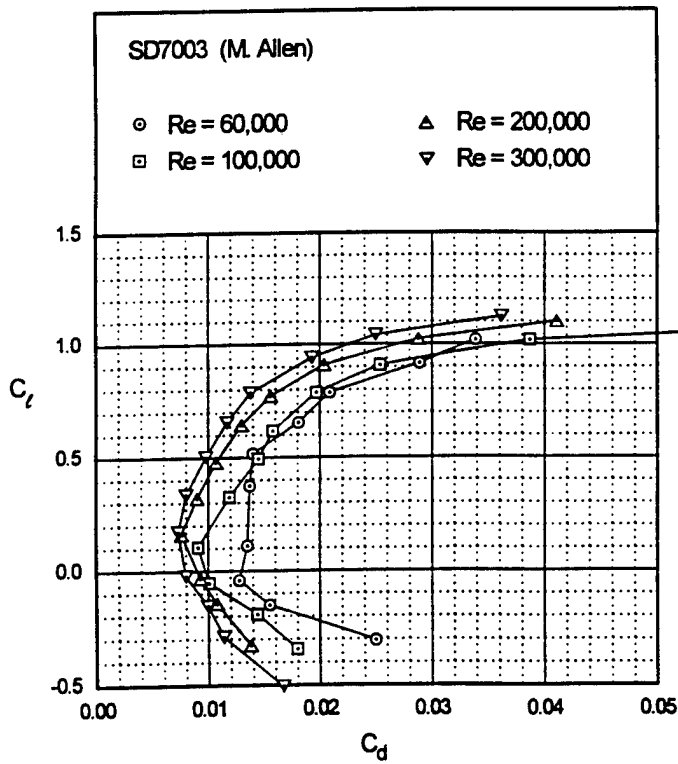
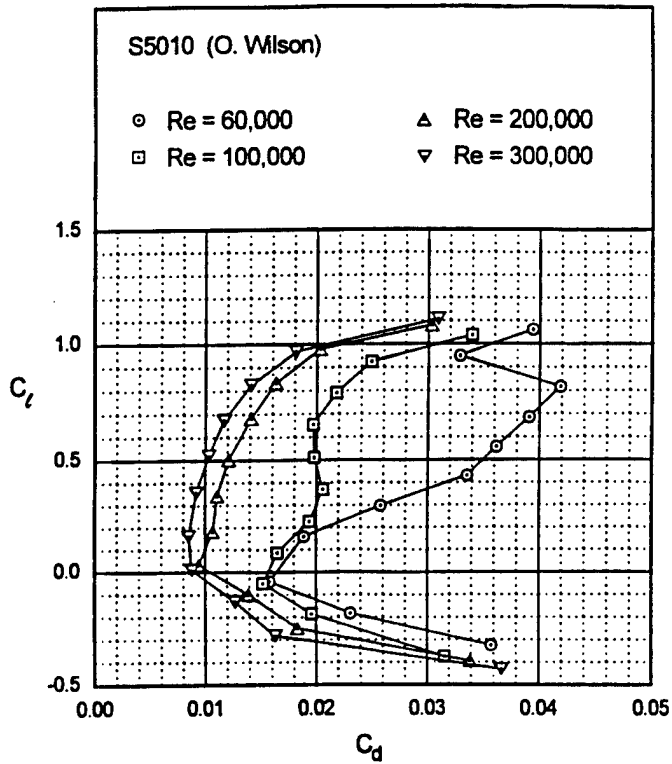


Figure 5.1 Geometry and Performance data for S5010 and SD7003 airfoils.  
(Taken from Selig<sup>13</sup> and Selig<sup>14</sup>)



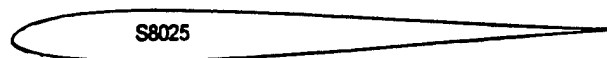
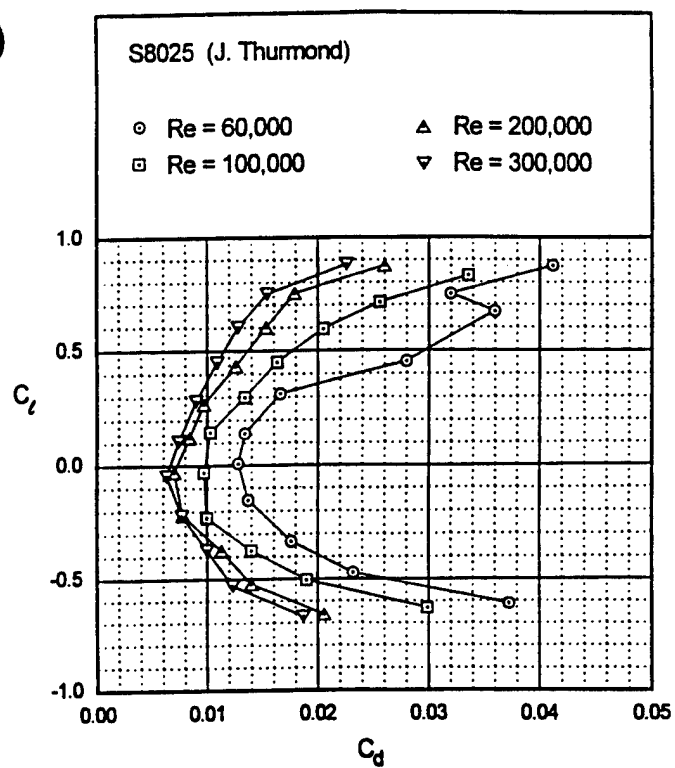


Figure 5.2 Geometry and performance data for S8025 airfoil.  
(Taken from Selig<sup>13</sup>)

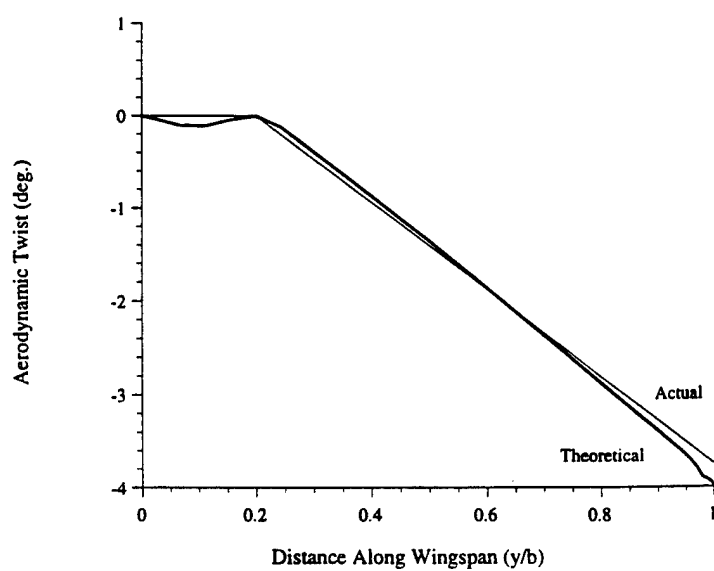


Figure 5.3 Plot of approximate twist distribution.

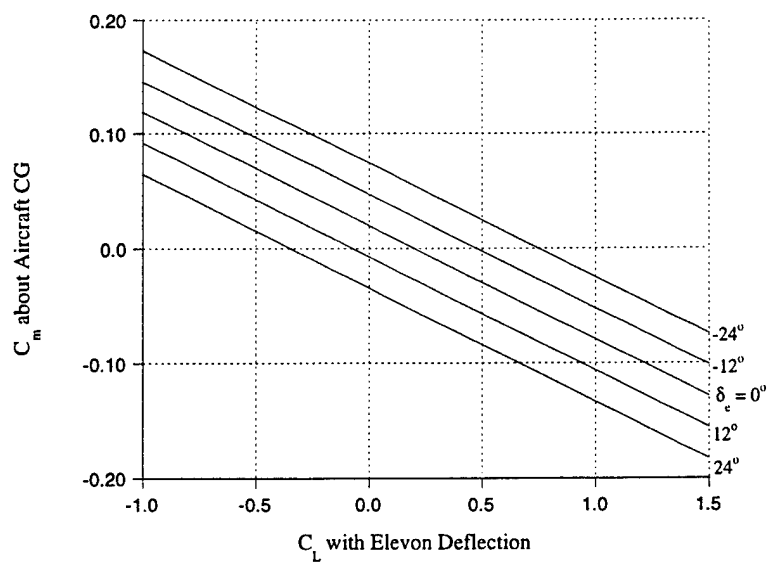


Figure 5.4 Longitudinal trim plot at cruise conditions using elevon deflection only.

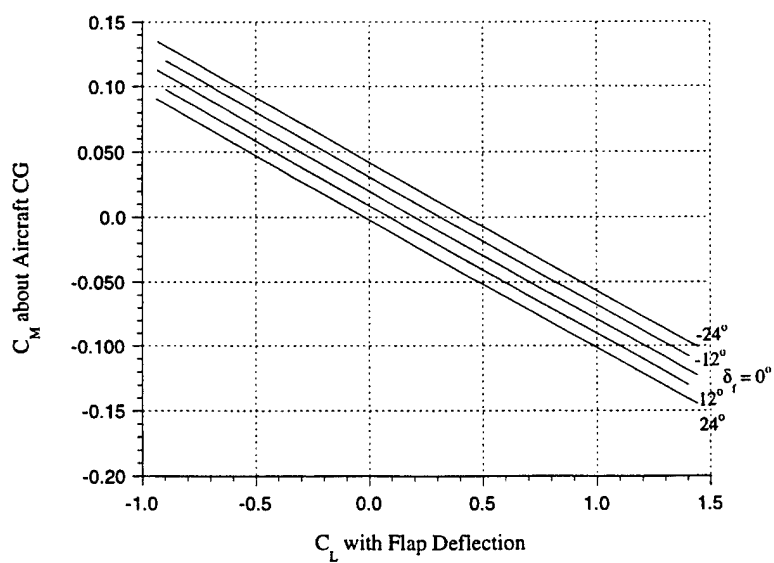


Figure 5.5 Longitudinal trim plot at cruise condition using flap deflection only.

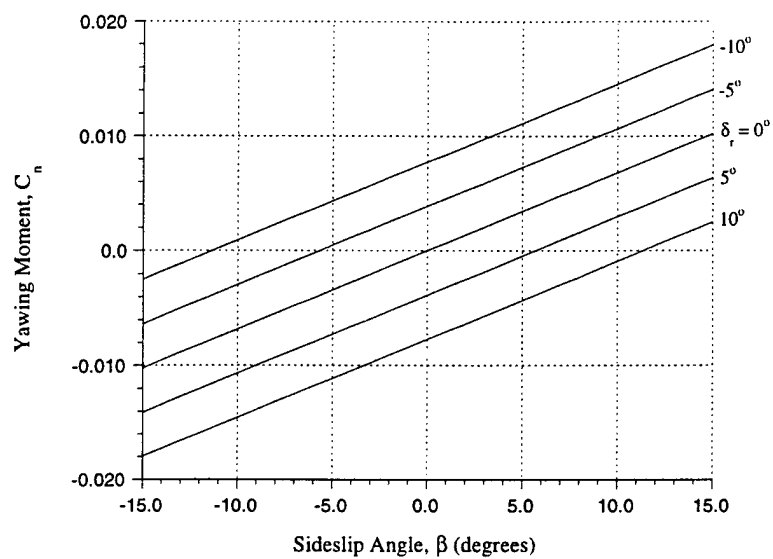


Figure 5.6 Rudder trim plot demonstrating ability to trim in sideslip conditions.

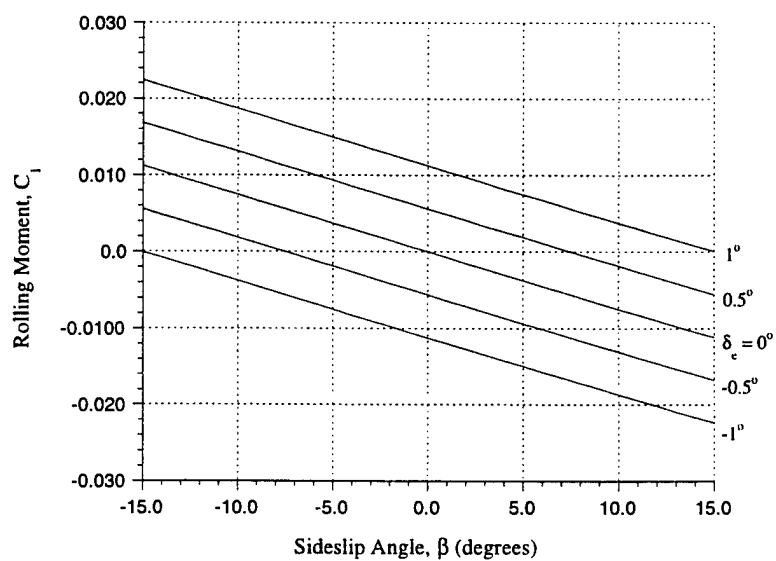


Figure 5.7 Elevon trim plot demonstrating ability to keep aircraft level in sideslip conditions.

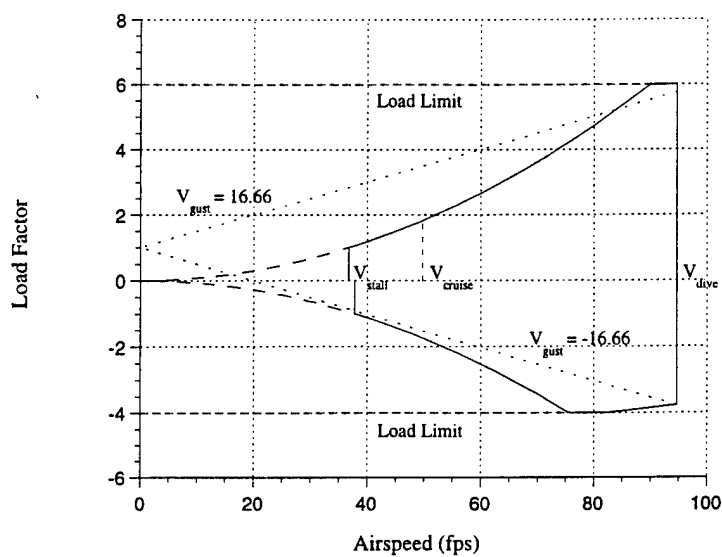


Figure 5.8 V-n diagram.

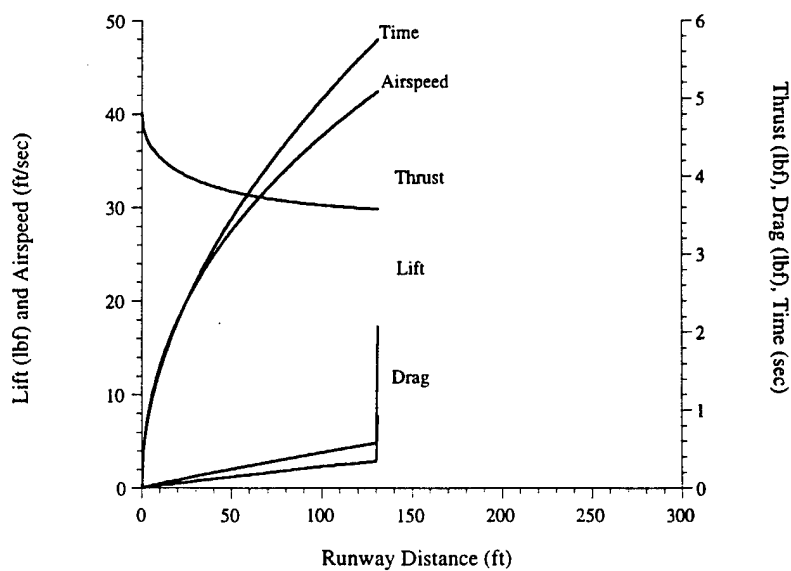


Figure 5.9 Take-off performance.

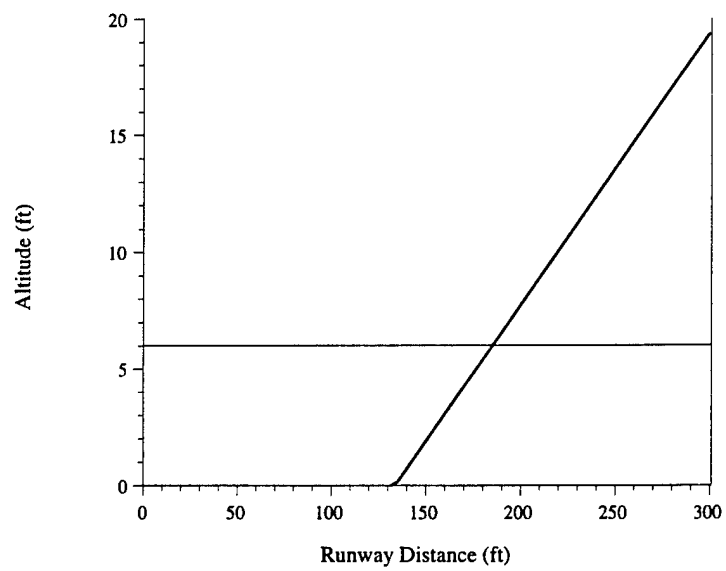
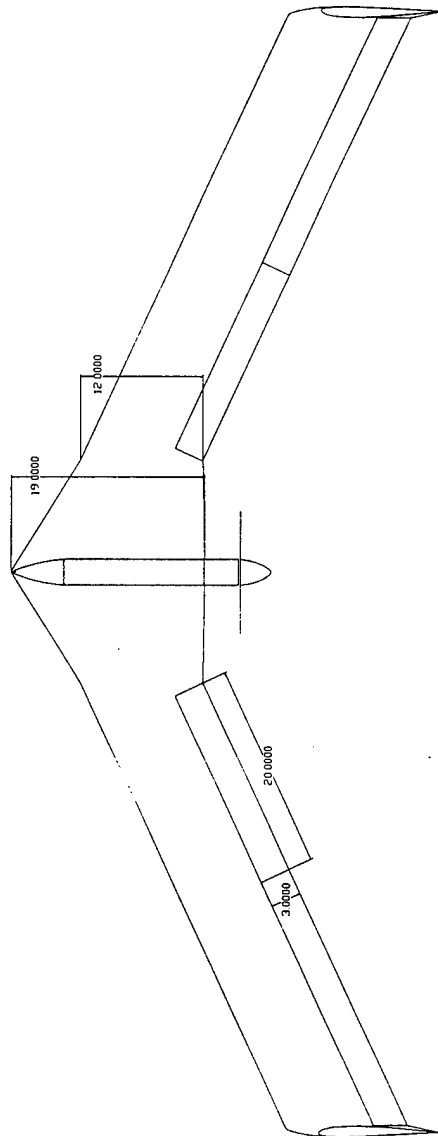
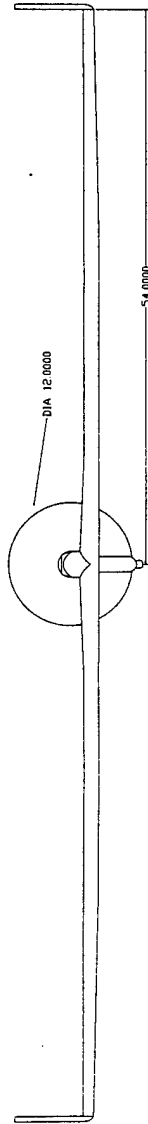
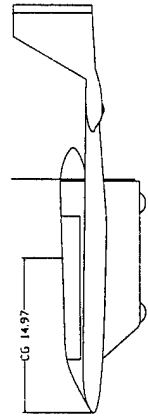


Figure 5.10 Climb performance.

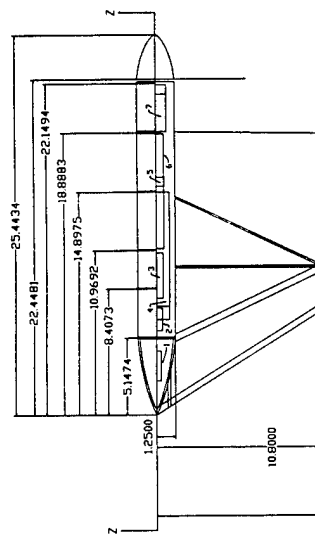


University of Illinois at Urbana-Champaign

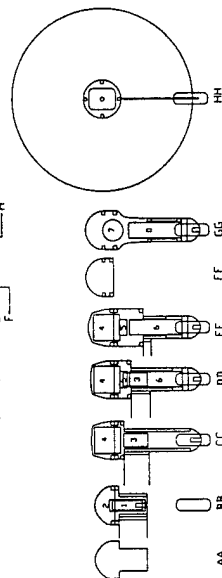
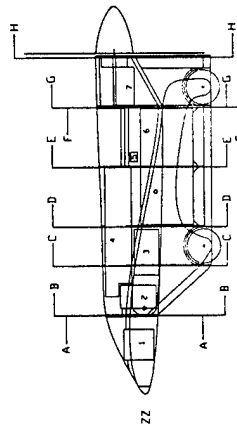
Aeronautical & Astronautical Engineering Department

AIAA Student Design/Built/Fly Competition 1997/1998

RPR-2 External Configuration (All dimensions in inches)



- 1 Receiver Battery
- 2 Receiver
- 3 Speed Controller
- 4 Battery
- 5 Switch
- 6 Payload
- 7 Motor
- 8 Servo



University of Illinois at Urbana-Champaign

Aeronautical & Astronautical Engineering Department

AIAA Student Design/Build/Fly Competition 1997/1998

RPR-2

Internal Configuration (All dimensions in inches)

## **6.0 Manufacturing Plan**

### **6.1 Component Requirements and Design Drivers**

The overall component requirements and design drivers used to select the manufacturing processes for the final design are:

- The components must satisfy structural requirements with an adequate safety factor.
- The components must be built as lightweight as possible, utilizing common manufacturing techniques while maintaining good accuracy.
- The components should be manufactured from readily available, low-cost materials.

In addition to these general requirements, there are special requirements unique to particular components. For example, the fuselage requires easy access to internal components as well as easy installation and removal of the payload. The component-specific requirements are discussed below, in connection with the manufacturing processes investigated.

### **6.2 Manufacturing Processes Investigated**

Several possible construction techniques were investigated for the fuselage, wings and the winglets/vertical stabilizers. These methods are quite common in model aircraft construction and helped to form the basis of the analysis tools discussed in this section.

#### **6.2.1 Wing**

In the selection process for the wing construction method, two important objectives were: (1) the need for high strength and stiffness for performing high-g turns and (2) the need for good contour accuracy for low profile drag. The methods investigated were combinations of foam core or built-up sections that were sheeted with balsa or thin plywood, with basswood or composite spars. In addition, foam cores with composite skins were considered.

#### **6.2.2 Fuselage**

Specific design requirements for the fuselage were (1) low frontal area, (2) structural integrity, and (3) easy access to internal components. To meet these requirements a pod-shaped fuselage was designed, with the payload located in the pod. The pod structure must transfer the inertia loads from the payload to the wing attachments, as well as handle the landing loads from



the wheels. Several manufacturing techniques were investigated for constructing the fuselage. They included (1) using structural plywood sides for the pod covered by non-structural fiberglass skins, and (2) using a structural composite shell built up over a foam plug that is later removed.

### **6.2.3 Winglets/Vertical Stabilizers**

The manufacturing processes considered for the winglets were essentially the same as those for the wing. The structural requirements, however, were less severe. Also, it was required that the construction method would allow removal of the winglets and/or replacement with winglets of larger or smaller size if indicated by initial flight-test results.

## **6.3 Figures of Merit**

Figures of merit (FOMs) for screening competing manufacturing processes were established based upon the component requirements and design drivers listed in Section 6.1. The quantitative value judgments for each of these FOMs are summarized in Table 6.1.

- **Structural Adequacy:** the ability of the resulting component to satisfy the structural requirements.
- **Weight:** the overall weight of the resulting component.
- **Skill Required:** the required skill level of the construction team necessary to execute a particular manufacturing process with high accuracy.
- **Contour Accuracy:** the ease with which a desired contour could be achieved and maintained.
- **Material Availability:** the ease and speed of acquiring the building materials.
- **Time Required:** the amount of time required to complete a particular component for a given manufacturing process.
- **Cost:** the cost of the materials required to use a given manufacturing process. This also accounts for the cost of "specialized" tools or equipment associated with a given manufacturing process.

## **6.4 Methods of Analysis Used to Screen Manufacturing Processes**

The analysis method for screening the manufacturing processes was evaluated based on past experience, instead of using elaborate manufacturing models. For example, the experience base built from the UIUC entry for the 1996-97 competition was utilized. This provided excellent design data in terms of evaluating strength, weight, construction time, cost, etc. More

specifically, past knowledge provided information regarding: (1) an evaluation of the skill of the construction team, (2) the speed at which materials could be obtained from certain suppliers and identification of new suppliers of materials, (3) construction times for various components, and (4) how well students with busy class schedules could work together to get the job done. Furthermore, the R/C modeling experience of this year's project team was utilized to make most of the manufacturing decisions. All of this experience was drawn upon during the evaluation of the figures of merit.

## **6.5 Results: Manufacturing Processes for the Final Design**

### **6.5.1 Wing**

The wing manufacturing process selected was a foam core cut with a hot-wire, carbon fiber spar caps, fiberglass shear webs and fiberglass skin. To assist with the transfer of loads from the spars to the fuselage, the wing/fuselage joint was reinforced with a plywood rib that was then bonded to two shorter spars "fanning" out from a point 20% along both the top and bottom spars (see Fig. 4.7). To absorb shearing stresses between the spars, two layers of 3-oz. fiberglass were used as a shear web. The fiberglass was bonded to the inner surface of each spar and then bonded to the foam cores at a chordwise location of 25% along the entire span of the wing. A cross-sectional layout of this configuration is also shown in Fig. 6.1. The primary factors for choosing this construction method were the need to maintain contour accuracy for low profile drag and the need for high strength and stiffness. The final ranking of the competing processes for the wing is shown in Table 6.2.

### **6.5.2 Fuselage**

The manufacturing process selected for the pod-shaped fuselage was to use plywood for the sides of the pod, and to cover it with a non-structural external shell. This decision was made because it was felt that the plywood would provide not only the structure for the inertia and landing loads, but also serve to support the non-structural composite shell that provides the external shape. The final ranking of the competing processes is shown in Table 6.3.

### **6.5.3 Winglets/Vertical Stabilizers**

The manufacturing process selected for the winglets was to use a hot-wire cut foam core with a fiberglass skin. Owing to their relatively small size and small aerodynamic loads, these winglets have no spars. It is felt that the skins provide sufficient strength to handle the aerodynamic loads. The final ranking of the competing processes is shown in Table 6.4.

## **6.6 Construction Details**

The cores for the wings and the winglets were cut from housing insulation foam using standard hot-wire techniques. The resulting wing cores were cut with a hot-wire along the span and the lay-up of the fiberglass shear webs was done. The 0.06"x0.50" inch rectangular pultruded carbon fiber spar caps were then bonded to the shear webs and the reassembled wing was sheeted with one layer of 3.7 oz. fiberglass. The winglets/vertical stabilizers were made removable to allow for fine-tuning that may be necessary after the initial flight tests.

As shown in the drawing package, the fuselage internal structure consists of two 3/16" thick plywood sheets that form the sides of the pod. Plywood formers at several longitudinal locations interconnect these plywood sheets. The outer shape is provided by a non-structural fiberglass fairing, which was laid up on the plywood sheets.

Figure 6.2 is a proposed and actual timeline for construction of the competition aircraft. At the time of the writing of this report, construction is proceeding on schedule. If everything goes as planned, the first test flight of the final aircraft, RPR-2, will be on April 4, 1998.

## **6.7 Cost Reduction Methods**

The choice of such a simple configuration was perhaps the most important cost reduction method. This was manifested in the manufacturing processes and material selection. All of the construction materials used are standard equipment in the R/C model community. They are commercially available from many different suppliers as well as obtainable in a matter of a few days to one week. Several of the building materials can be obtained directly from the local hardware store or building center. For example, the extruded polystyrene foam core was cut from a 4 x 8 foot sheet of home insulation purchased in town on the same day. The manufacturing processes require no special tools or machinery.

Table 6.1 Figures of Merit Used in Manufacturing Plan Formulation

Figure of Merit	Ranking		
	5	3	1
Structural Adequacy	high	average	low
Weight	light	average	heavy
Skill Required	easy to construct	average difficulty	difficult to construct
Contour Accuracy	easy to achieve	average difficulty	difficult to achieve
Material Availability	easily acquired	average availability	difficult to acquire
Time Required	short	average	long

Table 6.2 Final Ranking of Figures of Merit for Wing

Figure of Merit	Ranking	
	wood built up	sheeted foam
Structural Adequacy	1	4
Weight	5	3
Skill Required	3	4
Contour Accuracy	2	4
Material Availability	3	3
Time Required	3	5
Cost	4	3
Total	21	26

Table 6.3 Final Ranking of Figures of Merit for Fuselage

Figure of Merit	Ranking	
	structural shell	internal structure
Structural Adequacy	3	5
Weight	4	3
Skill Required	3	4
Contour Accuracy	3	3
Material Availability	3	3
Time Required	4	4
Cost	4	4
Total	24	26

Table 6.4 Final Ranking of Figures of Merit for Winglets

Figure of Merit	Ranking		
	wood built up	foam-wood	foam-glass
Structural Adequacy	2	5	4
Weight	5	2	3
Skill Required	2	4	5
Contour Accuracy	2	3	4
Material Availability	3	3	3
Time Required	1	1	4
Cost	4	3	3
Total	19	21	26

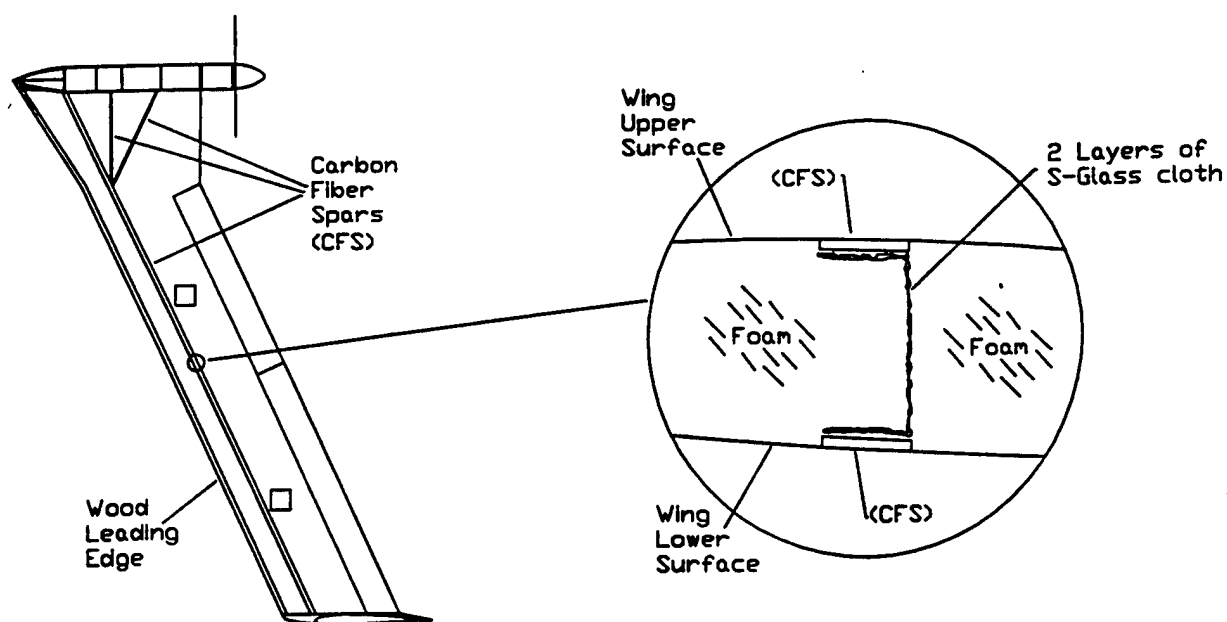


Figure 6.1 Placement of carbon fiber along wingspan and cross-sectional view.

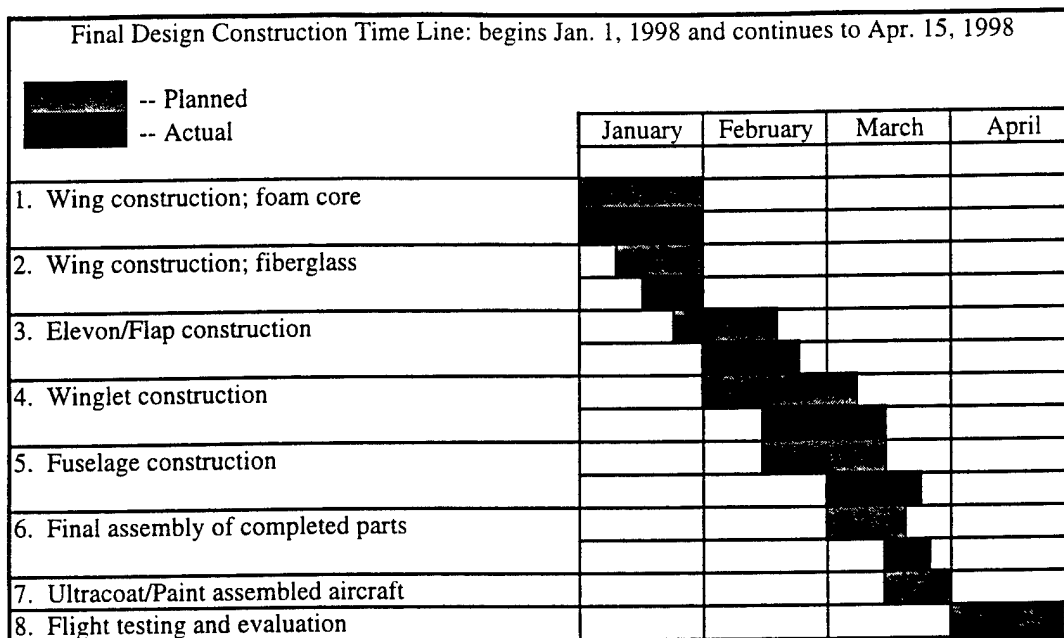


Figure 6.2 Project timeline for construction of RPR-2.

## REFERENCES

1. LinAir. Vers. 1.0. Computer software. Desktop Aeronautics, 1987. Macintosh.
2. DIRECT. Vers. 3. Computer software. Chris Lyon, 1997. PC, Matlab.
3. CRUISE. Vers. 7.2. Computer software. Chris Lyon, 1997. PC, C.
4. ElectriCalc. Vers.1.0. Computer software. SLK Electronics, 1996. PC.
5. Kern, R.A., Private Communication, Sept. 1996.
6. University of Illinois Design/Build/Fly Team. RPR-1 Jack Final Design Report. Champaign, 1997.
7. Nickel, K. and Wohlfahrt, M., *Tailless Aircraft in Theory and Practice*, translated by E.M.Brown, 1 st ed., AIAA Education Series, Washington, D.C., 1994.
8. Lyon, C.A., Broeren, A.P., Gopalarathnam, A., Giguere, P., and Selig, M.S., *Summary of Low-Speed Airfoil Data—Vol. 3*, SoarTech Publications, Virginia Beach, VA, Dec. 1997.
9. INVERSE. Vers. 3. Computer software. Chris Lyon, 1997. PC, Matlab.
10. Jones, Robert T. *The Spanwise Distribution of Lift For Minimum Induced Drag of Wings Having a Given Lift and a Given Bending Moment*. NACA TN 2249, 25 Sept. 1950.
11. Raymer, D.P., *Aircraft Design: A Conceptual Approach*, 2nd ed., AIAA Education Series, Washington, D.C., 1994.
12. Roskam, J., *Airplane Flight Dynamics and Automatic Flight Controls*, Roskam Aviation and Engineering Corporation, Ottawa, KS, 66067, 1979.
13. Selig, M.S., Lyon, C.A., Giguere, P., Ninham, C., and Guglielmo, J.J., *Summary of Low-Speed Airfoil Data—Vol. 2*, SoarTech Publications, Virginia Beach, VA, 1996.
14. Selig, M.S., Donovan, J.F., and Fraser, D.B., *Airfoils at Low Speeds*, SoarTech 8, SoarTech Publications, Virginia Beach, VA, 1989.

## **7.0 Lessons Learned**

This section details all of the modifications made to the aircraft since submission of the Design Report – Proposal Phase: the results of propulsion system and flight tests, a final cost assessment, and suggestions for improvement in the design and manufacturing processes.

### **7.1 Comparison of Final and Design Aircraft**

The final aircraft (shown in Fig. 7.1) is identical to that presented in the proposal phase of this report, with only minor modifications to component placement and small aerodynamic improvements. In order to balance the aircraft about the required CG location, approximately five ounces of lead weight were placed in the nose. Some components, such as the battery pack, were moved slightly from their initial location in the fuselage to further facilitate this balancing. To minimize flow separation at the rear of the fuselage, which would decrease the efficiency of the propeller, a small fairing was added to the wing, blending its contour with that of the fuselage.

The final aircraft weighs 15.59 lbs., which is very close to the proposal phase estimate of 15.22 lbs. The added weight is attributed to light-weight components that were not originally accounted for, and to the addition of the five ounces of lead weight. The weights for major components of the final aircraft are given in Table 7.1.

### **7.2 Cost Assessment**

The cost of the final aircraft, broken into subsystems, is summarized in Table 7.2. Experience with last year's project helped keep actual component costs in line with predictions made at the beginning of this project.

### **7.3 Propulsion System Tests**

Limited propulsion tests were performed in order to validate the results of ElectriCalc. The tests were done in the University of Illinois Instructional Subsonic Wind Tunnel with the motor mounted on a test rig. The motor was powered by the same battery pack that was used in the aircraft. A Zinger 11-10 pusher propeller with a 4.0:1 gearing was used. This represented one of the configurations considered for the final aircraft at the time.

Figures 7.2 and 7.3 show the results of the static test. The results show good overall agreement between the experiment and ElectriCalc. Figures 7.4 and 7.5 show the thrust and



endurance results for three cruise velocities. Again, the experiment and ElectriCalc agree reasonably well, especially in the 70 to 90 ft/sec cruise velocity range. This is the range in which the aircraft is expected to operate. The good agreement between the experimental data and ElectriCalc calculations shows that ElectriCalc can accurately predict the performance of the propulsion system that is used in the aircraft.

#### **7.4 Flight Tests**

The aircraft has been completed and successfully test flown. No payload was installed on the test flights in an effort to maximize the power available if the aircraft was to prove unwieldy.

The test flights yielded much useful data. First and foremost, the aircraft proved to be longitudinally stable. The pilot reported that it handled well and was much more responsive than last year's aircraft. The winglet rudders had little effect on the yawing moment, but they may aid in steering the aircraft when the full payload is carried. The aircraft also surpassed the take-off requirement. Unacceptable heating of the motor was resolved by cutting ducts in the fuselage shell for ventilation. Additional modifications to the fuselage shell are planned to further reduce the heating of the propulsion system.

While draining the battery packs on the ground, the MaxCim neodymium motor cut off. A diagnostic indicated a problem with the Hall Effect Device, and consultation with the manufacturer indicated that a magnet may have been thrown. The aircraft was then successfully flown with the MaxCim motor used last year and the current speed controller. The neodymium motor will be sent to the manufacturer for repair and magnet reinforcement with Kevlar.

#### **7.5 Areas for Improvement in Design and Manufacturing Processes**

The analysis and design tools used in the development of *RPR-2* have resulted in a vehicle capable of exceeding all of the specified requirements. However, some areas of refinement were identified.

- Conduct propulsion testing at an earlier date; the data could not be used to tweak the aircraft design because the aircraft was already built by the time of testing.
- Build a structural test specimen using the construction techniques implemented for the wing; the structural test specimens that were built and tested were not of the type used for the final wing.

- Get more people involved in the design process; too few on the design team caused delays since team members had very little detailed information about the design of the aircraft, requiring constant consultation with the designers on numerous minor details.
- Build a prototype; this would have given the team a handle on the things most difficult to predict (directional stability, ground handling, and cooling).

The manufacturing proceeded smoothly and successfully resulting in a reliably constructed aircraft. However, several suggestions can be made for improvement.

- Balance the workload more evenly throughout the team, and prevent a last minute rush in aircraft fabrication. More concrete deadlines for the construction tasks need to be established.
- Create more room in the fuselage for components. There is very little room to move components for CG adjustment. This can be resolved by various methods (longer fuselage, larger cross-sectional area, thinner padding, etc.)
- Find a better method for covering the wing. The application of UltraCote to the fiberglass skin of the wing proved to be difficult because a heating iron could not be used (this would melt the foam core). A coat of glossy paint may be a more desirable covering for the wing.

Improving the fabrication process should not impose a large additive monetary cost, since a well-stocked construction shop has already been set up. With extra time committed, worker craftsmanship can be greatly improved.

Making the suggested improvements will provide future University of Illinois Design/Build/Fly teams with reliable design tools. When combined with the experience the team members gained from participating in this project, these improvements will result in robust, quality designs that can meet the performance objectives of future competitions.

## 7.6 Conclusions

There are a few more general "lessons learned" from the entire project. The build-and-fly aspect of the project again taught many valuable lessons about engineering design that would otherwise have been overlooked. Correct assumptions and good calculations are essential. errors can lead to crashes. The demands of flying emphasize the need for a flexible d

that, during the final stages of assembly, components can be tweaked or moved slightly to prepare the aircraft for flight. While the design of *RPR-2* required much time and effort from every member of the project team, their contributions led to an aircraft that is well built and on schedule.

Table 7.1 Final Aircraft Weight Breakdown

Major Component	Minor Components	Weight (lbf)
Wing	Winglets, Servos, Outrigger Gear	3.48
Fuselage	Receiver, Servo Battery, Main Gear	1.26
Propulsion	Motor, Speed Controller, Spinner, Propeller	0.91
Main Battery		2.44
Payload		7.5
<b>Total</b>		<b>15.59</b>

Table 7.2 Aircraft Component Costs (rounded to nearest dollar)

<b>Propulsion System</b>	
motor and speed controller	490
battery packs (2)	300
*Misc. (propellers, spinner, wire, connectors, etc.)	35
Propulsion subtotal	825
<b>Wing</b>	
*Wood	45
Foam	40
*Misc. (fiberglass, epoxy resin, UltraCote, etc.)	60
Wing subtotal	145
<b>Fuselage</b>	
*Wood	20
Fiberglass	25
*Misc. (nuts and bolts, epoxy resin, washers, etc.)	10
Fuselage subtotal	55
<b>Other</b>	
Radio	400
Other subtotal	400
<b>Total</b>	<b>1425</b>

\* estimated

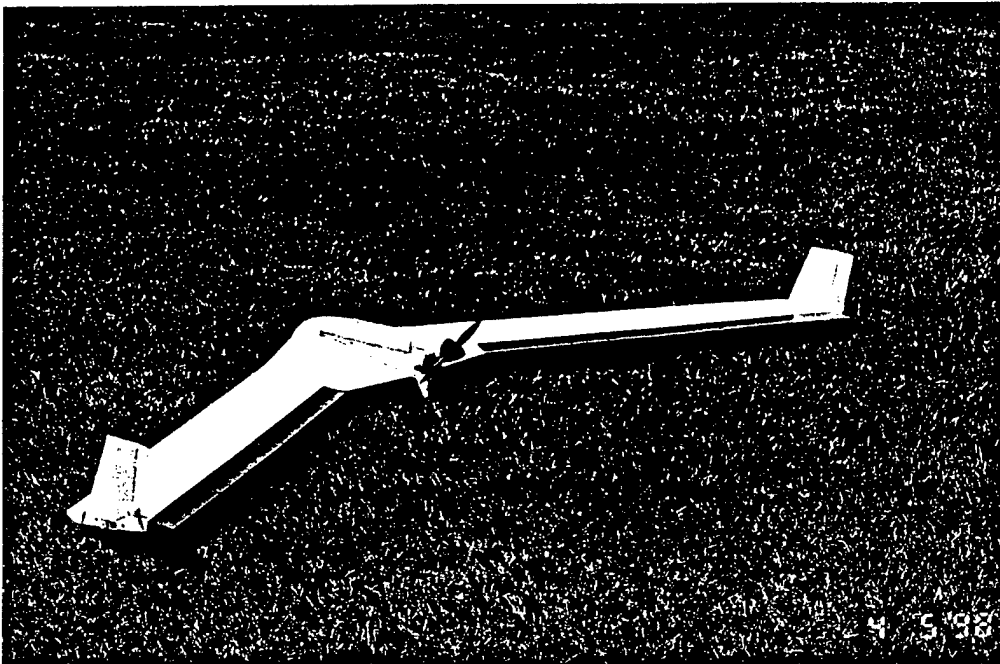


Figure 7.1: Completed competition aircraft.

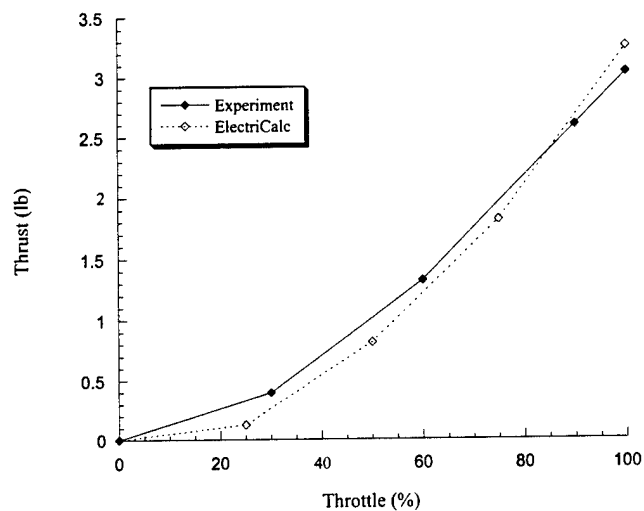


Figure 7.2: Static thrust curve. Zinger 11-10 pusher prop; 4.0:1 gear ratio.

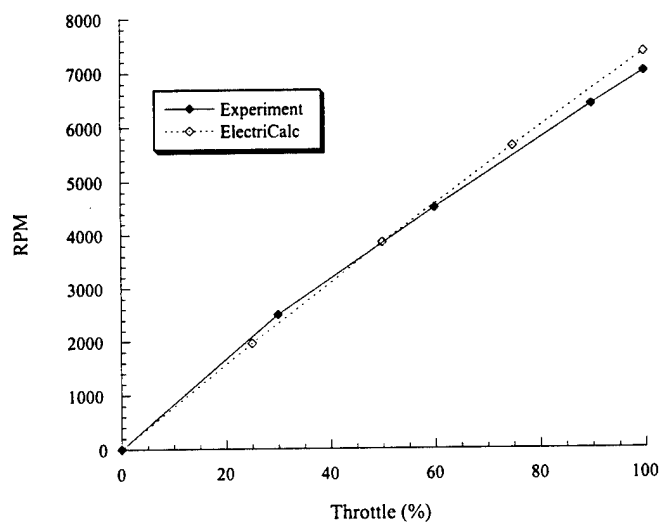


Figure 7.3: Static RPM curve. Zinger 11-10 pusher prop; 4.0:1 gear ratio.

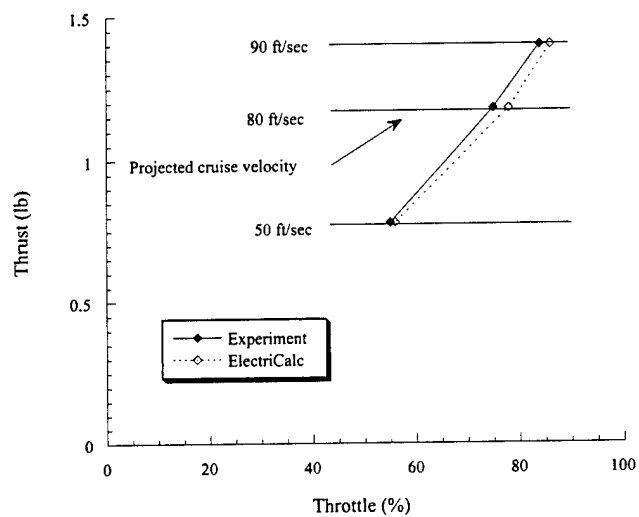


Figure 7.4: Cruise thrust curve. Zinger 11-10 pusher prop; 4.0:1 gear ratio.

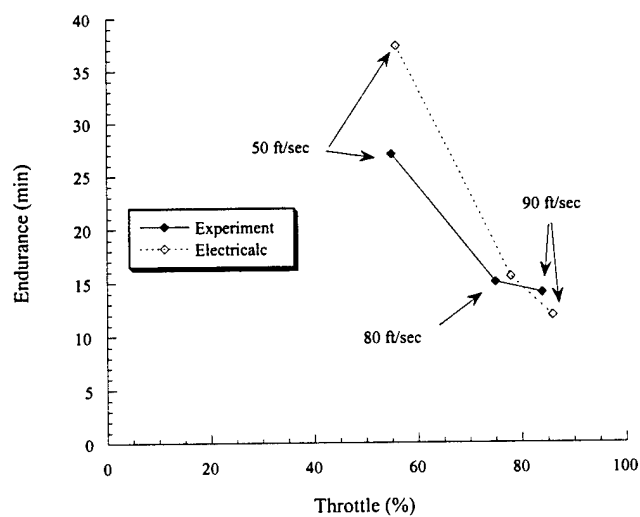


Figure 7.5: Cruise endurance curve. Zinger 11-10 pusher prop; 4.0:1 gear ratio.

# **Design Report**

## **1998 AIAA/Cessna/ONR Student Design/Build/Fly Competition**

**Team Name:  
MIT Aero-Astro**

**Team Members:**

**George Berkowski  
Eric Carreno  
Carl Dietrich  
Jacob Markish  
Phil Ogston  
T. Rivkin**

**Advisor: Pete Young, Col, USAF**

**March 16, 1998**

**Department of Aeronautics and Astronautics  
Massachusetts Institute of Technology  
77 Massachusetts Ave.  
Cambridge MA 02139**



## 1. Executive Summary

After learning about the 1998 AIAA Student Design/Build/Fly competition in the early Fall of 1998, MIT undergraduates in the Aeronautics and Astronautics Department became very enthused about entering this year's competition. Under the mentorship of Col Pete Young, the students organized into design teams, developed plans, established schedule milestones, and started the design efforts and analyses to develop a (hopefully) competitive proposal and aircraft. With only limited spare time during the school year to devote to this extra-curricular project, and keeping in mind that this project was the first complex model design and construction project for almost all the students, an important emphasis from the very beginning was to balance performance against the need to minimize technical and schedule risks.

During the Conceptual Design phase, numerous aircraft configurations and ideas were proposed and evaluated. The students quickly became aware that total flight performance was heavily influenced by the performance of the electric propulsion system, so initial emphasis centered on propulsion items such as the types of motors available, their power and efficiency, motor batteries, and motor gearboxes. In these assessments, the ElectriCalc performance spreadsheet program proved to be an invaluable aid to answering numerous design questions related to the runtime endurance of various electric propulsion systems under various design conditions. Towards the end of this initial design phase, the students selected a high wing monoplane as their baseline, and the details leading to this selection, as well as others, can be found in Section 3.

In the Preliminary Design phase which followed the Conceptual Design phase, more attention was paid to performance sensitivities as more detailed evaluations were conducted on wing airfoils, wing area, aspect ratio, and other key aerodynamic parameters. The choice of aileron control surfaces along with rudder and elevator, but not maneuvering flaps, was considered to be important to good handling around the turns which the team felt would be essential to consistent flight performance. In addition to the ElectriCalc program used in the previous design phase, the team relied heavily on the design and flight simulation capability of the NHP/CSM R/C Flight Simulator, a PC-based flight simulator which contains a very detailed aircraft design package. A key piece of analysis completed in this phase was a rigorous evaluation of 6 airfoils to assess their

effects around the race course. Based on the detailed results which are summarized in Section 4, the Clark Y airfoil was chosen for MIT's aircraft entry.

The Detail Design phase refined the design elements developed in the previous two phases into a final system configuration. A triple taper leading planform was chosen, consistent with the design practices used in competitive International Class sailplanes. A pod and boom fuselage configuration was selected for simplicity, functionality, and light weight. The MIT group decided that the best placement of the flight controls' servos was close to the control surfaces themselves to eliminate long linkage runs and possible flutter. During this phase, many hours were spent "flying" the flight simulator routines in the NHP/CSM flight simulator program, allowing candidate pilots to become familiar with the handling characteristics of the MIT aircraft and with the use of the Airtronics Stylus transmitter. Further details of the final design configuration, as well as predicted performance, can be found in Section 5 of this report.

The Manufacturing phase of the team effort evaluated several interesting construction approaches. After extensive discussions and screening evaluations, the final approach selected was balsa sheet over blue foam cores for the wing, and balsa and Monokote construction for the horizontal and vertical stabilizers. For most of the students, this was their first exposure to hot wire cutting of foam, vacuum bagging, and close tolerance construction of numerous components. As the project aircraft evolved to its final finished state, the students expressed great satisfaction as they saw their ideas become physical realities. Details of the various construction alternatives considered in this phase can be found in Section 6.

The first flights of the completed aircraft took place on March 8th at an auxiliary airfield approximately 20 miles west of Boston. Performance and handling characteristics of the MIT aircraft were very satisfactory and confirmed, at least initially, the performance predictions developed during the design phases. Further flight tests will take place as students' time permits to gain familiarity with the aircraft's flying characteristics with the 7.5 lb steel payload as well as under various weather conditions. All in all, this effort has been extremely interesting, very enjoyable, and most important of all, educational for all the team members involved.

## 2. Management Summary

An initial kickoff meeting was held on 30 October 1997 and team members were assigned to six main working groups. The six working groups were: aerodynamics, propulsion, structures, avionics, systems/project engineering and report writing. Design personnel and group assignments are as follows:

Aerodynamics:	Eric Carreno, Phil Ogston
Propulsion:	Carl Dietrich
Structures:	Carl Dietrich, Jacob Markish
Avionics:	George Berkowski
Systems:	Eric Carreno
Report Writing:	Tyra Rivkin, Jacob Markish
Advisor:	Pete Young

Each design group appointed a lead person responsible for coordinating and keeping efforts on track to support the entire team.

A master schedule was drawn up for the team at the onset of the design phase and updated every week thereafter. Scheduling was based upon a desire to spread design and construction over a long period of time to account for unforeseen circumstances and inevitable time constraints as the semester progressed. When necessary, critical path elements were identified and given special attention as required. A detailed schedule can be found in Figures 1 and 2. Figure 1 shows the schedule for the Fall 1997 semester. The Spring 1998 schedule appears on the following page in Figure 2. As expected, the team ran about a week to ten days behind schedule depending on the phase of the project for the fall term. Winter break helped move the project back on schedule and a few of the team members returned early in January to begin constructing the aircraft structure.

Once a baseline configuration was selected, all significant subsystem changes were discussed in the weekly project team meetings. All proposed changes were discussed and weighted by relative impact on overall performance, difficulty in implementation, and potential scheduling setbacks. If the team decided that a significant change was in fact necessary, the configuration and schedule were adjusted as required and work continued from that point.

### Section 3: Conceptual Design

During the Conceptual Design phase, the MIT Aero-Astro team sorted through a number of aircraft configurations using a combination of analytic and engineering judgment techniques to screen candidate aircraft configurations. As a first cut, the aircraft designs entered in the previous year's AIAA D/B/F competition were reviewed to benchmark competitive entries as well as to assess significant trends in design, propulsion, and airfoil selection. The team then "brainstormed" additional aircraft design parameters which were non-judgmentally carried forward for further detailed assessments.

#### *I. Design parameters investigated and their importance*

Number of electric motors: the principal advantage to having two (or more) electric motors is the increased thrust and propeller disc area offered which could benefit takeoff performance, level flight speed, and turning performance around the pylons.

Size and type of electric motor(s): the principal trade here was between ferrite, "rare earth", and "brushless" motors. Since the flight portion of the AIAA D/B/F competition rewards the entries completing the most pylon laps in a limited amount of time with a fixed mass of batteries, an important factor driving the size and type of electric motor(s) was the efficiency and output of the motor(s) to be installed into the competition aircraft. The propulsion team looked at the performance available from Astro ferrite, Astro Cobalt, Aveox, Max Cim, Ultra, Plettenburg, and Robbe electric motors.

Geared vs ungeared propulsion systems. Geared motor systems offer the capability to swing larger, more efficient propellers than an ungeared propulsion system and the increased disc area would enhance takeoff and turning performance.

Motor battery type, size and capacity: within the 2.5 lb. limit, it was important to be able to maximize the total electrical energy carried onboard the aircraft. Nickel Metal Hydride and Nickel Cadmium rechargeable batteries were the two battery technologies investigated. Additionally, the amp-hour cell capacities available from commercial battery suppliers were investigated to determine the best cell sizes and capacities.

Wing span, area, airfoil, and aspect ratio: these design parameters are a major determinant of aircraft performance for high aerodynamic efficiency, maximum level flight speed, and efficient turning performance.

Airframe weight: in order to optimize flight performance, it would be important to minimize airframe weight consistent with structural strength requirements.

V-tail controls could increase total performance by reducing the surface area, drag, and weight of the tail surfaces.

A T-tail configuration would increase the effectiveness of the horizontal stabilizer by raising it above the wake of the wing and propeller; as well as increase the effectiveness of the vertical stabilizer through endplate effects.

A "pusher" motor location is theoretically more efficient than a "tractor" configuration since the propeller slipstream flows directly back without impinging on the aircraft airframe causing extra drag.

Wing flaps, by increasing wing lift coefficients for a given angle of attack, have the beneficial attributes of increasing aircraft lift during takeoffs and landings as well as providing tighter turns around the pylons.

Rudder and elevator control only without wing flap or aileron controls, as used on recent highly placing SAE cargo lifting aircraft configurations, reduces the number of servos required along with the weight of their associated wiring and connectors, and provides a more efficient wing configuration unencumbered by the complexity and gap-induced drag losses of flap and aileron control surfaces.

## *II. Analytic methods used during Conceptual Design*

The principal analytic tool used during Conceptual Design was the ElectriCalc Version 1.0E spread sheet performance software program developed by Sid Kauffman, SLK Electronics, 2906 Charolais Drive, Greensboro, NC 27406. This computerized tool allowed the team to analyze electric motors, battery packs of varying size, aircraft weights and areas, propeller and gear box options, and other key parameters in a systematic manner. According to model aircraft electric propulsion experts that we checked with, ElectriCalc is accurate to between 5% and 7.5% on the conservative side, but we found the primary value of ElectriCalc during Conceptual Design was its ability to conduct performance assessments with multiple design parameters in a fast and efficient manner.

Figures of merit (FOMs) and supported mission features. To assist making systematic assessments of the design parameters detailed above, 5 weighted figures of merit were used to screen competing concepts. Singly or in combination, conceptual design concepts were scored

against these figures of merit linked to pertinent and significant mission features. A design completely satisfying all FOMs would score a maximum of 65 points.

- FOM #1, 15 pts: High aerodynamic efficiency. The team felt strongly that high aerodynamic efficiency was the key to completing a maximum number of laps within the stringent contest constraints. The mission features supported are range and endurance.
- FOM #2, 10 pts: Good handling characteristics. After a close review of the contest rules, the team concluded that good handling performance was key to having efficient turning performance around the pylons, an important factor considering the extra payload weight to be carried. Mission feature supported: minimum lap times.
- FOM #3, 15 pts: High electric propulsion system performance. The key factors here are the propulsion system's current drain, available voltage, amp-hour capacity, delivered thrust, motor and system efficiency, and run-time. The mission features addressed by this FOM are range and endurance.
- FOM #4, 10 pts: Minimum airframe weight. This figure of merit covers minimizing the weights of all components of the completed aircraft, including the radio equipment and electric propulsion system. The mission features addressed by this FOM are range and endurance.
- FOM #5, 15 pts: Minimizing technical and schedule risks. The undergraduate team chose a project philosophy to control technical and schedule risks by choosing conservative design approaches and architectures. The mission feature supported was availability: to produce a minimum risk design which would not present significant jeopardies during construction, flight tests, or to the overall schedule.

From the design factors listed above, the undergraduates synthesized four design configurations which were then reviewed in further detail. For baselining purposes, Nickel Cadmium motor batteries and geared brushless electric motors were common to all configurations. The results of the assessments of each design against the Figures of Merit are shown below in Table 1.

**Table 1: Figures of Merit and Design Point Selection**

Configuration	FOM #1 (15)	FOM #2 (10)	FOM #3 (15)	FOM #4 (10)	FOM #5 (15)	Total (65)	Rank
Moderate aspect ratio, conventional tail, ailerons	12	8	15	9	13	57	1
Moderate aspect ratio, V-tail, ailerons	12	4	25	13	7	51	2

**Table 1: Figures of Merit and Design Point Selection**

Configuration	FOM #1 (15)	FOM #2 (10)	FOM #3 (15)	FOM #4 (10)	FOM #5 (15)	Total (65)	Rank
High aspect ratio, conventional tail, ailerons	8	8	15	6	10	47	3
High aspect ratio, T-Tail, flaps, ailerons	15	4	15	5	5	44	4

The highest rated configuration to be evaluated has a moderate aspect ratio wing to balance efficient straightaway flight performance with good handling in the pylon turns. Ailerons, rudder, and elevator flight controls provide the desired 3-axis handling characteristics in pitch, roll, and yaw. Although maneuvering flaps offered potentially tighter turning, preliminary assessments concluded that significant velocity losses in the turns of this high wing loading, limited propulsion energy aircraft made flaps impractical for this year's effort. A removable horizontal and vertical stabilizer tail section facilitates any design changes resulting from flight tests with the heavy payload.

## 4. Preliminary Design

The preliminary design phase focused on optimizing overall theoretical performance of the aircraft. Once the basic configuration was agreed upon, the team began evaluating specific design points to estimate the potential degree of success associated with each. The basic design parameters and sizing trades investigated include: propulsion systems, airfoil candidates, aspect ratio, wing area, and control surface selection and sizing, and takeoff performance. Each parameter was chosen to support one of the following design or mission features: level flight speed, lap time, maximum laps completed in seven minutes, and turning performance.

### *1. Propulsion System Selection and Sizing*

The propulsion system was designed with the help of the ElectriCalc software program. Driving factors behind final system selection focused on current drain, overall system efficiency, cruise speed in level flight, overall thrust produced and climbout angle.

The team felt that propulsion system current drain was a significant factor in selecting a final propulsion system due to the allowed duration of the pylon portion of the flight--seven minutes. Selection of a propulsion system that would not drain the power supply in less than seven minutes (plus an additional margin of safety) was critical to satisfy flight constraints. Larger motor systems could potentially provide additional thrust and, therefore, increase flight speeds for short periods of time. However, this current drain would deplete the available power too quickly. Smaller systems could be relied on to last the duration of the race, but do not provide the desired thrust.

Initial calculations of available battery capacity and average current drain yielded valuable information and aided in propulsion system downselection. Inquiries to battery suppliers provided data that 19 Nickel Cadmium cells rated at 2000 mah (average) would produce 22.8 volts (average); 2000 mah was equivalent to 120 amp-minutes of total battery capacity. The team felt that the best strategy would be to deplete the 120 amp-minutes during the 7 minute timed portion of the flight, plus an extra minute of powered flight to account for extra current drain during takeoff and landing. With a baselined 8 minute flight, an average current drain of 15 amps was computed. This initial assessment was felt to be about 10% conservative since currently available



cells were rated at 2200 mah whereas 2000 mah was used in our calculations ( $2000/2200=.909$ , yielding the calculated 10% margin mentioned above). Preliminary sizing analysis was necessary during the preliminary design phase since an assessment of the duration and delivered power of the batter pack was critical to final mission planning and analysis.

Critical to meeting the team's goal of completing the maximum number of laps in seven minutes and efficient flight around the pylons is the cruise speed of the aircraft in level flight and the net thrust of the propulsion system itself. Again, a trade-off was necessary here to optimize the cruise speed while, at the same time, selecting a propulsion system that would provide both the required range and endurance.

Climbout angle was also evaluated and compared for various propulsive configurations. A high climbout angle allows the aircraft to reach the desired cruise altitude in a shorter amount of time. However, a higher climbout angle consumes more power and, therefore, leaves less energy for the 7 minute portion of the flight. Again, these trades were evaluated and the final system was selected to optimize each of the above constraints as much as possible.

## ***II. Airfoil Selection***

Airfoil selection was based on a rigorous set of performance analyses baselined around the competition course layout. Seven airfoils were analytically compared for their performance both in straight line cruising flight as well as pylon turning performance. Wing aspect ratio, wing taper, and wing twist were also evaluated as part of the performance evaluations.

The performance metric minimized and evaluated was the lap time for a constant power setting. From here, the aerodynamics team calculated the total number of laps the proposed airfoil design and baseline aircraft design could complete in the allotted seven minutes. The optimization strategy for the straight legs of the race called for the maximum attainable velocity in cruise for a given configuration. However, since traversing the course successfully includes turning, bank angles must be accounted for in the final airfoil selection. Minimum turning time requires a compromise between the bank angle and the cornering velocity. The goal is to maximize bank angle and velocity simultaneously to create a minimum turning radius and turn time.

One major problem with evaluating the turning legs and straight legs of the course independently is the velocity discontinuities at the flight boundaries. In reality, the aircraft would

experience an acceleration at the beginning of a turn that would provide a smooth transition between the two legs of the flight. For simplification, the aerodynamics team chose to include the velocity discontinuities and evaluate the airfoil configurations for each leg of flight independently.

The baseline airfoils evaluated are shown in Table 2 below along with their calculated straight leg and turn time. A rectangular wing shape was assumed for initial calculations. Table 2 also includes a rank of the evaluated airfoils based upon total calculated lap time:

**Table 2: Baseline Airfoil Rankings**

Airfoil	Straight Time [s]	Turn Time [s]	Total Time [s]	Rank
Clark Y	13.550	5.908	19.458	1
RG-15	13.400	6.094	19.494	2
E214	14.021	5.540	19.561	3
SD2030	13.506	6.155	19.661	4
E205B	13.605	6.215	19.825	5
E193	13.754	6.097	19.851	6
E374	18.334	6.576	19.910	7

From the baseline design rankings, the Clark Y airfoil was chosen to conduct further design modifications to optimize performance. The possible modifications centered around incorporating taper and geometric twist into the wing design. The initial efficiency factor for the rectangular Clark Y airfoil was around 0.9. Calculating the optimum efficiency versus taper ratio for the given wingspan and Clark Y performance approximations estimated that maximum efficiency (0.97) occurs at a taper ratio of 0.4. Adding an element of geometric twist into the wing design did not show significant reduction in lap time, and the team decided that the associated difficulty in manufacturing was not worth the nearly insignificant time advantage.

### **III. Aspect Ratio**

Closely parallel to selecting the airfoil was designing a wing with an appropriate aspect ratio. Using information about system efficiency versus a wing taper ratio, and keeping in

mind an estimate of desired wing area and wingspan, the aerodynamics team decided upon an aspect ratio of 12.8 to minimize lap time and maximize overall flight performance.

#### ***IV. Wing Area***

The total wing area was decided upon using two methods. First, the ElectriCalc program generated flight performance data based on a chosen propulsion system. The generated spreadsheet yielded information about stall criteria and maximum cruise speed. From ElectriCalc, the two initial estimates suggested by the design team, 750 in<sup>2</sup> and 1000 in<sup>2</sup>, were analyzed and compared. The calculations indicated that the smaller wing's higher wing loading would present takeoff, landing and handling problems. While the larger wing did not show the same problem, the overall cruise speed was less than what the team was attempting to achieve. With these factors in mind, the team decided to move forward with a total wing area of 830 in<sup>2</sup> in an attempt to compromise between the two design considerations mentioned above. The second method of analysis was the use of an electronic, PC-based simulator program, the NHP/CSM Radio Controlled Flight Simulator which has an extensive design library. Again, the mid-sized (830 in<sup>2</sup>) wing demonstrated the best overall handling and flight qualities.

#### ***V. Control Surface Selection and Sizing***

Four configurations were discussed and evaluated for the design of the control surfaces: flaps, V-tails, T-tails and ailerons. While reliable and relatively easy to build, the use of flaps indicated a degradation in speed around the pylons, and the team was not willing to intentionally compromise one of the most critical flight elements. Since this is the first MIT team to enter the competition, the overall design tended to be somewhat conservative, and the V-tail design was decided to be too risky for further consideration. The T-tail was more feasible in terms of flight performance, but was too damage-prone to be seriously considered for the final design. In the end, ailerons were selected as the control surface of choice due to its relatively predictable flight characteristics.

The size of the control surfaces was, again, simulated in the NHP/CSM program the same as was the case with the designing the overall wing area. Final numbers for these surfaces can be found in Section 5. Control surface size was decided upon to maximize turning performance and handling qualities and not detract from the overall goal of minimizing lap time.

The accuracies of Electri-Calc and the NHP/CSM analysis program was felt to be no better than 10% on the optimistic side due to various simulation assumptions. However, these two tools were invaluable in their ability to generate consistent trends in data for sizing, performance prediction and overall handling.

## 5. Detail Design

### 1. Component selection and systems architecture

MIT's final design is a high wing monoplane with a Clark Y wing airfoil, powered by a geared Aveox 1406/4Y brushless electric motor, and a "pod and boom" fuselage with a composite-reinforced plywood forward fuselage and a carbon fiber boom rear fuselage. The 103" span wing planform has an aspect ratio of 12.8 and features a triple tapered leading edge configuration with a straight trailing edge to provide a tailored spanwise lift distribution. The wing's main panel is a 70" long flat center section with an 11" root chord at centerline. Two tip panels mounted with 10 degrees dihedral enhances stability & control handling performance in the pylon turns. Total wing area is 930 square inches. The wing structure is hot wire-cut blue foam covered with 1/16" balsa vacuum bagged to the wing cores with West Systems epoxy, and with carbon fiber mat and a composite spar to carry bending loads. Without the 7.5 pound payload, the aircraft's wing loading is 18.6 ounces/sq ft; carrying the payload, the wing loading doubles to 37.2 ounces/sq ft.

The G-load capability of the aircraft's wing, the primary loads carrying member, was computed to have a 4.6 Safety Factor based on the compressive strength of the blue foam, the composite-reinforced main spar, carbon fiber mat reinforcement, and the balsa sheeting epoxied to the foam cores.

The electric propulsion system uses an Aveox 1406/4Y brushless electric motor with a power pack consisting of 19 Nickel Cadmium Sanyo 2000 SCRC cells. A 3.78:1 Planeta all-metal gear box provides the gear reduction required to turn large props while still maintaining a co-axial in-line motor configuration. An Aveox H-60 electronic speed control provides proportional speed control of the Aveox motor.

The radio control system chosen is an Airtronics Stylus computer radio transmitter driving an Airtronics 7 channel PCM receiver; receiver and servo power is provided by a Cermak 600 mah Nickel Cadmium battery. Lateral control is provided by two JR341 micro servos, mounted outboard in the wing panels, each driving separate wing ailerons. Elevator and rudder control is by JR341 micro servos mounted at the tail surfaces to minimize the control system complexity and flutter of long control linkages.

The ailerons, horizontal and vertical stabilizers were sized to provide excellent handling qualities throughout the flight envelope while carrying the required payload. The layout and



configuration of the wing's two ailerons is patterned after competition aircraft designed for FAI International Class F3B competitive glider events.

The 249 square inch horizontal stabilizer contributes to a 0.80 tail volume coefficient, deliberately conservative to provide strong stability & control attributes flying with or without the steel payload. The vertical stabilizer is similarly sized to provide strong stability contributions considered to be crucial for efficient pylon turns in varying wind conditions. The horizontal and vertical stabilizer are removable from the fuselage to facilitate transportation and handling.

## ***II. Predicted performance***

To provide the required endurance and a competitive range, the total aircraft design was optimized to provide high cruise speed, efficient turning performance, and sufficient performance margin to take off, complete a competitive number of pylon laps, and land within the specified landing zone. The predicted performance of MIT's entry, using a 11x7 APC composite propeller, is as follows:

Takeoff performance, rate of climb: 336 feet/min. @ 25 mph

Maximum speed in level flight: 52 mph.

Maximum number of laps in 7 minutes: 21

Stall speed: 23 mph

Propeller RPMs at maximum speed: 8410 rpm

Propulsion system action time: 8 minutes, 36 seconds

Payload fraction: 50%

Cost reduction steps: To hold down costs, readily available and inexpensive materials were used for primary construction. The wing cores were cut from blue plastic foam material ordinarily used for house insulation. The wing cores were sheeted with 1/16" balsa rather than

expensive layups of composite material. The heart of the main wing spar is a common hardware store yardstick positioned on its edge. The fuselage cargo section is made of 1/16" plywood. And the horizontal and vertical stabilizers are constructed from balsa wood and covered with Monokote left over from other student projects. Overall, the MIT entry is made up of extremely inexpensive materials.



## 6. Manufacturing Plan

Manufacturing processes investigated:

From the inception of the project, the undergraduate projects teams were very focused on the manufacturing processes required to construct their entry. After all, an ultra-high performance aircraft wouldn't be competitive if it wasn't completed in time for flight tests before the competition or in the worst case, not finished at all! The following manufacturing techniques were proposed and evaluated:

- a. All built up wing construction. This construction approach uses conventional "rib and spar" model aircraft construction to assemble the primary wing structure. Materials would consist primarily of balsa, spruce, and plywood, and covering would be Monokote for rigidity. The primary attribute of this approach was the potential for light structural weight. The principal disadvantages were the high skill levels required for assembly, the many hours required for the actual construction, and high repair times in event of significant damage.
- b. All composite wing structure over foam substrate. This construction technique uses several overlapping layers of fiberglass and carbon fiber vacuum bagged over a hot wire-cut foam substrate. Its primary attribute is the speed of assembly as well as high strength. A disadvantage is a degree of uncertainty of the selection of the proper number of composite layers applied as well as the choice of composite grades for optimum strength to weight characteristics.
- c. Molded composite wings. This approach fabricates top and bottom wing composite shells in custom molds, with the shells then joined with a single internal spar and at the leading edges and trailing edges. This technique offers extremely high dimensional accuracy and high strength-to-weight characteristics. Disadvantages are the time and effort required to fabricate the required molds, as well as the proper selection of the composite materials.
- d. Balsa sheeted wings vacuum bagged over foam substrate. This construction technique has the primary advantage of ease of fabrication as well as fast assembly time. A minor disadvantage is the requirement to edge glue and finish sand multiple sheets of balsa wood prior to the vacuum bagging processes.

e. Obechi sheeted wings vacuum bagged over foam substrate. This technique avoids the edge-gluing required for balsa sheet since obechi sheet can be ordered in sheets long and wide enough to cover entire wing panels with a single piece. A minor disadvantage is that due to its extreme thinness (approximately 1/32"), use of obechi requires that the foam cores be cut to an extremely high tolerance.

f. Fuselage: all composite forward fuselage. Fabrication of a custom mold for the forward fuselage would provide a low drag fuselage with high strength and minimum weight. A major disadvantage would be the first-time non-recurring design effort required for this approach.

g. Fuselage: reinforced plywood forward fuselage. This approach has the primary advantages of requiring fairly low skill levels and being relatively low cost, as well as being suitable for late-breaking modifications with minimum effort.

h. Horizontal and vertical stabilizers: composite over foam, balsa over foam, and built up structure. The principal trade here was between the aerodynamic advantages of wire cut foam structure, sheeted with a lightweight material, versus the speed, ease of fabrication, and light weight of a conventional balsa assembly.

The following FOMs were used to screen the candidate manufacturing processes described above. A perfect score would total 75 points.

- FOM #1, Availability (10 points). This criteria encompassed the time and effort required to procure the supplies, materials, and equipment needed for manufacture and assembly.
- FOM #2, Required skills (15 points). This item ranked various manufacturing processes against the craftsman skills needed.
- FOM #3, Materials cost (15 points). This metric assessed the costs of materials and adhesives required for each manufacturing process.
- FOM #4, Manufacturing time (10 points). Included in this metric was the setup time, actual construction time, and additional time required to final finish components.

- FOM #5, Repair and maintenance requirements (10 points). This factor assessed the possible time to repair aircraft items if damaged during testing.
- FOM #6, Minimizing technical and schedule risk (15 points). Similar to the FOM#5 used in Conceptual Design, this metric was a management assessment of the riskiness of each proposed manufacturing candidate.

**Table 3: Manufacturing Figures of Merit**

Config.	FOM #1 (10)	FOM#2 (15)	FOM#3 (15)	FOM#4 (10)	FOM#5 (10)	FOM#6 (15)	Total (75)	Rank
built up wing	10	4	12	4	2	3	35	4
all comp. wing, foam	8	10	5	7	7	5	42	3
molded comp. wing	2	3	2	2	3	5	17	5
balsa, foam wing	10	12	12	8	8	13	63	1*
Obe- chi, foam wing	7	10	10	6	6	10	49	2
all comp fuse- lage	6	5	8	10	5	7	41	2
rein- forced ply- wood fus.	10	10	15	12	9	14	70	1*

**Table 3: Manufacturing Figures of Merit**

Config.	FOM #1 (10)	FOM#2 (15)	FOM#3 (15)	FOM#4 (10)	FOM#5 (10)	FOM#6 (15)	Total (75)	Rank
comp., foam stabi- lizers	8	10	10	7	8	10	53	3
balsa, foam stabil.	10	12	12	8	8	13	63	2
built- up sta- bil.	10	15	15	8	9	14	71	1*

### *III. Results of final selection of manufacturing processes*

As shown in Table 3, the candidate manufacturing processes were evaluated against the 6 FOMs above. For the wing, vacuum-bagged balsa over foam was the final selection. For the fuselage, the low risk reinforced plywood approach won out over the all-composite fuselage approach. For the stabilizers, the ease, light weight, and minimum risk approach of an all-built-up structure was the final choice.

### *IV. Manufacturing Milestones*

Task	Time Span - planned	actuals
<b>Fuselage Construction</b>	6-20 January	6-20 January
- fab forward fuselage	6-10 Jan	8-10 Jan
- install carbon boom	10-12 Jan	12-15 Jan
- add composite reinf.	12-15 Jan	15-17 Jan
- install stab platform	15-17 Jan	17-20 Jan
- final cleanup	17-20 Jan	17-20 Jan
<b>Wing Construction</b>	13 Jan - 9 Feb	13 Jan - 17 Feb
- cut wing cores	13 Jan - 20 Jan	23 Jan - 2 Feb
- prep balsa sheets	13 Jan - 20 Jan	23 Jan - 26 Jan
- install spar and wiring	20 Jan - 25 Jan	27 Jan - 3 Feb

- vacuum bag ops        25 Jan - 28 Jan

3 Feb - 6 Feb

- final trimming, finishing 28 Jan - 9 Feb

8 Feb - 17 Feb

**Stabilizer Construction** 13 Jan - 20 Jan

20 Jan - 3 Feb

- layout and framing     13 Jan - 18 Jan

20 Jan - 25 Jan

- covering                19 Jan- 20 Jan

28 Jan - 3 Feb

**1997-1998 Cessna/ONR/AIAA  
Student Design/Build/Fly Competition**

**Design Report - Addendum Phase**

**Section 7: Lessons Learned:**

Progress to date on MIT's AIAA D/B/F project has in general fully met the expectations of the group. Although construction started later than initially planned, hard work between the Fall and Spring semesters produced an airframe that achieved first flight in early March, a satisfying and very key milestone in the overall program. Flight tests to date have confirmed satisfactory performance and handling characteristics, as well as allowing the team to gain experience with the Airtronics Stylus radio control system and the Aveox brushless electric propulsion system. The current emphasis is on accumulating flight experience with incrementally increasing payload weights and the team is cautiously optimistic that they will be able to successfully complete their official flights at the Wichita flyoffs in late April.

The basic design of MIT's final contest aircraft is unchanged from the design detailed in the Proposal. Based on the flight test program, there may be some minor changes to the landing gear due to the landing loads imposed by the ballast. There are no changes being planned for the aerodynamic surfaces or the fuselage structure.

For second generation designs to be flown in future competitions, the students have identified several promising areas of improvement for both design and manufacturing. In the area of design, the students plan to investigate improvements in streamlining, increased use of composite structures, aerodynamic improvements, and airfoils optimized for the competition's performance requirements. In the manufacturing sector, the MIT team intends to make only relatively minor changes to the basic manufacturing processes used on this year's first generation aircraft.

The design changes, aerodynamic improvements, and manufacturing changes being considered for a second generation

aircraft are relatively minor. At this time, the most significant manufacturing change being considered is to build a new wing, replacing the present balsa sheeting covering with fiberglass and carbon fiber laminates. The cost required to do this is estimated to be approximately \$25 for materials (composites, West Systems epoxy), and there should be a net time savings estimated to be approximately 10% due to less preparatory effort required.

Following the conclusion of the 1998 competition effort, the team will map out their plans for fielding an entry for the 1998-1999 competition. As the competition in Wichita is expected to be very intense, the MIT team will develop their development strategies based on the results

#### Manufacturers' List Prices for materials, components, and systems:

- a. Radio control equipment
  - Airtronics Stylus 8 channel radio; transmitter, receiver, battery \$700
  - 4 JR 341 micro servos @ \$50 \$200
- b. Electric propulsion equipment
  - Aveox 1406/4Y brushless motor \$152
  - Aveox M-60 electronic speed control \$200
  - Planeta 3.78:1 gearbox \$117
  - 3 19 cell Sanyo S2000 SCRC battery packs @ \$175 \$525
  - Astro Flight 112D digital peak charger \$165
  - APC 12x6 propeller \$ 4
- c. Structural material
  - blue foam \$ 10
  - 1/16" balsa sheeting \$ 20
  - carbon fiber boom \$ 5
  - 1/16" and 3/32" plywood \$ 8
  - Kevlar and fiberglass reinforcement \$20
  - plastic iron-on covering material \$12
- d) Miscellaneous
  - DuBro 3 1/2" wheels \$ 5
  - clevises, wheel retainers \$ 5

Compared to the cost estimates made during the design evaluations, the MIT team concluded that the uneventful development and flight test efforts did not cause significant cost changes to the basic approaches originally selected. The major percentage of the project's overall costs involved the electric propulsion system - the Aveox brushless motor, its speed control, flight batteries, and the digital peak detection charger - and the radio control system - Airtronics Stylus PCM transmitter, receiver, and micro servos. The actual cost of these components was satisfactorily covered by the budget estimates prepared at the onset of the program. The team's basic plan for next year is to re-use the radio control equipment and electric propulsion components purchased for this year's initial entry - thus the incremental expenses for assembling a new airframe should be quite low. These plans will change, of course, if there are significant changes in the competition rules for 1998-1999.



**Cessna / ONR**  
**Student Design/ Build/ Fly Competition**  
Proposal Phase



Submitted By:  
Oklahoma State University

Team Members:

Alan Anderson  
Adrianto Augustnine  
Joel Basler  
Anthony Boechman  
Ben Cantwell  
Joe Conner

Gary Lantz  
Yolanda Mack  
Jamie Morgan  
Vamsi Prakhya  
David Roberts  
Nick Scocos

## TABLE OF CONTENTS

EXECUTIVE SUMMARY .....	1
MANAGEMENT SUMMARY .....	3
PROJECT MILESTONES CHART .....	4
CONCEPTUAL DESIGN .....	5
PRELIMINARY DESIGN .....	8
DETAIL DESIGN .....	14
FINAL AIRCRAFT STATIC'S , PERFORMANCE AND DRAWINGS .....	15
MANUFACTURING PLAN .....	20
MANUFACTURING MILESTONES CHART .....	23

## LIST OF FIGURES AND TABLES

FIGURE 1 RANGE VERSUS LEVEL FLIGHT SPEED WITH VARYING ASPECT RATIOS .....	8
FIGURE 2 RANGE VERSUS LEVEL FLIGHT SPEED WITH VARYING WEIGHT .....	9
FIGURE 3 DRAG FORCE VERSUS REAR FUSELAGE LENGTH.....	10
FIGURE 4 POWER REQUIREMENTS VERSUS LEVEL FLIGHT SPEED WITH VARYING ASPECT RATIO .....	11
FIGURE 5 POWER REQUIREMENTS VERSUS LEVEL FLIGHT SPEED WITH VARYING WEIGHT .....	12
FIGURE 6 POWER REMAINING VERSUS GROUND ROLL DISTANCE WITH VARYING WEIGHT.....	13
FIGURE 7 POWER REMAINING VERSUS CLIMB-OUT DISTANCE WITH VARYING WEIGHT .....	13
TABLE 1 FUSELAGE FOM .....	5
TABLE 2 WING FOM.....	6
TABLE 3 TAIL FOM .....	6
TABLE 4 GEAR FOM.....	7
TABLE 5 MANUFACTURING METHOD FOM .....	20
TABLE 6 AIRCRAFT COST ESTIMATES .....	22

## Executive Summary

A group of engineering students from differing academic statuses and technical backgrounds were given the task of designing and building an aircraft that would complete and win the AIAA Student Design Contest. The first major step in the designing an aircraft is the conceptual design phase. During the conceptual design phase, we laid out the major requirements and restrictions for the aircraft to meet the contest regulations, which includes:

- Must be propeller driven.
- Must use over the counter batteries for propulsion power.
- Must have a removable 7.5 pound steel payload
- Must make an un-assisted takeoff within 300 feet and clear a six foot obstacle.
- Complete as many laps as possible within seven minutes.
- Must successfully land in with in the same 300 foot distance.

With all these major requirements found, the major governing equations for the differing flight phases were developed. The development of the equations was done mainly by hand, with the use of MathCAD to aid in simplification. These major equations can be grouped into three phases:

- Ground Roll

$$T - D - \mu \cdot F_n = \frac{W}{g} \cdot a$$

- Rate of Climb

$$\text{rate\_of\_climb} = \frac{(T - D) \cdot v}{W}$$

- Level Flight

$$R = v \cdot t = \frac{v \cdot \eta \cdot T \cdot \text{cap}}{P_{\text{req}}} = \frac{v \cdot \eta \cdot T \cdot \text{cap}}{D \cdot v} = \eta \cdot \frac{T \cdot \text{cap}}{D}$$

$$P_{\text{req}} = \frac{1}{2} \cdot C_{d0} \cdot \frac{C_l^2}{(\pi \cdot AR)} \cdot \rho \cdot v^3 \cdot S$$

Now that the major governing equations had been found, we began to look at the equations to determine the major factors of the equationse. We discovered that by analyzing the Level Flight phase we had three major factors which controlled range of the aircraft. These three items were:

1.  $\eta_T$  Propulsion system efficiency.
2.  $\text{cap}$  Total energy capacity of the battery pack.
3.  $D$  Total Drag on the aircraft.

It can clearly be seen that as  $\eta_T$  or *cap* are increased and D is decreased the range or number of laps will also increase. From this equation we found that the aircraft needed to have minimum drag, maximized propulsion system efficiency and energy capacity of the batteries. With this in mind we moved on to the next phase which required all team members to submit a sketch of their idea of the final aircraft. These ideas as well as some other historical ideas were then broken apart into the major components of an aircraft. These components are the fuselage, main wing, tail, propulsion system, and landing gear. All of the ideas for components were then 'scored' by factors such as drag, construction, and cost.

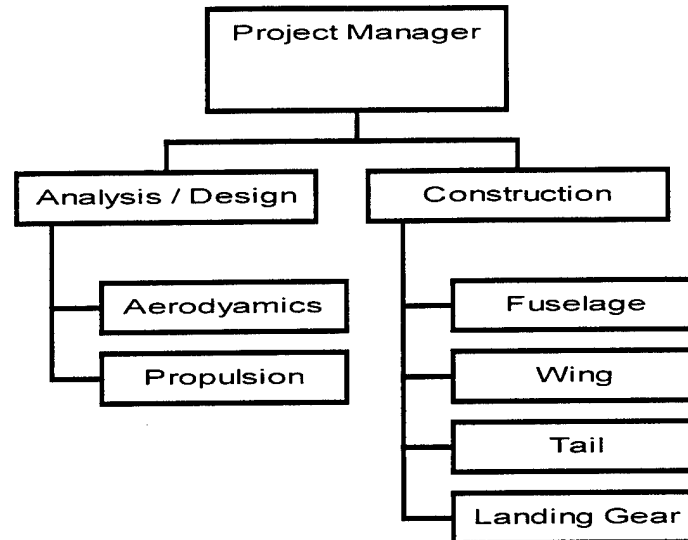
The next major step was the preliminary design phase. In this phase the major objective was to find out the power requirements for level flight for differing designs. In this step we made almost exclusive usage of a spreadsheet to analyze and graph the effect of major design elements of the wing such as aspect ratio, total weight, velocity, and time in flight on the range. It was found from these results that the only major factors on this phase of flight was time and velocity. Since the other factors did not appear to effect this phase of flight, we then analyzed the ground roll and rate of climb phases. Both of these phases also involved the use of a spreadsheet.

It was found that aspect ratio and total weight did effect both of these phases. The next major step was to tie these three phases together and try to find a final design that worked in all three phases, while still giving maximum range. This was also done in a spreadsheet so that changes made in the basic aircraft design could be seen in all three phases. Next the rear fuselage and tail, sizing was analyzed by use of a spreadsheet to find the minimum drag caused by a combination of the rear fuselage and tail surfaces. Finally, the best propulsion system was found by use of a FORTRAN program written to analyze the best combination of battery packs and motor. With these results we moved to the detailed design stage.

The detailed design phase was where all major components were sized and brought together for the first time. It is during this phase that the best propulsion system was used to size the remaining components. The main wing design used the same spreadsheet utilized in the preliminary design phase. The main objective for the main wing was to find a wing that would allow the aircraft to get off the ground with minimum power. After the main wing was found and sized, the tail surface was sized. To size the V-tail, the information from the best tail of the preliminary phase was used and then sized accordingly. With the tail now sized, the forward fuselage was sized. This was done so that the moment created by the tail surface was canceled by the moment created by the motor. This would have the effect of keeping the center of gravity where we needed it. Now that the entire fuselage length was known, the landing gear was designed and placed. This was done by simple analysis of rotation required for takeoff and prohibiting the tail from touching the runway. With all major components sized and location known, detailed AutoCAD drawings and a building materials list were created.

## Management Summary

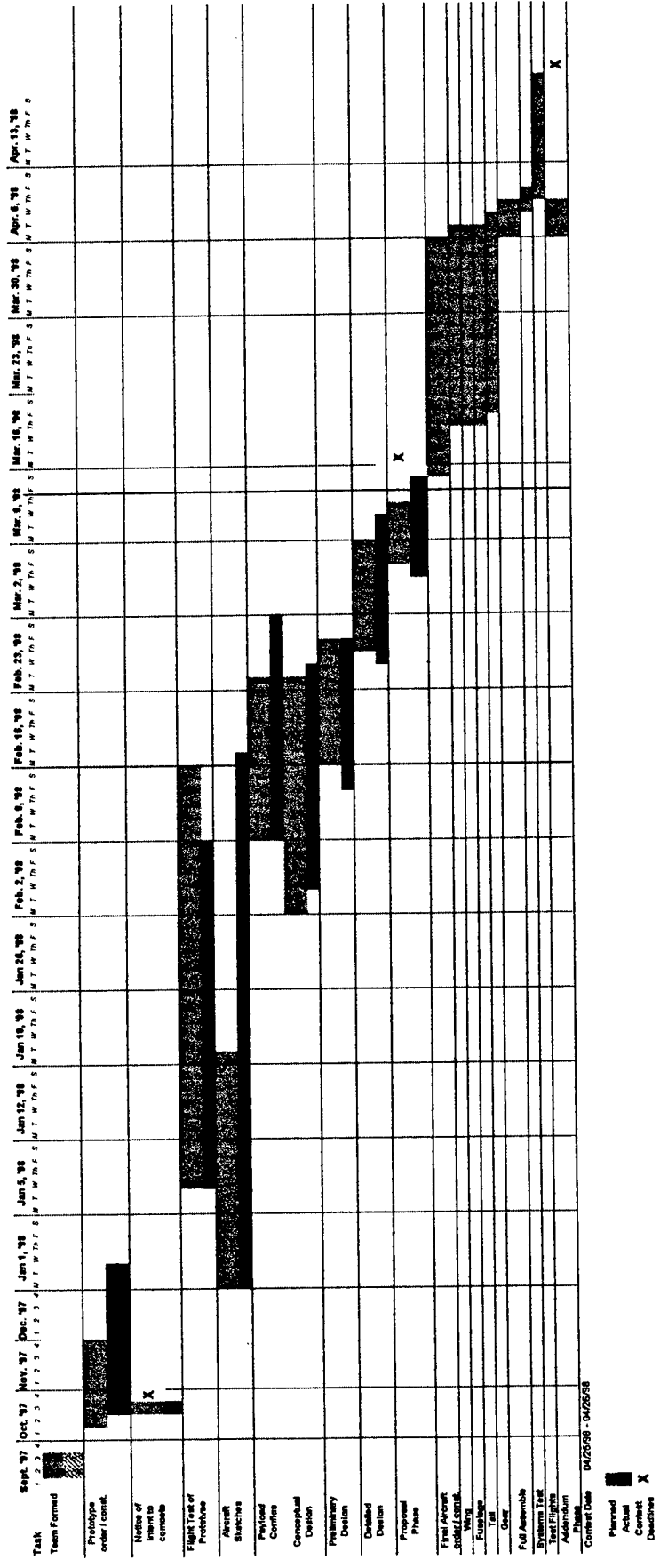
The team was broken into two major sections which were analysis/design and construction. While there were two sections, all member weres involved in parts of both sections depending on their knowledge and skill level. The basic team layout is as follows:



The team break down:

- Project Manager Joe Conner
- Analysis / Design
  - Aerodyamics Gary Lantz, Nick Scocos, Vamsi Prakhya
  - Propulsion Alan Anderson, Adrianto Augustnine
- Construction
  - Fuselage Ben Cantwell, Jamie Morgan
  - Wing Joel Basler, Yolanda Mack
  - Tail Anthony Boechman, David Roberts
  - Landing Gear Ben Cantwell, Anthony Boechman

While this is the assigned tasks for each member, no one was locked into the group of which they were assigned to; members could freely help out any group of which they found interest in. There were, however, some items such as airfoil research and conceptual sketches which were completed by all members. All of the major events which occured during this project are shown on the following milestone chart.

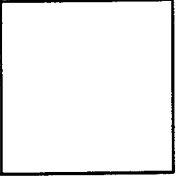
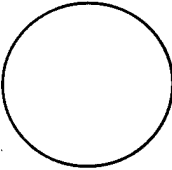
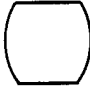


Project Scheduling (Milestones)

## Conceptual Design

Before this phase began, team members were asked to submit several sketches depicting their conceptualization of the plane. This information was then compiled and used to aid the conceptual design. The ideas from each sketch were then broken into the following components: fuselage, tail configuration, main wing shape, and landing gear. Each of the following were then analyzed for the effects on fabrication, drag, weight, controllability, and efficiency.

**Fuselage**

Shape	Advantages	Disadvantages
Square 	<ul style="list-style-type: none"> <li>• Easy to mount wing and land gear.</li> <li>• Easy to fabricate</li> <li>• High efficient fit for required payload shape.</li> <li>• Low Weight</li> </ul>	<ul style="list-style-type: none"> <li>• Low to Moderate Drag</li> </ul>
Circular 	<ul style="list-style-type: none"> <li>• Low Drag</li> </ul>	<ul style="list-style-type: none"> <li>• Difficult to fabricate</li> <li>• Low efficient fit for required payload shape</li> <li>• Difficult to mount wing and landing gear.</li> <li>• Stringers required</li> </ul>
Elliptic 	<ul style="list-style-type: none"> <li>• Low Drag</li> <li>• Easy to mount wing and landing gear.</li> <li>• Medium efficient fit for required payload shape.</li> </ul>	<ul style="list-style-type: none"> <li>• Difficult to fabricate.</li> <li>• Possible requirement of stringers in fuselage.</li> </ul>

**Table 1 Fuselage FOM**



## Wing



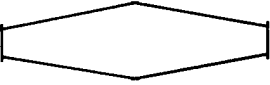
Shape	Advantages	Disadvantages
Elliptical 	<ul style="list-style-type: none"> <li>• Lowest induced Drag</li> <li>• Most efficient wing shape.</li> </ul>	<ul style="list-style-type: none"> <li>• Very Difficult to fabricate.</li> <li>• Entire wing stall at the same time.</li> <li>• Reynolds number varies across the span.</li> </ul>
Rectangular 	<ul style="list-style-type: none"> <li>• Constant Reynolds number across the span</li> <li>• Stalls at root first.</li> <li>• Very easy to fabricate</li> </ul>	<ul style="list-style-type: none"> <li>• Least efficient wing shape.</li> <li>• Heaviest wing shape</li> </ul>
Tapered 	<ul style="list-style-type: none"> <li>• Close to elliptical wing</li> <li>• High strength with optimum weight</li> <li>• Lighter than same size rectangular wing.</li> </ul>	<ul style="list-style-type: none"> <li>• Moderate to Difficult to fabricate.</li> <li>• Low Reynolds number effects.</li> <li>• Majority of the wing stall at the same time.</li> </ul>

Table 2 Wing FOM

## Tail




Shape	Advantages	Disadvantages
Conventional 	<ul style="list-style-type: none"> <li>• Adequate stability and control equations.</li> <li>• Lighter than T-Tail</li> <li>• Easy to fabricate.</li> <li>• Easy to control</li> </ul>	<ul style="list-style-type: none"> <li>• High Interference drag</li> <li>• Control surface shadowing on takeoff.</li> </ul>
T-Tail 	<ul style="list-style-type: none"> <li>• Moderate stability and control equations.</li> <li>• Allows smaller vertical Tail.</li> <li>• No shadowing on takeoff.</li> </ul>	<ul style="list-style-type: none"> <li>• Difficult to fabricate.</li> <li>• Heaviest tail.</li> <li>• Thickest vertical tail.</li> </ul>
V-Tail 	<ul style="list-style-type: none"> <li>• Lowest interference drag.</li> <li>• Easy to fabricate.</li> <li>• One less surface to build, but still same amount of surface area.</li> </ul>	<ul style="list-style-type: none"> <li>• Adverse roll effect if not designed correctly.</li> <li>• Fewer adequate stability and control equations.</li> </ul>

Table 3 Tail FOM

### Landing Gear

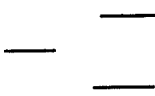
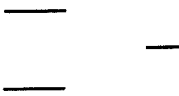
Shape	Advantages	Disadvantages
Tricycle Gear 	<ul style="list-style-type: none"> <li>• Easy to fabricate.</li> <li>• Very stable.</li> <li>• Lighter tail structure.</li> <li>• Easy to control</li> <li>• Low to Moderate Weight</li> </ul>	<ul style="list-style-type: none"> <li>• Moderate Weight</li> <li>• Moderate to Heavy Drag</li> </ul>
Tail Dragger 	<ul style="list-style-type: none"> <li>• Low Weight</li> </ul>	<ul style="list-style-type: none"> <li>• Moderate to fabricate.</li> <li>• Stability problems/ Ground looping</li> <li>• Heavier Tail structure.</li> <li>• More difficult to control.</li> <li>• Moderate Drag</li> </ul>
Retractable Gear	<ul style="list-style-type: none"> <li>• Low Drag</li> </ul>	<ul style="list-style-type: none"> <li>• Moderate to Difficult to fabricate.</li> <li>• Highest weight</li> <li>• Requires larger fuselage.</li> <li>• Requires onboard systems.</li> </ul>

Table 4 Gear FOM

Finally, each of the FOM were scored in the following order: Ease of fabrication, effect on drag, effect on weight, efficiency and finally controllability. From the above analysis we chose to investigate the following conceptual design:

Wing: Rectangular shape

Tail: V-Tail configuration

Fuselage: Square

Landing gear: Tricycle pattern

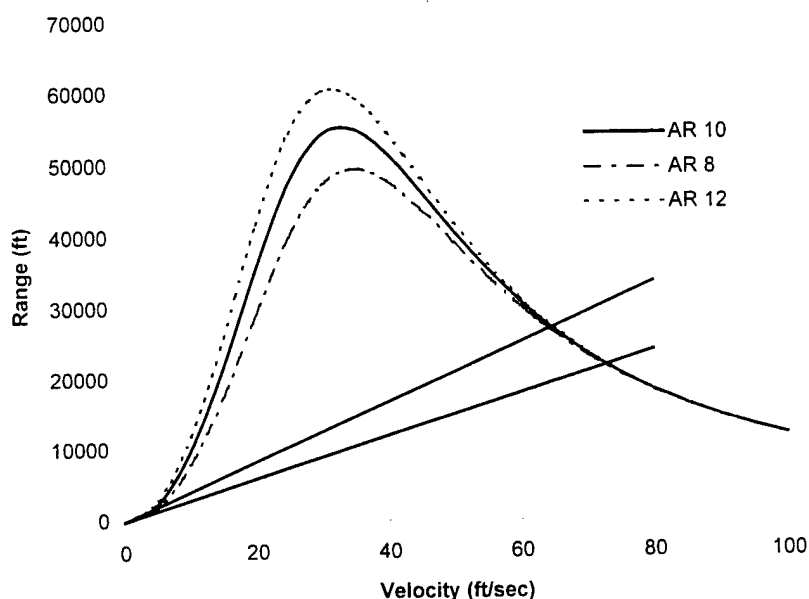
With this conceptual design, we next moved onto the Preliminary design.

## Preliminary Design

The major objective of this phase was to find out how to design each component of the aircraft to have the highest possible range and lowest drag effects. To do this we decided to divided the aircraft into the following major components: the wing, tail rear fuselage combination, and finally the propulsion system.

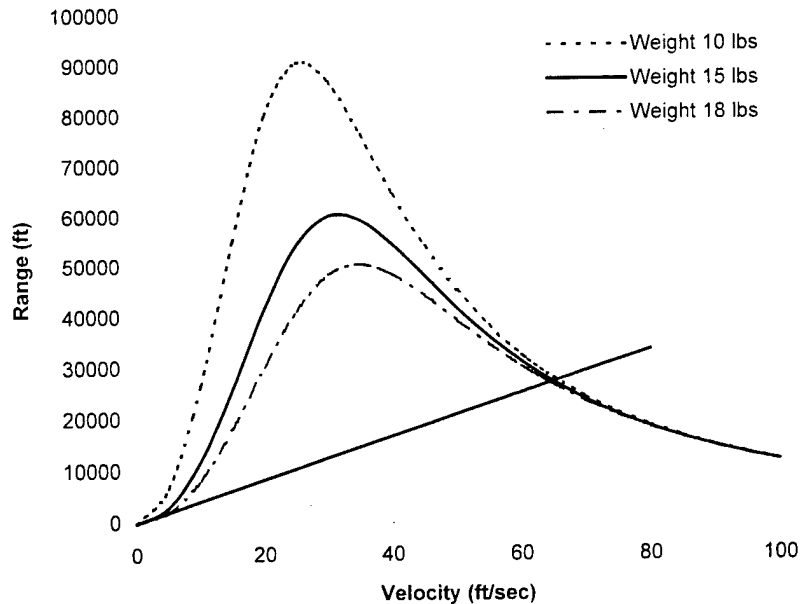
Since the wing was the major design component it was the first to be analyzed. The first item we analyzed was the effect of aspect ratio on the drag coefficient.. To do this, the aspect ratio was varied from a low of four to a high of seventeen. Simultaneously, the Reynolds number across the wing was also calculated. From this it was seen that an aspect ratio of 13 and above had a Reynolds number below 300,000 which leads to an increase in 'Wing Parasite drag'. It was also found that an aspect ratio of 7 and below was undesirable since the induced drag was very high in this region.

With this limit on aspect ratios found, the effect of the remaining aspect ratios on range was solved in a spreadsheet. This was done by varying the velocity from 0 to 100 ft/sec and then graphing the results. The results of this are shown in following graph:



**Figure 1 Range versus Level Flight Speed with varying Aspect Ratios**

The graph above clearly shows that aspect ratio has little or no effect at the maximum time of flight (7 min.). Since aspect ratio appears to have little effect on range, the total weight of the aircraft was investigated while holding the aspect ratio to be 10.



**Figure 2 Range versus Level Flight Speed with varying Weight**

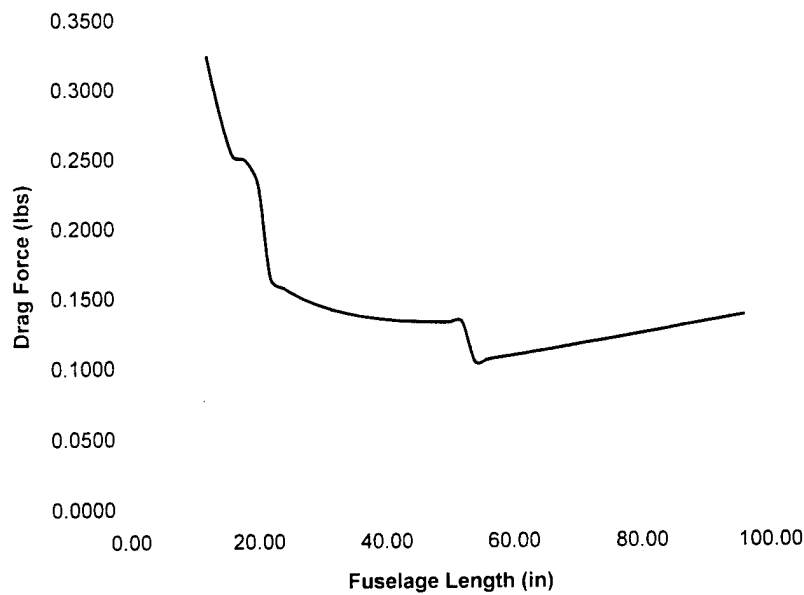
The results of the plot show that weight also has little effect at the seven minute time. However it was noted that both graphs appear to agree on the same velocity (approximately 65 ft/sec.) of flight at the given maximum time.

With the information gained from these two plots, a minimum coefficient of lift needed for level flight could be estimated. With this estimation a search for a feasible airfoil was made using the following Internet sites for airfoil characteristics and configuration:

- <http://beadec1.ea.bs.dlr.de/Airfoils/calcfoil.htm>
- [http://amber.aae.uiuc.edu/~m-selig/ads/coord\\_database.html#S](http://amber.aae.uiuc.edu/~m-selig/ads/coord_database.html#S)

With this preliminary configuration of the wing we then moved on to the tail surface.

Again, the major objective here was to minimize drag forces caused by the rear fuselage and tail surface. To do this, a spreadsheet was used to calculate the drag forces as a function of rear fuselage length. This analysis was done by finding drag forces of the fuselage and tail surfaces separately. The fuselage was modeled as a simple plate, of which the width was the fuselage perimeter and the length was the rear fuselage span. By varying the fuselage length from one to nine feet, the corresponding required tail surface was found by use of the standard stability and control equations. With the tail surface area now found we then calculated the drag force upon it by modeling the tail as a flat plate also. We then found the total drag force and plotted the results versus the rear fuselage length.



**Figure 3 Drag Force versus Rear Fuselage Length**

From the results of this analysis the minimum drag occurred at approximately 54 inches. Using this length, the corresponding vertical and horizontal tail surface areas were found to be 2.10 and 1.63 sq.ft. respectively, this gives a total tail surface area 3.72 sq.ft. Since a 'V' tail was chosen the dihedral angle of the V-tail needed to be found. The dihedral angle was found by using simple trigonometry.

With the preliminary design of the aircraft we headed for finding a propulsion system that supplied the needed power for the flight. Before we actually decided on the components of the system, we calculated the power requirements for every phase of the flight. We first calculated the power required for level flight using the spreadsheet for varying aspect ratios and then varying weight. The results are plotted in the graphs shown below.

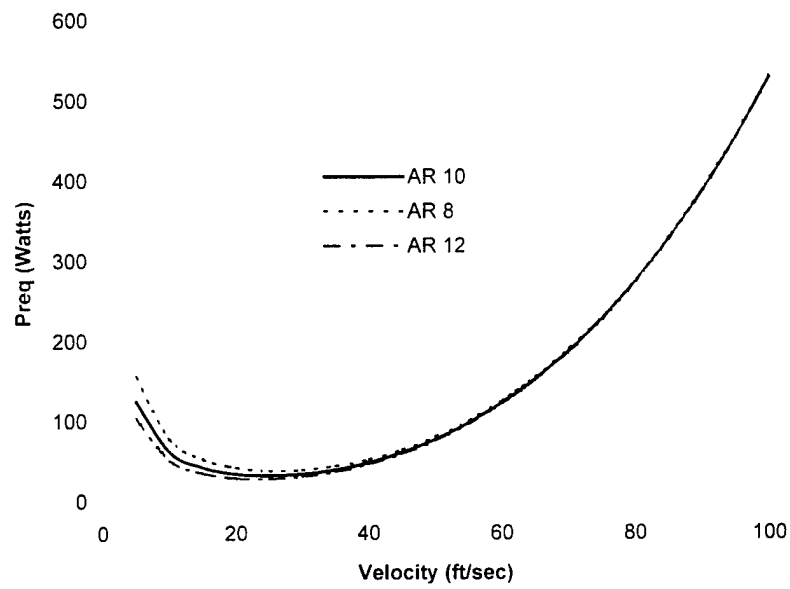
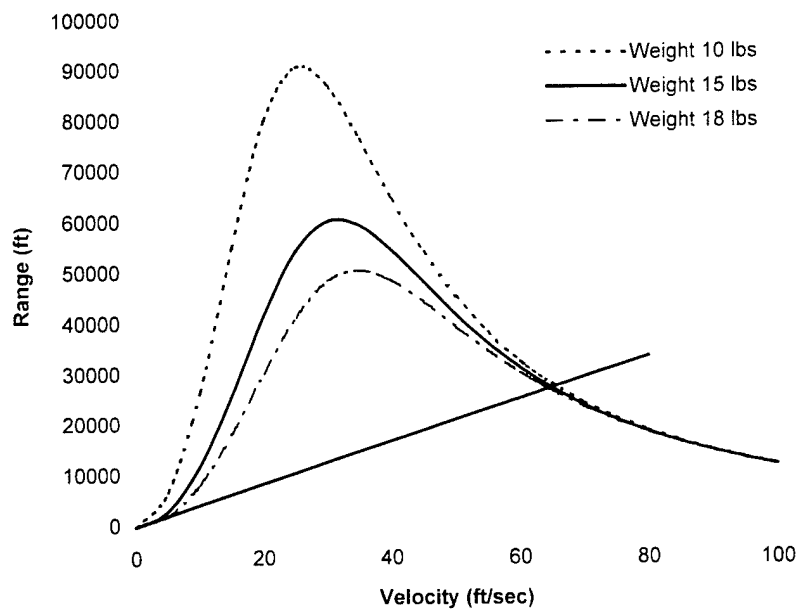


Figure 4 Power Requirements versus Level Flight Speed with varying Aspect Ratio



**Figure 5 Power Requirements versus Level Flight Speed with varying weight**

The above graph shows that at a flight velocity of approximately 65 ft/sec., the required power is approximately 175 watts.

With the required power estimated we searched for a motor-battery combination that could deliver the power most efficiently. This was done by using a FORTRAN program which analyzed hundreds of motor-battery combinations and filtered out combinations that had more than 20 batteries, lacked an endurance between five and eight minutes, less than at least 11.7 laps, and an overall efficiency below 78%. This limited the search to a low number of combinations which was then manually scanned to find the final combination.

With final power-pack found, we then analyzed the take-off phase. The take-off phase was broken into the two sub-phases, ground roll, and climb out.

The power required for both the phases can be found using standard equations. Power requirements found for these phases as well as the time involved results in the power remaining for level flight and landing. Results of weight on both phases can be seen in the graphs below.

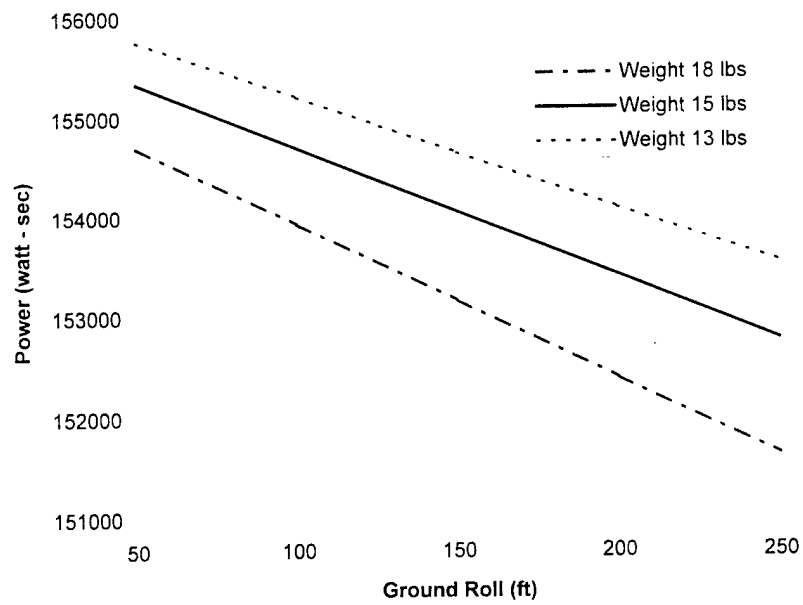


Figure 6 Power Remaining versus Ground Roll Distance with varying weight

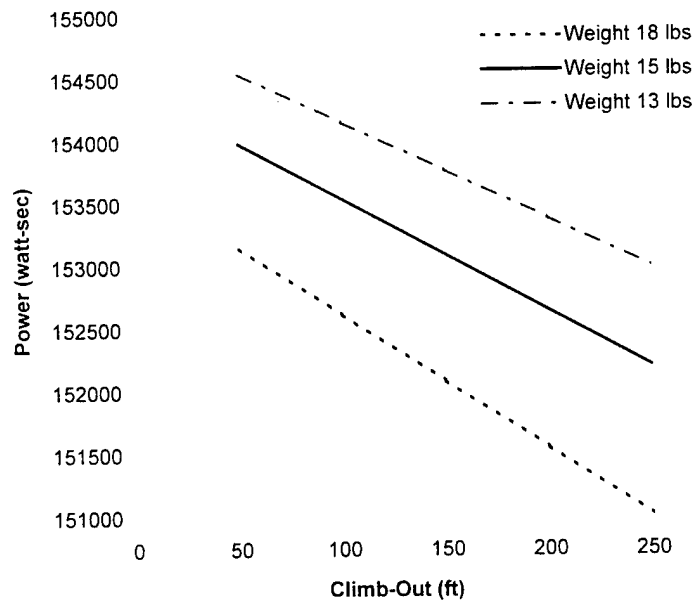


Figure 7 Power Remaining versus Climb-Out Distance with varying weight



## Detail Design

With the propulsion system selected and an overall system efficiency of 41 % (including the propeller losses and a large number of preliminary iterations) we decided to allow 325 watts for a level flight of 7 min., leaving 1.2 min. remaining for take-off and landing. To simplify controls, an aspect ratio of 10.5 was chosen so that the ground roll phase also require 325 watts, thus allowing a single throttle setting. With this power setting the flight speed was found to be 57.35 ft/sec. with a predicted weight of 15 lb. and a wing surface area of 12 sq.ft. The minimum coefficient of lift was found to be 0.32.

With these result the airfoil was selected, using the previous websites, to be one of several candidates: S3014, SD2030, and the SD2083. This group of airfoils allowed a safe maximum lift coefficient of 1.17 during take-off.. With this lift coefficient the ground roll distance was 150 ft. with a take-off velocity of 32.99 ft/sec. This ground roll distance leaves 150 ft. remaining to climb over the six foot obstacle. After a seven minute flight at 325 watts, a time of 0.85 min. remained for landing. In order to increase the wing's efficiency, lowering the induced drag but maintaining high Reynolds number across the majority of the wing, a taper at the wing tips was used. This taper begins at 3.5 feet from the root of the wing. To achieve the surface area previously established as well as the aspect ratio the root length was calculated to be 14.64 inches requiring the tip to be 6.88 inches. To aid in the manufacturing process, the rear of the wing will be held straight. Also, a dihedral angle of 6 deg. was chosen from historical records. With the main wing and tail now correctly sized, the length of the forward fuselage could then be calculated.

This was done by simply estimating the tail weight, then balancing the moments about the center of gravity caused by the motor and tail. This results in a forward fuselage length of 1.5 feet, and an overall fuselage length of 6 feet. The next major item to design was the spar.

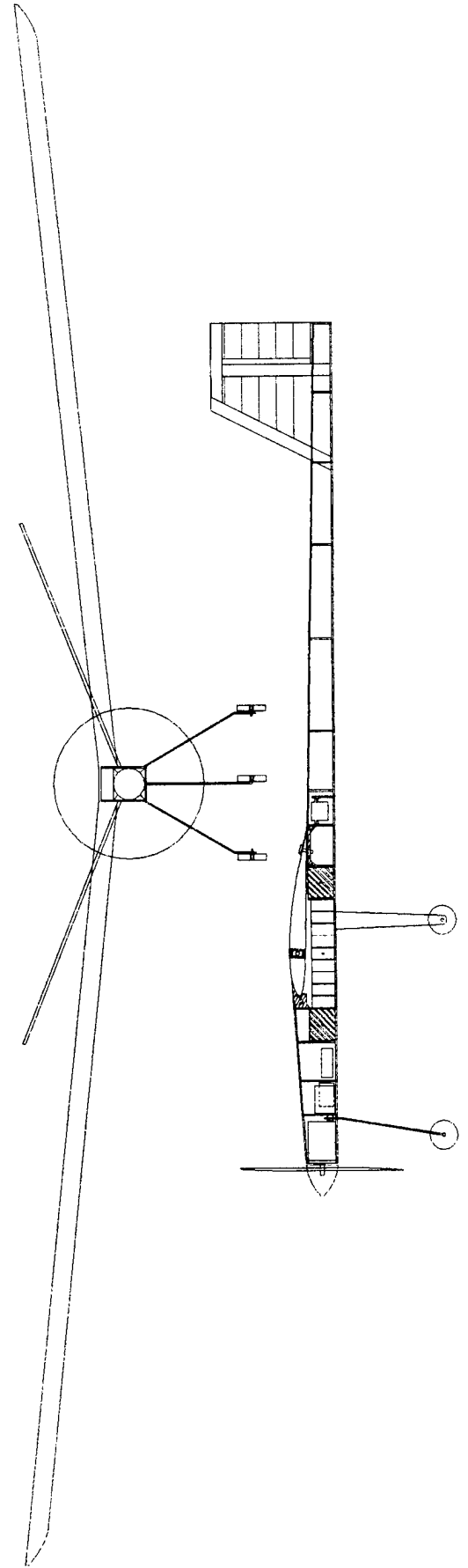
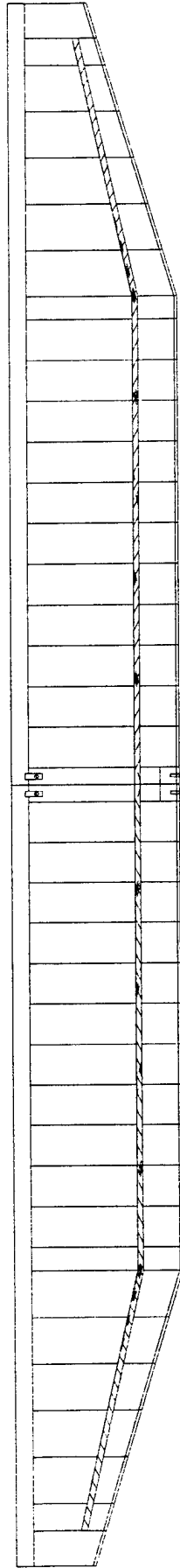
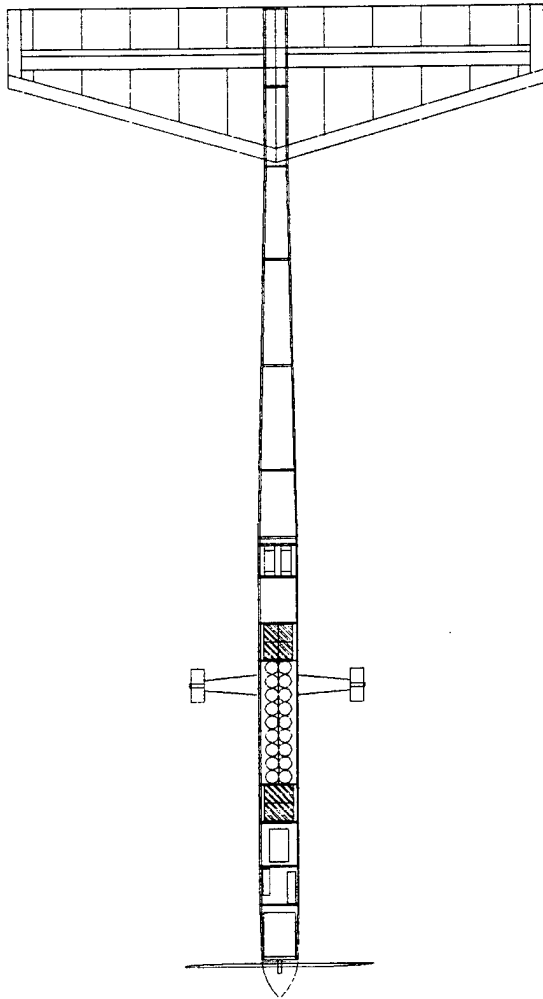
The spar is the main load bearing structure within the wing. To design this, the wing was modeled as a simple beam rigidly attached at one end. To accomplish this only half the wing span and half the total load would be modeled as a simple beam rigidly attached at one end. With this model established, and a load design of 2.5 g chosen the loads across the beam could be found. With this information, we found that the spar needed to be 0.5 inches in width and 1.5 inches in height. The candidate airfoils above were all eliminated except for S3014. The only other major item left to design was the landing gear.

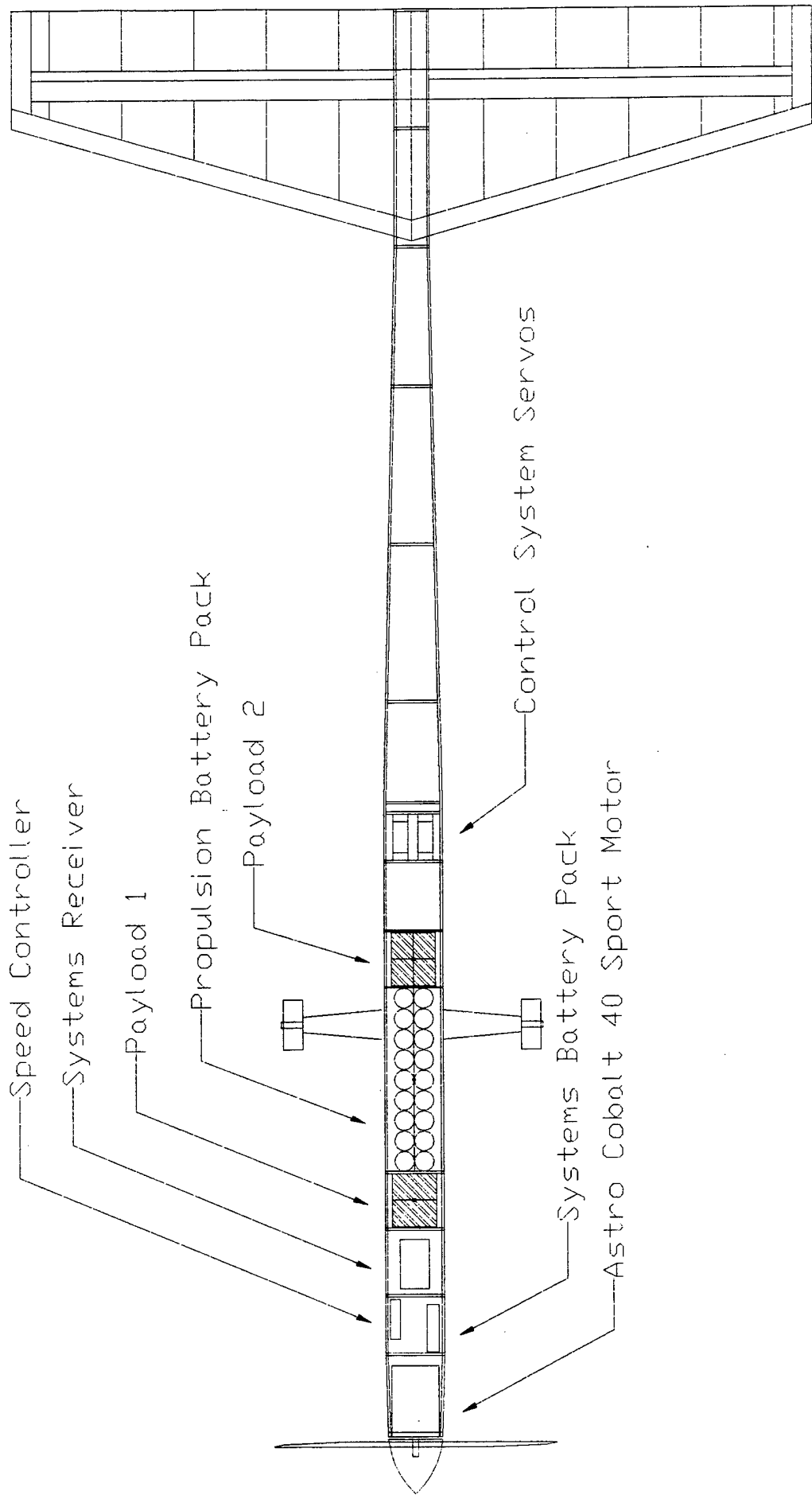
The location of the main gear is behind the center of gravity. The location was found by simply finding the intersect of a line which is rotated 15 degrees from the center of gravity (towards the tail) and the maximum tail down angle. The intersection of these two lines indicates the location of the main gear support. This location was found to be 2.8 inches behind the center of gravity. This gives the gear a height of 10.5 inches and a tread of 12 inches. The front gear will be placed near the rear of the motor mount that is 1.3 feet forward of the center of gravity. The wheels for the aircraft will be composed of wheels normally used in roller blades. This was chosen due to its strength, rolling

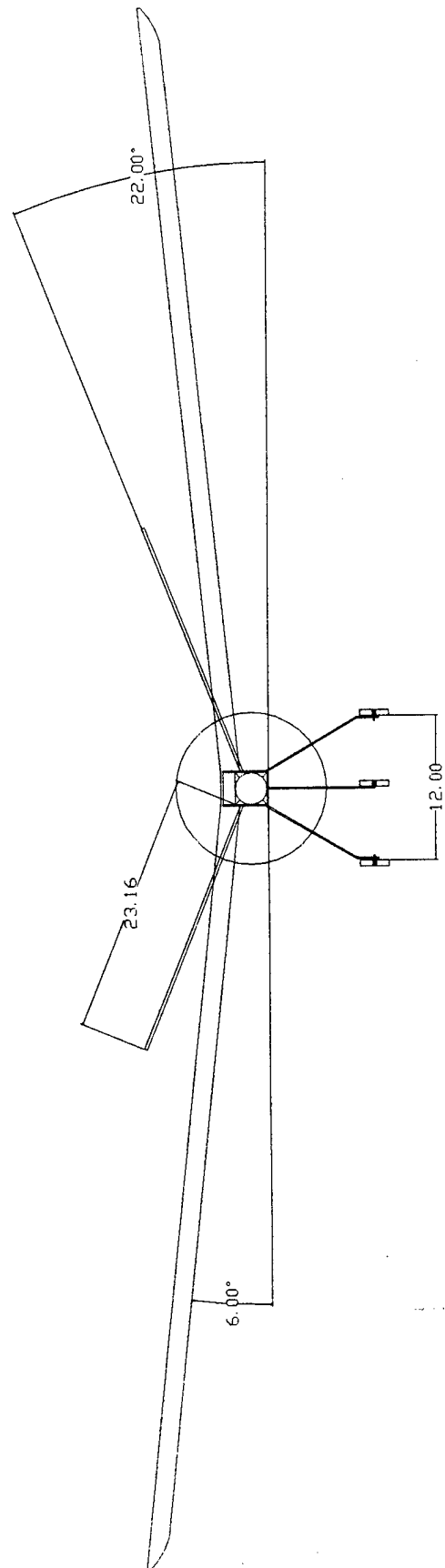
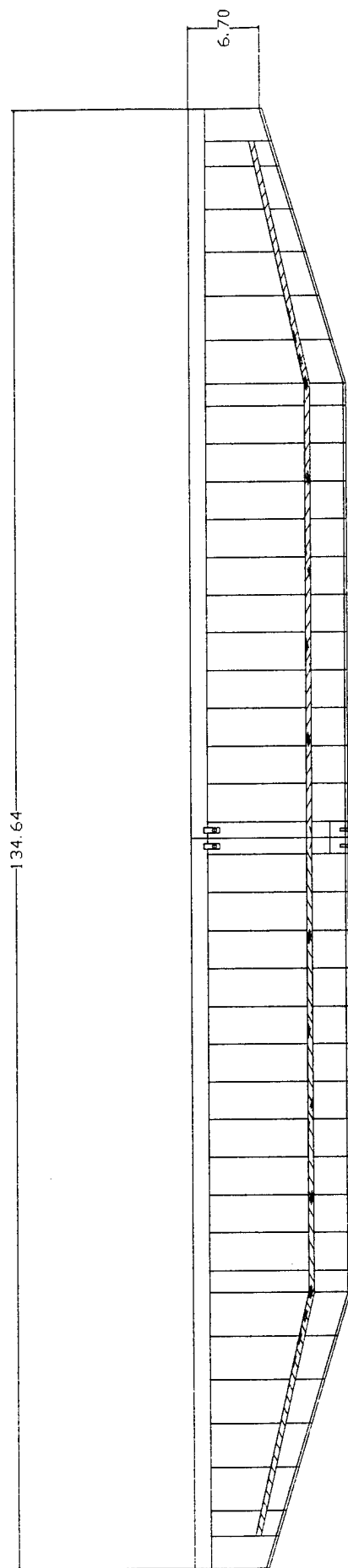
friction, size, and cost. The last item to be added was wheel pants in an effort to reduce the effects of drag caused by the wheel.

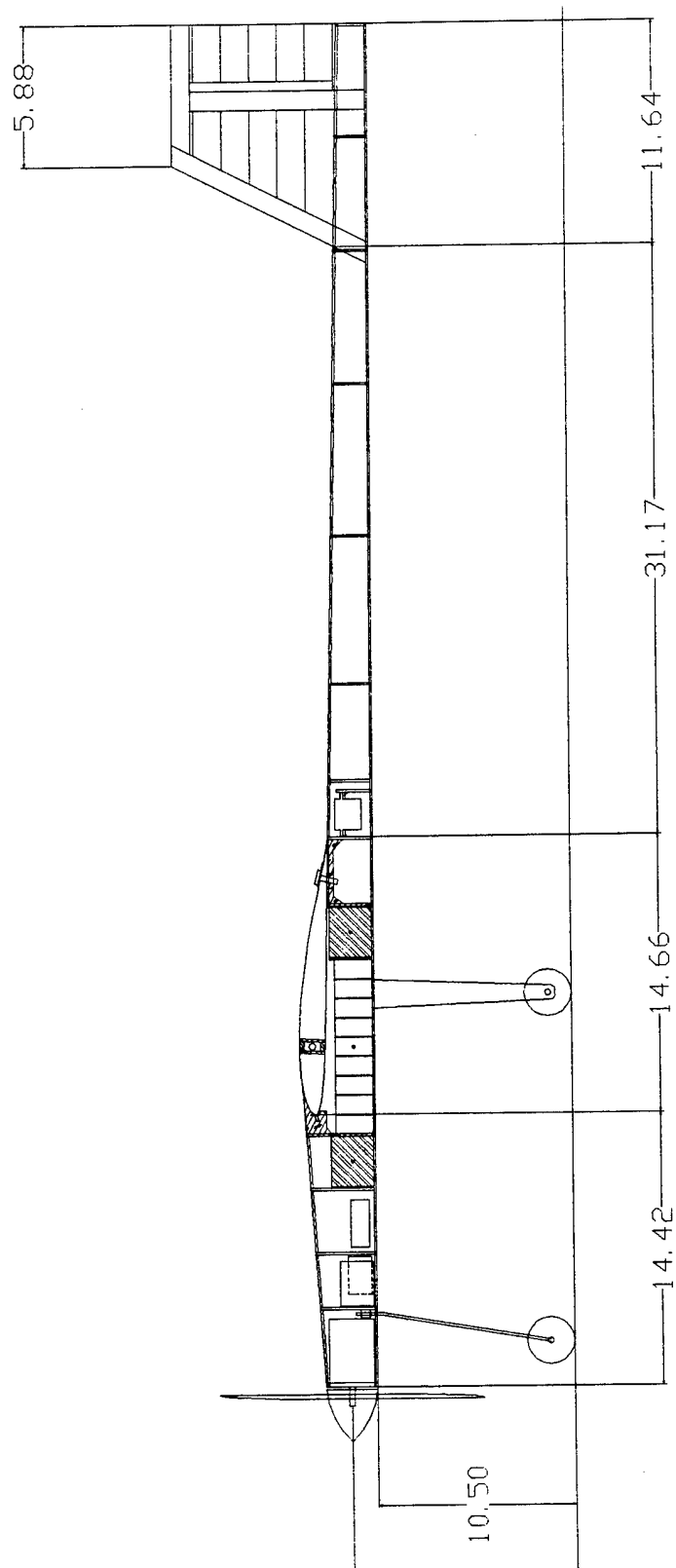
### ***Final Aircraft Static's , Performance and Drawings.***

- Weight:
  - Gross: 15.31 lb.
  - Empty: 7.81 lb.
  - Payload Fraction: 49%
- Wing:
  - Airfoil: S3014
  - Span: 11.22 ft.
  - Surface: 12 sq.ft.
  - Root Chord: 1.22 ft.
  - Tip Chord: 0.57 ft.
  - Dihedral: 6 deg.
- V-tail:
  - Surface: 3.72 sq.ft.
  - Span: 3.86 ft.
  - Root Chord: 0.97 ft.
  - Tip Chord: 0.49 ft.
  - Dihedral: 22 deg.
- Fuselage:
  - Length: 6 ft.
  - Maximum size: 2.75" x 3.04"
- Propulsion System:
  - Motor: Astro Cobalt 40 Sport
  - Speed controller: Astro 211
  - Batteries: 18 Sanyo 2300 SCE
- Ground Roll: 150 ft.
  - Time: 13.64 sec
- Takeoff velocity: 32.99 ft/sec
- Rate of Climb: 2.19 ft/sec
  - Time: 4.56 sec
- Flight Speed: 57.35 ft/sec
- Range: 23.000 ft
  - Time: 7 min
  - Load Factor in turns: 2g
  - Laps: 13
- Total endurance: 8.15 min.
- Maximum g Loading: 2.5









## Manufacturing Plan

The first major objective was to determine the type of construction techniques to be used. We found that most aircraft of this type can be broken into three types: composite, "built-up", and a combination of the two. Each of the manufacturing methods were then analyzed for the following: skill level, weight, cost, availability, time, and strength.

Method	Advantages	Disadvantages
Built-up	<ul style="list-style-type: none"> <li>• Low Weight</li> <li>• Easy to fabricate</li> <li>• Little time required</li> <li>• Not glue sensitive</li> <li>• Low cost for material and tooling</li> <li>• Easy to repair</li> <li>• Readily available materials</li> </ul>	<ul style="list-style-type: none"> <li>• Moderate strength to weight</li> </ul>
Composite 'Foam Core'	<ul style="list-style-type: none"> <li>• High strength to weight</li> <li>✎ <i>Low Weight *</i></li> <li>• Low to Medium cost for material and tooling.</li> <li>• Readily available materials.</li> </ul>	<ul style="list-style-type: none"> <li>• Moderate to Difficult to fabricate.</li> <li>• High time required.</li> <li>• Very glue sensitive.</li> <li>• Very Difficult to repair.</li> <li>✎ <i>Medium to High Weight if not done correctly. *</i></li> </ul>
Combination	<ul style="list-style-type: none"> <li>• Moderate to High strength to weight</li> <li>• Readily available materials.</li> <li>• Low to Medium cost for material and tooling.</li> <li>✎ <i>Low Weight *</i></li> </ul>	<ul style="list-style-type: none"> <li>• Moderate to Difficult to fabricate.</li> <li>• Moderate time required.</li> <li>• Area dependent glue sensitive.</li> <li>• Difficult to repair.</li> <li>✎ <i>Medium Weight if not done correctly. *</i></li> </ul>
* Indicates items <i>may</i> have a problem.		

**Table 5 Manufacturing Method FOM**

Finally, each of the FOM were scored in the following order: Ease of fabrication, time, weight, strength, cost, and then availability. From the above analysis we selected the "Built-up" approach for the majority of the manufacturing. Some of the major load bearing parts will be reinforced by use of the 'combination' method. At the end of this section you will find the planned manufacturing milestones chart. This chart contains the breakdown of construction of the major components. With this method chosen, we decided to look at each area of the aircraft in order to decided which materials to use. The wing was the first item to be considered. We decided for the wing to use a spruce spar as this offered a high strength to weight ratio. Other material, which was considered was: balsa, carbon-fiber arrow shafts, aluminum rods, and others. These were eliminated due

to one or more of the following: low strength to weight ratio, size, availability, little or no reliable property information, and final cost. We will, however, place a carbon fiber strip along a portion of the bottom of the spar, near the root, to increase its strength as this is the area of highest load. The shear webs will be made from balsa and will also run only a portion of the way on both sides of the spar. As the ribs serve mainly to hold the airfoil shape we decided to make them as light as possible.

Some of the material that was considered for the ribs were: foam-core poster board, balsa, and plastic. The poster board was eliminated because it is not only sensitive to glue but it is also sensitive to heat and not easily repairable. The plastic was removed due to its higher density when compared to balsa. This left us with balsa as the material for the ribs.

The material considered for leading edge of the wing was simple balsa leading edge stock, spruce leading edge stock, and final birch sheeting. The first two were eliminated due to the time and effort that must be placed into maintaining the correct airfoil shape. Instead of using a traditional leading edge stock, a small piece of balsa will be placed near the front of the airfoil to help maintain the rib spacing. The leading edge will be covered in 1/64 inch birch sheeting. This method should not only save weight but more importantly will allow for the airfoil shape to be maintained. The trailing edge is the remaining part of the wing, its area will be constructed from stock balsa.

The main reason this material was chosen is due to its exact fit to the trailing edge can be found in balsa stock. With this match, very little work will need to be done to fit it to the wing. Finally, the entire surface of the wing will be covered in a covering called MonoKote®, this covering will provide a very clean and smooth surface across the wing, which will help to reduce the drag across the wing, and the wing can be covered rather quickly.

We plan are to build the wing in two halves with a wing brace connecting the two halves. This design was chosen for two reasons, first it allows the wing to be easily transported to and from the flight field and it will also allow a quick change of the dihedral angle if flight tests indicate a need for this. The wing will attach to the fuselage by use of two small dowel rods which will slide into place in the front of the wing box, and the trailing edge will be held in place by two nylon bolts which will attach at the rear of the wing box. The tail will be constructed in a similarly fashion to the wing, except it will not contain a spar.

The fuselage for the plane will be constructed in the square configuration. The walls of the fuselage will be made from balsa sheeting which is 3/32" thick with an additional 1/16" thick sheeting added in the areas of high loading. The bulkheads, mainly used to hold shape, will be made from 3/32" balsa. The only area that contains bulkheads that will differ is the center section. This area will form the basis of the wing box and major load carrying area. Since this is an area of high stress, 3/16" balsa with a fiber-glass covering will be used. This will allow the strength and still maintain a low weight. Initially it was planned to use an aluminum box in this area, but it was soon found that it would weight more than needed and the loads in this area did not require this much strength.

The landing gear will be one area of which high strength is needed for this reason we chose to build the gear out of aluminum. The reason behind choosing this metal was



mainly due to its ease in manufacturing and high strength to weight ratio. The gear will be attached to the bottom of the fuselage directly to minimize interference effects and allow it to pass its load to the load bearing box contained inside this portion of the fuselage. Roller blade wheels will be used in the landing gear as they have both high strength and low rolling friction. The front gear will attach directly behind the mount and be constructed of a simple aluminum rod. This was chosen to limit the weight of the gear, and because the front gear will see only a small portion (15%) of the total landing load.

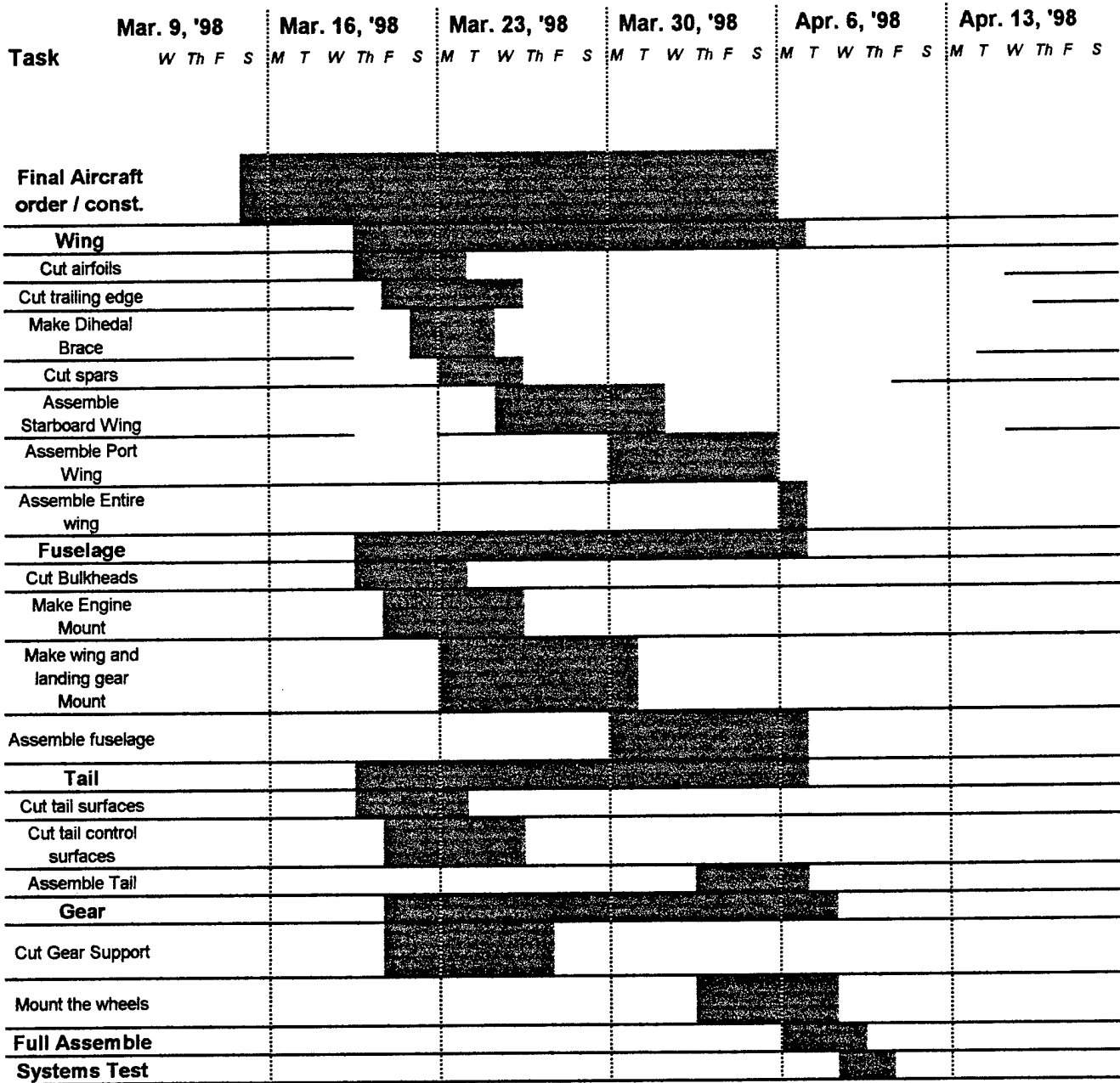
The required steel payload will be loaded through the top by use of hatches and the removable wing. The payload will be split into two pieces. These two pieces will be placed at an equal distance from the established center of gravity. This was done so that the aircraft's center of gravity will remain constant for both the loaded and unloaded conditions. The two pieces will be ordered as one large piece of steel bar stock that has the cross-sectional area of 2.25 x 2.25 inches. The bar will then be weighted to determine the length of bar needed to satisfy the required 7.5 lb. payload. While it is known that steel should have a density of 27 cubic in/lb, it is believed to be safer to order a bar longer than needed so as to insure the 7.5 pounds. After obtaining the true density of our steel, we will then cut it into the required length.

With all major design elements now found, we created an estimated cost list. The following is a summary of that list:

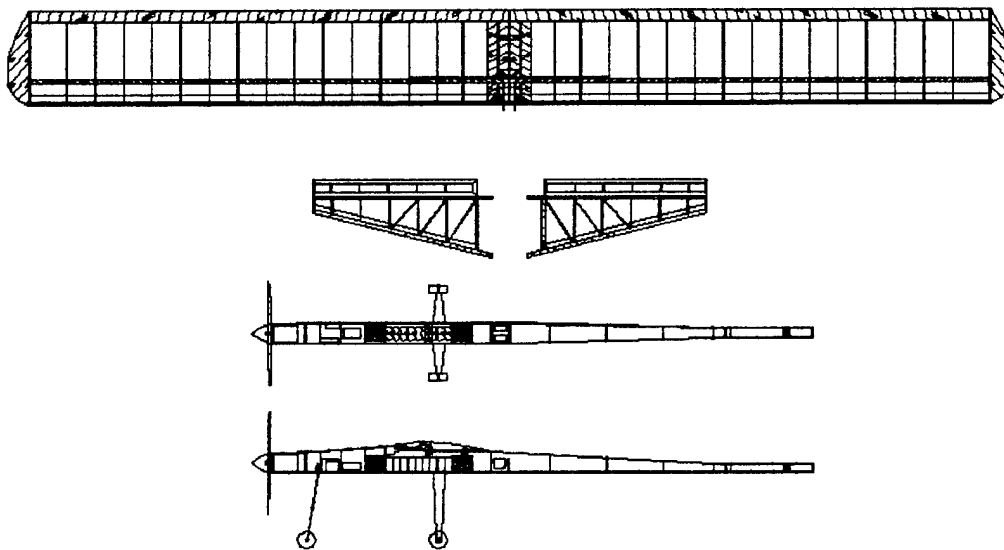
Group	Estimated Price
Motor and Accessories	\$280
Construction Materials	\$525
Batteries and Accessories	\$250
Control Systems	\$55
Payload	\$30
Miscellaneous	\$200
<b>Total Expected</b>	<b>\$1340</b>

**Table 6 Aircraft Cost Estimates**

# Manufacturing Schedule



**Cessna / ONR**  
**Student Design/ Build/ Fly Competition**  
Addendum Phase



Submitted By:  
Oklahoma State University

Team Members:

Alan Anderson	Gary Lantz
Adrianto Augustnine	Helen Hunt
Joel Basler	Steven Jones
Anthony Boechman	Yolanda Mack
Ben Cantwell	Jamie Morgan
Joe Conner	Vamsi Prakhya
	Nick Scocos

## TABLE OF CONTENTS

Lessons Learned.....	1
Design Changes .....	1
Next Generation Design .....	9
Aircraft Costs .....	9

## List of Tables , Drawings and Figures

Table 1 Cost Comparison .....	9
Table 2 Itemized Cost List .....	11
 Drawing 1 Main Wing Comparison .....	3
Drawing 2 Attachment Point Comparison .....	4
Drawing 3 Tail Control Surface Comparison .....	5
Drawing 4 Fuselage Comparison (above) .....	6
Drawing 5 Fuselage Comparison (side) .....	7
 Figure 1 Lift Versus Drag for Differing Planforms .....	1

## Lessons Learned

### Design Changes

The major changes in the final aircraft from the proposed design can be broken into the following components; the wing, tail control surfaces, and the fuselage. In the proposal phase it was determined to have a main wing with a constant chord section followed by a taper section near the tip. This design was changed to a straight rectangular wing for several reasons. First, after full size plans were drawn up, it was noticed that the tapered design would have lead to major construction and weight problem do to the transition at the start of the tapered section. Next, since the structural verification required the aircraft to be lifted at the wing tips the tapered section must be design to handle the 2.5 g load that would be induced. Finally, a vortex panel method was used to compare the lift versus drag of both planform. The results, which can be seen in figure 1, of this showed that the rectangular wing actually has better results. With this in mind, we decided to return to the original wing planform design of a rectangular wing. The design allowed the wing to be manufactured more quickly as only one airfoil pattern need to be manufactured. The next major change in the design of the wing was the attachment points.

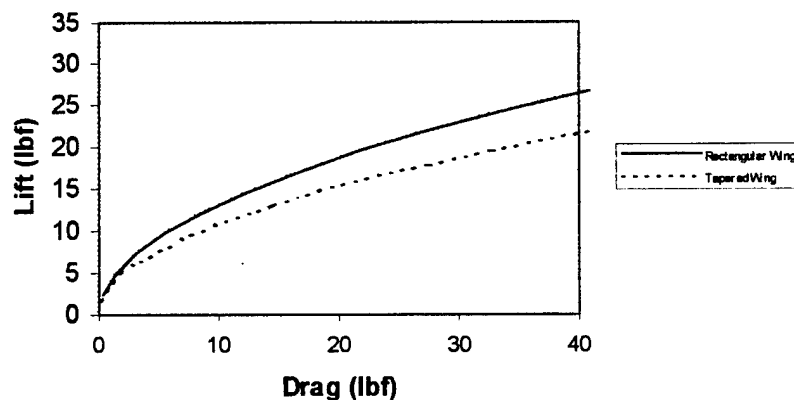
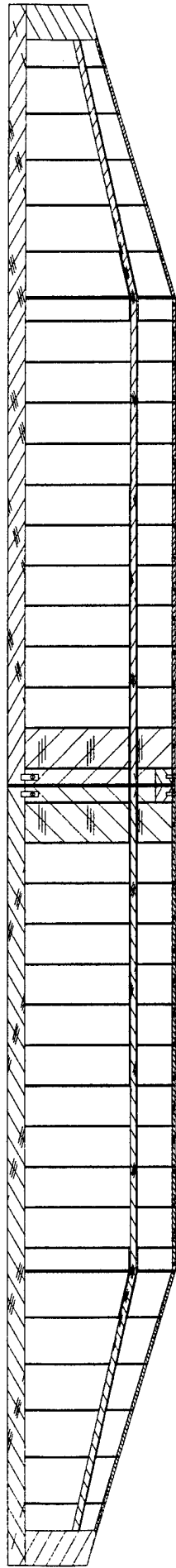


Figure 1 Lift Versus Drag for Differing Planforms

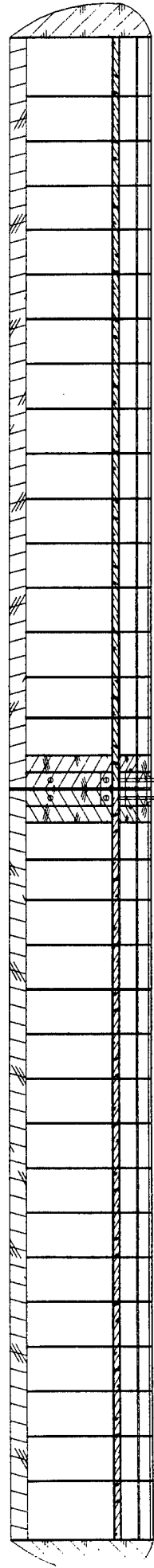
In the proposal phase we decided to go with a two point attachment. The attachment points would be a dowel rod at the leading edge of the wing and a bolt at the trailing edge. This design was also changed after the full size plans were drawn up and analyzed. After analyzing available attachment points we decided to manufacture a wing bolt box near the spar. This attachment point allowed a much simpler load path to be established; also this arrangement allowed for the center section of the wing to built with less material. The wing is still pinned at the leading edge by use of the dowel rod and the trailing edge by a bolt; however since these points were no longer major load bearing points the material requirements were lowered. The next area that was changed from the proposal phase was the size of the control surfaces.

The size of the control surface was decreased in size. The decision was made due to the flight tests conducted. From the tests we determined that the aircraft had more than enough control deflection to maneuver the required surface. With this information the

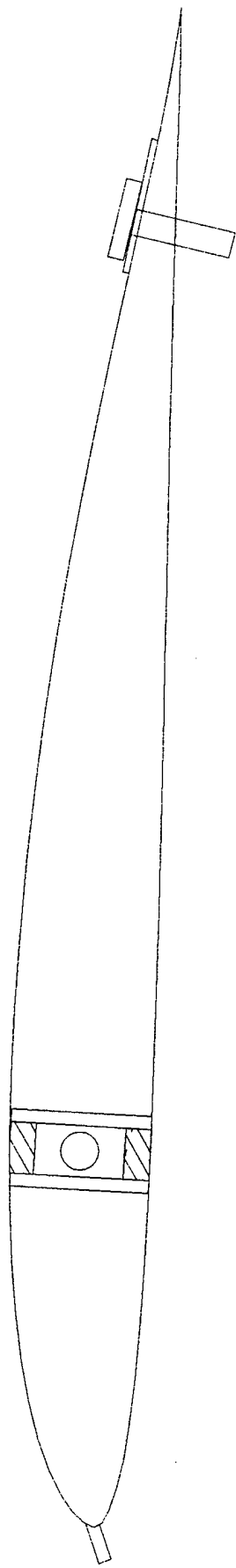
control surface was resized to half its original size. With the tail now fully sized, the fuselage was redesigned. This was done for two main reasons, first the weight of the tail during the proposal phase had to be estimated to determine the length of nose required to cancel out the moment created by it. Secondly, the area of the rear fuselage was redesigned around the minimum area needed to support the tail. After redesigning the fuselage, it was determined that we could lose weight in the fuselage by use of a light ply truss system with balsa over the surface. This new design allowed us to drop the weight of the fuselage from 20 ounces to just over 14 ounces. While the analysis did show that weight had little to no effect on range, the aircraft must still get off the ground before it can even enter the track to complete the laps. This along with the other changes can be seen in the drawings that follow this section. The only other small item that will be added, is the use of dry ice to aid in the cooling of the power packs. The cooling will be accomplished by use of a NACA inlet scoop placed in front of the forward steel payload. The steel payload will be stored in dry ice before each flight. The test run with this arrangement indicates an increase in output battery capacity as the batteries are kept cool and therefore their internal resistance does not increase throughout the flight.



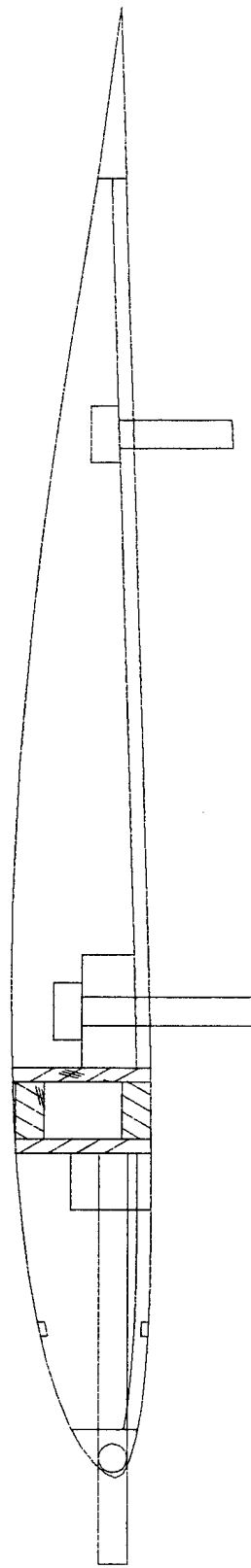
Original



Final

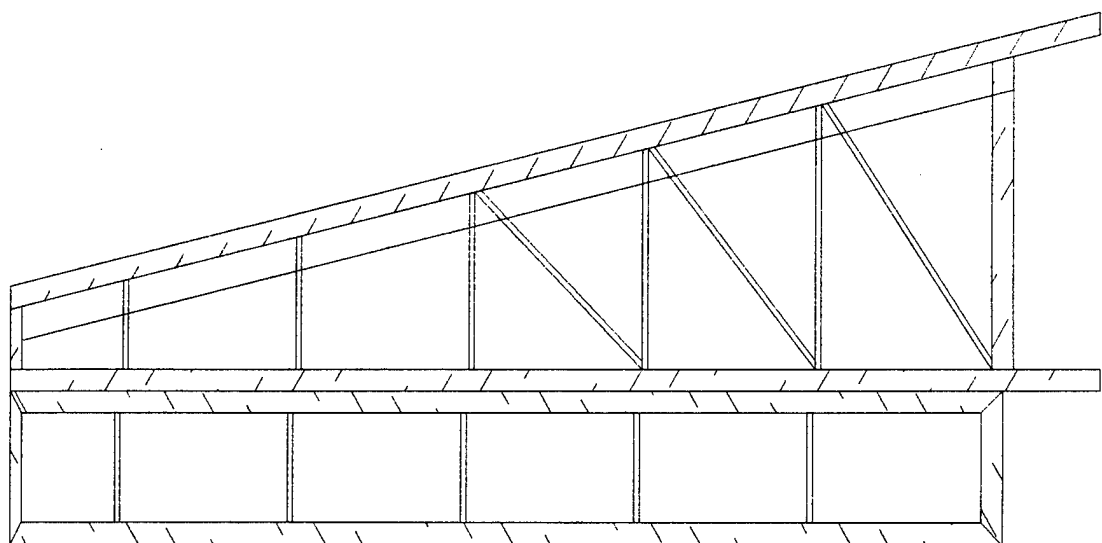


Original

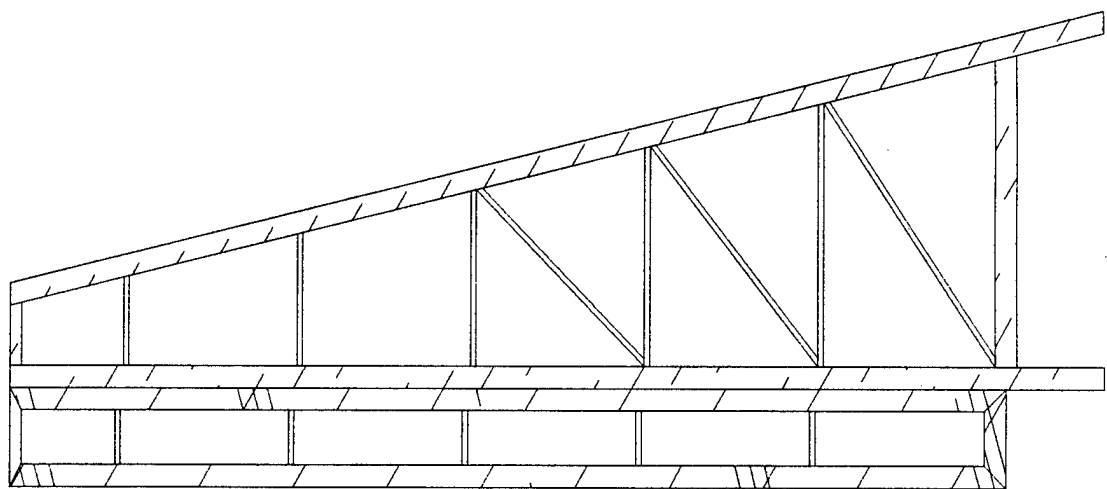


Final

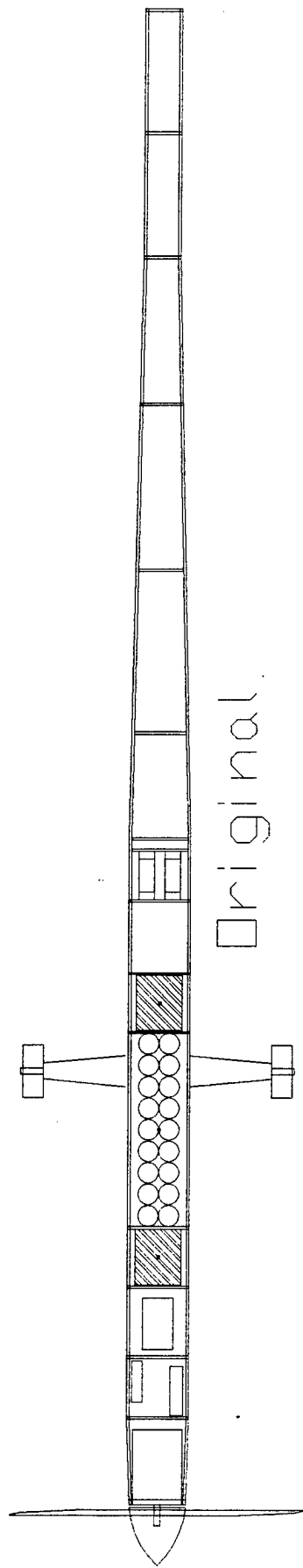




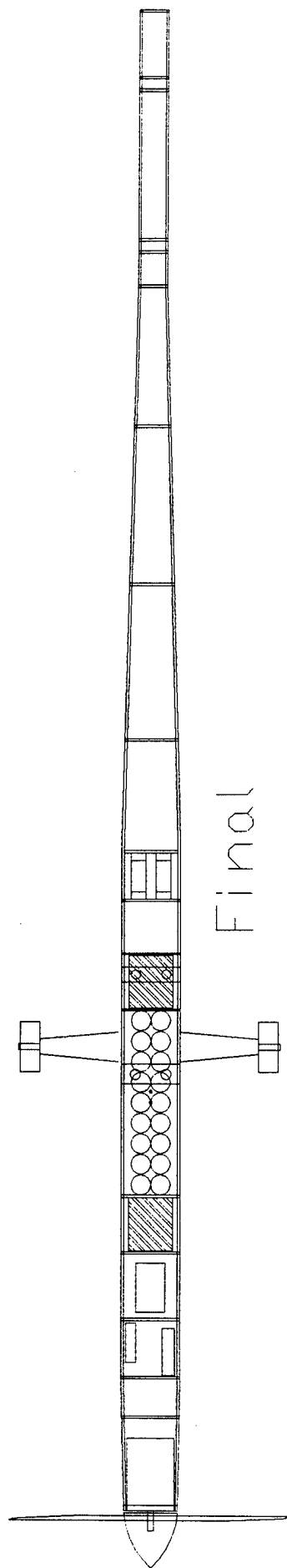
Original



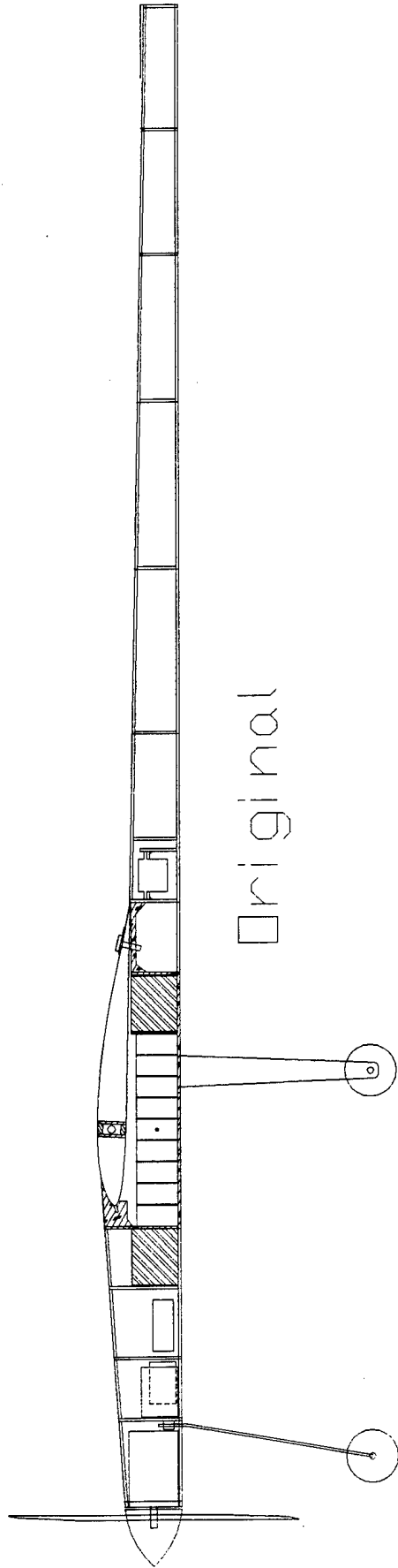
Final



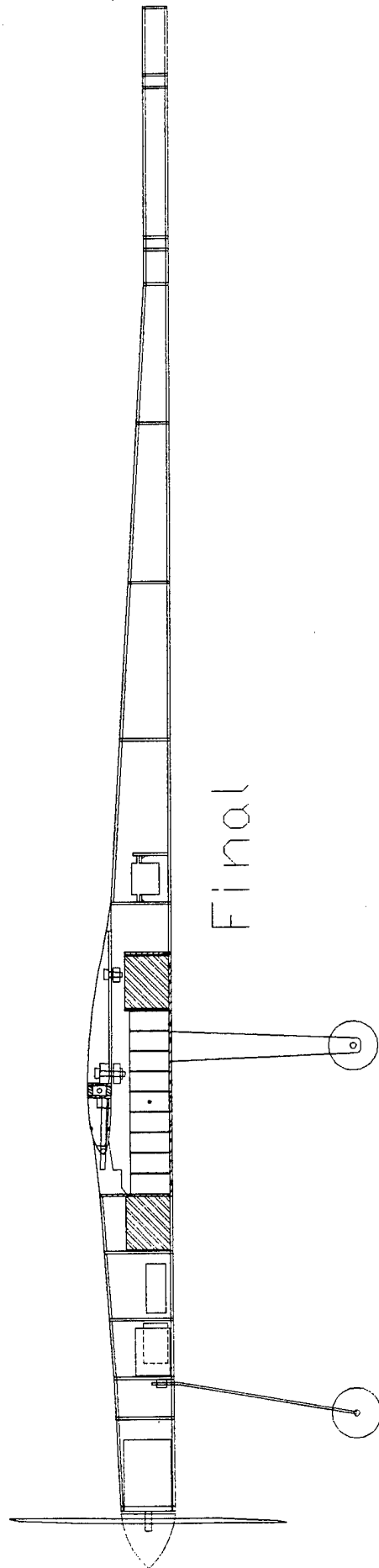
Original



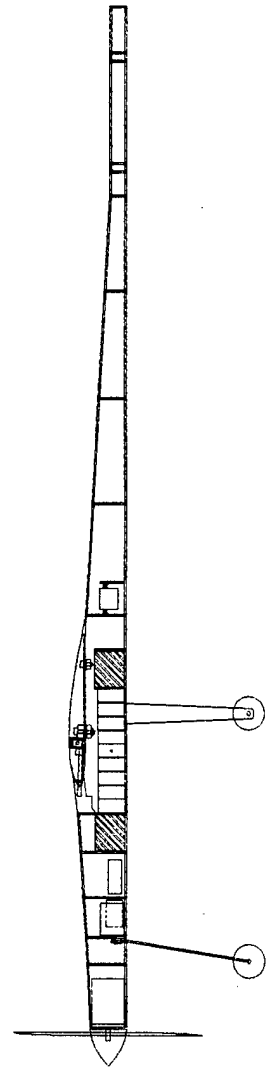
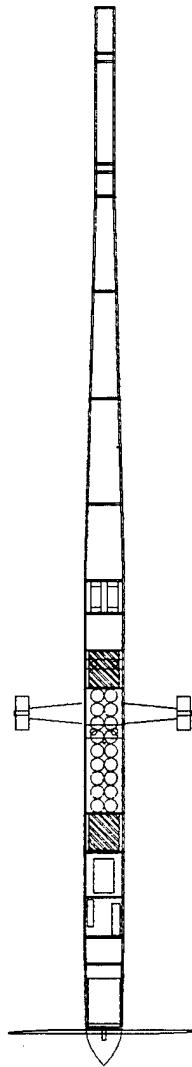
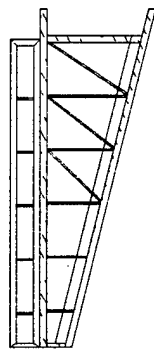
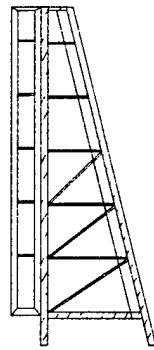
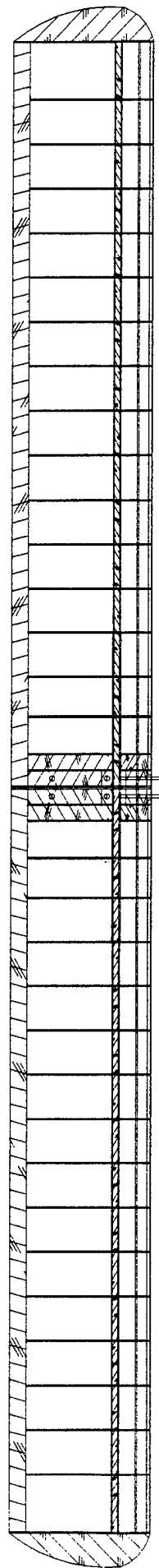
Final



Original



Final



### ***Next Generation Design***

At this time, the only area of improvement in the next generation design would be better material selection and information. To aid in the materials selection two major items are planned to be carried out. First is the creation of a material properties list. To create this list the density of all the material that was put into the aircraft was found and recorded. The next major item is to conduct a strength test on the differing types of material that can be used in the aircraft. This should allow a better weight estimate of any aircraft to be designed in the future.

### ***Aircraft Costs***

The following is a table showing a summary of the estimated versus actual costs.

Group	Estimated	Actual
Construction Materials	\$525.00	\$313.26
Motor and Accessories	\$280.00	\$297.95
Batteries and Accessories	\$250.00	\$228.00
Control Systems	\$55.00	\$93.06
Payload	\$30.00	\$30.00
Miscellaneous	\$200.00	\$68.02
<b>Total</b>	<b>\$1,340.00</b>	<b>\$1,004.04</b>
<b>Difference</b>		<b>\$335.96</b>

**Table 1 Cost Comparison**

As can be seen from the results shown in table 1, the a difference between the estimated and actual costs is \$335.96. This difference will be address by each grouping independently. Construction materials are lower than expected for two reasons, first is the supplier of materials. The estimated costs were done with one company in mind however a second company, Balsa USA, was located. This company specializes in model aircraft material. Not only did this company have a much larger selection of material but the material was of better quality and also had a lower cost. Secondly, the new wing design required less material than the proposed design. The motor and accessories did come out higher than estimated, however this was because of the decision to purchase the motor and two gear boxes of differing sizes. This was done to save money for any future designs. Propulsion batteries and accessories also come in under the estimated cost. This difference can also be attributed to a change in venders. The second vender not only had a large selection of batteries, but their low cost allowed us to purchase 40 batteries. This large number of batteries allowed us conduct several experiments and then build a pack out of the best batteries. The next area is the control systems. This area did come out higher than estimated mainly do to an over sight of the items required in this area. The estimated costs only included servos and control lines. The final cost included the following items; servos, control horns, control rods, control rod exits, and other items. The complete list of items

in this area can be seen in the itemized list that follows this section. The one item that did come it at exactly the estimated cost was the steel payload. This is mainly do to the fact that the steel payload was obtained from the lab. Finally the last item is miscellaneous. Miscellaneous items were items that did not fit into any of the other groups, but were still required for the project. An itemized list of the costs for each of the groups follows.

Item	Quantity	Price	Total	
1/8 x 6 x 24 Ply	15	\$1.25	\$18.75	
3/32 x 3 x 48	5	\$0.72	\$3.60	
1/4 x 4 x 42	1	\$1.73	\$1.73	
Nylon Bolts (10)	1	\$1.10	\$1.10	
Front Wheel 2.5	1	\$3.18	\$3.18	
Covering Black	3	\$6.95	\$20.85	
Covering Orange	3	\$6.95	\$20.85	
Covering White	3	\$6.95	\$20.85	
3/32 x 6 x 48 Ply	2	\$5.29	\$10.58	
Wing Skin 1/64 x 48 x 48	1	\$64.50	\$64.50	
3/32 x 4 x 48	5	\$1.20	\$6.00	
1/4 x 36	10	\$0.20	\$2.00	
3/32 x 4 x 30	5	\$0.70	\$3.50	
1/4 x 1 1/2 x 36	5	\$0.79	\$3.95	
1/8 x 12 x 24	1	\$2.43	\$2.43	
1/4 x 1/2 x 36	10	\$0.65	\$6.50	
2 x 3 x 36	1	\$4.36	\$4.36	
1/8 x 1/4 x 36	10	\$0.14	\$1.40	
1/4 x 1/2 x 48	5	\$0.42	\$2.10	
1/4 x 1/4 x 36	5	\$0.23	\$1.15	
1/8 x 6 x 48	1	\$2.40	\$2.40	
1/8 x 1/4 x 48	10	\$0.22	\$2.20	
Main Wheels	4	\$1.50	\$6.00	
Wheel Pwells	2	\$8.59	\$17.18	
Hinges	1	\$3.09	\$3.09	
CA+	4	\$7.49	\$29.96	
CA Activator	1	\$4.49	\$4.49	
Nose Gear	1	\$3.79	\$3.79	
Kevlar Ribbon	1	\$2.39	\$2.39	
Balsa Filler	1	\$4.99	\$4.99	
Fiber Glass 6oz.	1	\$5.49	\$5.49	
Carbon Fiber	1	\$11.00	\$11.00	
Plotter Paper	2	\$10.45	\$20.90	
				Construction Materials
				\$313.26
AstroFlight 640G	1	\$145.00	\$145.00	
Gear Box 3.1:1	1	\$49.95	\$49.95	
Speed Controller	1	\$90.00	\$90.00	
Silicon Wiring	1	\$10.00	\$10.00	
Arming Fuse	1	\$3.00	\$3.00	
				Motor and Accessories
				\$297.95
Battery Pack (Systems)	1	\$11.99	\$11.99	
Servos S148 (3)	1	\$50.00	\$50.00	
Control Horns (4)	2	\$0.70	\$1.40	
Control rod exits (2)	2	\$0.95	\$1.90	
Gold'n Rods 48" (2)	2	\$4.79	\$9.58	
Servo Extensions 1m	2	\$8.00	\$16.00	
External Switch	1	\$2.19	\$2.19	
				Control Systems
				\$93.06
Arming Fuse	1	\$3.00	\$3.00	
Zero loss Connector				
(battery side)	2	\$2.50	\$5.00	
Battery Propulsion (pack)	40	\$5.50	\$220.00	
				Batteries and Accessories
				\$228.00
Payload 2.25 x 2.25 x 6	1		\$30.00	
				Payload
				\$30.00
Drill Set	1	\$12.49	\$12.49	
MitreBox	1	\$14.49	\$14.49	
Dry Ice	5	\$5.25	\$26.25	
Knife/Blade Set	1	\$14.79	\$14.79	
				Miscellaneous
				\$68.02

**Total**  
**Price \$1,030.29**

**Table 2 Itemized Cost List**

# Project Backfire

AIAA  
SDSU  
Student Chapter



## **Table of Contents**

<b>Part 1: Executive Summary.....</b>	<b>p.1-2</b>
<b>Part 2: Management Summary.....</b>	<b>p.3</b>
<b>Part 3: Conceptual Design.....</b>	<b>p.4-5</b>
<b>Part 4: Preliminary Design.....</b>	<b>p.6-7</b>
<b>Part 5: Detail Design.....</b>	<b>p.8</b>
<b>Part 6: Manufacturing Plan.....</b>	<b>p.9</b>
<b>Bibliography.....</b>	<b>p.10</b>
<b>Appendix.....</b>	<b>p.11-31</b>

## Part 1 Executive Summary

The Backfire project started at weekly meetings. As a club we reviewed all the activities made available to us by AIAA. Entering this competition would satisfy many of our needs to apply what we have learned, improve engineering communication and demonstrate that SDSU can be competitive. Everyone at the meetings was made comfortable with the idea of actually producing something and competing.

After the club agreed that we could make a move, there was an announcement and order to submit proposals. At proposal time, everyone was free to think and research and offer a concept of a plane. They were allowed to work in groups with the additional understanding that they had to of course present their idea to the club as well. This presentation was to include a clear concept of a plane, explanatory drawings of that plane and demonstrate the understanding of the basic configuration and how it would perform. There was no direct emphasis on numbers or critical dimensions at this point. If someone came up with a proposal and did not present it in front of everyone in the club then it was not considered.

Of the 5 proposals that were turned in, there were three radically different designs. One of them we will call case1, this was a twin fuselage & engine design with a joined tail in the rear (similar to a Bronco). Then there is case2 which was somewhat similar to case1, but had a sweep back angle and lacked winglets. In addition case2 was a single engine pusher. Finally case3 was a canard configuration with a push propeller. After reviewing these cases the arguing began. Please refer to the appendix for clarity with these cases.

Each member who participated, had to defend their proposals against the other. This was done understanding the team would be run as a democracy in the first stages and would then vote into which direction to go. Running the club/team as a democracy was instrumental in the beginning stages to give ownership of the project to everyone and have a common sense of direction. The team came to vote case3 as the winner. There was a common concern that we must avoid as much propeller wash on the body as possible. In addition it was realized that we should pine away from making it so stable which is the tendency of students at our level. A "stable" plane is difficult to land and turn. Shortly after the vote organizational plans were made.

The experience of the club/team had to be assessed. Ultimately 3 divisions were created and these are: Aerodynamics(A), Flight Mechanics(FM), and Propulsion(P). Everyone was then given a choice as to which group to specialize in. Their choices were checked by the project leader who is also the president of the club. All members were given a composition book to record all that pertained to the project, that they contributed. With the division into groups they were given time to break off and research and compose estimates of performance and dimensions to their respective fields. They were to establish their own division's harmony and then we would all come back together to make compromises and integrate the disciplines together.

Many kinds of tools were used for each stage. In the conceptual stage there was an emphasis on non-CAD sketching and presentation delivery. In addition we all had to review the rules, last year's competitors designs and personal testimony. For the second phase we used benchmarking, observed last year's competitors vital statistics and dimensions, observed existing flying designs, Theory of wing sections book(and other various texts), Excel template programs, and most of all wind-tunnel testing. Then on the detailed design the many tools that we used included the use of AutoCAD, more benchmarking, Excel, Advanced Aircraft Analysis (AAA) program, and more important texts sited in the bibliography.

## Part 2 Management Summary

We began as a democracy to establish a common understanding of the directions. The basic concept and configuration was put up for voting. The members were asked to submit a paper indicating any of their experience of skills related to the project. This gives the project leader an idea of how much help we need to pull in; also it will help him to judge if they should be in the group that they've chosen. This was an instrumental part in assigning personal assignments and getting efficient and consistent results.

We broke the project into three areas, flight mechanics, aerodynamics, and propulsion. Activities such as field trips or campus activities break the ice and help us to keep a close communication. Early in the conceptual stage each member was given a composition book to record all of his or her thoughts pertaining to the project. This would not only serve as a record, but it would also ensure that all possible avenues are taken into consideration. During the preliminary planning each group was responsible for their realm. There was difficulty with communication when trying to explain ideas, because sketches were minimal and unclear. So as a result we designated drafters, Tim, Ryan, and Richard, in order to create a precise pictures of our plans. This would help the building process become more efficient since everyone would know what needs to be done.

The management structure consists of a project leader. This person is responsible for supplying each group with the materials and tools that they need. In addition he must over see all operations. Personal tasks were implemented only when precise drawings were available and competence was confirmed. Every team member was required to fill out the schedule form and place in the workshop. Configuration control of both the management and airplane structure was maintained through constant communication.

### Part 3: Conceptual Design

For our Conceptual Design we chose case 2 that has two side fuselages and two vertical tails with each vertical tail is attached to each end of the fuselage. They then connected with the horizontal tail section hanging on top of each tail. The ducted fan propeller will be mounted behind the center fuselage. This will produce a thrust vector that is free of windshear to any surface. This design will prevent the interference drag from the airplane's moving surface. Aspect ratio was chosen to be between 5.5 - 7.5 to give a considerate stall angle of attack while the aircraft still produce very little induce drag. This criteria works extremely well when the aircraft operate at 1.5 to 2.5 times the stall speed. All the stability data was estimated upon the previous existing airliners and transport aircrafts. Therefore, this aircraft will pose the characteristic of extremely high lift and low drag, but highly maneuverable.

There was also a main fuselage was designed to be in the center of the aircraft to provide room for cargo space and a mounting of the ducted fan. The wing planform is to center on the main fuselage. The cross-sectional area to length ratio of the main fuselage was chosen where the drag coefficient was less than 0.11. The side fuselages were relatively the same length of the main fueslage but their cross-sections were forty percent the size of the main fueslage. The drag coeffients were 0.14. Since the aircraft experinced pure laminar flow, all moving surfaces are very sensitive to any change in aerodynamics. The wing planform and the enpennage were designed with large moving surfaces

associated relative to the main fuselage, so that they provide extremely maneuverable aerodynamic characteristics.

We finally decided on case three. This design incorporates a canard configuration that we felt would increase maneuverability. It also has a lower coefficient of drag than case 2 and also it is also more stable due to the canard and the large wing planform area. It was also chosen because it has a level of instability to allow for superior maneuverability and speed. The design also has a propellor in the aft section hence the name Backfire. The stall angle is greater compared to case 2. This design, as with case 2, allows the aircraft to produce little drag and is as maneuverable, if not more so than case 2. The design also allows the aircraft to perform the same with or without the steel payload.

We also felt that this design's performance would far exceed that of case 2. Performance is a key factor for this competition because the plane has to fly so many loops around a preset course. We also felt that the idea of a propellor in the back would aid in the overall speed of the aircraft in that there will be less friction from air on the moving surfaces. This is also important because if there is less friction there is more room for error. The design also allows for steep and wide banking turns.

5

#### Part 4 Preliminary Design

We decided to go with a canard aircraft for several reasons. One is, because characteristically it is difficult to stall. The canard surface generally stalls before the main aft wing does. When the canard surface does stall the main wing is still unstalled and the plane tends to pitch down and recovers back to normal flight.

We have found from our research that wing's leading edge sweep back angle should below 17 degrees because when exceeding this there is a loss in capability to form natural laminar flow. With a larger sweep back angle the vortices shed from leading edge create turbulence that inhibits the natural laminar flow. Nevertheless we have decide to go with a sweep back angle of 20 degrees to increase stability.

The size of our main wing was decided through much study and careful research. The wing span is two meters, the root cord is 0.43 meters, the tip cord is 0.25 meters and the taper ratio ( $C_t/C_r$ ) is equal to 0.581 meters. We decided to have a high aspect ratio to produce a low induced drag. The coefficient of induced drag is inversely proportional to the aspect ratio. We opted for tapered wing, but we had to compromise between difficulty to produce wing platform and a simple rectangular wing, which has a lift distribution, which is far from optimum. From our schooling we know that winglets reduce the induced drag greatly and with only a minimal increase in bending moment. We also decided to have a sweep back angle of ten degrees. The center of gravity for neutral stability should be considerably ahead of the twenty-five percent point of the wing mean aerodynamic cord. The function of sweeping back the wing is to reduce instability. A wing that is swept back bends under and lifts the load in a direction that reduces or washes out incidence at the wing tips. It produces an automatic load relief and

6

improves directional stability and control wing ailerons. The aileron gap reduces the airflow from the high pressure under the surface under the wing the lower pressure of the upper wing surface, in turn reduces the drag.

Canard configurations have been revived in recent years in belief that trimming with an increasing load reduces the induced drag. Our canard has a span of 0.6 meters, a cord length of 0.11 meters, and an aspect ratio of six.

We also decided to use a pusher engine at the rear of the fuselage. This is because the propeller combination behind the airframe helps to maintain laminar flow on the canard foreplane, body, and wing. The propeller size is  $13/8$ , which means it has a thirteen-inch diameter and it moves forward eight inches for every revolution.



## Part 5: Detail Design

The overall design that we chose was case 3. This design is no different than the one chosen for our preliminary design because we felt that this design was perfect for our figures of merit. Our actual choice consisted of a canard, an engine that allows ~~eight~~ <sup>high</sup> feet per revolution. It also contains spaces for the servos in the fore part of the aircraft and motor batteries in the center of the fuselage. For the calculations please refer to the appendix.

## Part 6 Manufacturing Plan

The manufacturing plan is a mix of both early traditional techniques and advanced composites. The fuselage construction consists of traditional techniques meaning it is predominantly composed of Balsa. This approach included the standard of making formers and running stringers. The canard and main wing implement the new composites techniques.

Making these two components was approached by defining their basic structure in CAD the sectioning. We then printed out the sections that we needed they were used as templates. Traditional techniques, of using strategically placed stringers, was used for rigidity. The voids were then filled with pre-cut white polystyrene foam. This was then sanded down to conform to the formers. Now the we had the shape defined fiberglass and carbonfiber (both fine weave) along with polyester resin was used to laminate the wings shape. After the lamination(wet-lay-up) we contained and sealed it, to practice common vacuum bagging techniques in hopes that the part would be fairly homogenous and the excess resin extracted.

The interfaces between the canard/ fuselage and mainwing/fuselage were given extra attention for rigidity to carry the payload. This resulted in aluminum cross spars.

If time permits or if poor performance demands we will use the existing plane as a male plug. Form this it logically follows to make the female plugs and end up with a virtually mono-cock plane.

## BIBLIOGRAPHY

1. Abott, Ira H. Theory of Wing Sections: Including a Summary of Airfoil Data, Dover Publications, Inc. New York, 1959
2. Anderson, John D., Jr. Fundamentals of Aerodynamics. McGraw-Hill, Inc. New York, 1991
3. Baker, Frank B. "Varieze." RCM Dec. 1979: #784
4. Simons, Martin. Model Craft Aerodynamics, 3<sup>rd</sup> edition. Guildford & Kings Lynn, Great Britain, 1994
5. Renger, Larry. "Skyblaster." RCM July 193: # 1148
6. Kermode, A.C. Mechanics of Flight, 10<sup>th</sup> edition. Longman Group Ltd. , 1996 2.
7. Roberson, John A. Engineering Fluid Mechanics, 6<sup>th</sup> edition. John Wiley & Sons , Inc., New York, 1997
8. Simons, Martin. Model Craft Aerodynamics, 3<sup>rd</sup> edition. Guildford & Kings Lynn, Great Britain, 1994

# Backfi

## Management Part 2

Name	Phone	E-mail	Specialization
VICTOR Z. HUGO	428-0646	hugo@kahuna.sdsu.edu	Project Leader
CHARLES SMITH	225-1529	csmith@kahuna.sdsu.edu	Aerodynamics, Wing/fuselage interface Canard/Fuselage interface
CHARLIE JONES	536-9049	jones8@rohan.sdsu.edu	Aerodynamics, Wing, Winglets, Fundraising
RYAN CALL page	596-8637 910-5993	call@rohan.sdsu.edu	Drafter
JIM GLEDHILL	279-6201	gledhill@rohan.sdsu.edu	Propulsion, Pilot, Controls, Fuselage
SUNSHINE RUSSEL	265-5826	srussel@rohan.sdsu.edu	Aerodynamics, Fundraising
TIM HARDEN	689-1049	Hardenhouse@msn.com	Drafter, Payload
RICHARD GUNDERSON	462-3482	rgunder@travelin.com	Drafter, Pilot, Controls,

Every team member will share the responsibilities of:

Communication, Design Input, Windtunnel Studies  
Structures, Parts Fabrication, Reports, Cleaning Shop

Please fill in the hours  
when you are *unavailable*.

**Schedule**

Name \_\_\_\_\_

Phone \_\_\_\_\_

E-mail \_\_\_\_\_

The team will need you at the hours that you do not fill.  
Expect to be called upon.

	Sun	Mon	Tues	Wed	Thur	Fri	Sat
0600							
0700							
0800							
0900							
1000							
1100							
1200							
1300							
1400							
1500							
1600							
1700							
1800							
1900							
2000							
2100							
2200							
2300							
2400							

Normal people try to sleep after this time...  
Are you normal?  
If not, a special schedule will be made for you.

## Deadlines

	Planned	Actual
Conceptual Design	12-Nov-97	05-Nov-97
Research, Benchmarking (Info. Collecting)	26-Nov-97	29-Dec-97
Planning/Estimating (Preliminary design)	29-Dec-97	28-Jan-98
Finalize building plan (detailed design)	08-Jan-98	11-Feb-98
Strut Prototype Production	19-Jan-98	16-Feb-98
Wind tunnel model	28-Feb-98	06-Mar-98
Wind tunnel set-up	27-Feb-98	02-Mar-98
Wind tunnel studies	02-Mar-98	Pending
Rough Draft Proposal Report	03-Mar-98	11-Mar-98
Final Draft Proposal Report	10-Mar-98	12-Mar-98
Completion of Prototype	18-Mar-98	Pending
Pre-flight De-bugging	19-Mar-98	Pending
Maiden Flight	21-Mar-98	Pending
De-bugging Time	22-Mar-98	Pending
Ground crew practice	21-Mar-98	Pending
Rough Draft Addendum Report	04-Apr-98	Pending
Final Draft Addendum Report	08-Apr-98	Pending
Finalize Performance	14-Apr-98	Pending
Prepare for travel	23-Apr-98	Pending
Competition time	25-Apr-98	Pending

Management part -

## COST ANALYSIS

Windtunnel model		quantity	cost	total	acquisition status	
		by unit			yes	no
1	Door Skin	1	9.5	9.5	x	
2	Polystyrene foam					
	pink	remnant	0	0	x	
	white	remnant	0	0	x	
3	Bondo 3min epoxy	1	4	4	x	
4	scrap aluminum					
	mounting arm	remnant	0	0	x	
	variable canard mount	remnant	0	0	x	
	variable wing mount	remnant	0	0	x	
5	fine fiberglass weave	2	5	10	x	
6	disposables					
	safety	1	10	10	x	
	measuring	3	12	36	x	
7	1/2 gallon of polyester resin	1	50	50	x	
	Vacuum Bagging Accessories					
8	plastic	8	3	24		x
9	chromium(seal tape)	3	3	9		x
10	peel-ply	8	4	32		x
11	babycloth	8	5	40		x
		total cost		224.5		
		Funds needed=		105		

(K4)

*Managemen's for*

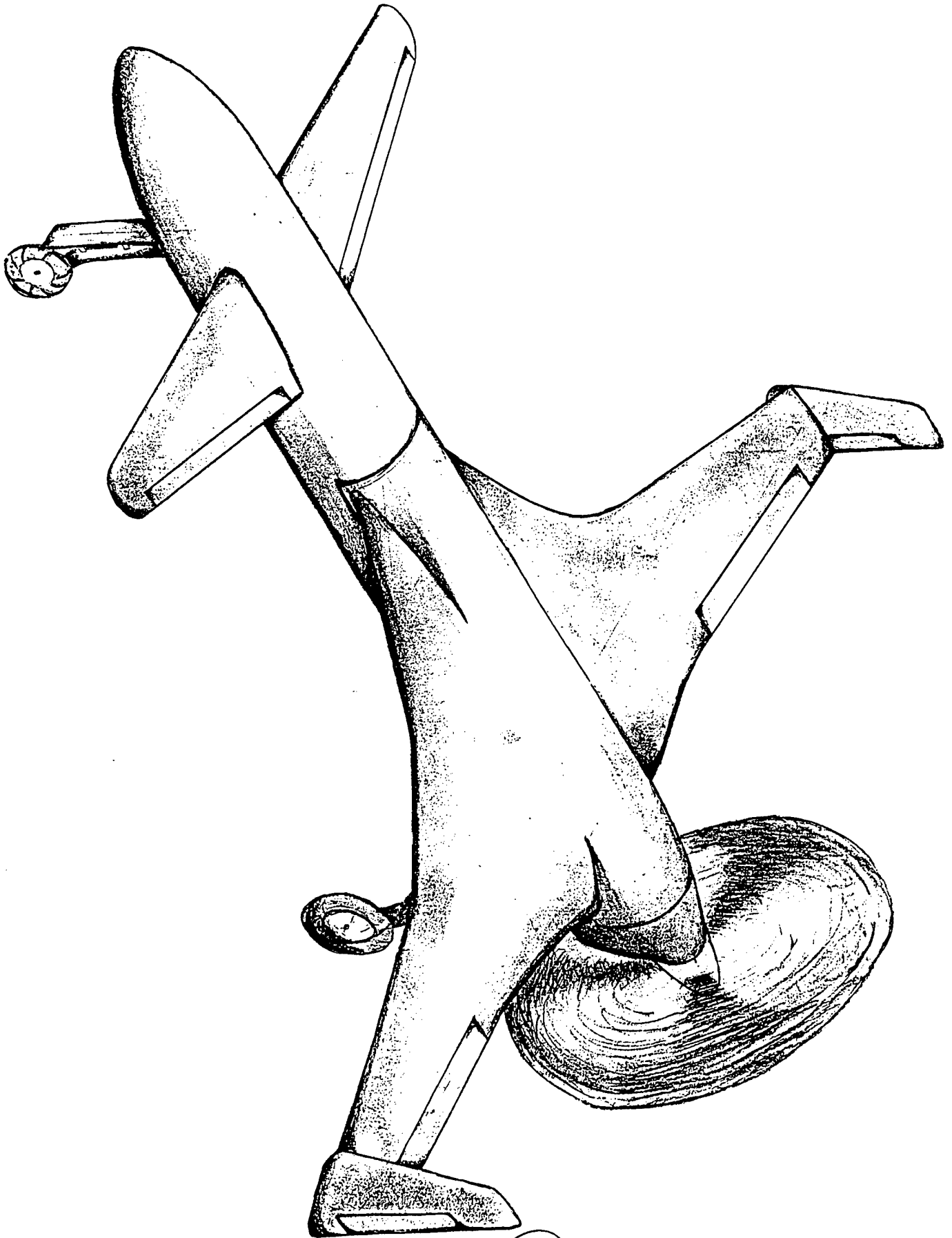
PROTOTYPE	QUANTITY BY UNIT	COST	TOTAL	ACQUISITION STATUS	
				YES	NO
1 Balsa wood	2	5	10		x
sheets	35	0.5	17.5		x
stringers	2	7	14		x
block	10	1	10		x
2 Spruce stringers	2	10	20		x
3 Zap(glue)	2	4	8		x
4 3min epoxy	1	75	75		x
5 Polyester laminating resin	3	5	15		x
6 fine fiberglass weave	3	21	63	x	
7 fine carbon weave					
8 Vaccum Bagging Accessories	16	3	48		x
9 plastic	6	3	18		x
10 chromium(stel tape)	16	4	65		x
11 peel-ply	16	5	80		x
12 babycloth	1	3.25	3.25	x	
13 front wheels	2	9	18	x	
14 rear wheels	2	4.15	8.3		x
15 front landing gear	1	25	25		x
16 rear landing gear	2	4.25	8.5		x
17 push rods	2	4	8		x
18 linking arms	2	10	20		x
19 Tie rods	1	5.75	5.75		x
20 hinges	2	5	10		x
22 3-blade push prop	2	4	8	x	
23 2-blade push prop	1	200	200		x
24 Futuba controler/servos	20	9	180		x
25 batteries-c size Nicad 200mah	1	210	210		x
26 Charger	0	0	50		x
27 Miscellaneous					

total cost 1198.3  
**Funds needed = 1106.05**

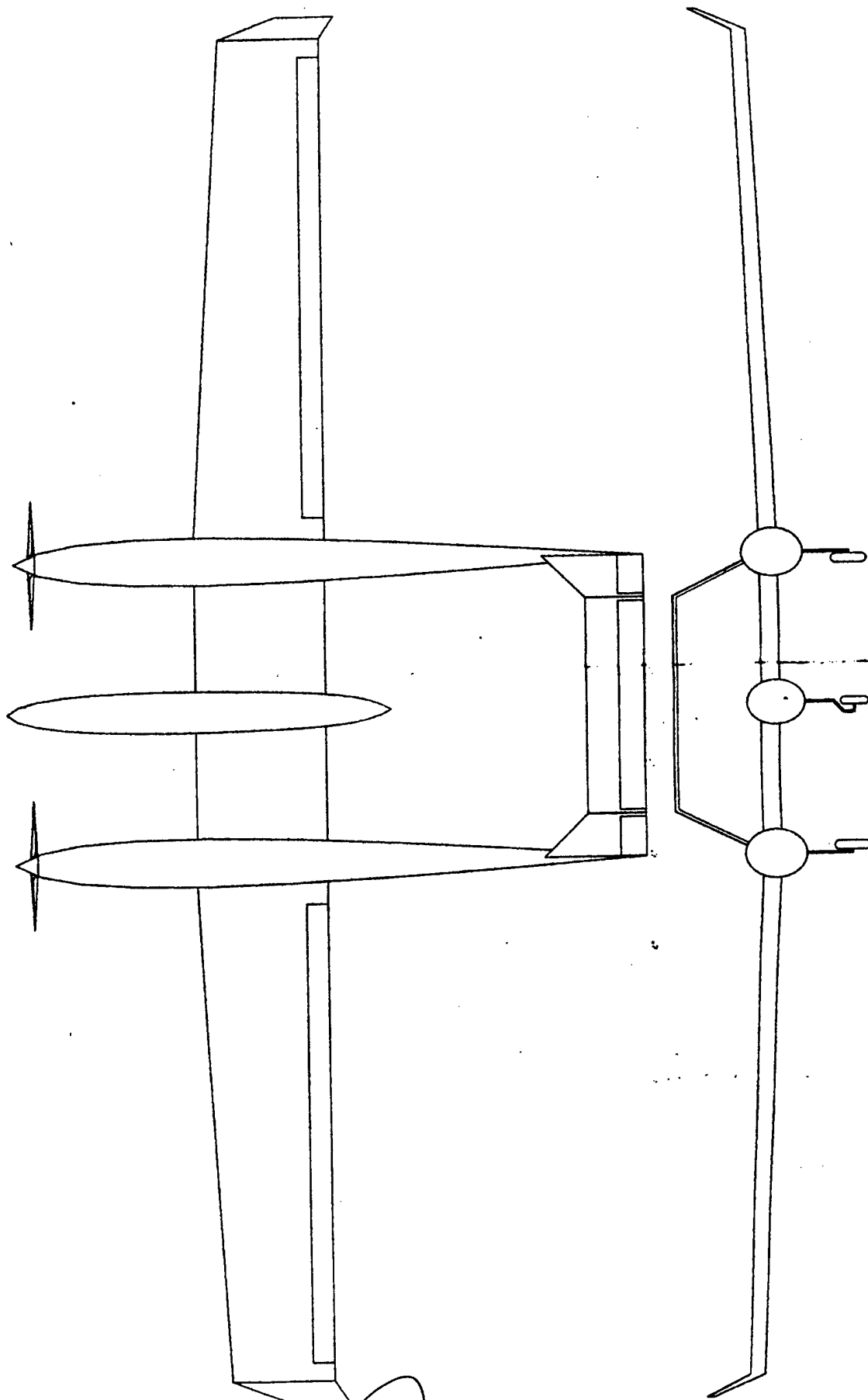
65



Conceptual part 3



Conceptual part 3



(17)

# Conceptual

part 3

$$C_R = .43 \text{ m}$$

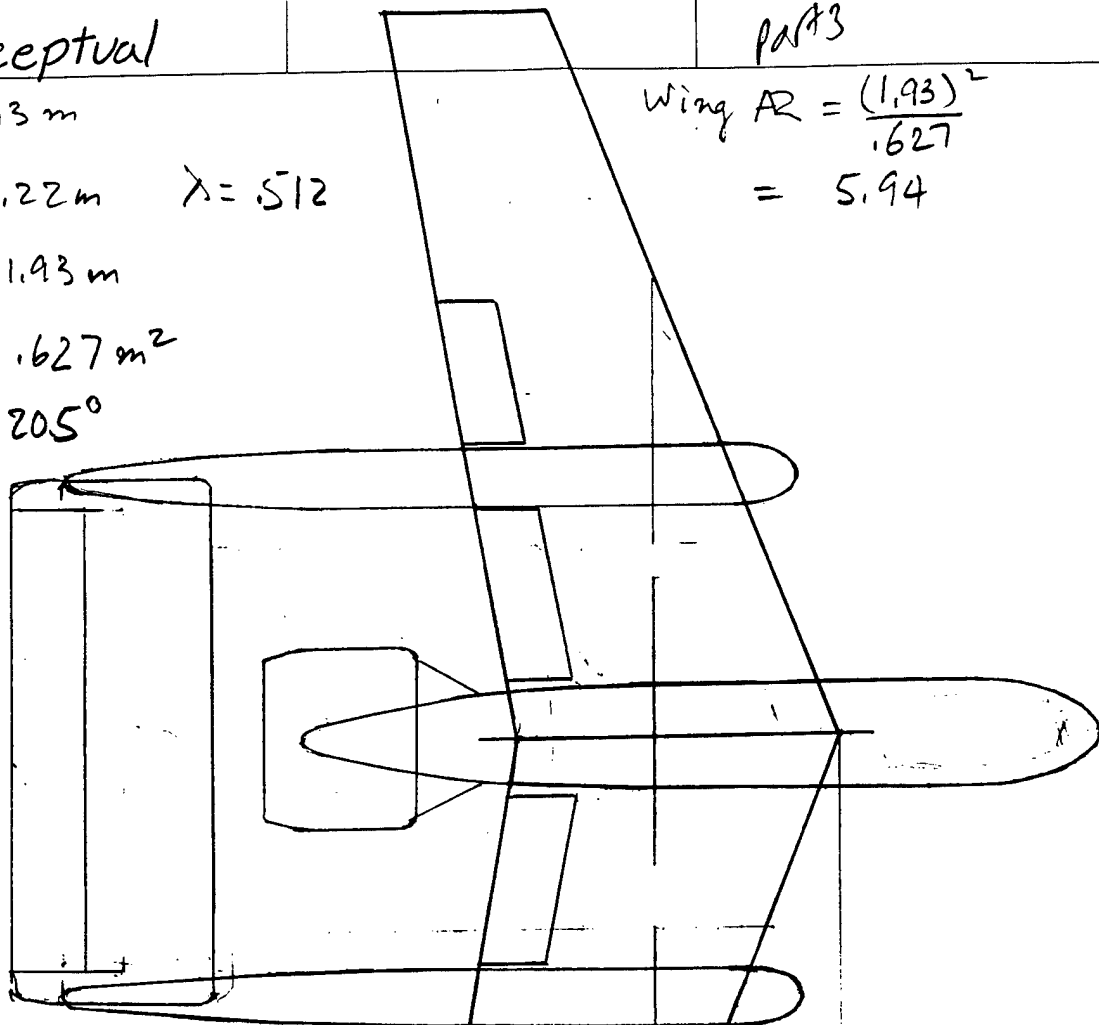
$$C_t = .22 \text{ m} \quad \lambda = .512$$

$$b = 1.93 \text{ m}$$

$$S = .627 \text{ m}^2$$

$$\Lambda = 20.5^\circ$$

$$\text{Wing } AR = \frac{(1.93)^2}{.627} = 5.94$$



Horizontal tail

$$\bar{C} = .27 \quad AR_t = 2.6$$

$$b = .7 \text{ m}$$

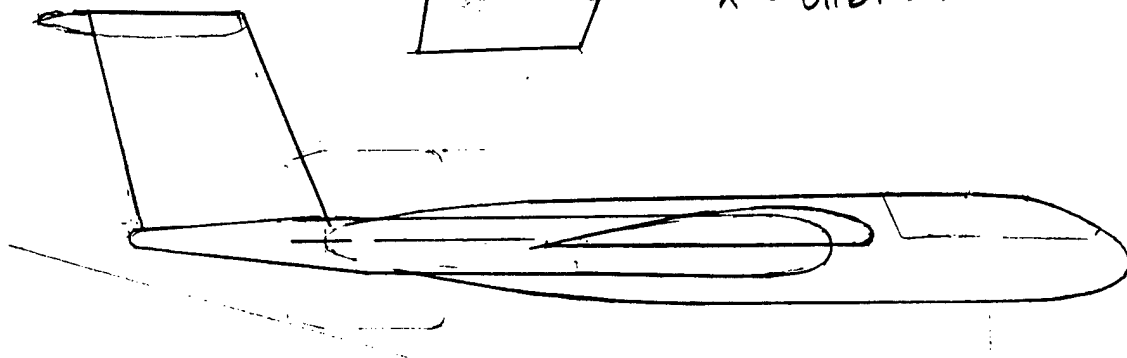
$$S_t = .189 \text{ m}^2$$

$$\bar{C} = \frac{2}{3} (.43) \left( \frac{1 + .512 + .512^2}{1 + .512} \right)$$

$$\bar{C} = .336 \text{ m}$$

$$X = \frac{b}{2} \frac{1}{3} \frac{1 + 2(.512)}{1 + .512} \tan 20.5$$

$$X = 0.161 \text{ m}$$

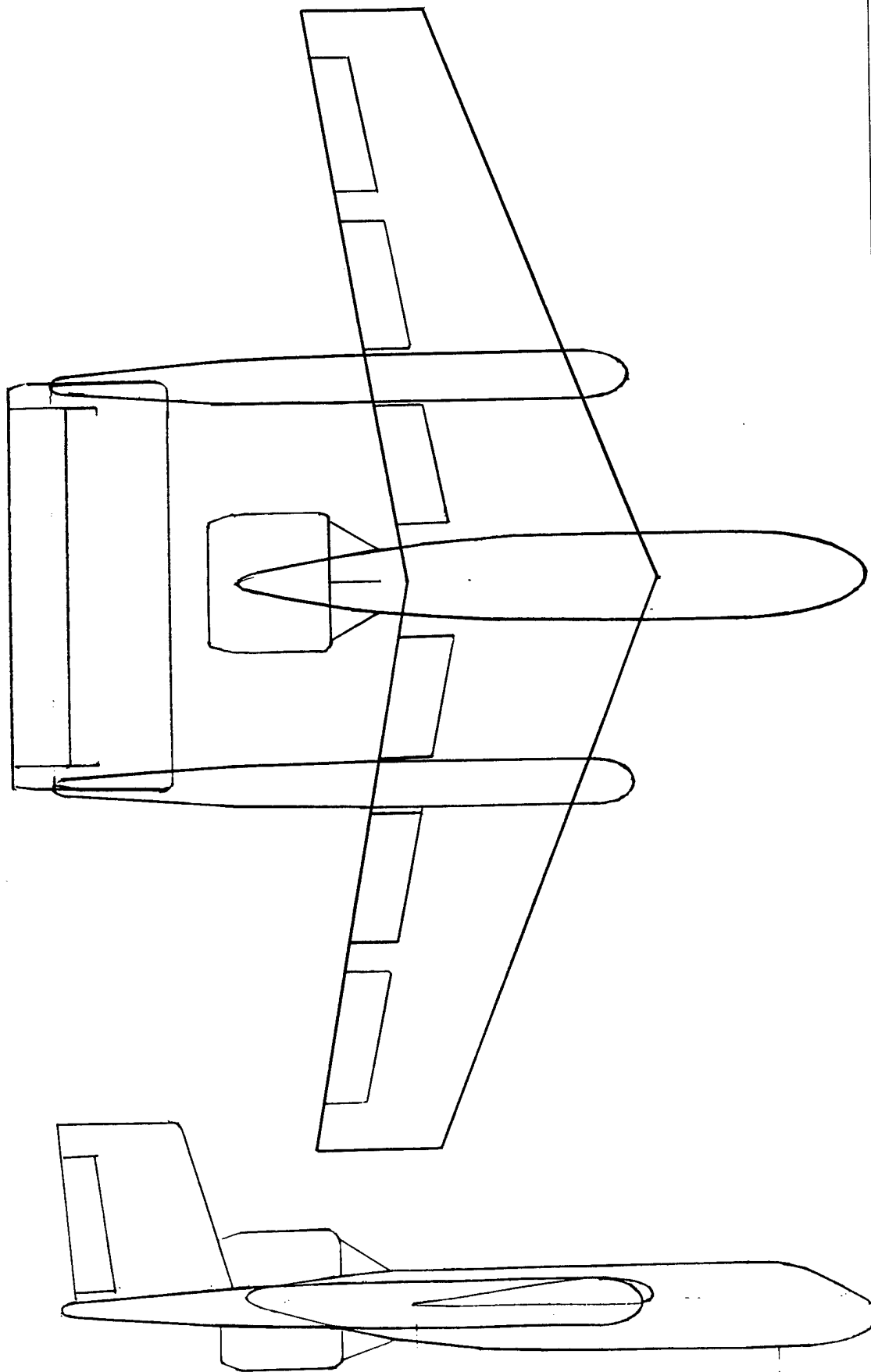


WING AERODYNAMICS CENTER

$$\frac{1}{4} (.336 \text{ m}) + 0.161 \text{ m} = .245 \text{ m}$$

(18)

Conceptual



# Preliminary / Detailed : part 4

**NACA  
0018**

ca=chord  
length

ca= 0.342523

x % of ca	y % of ca	X	Y
0	0	0	0
0.5		0.001712	0
1.25	2.841	0.004281	0.009731
2.5	3.922	0.008563	0.013433
5	5.332	0.017126	0.018263
7.5	6.3	0.025689	0.021578
10	7.024	0.034252	0.024058
15	8.018	0.051378	0.027463
20	8.606	0.068504	0.029477
25	8.912	0.085630	0.030525
30	9.003	0.102756	0.030837
40	8.705	0.137009	0.029816
50	7.941	0.171261	0.027199
60	6.845	0.205513	0.023445
70	5.496	0.239766	0.018825
80	3.935	0.274018	0.013478
90	2.172	0.308270	0.007439
95	1.21	0.325396	0.004144
100	0.189	0.342523	0.47368E

**NACA 63  
-018**

cb=chord  
length

cb= 1

x % of cb	y % of cb	X	Y
0	0	0	0
0.5	1.404	0.005	0.01404
0.75	1.713	0.0075	0.01713
1.25	2.217	0.0125	0.02217
2.5	3.104	0.025	0.03104
5	4.362	0.05	0.04362
7.5	5.308	0.075	0.05308
10	6.068	0.1	0.06068
15	7.225	0.15	0.07225
20	8.048	0.2	0.08048
25	8.6	0.25	0.086
30	8.913	0.3	0.08913
35	9	0.35	0.09
40	8.845	0.4	0.08845
45	8.482	0.45	0.08482
50	7.942	0.5	0.07942
55	7.256	0.55	0.07256
60	6.455	0.6	0.06455
65	5.567	0.65	0.05567
70	4.622	0.7	0.04622
75	3.65	0.75	0.0365
80	2.691	0.8	0.02691
85	1.787	0.85	0.01787
90	0.985	0.9	0.00985
95	0.348	0.95	0.00348
100	0	1	0

**NACA  
0024**

cc=chord  
length

cc= 1

x % of cc	y % of cc	X	Y
0	0	0	0
0.5		0.005	0
1.25	3.788	0.0125	0.03788
2.5	5.229	0.025	0.05229
5	7.109	0.05	0.07109
7.5	8.4	0.075	0.084
10	9.365	0.1	0.09365
15	10.691	0.15	0.10691
20	11.475	0.2	0.11475
25	11.883	0.25	0.11883
30	12.004	0.3	0.12004
40	11.607	0.4	0.11607
50	10.588	0.5	0.10588
60	9.127	0.6	0.09127
70	7.328	0.7	0.07328
80	5.247	0.8	0.05247
90	2.896	0.9	0.02896
95	1.613	0.95	0.01613
100	0.252	1	0.00252

**NACA  
63A006**

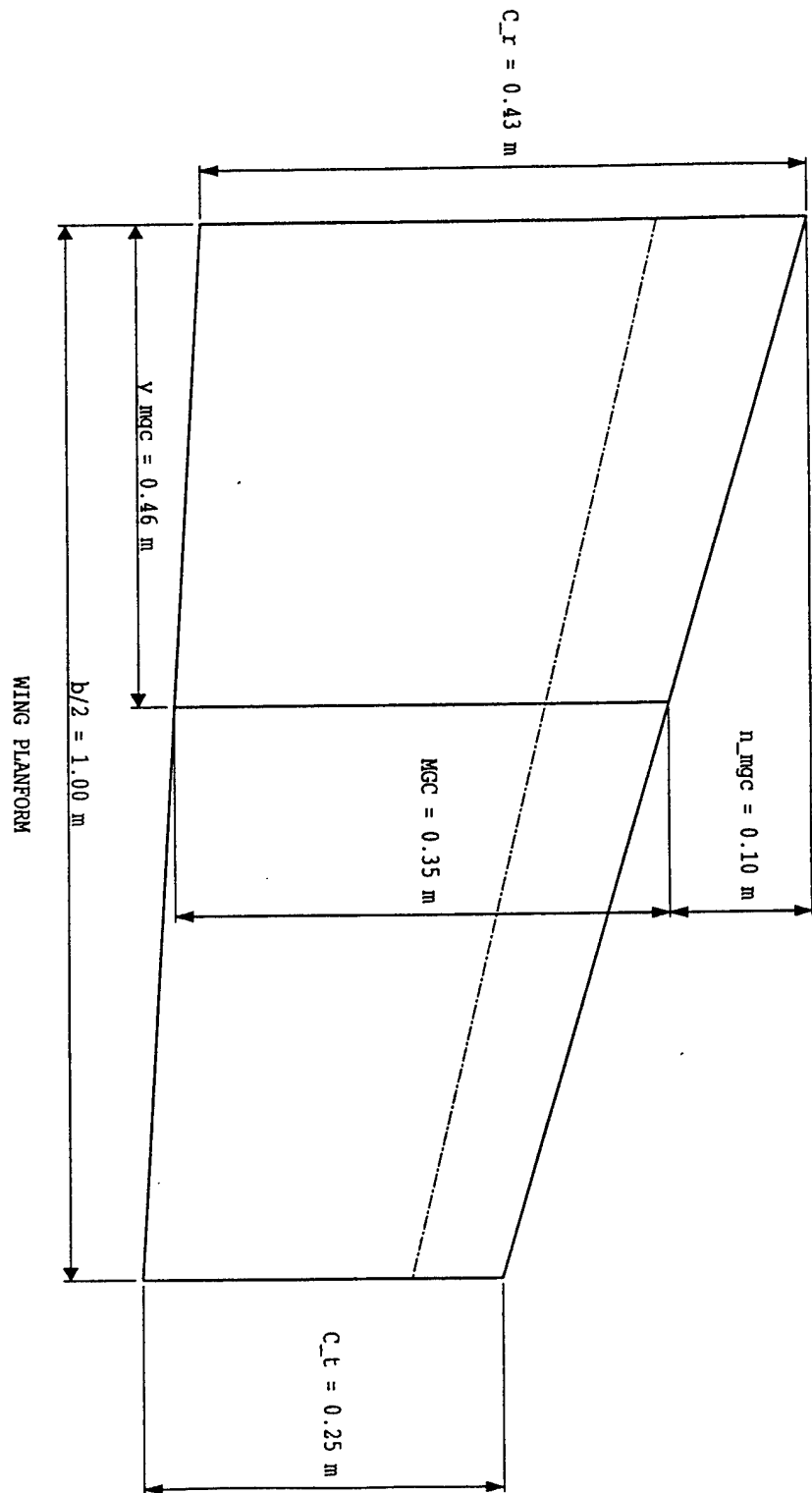
cd=chord  
length

cd= 1

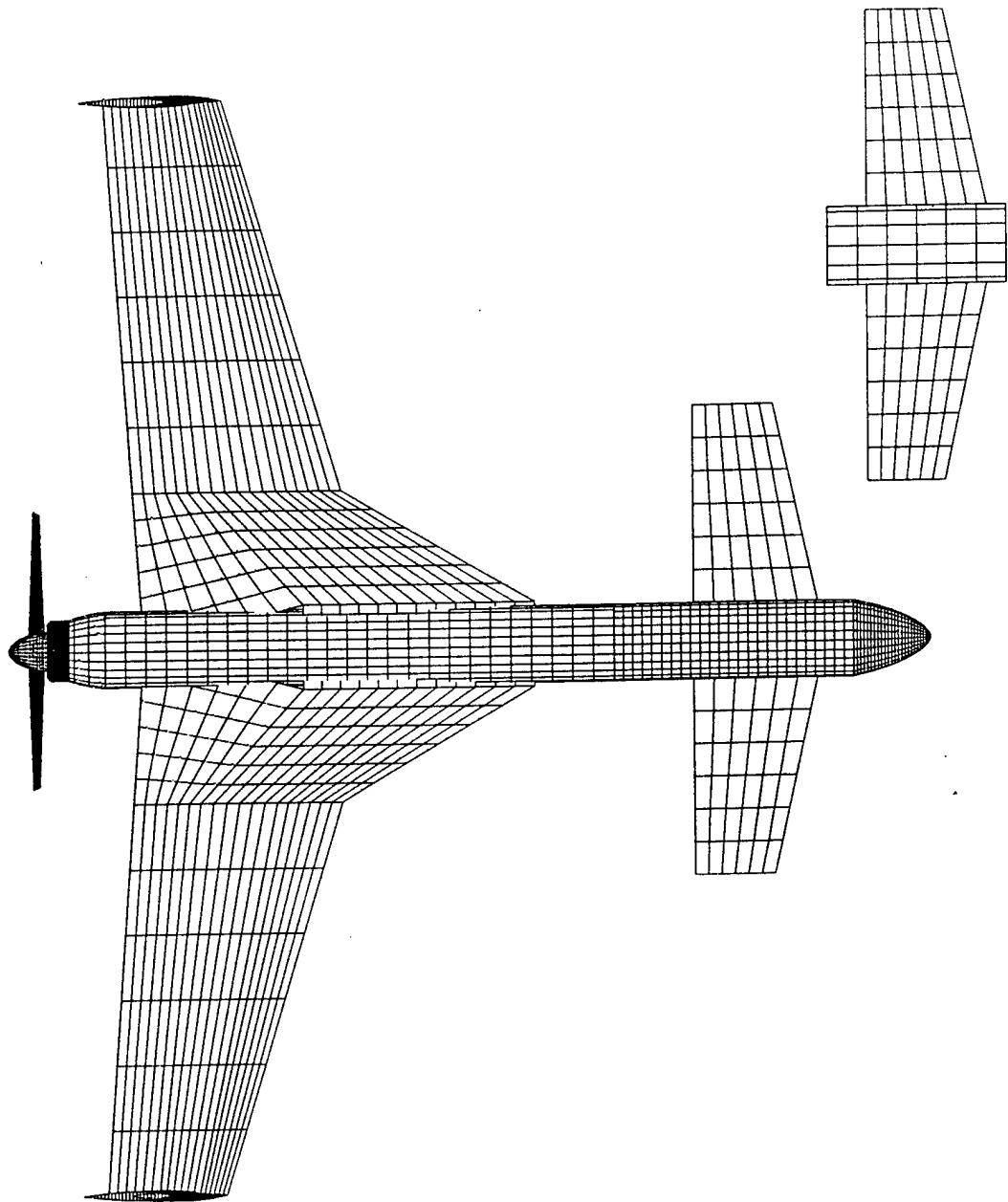
x % of cb	y % of cb	X	Y
0	0	0	0
0.5	0.495	0.005	0.00495
0.75	0.595	0.0075	0.00595
1.25	0.754	0.0125	0.00754
2.5	1.045	0.025	0.01045
5	1.447	0.05	0.01447
7.5	1.747	0.075	0.01747
10	1.989	0.1	0.01989
15	2.362	0.15	0.02362
20	2.631	0.2	0.02631
25	2.82	0.25	0.0282
30	2.942	0.3	0.02942
35	2.996	0.35	0.02996
40	2.985	0.4	0.02985
45	2.914	0.45	0.02914
50	2.788	0.5	0.02788
55	2.613	0.55	0.02613
60	2.396	0.6	0.02396
65	2.143	0.65	0.02143
70	1.859	0.7	0.01859
75	1.556	0.75	0.01556
80	1.248	0.8	0.01248
85	0.939	0.85	0.00939
90	0.63	0.9	0.0063
95	0.322	0.95	0.00322
100	0.013	1	0.00013

20

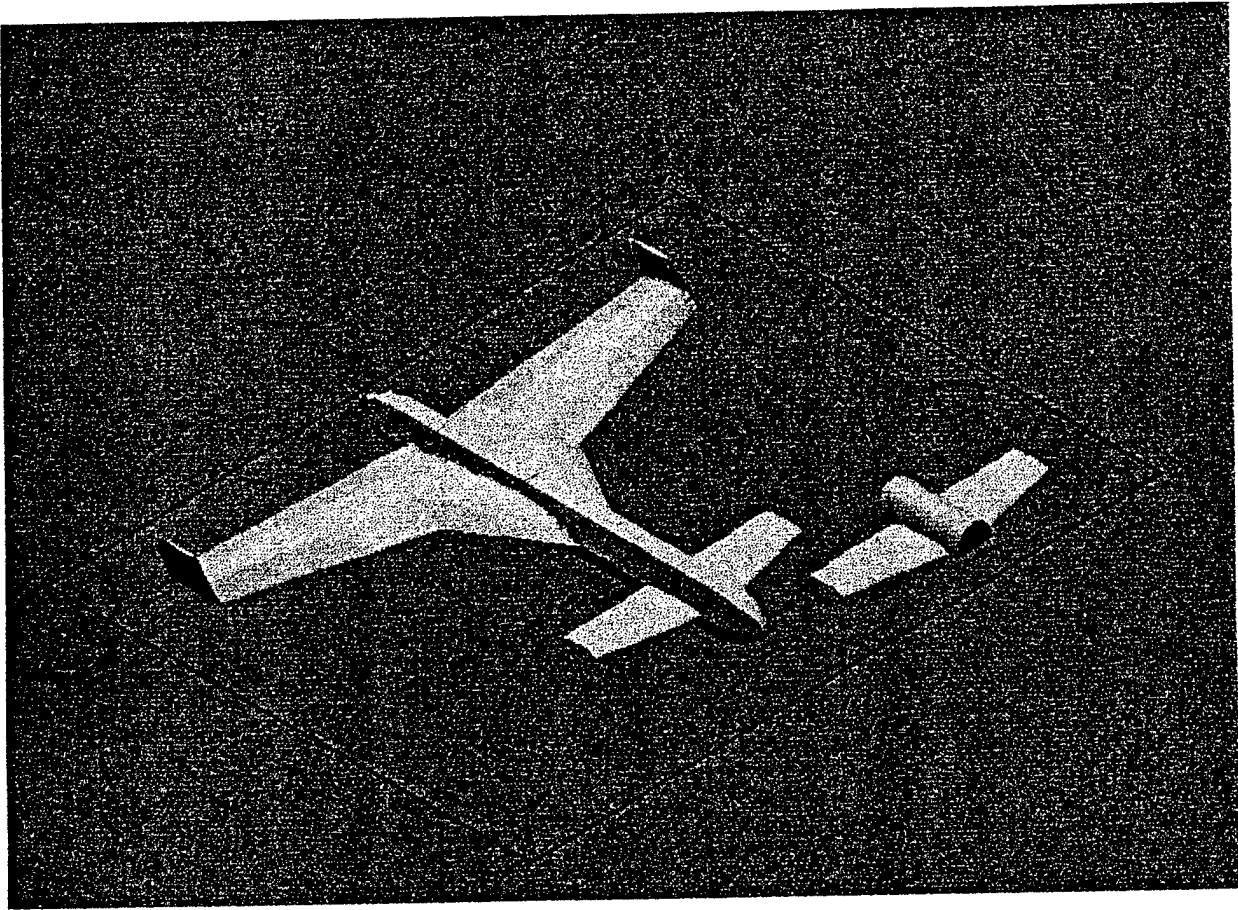
# Preliminary Design part 4



Preliminary Design part 4

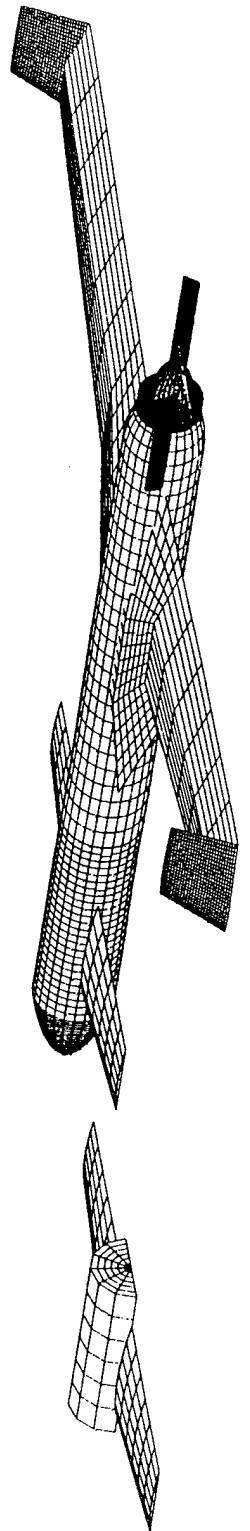


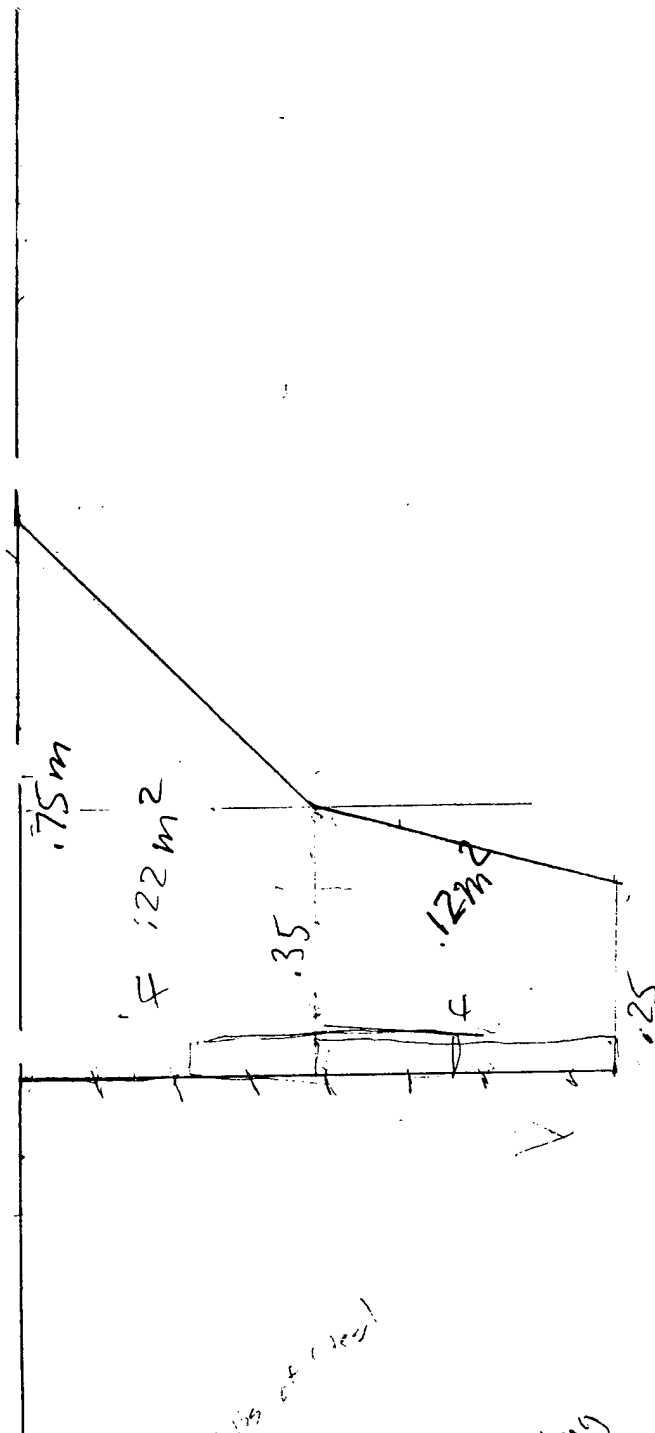
Preliminary Design part 4





# Preliminary Design part 4



Preliminary Design part 4

7.5 m of chord

$$F = m a$$

$$\frac{7.5}{32} = m$$

$$m = 0.2344$$

$$m = 3.9 \text{ kg}$$

(25)

Critical Dimensions

Backfire

Detail parts

## Detailed Design

FULL SCALE  
(Prototype)0.4 SCALE MODEL  
(Wind Tunnel Model)NACA 65<sub>3</sub>618  
(Rear Wing)  
Wingspan

2 m

0.8 m

 $C_r$ 

0.4282 m

0.17128 m

 $C_t$ 

0.252 m

0.1008 m

S

0.68 m<sup>2</sup>0.272 m<sup>2</sup>

AR

5.88

5.88

fuselage diameter

0.127 m

0.051 m

fuselage length

1.25 m

0.5 m

leading edge sweepback  
angle

20°

20°

NACA 4412  
(Canard)

Wingspan

0.66 m

0.264 m

Chord

0.11 m

0.044 m

AR

6

6

## Performance Data Calculations (Estimated)

Air Speed  $V_{\infty} = 30 \text{ mph} = 13.41 \text{ m/s}$  (standard sea level)

Takeoff Gross Weight  $W = L = 18.0 \pm 0.25 \text{ lb} = 80 \text{ N}$

Rear wing airfoil NACA 653618  $C_L = 1.8$  at  $\alpha = 0^\circ$   
 $C_{L_{\max}} = 2.6$  at  $\alpha = 9^\circ$

$$q_{\infty} = \frac{1}{2} \rho_{\infty} V_{\infty}^2 = \frac{1}{2} (1.23 \text{ kg/m}^3) (13.41 \text{ m/s})^2 = 110.6 \text{ N/m}^2$$

$$S = \frac{L}{C_L q_{\infty}} = \frac{80 \text{ N}}{(1.8)(110.6 \text{ N/m}^2)} = 0.40 \text{ m}^2 \text{ (minimum)}$$

- \* Prototype  $S$  increased to 0.68 to ensure lift capability  
 (Margin of Safety)

$$V_{\text{stall}} = \left( \frac{2L}{\rho_{\infty} S C_{L_{\max}}} \right)^{1/2} = \left[ \frac{2(80 \text{ N})}{(1.23 \text{ kg/m}^3)(0.68)(2.6)} \right]^{1/2} = 19.2 \text{ mph}$$

at  $\alpha = 9^\circ$

Design recommended  $C_D = 0.1$

$$\frac{L}{D} = \frac{C_L}{C_D} = \frac{1.8}{0.1} = 18$$

$$D = \frac{L}{18} = \frac{80 \text{ N}}{18} = 4.44 \text{ N}$$

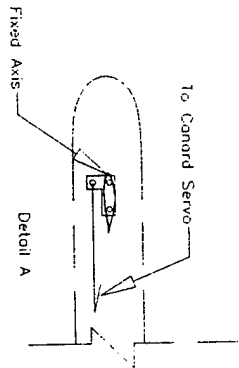
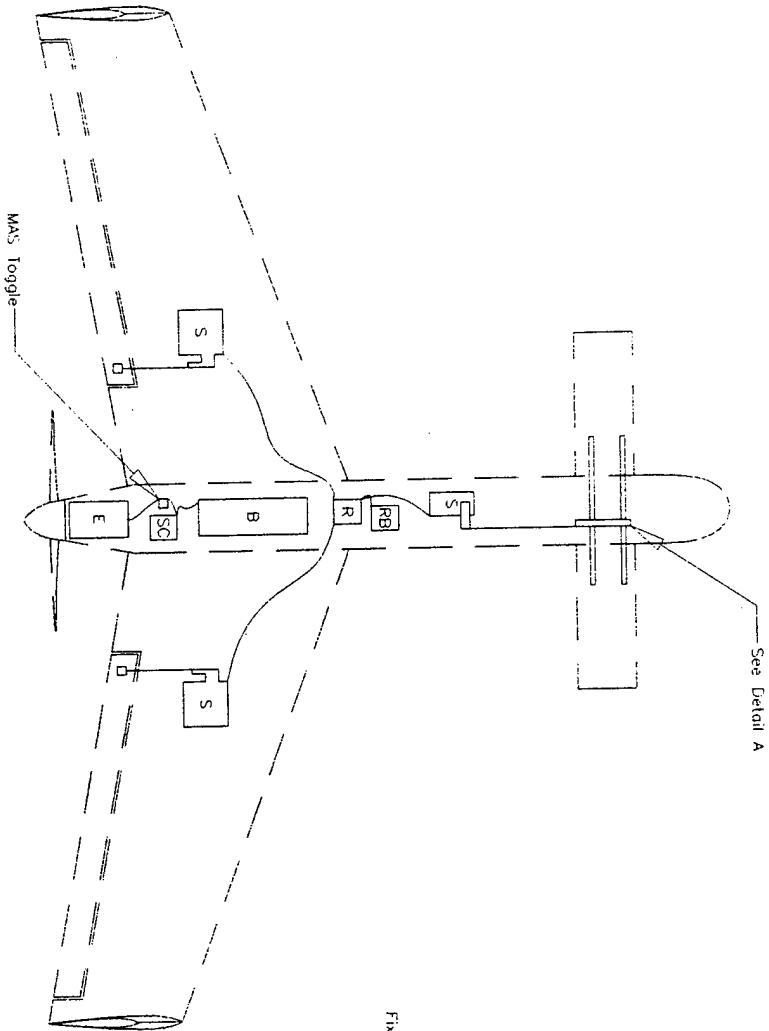
$$\text{Power Required} = D \cdot V = (4.44 \text{ N})(13.41 \text{ m/s}) = 59.5 \text{ (minimum)}$$

- \* Rear wing limited to  $C_L$  lower than foreplane (canard) to ensure that canard will stall first, therefore canard airfoil chosen for higher  $C_L$ .
- \* Nosediving pitching moment intrinsic to design counter-acted by lift capabilities of front canard.

Front Canard Airfoil NACA 4412

Detail part 5

- S = Servo
- R = Receiver
- RB = Receiver Battery
- SC = Speed Control
- E = Electric Motor
- B = Motor Battery



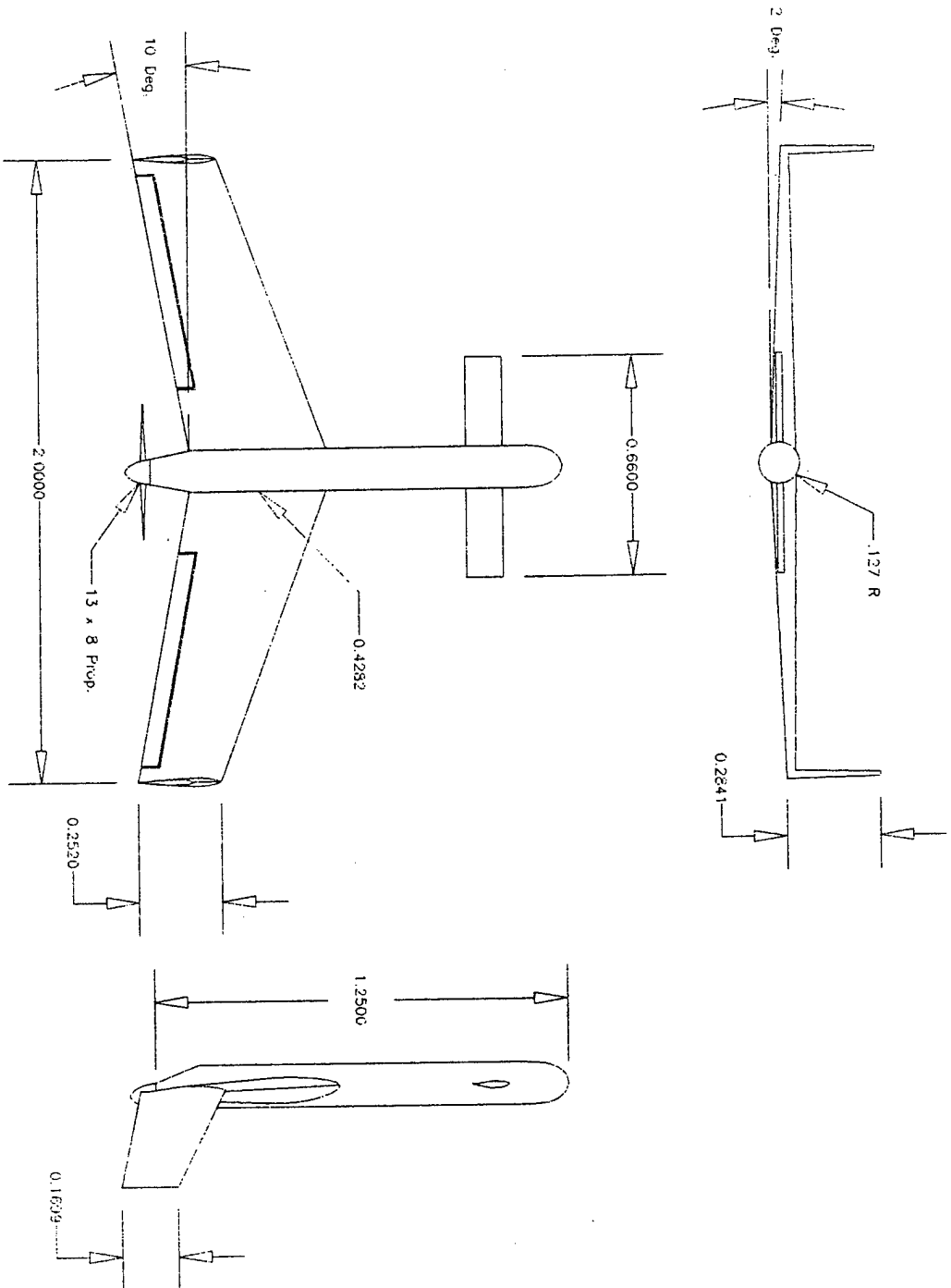
# BACKFIRE

(Control Layout Simplified)

Drawn By: Richard Gunderson 3/01/98

SDSU AIAA Student Design Project

Detail Part 5



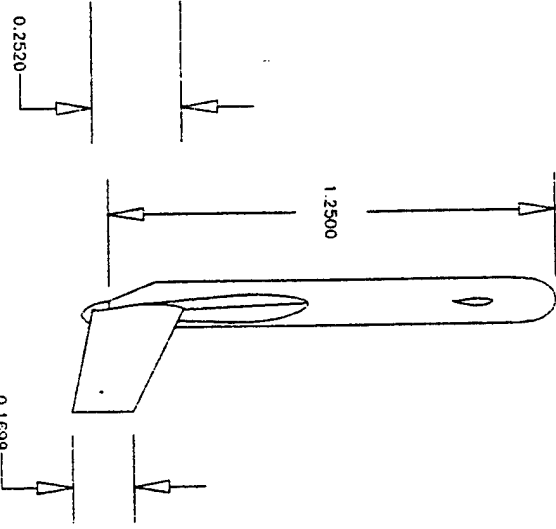
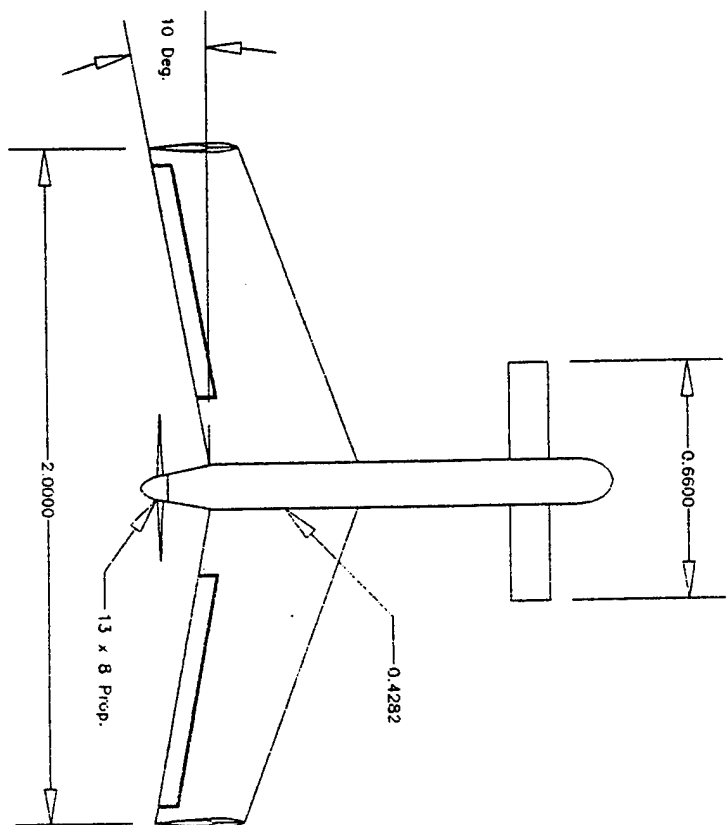
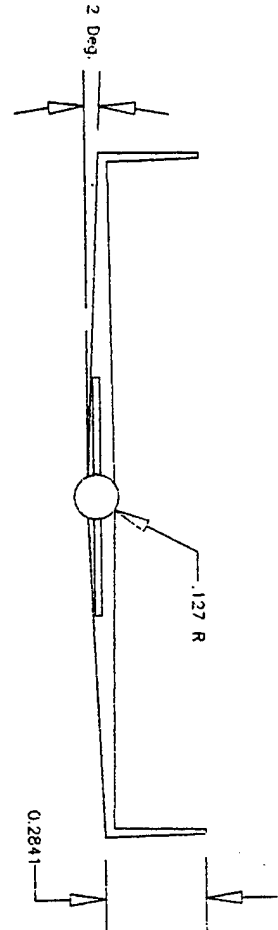
BACKFIRE  
(Three View)

Drawn By: Richard Gunderson 3/01/98

SDSU AIAA Student Design Project

29

Notes



# BACKFIRE

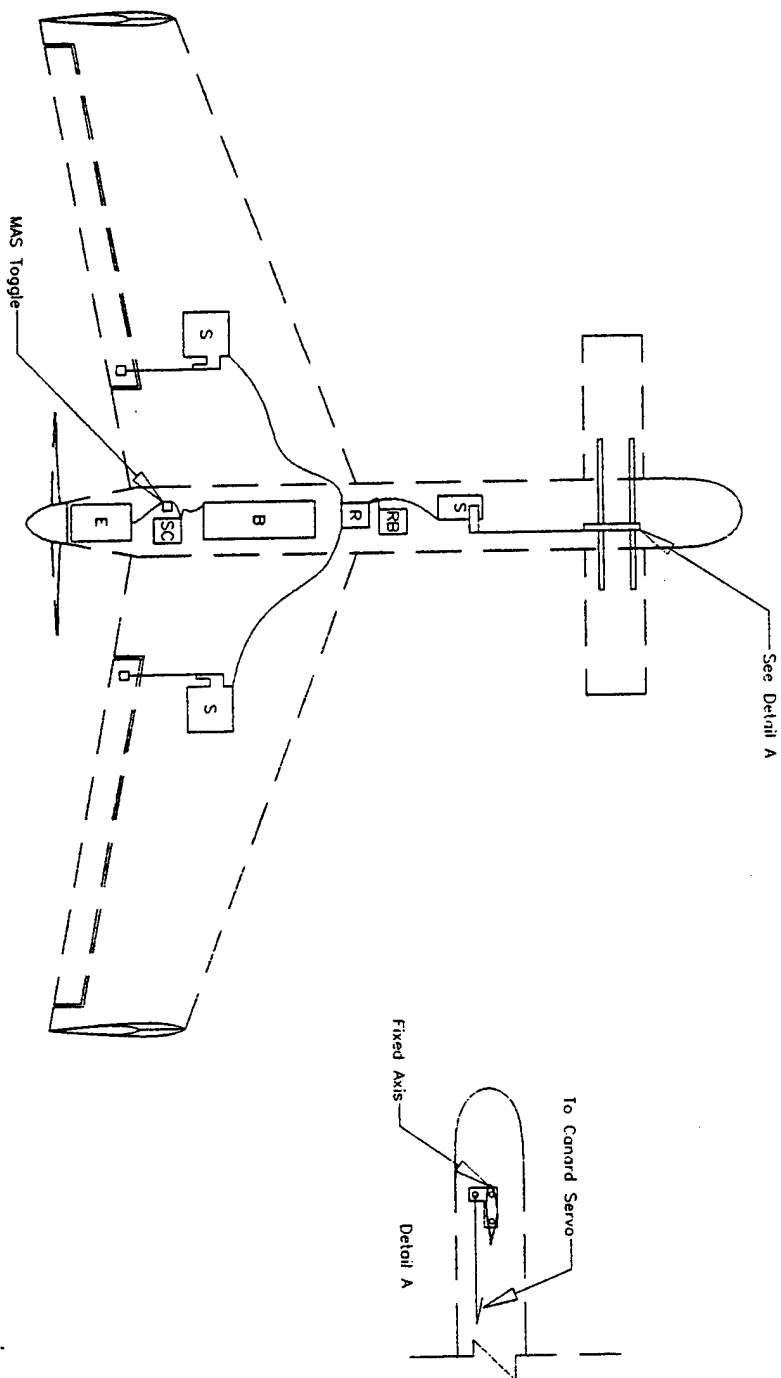
(Three View)

Drawn By: Richard Gunderson 3/01/98

SDSU AIA Student Design Project

30

Detail 1/6rt5-



S = Servo  
 R = Receiver  
 RB = Reciever Battery  
 SC = Speed Control  
 E = Electric Motor  
 B = Motor Battery

# BACKFIRE

(Control Layout Simplified)

Drawn By: Richard Gunderson 3/01/98

SDSU AMA Student Design Project

(31)



ADDENDUM PHASE REPORT  
For  
PROJECT BACKFIRE

Prepared by:  
SDSU's AIAA Student Chapter  
BACKFIRE TEAM  
4-13-98

## Table of Contents

	pages
1 Documented changes in PPR part 5	1
2 Documented changes in PPR part 6	2-3
3 Identified areas of improvement	3-4
4 Estimates of time savings from part3	4
5 Table of Manufacture's list prices	appendix
6 Narrative Assessment of costs	4
7 Bibliography	5
8 Summary of changes from PPR part 6	appendix
9 New detailed drawings of entire Backfire plane	appendix

Many lessons have been learned since the submission of the Proposal Phase Report(PPR). This whole project has taught us how much we really know about designing, flight, and the wonderful RC plane hobby. More importantly it has taught us more transcendental lessons about leadership(good & bad), cooperative learning, team work, engineering communication, fundraising, time management, and perseverance. All of these lessons would not have materialized if the Backfire Project was not undergoing changes or growth. The PPR was lacking in much of the required information. Let us now take a look at what we discovered about the definitions of some of the terms and what they amount to with respect to Backfire.

In part 5 of the PPR we were to state the values and characteristics of our plane , in short, detail design. We changed the handling qualities of our plane by changing dimensions of configuration and control surfaces. Case 3 was originally chosen because of its instability. However we "toned" down the inherent instability by keeping the canard and main wing as far apart as possible in both the lateral and longitudinal directions (ref. 1 page248). Another main configuration change happened in the dihedral angle which was increased to 5 degrees. Furthermore the winglets were placed further back to correct the location of the CG without the payload (ref. 2 page 165). The whole canard was going to be used as a control surface, instead it was positioned at a positive 2 degree angle of attack with elevators on the trailing edge. Finally another drastic change in the addition of flaps and reduction of aileron control surface. Rudders were added but are not manually controlled. The rudders are designed to only bend away from the fuselage, restricted by music wire.

The G-load capacity was determined by graph(ref.3 page 183). The G-load capacity ranges from 1-2( $\pm 0.3$ ). The true range, endurance, and payload fraction have not been determined quantitatively.

More changes have occurred in the components and systems architecture. These include: separable wings, canard, and winglets. This characteristic was desired for transportation purposes. With the use of aluminum plates shaped in the airfoil sections of the wing/fuselage

mating surfaces, we were able to reinforce the main aluminum cross spars. They connect in a sturdy lap joint fastened by four bolts in the center of the fuselage. The canard is one unit which is bolted in a slot in the front of the fuselage. The addition of flaps increases the amount of servos in the wing unit (please refer to the appendix). There is now one servo per control surface. In addition there is another servo operating the front landing gear for taxiing.

The PPR part 6, manufacturing plan, experienced many changes as well. At the time of the PPR it seemed our avenues were wide open. The rules had stated that propulsion components should be commercially available and not altered. This is sensible and makes it easier of course. The team made decisions that would divert us from "re-inventing the wheel". Not only did we buy the propulsion components over the counter, but many of the controls and linkages as well. The only avenue for creativity left is the fabrication of the plane. This is quite a wide avenue! Our manufacturing approach can be best observed when we view the different component systems. The component systems are divided into (in order from forward to aft): nose, canard, fuselage, wing/fuselage interface, wing, winglet, and rear fuselage taper. The nose was originally going to be done on a lathe and then we looked at stereo-lithography on campus. Further investigation showed this process to be quick and accurate, but costly so the final plan was to revert to using cross-section templates and fiberglass composite processes (FCP). The fuselage was originally being made with balsa wood construction, a traditional technique (TT). The production process drastically changed to using 4.5 inches (outside diameter) black ABS pipe to define the fuselage male mold. The interface was not mentioned in the earlier report because of its difficulty to manufacture. We solved the problem with same process as the nose by using cross-sections and FCP. The taper at the end of the fuselage also used this manufacturing plan. All of these parts compose a male mold that was then used to "pull off" the part.

The wing had many ways to be made which included traditional methods, Carbon fiber, and FCP. Originally we were going to use carbon fiber. However we found out that carbon

fibers can block out radio waves. We could not take the chance of this happening, so we went back to FCP. We used doorskin for the wing structure and "stuffed" it with foam, FCP and finally vacuum-bag.

The winglets were originally going to be made of aluminum. FOM's such as cost, availability and skill level caused us to change. We went to using 1/8 inch balsa and Monocoat. This would provide weight savings and "when" a crash occurs it would absorb the shock instead of twisting the whole wing. All these changes in manufacturing came about by learning from team agreement, consulting with hobby shops, consulting with professors and individual member's hobby experience. All of these changes were made for a better Backfire, but there are ways to improve even more(refer to appendix for summary list of this section).

There are many areas for improvement in design and manufacturing process. The design of a next canard configuration should include making the aircraft less heavy through advanced time consuming FCP. These processes include making a female tool. Extensive wind tunnel testing should be executed to optimize airfoils of the canard and main wing and their respective angles of attack. Another lacking among the many team members was an understanding of the propulsion system, particularly the propeller and the power plant (batteries). The engine should be mounted for high clearance and exposure to freestream air. All of these changes can easily be implemented with improvements in the manufacturing process.

Key improvements, in manufacturing process has to occur in better project leadership, engineering communication and a greater sense of team spirit. The mode of communication should be more professional with documentation of individual member's tasks, documentation of group decisions and most importantly sketches and drawings. Production of female tools requires time, but yields excellent results. This cannot be effectively practiced without the group having a minimal background in composite techniques. Furthermore knowledge of building materials is essential for ease of production and overall performance of a future Backfire or any plane.

These improvements would speed up the production process, but additional tasks and hours would have to be added for making female molds. The need for quality should override the saving of time, but of course still be within the deadlines. The effective hours, of an individual member on this project, is equal to 100days times 3hours plus 14days times 8 hours. This equals 472 hours. This time would only be minimized by at most 20%. Actually, based on current trends and attitudes there is no such thing as saving time. There is this thinking that most engineering can be improved upon or there is always room for optimization. Notice that all the knowledge of processes, design and materials does not save time, but expands it because with the knowledge it opens up more avenues of application. The predicted costs differ drastically from what was actually spent. Some things were simply not needed. Please refer to the appendix for the old cost analysis and actual Manufacture's list analysis.

The prices, of the components and production, were actually cheaper through asking for donations and discounts. However we still suffered with insufficient funds, most small items were obtained through personal funds. The most expensive item was the motor with speed controller and batteries. We did receive these at discount Internet prices. Funding for projects is difficult to acquire, especially when milestones are not reached in a timely manner, which unfortunately was the case with Backfire.

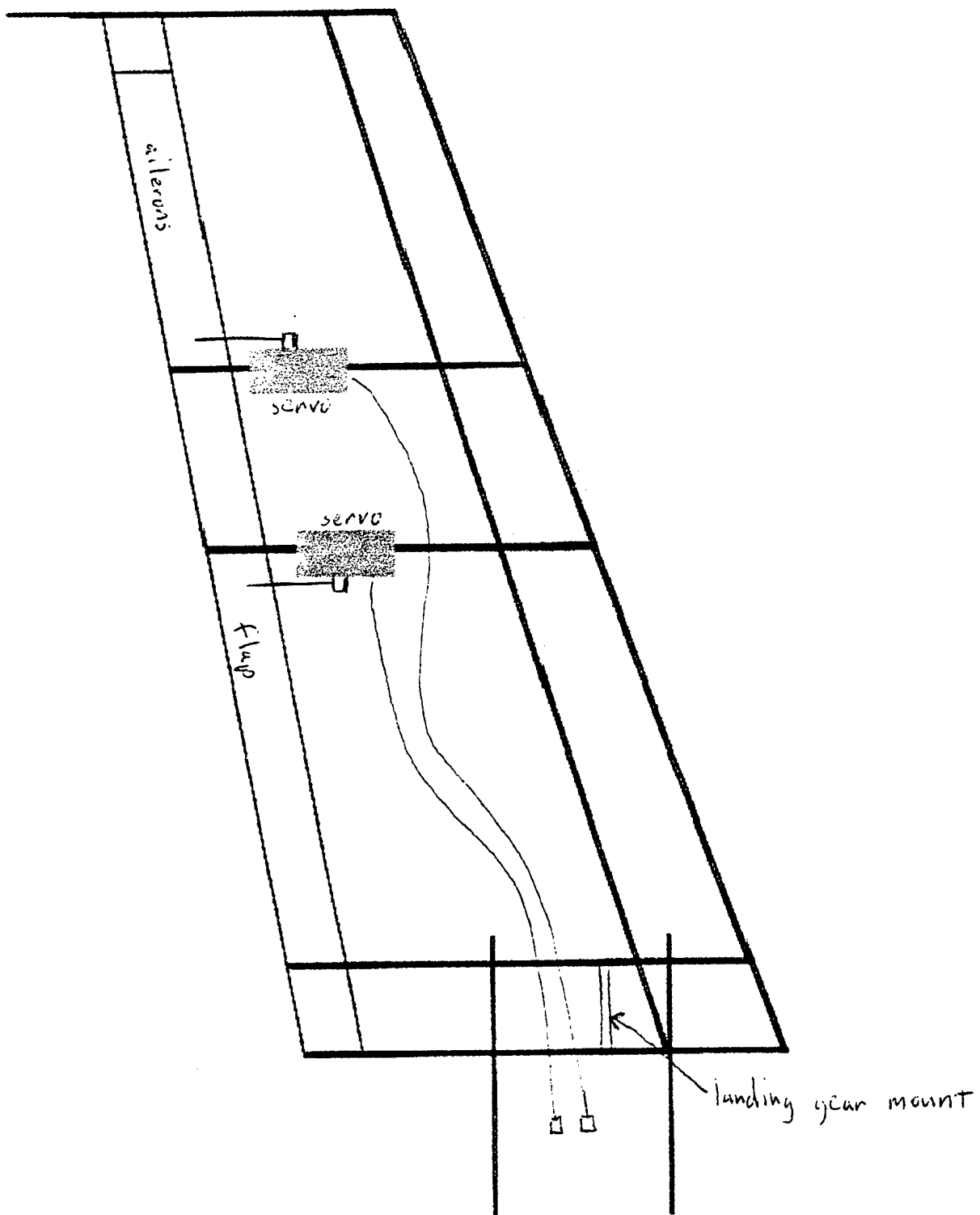
Much has been learned by those who participated in the Backfire project. We learned more important things than engineering and the spirit of competition. For those who persevered to the end, we learned the value of success and failure. The latter lesson is extremely important. This lesson is harsh, but important to be acquainted with now, than experiencing it in the workplace. From discussion and exploration we the remaining Backfire Team discovered that much of the problems we experienced, industry experiences as well, the only real difference is that the latter gets a paycheck.

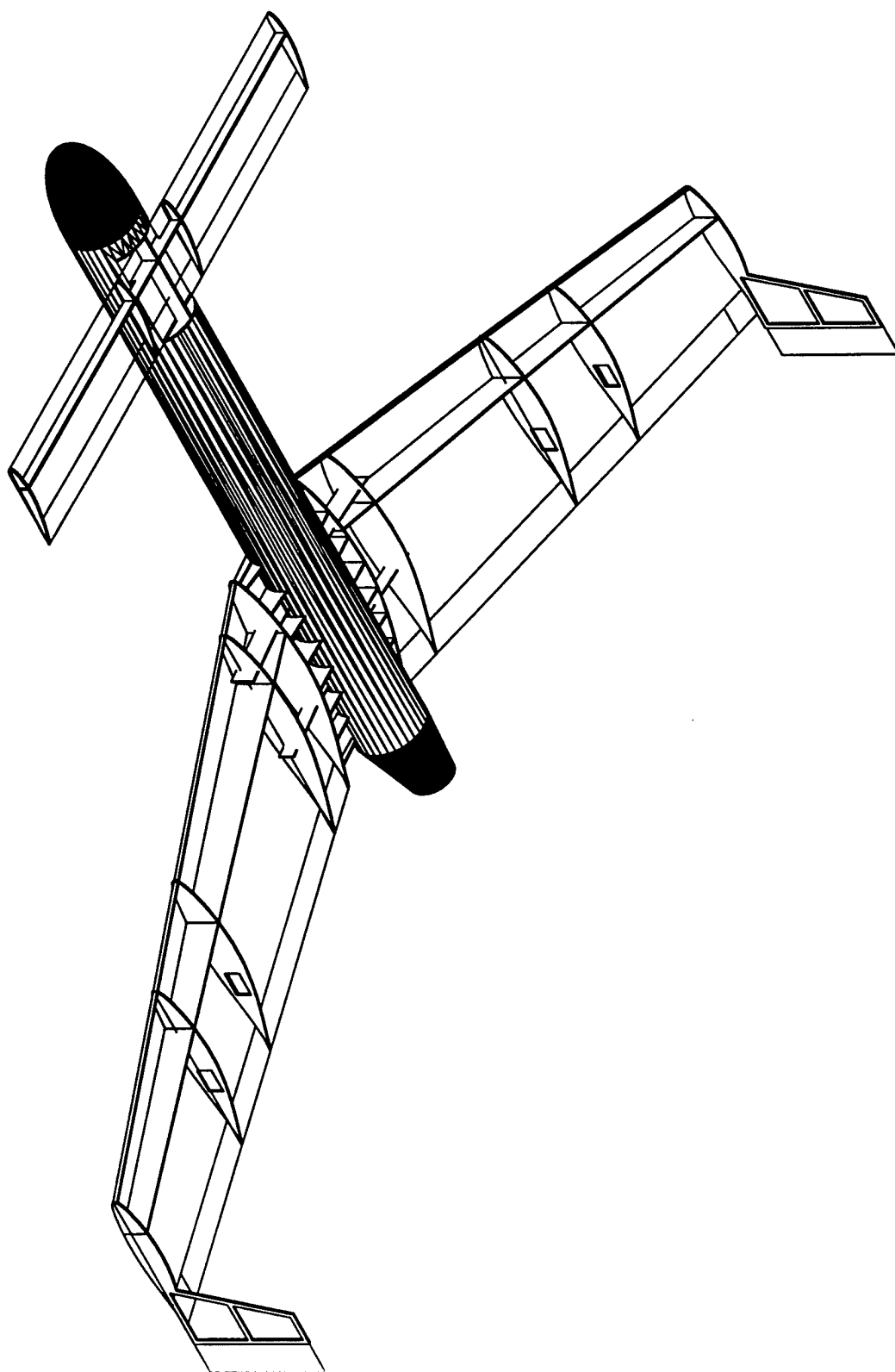
## Bibliography

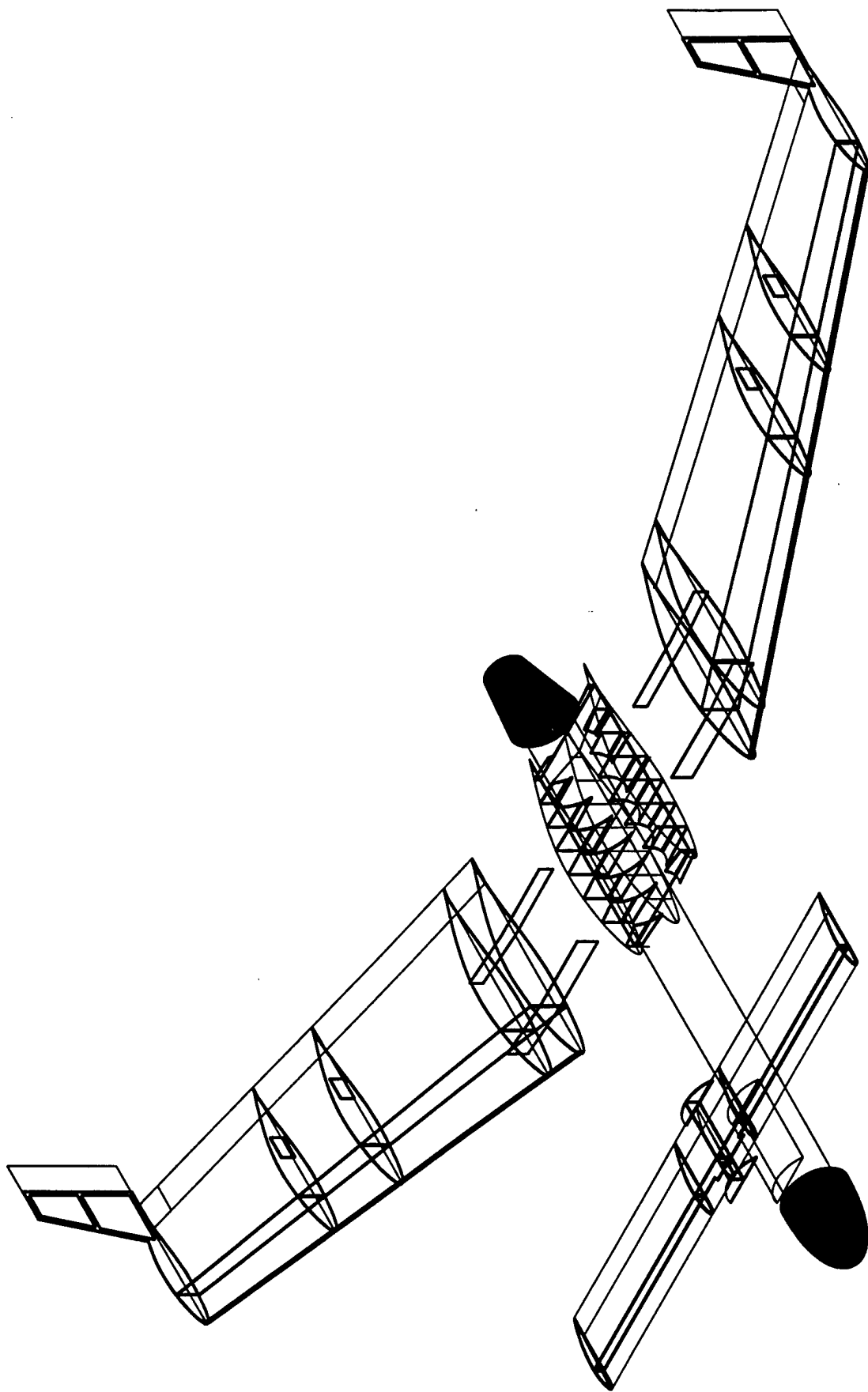
- 1) Abzug, Malcolm J. Airplane Stability and Control, Cambridge Aerospace Series, United Kingdom, 1997.
- 2) Simons, Martin. Model Aircraft Aerodynamics, 3<sup>rd</sup> edition. Guilford and Kings Lynn, Great Britain, 1994.
- 3) Smith, H.C. Illustrated guide to Aerodynamics 2<sup>nd</sup> edition. Tab Books, U.S.A., 1992.

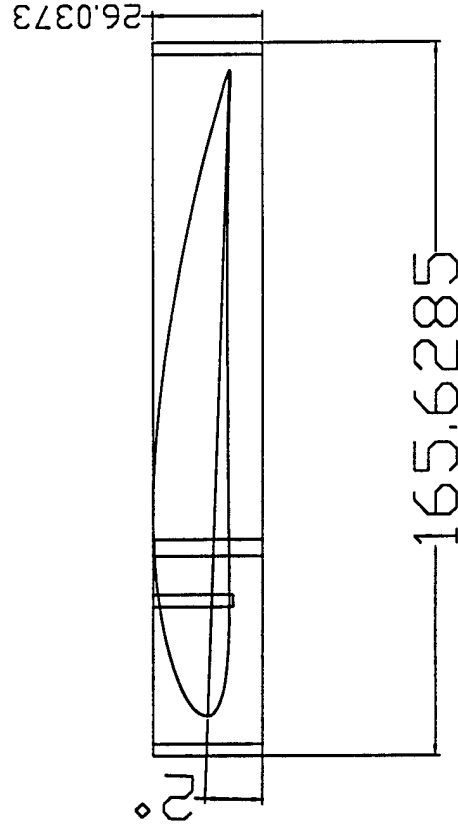
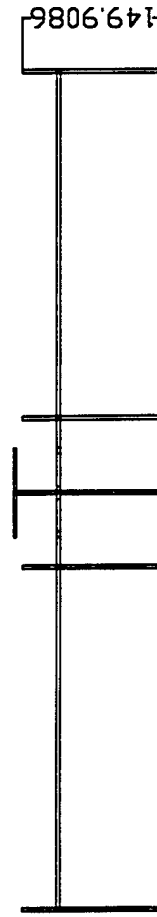
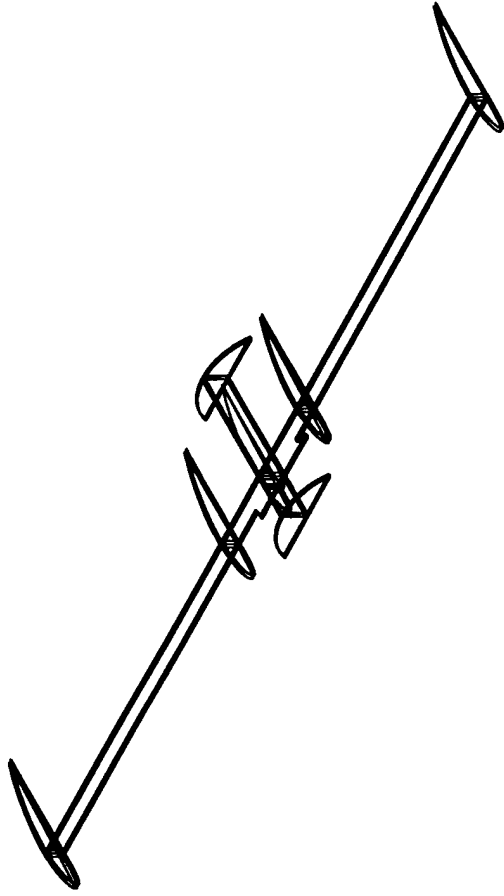
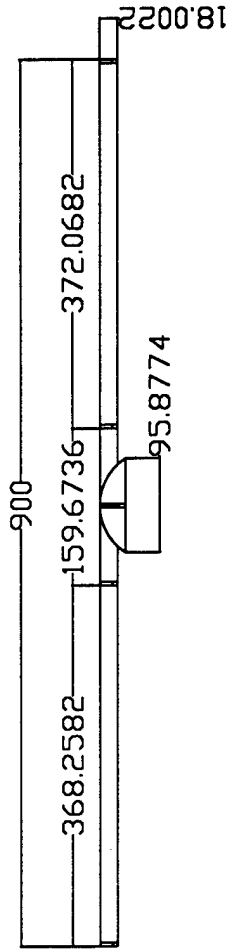
## Appendix

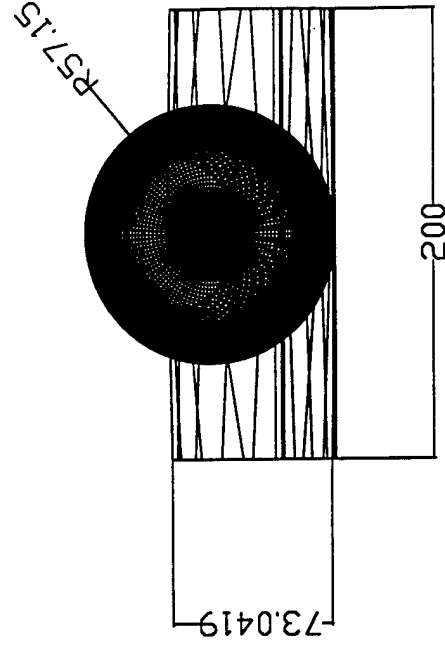
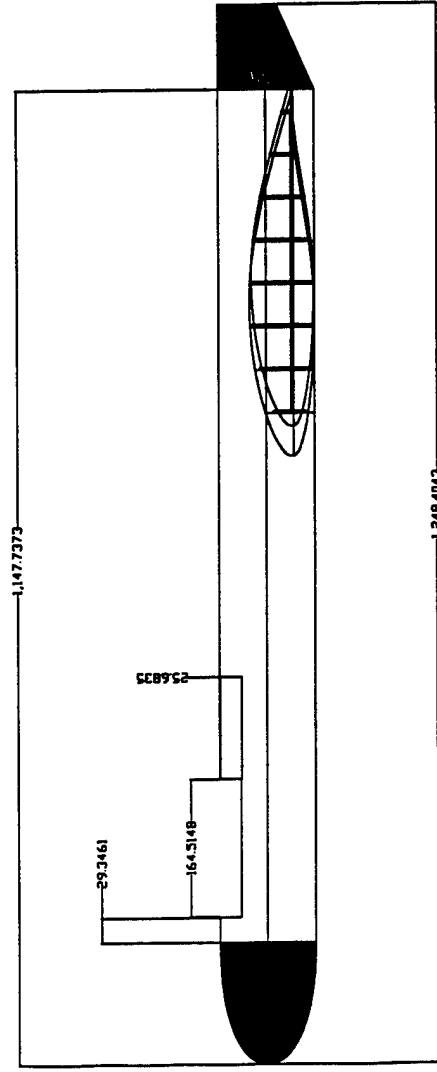
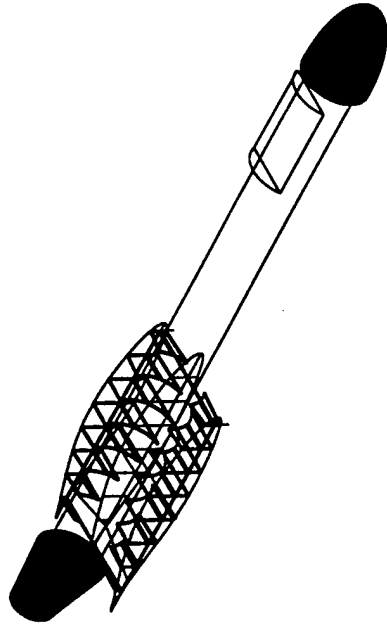
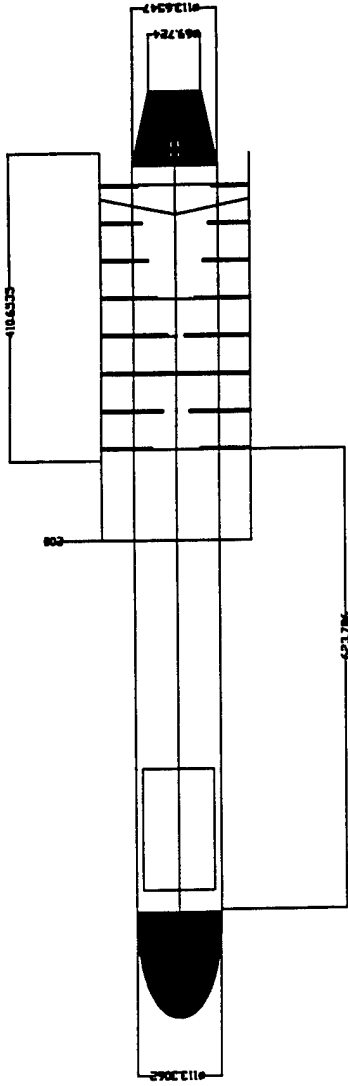


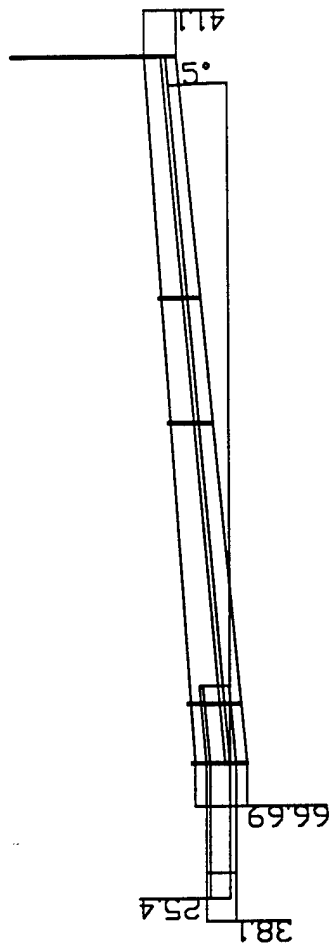
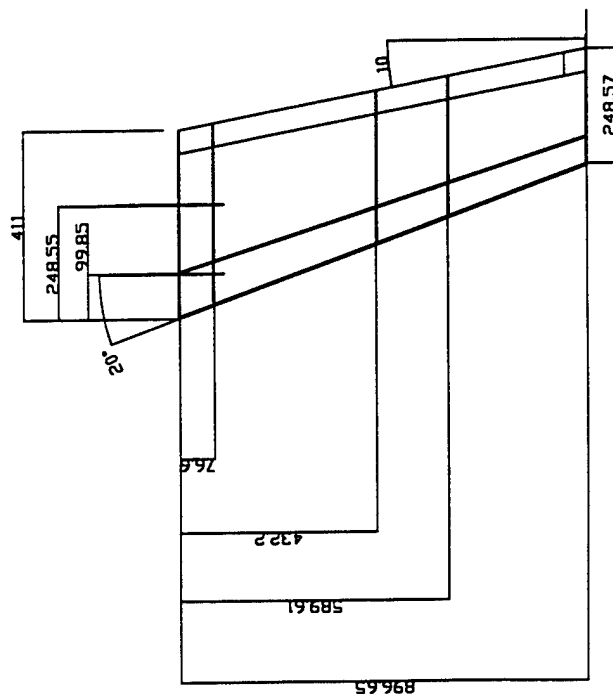
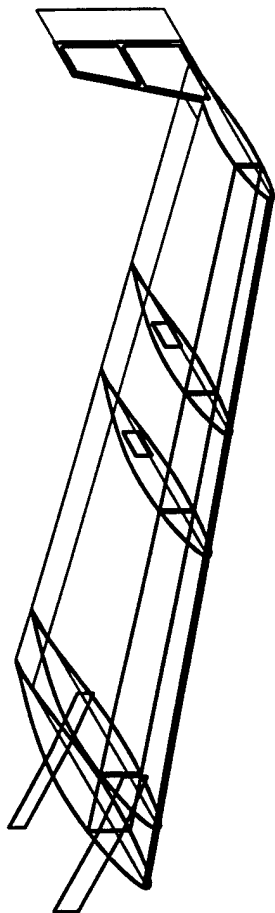
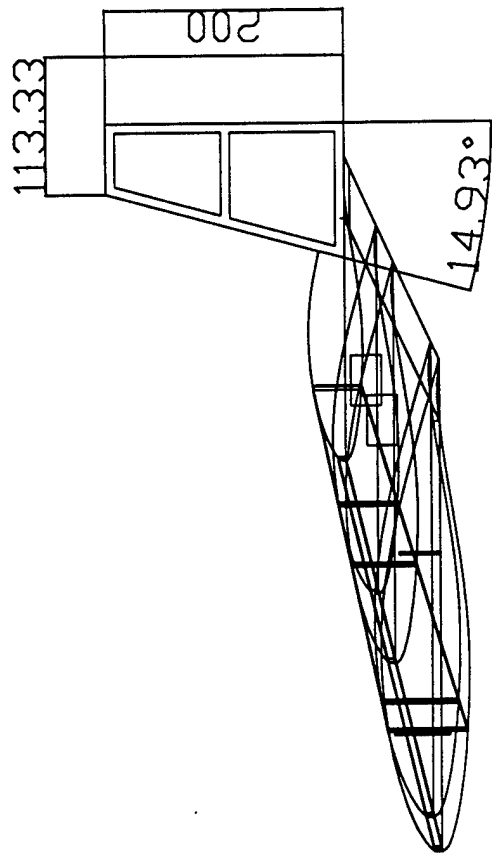












Cost analysis during PPR

PROTOTYPE	QUANTITY BY UNIT	COST BY UNIT	TOTAL	ACQUISITION STATUS	
				YES	NO
1 Balsa wood					
sheets	2	5	10	x	
stringers	35	0.5	17.5	x	
block	2	7	14	x	
2 Spruce stringers	10	1	10	x	
3 Zap(glue)	2	10	20	x	
4 3min epoxy	2	4	8	x	
5 Polyester laminating resin	1	75	75	x	
6 fine fiberglass weave	3	5	15	x	
7 fine carbon weave	3	21	63	NA	NA
8 Vacuum Bagging Accessories			0		
9 plastic	16	3	48	x	
10 chromium(seal tape)	6	3	18	x	
11 peel-ply	16	4	64	x	
12 babycloth	16	5	80	x	
13 front wheels	1	3.25	3.25	x	
14 rear wheels	2	9	18	x	
15 front landing gear	2	4.15	8.3		x
16 rear landing gear	1	25	25		x
17 push rods	2	4.25	8.5		x
18 linking arms	2	4	8	x	
19 Tie rods	2	10	20		x
20 hinges	1	5.75	5.75	x	
22 3-blade push prop	2	5	10	NA	
23 2-blade push prop	2	4	8	x	
24 Futaba controler/servos	1	200	200	x	
25 batteries-c size Nicad 2000mah	20	9	180		x
26 Charger	1	210	210		x
27 MAS switch	1	4	4		x
28 RFMSM components	2	30	60		x
29 West Systems Epoxy					
30 Part A Resin one gallon	1	80	80		x
Part B Hardener one quart	1	30	30		x
31 Measuring Pumps	2	7	14		x

total cost 1335.3  
Funds needed = 639.8

Addendum Cost Manufacture's list price cost analysis

PROTOTYPE	QUANTITY BY UNIT	COST BY UNIT	TOTAL	ACQUISITION STATUS	
				YES	NO
1 Balsa wood					
sheets	2	5	10	x	
stringers	30	0.5	15	x	
block	2	7	14	x	
2 Spruce stringers	10	1	10	x	
3 Zap(glue)	3	10	30	x	
4 3min epoxy	2	4	8	x	
5 Vacuum Bagging Accessories					
plastic	16	3	48	NA	
chromium(seal tape)	6	3	18	NA	
peel-ply	16	4	64	NA	
babycloth	16	5	80	NA	
6 front wheels	1	3	3	x	
7 rear wheels	2	5	10	x	
8 front landing gear	2	4.15	8.3		x
9 rear landing gear	1	25	25		x
10 push rods	2	3	6		x
11 linking arms	2	3	6		x
12 Tie rods	2	7	14		x
13 hinges	2	3	6	x	
14 2-blade push prop	1	3.75	3.75	x	
15 Futaba controler/servos	1	200	200	NA	
16 batteries-c size Nicad 2000mah	20	9	180		x
17 Charger	1	210	210	NA	
18 MAS switch	1	4	4		x
19 RFSM components	2	30	60		x
20 West Systems Epoxy					
Part A Resin one gallon	1	45	45		x
Part B Hardener one quart	1	16	16		x
Measuring Pumps	2	5	10		x
21 Paint cans	2	5	10		
22 Micro-fill Putty	2	5	10		
23 Doorskin	2	5	10		
25 Plywood hobby quality	1	10	10		
26 Music wire assorted	4	5	20		
27 Styro-foam insulating	4	5	20		
total cost			1184.05		



# Composites Process (CP)

# Traditional (T)

# (HW) hot wire all

nose

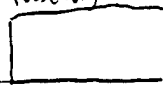
interface  
fuselage

interface

wing

winglet

tail



Plans 1) wood → luther (CP)

1) Wood foam

1) (T) monocoque

~~same as~~  
~~canard~~

Expend 2) Stereolithography

2) CP carbon low sections

3) Cross-sections (CP)

3) CP fiberglass

1) T

2) (CP)

1) (T) balsa wood

2) (T) w/ resin

1) aluminum

screw mounted

3) (CP) pipe/fuselage &  
male plug

2) wood ply (T)

3) (CP) foam ply sandwich

Originally planned

2)

2)

1)

2)

1)

2)

Now

3)

3)

1)

3)

2)

2)

canard

1) (T) monocoque

2) (CP) carbon & foam

3) (CP) fiberglass

2)

3)

1)

# **1998 AIAA DBF Competition Design Report**

————— *Proposal Phase* —————



***Queen's University at Kingston***

*Department of Mechanical Engineering*

*Department of Engineering Physics*

*March 16, 1998*

## Table of Contents

---

<b>Nomenclature</b>	<b>3</b>
<b>1.0 Executive Summary</b>	<b>5</b>
<b>2.0 Management Summary</b>	<b>7</b>
<b>3.0 Conceptual Design</b>	<b>8</b>
3.1 Design Parameters	8
3.2 Figures of Merit	9
3.3 Concept Evaluation	10
<b>4.0 Preliminary Design</b>	<b>11</b>
4.1 Take-off Gross Weight (TOGW) Estimation	11
4.2 Propulsion Systems Selection	11
4.3 Wing Area and Airfoil Selection	11
4.4 Aspect Ratio	12
4.5 Tail Sizing	19
4.6 Airframe and Fuselage Sizing	14
4.7 Landing Gear Sizing	15
4.8 Summary of Key Features	15
<b>5.0 Detail Design</b>	<b>16</b>
5.1 Drag Estimation	16
5.2 Take-off Performance	17
5.3 Handling Qualities	18
5.4 G-Load Capability	18
5.5 Turning Radius	19
5.6 Endurance and Range	19
5.7 Payload Fraction	20
<b>6.0 Manufacturing Plan</b>	<b>21</b>
6.1 Wing	21
6.2 Landing Gear	22
6.3 Tail Surfaces	22
6.4 Airframe	22
6.5 Figures of Merit	23
6.6 Evaluation and Selection	24
<b>Appendix A: Longitudinal Stability Calculation Values</b>	<b>26</b>
<b>Appendix B: References</b>	<b>27</b>
<b>Appendix C: Drawing Package</b>	<b>28</b>

## Nomenclature

---

A	parasite drag coefficient
$A_{\text{wetted}}$	wetted area
AOA	angle of attack
AR	aspect ratio
$a_m$	average acceleration on ground roll
ac	aerodynamic centre
B	induced drag coefficient
c	chord
$C_D$	coefficient of drag
$C_{D\text{Para}}$	coefficient of parasite drag
$C_{D\text{Induced}}$	coefficient of induced drag
$C_f$	skin friction drag coefficient
CG	center of gravity
$C_L$	coefficient of lift of wing
$C_L$	coefficient of lift of stabilator
$C_{L\alpha}$	derivative of $C_L$ with respect to AOA
$C_{L\text{max}}$	maximum coefficient of lift
$C_M$	coefficient of pitching moment
$c_p$	power coefficient
$c_t$	thrust coefficient
D	fuselage diameter
D	propeller diameter
D	drag
$d_c$	climb-out distance
$d_r$	ground roll distance
$d_{\text{TO}}$	take-off distance
e	wing efficiency factor
g	acceleration of gravity
h	altitude
I	mass moment of inertia
k	form factor
L	lift
M	mass
M	pitching moment
R	turning radius
Re	Reynold's number
$S_h$	stabilator planform area
$S_w$	wing planform area
T	thrust

TOGW	takeoff gross weight
$t$	maximum airfoil thickness
$V$	velocity
$V_{\max}$	maximum cruise speed
$V_{\min}$	minimum cruise speed (stall speed)
$V_{\text{mean}}$	mean velocity on takeoff roll
$V_{\text{stall}}$	stall speed
$V_{\text{TO}}$	takeoff speed
$W$	weight
$X_{\text{CG}}$	position of CG
$X_{\text{ACW}}$	position of wing aerodynamic center
$X_{\text{ACH}}$	position of stabilator aerodynamic center
$X_{\text{NP}}$	position of stability neutral point
$\alpha$	angle of attack
$\beta$	angle of bank
$\rho$	air mass density
$\sigma$	maximum stress
$\varepsilon$	downwash angle
$\eta$	efficiency
$\mu$	dynamic viscosity
$\gamma$	kinematic viscosity

## 1. Executive Summary

---

This year marks Queen's University's first entry in the AIAA DBF Competition. For the past eight years, the student aerospace enthusiasts that compose Queen's Aero Design Team have designed and built a plane to compete in a cargo aircraft competition organized by the Society of Automotive Engineers (SAE). The SAE competition had been focused solely on one design parameter—payload capacity—and that focus did not change from year to year. When combined with a confining set of sizing and propulsion restrictions, this led to a homogeneity of aircraft designs and left the engineering emphasis primarily on materials and construction techniques. For this and other reasons, the team decided this year to switch competitions in 1998 and participate in the relatively new AIAA DBF contest.

The challenge for this year's team was to translate the knowledge gained from the SAE heavy-lift competition into a successful design for an aircraft with entirely different mission objectives. Previous aircraft had been built with a focus on structural ruggedness and good stability. In competition, each plane was given successively heavier payloads until it either could not take-off or until it crashed catastrophically and could not be flown again. A successful plane needed to retain good handling characteristics even when excessively loaded and had to be tough enough withstand the abuse of an impact under these same conditions.

In contrast, the objective of this year's AIAA competition put a focus on speed, while the battery requirement necessitated both aerodynamic and motor efficiency. Early in the conceptual design phase, concern was expressed over the relative thrust produced by electric motors with respect to the 0.61 cu. in. gas engines that powered previous aircraft. The team had no experience with electrically powered flight, and some team members were therefore assigned to research the basic principles of motor and battery selection, gear reduction, and electronic speed control. The conceptual design phase began with two brainstorming sessions in which all team members were asked to submit their ideas for the plane. Some participants submitted sketches of entire aircraft configurations, while others simply shouted out ideas they had for one particular design aspect or component of the plane. Simple sketches were made to illustrate design concepts as needed. Innovative concepts were strongly encouraged, even if considered impractical. For instance, some of the most creative ideas included:

- installing a ballistic parachute for emergency descents (somewhat pessimistic);
- attaching the motor mount to a servo to generate vectored thrust;
- employing methods of passive flow control, such as skin riblets or a boundary layer trip on the wing.

(None of these concepts were considered workable or advantageous enough to warrant a figure of merit screening.) Little evaluation was done of any design concept during these sessions. All ideas were instead recorded, and a list of possible design features was compiled. Concepts were categorized along the major design parameters of the plane. After brainstorming had exhausted the generation of new ideas, evaluation began on the concepts. At the conceptual stage, this evaluation was almost purely qualitative in nature and took place mostly in the form of advantage/disadvantage weighing. Some concepts were eliminated very quickly, while others required extensive debate. Among the alternatives most intensively investigated were:

- pusher propeller vs. tractor configuration,

- high wing vs. low wing,
- tricycle gear vs. taildragger configuration,
- location of payload (fuselage vs. wing mounting).

The concepts that make up the final configuration were eventually selected in a more formalized process. The benefits and detriments of design concepts were categorized into figures of merit and then ranked according to their relative importance. Competing concepts were then evaluated based on the sum of their overall scores in each figure of merit.

The preliminary design phase was concerned with the initial sizing of major aircraft components and with the estimation of critical performance values necessary for the sizing. At this point, the general configuration of the aircraft was “frozen” so that quantitative analysis could begin. Simplified methods were used to give very rough estimates of take-off gross weight, cruise speed, and available thrust. Commercial software packages aided in the selection of a propulsion system by providing estimates of engine performance. The internal arrangement of batteries, payload, and electrical systems was developed. For every sizing parameter and performance estimate, historical data from previous aircraft was used to provide both “first-iteration” values and final validation of numerical results. In this way, the team’s experience with other competitions proved to be a major time-saving factor.

In the detail design phase, the plane was “broken down” into its individual components and design proceeded separately on each element. Component interfacing issues were addressed. In many ways, this design phase was integrated with the development of the manufacturing plan. Team members were aware at every step that their designs needed to be practical and cost-effective to build. Since the same team members who designed a component would also be largely responsible for constructing it, effort was taken to ensure that detail designs never required more skill or time to build than was available. Materials were selected based not just on their mechanical properties, but also on their cost and availability as well. In many cases, test components were built in order to gain empirical data on the workability of a particular design or manufacturing process before final decisions were made. A major undertaking was made to cut weight off this year’s aircraft wherever possible, due both to the reduced structural loads being placed on it and to the reduced thrust available from the electric motor. The detail design phase concluded with a more rigorous estimation of the aircraft’s predicted performance, using several published sources to obtain the necessary calculations. A final three-view assembly drawing of the finished aircraft design was produced using AutoCAD software.

Although Queen’s University does not have an Aerospace Engineering program, many students in related disciplines of the Applied Science program have a strong interest in this field. The Queen’s Aero Design Team provides an opportunity for these students to learn the engineering principles associated with powered flight and to gain hands-on experience with an actual aircraft design problem. At the educational level, a truly successful project is one in which risks are taken, mistakes are sometimes made, and valuable lessons are learned. It is hoped that Queen’s Aero Design Team will continue to find success at this year’s competition.

## 2. Management Summary

Queen's Aero Design Team is managed with a project-matrix structure, under a single project manager. The preliminary design of this years' plane was discussed and judged by managers and group leaders. (Table 2.1) Upon completion of preliminary designs and calculations, the details of the design were discussed among all team members. Section leaders control the design, configuration, and construction of their respective section, with collaboration as necessary, while managers retain responsibility for all portions of the aircraft. Control of scheduling lies with the Project Manager. Planned schedules were set during the conceptual design stage. (Table 2.2)

**Table 2.1. Queen's Aero Design Team architecture, 1997-98**

<i>Name</i>	<i>Position</i>	<i>Name</i>	<i>Position</i>
Mike Crump	<b>Project Manager</b>	Richard Montgomery	Airframe
Bruce Haycock	<b>Construction Manager</b>	Mike Grierson	Wing
Alexis Stoller	<b>Wing Leader</b>	Ed Birchnall	CAD
	<b>Business Manager</b>		
Phil Laird	<b>Airframe Leader</b>	Hubert Chow	Wing
Jason Millar	<b>Tail Leader, CAD</b>	Matt Olmstead	Landing Gear
Rick Andruchow	Landing Gear	Steve Devlin	Wing
Melissa Clarke	Airframe, CAD	Pieter-Jan Dejaeghere	Electrics, Motor

**Table 2.2. Project Schedule & Timing**

<i>Milestone</i>	<i>Planned Date (month / week)</i>	<i>Actual Date (month / week)</i>
<b>1.0 Conceptual Design Phase</b>	9 / 2	9 / 2
1.1 Evaluation of desired properties	9 / 2	9 / 2
1.2 Discussion and evaluation of design concepts	9 / 3	9 / 3
<b>2.0 Preliminary Design Phase</b>	10 / 2	10 / 2
2.1 Evaluation of available motors	10 / 3	10 / 3
2.2 Preliminary calculations (Vmax, Vmin, Thrust)	10 / 3	10 / 4
2.3 Sizing of major components	10 / 4	11 / 2
<b>3.0 Detailed Design Phase</b>	11 / 1	11 / 3
3.1 Section Leaders and teams chosen	11 / 1	11 / 3
3.2 Wing Design		
3.2.1 Select manufacturing method	11 / 1	11 / 4
3.2.2 Design attachment method to airframe	12 / 1	12 / 1
3.3 Landing Gear		
3.3.1 Select manufacturing method	11 / 2	11 / 4
3.4 Tail		
3.4.1 Selection of boom material/manufacturing method	11 / 2	11 / 4
3.4.2 Design/dimensioning of tail surfaces	11 / 3	12 / 1
3.5 Airframe		
3.5.1 Select manufacturing method	11 / 1	11 / 3
3.5.2 Weight, battery configuration; calculation of C of G	1 / 2	1 / 4
<b>4.0 Written Report</b>	2 / 1	2 / 3
4.1 Writing and AutoCAD drawing begin	2 / 1	2 / 3
4.2 Editing and revision of final report	3 / 1	3 / 2



### 3. Conceptual Design

---

The absence of restrictions on planform area allowed the team to consider some concepts that had been immediately rejected in previous designs. To encourage innovation, a “clean-paper” approach was taken to the design of this year’s aircraft, starting with a review of the mission requirements of the new competition. During the most initial stage of the design process, team members were encouraged to put forward any innovative conceptual ideas they might have, whether they be for a complete aircraft configuration or for specific design parameters. From these brainstorming sessions, a collection of design concepts was quickly cultivated for each major design parameter.

#### 3.1 Design Parameters

##### 3.1.1 Tail Configuration

Three tail configurations were considered: a conventional tail, a T-tail, and a twin boom-mounted tail. (A V-tail configuration was also proposed, but quickly rejected from further consideration due to its inherent control-actuation complexity.) The conventional tail is relatively easy to build and has proven to provide adequate stability and control at a very light weight. It was argued that the T-tail, on the other hand, helps to elevate the horizontal stabilator out of the propwash and into “clean” air. The T-tail was also favoured for its aesthetic quality. Concern was expressed over the problem of attaching push-pull rods to actuate the stabilator of a T-tail. Finally, the twin boom-mounted tail arrangement was proposed to allow the inclusion of a pusher-propeller configuration. Although the twin boom tail would provide additional stability and control, it would also increase overall weight and drag.

##### 3.1.2 Engine Placement

Both a tractor configuration and a pusher-propeller concept were discussed. The pusher-propeller was considered in conjunction with the twin tail boom concept. It was thought that a push-prop configuration could reduce viscous drag by allowing the fuselage to fly in air undisturbed by the propeller. This configuration came with several drawbacks, however. It reduces the clearance of the prop during take-off rotation, and could consequently require larger, heavier landing gear. The push prop lacks the inherent stability of the tractor configuration, due both to the location of the thrust vector behind of the centre of gravity and to the aftward shifting of the centre of gravity. Finally, while the push-prop may allow the aircraft body to fly in undisturbed air, it places the propeller itself in the turbulent wake of the fuselage, reducing its aerodynamic efficiency.

##### 3.1.3 Wing Placement

Consideration was given to high, mid, and low wing configurations. The high wing was considered superior in lateral stability and offered the advantage of greater wing tip clearance on take-off and landing. It was argued that a mid-wing placement could decrease interference drag, while a low wing would be superior from a structural standpoint, by allowing direct load transfer from the spar to the landing gear.

##### 3.1.4 Landing Gear Configuration

Both the taildragger and tricycle landing gear configurations were investigated. The

taildragger arrangement was favoured for its lighter weight, reduced drag, and greater prop clearance. Tricycle gear, on the other hand, has proven to provide far more control authority on the ground. On many occasions, the team pilot has expressed a strong preference for the handling characteristics of the tricycle gear arrangement.

### *3.1.5 Payload Placement*

One innovative concept to reduce both weight and drag called for locating the steel payload inside the wing of the aircraft, perhaps inside a hollow spar. This would eliminate the need for structural strengthening of the fuselage and reduce the overall size of the body. Concern was expressed for the effects this arrangement might have on lateral control authority and lateral stability. There was also concern about the bending load this would place on the wing during high-g manoeuvres or hard landings. Finally, it was argued that by placing the steel inside the fuselage, it could be made to act as a heat sink to help regulate battery temperature.

## **3.2 Figures of Merit**

At the conceptual stage, figures of merit were kept qualitative. A description of the figures of merit used to evaluate design concepts is given here, along with the relative "importance factor" of each FOM.

### *3.2.1 Drag Penalty*

This is a measure of the relative drag penalty each concept was estimated to have over the others. Increased drag would most strongly affect the maximum speed, take-off distance, range, and endurance of the aircraft. This FOM was assigned an importance factor of 3.

### *3.2.2 Weight Penalty*

This is a measure of the relative weight penalty each concept was estimated to have over the others. Increased weight would most strongly impact the take-off distance of the aircraft. This FOM was assigned an importance factor of 4.

### *3.2.3 Handling Quality*

This is a measure of the relative "flyability" of each concept, from a pilot's perspective. The affects of each concept on stability and control authority were considered. Handling quality critically affects all aspects of the mission and is especially important since the pilot will not have extensive time to practice flying the plane. This FOM was assigned an importance factor of 5.

### *3.2.4 Survivability*

This is a measure of the relative ruggedness of each concept (the real emphasis here is on crashworthiness). Experience in previous competitions has shown that often the winning aircraft is the one that can be flown again (usually with minor repairs) after a mishap. It was felt that this FOM would be less important in this competition, however, as the aircraft would not be purposely flown past its design limitations. This FOM was assigned an importance factor of 1.

### *3.2.5 Ease of Construction*

This is a measure of the relative difficulty involved in the construction of each concept. The necessary experience, skill, time, and cost of construction for each concept was considered.

This FOM was assigned an importance factor of 2.

### 3.3 Concept Evaluation

#### 3.3.1 Analytical Method

Evaluation of competing concepts under each design parameter was made by rating each concept on a “goodness” scale of 0 to 5 for each FOM, based on the qualitative considerations described above. The ratings were then multiplied by their FOM “importance factors” and added up to provide a final score for each concept (see Table 3.1).

*Table 3.1. Conceptual design evaluation. Selected design concepts are shaded.*

	<b>Drag Penalty</b>	<b>Weight Penalty</b>	<b>Handling Quality</b>	<b>Survivability</b>	<b>Constructio n Difficulty</b>	<b>Total Score</b>
<b>Engine</b>						
<i>Tractor</i>	3 × 3	5 × 4	5 × 5	4 × 1	5 × 2	68
<i>Push-Prop</i>	4 × 3	5 × 4	3 × 5	4 × 1	4 × 2	59
<b>Tail</b>						
<i>Conventional</i>	4 × 3	4 × 4	4 × 5	4 × 1	5 × 2	62
<i>T-Tail</i>	4 × 3	4 × 4	4 × 5	5 × 1	3 × 2	59
<i>V-Tail</i>	5 × 3	4 × 4	3 × 5	4 × 1	0 × 2	50
<i>Twin Boom</i>	2 × 3	2 × 4	5 × 5	4 × 1	3 × 2	49
<b>Wing</b>						
<i>High</i>	3 × 3	3 × 4	5 × 5	5 × 1	4 × 2	59
<i>Mid</i>	5 × 3	3 × 4	4 × 5	3 × 1	3 × 2	56
<i>Low</i>	4 × 3	3 × 4	3 × 5	1 × 1	4 × 2	48
<b>Landing Gear</b>						
<i>Tricycle</i>	2 × 3	2 × 4	5 × 5	4 × 1	3 × 2	49
<i>Taildragger</i>	5 × 3	3 × 4	2 × 5	3 × 1	3 × 2	46
<b>Payload</b>						
<i>Fuselage</i>	3 × 3	3 × 4	5 × 5	4 × 1	4 × 2	58
<i>Wing</i>	4 × 3	4 × 4	3 × 5	2 × 1	3 × 2	51

## 4. Preliminary Design

---

### 4.1 Take-off Gross Weight (TOGW) Estimation

The first step in the preliminary design phase was estimating the gross weight of the aircraft. This parameter is of course critically important to both the sizing and the final performance of the plane. TOGW estimation in the preliminary phase was done primarily through the examination of historical data. The empty weight of our 1997 cargo aircraft had been 8 lb. It was estimated that at least 1.5 lb. of structural weight could be saved on this year's plane, based on the altered mission objectives of the new competition. When this weight was added to the 10 lb. payload + battery requirement, a take-off gross weight value of 16.5 lb. was estimated. This figure seemed reasonable when compared to the published data for the inaugural AIAA DBF entries (average TOGW  $\approx$  16.6 lb.). The expected accuracy of the estimate at this stage of the design was  $\pm 1.5$  lb.

### 4.2 Propulsion Systems Selection

The propulsion system was selected so as to give the maximum possible thrust and a high efficiency to make the best possible use of available battery power. MaxCim, Aveox, and Astroflight motors were compared based on their published efficiencies, predicted performance, cost, and their performance in past competitions. In addition, MotoCalc and ElectriCalc commercial software packages were used to compare the various possible configurations of motor, controller, gearbox, propeller, and batteries for their efficiency, thrust, and estimated run-time. All of the high-performance motors had comparable costs, and this was considered of less importance than performance. The batteries were selected by comparing weight (and therefore number of cells), capacity, and internal resistances leading to ohmic losses. These considerations led to the choice of 20 SR 2000Max cells. Each of these cells weighs 1.8 oz., leaving 4 oz. for all connections, shrink-wrap, and wires. The software analysis indicated that a MaxCim MaxNEO 13Y motor, combined with the Maxμ 35A-25NB speed controller, a 4:1 gear ratio, and a 12-8 propeller would give the best overall performance. This arrangement resulted in an estimated static thrust of 15.6 N (3.51 lbf) and a dynamic thrust of 12.5 N (2.81 lbf) at 15 m/s (34 mph). These numbers were later validated using classical propeller performance equations.

### 4.3 Wing Area and Airfoil Selection

The wing area and airfoil were chosen based on the lift requirements at the expected cruise speed, as well as take-off performance, stall characteristics, and induced drag estimates. The FOMs used in the selection are as follows.

#### 4.3.1 $C_L$ at the Best Lift to Drag (L/D) Angle of Attack

The  $C_L$  at best L/D was used to gain insight into the amount of lift the wing would produce while operating at peak efficiency. This was considered important since the more lift the airfoil generates, the smaller the wing area can be, thus reducing drag.

#### 4.3.2 Maximum $C_L$

The maximum  $C_L$  was considered to be important as this determines the stall speed, take-off speed, and maximum g-loading for a fixed wing area. Due to the requirement for take-off

within a limited distance and the energy advantage obtained by minimizing the amount of time in climb, a high  $C_L$  was considered significantly advantageous. In addition, this also allows for high-g manoeuvres without the onset of an accelerated stall, giving the aircraft the ability to use a minimal turning radius and effectively shortening each lap.

#### 4.3.3 Stall Characteristics

Like many other parameters, this FOM arises from past experience. An airfoil with a more docile stall is considered to be significantly advantageous in the event of an unplanned circumstance. Accidentally over-banking the aircraft and stalling the wing can lead to disaster with an aggressive-stalling airfoil. A gentler stall will increase the time available to react and increase the likelihood of recovery. The stalling characteristics were compared based on published lift and drag data, and on previous experience in observing the in-flight stall characteristics of most of the airfoils considered.

#### 4.3.4 $C_D$ at Expected Cruise AOA

Due to the restrictions on available battery power, once a maximum thrust is achieved through careful selection of a motor and electrics, the top speed can only be increased through drag reduction. The airfoils were compared at the expected cruise  $C_L$ , where the drag will have the most influence on performance.

The airfoil was selected based on these criteria, along with initial calculations for the estimated gross weight and airspeed. The gross weight was taken as 73.6 N (16.5 lb.), as estimated in section 4.1. The cruise speed was estimated based on an initial thrust estimate of 12.5 N (2.81 lbf), and an overall "worst-case"  $C_D$  of 0.06 (0.03 parasite + 0.03 induced), using the modified equation:

$$V_{\max} = \sqrt{\frac{2T_{\max}}{\rho C_D S_w}}$$

Initially, the surface area was taken as 0.929 m<sup>2</sup> (10 ft<sup>2</sup>). This gives a top speed of 19.2 m/s (63±3 ft/s or 43±2 mph). From this, the  $C_L$  at cruise is determined from the standard lift equation, modified slightly to account for three-dimensional effects reducing the overall lift of the wing:

$$C_{L\min} = \frac{2L}{\eta \rho S_w V_{\max}^2}$$

where  $\rho$  is the efficiency of the wing, assumed to be 0.75, and  $L$  is the total lift required (equal to the gross weight). This gives a required  $C_L$  of 0.6±0.1. Take-off speed, stall speed, and maximum g-loading were examined next to define the required limits on the  $C_L$ . The desired stall speed was estimated 55% of the cruise speed, giving a lift-off speed 63% of the cruise speed. Using the same  $C_L$  formula as above, replacing  $V_{\max}$  with  $V_{\text{Stall}}$  gives a required maximum  $C_L$  of 1.6±0.1. It was also desired to have an aircraft capable of manoeuvring with a g loading of 2, which gives a required maximum  $C_L$  of 1.2. As such, the airfoil was required to have a  $C_{L\min}$  of 0.6 and a  $C_{L\max}$  of 1.6. Airfoil lift and drag data was obtained from the UIUC Low-Speed Airfoil Test program. The airfoil could then be chosen from the extremely wide number available, using the FOMs listed above and the desired values calculated. The final selection made was the **S1210**, with a  $C_L$  of 0.7 and a  $C_D$  of 0.014 at its minimum drag angle of -2°.

and a maximum  $C_L$  of 1.7 as the angle of attack approaches the critical angle of approximately  $12^\circ$ . In addition, the S1210 has relatively good stall characteristics, with a gentle approach and fall from the  $C_{LMax}$ .

#### 4.4 Aspect Ratio

A higher aspect ratio will reduce the induced drag of the aircraft, thus allowing for a faster cruise speed. However, manoeuvrability is compromised due to an increased moment of inertia about the longitudinal axis. As well, a longer wing experiences higher bending moments and is more likely to flex under loading. This makes its construction more difficult and structurally heavier than that of a shorter wing. Since the wing area had been previously selected as  $10 \text{ ft}^2$  ( $0.929 \text{ m}^2$ ), defining the wing span also sets the aspect ratio. For induced drag considerations, the aspect ratio is desired to be as large as feasible. A  $3.048 \text{ m}$  ( $10 \text{ ft}$ ) span is near the limit that can be properly constructed in readily available facilities, can be constructed to be sufficiently stiff so as to minimize deflection at the wingtips, and built with a specific weight comparable to that of a shorter wing. The wing span was therefore set at  $3.048 \text{ m}$  ( $10 \text{ ft}$ ), with a chord of  $0.3048 \text{ m}$  ( $1 \text{ ft}$ ) and an aspect ratio of 10.

#### 4.5 Tail Sizing

The design considerations used to determine the required tail surface dimensions are stability and control authority. The airfoil is capable of approximately  $2.4g$  before stalling (see section 5.4.2), and has a coefficient of moment of approximately 0.25 (estimated based on data for similar airfoils, as no pitching moment data is available for the S1210). The stabilator must be capable of overcoming both the pitching moment of the wing and the moment caused by a finite separation between the centre of gravity and the centre of pressure (assumed for now to be within  $0.0127 \text{ m}$  or  $0.5 \text{ in.}$  of each other) and still provide enough torque for control. This leads to the inequality:

$$X_{ach} \frac{1}{2} C_{Lh} \rho S_h V^2 \geq \frac{1}{2} C_M \rho S_w V^2 c + 2.4 X_{acw} W + I \alpha$$

From this, the product of stabilator maximum coefficient of lift, surface area, and distance from the centre of gravity ( $X_{ach} C_{Lh} S_h$ ) can be found. In order to minimize its size and reduce drag, the tail is placed as far aft as feasible to give it a large moment arm on which to act. It has been found that a  $0.062 \text{ m}^2$  ( $96 \text{ in}^2$ ) stabilator located  $1.016 \text{ m}$  ( $40 \text{ in.}$ ) from the CG, with an inverted E212 airfoil ( $C_{Lmax}$  of 1.3), provides the desired qualities. In addition, this combination produces a torque equal to the estimated pitching moment of the wing at an AOA of  $0^\circ$ , near the angle of minimum drag for the E212 airfoil.

Unlike the stabilator, the rudder does not need to overcome a large pitching moment at any time. Therefore, a symmetrical airfoil with relatively low drag was desired, leading to the selection of a NACA 0009 section. The rudder is located ahead of the stabilator to avoid physical interference between the surfaces. This placement sets the distance for the rudder from the CG. Sizing was accomplished by ensuring the rudder would be capable of providing sufficient torque to allow positive directional control and maintain directional stability. Based on historical data, a rudder  $0.031 \text{ m}^2$  ( $48 \text{ in}^2$ ), or half the size of the stabilator, was thought to be more than adequate for both control authority and directional stability.

#### 4.6 Airframe and Fuselage Sizing

The sizing parameters used in the development of a fuselage profile includes the total length, cross-section shape, and the cross-sectional dimensions. Alternative designs are evaluated mostly on how well they can contain all of the required components (payload, batteries, control system) while minimizing parasite drag produced the fuselage. All necessary components were initially assigned an initial location within the fuselage, with the possibility of later rearranging the internal configuration to ensure correct centre of gravity placement. The initial configuration is as follows:

- ☒ The batteries were arranged in 4 rows of 5 cells, with 2 rows per battery pack. These packs were placed along the sides of the fuselage, with their centre chosen to be the proposed centre of gravity. Dimensions required: 0.254 m (10 in.) length, 2 packs each with a  $0.0254 \times 0.0508$  m (2×1×2-inch) cross-section.
- ☒ The cargo was placed between the two battery packs, as a  $0.0508 \times 0.254 \times \sim 0.0343$  m<sup>3</sup> (2 × 10 × ~1.35 in<sup>3</sup>) block, increasing the required dimensions to 0.254 m (10 in.) length, 0.1016 × 0.0508 m (4×4-inch) cross-section. The speed controller was placed on top of the cargo using a mounting bracket. This was done so both the batteries and cargo, the main sources of weight, could be located over the CG. In addition, the steel block can be cooled prior to each flight to act as a heat sink, thereby increasing the overall efficiency.
- ☒ A firewall with a hole to allow cooling airflow was added in front of the batteries and cargo, and the motor attached to this firewall, adding 0.0826 m (3.25 in.) to the length, including the gearbox.
- ☒ A partial firewall was added behind the batteries and cargo to secure them in place, and the receiver and servo battery pack were placed behind this firewall. This added 0.0826 m (3.25 in.) to the length.
- ☒ The tail boom was attached aft of the servo battery pack, the stabilator and rudder servos were mounted on the tail boom, and a final support for the tail boom was added at the rear. This added a further 0.1143 m (4.5 in.) to the length.
- ☒ Vertical supports were placed along the sides secure the components in place, adding 0.0127 m (0.5 in.) to the width. This gave final required dimensions of  $0.0572 \times 0.1143 \times 0.5334$  m<sup>3</sup> (2.25 × 4.5 × 21 in<sup>3</sup>)
- ☒ The airframe box is then covered with an streamlined, non-load-bearing cowling to reduce drag. The cross-section was the smallest possible that could cover the box and still allow cooling airflow over the motor, controller, and batteries. A  $0.106 \times 0.152$  m (4×6-inch) elliptical cross-section was used with a total length of 0.6096 m (24 in).

#### 4.7 Landing Gear Sizing

The landing gear was required to be large enough to provide adequate propeller clearance, give good stability on the ground, and be capable of withstanding the loads incurred during rough landings. To meet the propeller clearance requirement, the total landing gear height, from the bottom of the airframe box to the ground must be 0.1461 m (5.75 in.). The required gear strut dimensions were obtained using

estimated bending moments imposed under a 3g loading, using Kevlar-wrapped around a foam core (see section 6.2.2) as the strut material. With a rectangular cross-section and constant curvature of 0.1016 m (4 in.) in transition from horizontal to vertical, the safety factor (actual stress / yield stress) was found to be 1.53 for a width of 0.0508 m (2 in.), which was considered to be sufficient for this application.

#### **4.8 Summary of Key Features**

##### **4.8.1 Propulsion**

- Motor: MaxNEO 13Y Brushless DC
- Speed Controller: Maxμ 35A-25NB
- Cells: 20 SR 2000Max
- Gear Box: MaxGR 4:1
- Propeller: 12-8 APC

##### **4.8.2 Wing**

- Span: 2.54 m (10 ft.)
- Aspect ratio: of 10
- No taper, no sweep
- Airfoil: S1210
- 0.102 × 0.61 m (4 × 24-inch) differential ailerons

##### **4.8.3 Stabilator**

- Span: 0.61 m (24 in.)
- Chord: 0.102 m (4 in.) (Aspect Ratio = 6)
- Airfoil: E212 (inverted)

##### **4.8.4 Rudder**

- Span: 0.305 m (12 in.) span
- Chord: 0.102 m (4 in.) chord (Aspect Ratio = 3)
- Airfoil: NACA0009

##### **4.8.5 Fuselage**

- 0.102 × 0.152 m (4 × 6-inch) elliptical cross-section
- Length: 0.61 m (24 in.)

##### **4.8.6 Landing Gear**

- Base: 0.305 m (12 in.)
- Strut Width: 0.0508 m (2 in.)
- Height: 0.146 m (5.75 in.)



## 5. Detail Design

Drawings of the final aircraft assembly, indicating size and location of all major components, are attached in Appendix C. Detail drawings are provided for the wing structural assembly.

### 5.1 Drag Estimation

Before performance of the aircraft can be predicted, it is necessary to estimate the drag forces acting on the aircraft. In this basic estimation, total drag is taken to be the sum of parasite drag and induced drag, given by the equation  $C_{DTotal} = A + B \times C_L^2$ .

#### 5.1.1 Parasite Drag

Parasite drag is estimated using the “component build-up” method. A flat-plate skin friction drag coefficient ( $C_f$ ) is calculated for each major component of the aircraft and then multiplied by a “form factor” ( $k$ ) to that estimates losses due to form drag:

$$C_{dPara} = \sum \left[ \frac{k \times C_f \times A_{wetted}}{S_w} \right]_{component}$$

where

$$C_f = \frac{0.455}{(\log_{10} Re)^{2.55}} \quad \text{and} \quad Re = \frac{V \times Length}{\gamma}$$

Interference drag was neglected for this estimate. Values of each component for each variable are given in Table 5.1.

**Table 5.1. Parasite drag estimation using “component build-up” method.**

	$A_{wetted} (m^2)$	$Re (\rho VL/\mu)$	$C_f$	Form factor, $k$	$C_{DPara}$
<b>Wing</b>	1.858	$3.74 \times 10^5$	$5.69 \times 10^{-3}$	1.26 ( $t/c = 0.12$ )	0.0143
<b>Fuselage</b>	$2.43 \times 10^{-1}$	$7.48 \times 10^5$	$3.98 \times 10^{-3}$	1.24 ( $L/D = 4.8$ )	$1.291 \times 10^{-3}$
<b>Wheels</b>	$2.74 \times 10^{-2}$	$9.35 \times 10^4$	$4.78 \times 10^{-3}$	$\sim 1.3$	$1.833 \times 10^{-4}$
<b>Gear Struts</b>	$1.55 \times 10^{-2}$	$6.23 \times 10^4$	$8.36 \times 10^{-3}$	$\sim 1.25$	$1.744 \times 10^{-4}$
<b>Stabilator</b>	$1.23 \times 10^{-1}$	$1.25 \times 10^5$	$7.16 \times 10^{-3}$	1.22 ( $t/c = 0.105$ )	$1.157 \times 10^{-3}$
<b>Rudder</b>	$6.19 \times 10^{-2}$	$1.25 \times 10^5$	$7.16 \times 10^{-3}$	1.17 ( $t/c = 0.09$ )	$5.582 \times 10^{-4}$
<b>Tail Boom</b>	$7.75 \times 10^{-3}$	$5.42 \times 10^4$	$8.63 \times 10^{-3}$	$\sim 1.5$	$1.080 \times 10^{-4}$
<b>Total</b>					<b>0.0178</b>

#### 5.1.2 Induced Drag

Induced drag is estimated using the “wing efficiency” method. The induced drag coefficient is given by:

$$C_{dInduced} = \frac{C_L^2}{\pi \times AR \times e}$$

$$e = 1.78(1 - 0.045 \times AR^{0.68}) - 0.646$$

When a cruising  $C_L$  of 0.7 is used (as estimated in section 4.3), this method yields values of  $e = 0.76$  and  $C_{DInduced} = 0.0205$ .

### 5.1.3 Total Drag

The total drag coefficient ( $C_{DTotal}$ ) of the aircraft in cruise is therefore given by:

$$C_{DTotal} = 0.0178 + 0.0205 = \mathbf{0.0383}$$

## 5.2 Take-off Performance

Take-off distance is broken into three components: ground roll, rotation distance, and climb-out distance. Rotation distance is assumed to be negligible for this calculation.

### 5.2.1 Ground Roll

The ground roll distance ( $d_r$ ) of the aircraft is given by:

$$d_r = \frac{V_{TO}^2}{2 \times a_{mean}}$$

where

$$M \cdot a_{mean} = \left[ T_{mean} - \left( A + B \cdot C_{Lg}^2 \right) \frac{1}{4} \rho V_{TO}^2 S_w - \mu \left( W - C_{Lg} \frac{1}{4} \rho V_{TO}^2 S_w \right) \right]$$

Take-off speed ( $V_{TO}$ ) is taken as 15% above stall speed:

$$V_{TO} = 1.15 \times V_{stall} = 1.15 \times 0.55 \times V_{max} = 10.6 \text{ m/s}$$

Static thrust is estimated from the available motor data using propeller performance equations given in ref. 6:

where

$$T = \frac{0.7376 \times Power}{RPM \times Diam} \times \frac{c_T}{c_p}$$

$$c_p = \frac{0.7376 \times Power}{\rho \times RPM^3 \times Diam^5}$$

With the motor/prop/gear/battery arrangement used in the aircraft, ElectriCalc software calculates 384 W of power supplied to the propeller and a rotational prop speed of 8,003 RPM (after gear reduction). Substituting these values into the above equations and referring to Fig. 13.8 of ref. 7 to estimate  $c_T/c_p$ , a static thrust of 15.8 N (3.55 lbf) is estimated. This result validates the figure thrust figures given by ElectriCalc (3.1 lbf at 8.5 m/s). For take-off performance,  $T_{mean}$  is taken as 14.6 N (3.28 lbf). The coefficient of rolling resistance ( $\mu$ ) is estimated at 0.015. Substituting these values into the above equations yields  $a_{mean} = 1.70 \text{ m/s}^2$  (5.58 ft/s<sup>2</sup>) and  $d_r = 33.0 \text{ m}$  (108 ft).

### 5.2.2 Climb-Out

The climb-out distance ( $d_c$ ) needed for the aircraft to clear an obstacle of height  $h$  is given

$$\text{by: } d_c = \frac{h}{\left( T/W \right) - \left[ \left( A + B \cdot C_{LMax}^2 \right) / 1.15^4 / \left( C_{LMax} / 1.15^2 \right) \right]}$$

The required height for this mission is 1.83 m (6 ft). Substituting in values of thrust, taken as 13.5 N (3.04 lbf) during climb-out, and  $C_{L_{Max}}$  (1.7 for this airfoil), this method gives a climb-out distance of  $d_c = 15.0$  m (49 ft).

### 5.2.3 Total Take-off Distance

The total take-off distance ( $d_{TO}$ ) of the aircraft is therefore given by:

$$d_{TO} = 33 + 15 = \mathbf{48 \text{ m (157 ft)}}$$

## 5.3 Handling Qualities

### 5.3.1 Longitudinal Stability

The aircraft's static longitudinal stability was calculated using methods presented in ref. 6. The neutral-point ( $X_{np}$ ) estimated was calculated using the following equation:

$$\bar{X}_{np} = \frac{C_{L\alpha} \bar{X}_{acw} - C_{m\alpha_{fus}} + \eta_h \frac{S_h}{S_w} C_{L\alpha_h} \frac{\partial \alpha_h}{\partial \alpha} \bar{X}_{ach}}{C_{L\alpha} + \eta_h \frac{S_h}{S_w} C_{L\alpha_h} \frac{\partial \alpha_h}{\partial \alpha}}$$

Derivations of the values used for each variable are given in Appendix B. This equation predicts that the aircraft neutral point,  $X_{np} = 1.18$ . The estimated centre of gravity for the aircraft is  $X_{CG} = 1.02$ . Thus, the aircraft has a positive static margin of  $1.18 - 1.02 = 0.16$ , or 16%. This is considered a very high value for any aircraft, and indicates that the plane is very statically stable in the pitching direction.

## 5.4 G-Load Capability

In predicting the maximum g-load the aircraft is capable of handling, two major parameters were investigated. Firstly, the aircraft's structural capabilities were estimated with a calculation of the spar's maximum allowable bending stress. Predictions were then made on the accelerated stall properties of the wing, using published lift data for the selected airfoil.

### 5.4.1 Structural Loading

The wing's manufacturing plan calls for two  $\frac{1}{4} \times 1$ -inch balsa wood planks, each wrapped in layers of carbon fibre, to serve as the main structural spars (see section 6.1.3). It is assumed that these spars will experience higher stresses than any other component of the aircraft during g-loading. Thus, the maximum bending stresses these elements can handle will determine the g-load capability of the plane.

The spars are placed at the  $\frac{1}{4}$ -chord of the wing and are spaced apart by  $\frac{3}{4}$ -inch of vertical separation (see drawings). One is located near the top surface, and the other near the bottom surface of the airfoil. Bending stress within the spars was estimated by modelling them as a single structural entity, both deflecting about a common neutral axis which exists at a point halfway between the two. The maximum stress due to bending occurs at the upper surface of the top spar and the lower surface of the bottom spar, which are the maximum distances ( $z$ ) from the neutral axis. This stress is given by:

where  $I_y$  is the spars' moment of inertia about the neutral axis. By assuming a carbon

$$\sigma_x = \frac{M_z z}{I_y}$$

fibre/epoxy layer thickness of 0.5 mm and an average Young's modulus of 145 Gpa ( $21 \times 10^6$  psi), it was found that a **4g loading** of the aircraft would produce a 20 cm (7.9in) deflection of the wing at each tip. This loading would cause stresses within the spars to reach 77% of their failure point. This was taken to be the maximum allowable structural loading for the aircraft.

#### 5.4.2 Accelerated Stall Characteristics

The maximum g-load that can be produced by the aircraft in a controlled level turn is given by the ratio of the maximum lift available from the airfoil to the lift generated in steady level flight. This is equivalent to the ratio of  $C_{LMax}$  to  $C_L$  at cruise. For our aircraft, this ratio is 1.7 to 0.7, or **2.4g**. Thus, if the aircraft is turned any harder than 2.4g, the maximum lift available from the wing will be exceeded and an accelerated stall will occur.

### 5.5 Turning Radius

In level flight, the lift generated by the wing equals the total weight of the aircraft. In a level turn, however, the wing must also provide a horizontal component to change the aircraft's direction while still providing enough vertical lift to balance the aircraft's weight. Thus, the maximum angle of bank ( $\beta$ ) that the aircraft can handle is governed by the amount of lift its wing can generate. Specifically, the angle is given by:

$$\cos \beta = \frac{C_{L @ \text{cruise}}}{C_{LMax}} = \frac{1}{2.4}$$

Thus, it is estimated this aircraft can maintain  $65^\circ$  of bank without causing the onset of an accelerated stall. This figure can be used to estimate the turning radius of the aircraft, first by calculating the lateral acceleration ( $a_c$ ) provided by the wing's lift at that angle:

This produces a value of  $a_c = 2.21g = 21.7 \text{ m/s}^2$ . Radius of turn is given by:

$$\tan \beta = \frac{a_c}{1g}$$

$$R = \frac{V^2}{a_c} = \frac{(19.2 \text{ m/s})^2}{21.7} = \mathbf{16.6 \text{ m (55 ft)}}$$

### 5.6 Endurance and Range

#### 5.6.1 Endurance

The aircraft achieves maximum endurance when flying at its minimum throttle setting, which provides sufficient thrust for the plane to achieve a velocity just above its stall speed ( $V_{\text{stall}}$ ). Thus, endurance is highly dependant on the motor and electrical system used.

The ElectriCalc commercial software package is used to estimate the endurance of the aircraft with the selected motor and battery arrangement. Electrical specifications for both the MaxNEO 13-Y motor and the SR 2000Max cell pack are used as ElectriCalc's input. ElectriCalc then calculates the operating characteristics of the propulsion system as a function of throttle setting. Included among the output parameters are current draw, motor power and efficiency, and run-time at the calculated RPM and velocity (estimated by ElectriCalc from wing loading and  $C_{DParasite}$ ). It was found that an airspeed of 10.7 m/s could be achieved with a

minimum throttle setting of 50%. At this setting, ElectriCalc estimated a run-time of **41 minutes**. This endurance estimate neglects power needed for take-off, climb-out, and landing.

#### 5.6.2 Range

The maximum range characteristics of an electrically-powered aircraft differ from those of a gas-powered plane, as motor efficiency drops at increased throttle settings. Losses caused by higher current draw reduce the effective range of the aircraft as throttle setting is increased. Thus, the maximum range of the aircraft is achieved not at the best lift-to-drag velocity, but at the lowest possible throttle setting—at the endurance throttle setting. To calculate the range, the endurance prediction of 41 minutes is multiplied by the speed at this value (10.7 m/s, just above  $V_{stall}$ ). This method produces a maximum range value of **26.3 km (16.5 miles)**. This value seems remarkably (and suspiciously) high given the performance of the aircraft at last year's competition, which were purposefully being flown to achieve maximum range. The best of these entries achieved an estimated ranges of about 13 km (8 miles).

### 5.7 Payload Fraction

Payload fraction is a measure of the payload's contribution to the take-off gross weight of the aircraft. It is given by:

$$\text{Payload Fraction} = \frac{W_{\text{payload}}}{TOGW}$$

The payload fraction of this aircraft is therefore predicted to be 7.5/16.5, or **0.45**.

## 6. Manufacturing Plan

---

### 6.1 Wing

From a manufacturing perspective, the wing is by far the most critical component of the aircraft. It not only bears the highest loading, but also must be built to the exact shape of the airfoil. The alternative manufacturing plans evaluated for construction of the wing are described here.

#### 6.1.1 Built-up Construction

This is the manufacturing process that has been used on the team's previous three aircraft. The selected airfoil is printed onto paper which is in turn glued to a piece of plywood. The plywood is cut around the paper using a jigsaw and then sanded down to the exact airfoil shape. The finished product is then used as a template to construct subsequent airfoils by the same process.

The spar is a single piece of  $\frac{1}{4} \times \frac{3}{4}$ -inch spruce running the length of the wing at the  $\frac{1}{4}$ -chord point. Medium density (blue) foam is cut to the airfoil shape using a home-made hot-wire cutter. Two plywood ribs are used as templates and guide the hot-wire around the airfoil shape. The wing is assembled around the spar, with each piece of foam being sandwiched between two plywood ribs spaced 8 inches apart. The whole wing is then sheeted with  $\frac{1}{32}$ -inch balsa wood and sanded down to remove irregularities. Finally, a smooth plastic MonoKote film is applied to the wing.

This process has proven very successful in previous competitions because it produces an extremely strong, resilient wing capable of withstanding moderate impacts. Although it is quite a time-intensive process, it is one with which the team has lots of previous experience. It is relatively inexpensive and requires materials easily obtained at most local hobby and hardware stores.

#### 6.1.2 Pultruded Carbon Spar

This method proposed to save weight by removing most of the foam core from the wing. A single pultruded carbon-fibre spar is inserted through alternating plywood and balsa wood ribs spaced 4 inches apart. Blue foam is cut only for the leading edge of the wing (forward of the spar). Behind the  $\frac{1}{4}$ -chord point, the wing is hollow and covered directly with a plastic MonoKote film. A thin balsa stringer is used at the trailing edge to hold the MonoKote to the airfoil shape.

By removing the blue foam from the wing, a significant weight savings is achieved. However, a pultruded carbon fibre spar is difficult and very expensive to obtain in the required shape and length. While incredibly rigid, the pultruded carbon fibre is also slightly heavier than desired.

#### 6.1.3 Carbon-Wrapped Balsa Spars

This process is quite similar to the first "hollow wing" process, but replaces the single pultruded carbon fibre spar with multiple composite spars. Two  $\frac{1}{4}$ -chord spars are constructed from 36-inch planks of  $\frac{1}{4} \times 1$ -inch balsa wood. Each is then wrapped with three layers of uni-directional carbon fibre cloth in a wet lay-up process. The  $\frac{1}{4}$ -chord spars are placed as close as possible to the top and bottom surfaces of the airfoil. Two smaller  $\frac{1}{4} \times \frac{1}{2}$ -inch spars, identically

constructed, run along the  $\frac{3}{4}$ -chord point to provide further structural rigidity. These aft spars are each 6 feet long, stopping at the aileron of each wing. Once again, blue foam is sandwiched between plywood and balsa ribs forward of the  $\frac{1}{4}$ -chord spar and the whole assembly is covered with plastic MonoKote.

This process retains the weight-saving benefits associated with the first "hollow wing" process while significantly reducing the cost to build. However, it is by far the most difficult to construct and requires more time and skill than either of the alternatives.

## 6.2 Landing Gear

alternative manufacturing plans evaluated for construction of the landing gear were:

### 6.2.1 *Aluminium Gear*

Historically, an all-aluminium landing gear assembly has been used, mainly for its strength. This process requires a single main gear strut assembly to be cut from  $\frac{1}{4}$ -inch aluminium and bolted to the airframe. Aluminium wheels are used.

Although an assembly left over from a previous aircraft would could in theory be incorporated directly into this year's plane at incidental cost, an all-aluminium gear assembly would be far stronger than needed for this competition and comes with a significant weight penalty.

### 6.2.2 *Composite Gear*

An alternative manufacturing process proposed that a single piece of blue foam be cut to the desired strut shape and then wrapped in Kevlar and fibre-glass using a wet lay-up process. Small plastic or rubber wheels are used in place of aluminium.

This process produces a gear that is relatively light, while still being strong and tough enough for this mission. It is also relatively easy to build. The landing gear must be built tough, but preferably not too rigid.

## 6.3 Tail Surfaces

The alternative manufacturing plans evaluated for construction of the tail surfaces were:

### 6.3.1 *Foam Core*

Previous planes used a simple foam core construction for the tail surfaces. Blue foam is cut to the airfoil shape using plywood templates and is then sheeted with  $\frac{1}{32}$ -inch balsa wood for structural rigidity.

This assembly has always provided good impact resistance for the tail on previous aircraft. It is extremely simple to build. However, the epoxy and balsa used in the sheeting does make it heavier than preferred for this mission.

### 6.3.2 *Rib and Spar*

This process uses an epoxy tube as the main structural member of each tail surface. Plywood ribs are cut and sanded to shape, then bonded to the spar with epoxy. The entire assembly is covered in MonoKote.

Again, a weight-savings is achieved through the elimination of balsa sheeting. This method does require more skill and time than the foam core alternative.

## 6.4 Airframe

The alternative manufacturing plans evaluated for construction of the airframe were:

### 6.4.1 *Nomex Wrapped in Fibre-glass*

This manufacturing process involves the construction of a mold for the desired airframe shape. A Nomex honeycomb core is sandwiched between several layers of fibre-glass in a wet lay-up process.

The resulting airframe structure is extremely strong and very light. However, previous experience has proven that Nomex is a very difficult material with which to work. It is also relatively difficult to obtain.

### 6.4.2 *Balsa Wrapped in Fibre-glass*

This method is very similar to the one described above, except that balsa wood replaces Nomex as the composite core. A mold is not necessary; the frame is simply constructed from 1/4-balsa and then wrapped in layers of fibre-glass, again using a wet lay-up process.

This method produces an airframe that is comparable in weight and strength to the Nomex core, but much easier to build. Balsa wood can be obtained easily and cheaply at any local hobby shop.

### 6.4.3 *Ribs and Stringers*

The most traditional method of building a model aircraft airframe is with the use balsa wood and aircraft plywood. Structural loads are supported by plywood ribs, while the shape of the fuselage is held by balsa stringers. The assembly is joined together with epoxy and covered in MonoKote.

This process produces the lightest airframe of all the alternatives considered. It is also the most fragile and requires a lot of time and skill to construct properly.

## 6.5 Figures of Merit

At the conceptual stage, figures of merit were kept qualitative. A description of the figures of merit used to evaluate design concepts is given here, along with the relative "importance factor" of each FOM.

### 6.5.1 *Skill Level Required*

This is a measure of the amount of experience needed to build a high-quality component using alternative design methods.

### 6.5.2 *Cost/Availability*

This is an estimate of the cost required to build a component using alternative manufacturing processes. Since all labour is done by student team members (at no cost), this FOM essentially compares the relative cost of procuring materials needed for each process. Materials which are available in Canada were preferred due to the relative weakness of the Canadian dollar in early 1998 and the added cost and delay of shipping materials through customs. The team operates on a very tight budget. This year, the cost of purchasing an electric motor and batteries accounted for about 70% of the plane's total cost.

### 6.5.3 *Time Required*



This is an estimate of the man-hours required to complete the component using alternative manufacturing processes. This is an important consideration because every component is built by engineering students with full academic course loads.

#### 6.5.4 Design Benefits

In evaluating manufacturing processes, design considerations typically revolve around strength and weight. In this year's plane, every effort was made to reduce unnecessary structural weight.

### 6.6 Evaluation and Selection

#### 6.6.1 Analytical Method

Each of the competing alternatives was evaluated concept for each FOM. The cost of each process was estimated by tallying retail prices of all materials required (in some cases, this cost had to be estimated). Required skill level is represented by a score taken from a scale of 1 to 3. Time required is an estimate of the number of man-hours required to complete each process. Design benefits (in weight reduction and structural enhancements) are represented by a score taken from a scale of 0 to 5.

Total scores were tabulated using the following equations, which illustrates the relative importance placed on each FOM:

$$\text{Total Score} = 50 - \left( \frac{\text{Cost}}{5} \right) - (\text{Skill Level} \times 3) - \left( \frac{\text{Time}}{6} \right) + (\text{Design Benefits} \times 5)$$

Table 6.1. Manufacturing process evaluation. Selected methods are shaded.

	Cost/ Material Availability Can\$ (US\$)	Skill Level Required	Time Required (man-hours)	Design Benefits	Total Score
<b>Wing</b>					
Built-up Wing	125 (87 US\$)	2	110	1	6
Pultruded Carbon Spar	250 (153)	1	60	4	7
Carbon-Wrapped Balsa Spar	130 (90)	3	85	4	21
<b>Landing Gear</b>					
Aluminum	40 (28)	2	6	0	35
Composite	30 (21)	2	10	4	56
<b>Tail Surfaces</b>					
Foam core	10 (7)	1	6	4	64
Rib-and-Spar	7 (5)	2	10	4	66
<b>Airframe</b>					
Composite Nomex	100 (70)	3	80	5	33
Composite Balsa	60 (42)	2	65	4	42
Rib and Spar	55 (38)	3	100	2	23

Table 6.2. Manufacturing Milestones

Milestone	Proposed Date (m / wk)	Actual Date (m / wk)
<b>1.0 Wing</b>		
1.1 Support ribs cut and sanded	1 / 1	2 / 1
1.2 Spar construction begins	1 / 3	2 / 3
1.2.1 Balsa sections cut and glued	1 / 3	2 / 3
1.2.2 Balsa wrapped in composite	2 / 1	3 / 1
1.3 Foam sections cut	2 / 3	2 / 2
1.4 Wing attachment assembly made	2 / 4	3 / 3
1.5 Final construction of wing	3 / 1	3 / 4
<b>2.0 Landing Gear</b>		
2.1 Foam cut	3 / 1	3 / 2
2.2 Kevlar wrapped	3 / 2	3 / 3
2.3 Assemble wheels and gear	3 / 3	3 / 4
<b>3.0 Tail</b>		
3.1 Elevator and rudder ribs cut and sanded	2 / 1	2 / 1
3.2 Foam sections cut	2 / 2	2 / 2
3.3 Attachment assembly made	2 / 3	2 / 4
3.4 Tail sections attached to boom	2 / 4	2 / 4
<b>4.0 Airframe</b>		
4.1 Balsa cut and sanded to desired shape	2 / 2	2 / 2
4.2 Composite wrapping	2 / 3	2 / 3
4.3 Preparing fuselage attachment points	2 / 4	2 / 4
4.4 Packing fuselage	3 / 1	3 / 2
4.4.1 Mounting engine	3 / 1	3 / 2
4.4.2 Secure battery packs	3 / 1	3 / 2
4.4.3 Install and test servos	3 / 1	3 / 2
4.5 Attach components	3 / 4	3 / 4
4.5.1 Attach wing at angle of incidence	3 / 4	3 / 4
4.5.2 Attach tail	3 / 4	3 / 4
4.5.3 Attach landing gear	3 / 4	3 / 4
<b>5.0 Pre-flight testing</b>		
5.1 Confirm center of gravity	4 / 1	4 / 1
5.2 Test servos for accurate response	4 / 1	4 / 1
<b>6.0 Flight Test</b>	4 / 2	4 / 2

## Appendix A: Longitudinal Stability Calculation Values

The equation used to calculate the neutral point position is:

- $C_{L\alpha}$  is found by taking the slope of the “ $C_L$  vs. AOA” chart from published airfoil data for S1210

$$\Rightarrow C_{L\alpha} = 5.17 \text{ per radian}$$

$$\bar{X}_{np} = \frac{C_{L\alpha} \bar{X}_{acw} - C_{m\alpha_{fus}} + \eta_h \frac{S_h}{S_w} C_{L\alpha_h} \frac{\partial \alpha_h}{\partial \alpha} \bar{X}_{ach}}{C_{L\alpha} + \eta_h \frac{S_h}{S_w} C_{L\alpha_h} \frac{\partial \alpha_h}{\partial \alpha}}$$

- $X_{acw} = 1.04$

where  $k_f$  is the empirical pitching factor estimated from Fig. 16.14 of ref. 7.

- $\eta_h^{max} = \frac{k_f \cdot W_f^2 \cdot L_f}{C_{L\alpha} S_w} \frac{0.6 \cdot 0.5^2 \cdot 2}{(tail \text{ is placed well above wing})} = 0.06$

- $C_{L\alpha_h}$  is found by taking the slope of the “ $C_L$  vs. AOA” chart from published airfoil data for E212

$$\Rightarrow C_{L\alpha_h} = 5.84 \text{ per radian}$$

where  $\delta\epsilon/\delta\alpha$  is estimated from Figure 16.12 of ref. 6.

$$\frac{\partial \alpha_h}{\partial \alpha} = 1 - \frac{\partial \epsilon}{\partial \alpha} = 1 - 0.1 = 0.9$$

- $X_{ach} = 3.88$

- $X_{CG} = 1.02$

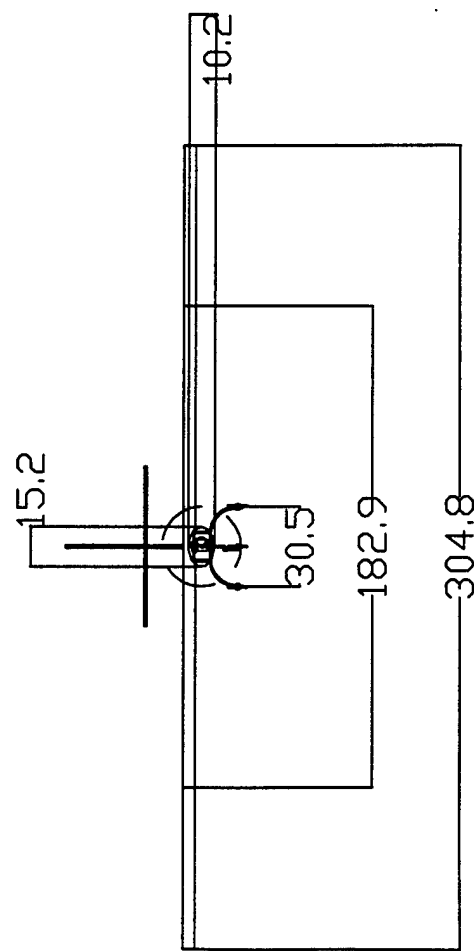
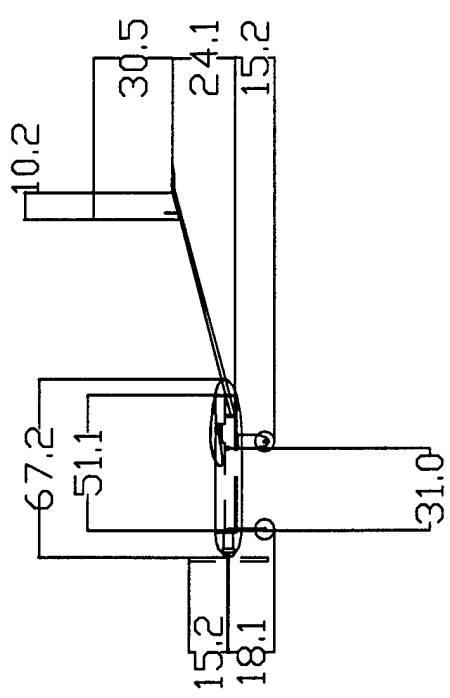
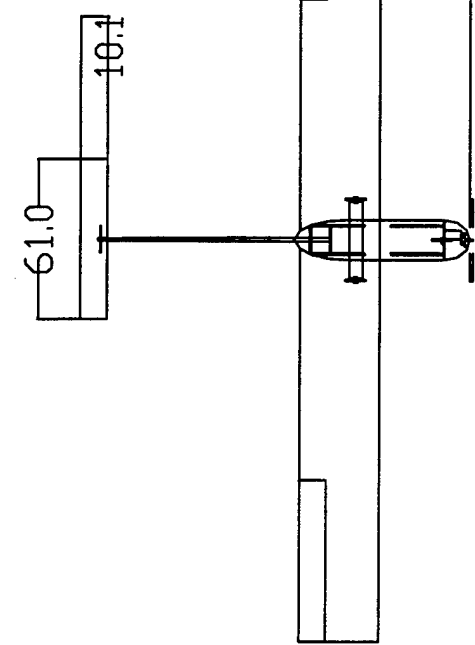
## Appendix B: References

---

1. Eppler, Richard. Airfoil Design and Data. Springer-Verlag: Germany. 1990.
2. Foster, Steve. "*Undercarriage Design for Queen's Cargo Aircraft*." Undergraduate Thesis Project, Department of Mechanical Engineering. March, 1994.
3. Horton, Johanna Lisa. "*Cargo Aircraft Stability Analysis*." Undergraduate Thesis Project, Department of Mathematics and Engineering. April, 1993.
4. McCormick, Barnes. Aerodynamics, Aeronautics, and Flight Mechanics, second edition. John Wiley & Sons, Inc.: New York. 1995.
5. Munson, Young, and Okiishi. Fundamentals of Fluid Mechanics, second edition. John Wiley & Sons, Inc.: New York. 1994.
6. Raymer, Daniel. Aircraft Design: A Conceptual Approach. AIAA Education Series. American Institute of Aeronautics and Astronautics, Inc.: Washington, D.C. 1989.

**Appendix C: Drawing Package**

REVISIONS			
ZONE	REV	DESCRIPTION	DATE



NOTES:

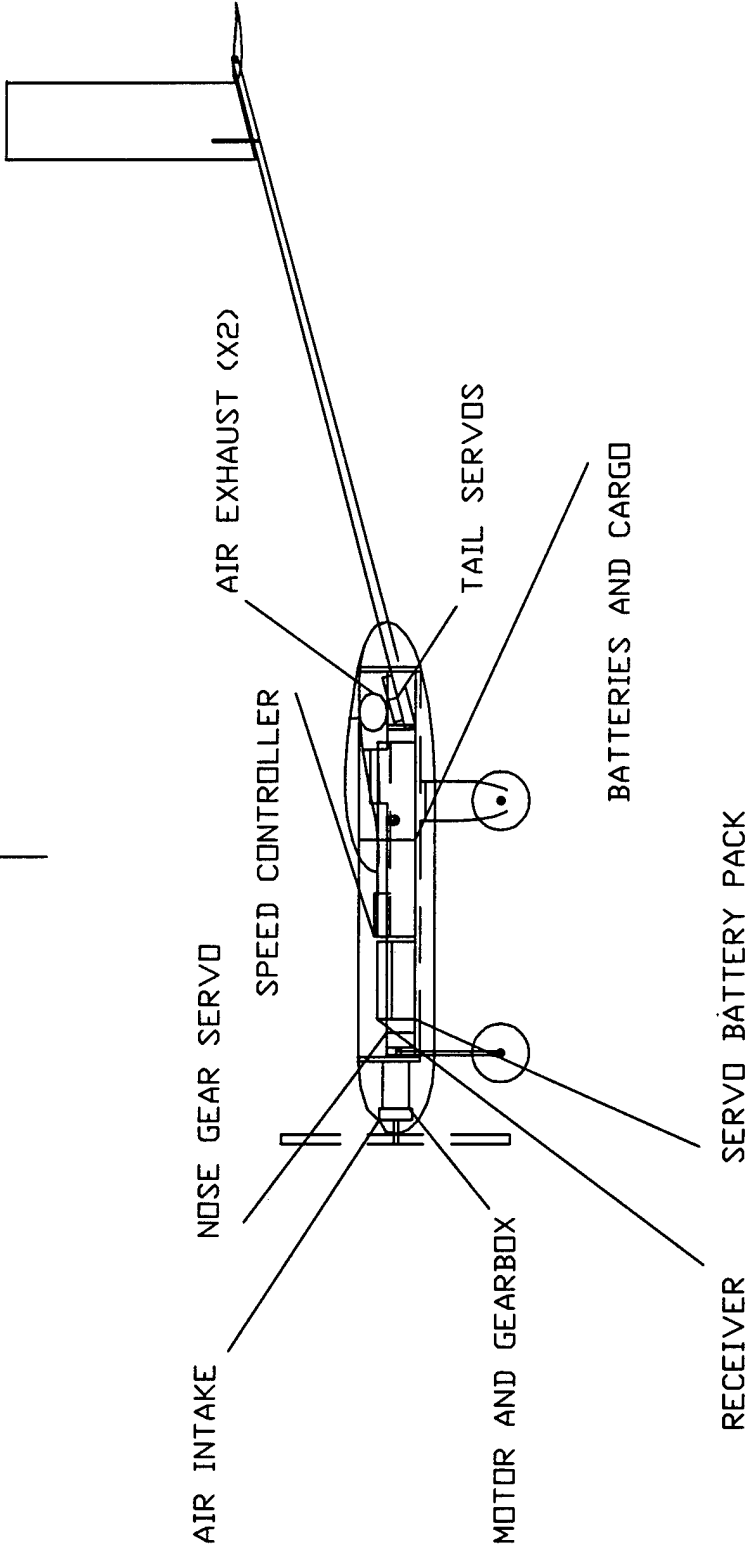
QUEEN'S AERO DESIGN TEAM

ASSEMBLY DRAWING

ALL DIMENSIONS IN CM

SIZE	FSCM NO.	DWG NO.	REV
		QAD01A	A
Scale		Sheet	

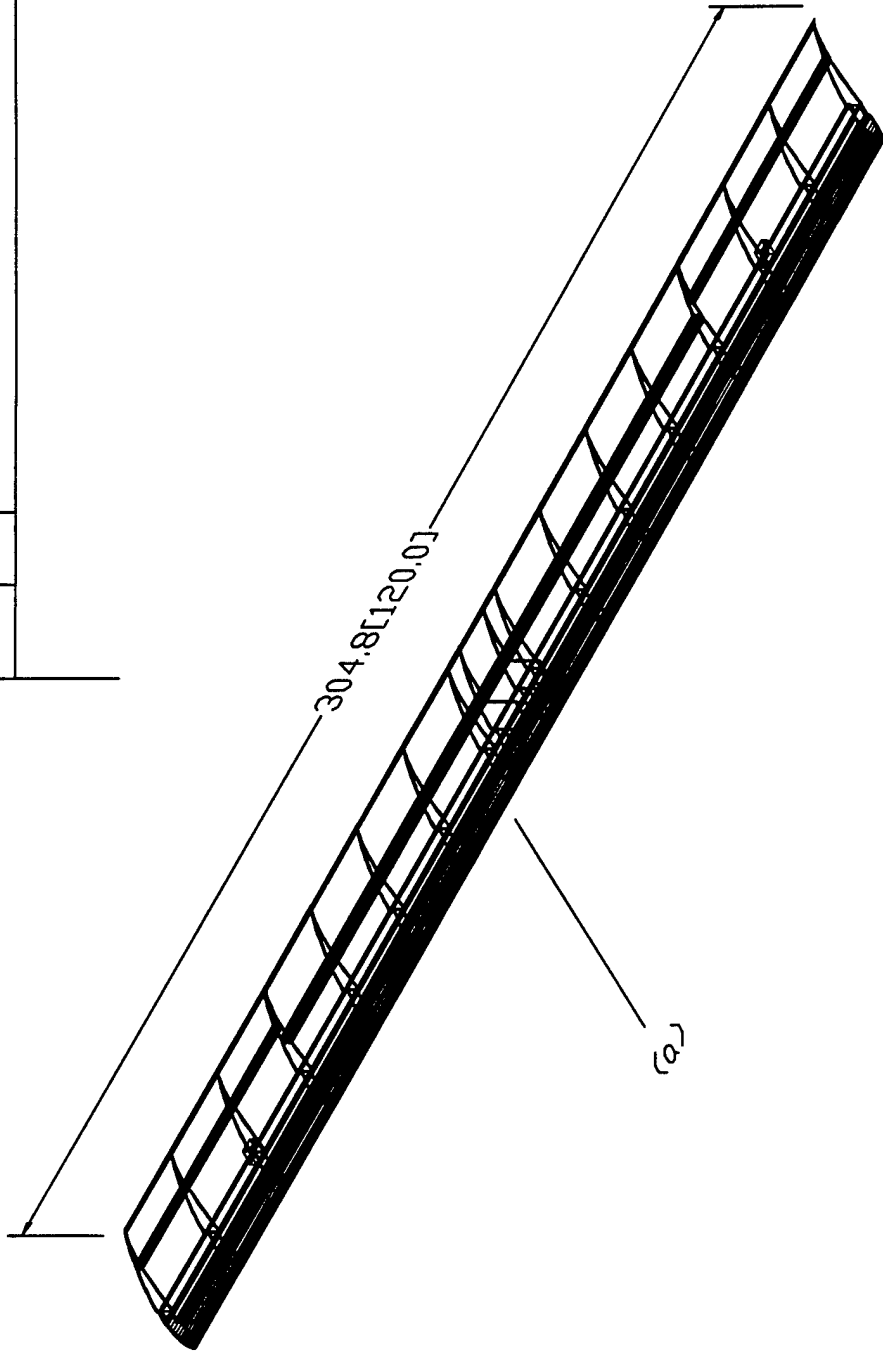
REVISIONS			
ZONE	REV	DESCRIPTION	DATE
			APPROVED



SEE DRAWING QAD02A FORAILERON SERVO LOCATION

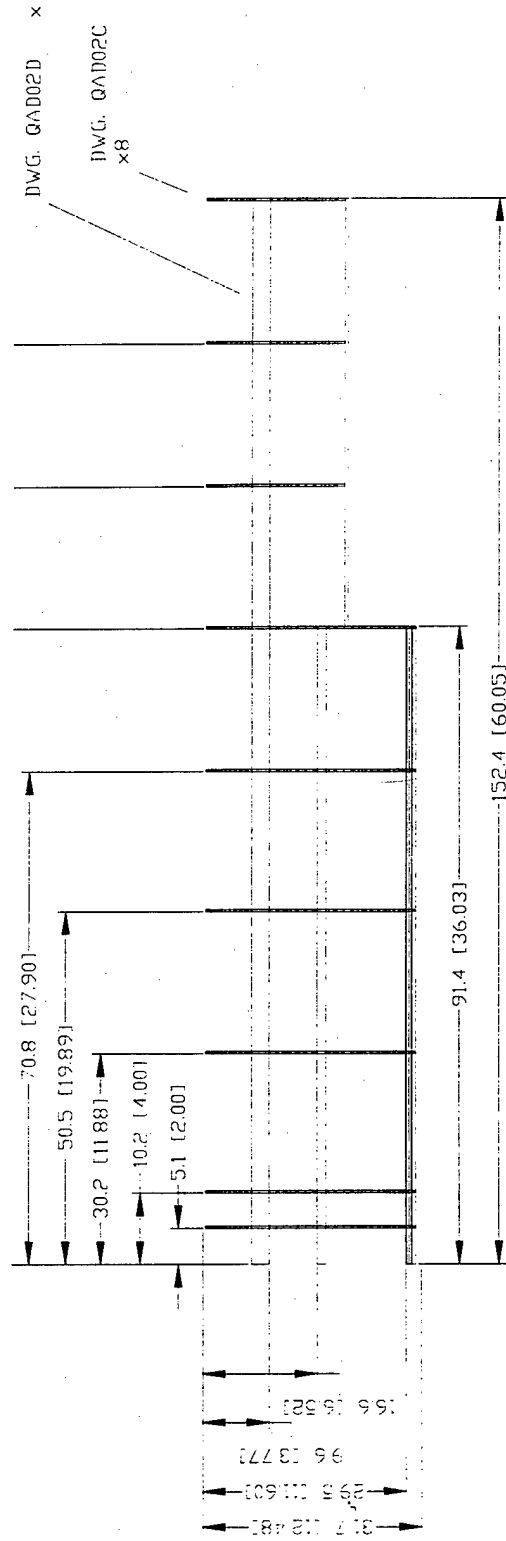
NOTES	QUEEN'S AERO DESIGN TEAM			
	SYSTEMS AND CARGO LOCATION			
SIZE	FSCM NO.	DWG NO.	REV	
		QAD01B	A	
Scale		Sheet		

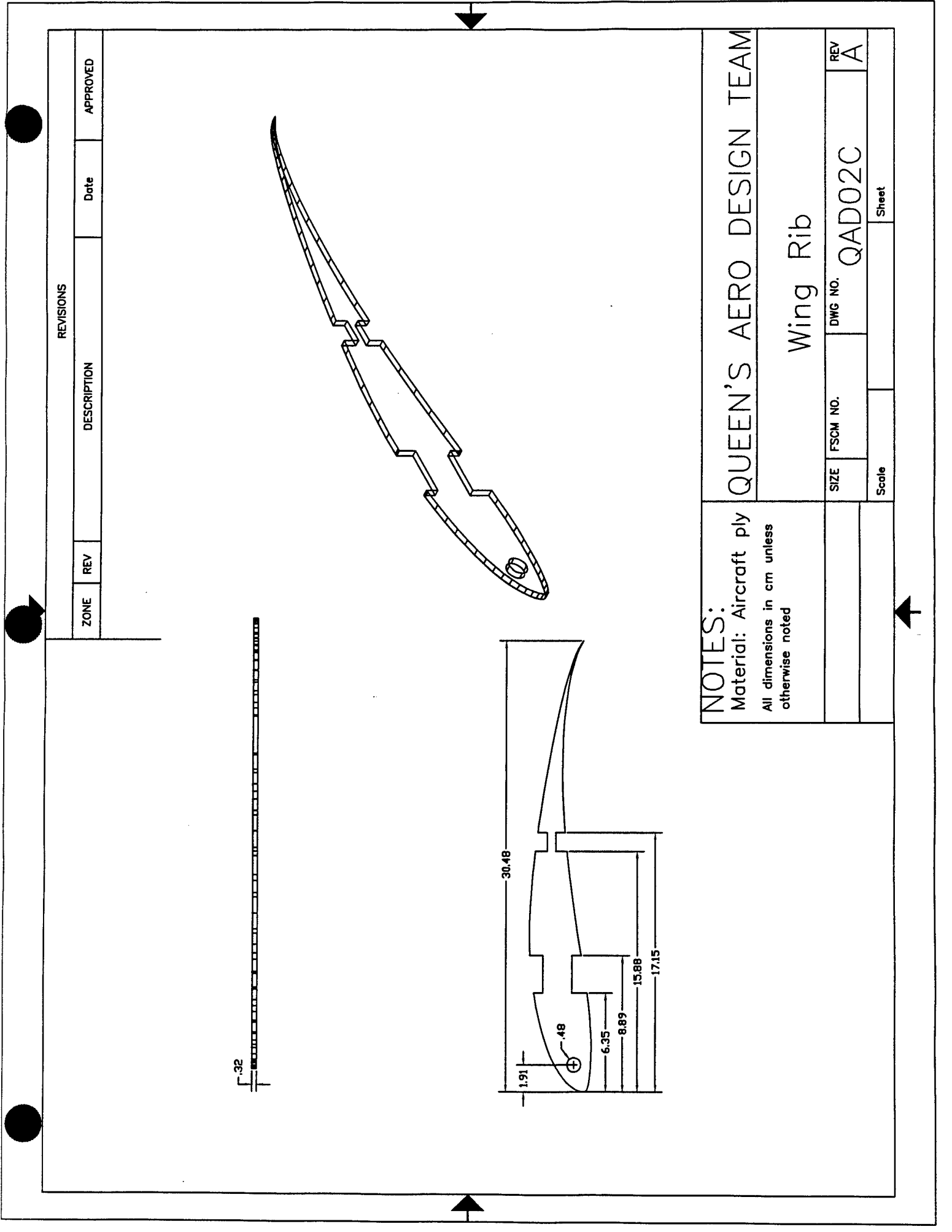
REVISIONS			
ZONE	REV	DESCRIPTION	DATE
			APPROVED



<p>NOTES:</p> <p>Materials</p> <p>(a) blue foam</p>		<p>QUEEN'S AERO DESIGN TEAM</p>	
<p>All dimensions in cm (in)</p>		<p>WING, STRUCTURE</p>	
SIZE	FSCM NO.	DWG NO.	REV
		QAD02A	A
SCALE		SHEET	





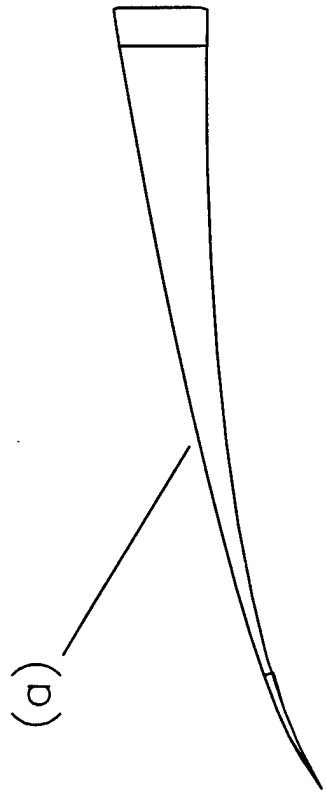
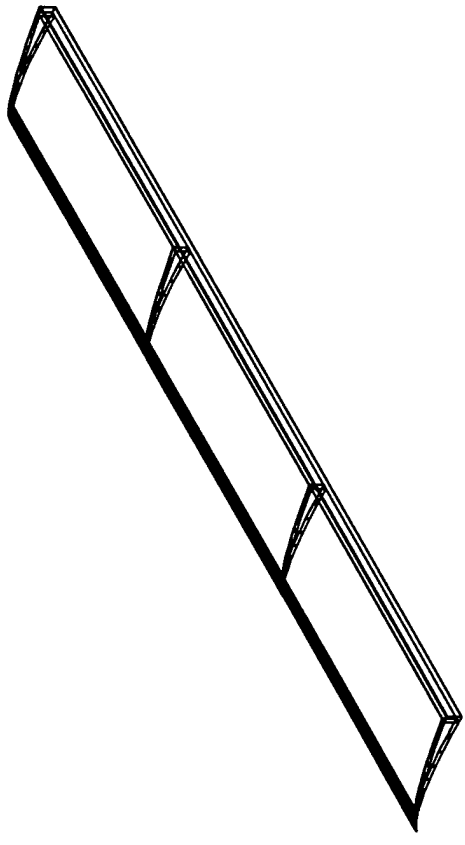
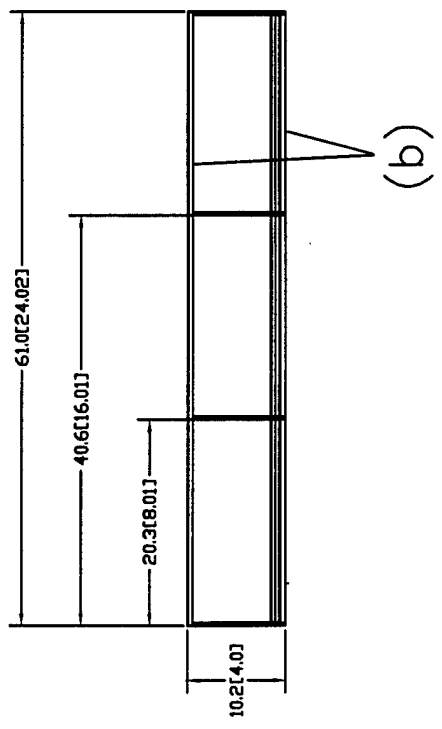


NOTES:  
Material: Aircraft ply  
All dimensions in cm unless  
otherwise noted

QUEEN'S AERO DESIGN TEAM			
Wing Rib			
SIZE	FSCM NO.	DWG NO.	REV
		QAD02C	A
Scale		Sheet	

REVISIONS

ZONE	REV	DESCRIPTION	Date	APPROVED
------	-----	-------------	------	----------



NOTES:

Materials  
(a) Balsa (b) plywood  
All dimensions in cm unless  
otherwise noted

QUEEN'S AERO DESIGN TEAM

AILERON (RIGHT)

SIZE	FSCM NO.	DWG NO.	REV
		QAD02D	A

Scale Sheet

# **1998 AIAA DBF Competition Design Report**

———— *Addendum Phase* ————



***Queen's University at Kingston***

*Department of Mechanical Engineering*

*Department of Engineering Physics*

*April 13, 1998*

## 7. Lessons Learned

---

### 7.1 Changes from the Proposal

Several modifications have been made to the aircraft design and manufacturing plans since submission of the Proposal Phase. Most significant of these is the change from a tricycle gear configuration to a taildragger design. As stated in the proposal phase, tricycle gear was originally selected for its handling qualities during the takeoff and landing runs. In addition, nose gear greatly reduced the danger of a prop strike during these phases of flight. The decision to switch to a taildragger configuration, however, was prompted by the need to reduce drag. Since most teams will most likely be using very similar propulsion and electric systems, a large portion of this competition is essentially about drag reduction. The plane with the least drag should have the highest range and speed, and should therefore be able to complete the most laps. In addition to reducing drag, the taildragger configuration also saves weight and increases prop clearance during ground operations. The decrease in controllability on the ground was therefore deemed to be a necessary evil, and was sacrificed to improve in-flight performance. Thus, the initial opposition to this configuration eventually gave way and an evaluation was done to investigate the feasibility of changing designs. It was discovered that the actual changes to be made were relatively minor. Firstly, the angle of the tail boom with respect to the horizontal was reduced from  $15^\circ$  to  $10^\circ$ . This put the plane at a  $15^\circ$  AOA during ground operations. Secondly, a small,  $\frac{3}{4}$ -inch-diameter tail wheel (commercial off-the-shelf) was mounted to the end of the tail assembly.

The second major design change was that of the main landing gear. It was proposed in the original design to use Kevlar-wrapped foam as the main load-bearing strut during landing. Actual manufacturing and testing of this design, however, indicated that we had greatly underestimated the difficulty in constructing it properly. To obtain a good bond between the Kevlar and foam, a vacuum bagging procedure was needed. A simple wet lay-up process resulted in delamination of the Kevlar during simulated hard landings, and subsequent failure of the gear. Vacuum bagging equipment is not readily available to the team, especially on short notice. It was therefore decided to discard the Kevlar-foam design altogether. Two alternatives were considered in its place: commercial off-the-shelf fibre-glass landing gear, or the same simple aluminium gear that had been used successively in previous competitions. For the same reasons outlined in section 6.2.1 of the Proposal Phase, aluminium gear was not favoured. Fibre-glass gear, rated by the manufacturer for a 15-pound model aircraft, was therefore selected. Small, foam-filled wheels were

simultaneously purchased, as well as a pair of plastic wheel pants to reduce parasite drag.

The final change is a relatively small detail design modification, not apparent from visual inspection. The manufacturing plan for the tail surfaces (rudder and stabilator) called for a "built-up" construction process in which balsa and plywood ribs are a bonded to an epoxy-tube spar and then covered with MonoKote. It was found, however, that covering this assembly with MonoKote was nearly impossible, because the plastic shrinks significantly more than expected as it is applied. This caused significant "sagging" at the leading and trailing edges and a disappointing overall product. The addition of a thin balsa sheet "skin" around the assembly, however, eliminated the problem. The balsa sheeting also made the tail surfaces much more rigid and resistant to light impact.

A similar technique was employed to reinforce the trailing edge of the wing. A one inch strip of balsa sheeting now covers the trailing edge, helping to stiffen against the shrinking force of the MonoKote covering and has the added advantage of making the wing more robust with very little extra weight.

## **7.2 Improvements for 2<sup>nd</sup>-Generation Design**

The first improvement to be made in the second generation design is replacement of the Selig high-lift airfoil with another airfoil such as the Clark Y. The two main reasons for this are ease of construction and drag reduction. The Selig high lift foil has a very distinct thin trailing edge. This makes it quite challenging to build properly while still retaining rigidity and strength. A less cambered airfoil should be able to provide sufficient lift for cruise, although a slight decrease in acceptable wing loading would result from the decreased coefficient of lift. This airfoil would have a lower coefficient of drag than the Selig foil allowing for a higher top speed. Implementing this change in a second generation design would have a negligible impact on cost, while simultaneously saving the team lots of time in cutting and sanding ribs.

The next modification involves the manufacturing method used for the tail surfaces. The current method produced an acceptable product, once they were sheeted. However, the process was fairly labour intensive, requiring a significant amount of time to construct and assemble. This could be improved using surfaces cut out of foam and wrapped using a composite material, most likely fibreglass, which is vacuum bagged to obtain good bond and a smooth finish. Such a change would improve strength and impact resistance. Although the method would save time, (estimated at 10 to 15 man-hours), acquiring the necessary materials and equipment

would likely be more costly than the current construction method. It is estimated that about \$20 worth of fibreglass cloth (plus some epoxy) would be needed, as opposed to the ~\$7 worth of wood and epoxy tubing in our current design. Additionally, vacuum bagging materials would require an additional investment.

The final modification we would make is the increased use of aerodynamic fillets and rounding to reduce form and interference drag from attachments and joints. In order to implement this final modification, the aircraft would have to be built faster to allow sufficient time for aerodynamic testing to identify problem areas. Proper wind-tunnel testing (if we had the required wind tunnel and flow visualization apparatus) would be an extremely time-intensive process. In combination with the smoothing and fillet construction, it is estimated an additional 50 man-hours would be required to implement this improvement. Cost would be minimal, once access to appropriate facilities could be obtained.

### 7.3 Cost Estimate

Costs are broken down for each section of the aircraft. For comparison, both manufacturer's list price and actual procurement cost (which includes donations, discounts, taxes, shipping, and customs charges) are provided. Costs marked with an asterisk (\*) are estimated. All figures have been converted to US dollars at an assumed exchange rate of \$1 US = \$1.44 Canadian.

**Table 3.1. Cost Estimate.**

	<b>Manufacturer's List Price</b>	<b>Actual Procurement Cost</b>
<b>Wing</b>		
Blue foam	7*	0 (leftovers)
EconoKote	17	16
Uni-directional carbon fibre	49	59
<b>Tail</b>		
Al-Carbon-Al tail boom (×2)	54	73
Epoxy tube	5*	5*
Push-pull rods and attachments	7	5
MonoKote	5	4

<b>Fuselage</b>		
<i>Kevlar</i>	32*	0 (leftovers)
<i>Fibreglass</i>	20*	0 (leftovers)
<b>Landing Gear</b>		
<i>Fibreglass main strut</i>	17	20
<i>Main wheels</i>	11	13
<i>Wheel pants</i>	20	23
<i>Tail wheel</i>	2	3
<i>Tail wheel assembly bracket</i>	3	4
<b>Motor and Electrics</b>		
<i>MaxNEO 13-Y Motor</i>	220	208
<i>Motor controller</i>	190	180
<i>Gearbox</i>	56	53
<i>Motor mount</i>	13	12
<i>Motor Battery pack</i>	190	206
<i>Radio Receiver</i>	120*	0 (borrowed)
<i>MicroServos (*4)</i>	130	114
<i>Servo battery pack</i>	30*	0 (borrowed)
<i>Wiring</i>	5*	0 (donated)
<b>Other</b>		
<i>Epoxy</i>	10*	10*
<i>Balsa wood</i>	22	16
<i>Aircraft plywood</i>	16	12
<i>Paint</i>	4*	3*
<i>Propeller</i>	4	3
<i>Miscellaneous nuts and bolts</i>	5*	5*
<b>TOTAL</b>	<b>\$ 1264</b>	<b>\$ 1045</b>

In retrospect, our actual costs match relatively well to our estimated costs from section 6.6 of the Proposal. Notable exceptions include the main landing gear, which ran about \$40 over the estimated costs due to the last-minute change in design. Many costs from the estimate above were not included in the Proposal as they were not relevant considerations in selecting one design or process over another (ie: paint, propeller, battery pack).

In many instances, actual procurement costs varied significantly from manufacturer's list prices. This is due to several factors. The team has long-standing relationship with local hobby shops and receives a discount on most standard materials. Many materials cannot be bought in the small quantities required for this aircraft, and thus leftovers from previous years are always available. This year, most of the composite fabrics, such as Kevlar and



fibreglass, were obtained in this manner. Finally, the weak Canadian dollar, in combination with foreign shipping and customs charges, heavily affected the actual price of any item purchased outside Canada. For example, the team received a discount on the motor equipment from MaxCim which was effectively neutralized by currency exchange and shipping costs.

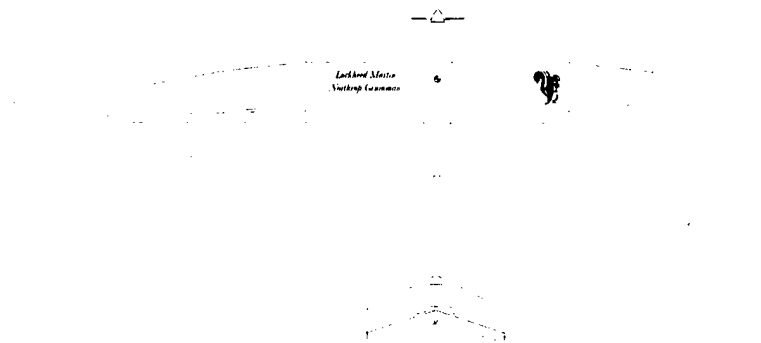
# Design Report - Proposal Phase

March 13, 1998

1997/1998 AIAA Student Design/Build/Fly Competition



*The University Of Southern California*



## UNDERGRADUATE TEAM MEMBERS

Philip Haworth- Editor, Propulsion  
Ryan Romo- Editor, Configuration  
Stuart Sechrist- Weight Analysis, Structures  
QiHuan Chen- Aerodynamics, S&C  
David Sandler- Editor, Mission Performance  
Jacob Evert- Conceptual Design  
Kevin Helm- Support Equipment  
Nathan Palmer- Landing Gear

## FACULTY ADVISOR

Dr. Ron Blackwelder

## INDUSTRY ADVISORS

Blaine Rawdon- Boeing  
Mark Page- All American Racing

## SPONSORS

Lockheed Martin Skunk Works  
Northrop Grumman

## 1. EXECUTIVE SUMMARY

### 1.1 Introduction

To solve the problem designed for contestants of the AIAA Student Design/Build/Fly competition, the University of Southern California team chose to divide it into five major areas: Configuration, Aerodynamics, Structures and Weights, Propulsion, and Mission Performance. Configuration focused on the layout of the

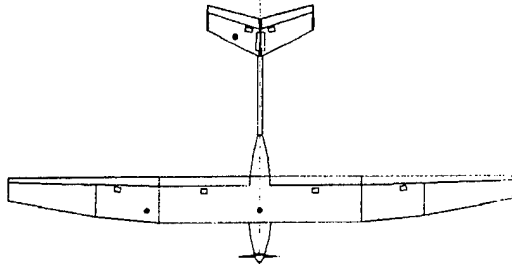


Figure 1.1 Plan View of Final Design

aircraft, and drawings and blueprints used in both the design and manufacturing stages of aircraft development. Aerodynamics aimed its efforts to determine the aerodynamic characteristics of the airplane and found suitable airfoils for use in the competition. Weights calculated the weights of materials and payload in the aircraft, located the center of gravity, analyzed the moments and forces of the final configuration, and chose the structural materials to be used in the final construction. Propulsion created the most efficient system to propel the aircraft and chose the best combination of propeller, motor and battery. Mission Performance tied the Aerodynamics, Weights, and Propulsion sections together to provide the complete platform from which different configurations were compared and contrasted.

The final configuration of the aircraft includes a flapped S7012 airfoil, no gearbox, an 8-inch propeller, and 26 Sanyo KR-1700AE batteries. The wing has an area of 5.3 ft<sup>2</sup> and an aspect ratio of 13. The predicted performance of the 13.77 lb. airplane is 25.3 laps.

### 1.2 Range of Design Alternatives

Multiple design alternatives were considered. Primary design alternatives compared choices of wing, tail, and motor configuration. These alternatives were explored in an attempt to maximize propulsive efficiency and turning performance, minimize construction, mechanical complexity, weight and overall drag, and to maintain stability.

Wing types considered were swept, low wings, anhedral and dihedral configurations. Tail alternatives

that were investigated included a V-tail, T-tail, along with different kinds of tailskids. Various motor configurations included alternatives such as using more than one motor, having a pusher propeller, or a more conventional tractor propeller.

Secondary, more detailed design alternatives looked at included payload configurations, wing mounting techniques, and layout of all essential hardware. Different payload configurations examined had variations in location, accessibility, and dimensions. There were three ways considered to mount the wing: a two-piece wing that plugs into the side of the fuselage, a one-piece wing bolted to the fuselage from the top, and a wing that slides into place from front to back. Different layouts of the essential electronics and cargo were based on available space and center of gravity considerations.

### 1.3 Design Tools

The two main design tools used in development of the design were Microsoft Excel spreadsheets and AutoCAD v.14. While still

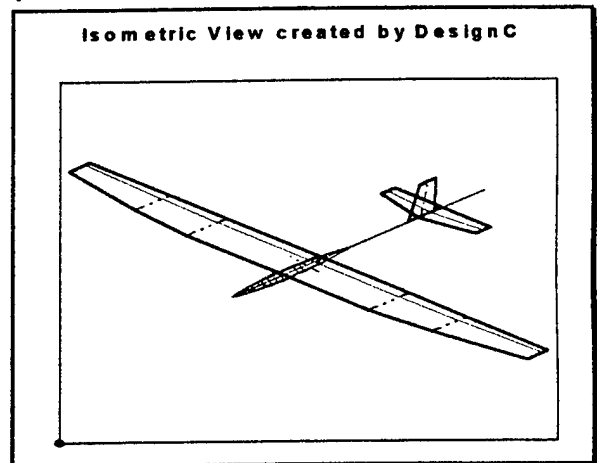


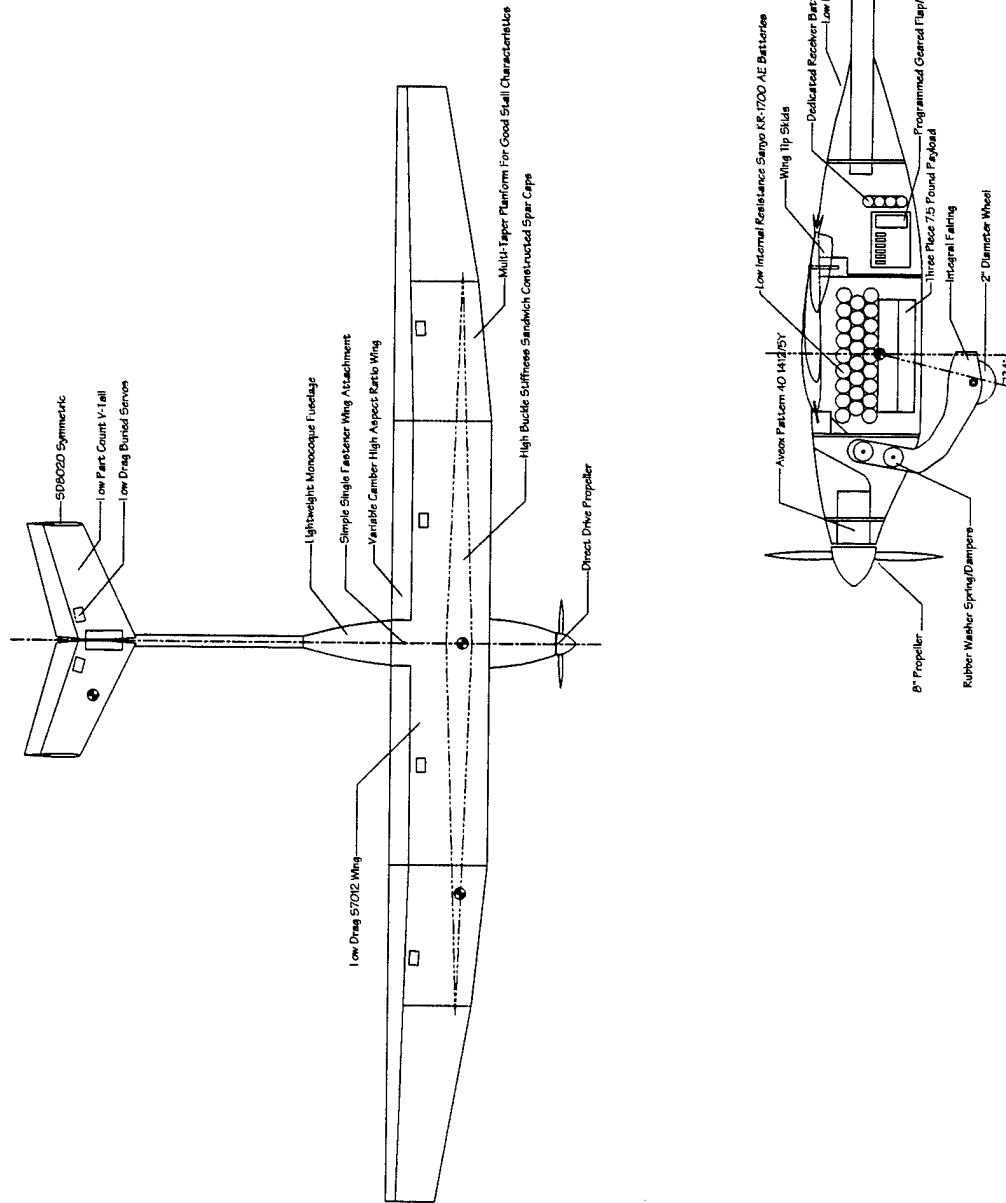
Figure 1.2 Isometric of Final Design Prior To Inclusion Of V-Tail

developing concepts for the design, Aerodynamics and Propulsion chose numerous airfoils, batteries, motors, and gearboxes, to examine in the preliminary and detailed stages of development. Weights researched electronic components involved and the materials to be used in the manufacturing process, and began building the code for an Excel spreadsheet. Configuration used AutoCAD to draw preliminary drawings for analysis and adjusted to specific constraints. Mission Performance gathered the equations from the other team divisions to enter in to a spreadsheet designed to connect the spreadsheets from the Weights, Aerodynamics, and Propulsion areas.

The preliminary design connected the completed Excel spreadsheets from each team division

# PEPS

*The University Of Southern California*



through the Mission Performance spreadsheet into a final workbook, after which time various configurations, including variations in wing area, aspect ratio, gearbox, motor, batteries, and airfoils were tested and compared. AutoCAD was used by Configuration and created the drawings of the airplane based of the Excel spreadsheet tests. After the major design characteristics were finalized, Configuration made more accurate drawings (blueprints) to be used in analyzing and manufacturing the design.

In addition to Excel and AutoCAD, the detailed design process enlisted the use of DesignC, a commercially available model sailplane design geometry program, in Excel format, created by Blaine Rawdon. This program was used and developed a 3-D drawing of the complete airplane that was easily modified to adjust the geometry of the wing and tail. Another use of Excel was to calculate specific performance characteristics that included take off performance, range, and endurance. Also, AutoCAD was used extensively to finalize the internal layout of the hardware and provided the schematics from which the plane was manufactured.

## 2. MANAGEMENT SUMMARY

### 2.1 Team Architecture

Management of the team was determined by experience and patterned after a corporation. Two industry professionals, Blaine Rawdon and Mark A. Page, agreed to share their time and knowledge to advise the group, held the roles of project managers and provided essential information and data needed to make the calculations for design. Dr. Blackwelder, who managed the funding, filled the chief financial officer role. He found the sponsors for the USC entry: Lockheed Skunk Works Corporation and Northrop Grumman. Assignments for various design sections (role of associate engineers) of the project were done on a volunteer basis of students, granted according to experience, responsibility and ability.

### 2.2 Design personnel and assignment areas

The responsibilities assigned rested in the 8-student team members. Ryan Romo produced configuration and drawings of the aircraft, while Qi Chen researched airfoils and developed the aerodynamics spreadsheet. Stuart Sechrist did structural testing, wrote the weights and structures spreadsheet, and directed the manufacturing process. Phil Haworth researched batteries, motors, gearboxes, and propellers, and prepared the propulsion spreadsheet. David Sandler connected the different sections together through the mission performance spreadsheet into one workbook. Finally, Nathan Palmer provided landing gear research as Kevin Helm and Jacob Evert researched alternative designs during the conceptual design phase.

### Management Architecture

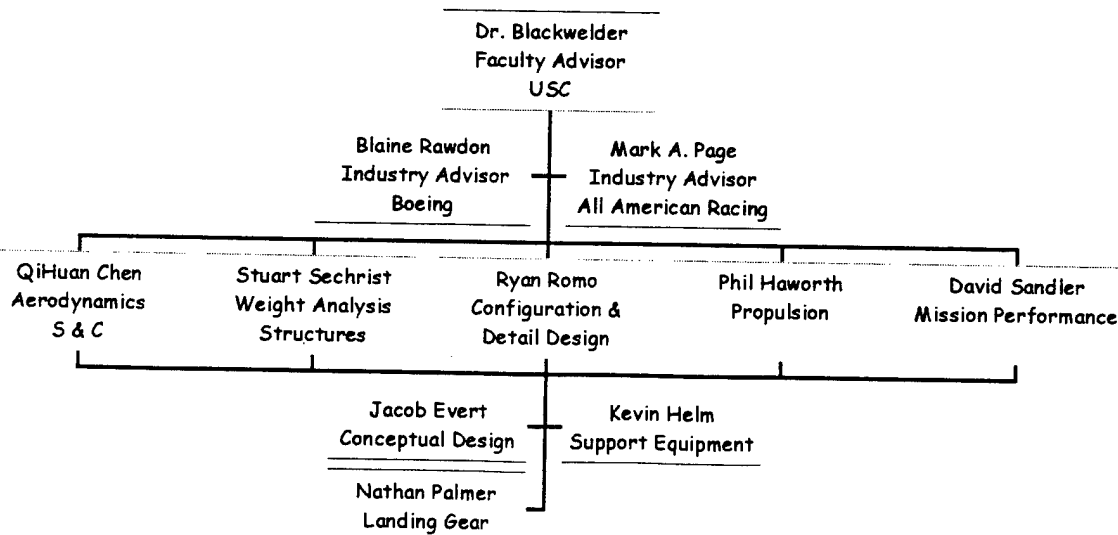
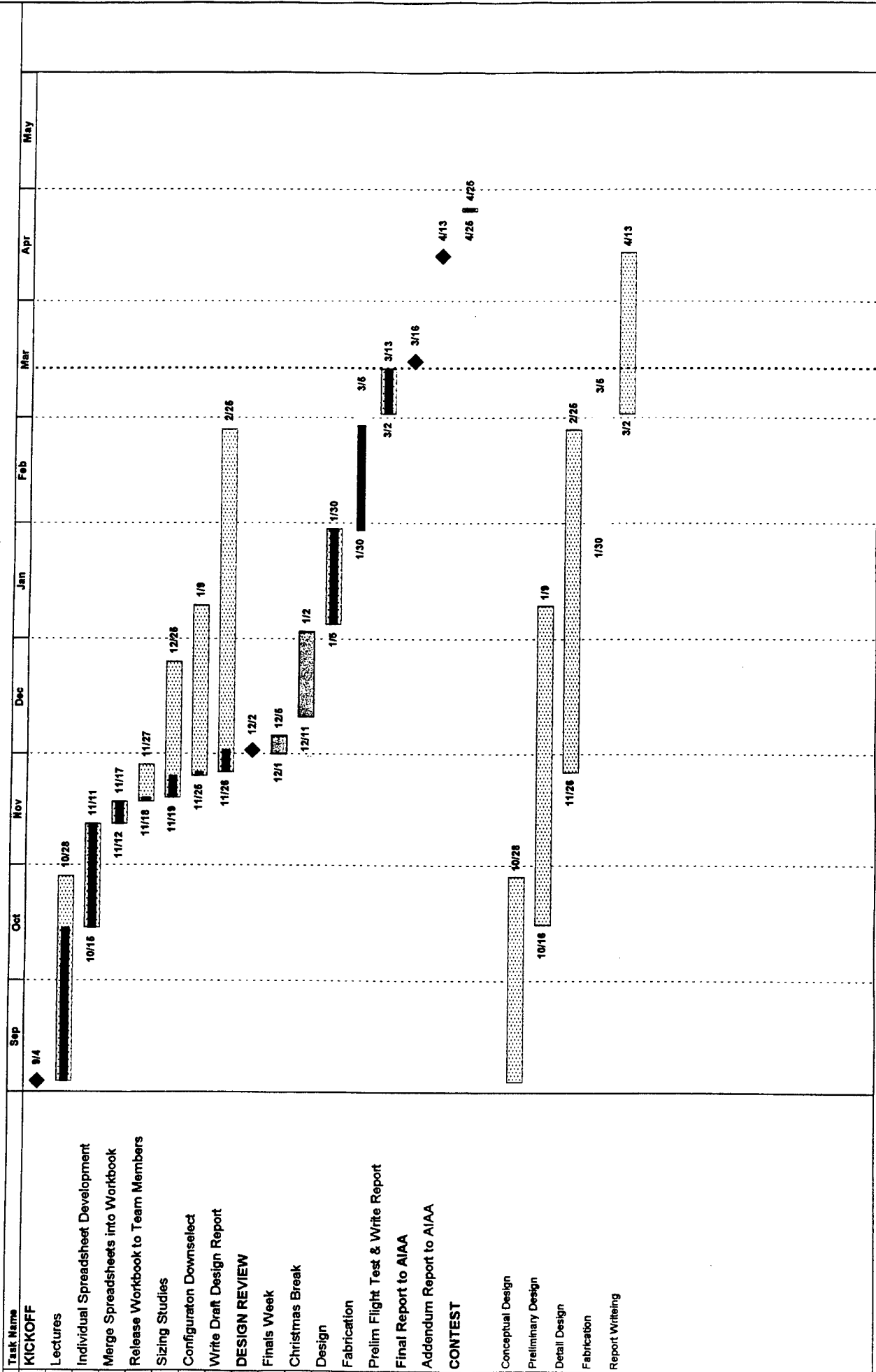


Figure 2.1 Team Organizational Chart

# USC AIAA Student Design/Build/Fly Competition

## MASTER SCHEDULE



## 2.3 Management structures

Setting group goals and a loose timeline, determined by the project managers, achieved a schedule control that met AIAA deadlines. Specific items and details of the configuration were addressed weekly as problems and new ideas arose. Most of the important decisions involving the plane were done as a group at weekly meetings. The milestone chart developed by the group is shown in Figure 2.2. Selection of the final airplane from the spreadsheets took longer than expected and held up all progress for several weeks.

## 3. CONCEPTUAL DESIGN

### 3.1 Design Parameters

The goal decided upon by the team was to design a plane with the shortest lap time possible. To achieve this goal, the highest straightaway and minimum turn radius (contributing to a decreased total lap distance) were obtained.

### 3.2 Figures of Merit

It was decided that the six most important variables for this mission were: turn rate, roll rate, weight, Lift-to-drag ratio (proportional to energy efficiency), simplicity of the plane, and flying characteristics. Turn rate determined how sharp the turn was, and is dependent on the load factor and  $C_L$  capability. Roll rate is important for entering and exiting the turns quickly and to reduce turn distance. Weight and L/D are important because of affects on the energy consumption rate. Maximizing the L/D ratio and thereby minimizing the drag maximizes the speed of the aircraft as desired.

Time constraints and mission requirements determined that simplicity allowed for the easiest design and manufacturing. If major problems were discovered during testing, there was time to make modifications on the design. Human error is to be a factor in the flying of this airplane, so an aircraft that is easier to handle will put less stress and possible problems in the hands of the pilot, reducing the risk of a mistake during competition. Also, because of the decision to pull up to near stall velocity twice during each lap, stall and recovery characteristics are very important.

#### 3.2.1 FOM Rankings

Agreeing that the turn is the most important part of the mission, the load factor capability (or turn rate)

was the feature most important for the plane. L/D was second because the batteries needed to last the whole seven minutes of the race. Next, due to a tight schedule, simplicity was ranked third, which gave the simpler designs an advantage. Roll rate ranked fourth because it has a smaller overall effect on the turn than the first three categories. Flying characteristics was set fifth since it mostly depends on the pilot. Weight was categorized as least important because an accurate depiction of weight could not be determined at this early stage of development.

### 3.3 Analytic Methods Used

The method of gathering ideas for the design of the aircraft was to put every idea on the board. From this pool, each was evaluated and ranked. Evaluations were based on our figures of merits using judgment calls and observation by inspection, and the pool was reduced to six planes

### 3.4 Initial Concepts

Plane A is a biplane; B resembles the Lockheed P-38 with three fuselages and the propulsion unit in the middle; C is a variation on B with an optional middle fuselage and two smaller propulsion units on the outside fuselages; D is a flying wing; E is a traditional, single wing with one motor, airplane; F is a variation of E, but its landing gear is wheels on the wing tips, with a downward bend in the wings for propeller clearance. Refer to Figures 3.1 through 3.6

### 3.5 Rankings

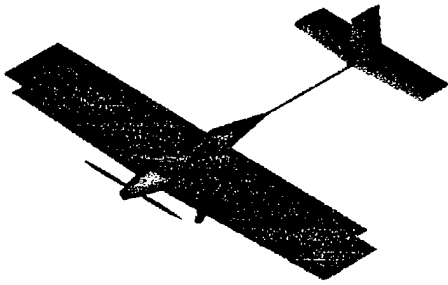
Each plane was ranked for all categories and one was selected. The plane with the lowest totals, plane E, our initial and simplest idea, was focused upon for the rest of the meetings.

#### 3.5.1 Turn Rate

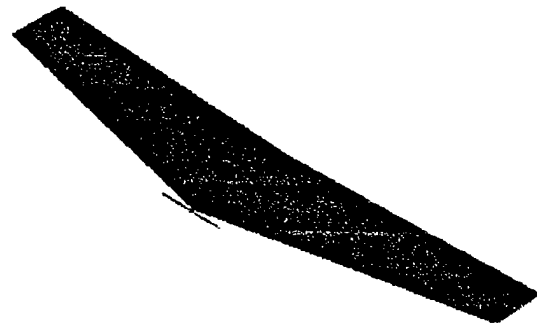
Turning rate, or load factor and  $C_L$  capability, will determine how tight the turn will be. All planes except D were able to perform sharp turns; they made use of flaps and similar airfoils. Plane D ranks last because of its short tail arm, while the rest had equal scores in this category.

#### 3.5.2 L/D (Energy Efficiency)

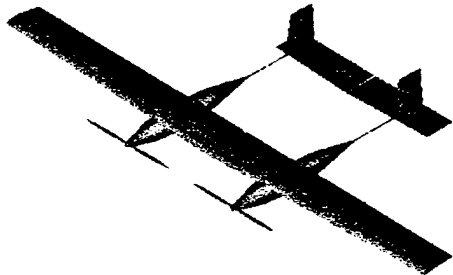
Aspect ratio ( $\text{Span}^2/\text{Wetted area}$ ) was compared on all the airplanes. Plane A had the smallest wingspan and a large wetted area, and ranked last in the category. Planes B and C were ranked 5<sup>th</sup> and 4<sup>th</sup> respectively.



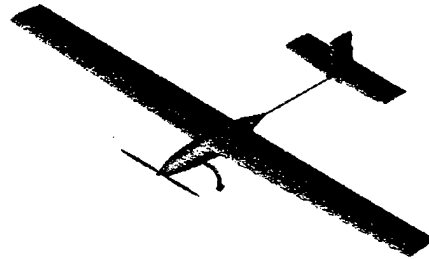
*Figure 3.1 Proposed Biplane Configuration*



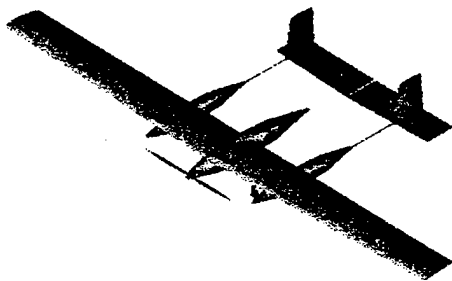
*Figure 3.4 Proposed Blended Wing Configuration*



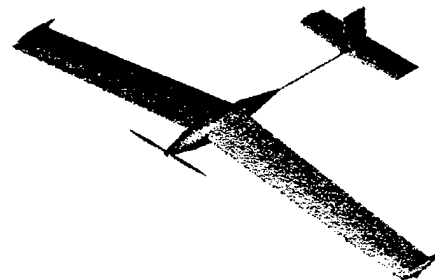
*Figure 3.2 Proposed Double Fuselage Configuration*



*Figure 3.5 Proposed Traditional Airplane Configuration*



*Figure 3.3 Proposed Triple Fuselage Configuration*



*Figure 3.6 Proposed Anhedral Wing Configuration*



Though they possessed a larger span than A, they also had a larger wetted area than the other planes because of the three fuselages. Plane C ranked better than B because the third middle fuse is optional, reducing the wetted area. Plane D ranked first because it had a large span and a very low wetted area. Planes E and F scored about the same, but since F uses the wing tips as landing gear, the wetted area is a little bit smaller than E.

### 3.5.3 Simplicity

Simplicity was scored by summing up the total number of sub-assemblies required to build for the plane. A had the most parts of the six: fuselage, propulsion unit, two wings, two ailerons, wing struts, vertical tail, rudder, h-tail, elevator, and a main gear, for a total of 12 sub-units. This tied for a rank of 4th. B and C were the most complicated of the six because of integration of three fuselages would prove to be a difficult task, and they consisted of 13 and 12 sub assemblies respectively. D is rather simple, and consisted of a wing, 2 elevons, 1 rudder, 1 propulsion unit, nose gear and a main gear totaling seven and ranking it first. E and F were the next two simplest planes with E having 10 and F having 11 sub assemblies. It was decided that the wing structure for plane F would require a complicated joining system, and so would attaching the wheels to the wing-tips.

### 3.5.4 Roll Rate

Roll rate is important for entering and exiting the turn quickly and it reduced the turn distance. Plane A's shorter wing span allows for an excellent roll rate, which is inversely proportional to wing span, and ranked first amongst the other designs. The other planes are all quite similar with B and C being slower due to mass further away from the center of roll for the plane. Planes E and F will be similar, but slower still, and D is the slowest of them all because of the lack of a tail.

### 3.5.5 Flying Characteristics

Handling qualities are a very important part of the mission since the plane will pull up to near stall twice each lap. Plane A has excellent stall characteristics and ranks first because it recovers nicely due to the high lift. B, C, E, and F all will handle quite well, as the tail will help with pitch damping. Proper center of gravity (c.g.) location also gave each equal static stability. Only plane D did not perform well in this category. The lack of a tail reduces pitch damping, and, being a flying wing, has less predictable stall characteristics.

### 3.5.6 Weight

Weight was difficult to estimate. Because D has the most volume, it was considered to be the heaviest of the group. Following was C because of the two propulsion units, and then came A because of all the bracing required for a bi-plane. B was 3<sup>rd</sup> because of the extra fuselages, and E was second after F because of its extra weight from the landing gear.

## 3.6 Overall Rating

The rankings concluded that plane E would be the base design. F followed in second, while third and fourth place went to planes A and B. Planes D and C tied for last in the overall category. In following meetings, improvements and small design changes were done to create our current design. The chart below shows each plane and their ratings.

<u>FOM's</u>	<u>A</u>	<u>B</u>	<u>C</u>	<u>D</u>	<u>E</u>	<u>F</u>
<i>Turn Rate</i>	1	4	5	6	2	3
<i>L/D</i>	6	5	4	1	3	2
<i>Simplicity</i>	5	6	4	1	3	2
<i>Roll Rate</i>	1	4	5	6	2	3
<i>Flying</i>	2	3	4	6	1	5
<i>Characteristics</i>						
<i>Weight</i>	4	3	5	6	2	1
<i>Sum total</i>	<b>19</b>	<b>25</b>	<b>27</b>	<b>26</b>	<b>12</b>	<b>17</b>
<i>Overall</i>	<b>3rd</b>	<b>5th</b>	<b>6th</b>	<b>4th</b>	<b>1st</b>	<b>2nd</b>
<u>Ratings</u>						

## 4. PRELIMINARY DESIGN

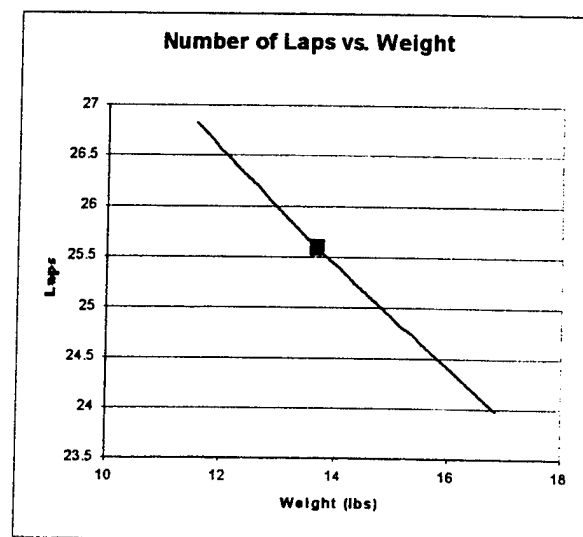


Figure 4.1 Laps vs. Weight

Weights Inputs		Total Weight lbs.	13.77 lbs.	
				% of plane
	Cargo	7.50		54.48%
Propulsion fudgeF	Motor from propulsion Battery weight	0.6375	Propulsion TOT	3.435
1	Wiring	2.50		24.95%
	Speed control	0.10		
	Prop	0.14		
		0.06		
Wing fudgeF	core density lb/ft^3	2.25	Wing TOT	1.069
	core volume ft^3	0.20067774	Weight w/o spar	7.77%
1.1	Area DesignC in^2	763.20		5.37%
	calculated spar wt.	0.299591311		
Tail fudgeF	core density lb/ft^3	2.25	Tail TOT	0.063
	core volume ft^3 design	0.010390		0.39%
1.1	AreaH DesignC in^2	86.40		
	AreaV DesignC in^2	86.40		
Radio fudgeF	receiver	0.125	Radio TOT	0.813
	servos	0.5		5.91%
1	battery?	0.188		
LandingGear fudgeF	gear	0.386497065	LandingGearTOT	0.464
	3% of total plane			3.37%
1.2				
Fuselage fudgeF	wetted area DESIGNC	147.5781634	Fuse TOT	0.342
	thickness in	0.02		2.49%
2	density lb/in^3	0.058		

## 4.1 Weights

In design of an aircraft, one of the most important factors is the total weight and its minimization because of the limited energy budget and needing to maximize range in a short time. Many of the plane's components were known to have a specific weight, including the radio, batteries, and steel. These known values of the hardware and materials were entered into the Weights portion of the spreadsheet. Excel was then used to test slightly different configurations in order to create the best possible airplane and come to a quick total weight calculation. Figure 4.1 shows the effect of weight on total laps. The result is that a 3.6 % increase in weight decreases the number of laps by 1%. Inputs for this spreadsheet came from geometry calculated by DesignC and other major design criteria such as the airfoil and the type of motor selected. Weights computed by this sheet included the foam core of the airfoils for the tail and wing, different motor weights, and wing spar weight calculation.

After this sheet was completed it was found that results were not as expected. Wing spar weight was not nearly as high as expected, and given different airfoils, the calculated spar weight did not change much. Figure 4.2 shows the effect of aspect ratio on the weight of the wing spar for four different airfoils considered. Another consideration was a change in performance of the plane due to a weight of plane slightly different than that calculated. Doing this gave an idea of how the plane would perform if the actual weight of the competition aircraft was not the same as the one calculated. A breakdown of components by weight and percentage of total weight is supplied in Table 4.1.

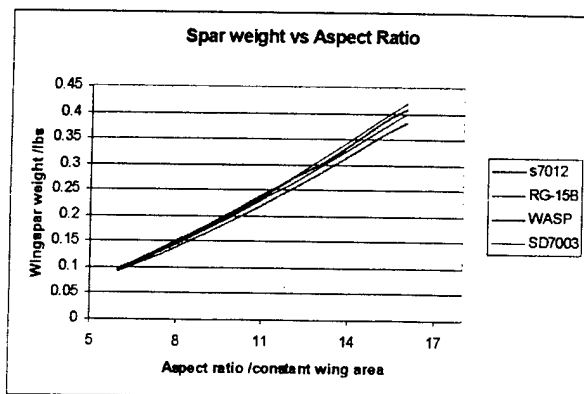


Figure 4.2 Spar Weight For Given Aspect Ratio

Component	Weight in Pounds
<b>Fuselage</b>	<b>0.342</b>
<b>Wing</b>	<b>1.269</b>
Wing foam	0.740
Wing spar	0.329
Wing servos	0.2
<b>Tail</b>	<b>0.4405</b>
Tail Foam	0.53
Tail Boom	0.1875
Tail servos	0.1
<b>Propulsion</b>	<b>1.3425</b>
Motor	0.6375
Wiring	0.2
Propeller	0.06
Receiver	0.125
Battery for Receiver	0.188
Speed Control	0.14
<b>Landing Gear</b>	<b>0.375</b>
<b>Empty Weight</b>	<b>3.769</b>
Payload	7.5
Batteries	2.5
<b>Total Weight</b>	<b>13.769 lbs.</b>

Table 4.1 Weight Breakdown by Component

## 4.2 Propulsion

### 4.2.1 Propulsion Design Parameters

The design parameters investigated in the propulsion area of the project were the following: propellers, motors, gearboxes, and batteries. The propeller to be used was an important parameter to be matched to the performance required of the propulsion system. The chosen propeller's Design Advance Ratio should most closely match the actual Advance Ratio achieved in order to provide the most propeller efficiency. The choice of motor is critical for the most torque and power to deliver to the propeller to provide the thrust. Gearboxes were also considered in case the optimum performance characteristics of the propellers and motors operated at different revolutions per minute (r.p.m.). The battery choice needed to be cells that provided the most electrical energy in 2.5 lbs. of cells.

### 4.2.2 Propulsion variables

The propeller data used to provide the characteristics of each type of propeller configuration was provided in Excel format by Mark A. Page. The specifications for the four motors considered in the final design were provided on the Aveox World Wide Web page. The ratios for the eight gearboxes considered were provided by the Astroflight and Aveox World

Wide Web pages. The statistics for the seven batteries under consideration were provided by ElectricCalc, a commercially available electric propulsion model airplane program purchased from Aveox. All of the statistics were entered into worksheets that were to be referenced by the Propulsion and Mission Performance spreadsheets.

#### 4.2.3 Propulsion spreadsheet

An Excel spreadsheet was created that matched the propeller and the electric propulsion system. It was divided into two halves, one for the propeller inputs and outputs, and the other for the motors, batteries, and gearboxes. The propeller side contained the variable inputs: Design Advance Ratio, number of propeller blades, diameter of the propeller, operating velocity, and the required thrust. The outputs were the torque, rpm and power required, along with propeller efficiency, thrust coefficient, and power coefficient. These outputs were connected to the second half of the spreadsheet by matching the torque and rpm provided by the propeller side to the torque and rpm that the motor-gearbox-battery system needed to provide. With these inputs and constants provided by the specifications of certain batteries, motors, and gearboxes, the following quantities could be determined: voltage, current, battery life, power output, and throttle setting.

#### 4.2.4 Findings of Propulsion spreadsheet

The selected battery pack consisted of 26 KR-1700AE cells. It was discovered that batteries with a higher capacity had a higher internal resistance, and provided less total energy than cells with less capacity and less internal resistance. The increased weight of the higher capacity cells was a driving factor in selecting the lower capacity, lower internal resistance, KR-1700AE batteries.

The maximum current of the system,  $I=40A$ , was not a limit approached by any of the design configurations. The maximum voltage, however, was one of the drivers in selecting  $J$ , the design advance ratio, and the propeller diameter. As  $J$  or propeller diameter decreases, the voltage required to produce the necessary thrust increased.

The advance ratio of 0.833 was chosen because any advance ratio smaller than that would have required a voltage greater 32.5 volts, which is the maximum voltage available with 26 cells. Figure 4.4 shows the effect of Design Advance Ratio on the total number of laps. Of the four advance ratios researched, the optimum was the greatest value without exceeding maximum voltage. Figure 4.5 shows the relationship between total laps and propeller diameter. The propeller diameter of 0.68 ft, or approximately 8 inches, was chosen because it was found to be the peak of the laps vs. propeller diameter curve, and required the

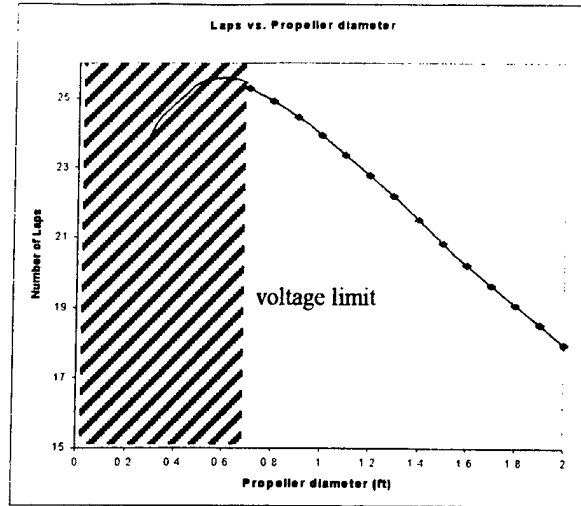


Figure 4.3 Laps vs. Propeller Diameter

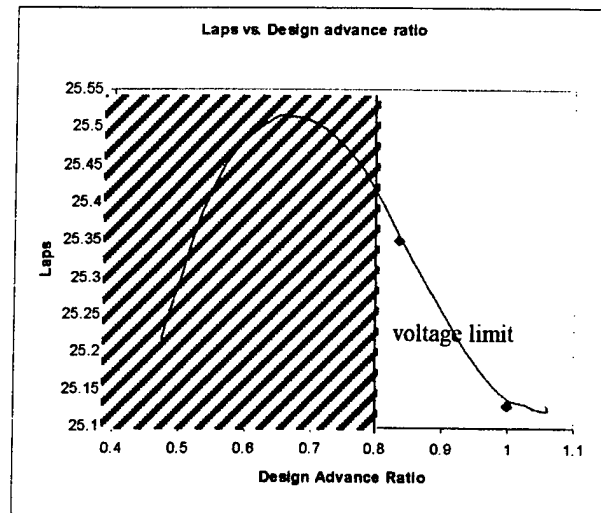


Figure 4.4 Laps vs. Advance Ratio

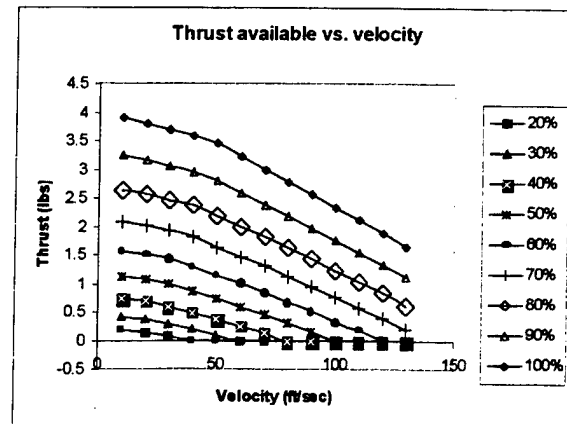


Figure 4.5 Available thrust vs. velocity

# Propulsion Spreadsheet

## Inputs

Velocity (ft/sec)	120.1355168
Air density (slugs/ft^3)	0.0023769
Thrust at cruise, lbs	1.991669761
Blade Count	2
Design J	0.833
Input - Actual J	0.661929248
Dprop (ft)	0.682

## Inputs

Motor Number	2
Battery Choice	6
Gearbox choice	1
Gear ratio (# : 1)	1

Actual J (V/nD) = 0.661027  
Delta J (input-output)= 0.000903

## Outputs

RPM - cruise	15,989
Power (hp)	0.534
Torque (ft-lb)	0.175
Ct -actual	0.0545
Cp	0.0440
Prop efficiency	0.814473468

## Outputs

Motor Shaft Power (hp)	0.534133
Motor Torque Req'd (ft-lb)	0.175454
motor RPM	15,989
I @ max pwr (amps)	47.86
I @max eff. (amps)	6.90
Input Power (hp)	0.657
Efficiency	0.814
Batt. Pack Life (min)	7.36
K1- motor torque constant (ft-lb/amp)	0.012036
K2- motor RPM constant(RPM/Volt)	585
I (amps)	15.08
Io (amps)	0.500
Battery voltage (volts)	32.500
Ro = armature resistance (ohms)	0.341
Throttle fraction	1.00
Voltage (volts)	32.47

Required Voltage 32.47

Selected Motor 1412/5Y  
Selected Gearbox no gearbox  
Selected Battery KR-1700AE

# Motor, Gearbox, and Battery Worksheet

## Motors

Motor Samples (All are AVEOX motors)

Motor Designation for MAIN worksheet	1	2	3	4
Motor model	1412/4Y	1412/5Y	1415/2Y	1415/3Y
Speed constant (RPM/volt)	725	585	1190	795
Torque constant(in-oz/amp)	1.865	2.311	1.136	1.699
Motor resistance (ohms)	0.065	0.105	0.02	0.05
No load Amps	0.7	0.5	1.8	1.2
Continuous current	22	17	50	40
Motor Weight	0.6375	0.6375	0.7625	0.7625
Length	0.196666	0.196666	0.2216666	0.2216666
Diameter	0.1225	0.1225	0.1225	0.1225

## Gearboxes

Gearbox #	1	2	3	4	5	6	7	8
Manufacturer		astro flight	astro flight	astro flight	astro flight	astro flight	astro flight	aveox
Description	no gearbox	model 710	model 711	model 712	model 713	model 714	model 714	
Ratio (# to 1)	1	3.27	4.36	3.69	3.1	3	2.7	3.7

## Batteries

Battery # 6      Model Name KR-1700AE      Tot. Energy (ft-lb) 159644.9

Number for worksheet	1	2	3	4	5	6	7
Model Name	N-1700SCRC	KR-1000AEL	KR-1100AEL	KR-1200AE	KR-1400AE	KR-1700AE	RC-2000
Milliamp-hours	1950	1100	1200	1300	1450	1850	2000
Milliohms per cell	5.5	9.5	10.5	9.1	11.5	8.5	7
Milliamp-hours per ounce	1005	1155	1215	1228	1326	1249	1012
Weight	1.94	0.95	0.99	1.06	1.09	1.48	1.975
Number allowed	20	42	40	37	35	26	20
Total Batt. mOhms	110	399	420	336.7	402.5	221	140
Milliohms speed control, etc.	15	15	15	15	15	15	15
power supply resistance	125	414	435	351.7	417.5	236	155
amp-minutes	2340	2772	2880	2886	3045	2886	2400
total energy (ft-lb)	129441.78	153338.724	159312.96	159644.862	168440.265	159644.862	132760.8

maximum voltage, or full throttle. It was discovered through the design process that having a gearbox, while reducing propeller rpm and increasing propeller diameter and efficiency, provided neither more nor less laps than gearing the propeller directly to the motor. This was due to the assumed 3% transmission loss due to the gearbox and the gearbox's weight. It was decided that if there were no gain by having a gearbox, there would be an advantage to having no gearbox and a smaller propeller diameter. Figure 4.5 shows the thrust available from the propeller at various velocities at throttle settings from 20% of maximum to 100% of maximum.

### 4.3 Aerodynamics

Aerodynamic characteristics, key to every aircraft, are based on its wing(s), tail, and fuselage dimensions as well as their shapes. The aerodynamics worksheet analyzed various airfoils and determined the aerodynamic characteristics necessary to predict performance when combined with the other worksheets.

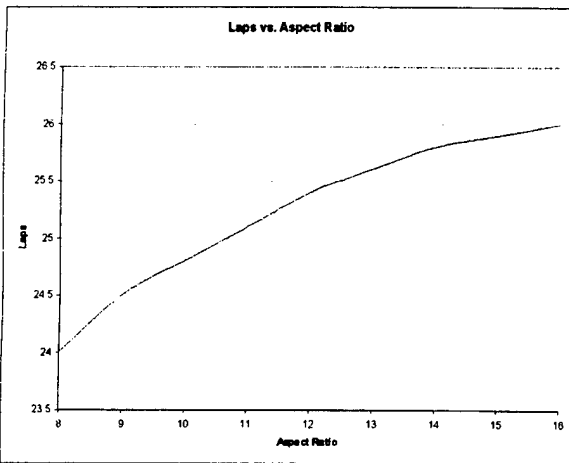


Figure 4.5 Laps vs. Aspect Ratio

In this case the task was to create an aircraft which flies at a maximum possible velocity provided the highest bank angle possible for the highest velocity in the turns.

#### 4.3.1 Wing

In designing the wing, it was decided that a low drag/moderate lift airfoil would perform the best for the contest requirements. A low-drag airfoil allowed the airplane to fly through the straight-aways with as much velocity as possible, and a high lift airfoil allowed high bank angles in the turns, reducing the turn radius around the pylons and the time to go around. A trade-off between having a high lift and low drag airfoil was made, even though a high camber airfoil gave the highest lift. However, the higher camber produced the most drag, while a thin low camber airfoil produced the

least lift, but also the least drag. The decision was made to have a thin low camber airfoil, to take advantage of its low drag and to add a flap to it to increase its lift characteristics in the turns.

In choosing an airfoil, designs were taken from Dr. Michael Selig's "Summary of Low-Speed Airfoil Data - Volume One". From this resource, airfoils were chosen based on their moderate lift characteristics. These airfoils were then analyzed using Dr. Martin Hepperle's World Wide Web page (<http://beadec1.ea.bs.dlr.de>), which has an airfoil analysis program. This data was then entered into a spreadsheet designed by the team to analyze the plane. The spreadsheet calculated the lift, induced drag coefficients, total drag of the wing, total drag of the airplane, and the total lift to drag ratio of the airplane. These calculations were made using the assumption that flow over the plane was incompressible. Initial data used for the calculations were the two-dimensional drag and lift coefficients of the airfoils.

The final seven airfoil designs analyzed were the RG15, SD7037, WASP, E387A, K3311, S7012, and the E374. These seven were then analyzed, again using Dr. Hepperle's web page, adding flaps of various sizes (in percent of the airfoil chords), at various deflection angles. This was done in order to determine how adding a flap would affect the lift and drag characteristics of the airfoils. The S7012 had the second highest lift coefficient (1.5 vs. 1.6 - the E387A), the lowest drag coefficient at straight and level flight (.008 vs. .0082 for the next best - the RG15B), and the highest L/D of all the airfoils tested (21.4 vs. 20.6 for the E374B, at the turns). The final aircraft has both ailerons and inboard flaps.

In determining the wing dimensions, many factors were taken into account. First, though it would

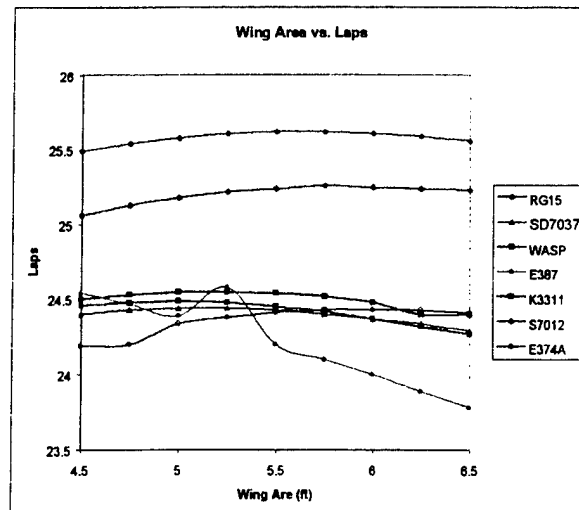


Figure 4.6 Laps vs. Wing Area

## Aerodynamics Spreadsheet

CL	Cdo-wing	Cdi	CD-wing	CD-total	L/D-wing
0.1	0.008	0.000265144	0.008265144	0.01420854	12.09900245
0.2	0.008	0.001060577	0.009060577	0.015003973	22.07364981
0.3	0.008	0.002386298	0.010386298	0.016329694	28.88420918
0.4	0.0082	0.004242307	0.012442307	0.018385704	32.14837812
0.5	0.0088	0.006628605	0.015428605	0.021372001	32.40733653
0.6	0.0095	0.009545191	0.019045191	0.024988588	31.50401516
0.7	0.0115	0.012992066	0.024492066	0.030435462	28.58068389
0.8	0.012	0.016969229	0.028969229	0.034912625	27.61550863
0.9	0.012	0.021476681	0.033476681	0.039420077	26.88438578
1.1	0.0125	0.032082449	0.044582449	0.050525845	24.67338659
1.2	0.013	0.038180766	0.051180766	0.057124162	23.44630804
1.3	0.0135	0.044809371	0.058309371	0.064252767	22.29487266
1.4	0.014	0.051968265	0.065968265	0.071911661	21.22232576
1.5	0.0145	0.059657447	0.074157447	0.080100843	20.22723368
1.6	1	0.067876917	1.067876917	1.073820313	1.498300014
1.7	1	0.076626676	1.076626676	1.082570072	1.579006018
1.8	1	0.085906723	1.085906723	1.091850119	1.657600936
1.9	1	0.095717059	1.095717059	1.101660455	1.734024295
2	1	0.106057683	1.106057683	1.112001079	1.808223957
CL-max 2D	1.5				
	1	2	3	4	5
	RG-15B @300k	SD7037B @300k	WASP @300k	E387A @300k	SD7003 @300k
CL-max 2D	1.1	1.3	1.2	1.1	1.1
t/c =	0.0892	0.092	0.0935	0.0906	0.0851
0.1	0.008	0.011	0.011	0.018	0.0078
0.2	0.0082	0.0105	0.0088	0.0098	0.007
0.3	0.0078	0.0078	0.0083	0.0085	0.008
0.4	0.0079	0.008	0.0081	0.009	0.0085
0.5	0.0082	0.0082	0.0092	0.0095	0.0085
0.6	0.0094	0.009	0.01	0.011	0.0092
0.7	0.011	0.0098	0.011	0.015	0.01
0.8	0.0123	0.0118	0.012	0.015	0.0115
0.9	0.016	0.013	0.0138	0.018	0.0118
1.1	0.022	0.0158	0.015	0.021	0.0123
1.2	0.04	0.0182	0.0175	0.021	0.013
					0.016
				K3311 @300k	S7012 @300k w/f
				1.1	1.1
				1.5	1.5
					0.0875
					0.008
					0.008
					0.008
					0.0082
					0.0088
					0.0095
					0.0095
					0.01
					0.0115
					0.012
					0.014
					0.018
					0.022
					0.032



be ideal for wing to have an infinitely high aspect ratio (AR) and longest span possible, limits are imposed by the structural abilities of available materials. Another factor taken into consideration was shipping. The maximum length allowed by commercial parcel companies is nine feet, so not exceeding that allows for safer, simpler travel of the wing. A third consideration was that it was better to have a low span aircraft for the straight-away segments of the course.

The team imposed an AR of 16, fearing structural instabilities such as flutter and wing bending past it, and the original design had a wing with an aspect ratio of 16, a wingspan of 10.2 feet, and a chord length of 9.1 inches. After some adjustments in the design spreadsheet, it was found that the aspect ratio could be lowered to 13 and the wing span could be trimmed down to 8.3 feet with a chord length of 8.8 inches. The original configuration allowed the plane to perform an estimated 26.1 laps in the seven-minute time limit. The final configuration gave an estimated performance of 25.3 laps. Figure 4.5 shows the effect of aspect ratio on the number of laps. There is no obvious optimum for the aspect ratio. The shorter wing span was favorable because it fit under the 9 feet maximum length limit for packages set by commercial parcel services. This allowed for a single piece wing as opposed to the 2-piece wing required for the 10.2 foot span, which is favorable because it does not require a joiner setup to connect 2 pieces together.

A joiner would add unwanted weight, canceling the effects of reduced aspect ratio. The lowered aspect ratio was a result of the shorter span length, but even in doing so from the original 16 to 13, the chord length of the wing was essentially maintained. It was necessary to retain a sizable chord length for the structural stability. A longer chord length produces a thicker wing, and thickness adds stiffness.

Figure 4.6 shows the effect of wing area on the number of laps for seven different airfoils. All the airfoils have flat optima, and the S7012 airfoil yields the most laps. Figure 4.7 shows the drag versus velocity curve for the S7012 airfoil at different total airplane weights. Figure 4.8 shows the chosen airfoil shape.

The final part of designing the wing was to configure it. Elliptical wing loading was most preferable but nearly impossible to manufacture. To make the wing loading near elliptical, it was necessary to taper the wing. The tapers were designed to allow the wing to stall near center span as opposed to the tips. Center stall precludes roll-off and ensures downward pitch. If the tips stalled, the task of rebalancing and regaining control of the plane would be entirely up to the pilot, a task that would be extremely difficult at the low altitude and high speeds in which the plane will be flown. It was decided that the wing would have four taper breaks, two on each side of the wing, which allowed three

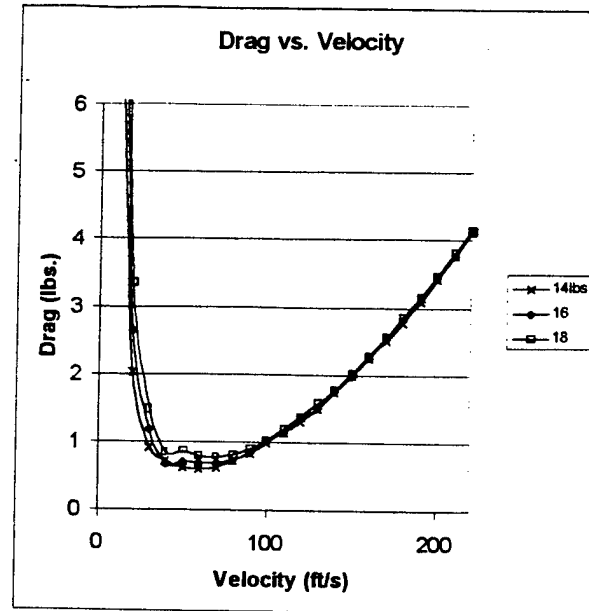


Figure 4.7 Drag vs. velocity

panels on each side. The breaks were at 40% and 65% of each side of the wing, measured from the center. The first panel was not tapered while the second panel was tapered from 100% to 85% of the root chord. The wing tip was tapered from 85% to 50% of the root chord. This three-panel configuration on each side allowed for the most favorable wing lift distribution.



Figure 4.8 S7012 Airfoil

#### 4.3.2 Tail

In designing the tail, a symmetric airfoil was chosen because it does not produce lift at zero angle of attack but would produce the necessary upward or downward lift for control with the proper flap deflection. Thus, the symmetric airfoil chosen for the tail was the SD8020, as shown in Figure 4.9. A V-tail configuration was chosen over the more conventional low horizontal – flapped and full flying tail – with a



Figure 4.9 SD8020 Airfoil

vertical stabilizer and a T-tail configuration because it was simpler than the other configurations. It had two identical sections bonded at a set angle, and in has two surfaces. This is different the other configurations

which had three effective surfaces. Also taken into consideration was that a V-tail had the clearance required for ground rolls that the plane would experience due to the single wheel landing gear configuration. A low horizontal would scrape the ground, while a T-tail would clear it but would be difficult and more complicated to implement.

#### 4.3.3 Fuselage

The fuselage of the aircraft needed to have certain minimum dimensions in order to hold the necessary payload (7.5 lbs. of weight, 2.5 lbs. of batteries, radio receiver equipment and all necessary padding). It was desirable to make the smallest fuselage possible to reduce the drag that it produces, which turned out to be 20% of the overall drag. The box dimensions of the fuselage were 4.25" x 7.00" x 5.25" and were used to design the main cargo sections. The rest of the fuselage was tapered from these dimensions to a 1-inch diameter circle for the tail to be placed into, as well as tapered forward to accommodate the motor.

#### 4.3.4 Stability and Control

The objectives were to give the pilot a predictable airplane, i.e. high stability and good pitch damping. The static margin was chosen to be 20% $\bar{mac}$ , while the tail arm was chosen to be one third the wingspan, which is derived from competition sailplane practice. It was decided that 33.2 inches was a good length for the arm because it was relatively short and allowed for a tail that did not require too much structural rigidity. The final tail volume was 0.85 square feet, which translated to a tail span of 27 inches.

The control of the aircraft was thought to be a problem due to the V-tail configuration of the tail, but it was decided that the problem could be resolved by using the mixing capabilities of commercial radio transmitters used for operating model planes, and doing so on the elevator and rudder functions. The flaps of the wings would be the slave control of the elevator function and would also be dependent on the ailerons. Deployed for takeoff, the flaps would follow the ailerons in the turns.

#### 4.4 Mission Performance

The mission performance portion of the spreadsheet was designed to utilize all the other pages of the spreadsheet (Weights, airfoil data, etc.) to combine all performance and design aspects into a single airplane. In doing so, various models of aircraft type and their results could be determined and compared.

The different models of aircraft were changed by the input variables. Primary inputs consist of the airfoil

data, aspect ratio, wing area, motor, battery and gearbox type. Secondary inputs are the percentage of maximum lift coefficient in the turns, diameter of the propeller, design of the J propeller and fuselage area. Final inputs include the areas of the wheels, struts, tails and the density of the air ( $\rho_{Wichita} = 0.0023769$  slugs/ft<sup>3</sup>).

Once all the data inputs have been selected, the spreadsheet is ready to solve for its output variables. The airfoil chosen is run through an iteration process to determine the coefficient of lift in the straightaway and another in the turns. At the same time, the weights page uses all the airplane sizing (wing area, fuselage area, etc.) and powerplants (batteries, motor and gearbox type) to determine the weight of the plane, while the DesignC page uses only the sizing values to picture what the plane will look like. The spreadsheet is designed as a program to run all variables and calculate all outputs based on the input data and their linked equations.

The outputs of the configuration page are positioned into 3 categories: vehicle, propulsion and mission performance. Vehicle performance gives the weight of the plane, all coefficients of lift needed (2-D  $C_{Lmax}$ , 3-D  $C_{Lmax}$ , in the turn and in the straightaway), the lift-to-drag ratios in the straightaway and in the turn and the number of g's in the turn. Propulsion performance involves the solution for thrust, propeller and motor rotations per minute, the horsepower of the motor selected, the voltage of the battery (and current running across it), and the percentage of throttle being used. The percentage of throttle is desired to be at, but no greater than 100%. Inputs are adjusted in an attempt to reach this level for a maximum number of laps. This number of laps is produced in the mission performance section. Also shown are the distance and work per lap, propeller efficiency, total energy of the battery, the take-off field length and the airspeed velocity (ft/s). The most valuable number, again, is the number of laps. The critical elements in determining the maximum number of laps are the combination of the battery, motor and gearbox, along with selecting an airfoil and adjusting its area and aspect ratio. The propeller efficiency is 81.2% and the efficiency of the motor-gearbox-battery system is 81.9%. The total number of complete laps predicted is 25. The average airspeed for the entire mission is 120 feet per second.

## 5. DETAIL DESIGN

### 5.1 Performance Predictions

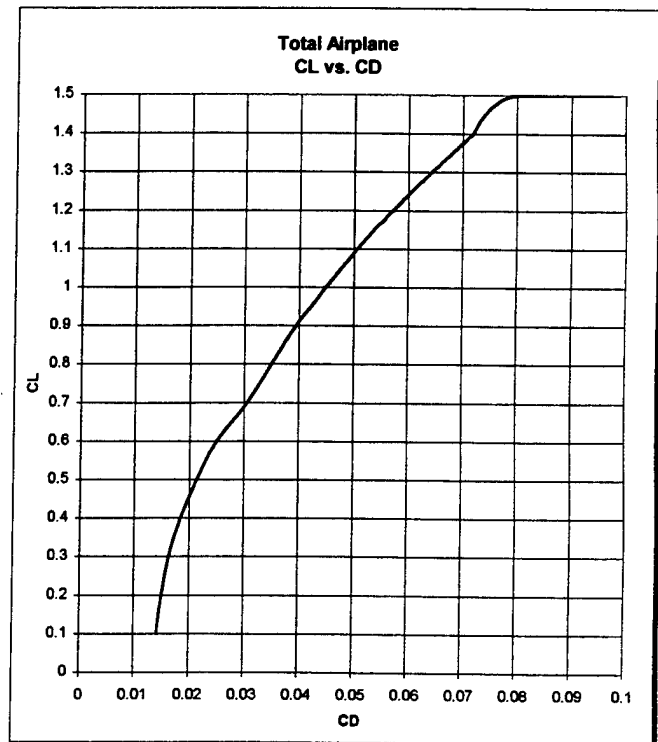
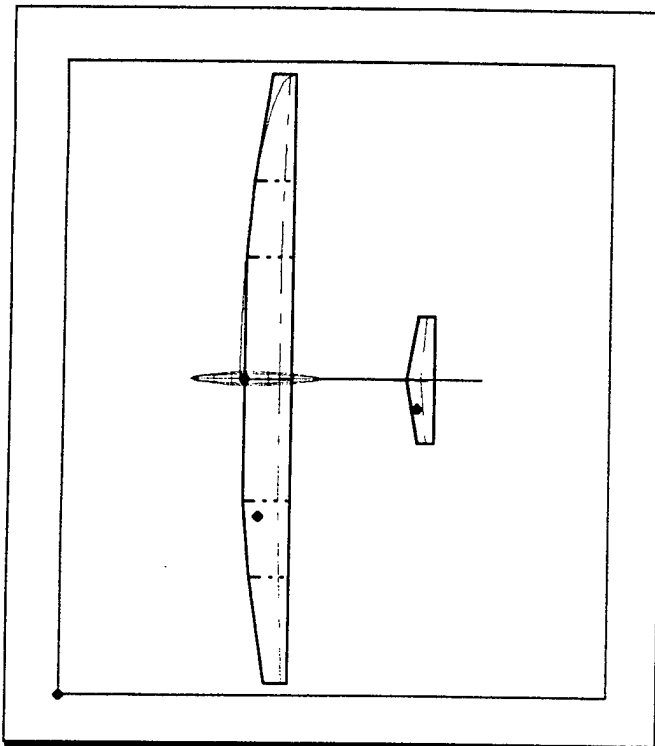
The overall performance guidelines included an airspeed of 120.1 feet per second, a range of 25.3 laps, a weight of 13.77 pounds and a force of 7.56 g's in the turns.

## USC AIAA97 Contest Design Spreadsheet

Enter inputs (red), then Cntrl-b for converged solution

DESIGNER INPUTS							
Airfoil # (#1-8) 7 <small>57012 @300k w/ flap</small>	%CL max(turns) % 85.00%	Sw ft2 5.3	ARw n.d. 13	Sh ft2 0.60	Sv ft2 0.60 <small>not yet DesignC</small>	Swet fuselage ft2 2.00	Wingspan ft 8.300602388
Swheels+frngs frontal ft2 (all) 0.05	Sstruts frontal ft2 (all) 0.01	Dprop ft 0.682	Design Jprop 333, .5, .666, .833, 1.000 0.833	Motor type (#1-4) 2 14125Y	Battery type (#1-7) 6 KR-1700AE	Gearbox type (#1-8) 1 1	Rho(S.L.) slugs/ft3 0.0023769

Vehicle Performance							
Weight lbs 13.68	CL max -2D n.d. 1.5	CL max -3D n.d. 1.35	CL straight n.d. 0.150	CL turn n.d. 1.15	L/D straight n.d. 10.30	L/D turn n.d. 21.38	n turn g's 7.63
Propulsion Performance							
Thrust=avgDrg lbs 1.99	Actual J n.d. 0.661	Prop RPM revs/min 15,969	Motor RPM revs/min 15,969	Motor Hp shp 0.53	% Throttle %batt voltage 99.9% <small>(must be &lt;100%)</small>	Voltage V Volts 32.47	Current I Amps 15.08 88.69%
Mission Performance							
Distance/Lap ft 1,993	Work/Lap ft-lbs 3,969	Total E-Battery ft-lbs 159,645	Prop Efficiency % 81.4%	Mtr+Batt+Gbx $\eta$ % 81.4%	Total Laps n.d. 25.32	TOFL ft TBD	Airspeed V fps 120.14



### 5.1.1 Takeoff Performance

$$\frac{(V_{cli}/V_{sta})^2 W^2}{g \rho S C_{L_{max}} [T - [D + \mu_r (W - L)]_{avg}]} = S_{lo}$$

- $\rho$  = density of air  
 $W$  = weight of airplane = 18 pounds (with 1.3 SF)  
 $g$  = gravitational acceleration  
 $S$  = wing surface area = 5.3 ft.<sup>2</sup>  
 $C_{L_{max}}$  = Maximum Lift Coefficient = 1.15  
 $T$  = thrust = 3.93  
 $D$  = drag = 1.54  
 $\mu_r$  = coefficient of rolling friction  
 $S_{lo}$  = distance to clear 6' obstacle  
 $L$  = lift  
 $V_{cli}/V_{sta}$  = Climb Velocity / Stall Velocity = 1.2

Equation 5.1 Takeoff Distance Equation

The total takeoff distance, including the distance to clear a six-foot obstacle at the end of the runway, is 300 ft. This is the distance calculated for an airplane weighing 18 pounds, or a safety margin of 1.3.

### 5.1.2 Handling Qualities

Handling qualities were integrated directly into the aircraft to reduce the demands placed upon the pilot. To begin with, the aircraft was constrained to a static margin (S.M.) of 20%, the same as sail pilots use, so pilots can adapt to flying the plane. Also, per competition sailplane practice, directional stability ( $C_{n\beta}$ ) was given a value greater than or equal to 0.00201 degrees for low snaking (snake-like movement in the air that is difficult to control). Next, high pitch damping was added through use of a longer tail boom (increased length results in more damping), which helps the plane correct itself in flight when upward gusts strike the tail. Fourth, the airplane utilizes a geared flap to elevator, which increases  $C_L$  in the turns to 1.15, helping to prevent stall in the turns designed for a radius of 59.5 feet. Fifth, the  $\delta_{elevator_{MAX}}$  (maximum change of elevator) is limited to 85% of the wing's  $C_{L_{max}}$ , no matter how hard the pilot pulls on the stick, eliminating worry for the pilot in overchanging the elevator. Sixth, a neutral stick was set for straightaway trim, allowing the pilot to let go of control with the knowledge that the plane is flying true. A seventh parameter applied was to set the plane at maximum throttle for the duration of the flight, including climb and descent. Eighth, full span

ailerons were built for a high roll rate to quickly get into the roll angle the plane is designed to fly at. Finally, it was determined that the pilot should actively control bank angle. Therefore, dihedral stability is not a big issue and the dihedral = 0°.

### 5.1.3 G Load Capability

The maximum g load encountered in the turns is 7.63g. For a safety factor of 1.5, the wing spar is designed to withstand a load factor of 11.44g.

### 5.1.4 Range and Endurance

The maximum endurance of the airplane is 3500 seconds (58 minutes) at an average velocity of 50 feet per second. The predicted maximum range of the airplane is 177,380 feet (33.6 miles) at 60 fps.

### 5.1.5 Payload Fraction

Table of Weight per Section of Aircraft

Section	Percentage
Steel payload	54.4
Fuselage	2.5
Wing	9.2
Tail	3.2
Propulsion	9.8
Landing gear	2.7
Batteries	18.2
<b>TOTAL</b>	<b>100.0</b>

## 5.2 Component Selection

The final design created with the use of the Excel workbook dictated the component selection. The selected propeller was an 8X6 propeller. The battery pack was one 26-cell, Sanyo KR-1700AE pack. The motor was the Aveox 1412/5Y, and did not require the use of a gearbox. The selected airfoil was the S7012 airfoil with 20% flaps.

## 5.3 Configuration Process

### 5.3.1 Selection of Building Materials

The final design for the University Of Southern California's entry into the AIAA competition was developed over time by weighing, comparing, and discussing all thoughts, ideas and results.

From the beginning a general consensus was formed by the group that the use of composites in construction was to be done in order to achieve a lightweight yet strong design. Composites were used to make a carbon fiber fuselage, Spyder-foam core wing

and carbon fiber landing gear provided superb levels of strength while maintaining minimal weight. A high strength to weight ratio was the key factor in the decision to go this route, in addition to ease construction, being easily formed into very difficult shapes, as opposed to balsa wood frames which must be cut to the appropriate shape. Another benefit offered by composites is their reproducibility, often an overlooked benefit. Once a mold has been produced, a piece (such as a fuselage) can be made in about the time it takes for the epoxy (glue) to dry. Besides composites' obvious structural and design benefits, they were chosen based on past experience in competition with them, as attested by annual entries in the SAE Cargo Plane Competition.

The plane's look took shape over many brainstorming sessions, as the basic process consisted of altering and improving a drawing of a plane brought to meetings. Over the course of time, a final design was developed. The preliminary shape was assumed by referencing past competition planes, with slight modifications made for a long and narrow fuselage, chosen for its ability to carry all necessary items without incurring excess drag. With a fuselage set, the rest of the plane was designed.

### 5.3.2 Wing-Fuselage Integration

The wing was chosen based on spreadsheet calculations, which showed that the Selig S7012 with 20% flaps provided the largest  $C_{Lmax}$ . Besides the amount of work that went into choosing an airfoil, the structural system of the wing involved structural testing and research. The final design for the wing does not include a conventional spar, rather a carbon fiber and 1/32" plywood lay-up on the upper surface of the wing. This design required much thought into how to connect the wing and the fuselage. Much of the forces from the wing were transferred to the center section, and it was key not to compromise the surface of the wing anywhere near the carbon and plywood spar. The final design called for two dowels that protrude from the leading edge of the wing and are then accepted by two holes in a bulkhead of the fuselage. The final point of restraint for the wing is a bolt towards the trailing edge of the wing that effectively clamps the entire wing assembly to the fuse. This system allows for quick removal of the wing as well as providing access to the interior of the fuselage, preventing the fuselage's aerodynamic shape from being compromised by unnecessary access holes.

### 5.3.3 Landing Gear design

#### 5.3.3.1 General landing gear configuration

The design of the landing gear was driven by the twin criteria of drag reduction and maximum simplicity, one major criterion. The spreadsheet revealed that cutting landing gear drag in half resulted in another theoretical lap, a significant improvement in performance. Using these criteria, a tricycle landing gear was eliminated because of the drag incurred if left extended and the complexity involved if it were made retractable. Also eliminated was a bicycle configuration because it offered few benefits over a simpler taildragger arrangement. Thus, a taildragger arrangement was decided as the basic layout for landing gear.

#### 5.3.3.2 Number of Wheels

The question of how many wheels to use and their placement remained. Early on, the benefits and drawbacks of a single, centrally mounted wheel were considered. Having a single landing gear in front instead of a conventional taildragger arrangement does away with one wheel and strut, potentially resulting in half the drag. Also, such a system is potentially half as complicated as a two-wheel arrangement. It makes takeoffs and landings more difficult, but the promised simplicity and drag reductions overrode this argument. It was decided to go ahead with the single landing gear concept.

#### 5.3.3.3 Landing Gear Retracts

As it became more defined, the plan for the landing gear underwent several modifications. Originally planned was to have the wheel retract into the rear of the fuselage. After sizing the wheel and the plane more precisely, it was discovered that gear retraction would require a weighty servo system and would be difficult geometrically to retract the gear and strut completely into the fuselage. Retracting the gear but leaving it exposed might have reduced drag compared to leaving it fully extended, but the expected drag reduction was deemed insufficient to justify the weight, complexity, and lack of robustness inherent in such a design. Thus, the decision was made to use a fixed single landing gear with a fairing plus a tailskid.

#### 5.3.3.4 Landing Shock Absorbed by the Gear

At this point shock absorption became an issue. Calculations showed that maximum expected landing

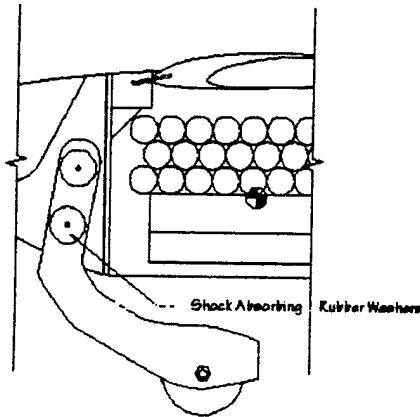


Figure 5.1 Detail of Landing Gear Shock Absorber

loads needed to be between 20 and -2 g's, assuming a vertical landing velocity of 4 feet per second (fps). Very rigid carbon fiber strut anchored to the plane with shock-absorbing rubber grommets was used to solve the problem. The strut uses two carbon bars that sandwich a core of light balsa wood. This H shaped strut, created by the sandwich, provided a pocket for both the wheel itself and its attachment to a bulkhead inside the fuselage. The drag of this strut was greatly reduced by applying a balsa faring to the strut and around the wheel, essentially turning the strut into another wing surface, reducing pressure drag.

#### 5.3.3.5 Takeoff and Landing Skids

With a single wheel gear, the problem of stability on landings and takeoff became yet another concern. For takeoffs it was assumed that a skilled pilot could easily control the plane, but landing was not so easily controlled. The solution was to place skids at critical points on the plane and prevent scraping of the wing and tail during landing by placing skids on both tips of the wing as well as on the rear of the tail boom. Then the material for the skids became another design decision. Metal hoops were rejected since they created too much drag and were hefty in weight. The final design called for the skids to be made of circuit board, which is light in weight and creates a considerably less amount of drag than steel rings.

#### 5.3.4 Tail Boom Design

The tail boom was the only part of the plane to remain constant throughout the entire design process. The carbon fiber tube was chosen because of its strength

characteristics and aerodynamic shape. It also acts as a conduit for the wiring of servos in the tail, eliminating the need for a push-rod assembly. The connection of the tail boom to the fuse was based on a simple plumbing principle. A carbon fiber tube with a inner diameter slightly larger than the outer diameter of the tail boom receives the tail boom. The larger carbon fiber tube, which is permanently attached to the fuselage, has slots cut at two of its quadrants. The clamping power of this system is derived from a simple hose clamp, which effectively locks the tail boom into place by compressing the outer tube around the inner.

#### 5.3.5 Tail Design

The design of the tail was based on landing gear considerations, stability, and control. The design concept behind the v-tail versus the t-tail included many factors, the first of which was weight, a v-tail possessing less. Second was a concern that a hard landing on our single gear might cause a t-tail to separate from the tail boom. Third, in keeping with the main focus that the contest is a competition, not a long term usage type of mission, the v-tail's handling aspects would suit this mission perfectly.

## 6. MANUFACTURING PLAN

### 6.1 Introduction to Manufacturing Process

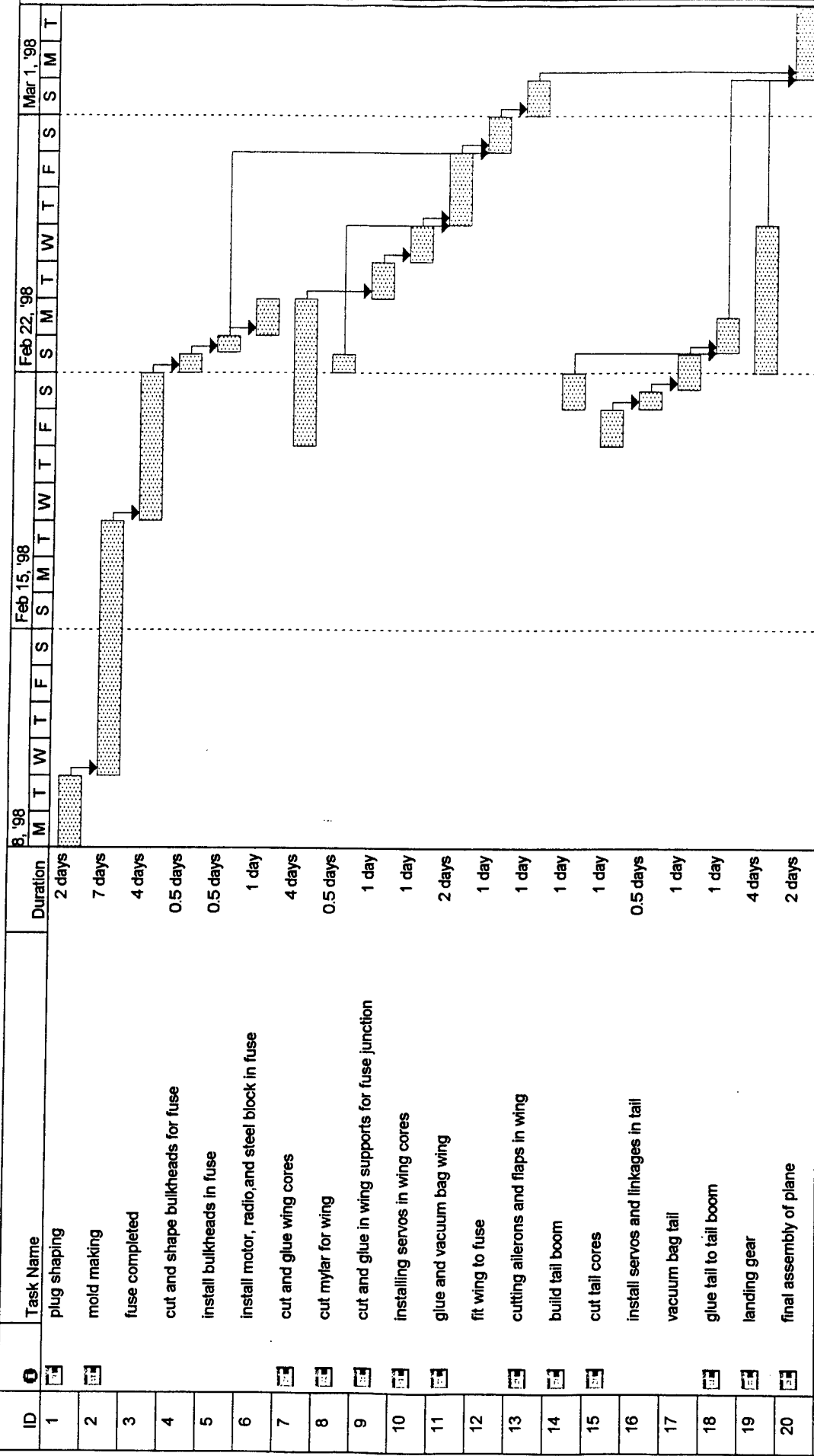
Considerations for material selection and overall process of building the plane were cost, speed, transportation, and quality. Since many of the team members have built and flown airplanes before, their skill level and experience were also considered. Many students in the group also had experience using composites to build airplane parts. Although many of these composites are not cheap, they are very light and strong, can be molded into intricate parts, and be made quickly. They are also more durable to bumps and accidents which come from competition, landing, and being transported half way across the country. The skill required to make many of these parts is minimal compared to the quality and reliability they ensure; nevertheless, building the major components of the plane (fuselage, wing, landing gear, tail) is a skilled process.

### 6.2 Fuselage Construction

The carbon fiber fuselage with aircraft plywood reinforcing hard points was to be molded. This carbon fiber shell can be very strong and lightweight. Hard points made out of aircraft plywood transfer concentrated loads into the strong carbon shell.

# USC AIAA Student Design/Build/Fly Competition

## Manufacturing Schedule



Project: Fabrication  
Date: 2/1/98

Progress

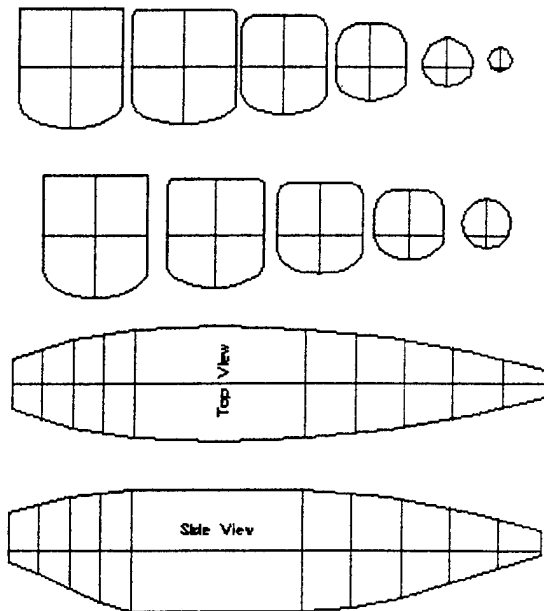


Figure 6.1 Sections and Views of Wood Plug

This carbon fiber shape is made by first making a plug out of wood. The plug or shell can be machined to the exact shape desired, but this method was not chosen because the process is expensive; instead the plug was shaped by hand in about 15 hours. A shell is made around the plug out of fiberglass in two pieces so that the plug can be removed. This shell was divided into top and bottom halves. When the halves were joined, an inch strip of carbon fiber cloth was added. Having these two joiners run along the sides of the fuselage added strength needed when the cut out for the mount of the wing was done. A layer of carbon fiber cloth and epoxy is laid up inside each side of the shell, and a one-inch fiber stinger is run down the inside to join the two halves.

Once the carbon has cured, the two shells can be pulled off the finished part. This whole procedure takes about 40 man-hours but each successive part only takes about 5 hours to reproduce. Hard points made out of quarter inch aircraft plywood were shaped to the fuse and glued in with 30-minute epoxy. These were cut out by hand on a scroll saw using a printout as a guide. The aircraft plywood is cheap, easy to work with, and has the strength required for the loads this airplane will encounter.

This process of making the fuselage is inexpensive and creates excellent parts that are very strong and durable. Materials such as carbon fiber and plywood are easily available from hobby stores and specialty shops such as C.S.T. There are several drawbacks of this procedure, including that the construction of the first part is time consuming. Another

problem is that creating a plug by sanding and carving may lead to imperfections which were not designed for, possibly creating a fuselage that is not as light as a built up balsa fuse. However, the durability of the finished product over many hard landings and "hangar rash" is well worth the small increase in weight.

## 6.3 Wing Construction

### 6.3.1 Concept for wing construction

There are many ways to build a small, light wing. Instead of a balsa wing or a molded composite wing, foam as a core and a composite, vacuum-bagged skin for strength was used. Plywood was shaped for hard points and aluminum dowels and a Teflon screw was to be used to attach the wing to the fuselage. A foam core wing and composite skin were considered because they take less time to build and make a very high quality wing. The major disadvantage of this choice was the flight load.

### 6.3.2 Wing skin structural tests

There was little data on how to produce foam core wings that have a skin able to take 7.56-g flight loads, so it was decided that spending time for tests on sample wing skins was needed to assure the plane's safety. Spyder foam was selected because it possesses the highest compression to weight ratio of many polystyrene foams. Twelve samples were created with varying compression skins under loading. Some of the skins had a 1/64" plywood stiffeners in them. Each sample was crushed in an Instron machine, the time for usage donated by the Mechanical Engineering department at USC. The results were accurate and very helpful in determining the lay-up for the spar to be in the wing skin. It was found that adding a sandwich of carbon, (1/64) plywood, and carbon gave a great increase in load-failure over conventional layers of carbon of the same weight.

### 6.3.3 Wing construction methods

Taking a block of foam and passing a hotwire over an airfoil shaped block on each side cuts out the shape of the wing by melting out the styrofoam. The process is quick (about 10 minutes) and produces excellent wing shapes that are nearly identical to those described in the design. The servos for the plane are glued into a cavities cut out of the core to hide them and reduce drag. Once the entire wing has been hot-wired out, glued together and hard-points installed, the composite skin can be applied. In this case another small indent was made in the upper surface to lay in a



flush wing spar. The composite skin is epoxied to a sheet of Mylar that is shaped to fit and cover the wing. Once the Mylar sheet has been completely covered and the spar has also been glued on, the Mylar is wrapped around the core and placed in a vacuum bag until it is cured. This process is highly skilled and creates excellent parts. Some of the students on the team have experience doing this, and it was not a problem to produce parts and train less experienced students at the same time. Equipment such as a vacuum pump and hotwire are expensive, but the quality of the final product is worth it.

#### *6.3.4 Tail and landing gear construction*

The tail was made in a similar to the wing using a foam core and composite skin for strength. It was, however, easier to make because there was no spar, connected to the tail boom with epoxy.

Drawings for the landing gear called for a  $\frac{1}{4}$ " plywood sheath with a carbon fiber coating on each side. The shape of the landing gear was cut out of plywood by hand using plans as a guide. Carbon fiber was glued on either side and vacuum-bagged to ensure no delamination. A wheel fairing was to be made out of something lightweight and inexpensive, so a sanded and shaped piece of foam was used.

#### *6.3.5 Summary of construction process*

The plane had to be built on a limited amount of time and at a reasonable cost. With limited resources and time, the best job thought possible was done. The schedule made for building the plane was reasonably kept, and the high quality end result was well worth the time and efforts.

The quality came from hard work throughout, especially at the inception. Beginning with a 'class' on how to design a model airplane, students began to develop thoughts and ideas for what was a plane built from scratch. Once a thorough academic background was in place, a schedule for design and building was set up.

Design of the aircraft was performed using computers. This was invaluable as several hundred combinations of configurations were analyzed using an extensive Excel spreadsheet, a near impossible and very tedious task if done by hand. However, it was discovered that at least one hand calculation should be done to be sure that there were no mistakes done in developing the software package utilized. Simple mistakes in equations caused serious differences in output results of weight. Once the problem was discovered, better results led to good comparisons of various aircraft based on primary design of the plane.

During the building phase of the schedule, it turned out to be very important to stay on pace. Our team almost got completely off schedule before a long work session caught us up. Academic constraints made the entire team susceptible to delays, but due to previous experience, it was deemed absolutely necessary to complete the plane as scheduled.

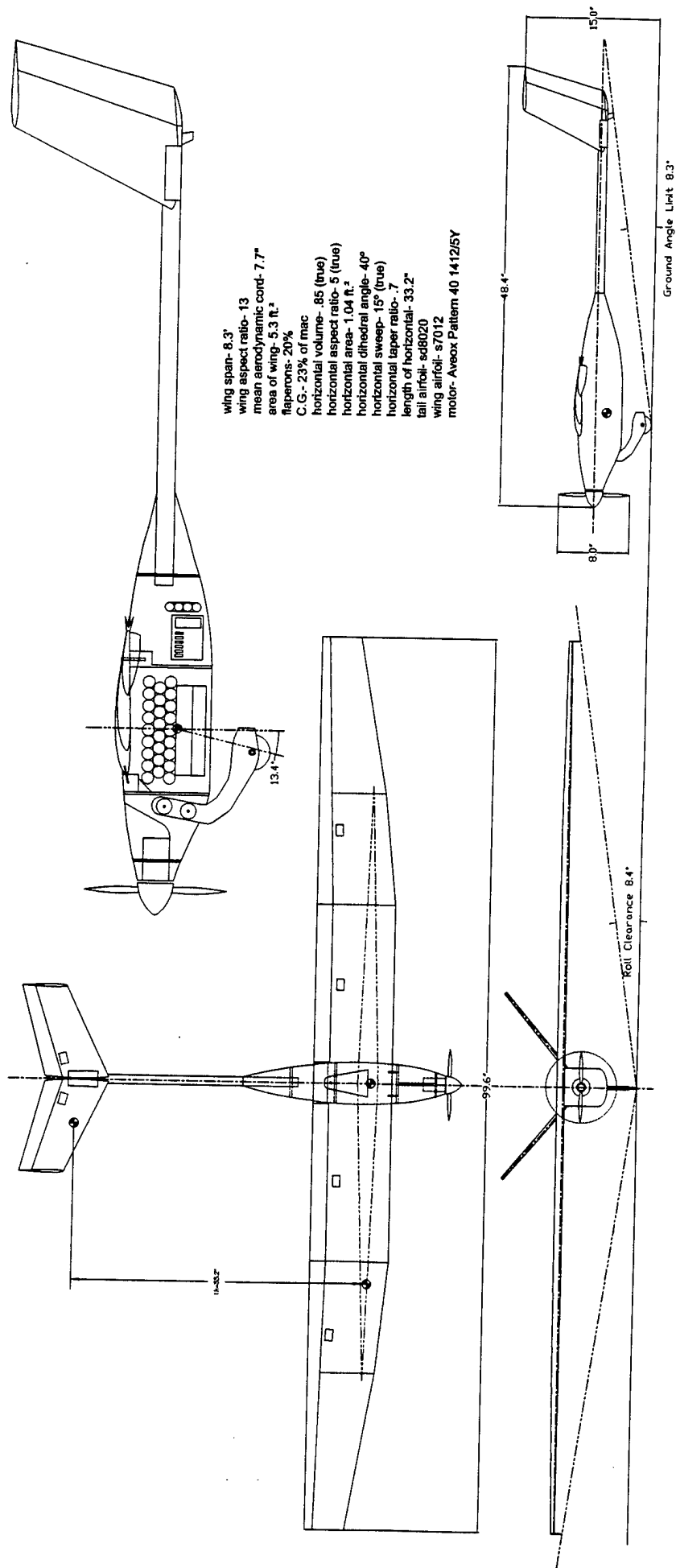
There is room for concern that the airplane will not perform as predicted. Further tests of the live aircraft still need to be completed, and it is possible that the aircraft built is not as clean as the aircraft designed on paper. In addition, there is no guarantee that the propeller selected in design will work as efficiently as other similar propellers, so further studies will be done using different props at future test flights. Also, if a larger propeller selected, a gearbox might be used, leading to questions of capability that cannot be answered at this time.

Another question that must be answered is how well the plane will handle with only one wheel. The pilot may deem the takeoff and landing gear too difficult to manage and require a change. Again, further answers will be discovered on future test flights.

Limited time to develop the plane was also a result of a fewer number of participants compared to years past. With only eight students involved throughout the year, and less than half with experience building anything, more teaching was necessary and mistakes were made. But, the team came together due to its commitment, and the performance as a whole was far beyond what has been seen in several years.

Thanks need to be given to our sponsors, Lockheed Martin Skunkworks and the Northrop Grumman Corporation, whose financial support allowed us the freedom to create the envisioned design. In addition, gratitude is given to Blaine Rawdon and Mark A. Page for the countless hours they spent driving to USC, teaching the fundamentals of model (and real) airplanes, and working out errors made during the course of the design process. Without them, the plane would be far different than the one built at present.

Final praise is given to the University of Southern California's Aerospace Department and to Dr. Blackwelder, whose continual support, efforts and experience proved invaluable.

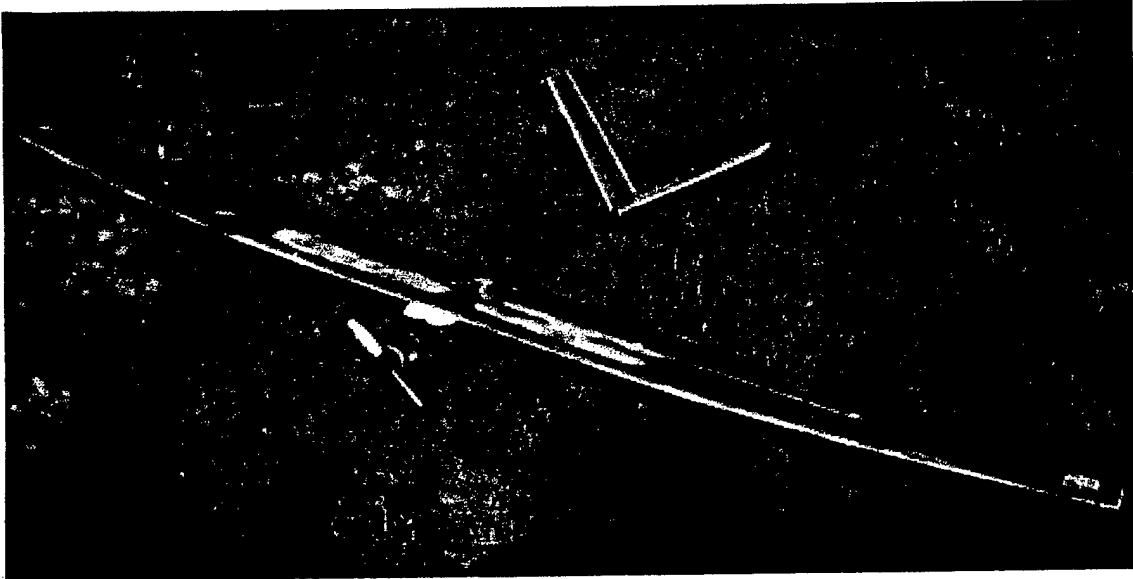


# Design Report – Addendum Phase

*University of Southern California*

April 13, 1998

1997/1998 AIAA Student Design/Build/Fly Competition



## UNDERGRADUATE TEAM MEMBERS

Philip Haworth (Editor)

Stuart Sechrist

Ryan Romo

Qi Huan Chen

Nathan Palmer

David Sandler

Jacob Evert

Kevin Helm

## FACULTY ADVISOR

Dr. Ron Blackwelder

## INDUSTRY ADVISORS

Blaine Rawdon – Boeing

Mark A. Page – All American Racing

## SPONSORS

Lockheed Martin Skunk Works

Northrop Grumman

## 7. LESSONS LEARNED

### 7.1 Differences between final and proposal design

#### 7.1.1 Fillets

Upon closer inspection of the proposal design, it was discovered that there were sharp corners in the airplane surface. These corners, located at the wing-fuselage junction on each side of the airplane, would create horseshoe vortices that would increase the drag on the airplane.

Fillets were then proposed to alleviate these horseshoe vortices. A brief drag calculation was done and the fillets were shown to reduce the drag by about 3%. These fillets were made of balsa wood, shaped and sanded by hand, and then

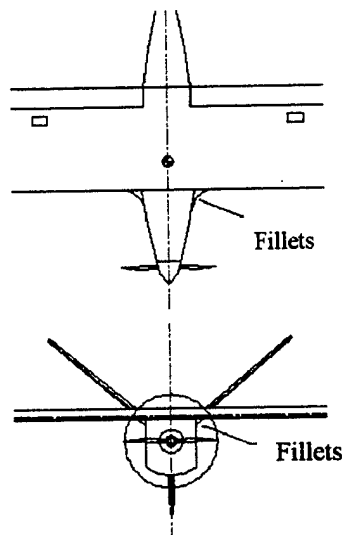


Figure 7.1 Fillets under wing

attached to the fuselage with epoxy at the locations shown in Figure 7.1. The time required to implement this change was six man-hours, and the cost was only for the balsa wood, which was ten dollars.

#### 7.1.2 SD7003 Airfoil

In the course of the design phase and early into the manufacturing stage, research continued to ensure that the airfoil and other components selected in the design phase provided the best performance. During this research, another airfoil, the SD7003 with flap, was shown to perform half a lap better than the S7012 airfoil when entered into the Excel design spreadsheet.

Although foam cores had already been cut for the S7012 airfoil, it was decided that the half lap increase was enough to warrant the purchase of new foam and to justify switching the airfoil completely. The cost of changing airfoils was \$46.25, the cost of the new spyder foam, since no other parts had been installed in the wing at that point. This cost was not an issue in the decision to

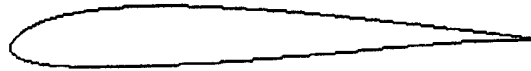


Figure 7.2 SD7003 airfoil

make the change. The main issue debated was the time to get the new airfoils cut out of the foam and the wing construction back on schedule. The time to cut the new airfoils was one week, because new foam needed to be ordered and received before any actual cutting was done. It was decided that the predicted half lap increase in performance was worth the one week delay. In reality, very little time was lost, as the manufacturing focus was redirected towards the fuselage, tail boom and the tail, which were all constructed during that week.

#### 7.1.3 Wingtip Washout

During the turns, the airplane is designed to pull up to 85% of  $C_{L_{max}}$ . In the event that the airplane passes the limit of  $C_{L_{max}}$ , good stall characteristics are necessary for the pilot to recover control and continue the flight. To this end, the wing was designed to have a 3° washout at the wingtips. This would help guarantee that the wingtips would stall after the center section of the wing stalls. This decision was made before the wing core sections were cut, so there was no increase in time required or cost to put washout in the wingtips.

### 7.2 Static load tests

When the wing and the wing spar caps were completely constructed, a static wing load test was done on the wing. The wing spar caps are several sandwiched layers of carbon fiber and 1/64" plywood inlaid into the wing. A picture of the layers are shown in Figure 7.3.

The predicted flight of the airplane included turns at 7.6g's. The static load test was designed to determine if the wing and the wing-fuselage junction would withstand a 9g turn. The wing was attached to the fuselage so as to test the strength of the wing and the wing-fuselage attachment. The fuselage and wing were suspended



*Figure 7.3 Carbon fiber and plywood layers laid out separately. The layers were then inlaid in the top of the wing to be used as the wing spar. A similar lay-up was used in the bottom surface of the wing.*



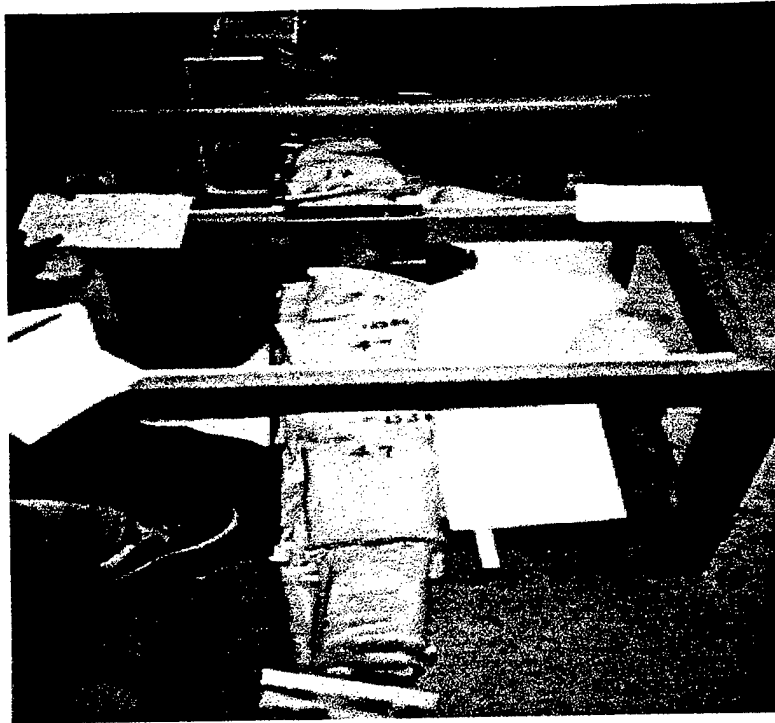
*Figure 7.4 Fuselage and wing suspended from workbench in preparation for static load test*

in an inverted configuration from a wood frame with duct tape. Figure 7.4 shows the experimental setup without applied loads. The position of the wingtips were recorded without any loads. Sandbags were used for weight and were applied to the wing in an approximately elliptical loading pattern. At the weight distribution that simulated a 9g turn, the wingtips deflected 4.25 inches. Figure 7.5 shows the wing with the maximum elliptical load pattern applied. There was some local buckling of the wing skins, and a wave on the secondary structure of the wing, but neither the

wing spar caps nor the foam structure of the wing failed.

### **7.3 Landing gear shock test**

One of the concerns raised when the decision was made to build a single strut, single wheel landing gear was the ability to absorb the shock of a hard landing. The design landing gear was built and tested for strength in a seven inch vertical drop that simulated a rate of sink of 6 ft/s. When subjected to the seven inch drop, the landing



*Figure 7.5 Fuselage and wing with simulated 9g load factor*

gear completely absorbed the load. No parts were damaged, and the gear did not bend back and hit the underside of the fuselage.

## 7.4 Areas for improvement

### 7.4.1 Design Process

Improvements that will be made in the next design process will be mainly adjustments to the Excel design spreadsheet. The first area for improvement is the range of alternatives investigated. For example, only four motors and seven types of batteries were included in the spreadsheet workbook. The addition of more motors and battery types would introduce more flexibility in the final design and could produce better performance results.

Another area for improvement in the design process is in the scope of what the Excel spreadsheet can do. More graphical outputs based on the spreadsheet's calculations would be helpful in the selection of various components of the aircraft.

Optimization of the parameters examined in the spreadsheet was done manually, and as a result, delayed the design process. A third improvement that could be made in the design process is the automation of spreadsheet optimization. If the spreadsheet could be programmed to locate the design that produces the

maximum number of laps, the selection time of the components would be greatly reduced. This would have allowed for an earlier start on construction and detailed design.

### 7.4.2 Manufacturing Process

One manufacturing technique that can be improved is the inclusion of wingtip washout. In the current wing, the washout was cut into the foam cores. In the vacuum bagging process, weight was applied to the top of the wing to make sure it cured without any large amount of wing twist. The weight applied at the wingtips, however, prevented all wing twist, including the 3° washout desired in the wingtips. This problem will be solved in the future by laying the vacuum bagged wing into the airfoil-shaped beds before applying any weight to the top of the wing. Uniformly cut beds will ensure that the washout will not be twisted out and also will provide a flat surface upon which to lay weight down on the wing.

In order to correct the washout of the current wing, a slit was cut along the leading edge of the wing, greatly reducing torsional rigidity, and weights were hung off the leading edge to twist it to the desired amount. Fiberglass was reapplied to the leading edge fixing the weak edge caused by the initial cut.

Experience was the most important asset in the construction of the airplane. Over half the

team had at least two years fabrication experience. Knowledge of carbon fiber and fiberglass construction techniques resulted in higher product quality. This quality was apparent in weight reduction without loss of strength. Experience also decreased construction time, as parts were constructed correctly the first time. The end result was a very clean aircraft fully constructed in a month.

### **7.5 Cost comparisons**

The actual costs of the materials and components of the airplane were about the same as the predicted costs. There was an increase in cost (\$56.25) due to the cost of the extra spyder foam purchased after the new airfoil was selected and the cost of the balsa wood for the fillets. There was a reduction in cost due to the decision to build the carbon fiber tail boom as opposed to purchasing a commercially available tube. This resulted in a savings of \$50. All the other costs involved in materials, electronics, and hardware were as expected from retail prices.

## Manufacturers List Price

<i>Component (quantity)</i>	<i>Total Price (\$)</i>
<b>Propulsion Systems</b>	<b>\$981</b>
Aveox 1412/5Y motor (2)	420
Aveox motor controller (1)	250
Batteries (26)	117
Battery charger (1)	149
propellers (3)	20
spinner (1)	5
propeller adapters (2)	20
<b>Building Materials</b>	<b>\$691</b>
Wood	100
Epoxy	110
Releasing Agents	40
Spyder Foam	74
Carbon fiber	224
Fiberglass	63
glue	80
<b>Other</b>	<b>\$1146</b>
Radio (1)	459
Servos (7)	406
servo links (12)	20
steel weight (3 pieces)	20
shrink wrap	20
paint	7
digital scale	100
vacuum bagging material	83
miscellaneous	31
<b>TOTAL</b>	<b>\$2818</b>



# PROPOSAL FOR THE DESIGN OF AN UNMANNED AIR VEHICLE

*Prepared for Gregory Page*

*Submitted 16 March 1998*

*by the Syracuse University Chapter of the American Institute of Aeronautics and Astronautics*

## *Design Team Members:*

*Kevin Bendowski*

*Kevin Bishop*

*Nick Borer*

*Marc Brock*

*Jarrold Cafaro*

*Arun Chawan*

*Garvin Forrester*

*Tom Jones*

*Dr. Hiroshi Higuchi, Advisor*

## TABLE OF CONTENTS

<b>1. Executive Summary</b>	<b>1</b>
1.1 Development	1
1.2 Design Tool Overview	1
<b>2. Management Summary</b>	<b>3</b>
2.1 Design Team	3
2.2 Management Structure	3
<b>3. Conceptual Design</b>	<b>4</b>
3.1 Design Parameters	4
3.2 Conclusions	6
<b>4. Preliminary Design</b>	<b>7</b>
4.1 Weight Estimation	8
4.1.1 The Wing	8
4.1.2 The Empennage	9
4.1.3 The Fuselage	9
4.1.4 The Landing Gear	9
4.1.5 Fixed Systems and Miscellaneous	9
4.2 Airfoil Selection	10
4.2.1 Airfoil Characteristics at Low Reynolds Number	10
4.2.2 Airfoil Tradeoffs	10
4.2.3 Final Airfoil Choice	11
4.3 Initial Performance	11
<b>5. Detailed Design</b>	<b>14</b>
5.1 Stability and Control	14
5.1.1 Dynamic Stability	14
5.2 Production of Thrust	14
5.3 Propeller Analysis	16
5.4 Thrust Charts	16
5.5 Drawing Package	17

<b>6. Manufacturing Plan</b>	<b>18</b>
6.1 Wing and Emennage	18
6.2 Fuselage	19
6.3 Boom	21
6.4 Assembly	21

---

## APPENDICIES

Appendix I. <i>Design Guidelines and Performance Specifications</i>	I-1
Appendix II. <i>Weight Estimation Program</i>	II-1
Appendix III. <i>Drag Polar Characteristics of a Flat Plate</i>	III-1
Appendix IV. <i>NACA 23012 Wing Section</i>	IV-1
Appendix V. <i>Low Speed Airfoil Characteristics</i>	V-1
Appendix VI. <i>Calculation of Center of Gravity Location</i>	VI-1
Appendix VII. <i>Motor Static Analysis</i>	VII-1
Appendix VIII. <i>Motor Performance</i>	VIII-1
Appendix IX. <i>Performance Calculations</i>	IX-1
Appendix X. <i>Specific Fuselage Material Cost Estimations</i>	X-1

## LIST OF FIGURES

Figure 4-1. <i>Airplane Forces During Flight</i>	7
Figure 5-1. <i>Takeoff Obstacle Diagram</i>	15
Figure 6-1. <i>Finite Element Model of Composite Fuselage</i>	20
Figure 6-2. <i>Finite Element Model of Wooden Boom Section</i>	21

## LIST OF TABLES

Table II-I. <i>Team Member Assignments</i>	3
Table II-II. <i>Milestone Chart</i>	3
Table III-I. <i>Propulsion FOMs</i>	4
Table III-II. <i>Fuselage FOMs</i>	5
Table III-III. <i>Wing Placement FOMs</i>	5
Table III-IV. <i>Wing Shape FOMs</i>	6
Table IV-I. <i>Wing Loading as a Function of Lift-Off Speed (<math>C_l=1</math>)</i>	8
Table IV-II. <i>The Comparison of MTOW to the Wing Loading</i>	11
Table IV-III. <i>Wing Dimensions and Variation of Plane Drag at Different Wing Loadings</i>	12
Table IV-IV. <i>Variations of Coefficients with Wing Loadings</i>	13
Table VI-I. <i>Wing Materials</i>	18
Table VI-II. <i>Qualitative Fuselage Materials Comparison</i>	20
Table VI-III. <i>Manufacturing Schedule</i>	22

# 1. EXECUTIVE SUMMARY

## 1.1 Development

In September of 1997, several members of the Syracuse University chapter of the American Institute of Aeronautics and Astronautics met to discuss the possibility of competing in the 1997-1998 Cessna/ONR Design/Build/Fly competition. Some of the members, who competed in the previous year's contest, came forward to heap praise upon it. After some discussion, many of the members decided to commit themselves to the new project, and many of those members have remained committed in the months since.

The design of any aircraft, whether it be a small radio-controlled model or an enormous cargo jet, involves many first steps. The basic concept must be determined before work is done on specific sections of it. This process, referred to as conceptual design, occupies the intellect of the assembled group until a consensus is reached among them. In the Syracuse University design team, this process took approximately two months.

In this two month span, many alternative ideas were expressed for the overall configuration of the UAV (unmanned air vehicle). These ranged from general propulsion requirements to wing shape. Some ideas were dismissed outright due to knowledge of the situation, but most required further thought and research. Much of this time was spent either meeting as a group or researching various concepts. Once the ideas had been narrowed down, detailed research began, resulting in team-wide debates. As more information became available, the same picture of the UAV began to circulate through the teams' collective head.

Since the motor was arguably what the aircraft needed to be designed around, a specific type needed to be chosen. Doing this would form the basis of the calculations necessary for preliminary design. Thus, before the end of the Fall Semester, the electronic components of the UAV were chosen and ordered, so preliminary design could start at the beginning of the next semester.

The next month was spent calculating the performance and dimensions of the aircraft, based upon the results of the conceptual design phase. At the end of this period, the team had a good idea as to how much the UAV would weigh, as well as its linear dimensions. These figures paved the way for the detailed design phase that followed.

In detailed design, the UAV was drawn up on a CAD program with the dimensions specified from preliminary design. Its performance and handling characteristics were also determined from the aforementioned data. While the data was being scrutinized, other team members discussed the materials that would comprise the aircraft's fuselage, boom, empennage, and wing. Members who advocated different materials again returned to research, and discussions ensued. It was at this point that the materials were priced, selected, and ordered in sufficient quantity to construct the aircraft.

Once the parts arrived, construction began. This was the last major phase started before the design report was submitted. Following the completion of the UAV, flight testing will occur to ensure that the design will perform to standards.

## 1.2 Design Tool Overview

The use of dedicated design tools was essential to the completion of the UAV. As a result, a vast array of resources were tapped to complete the various design phases.

For conceptual design, the tool utilized most often was the Internet. It proved to be an invaluable asset in the research of various propulsion systems, and was helpful in securing information on aircraft configurations. Every aspect of this phase was, in some way, connected to it. Indeed, it was on the Internet that the data for the brushless motor were found and utilized. The AVEOX home page included a "static test stand" to test the thrust and current draw of various motors connected with different propeller sizes and pitches. This was very helpful in providing information as to which motor to buy, as well as the base information of the preliminary design phase.

Research was not limited to the Internet. Configurations of full-size aircraft were sought through books such as Jane's all the World's Aircraft, as well as others. Specialty books on radio-controlled aircraft

provided answers when Internet research did not. As powerful a tool as the Internet is, it is sometimes hard to beat what the local library has to offer.

For the preliminary design stage, more advanced design tools were necessary to obtain meaningful results. Many of the desired results required iterative solutions, so the most efficient way to get answers was to write computer code. Most of the coding was done using C++, and checked by a simple mechanical process using MATCHAD software. Spreadsheet work was extensively used in predictions and comparison, and EXCEL was the choice program. Text on aerodynamic design and performance were invaluable as well. The two main books used were Aerodynamics, Aeronautics, and Flight Mechanics by Barnes McCormick, and Introduction to Flight, by John Anderson.

The final detail design relied mostly on the use of EXCEL, since estimations of performance were strictly formula based. A motor prediction program called MOTOCALC was used to predict the behavior of electric powered motors on an aircraft.

## 2. MANAGEMENT SUMMARY

### 2.1 Design Team

The number of people actively involved in the design team has decreased since the letter of intent was sent last October. There are currently eight members of the Syracuse University chapter of the AIAA involved with design and production of this UAV. Garvin Forrester and Marc Brock, both seniors, contributed their considerable knowledge in the field of aeronautics. AIAA chapter president and team leader Kevin Bendowski, a junior, gave both his experience gained with radio-controlled aircraft and of last year's competition to the team. Tom Jones, also a junior, proved to be a valuable asset due to his knowledge of composite materials and of computerized stress analysis tests. Sophomore Arun Chawan applied lessons learned in last year's competition to the current design. Sophomores Nick Borer and Jarrod Cafaro, as well as freshman Kevin Bishop, added their problem-solving skills and basic know-how to the team. Dr. Hiroshi Higuchi, AIAA chapter faculty advisor, lent his talents to the mix of students.

### 2.2 Management Structure

Specific aspects of the UAV design were delegated to specialized design teams. Obviously, those with more experience in a given field were assigned to that corresponding area. For example, the seniors of the team (who have the most experience in aircraft design) provided the dimensions of the aircraft, as well as its performance characteristics. The list of team assignments are given in Table II-I.

<u>Assignment</u>	<u>Team members</u>
Sizing & Performance Characteristics	Forrester, Brock
Wing & Empennage Design	Forrester, Brock, Bendowski, Chawan
Fuselage Design & Component Placement	Jones, Borer, Cafaro, Bishop
Fuselage Material Selection	Jones
CAD Drawings: Wing & Empennage	Chawan
CAD Drawings: Fuselage	Chawan, Bishop

**Table II-I. Team Member Assignments**

Timing was essential to the team's readiness. At the beginning of the project, team members came up with a schedule or "milestone chart" (Table II-II). This chart was used as a guide to keep the project on track. The detailed design took longer than anticipated; therefore, the project was delayed for more than a month. This, in turn, delayed the design proposal, but that time was almost made up for in the end due to the efforts of the team members.

<u>Item</u>	<u>Proposed Date</u>	<u>Actual Date</u>
Letter of intent submitted	10/22/97	10/26/97
Conceptual design complete	12/1/97	12/9/97
Electronic components ordered	12/16/97	12/9/97
Preliminary design complete	1/20/98	2/5/98
Detailed design complete	1/31/98	3/5/98
All materials ordered	2/6/98	3/6/98
Design proposal complete	3/8/98	3/12/98
Design proposal submitted	3/10/98	3/13/98
Construction complete	3/28/98	TBA
Flight testing	3/29/98	TBA

**Table II-II. Milestone Chart**

### 3. CONCEPTUAL DESIGN

#### 3.1 Design Parameters

Deciding the basic concept for the UAV was the first major hurdle on the path to its completion. In this initial phase of the project, the design team met once a week to discuss various ideas that would pertain toward a particular facet of the aircraft. Ideas were given, discussed, and either rejected outright or left for later discussion. In this fashion, the basic concepts for propulsion, fuselage shape, and wing configuration were born. These basic concepts trickled down to others, such as the number of motors required. The concepts were discarded or adopted based on the general knowledge of team, and, when necessary, further research was made into the matter.

Propulsion was the first item considered, since it had the most number of limiting factors (according to the rules). These include the type (electric), the weight of the power source (no more than 2.5 pounds, or about 20 cells), and the endurance (seven minutes of flight plus a reserve). From these limiting factors, the team concluded that a powerful and efficient electric motor was necessary to be competitive. Another consideration was how the motor choice would effect the design of the internal structure of the aircraft. Weight and cost completed the figures of merit (FOMs) required in motor selection. Table III-I shows a comparison of motor configurations versus the various FOMs.

First considered was the use of a direct drive standard electric motor connected to an external propeller. As this was used on last year's UAV, some of the team members were able to list the good and bad qualities of this configuration. It was powerful, yet it drew too much current, limiting the endurance of the aircraft. Thus, this configuration failed the efficiency test, yet passed the power test. However, these motors are the cheapest of the lot.

Next a direct drive brushless electric motor connected to an external propeller was considered. It was discovered through research that brushless motors could be as powerful as their brushed counterparts, yet not draw as much current. Power could also be increased by combining the motor with a gearbox, at little cost in current draw. Therefore, the brushless electric motor with a gearbox passed both the power and efficiency tests. The only drawback seemed to be the higher cost.

The next idea was to utilize an electric ducted fan to propel our UAV. Essentially, a ducted fan is a direct drive electric motor connected to an internal propeller. The amount of thrust provided through such a configuration was in question, however, and it would complicate the design of the airframe. The more powerful ducted fans drew quite a bit of current. Ducted fans were also quite expensive.

After direct drive motors, belt-driven electric motors connected to an external propeller were considered. The main concern was that the belt would be susceptible to slipping, which would reduce the power of the aircraft. Also, a belt could break, robbing the UAV of thrust completely. The only redeeming quality of a belt-driven motor was the lower RPM the motor would need to acquire.

The use of multiple motors was the final consideration. This would increase power, but would also increase weight, drag, and current draw. This would result in a more powerful aircraft, but at the expense of endurance. Also, this would be quite an expensive undertaking, doubling the cost of the motor chosen, while not doubling the amount of thrust.

Type	Power	Efficiency	Cost	Weight	Ease of Design	Total
Standard Electric Motor	3	2	4	3	4	16
(With Belt Drive)	3	1	3	3	3	13
Brushless Electric Motor	3	4	3	3	4	17
(With Belt Drive)	3	3	2	3	3	14
Ducted Fan	3	3	2	3	1	12
Multiple Motors	4	2	1	1	2	10

4-Excellent 3-Good 2-Fair 1-Poor

Table III-I. *Propulsion FOMs*



Once the team had decided what would power the aircraft, the fuselage configuration was looked into. Considerations (and thus the FOMs used) were weight, drag, strength, and ease of manufacture. At this stage, the team opted not to take material into consideration.

The design team decided to approach the fuselage from a "minimalist" point of view. In doing so, the fuselage would have as small a cross-sectional area as possible, while still containing all of the necessary components: the motor, batteries, speed controller, servos, weights, and the radio receiver. The empennage would be attached to the main body of the fuselage with a boom or booms. This would reduce both weight and drag.

This decision left few options. The body could be rectangular or cylindrical, and attached to the tail using one or two booms. The rectangular body would be easier to manufacture, but would do so at a cost of extra drag, and perhaps extra weight as well. A cylindrical body would be a bit harder to manufacture, but would reduce drag, weight, and increase the overall strength (see Table III-II).

The number of booms was similarly scrutinized. Two booms would keep the tail from twisting as much, but at a cost of additional weight. A single boom would reduce both weight and drag while maintaining enough strength to prevent significant tail twist (see Table III-II).

Type	Weight	Drag	Strength	Ease of Manufacture	Total
Rectangular Body	2	3	2	3	10
Round Body	3	4	3	2	12
Twin Boom	2	2	4	2	10
Single Boom	3	3	3	3	12

4-Excellent 3-Good 2-Fair 1-Poor

**Table III-II. Fuselage FOMs**

Wing placement was the next item discussed. This would have an effect on the design of the fuselage as well as the wing, so it was necessary to discuss in detail. There were only three possibilities available: low, middle, or high placement. The FOMs were similar to those used for determining wing position on full-size cargo planes (see Table III-III). However, some adjustments were made (from full-size aircraft) out of necessity. For example, cabin visibility was not considered, for obvious reasons.

Placement	Drag	Stability	Landing Gear	Crash Worthiness	Wing Structure	Total
High	2	3	1	3	3	12
Middle	3	2	2	2	1	10
Low	1	1	3	1	2	8

3-Best 2-Okay 1-Poor

**Table III-III. Wing Placement FOMs**

The final area addressed during the conceptual design phase of the UAV was the wing configuration. Three FOMs from the fuselage selection carried over: weight, drag, and ease of manufacture (see Table III-IV). Lift was also considered as an important figure of merit. Four possibilities were discussed for the wing design.

The first idea presented was to utilize a straight wing to provide lift for the aircraft. This was similar to the wing used in the previous year, allowing previous participants to provide useful insight. This type of wing would provide ample lift and would be easy to manufacture, at a cost of additional weight and drag.

A tapered wing was discussed next. Using this configuration, a decrease in weight would be achieved while maintaining lift comparable to the straight wing. There was minimal difference in drag between the two, but a tapered wing would be harder to manufacture.

Next addressed was the idea of a swept wing. This would give some relief from drag by reducing the amount of wing viewed head-on, and would weigh about the same as the other configurations

considered. However, a swept configuration would make the center of gravity calculations much more difficult, and thus the eventual design and manufacture of the wing and fuselage. This, coupled with the fact that the drag relief would be very small at the low speeds attained by UAVs, made this configuration undesirable.

Finally, a hybrid delta wing in a diamond configuration was considered. Again, this would give enough lift, but would complicate the design. Unfortunately, there was no available background information for such a configuration. Also, there was minimal time available to develop research data necessary for such an undertaking.

Because the drag encountered by the aircraft would be relatively small in comparison to the other characteristics, it was given less weight than the other FOMs. While drag and wing sweep are important to full size high speed aircraft, they are of little consequence to a UAV that cannot attain more than seventy miles per hour. Therefore, the design team decided to focus more on keeping weight and other design difficulties low.

Type	Lift	Weight	Drag	Ease of Manufacture	Total
Straight	4	2	2	4	12
Tapered	4	4	2	3	13
Swept	3	3	3	2	11
Hybrid Delta	3	3	3	1	10
4-Excellent 3-Good 2-Fair 1-Poor					

Table III-IV. *Wing Shape FOMs*

### 3.2 Conclusions

At the end of much debate and discussion, the team tallied its results to yield the concept used for the UAV. It would be propelled by a brushless electric motor with a gearbox. Around this choice, the exact dimensions and speeds the aircraft could be determined. The fuselage would be as small as possible to contain all of the necessary components, and would be cylindrical to reduce drag. The wing would be attached to the upper part of the fuselage, for reasons discussed earlier. A single boom would connect the fuselage to the empennage. The wing would be without sweep, but would hold some degree of taper so weight would be reduced.

The brand and type of motor were then selected so that work could begin on the rest of the aircraft. This would provide the basis for the preliminary design of the UAV.

#### 4. PRELIMINARY DESIGN

Early aeronautical engineers were only concerned with lifting and propelling aircraft from the ground; what happened after that was viewed with little importance. However, the sweeping movements in aviation during the pre-World War I era caused the airborne performance of the airplane to come under more intense scrutiny.

Questions arose such as: What is the maximum speed of the airplane? How fast can it climb to a given altitude? How far can it fly? How long can it stay in the air? Answers to these questions constitute the study of airplane performance, and contribute to the sizing and powering of a vehicle.

The first consideration of flight is much like our predecessors, getting it airborne:

From the free body diagram of an airplane, as sketched in Figure 4.1, the lift of the airplane must equal the weight for a level flight ( $L = W$ , Equation 4.1), where  $L$  is the lift of the airplane and  $W$  is the weight.

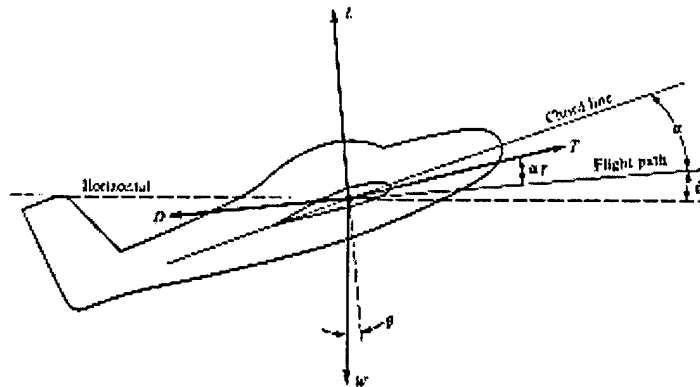


Figure 4-1. Airplane forces during flight

Equation (2) arises from basic aerodynamics, and gives the relation between the necessary lift coefficient of an airplane and the weight at a given altitude.

$$c_L = \frac{W}{0.5\rho_\infty V_\infty^2 S} \quad (2)$$

Where,  $c_L$  is the lift coefficient,  $V_\infty$  the freestream velocity and  $S$  the wing area.

Using equation (2), a useful relation for an airplane at sea level conditions at take-off can be achieved (equation 3, using the English System of units). Here,  $C_{L_{\max}} = 1$  is assumed, as is discussed later. Since the aircraft is restricted to low altitude for reasons of visibility, the sea level condition of air will be used for the necessary calculations.

$$\left( \frac{W}{S} \right) = \frac{V_\infty^2}{841.4} \quad (3)$$

Here, the Wing Loading is a defined factor that is labeled as:

$$\frac{W}{S} \equiv \text{wing loading}$$

This quantity is quite important, since the design wing loading of an airplane is usually determined by factors such as range, maximum velocity, and payload. Also from equation (3) the velocity at which the aircraft can reasonably lift-off (stall velocity) can be iteratively chosen for a given wing loading at a  $C_{LMAX} = 1$ . Table IV-I shows a list of required wing loading at a specified speed. Note that for higher wing loading, greater take-off speed is necessary.

Take off Speed (ft/s)	Wing Loading (W / S , lb / ft <sup>2</sup> )
20	0.48
40	1.90
50	2.97
60	4.28
70	5.82

**Table IV-I. Wing Loading as a Function of Lift-Off Speed ( $C_L=1$ )**

In almost all designs of aircraft, it is essential to know the maximum take-off weight (**MTOW**) of the airplane to achieve the functionality/performance and sizing of the airplane. The MTOW is not often a given parameter, however, and design for such becomes an iterative process. For example, a commercial airline design must take into account the transport of  $x$  amount of passengers and their baggage, the fuel to get to its destination, the effects of altitude and compressibility on the wings' airfoil, etc. These parameters and others contribute to the final weight of the airplane.

For this airplane, there are preset guidelines (Appendix I) that must be met in order to build a successful aircraft. These guidelines, as alluded to before, contribute to the MTOW of the airplane. For example, the aircraft must carry a simulated passenger payload of 7 1/2 pounds, so the next important stage of design is to predict the MTOW.

#### 4.1 Weight Estimation

Unavoidable load contributions in the design of an aircraft come from the structural weight of the vehicle and the weight of the propulsion device (powerplant). The structural weight includes the weight of the wing, empennage, fuselage and landing gear. The powerplant in this case includes the weight from the motor, batteries, propeller and gear. Fixed system and miscellaneous weights from items such as servos and connectors also need to be estimated.

Components can be estimated by using relations compiled over the years for real aircraft. These calculations initially require realistic assumptions of the airplane dimensions, and are highly iterative since the equations include the final MTOW as a parameter. Notice that the wing loading is an important parameter in these equations, which means that these evaluations produce useful aircraft dimensions.

A computer program (Appendix II) was necessary to compute the weights for each component, and thus the total take-off weight.

##### 4.1.1 The Wing

The wing weight is estimated from its planform dimensions when  $k_u = 0$  as follows:

$$W_{\text{wing}} = \frac{(1 + k_{ts}) (0.00945) (\text{MTOW})^{1.195} (A)^{0.8} (1 + \lambda)^{0.25} k_w(n)^{0.5}}{(t/c)^{0.4} \cos(\Lambda_{c/4}) (W/S)^{0.695}} \quad (4)$$

$k_{ts}$  is the coefficient used when there are engines either mounted on the wing or aft of the fuselage, thus  $k_{ts}=0$ ;  $A$  is the aspect ratio,  $\lambda$  is the taper ratio;  $k_w=1$ ,  $n$  is the ultimate load factor (1.5 is used for small aircraft),  $t/c$  is the average thickness to chord ratio; this parameter usually predicts a sensitive choice of airfoil section at high Reynolds numbers at speeds above the critical Mach number. Thus, thin wings with high sweep are used to reduce wave drag. However, this is not a concern since the Mach number and Reynolds number will be quite low throughout the entire mission flight and  $t/c$  will strictly be inherited by the choice of airfoil section.

$\Lambda_{c/4}$  is the angle of sweep at the quarter chord (because of low subsonic speed, the sweep is not necessary to delay drag divergence).

#### 4.1.2 The Empennage

The empennage is typically about 17% of the total wing weight:

$$W_{\text{empennage}} = 0.17 W_{\text{wing}} \quad (5)$$

#### 4.1.3 The Fuselage

The fuselage weight depends mostly on its length ( $L$ ) and the maximum diameter ( $D$ ):

$$W_{\text{fuselage}} = 0.6727 k_f(n)^{0.3} (\text{MTOW})^{0.235} (L)^{0.6} (D)^{0.72} \quad (6)$$

For aircraft that carry passengers,  $k_f$  is a necessary coefficient that depends on the number of passengers, assume  $k_f=1$ . It is kept in mind while dimensioning the fuselage that the payload needs to sit inside and must be readily accessible. An initial estimate of 9.6 inches was used.

#### 4.1.4 The Landing Gear

The landing gear does not contribute much to the total weight of the aircraft, since it is typically assumed to be only 4% of the total airplane weight:

$$W_{\text{LANDING GEAR}} = 0.04 (\text{MTOW}) \quad (7)$$

#### 4.1.5 Fixed Systems And Miscellaneous

These extra components can be assumed to take up only 3.5% of the total plane weight:

$$W_{\text{system}} = 0.035 (\text{MTOW}) \quad (8)$$

As a result, the total plane weight is given by:

$$\begin{aligned} \text{MTOW} = & \frac{(1 + k_{ts}) (0.00945) (\text{MTOW})^{1.195} (A)^{0.8} (1 + \lambda)^{0.25} k_w(n)^{0.5}}{(t/c)^{0.4} \cos(\Lambda_{c/4}) (W/S)^{0.695}} + 0.0627 k_f(n)^{0.3} (\text{MTOW})^{0.235} \\ & + (L)^{0.6} (D)^{0.72} + 0.04(\text{MTOW}) + 0.035(\text{MTOW}) + W_{\text{payload}} + W_{\text{powerplant}} \end{aligned} \quad (9)$$

where  $W_{\text{payload}}$  is the payload weight and  $W_{\text{powerplant}}$  is the contributing weight of the propulsion components described above.

## 4.2 Airfoil Selection

### 4.2.1 Airfoil Characteristics at Low Reynolds Number

In many applications, it is not uncommon to have the need arise for airfoil characteristics at Reynolds number ( $R$ ) values much lower than those for which most of the NACA and NASA data were obtained for. These data were obtained at  $R$  values of  $3 \times 10^6$  or higher.

Experiments have been carried out to predict airfoil behavior at low  $R$  ranges. NASA affiliates R. Eppler and D.M. Somers wrote a program for the design of low speed airfoils. It was found that the form of the lift curves change substantially, over the  $R$  range from  $4.2 \times 10^5$  to  $0.42 \times 10^5$ . Particularly at the lowest Reynolds number, the  $C_l$  versus  $\alpha$  plot is no longer linear. The flow separates at all positive angles just downstream of the minimum pressure point, near the maximum thickness location.

A more recent experimental and numerical study was performed by two engineers, (Donovan, J.F., and Selig, M.S., *Low Reynolds Number Airfoil Design and Wind Tunnel Testing at Princeton*). Using Eppler and Somers Airfoil Code, Donovan and Selig investigated a number of airfoils followed by wind tunnel testing. The study included new airfoils designed to tailor the chordwise pressure distribution at low Reynolds numbers to promote low drag. At  $R$  values less than approximately  $5.0 \times 10^5$ , an extensive laminar separation bubble can form on either surface, which significantly increases the drag. Therefore, the study examined means to shorten the bubble or promote transition to a turbulent boundary layer at a low value of  $R$ .

### 4.2.2 Airfoil Tradeoffs

Keeping in mind the discussion above, an airfoil section can now be chosen. Two choices exist at this stage;

(i). Typically, conventional airfoils without any special lifting devices will deliver  $C_{lmax}$  values of approximately 1.3 to 1.7, depending on Reynolds number, camber, and thickness distribution.

An existing airfoil can be chosen and its drag polar ( $C_{d,p}$ ) corrected for low Reynolds numbers.  $C_{d,p}$  can further be estimated as a flat plate (drag polar data is available in Appendix III for a flat plate) for  $R$  values less than 150,000. This should be a good estimation since by adding thickness to a thin, cambered plate and providing a rounded leading edge, the performance of the plate is improved over a range of angles, with the leading edge separation being avoided all together. Thus, in a qualitative sense we have defined a typical airfoil shape. Camber and thickness are not needed to produce lift (a **flat plate** can produce lift), but are instead used to increase the maximum lift that a given wing area can deliver.

It is appreciated that  $C_{lmax}$  is dependent on  $R$ . Thus, looking at two typical airfoils, the GA(W)-1 and the NACA four-digit airfoils, the variation of  $C_{lmax}$  can be compared. Experimental data shows that  $C_{lmax}$  as a function of  $R$  and thickness ratio ( $t/c$ ) for NACA four series increases with  $t/c$ . At an intermediate thickness ratios of around 0.12, the variation of  $C_{lmax}$  with  $R$  parallels that of the 17% thick GA(W)-1 airfoil. Note at least for this camber function that a thickness ratio of 12% is about optimum and the increased design maximum lift coefficient is a better tradeoff with a larger chord length. Also the data also shows that around  $t/c = 0.16$  values of  $C_{lmax}$  become linear and are maximum.

On further inspection, the NACA five-digit series uses the same thickness distribution as the four-digit series. The mean camber line is defined differently, to increase  $C_{lmax}$ . In fact, for comparable thickness the five series  $C_{lmax}$  is of the order 0.1 to 0.2 higher. The 23012 airfoil would therefore be a good choice, having a design  $C_l=0.3$  and  $C_{lmax}=1.8$ . Further characteristics of the airfoil are presented in Appendix IV.

(ii). The previously mentioned study produced an airfoil shape designated E374, which is pictured in Appendix V along with its lift and drag characteristics. It is designed to operate at a lift coefficient of 0.55 and  $C_{lmax}=1.0$ . However, below an  $R$  of 150,00 the drag coefficient rises rapidly.

#### 4.2.3 Final Airfoil Choice

The decision was made to go with the NACA 23102 airfoil, whilst accommodating for necessary drag as discussed beforehand, since at the time of the "close" of the design stage the optimum low speed airfoils were not found.

An average thickness ratio of 16% was chosen and hence fixed the average geometric chord at 0.75 ft for the 12% thick airfoil.

Note: Initial estimates used for the program were:  $b=6.5$  ft,  $\lambda=0.5$  (for small aircraft the root chord is recommended to be twice the tip chord length),  $A=8.67$ ,  $t/c=0.16$ ,  $c=0.75$  ft,  $c_t=0.5$  ft,  $c_o=1$  ft..

Wing Loading (W/S, lb/ft <sup>2</sup> )	2	2.5	3	4
Component	Weight(lbs.)			
WING	2.796	2.303	1.975	1.563
EMPENNAGE	0.475	0.391	0.336	0.266
FUSELAGE	2.681	2.660	2.647	2.629
LANDING GEAR	0.692	0.685	0.655	0.637
TOTAL STRUCTURAL WEIGHT	6.644	6.025	5.613	5.094
MOTOR	0.43			
BATTERIES	2.50			
PROP & GEAR	0.10			
TOTAL POWER PLANT WEIGHT	3.03	3.03	3.03	3.03
TOTAL PAYLOAD WEIGHT	7.5	7.5	7.5	7.5
FIXED SYSTEMS AND MISC.	.606	.586	.573	.557
Maximum Take-off Weight	17.78	17.141	16.716	16.18

Table IV-II. The Comparison of MTOW to the Wing Loading

#### 4.3 Initial Performance

Table IV-II presents some critical design considerations, but they are nothing without investigating the effect on parameters such as the lift coefficient,  $C_L$ , and total drag,  $C_D$ , of the aircraft at the varying wing loading as presented in Table IV-III.

The estimation of the total drag of an airplane is difficult, even for the simplest configurations. The following possible drag modes partly reveal why this is so.

**The induced drag,**  $C_{Di}$ , is the drag that results from the generation of a trailing vortex system downstream of a lifting surface of finite aspect ratio.

$$C_{Di} = \frac{C_L^2}{\pi e A} \quad (10)$$

$$e = 0.95.$$

$$C_{di} = k C_L^2, k = 1/\pi e A$$

**The parasite drag,**  $C_{D,o}$ , is the drag of the airplane not directly associated with the production of lift, and includes many drag components, such as, the skin friction drag, form drag, interference drag, trim drag, profile drag and cooling drag. The parasite drag can be estimated in terms of the total wetted area of the plane and its MTOW.

$$C_{D,o} = \frac{f}{S} \quad (11)$$

where  $f$  is calculated as shown below.

$$\log_{10} S_{wet} := 0.0199 + 0.7531 \log(MTOW)$$

$$\log f := \log_{10} S_{wet} + -2.5229$$

$$f := \exp(\log f) \cdot 2.3025$$

Since it is apparent that the 2-D airfoil section will see more skin friction and form drag, it is estimated from the charts in Appendix IV.IV & V and corrected for thickness. The profile drag should be more than the parasite drag as a check for correctness.

$$C_{d,o} = C_{d,p} (Re = 5 \times 10^6) \quad (12)$$

Now, the total drag can be estimated:

$$C_D = C_{d,o} + C_{di} \quad (13)$$

W/S, lb/ft <sup>2</sup>	MTOW, lbs.	S, ft <sup>2</sup>	b, ft	log <sub>10</sub> (S <sub>wet</sub> )	log <sub>10</sub> f	f, ft <sup>2</sup>	C <sub>D,o</sub>
2	17.78	8.89	11.85333	0.952	-1.571	0.027	0.003037
2.5	17.14	6.856	9.141333	0.942	-1.581	0.026	0.003792
3	16.7	5.566667	7.422222	0.934	-1.588	0.026	0.004671
4	16.18	4.045	5.393333	0.9245	-1.588	0.025	0.006

**Table IV-III. Wing Dimensions and Variation of Plane Drag at Different Wing Loadings**

Now, there exists a tradeoff for vehicle sizing. It is seen that the maximum take-off weight of the vehicle increases as the wing span increases. However, from Table I, a small W/S allows the vehicle to be airborne sooner, which makes a take-off speed of 40 ft/s a tempting choice. This requires a W/S close to two. As Table IV-III clearly shows that at this W/S the vehicle would require a wing span of nearly 12 feet, which would raise questions of deflection failure and overall strength of the wing.

Not shown in the tables, but easily interpolated from equation 2, is the fact that  $C_L$  needs to increase with W/S. The only drawback is that  $C_{di}$  increases also. Since the profile drag of the airfoil is going to drive the contribution of the parasite drag, the induced drag is the main contributor to the overall drag. An optimum choice from the preceding discussion would be a wing loading between 3 - 4 lb/ft<sup>2</sup>, representing realistic take-off velocities from 50 to 60 ft/s.

The variation of the drag with lift over these ranges of W/S are looked at in Table IV-IV. The final contributing factor is the thrust required by the plane to lift-off. This parameter contributes to the sizing of the power plant and thus the lift-off distance and in-flight performance:

$$T_R = \frac{W}{L/D} \quad (14)$$



W/S	Velocity(ft/s)	Re	C <sub>L</sub>	C <sub>DI</sub>	C <sub>d,o</sub>	C <sub>D</sub>	L/D	T <sub>R</sub> (lbs)
3	50	250,592	1.01	0.0394177	0.108	0.1474177	6.849	2.438
3	55	275,651	0.83	0.0269228	0.1104	0.1373228	6.077	2.748
3	60	300,710	0.70	0.0190093	0.009	0.0280093	25.033	0.667
3	65	325,769	0.60	0.0138012	0.00852	0.0223212	26.766	0.624
4	50	250,592	1.35	0.070076	0.108	0.178076	7.560	2.140
4	55	275,651	1.11	0.0478628	0.1104	0.1582628	7.030	2.302
4	60	300,710	0.93	0.0337944	0.009	0.0427944	21.846	0.741
4	65	325,769	0.80	0.0245356	0.00852	0.0330556	24.098	0.671

**Table IV-IV. Variations of Coefficients with Wing Loadings**

From here it can be seen that a W/S of 4 yields slightly better results, requiring less thrust at lift-off. On closer inspection, however, increasing the W/S decreases the wing area. Looking at Equation (15) for the lift-off distance,  $s_{LO}$ , of an aircraft, the  $s_{LO}$  is decreased by increasing the wing area, increasing  $C_{L,max}$ , and increasing the available static thrust,  $T$ . Lift-off distance is very sensitive to weight, and looking at equation 16, the necessary thrust is increased with higher W/S. Since the weight difference between the two wing loadings are minimal a W/S of 3 would be the ideal choice.

$$s_{LO} = \frac{1.44W^2}{g\rho SC_{L,max}T} \quad (15)$$

In fact, knowing the field distance, a relation for least available thrust for take-off as a function of W/S can be compiled. Assume that  $C_{L,max}$  is limited to 1.

$$T_{min} = \frac{18.814W}{300} (W/S) \quad (16)$$

From here it can be seen that the minimum thrust increases with wing loading, so at a W/S equal 3,  $T_{min}$  required is 3.14 lbs (50 ounces).

As of this stage the vehicle sizing looks as follows:

Wing Loading, lb/ft <sup>2</sup>	3.00
MTOW, lbs	16.7
Wingspan b, ft	7.4
Wing Area S, ft <sup>2</sup>	5.67
Aspect ratio, A	8.67
Root Chord, ft	1
Tip Chord, ft	0.5
Fuselage Diameter, ft	0.8
Mean Chord(geometric), ft	0.75
Mean Chord (dynamically), ft	0.788
T <sub>mino</sub> (lbs.)	3.14 (50.24 ounces)

This closes the section on the preliminary design of the vehicle. Now the question of producing necessary thrust for the vehicle arises. Also, dimensioning will change as the optimum performance of the aircraft is zeroed in on. Components may decrease or increase in number and size as performance optimization is explored. The time of flight will depend on the number of battery cells and other factors which will contribute to affecting the total weight. These and other factors are explored in the next section.

## **5. DETAIL DESIGN**

As of the start of this stage of the design, the payload dimensions were modeled reducing the fuselage diameter to 0.33 ft. Re-estimating the weights as in the previous section the weight was reduced and the final configuration and performance calculations are shown in Appendix V.

The aircraft's control surfaces were estimated following the discussion on stability and control in the next section and then the propulsion of the vehicle.

### **5.1 Stability and Control**

Stability of an aircraft refers to its movement in returning, or tendency to return, to a given state of equilibrium, frequently referred to as trim. More specifically, an aircraft can experience two types of stability phenomena. Static stability refers to the tendency of an aircraft under steady conditions to return to a trimmed condition when disturbed rather than any actual motion it may undergo following the disturbance. The forces and moments are examined to determine if they are in the direction to force the aircraft back into equilibrium. If so, the aircraft is statically stable.

#### **5.1.1 Dynamic stability**

There are three basic controls on an airplane: the ailerons, elevator, and rudder -- which are designed to change and control the moments about the x, y, and z axes. These control surfaces are flaplike surfaces that can be deflected back and forth at the command of the pilot.

##### **Vertical Stabilizer**

A fin area from 7% to 12 % of the wing's area is recommended

##### **Rudder Area**

A rudder area of 30% to 50% of the total fin area will work well.

##### **Horizontal Stabilator**

The total area of the horizontal stabilator should be about 20% to 26% of the total wing area. For a fin of 7% make the stabilator 20% of the wing area.

##### **Elevators**

Normally 25% to 30% of the total stabilizer area.

##### **Engine location**

An engine located 21% to 27% of the wing span is suitable. A nose moment of 25% of the wingspan is a good average. The actual engine location is usually measured from the C.G. to the propeller. The distance used was measured from the leading edge of the wing to the propeller.

##### **Neutral Point**

For an aircraft to be statically stable, the cg must be ahead of the neutral point. A static margin of at least 5% is recommended to maintain static longitudinal stability. The calculation for the location of the center of gravity is found in Appendix VI.

### **5.2 Production of Thrust**

Now it is obvious that the necessary thrust has to be produced from the motor in Appendix I. This requires gearing and placing the right propeller dimensions and battery cells to produce the required thrust for a certain amount of time. This is important since, as shown before, more thrust equals a shorter takeoff distance and the aircraft has to (1) get off the ground and (2) fly for at least 7 minutes also the number of

battery cells influences the planes total weight. Hence it is necessary to determine the optimum propeller size and cell configuration for the best static and in-flight thrust characteristics of the plane.

Importantly, the  $s_{LO}$ , must accommodate for a safety clearance of 6 feet after takeoff. Assuming that a 6 foot obstacle is placed at the end of the 300 foot runway, then a minimum lift-off distance  $x$  and climb angle must be achieved at a minimum climb thrust.

$$\text{From eq.(16), } T_{\min \text{ object}} = \frac{18.814W}{300 - x} (W/S) \quad (16a)$$

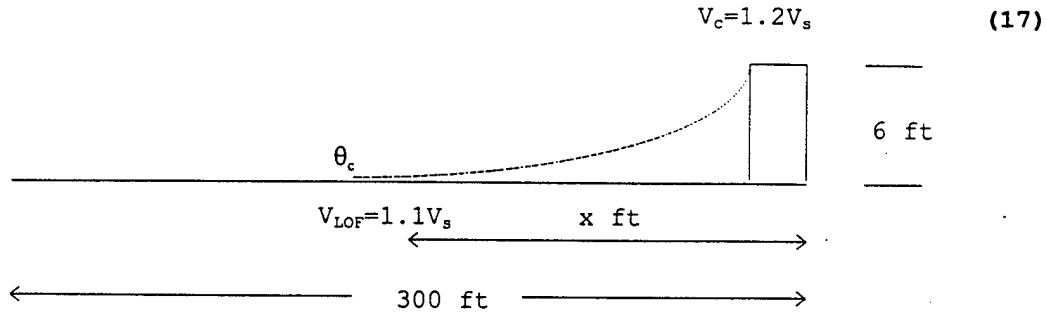


Figure 5-1. Takeoff Obstacle Diagram

The necessary climb angle  $\theta_c = \tan^{-1}(6/x)$  eq. (17). This correlation is also related to the velocities during the climb of the vehicle as follows:

$$\theta_c = \tan^{-1} V_c/V \quad (18)$$

$V_c$  (R/C) is the climb velocity(fps) at the climb rate and can be estimated as given by FAA rules for climb over a 35 ft obstacle as  $1.2V_s$ , where

$$V_s = \sqrt{\frac{2W}{\rho S C_{L, \max}}} \quad (19)$$

$C_{L, \max} = C_{L_0} + C_{L_\alpha} \alpha$ , however, in ground roll estimate  $C_{L, \max} = 1$ , since the angle of attack of the plane is restricted such that the tail doesn't drag the ground.  $V$  is the ground speed which could be estimated as the lift-off speed,  $V_{LOF}$ .

Thus from Eq's (17) & (18),

$$x = \frac{6}{\left(\frac{RC}{60} / V_{LOF}\right)}$$

$$\text{The rate of climb R/C at } T_{\min} \text{ is given by: } 60[V_c(T_{\min} - D)]/W \quad (20)$$

where  $D$  is the drag at that time and  $W$  is the weight of the plane.

From the value of  $V_s$  (from Appendix IX) and equation (17), the climb velocity is 59.8 ft/s.  $D$  is 0.67 lbs and the R/C = 533.2 fpm at  $9.2^\circ$ . Thus, the minimum takeoff distance for the aircraft is  $x = 37$  feet.

From equation (16a), and a couple of iterations the static thrust of the prop must be equal to at least 3.5 lbs (57.34 ounces) to clear the object leaving the ground at  $x = 32$  feet before the obstacle. Hence, the plane should leave the ground at least 268 feet down the runway.

### 5.3 Propeller Analysis

The airflow seen by a given propeller section is a combination of the airplane's forward motion and the rotation of the propeller itself. The net thrust of a propeller when summed over its entire length of the blades, yields the net thrust available which drives the airplane forward. The propeller is analogous to a finite wing that has been twisted. The propeller efficiency,  $n$ , is defined as

$$n = P_A/P \quad (21)$$

where  $P$  is the shaft brake power (the power delivered to the propeller by the shaft of the engine) and  $P_A$  is the power available from the propeller.

The power input would simply be the total current available x the terminal voltage. The output power would be affected by the heat dissipated by the batteries.

The efficiency for an electric motor can be determined in terms of its power loading. Hence the available power would be in terms of the output power loading ( $W/lb$ ) and the shaft brake power an input power loading ( $W/lb$  or  $W/kg$ ).

The power available is an aerodynamic phenomenon which is dependent on the angle of attack and pitch angle of the propeller airfoil. So the pitching of the propeller is important to the thrust it produces.

The propeller may become stalled if the propeller blades are producing far less thrust than predicted (they are basically just beating the air and absorbing a lot of power from the motor). This is typical with high pitch:diameter ratio propellers at low flight speeds.

An effective propeller pitch (in inches or centimeters) also has to be looked at, and indicates the effective pitch of the propeller at the indicated airspeed (as the plane gains speed and begins to move through the air, the propeller works as if it had a reduced pitch). Another contributor to the time of flight is the predicted pitch speed, in miles per hour or meters per second. This is the speed of the air as it leaves the back of the propeller, relative to the plane (i.e. the excess pitch speed, beyond the speed at which the plane is flying).

### 5.4 Thrust Charts

The static thrust for a motor is given by:

$$T = P_{io}^{2/3} (2\rho A)^{1/3} \quad (17)$$

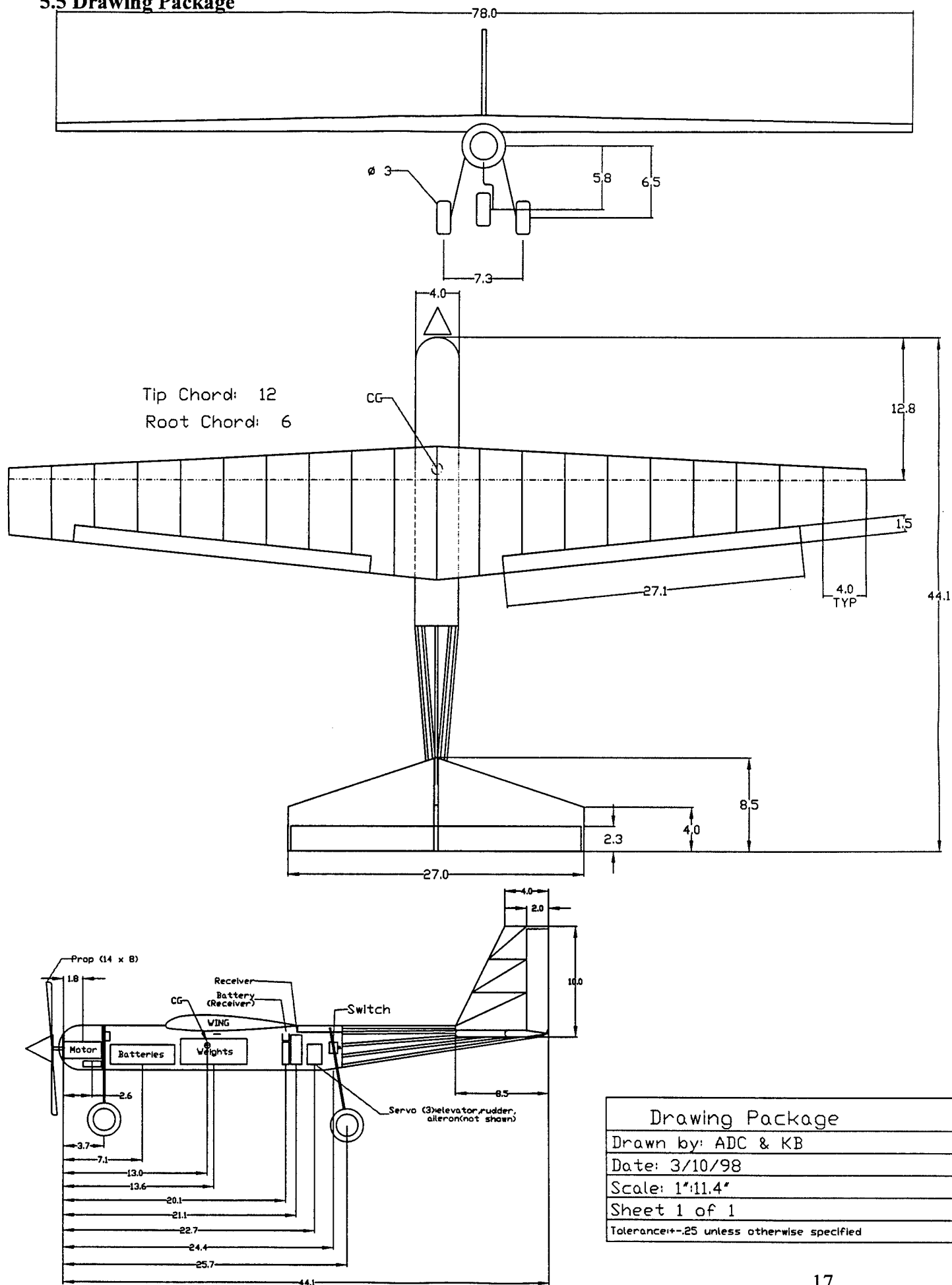
where  $A$  is the cross-sectional area of the blade and  $P_{io}$  is the motor output power.

Prediction of the motor performance is a little complex, hence, the aid of a computer program was rendered. Appendix VII shows data used to screen possible configurations. The battery cell count was minimized to from 15 - 19 cells, since one cell weighs about 2.05 oz. The motor has already been geared and as such, a range of propeller diameters and pitch lengths have been specified in Appendix I.

Looking at Appendix VII, the table shows that there is not sufficient static thrust available without possible stall of the blades at a diameter of 11 inches over the entire range of available pitch. Therefore, a higher blade diameter has to be used. On continuing iterations of the propeller versus the pitch and diameter of the blades an optimum thrust and time of flight at level flight was found to be for a 14 x 9 propeller on seventeen battery cells at a static thrust of 84.2 ounces. Results in Appendix VIII show that maximum flight time at 87% throttle to be 12 minutes at a maximum speed of 60 MPH. At 100% throttle the flight time is reduced to 8 minutes at level flight at the maximum speed of 70 MPH.

Appendix IX shows that performance calculations of the plane. They indicate a level speed of 41 MPH and a stall speed of 34 MPH. A take-off distance of 168 feet is estimated.

## 5.5 Drawing Package



### Drawing Package

Drawn by: ADC & KB

Date: 3/10/98

Scale: 1"=11.4"

Sheet 1 of 1

Tolerance:  $\pm .25$  unless otherwise specified

## 6. Manufacturing Plan

### 6.1 Wing and Empennage

The final manufacturing process for the wing and empennage was selected after researching three possible procedures. A polystyrene core wing with balsa sheeting, a traditional balsa wood wing with ribbed internal structure, and a graphite composite structure were considered. The factors which determined the selection of a final procedure were cost, availability, reparability, and skill level required to manufacture the material. A traditional balsa wing turned out to be the best overall option according to these parameters.

Characteristics for each material were researched and charted in comparison to each other.

	Foam	Balsa	Graphite
<b>Availability</b>	Excellent	Excellent	Excellent
<b>Reparability</b>	Average	Excellent	Poor
<b>Skill Level</b>	Moderate	Low	High
<b>Density</b>	1.0 g/cm <sup>3</sup>	0.15 g/cm <sup>3</sup>	1.8 g/cm <sup>3</sup>
<b>Tensile Strength</b>	40 MNm <sup>-2</sup>	35 MNm <sup>-2</sup>	650 MNm <sup>-2</sup>
<b>Cost</b>	\$45.00	\$53.00	\$200.00

Table VI-I. *Wing Materials*

Each material was readily available through mail order or local hobby supply shops, and therefore was not a determining factor in selecting one material over another. The reparability factor was more influential in the final selection. The wing must have the capability to be quickly repaired during competition in case of damage sustained during a hard landing or crash. Polystyrene foam is not easily mended because many adhesives deteriorate it. Graphite composite is difficult to repair in the field because the process used to form any graphite composite part is time consuming. Balsa has the best reparability characteristics because it can quickly and easily be mended in the field using cyanoacrylate (CA) glue.

The skill level required to manufacture the material was also an influential factor because time is a constraint. Polystyrene is moderately difficult to work with because a hot wire must be used to shape it. Graphite composite is an advanced material which was not considered for the wing and empennage because the time requirements necessary for design and construction of a mold were not acceptable. Balsa was the easiest material to manufacture because no special tools are needed to shape it.

The cost of graphite composite was a major factor in eliminating it from possible contention even though it has a higher tensile strength than either balsa or foam. Balsa and polystyrene are comparable in cost, and balsa was the better choice due to its favorable reparability characteristics and ease of construction.

The fabrication process for balsa was created by researching radio control model airplane books and manuals. The dimensions of the ribs are critical to the construction of the wing because they hold the shape of the airfoil. ModelCalc, an airfoil program, was used to produce accurate full scale plots of the various size ribs for the tapered wing. The wing was drawn on AutoCad R13 and plotted full scale to be used as direct reference during construction. The wing plans include placements of spars, ribs, sheeting, ailerons, and the leading and trailing edge. This reduced the cost of manufacturing by eliminating the need to buy full scale blueprints at a cost of \$9.00 per drawing. The drawings are covered with wax paper and placed on an angled surface due to the wing taper. The wood must be prepared prior to beginning construction. The ribs are cut by placing balsa wood sheets under the full scale rib plots and cutting the pattern for each individual rib. In order to reduce weight, the unnecessary interior area of each rib is removed. The balsa spars are cut to length and strengthened by adding strips of graphite fiber to two opposite sides. This technique gives it added strength with a minimal weight increase of 0.2oz.

The wing is constructed of two symmetric halves. The bottom spar and trailing edge are pinned into place on top of the plans. First, the trailing edge is attached to a jig which ensures that the ribs are

aligned in proper orientation. Next, each rib is glued to the trailing edge and spar. Then, the top spar is attached, and webs are glued into place for reinforcement. The leading edge and sheeting are now glued into place. Wingtips are made by carving blocks of balsa, and are small in size due to the tapered wing. The ailerons are the only moving parts on the wing, and attach to the trailing edge by CA hinges. The second half of the wing is built, and the two halves are joined using epoxy and fiberglass.

The construction of the empennage is much more simple than the wing because it is not designed as an airfoil. The plans for the empennage truss design were drawn on AutoCad, and were plotted to be used as reference for construction. In order to minimize weight, the vertical and horizontal stabilizer are built by constructing a frame, and reinforcing it with a simple truss. The elevator and rudder must be attached with control rods and CA hinges by a similar procedure used for the ailerons.

## 6.2 Fuselage

During the preliminary design phase for the fuselage, there were four material choices available to the team. The material choices were: 1) Balsa, 2) Fiberglass, 3) Kevlar, and 4) Graphite. These four materials were compared on the basis of a series of criteria that would be applicable for this project. The qualitative comparison is shown below in Table VI-II.

A preliminary construction plan was necessary at this time to assist in the evaluation of the material selection. However, a wooden fuselage would have to be constructed differently than a composite fuselage. Therefore, both wooden and composite construction plans needed to be developed. In comparison to the design from the previous year, a wooden fuselage would be constructed as a box from four planes. Whereas, typically, high strength, light weight composite materials are cast from molds pulled off precision made plugs. However, due to the construction phase time constraints, a more expedient method of construction would be required if a composite material was to be chosen. This resulted in a study into alternate means of composite construction.

These alternate means consisted of moldless construction and pre-made molds, in addition to the typical mold casting process. Moldless construction is a method typically utilizing a foam core with composite materials draped over top of the foam. Whereas a pre-made mold would have to be already in existence and be exact to the specifications of the fuselage required.

A radical, low cost, fast construction method was suggested for composite molding by one of the members of the team. Instead of building a mold to fit the needs of the fuselage, a section of 4 inch diameter PVC piping could be cut lengthwise to reveal two half cylinders, which then could be surface finished as typical composite molds and used as the final molds. These two molds would produce two composite half cylinders which would then be placed back into the molds and attached together to produce a thin walled composite cylinder for use as the fuselage. It was suggested that the curing time could be shortened by heating the molds during the cure cycle. This would require an oven. An additional radical method was conceived to shorten the manufacturing time by this heating procedure. A steel cabinet with a space heater placed inside was suggested for use as an oven. A thermometer must be placed inside the cabinet for use as the thermostat. The setting of the space heater was altered until a constant temperature of roughly 100°F was reached. This mold making procedure would be effective at a low cost, and would produce a product with minimal construction time.

A comparison as to the overall strength of each material was also necessary. Balsa, being the least strong, would be comparable to fiberglass. Kevlar was shown to be roughly twice as strong. Graphite would then be stronger still, at roughly three times the strength of fiberglass. Each of these materials are however differ in other various properties; kevlar has high impact resilience, while graphite has high flexural strength.

It was believed that cost would weigh greatly into the material selection. However, after a series of detailed studies, it became apparent that the three composite materials would all be comparable, with a balsa configuration being marginally less expensive (see Appendix X).

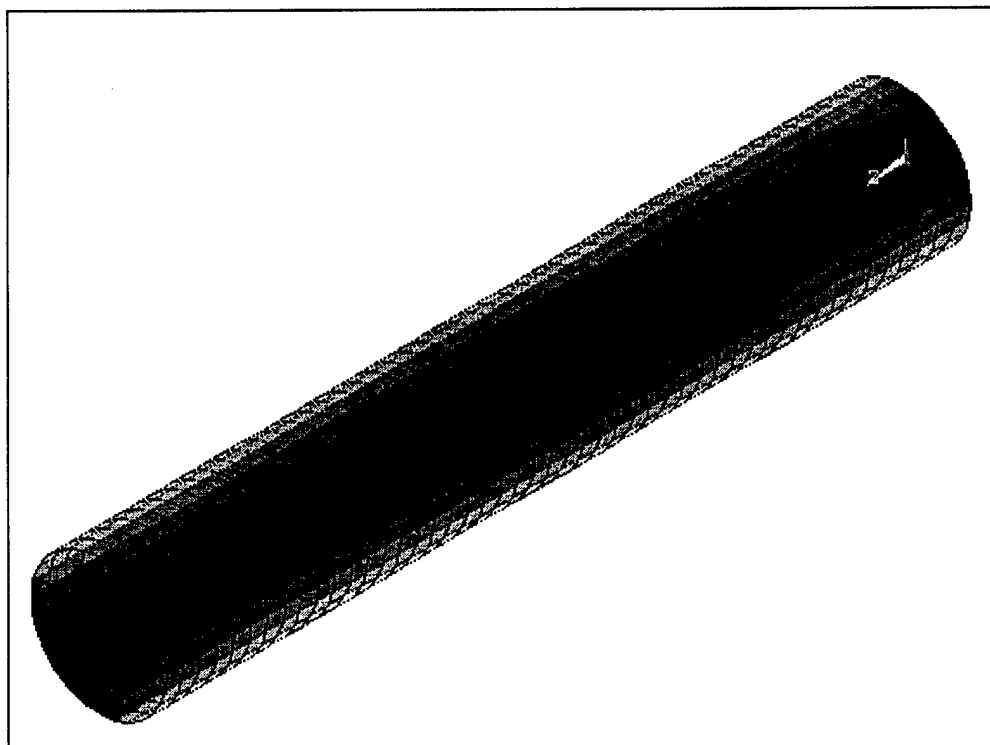
After taking all things into account (as shown in Table VI-II), Graphite became the material of choice. It was also decided to use the PVC molding method as described above. This was expected to produce a strong lightweight fuselage at a lower cost than typical molding techniques. This would then be used as the structural member of the airframe.

	Balsa	Fiberglass	Kevlar	Graphite
Cost	3	3	2	1
Strength to Weight	2	2	3	4
Elastic Strength	2	2	3	4
Flexural Strength	2	3	2	4
Availability	3	3	3	3
Workability	3	2	2	2
Prerequisite of Experience	3	2	2	2
Time of Manufacture	3	2	2	2
Knowledge Gained	2	3	4	4
Design Improvement Over Previous Year	1	2	3	4
Total	24	24	26	30

4-Excellent 3-Good 2-Fair 1- Poor

**Table VI-II. Qualitative Fuselage Materials Comparison**

A finite element model was developed to determine the specific number of layers and orientation of the plies of graphite needed to withstand the loads that the fuselage would see in flight (see Figure 6-1). This model suggested that the fuselage could be constructed with only two layers and still withstand to in-flight loads. However, a decision was made to use three layers, in order to account for any fabrication errors.



**Figure 6-1. Finite Element Model of Composite Fuselage**



### 6.3 Boom

Connection of the fuselage to the empennage was another major consideration to take into account. A similar PVC molding method was considered for fabrication of a boom which would connect the fuselage to the empennage. However, it was decided that there would be too many places for error in the fabrication phase of a tapered boom which could result in an in-flight failure. Another consideration was a wooden dowel for use as the boom. This idea was ruled out after weight consideration. This led to the decision of designing a balsa wood boom to connect the fuselage to the empennage. A design for this boom was developed utilizing a finite element model (see Figure 6-2). This boom would be connected to the interior of the finished fuselage and it would run to the empennage. The boom was designed such that the vertical tail and horizontal stabilizer could be inserted into the rear section of the boom through sized cutouts. It was decided to use a frame of eight balsa beams that would connect together at the rear of the aircraft and connect directly to the fuselage.

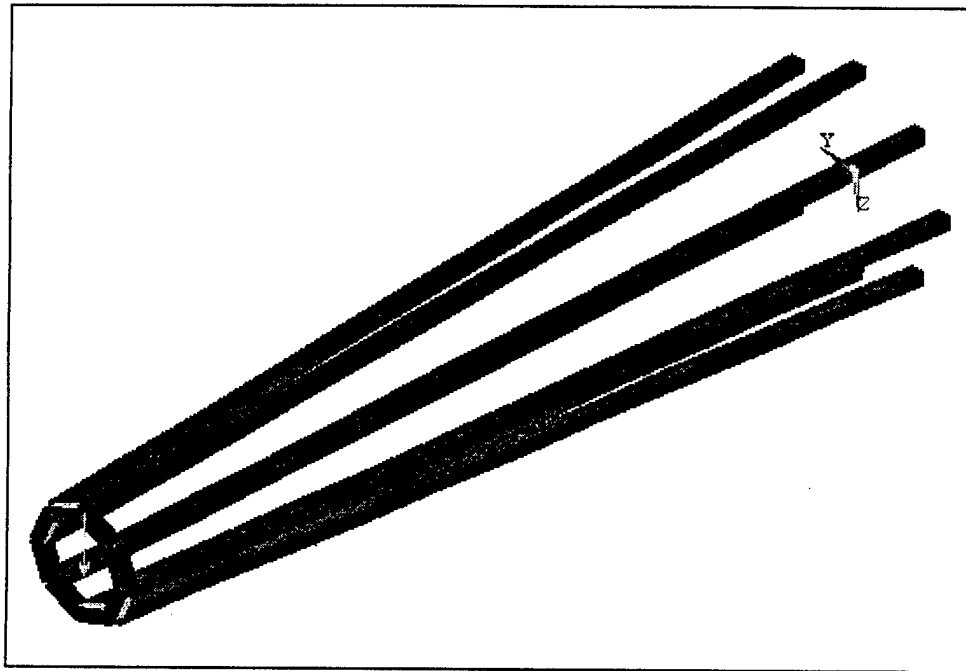


Figure 6-2. *Finite Element Model of Wooden Boom Section*

### 6.4 Assembly

Following construction of all necessary components, the aircraft would have to be assembled. In order to reduce any unforeseen assembly problems an assembly plan was conceived. This determined the steps in manufacturing, and resulted in a manufacturing schedule (see Table VI-III). This schedule was to coincide with the Management milestone schedule.

It was decided that the fuselage should be constructed first, as every part of the aircraft, except the empennage, will be attached to it directly. This would take at least a week to construct, as each molded piece takes 24 hours to cure. Also, if there are any unforeseen problems in utilizing the radical molding procedure, there would be ample time to correct for them. Shortly after beginning construction of the fuselage, there would be sufficient time to begin construction of the wing.

Task	State	Proposed Date	Actual Date
Ordering of Parts	Begun	2/6/98	3/6/98
Ordering of Parts	Completed	2/13/98	3/10/98
Fuselage Construction	Begun	2/13/98	3/9/98
Wing Construction	Begun	2/17/98	3/10/98
Fuselage Construction	Completed	2/20/98	TBA
Nose Construction	Begun	2/20/98	TBA
Nose Construction	Completed	2/24/98	TBA
Wing Construction	Completed	3/6/98	TBA
Wing Cutout	Completed	3/9/98	TBA
Boom Construction	Begun	3/9/98	TBA
Empennage Construction	Begun	3/10/98	TBA
Empennage Construction	Completed	3/17/98	TBA
Boom Construction	Completed	3/17/98	TBA
Boom/Empennage Integration	Begun	3/18/98	TBA
Boom/Empennage Integration	Completed	3/23/98	TBA
Electronics Integration	Begun	3/24/98	TBA
Landing Gear Integration	Begun	3/24/98	TBA
Landing Gear Integration	Completed	3/28/98	TBA
Electronics Integration	Completed	4/1/98	TBA
Control Rod Integration	Begun	4/3/98	TBA
Control Rod Integration	Completed	4/6/98	TBA
Final Manufacturing & Painting	Completed	4/13/98	TBA

**Table VI-III. Manufacturing Schedule**

As soon as the fuselage is completed, extra attention should be given to the wing. As soon as the wing is completed, the cutout of the fuselage for the wing must be done. It must be done as soon as possible so that the boom can be attached to the fuselage section. Also at this time, the nose can be manufactured. This nose piece will assist in the aerodynamic flow from the spinner to the main fuselage. It is to be carved out of four pieces of balsa and sanded down to create a smooth surface. It must be made to fit just inside the fuselage cylinder and still have a flush transition from the one piece to the next.

Soon after completing the fabrication of the nose piece, the wing fabrication should be completed. This will now allow for the removal of the section of the fuselage which will be replaced by the wing in the final construction phase. If the wing is not complete at this time, the dimensions of the cutout section can be found using the dimensions of the wing ribs. This construction alternative assist in keeping the construction phase moving if there are setbacks in wing fabrication. After the wing cutout has been removed from the fuselage, construction can begin on the boom.

After the boom construction has begun, the empennage construction can also begin. These two components should be completed in similar intervals of time. Thus the integration of these two components can begin as soon as they are both completed. At the completion of this manufacturing step, there will be a fuselage with a nose, a boom, an empennage, and a fully fabricated wing.

At this stage the electronics and weights will be mounted inside the fuselage utilizing conformed pieces of balsa to distribute loading on the composite cylinder shell. Also, all control rods must be installed inside the fuselage at this time. Following this installation and the connection of the wing to the fuselage, the aircraft will be ready for aesthetic alterations, such as painting and covering with monocothe. After this stage, the aircraft will be ready for ground testing and then flight testing.

---

---

APPENDIX  
I

---

DESIGN GUIDELINES AND PERFORMANCE SPECIFICATIONS

Payload	=	7.5 pounds
Battery Pack	=	2.5 pounds*
Field Length	=	300 feet
Scheduled flight time	=	7 minutes

---

Baseline Motor		Aveox 1406/4Y
Gear Box		Aveox/Robbe 3.7:1
Recommended pitch		7 - 13 inches
Recommended diameter		11 - 16 inches
Turns	=	4
Speed constant	=	1500 RPM/V
Continuous/Peak current	=	18A/41A
Resistance	=	.06 Ohms
Idle Current	=	1.2 Amps
Weight	=	6.9 ounces (0.43 pounds)

**Notes:** A six foot obstacle must be cleared within the field length takeoff.

\* The maximum battery pack weight allowed.

---

---

## APPENDIX

## II

---

### WEIGHT ESTIMATION PROGRAM

```
#include<iostream.h>
#include<math.h>
#include<stdlib.h>
#include<conio.h>
#include<stdio.h>

double ar, tr, tc;
double mc, s;
double W, WL, lf;
double L, D, payload, motor, battery, prop;

double Max_Weight(double MTOW, double aspect_ratio, double taper_ratio,
double n, double thick_chord, double sweep, double wing_loading, double
Length, double Diameter)

{

    cout << "\n\nEnter the total payload weight (pounds): " ;
    cin >> payload;

    cout << "\n\nEnter the motor weight (ounces): " ;
    cin >> motor;

    cout << "\n\nEnter the max. battery pack weight (pounds): " ;
    cin >> battery;

    cout << "\n\nEstimate the gear and prop weight (ounces): " ;
    cin >> prop;

    double WING = ((0.00945)* pow(MTOW,1.195) * pow(aspect_ratio,0.8)
* pow((1+taper_ratio),0.25) * pow(n,0.5))/ (pow(thick_chord,0.4) *
cos(sweep) * pow(wing_loading,0.695));
    double EMPENNAGE = 0.17 * (WING);
    double FUSELAGE = 0.6727 * pow(n,0.3) * pow(MTOW,0.235) *
pow(Length,0.6) * pow(Diameter,0.72);
    double LANDING = 0.04*(MTOW);
    double SYSTEM = 0.035*(MTOW);

    double STRUCT = WING + EMPENNAGE + FUSELAGE + LANDING;

    double PAYLOAD = payload;
    double POWER = motor/16 + battery + prop/16;
```

```

        cout << "\n\nThe wing weight = " << WING << " pounds " ;
        cout << "\n\nThe empennage weight = " << EMPENNAGE << " pounds ";
        cout << "\n\nThe fuselage weight = " << FUSELAGE << " pounds ";
        cout << "\n\nThe landing gear weight = " << LANDING << " pounds
";
        cout << "\n\nThe total structural weight = " << STRUCT <<
"pounds";
        cout << "\n\nThe total payload weight = " << PAYLOAD << " pounds
";
        cout << "\n\nThe fixed system weight = " << SYSTEM << " pounds ";
        cout << "\n\nThe total power plant weight = " << POWER << "
pounds ";

        cout << "\n\nThe total plane weight = " << PAYLOAD + SYSTEM +
STRUCT << " pounds ";

        cout << "\n\n\nThe required wing area = " << (MTOW/wing_loading)
<< "feet";

        return WING,EMPENNAGE,LANDING,SYSTEM;
}

void main ()
{

    double span;
    double ct, co, t;

    cout << "\nEnter the wingspan(feet): ";
    cin >> span;

    cout << "\nEnter the root chord (feet): ";

    cin >> co;

    cout << "\nEnter the tip chord (feet): ";
    cin >> ct;

    cout << "\nEnter the thickness of the airfoil section (12% is
recommended): ";
    cin >> t;

    cout << "\nEnter the sweep angle at the quarter chord(degrees): ";
    cin >> s;

    cout << "\nEnter the length of the fuselage (feet): ";
    cin >> L;

```

```

tr = ct/co;
mc = co*(1-(1-(tr)) * (span/2)/span);
tc = (t*.01)/mc;
ar =(2 * span)/ (co * (1 + tr));

cout << "\n\nThe taper ratio of the wing = " << tr;
cout << "\n\nThe mean geometric chord      = " << mc;
cout << "\n\nThe thickness to chord ratio = " << tc;
cout << "\n\nThe aspect ratio = " << ar;

cout << "\nEnter a guess for the total weight (lbs): ";
cin  >> W;

cout << "\nEnter the wing loading(lb/sq.feet): ";
cin  >> lf;

lf=1.5;

Max_Weight(W,ar,tr,lf,tc,s,WL,L,D);
}

```

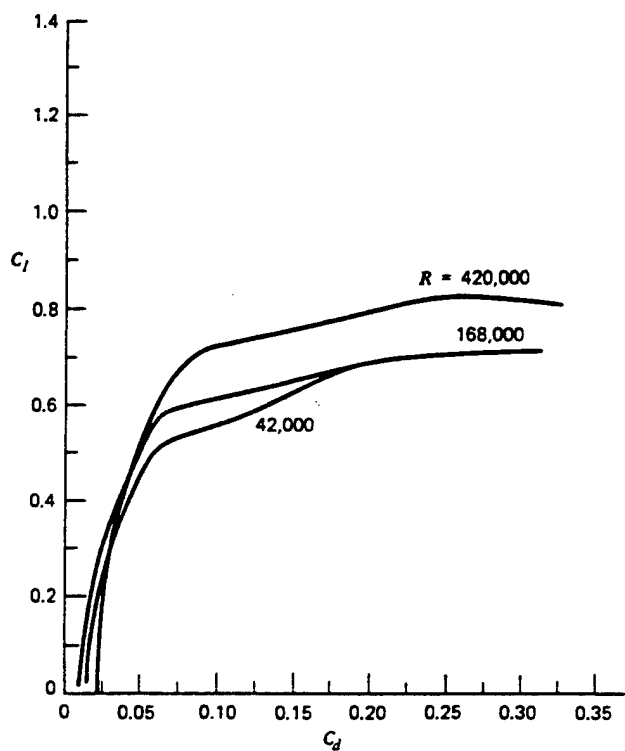
---

---

APPENDIX  
III

---

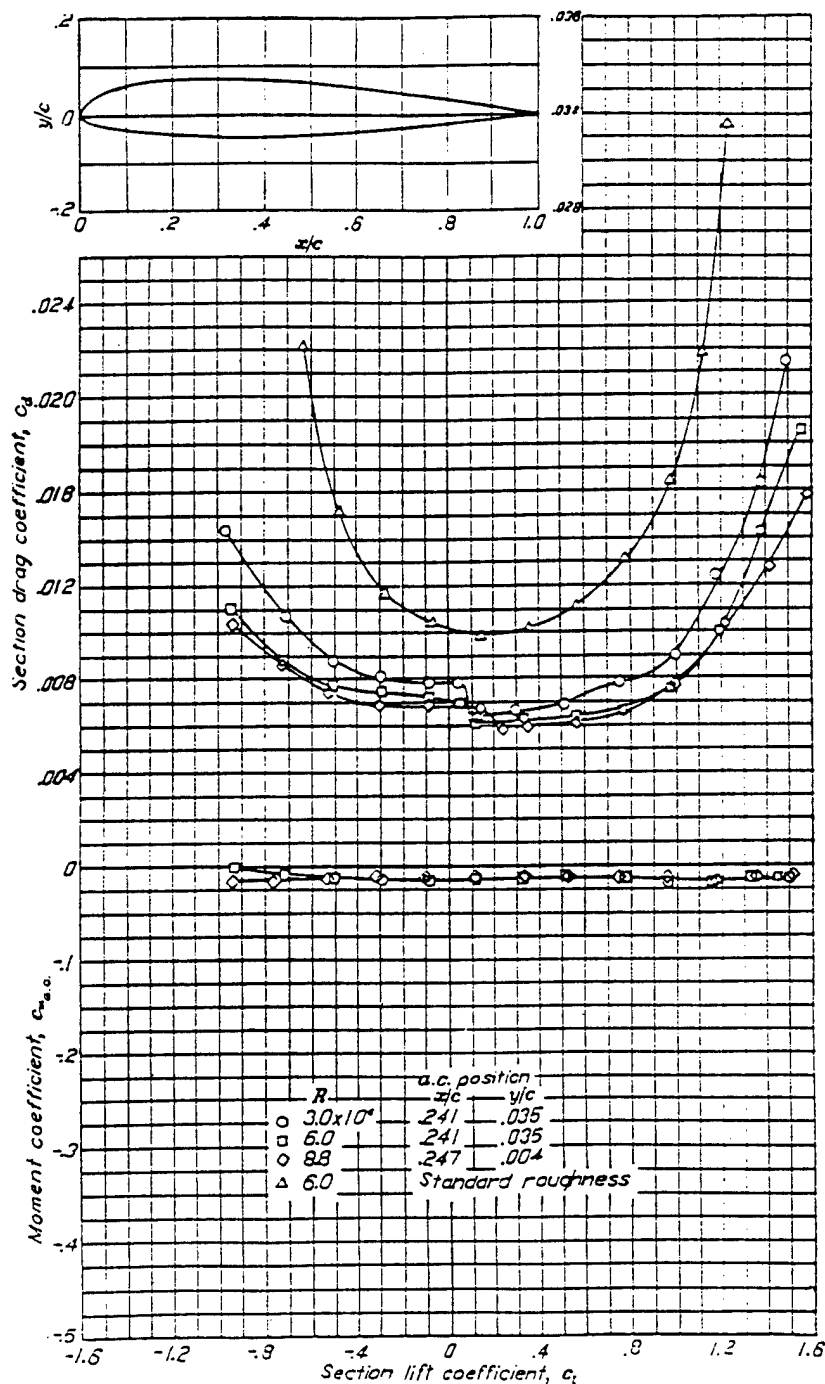
DRAG POLAR CHARACTERISTICS OF A FLAT PLATE



Drag polar for the flat-plate airfoil at low Reynolds numbers.

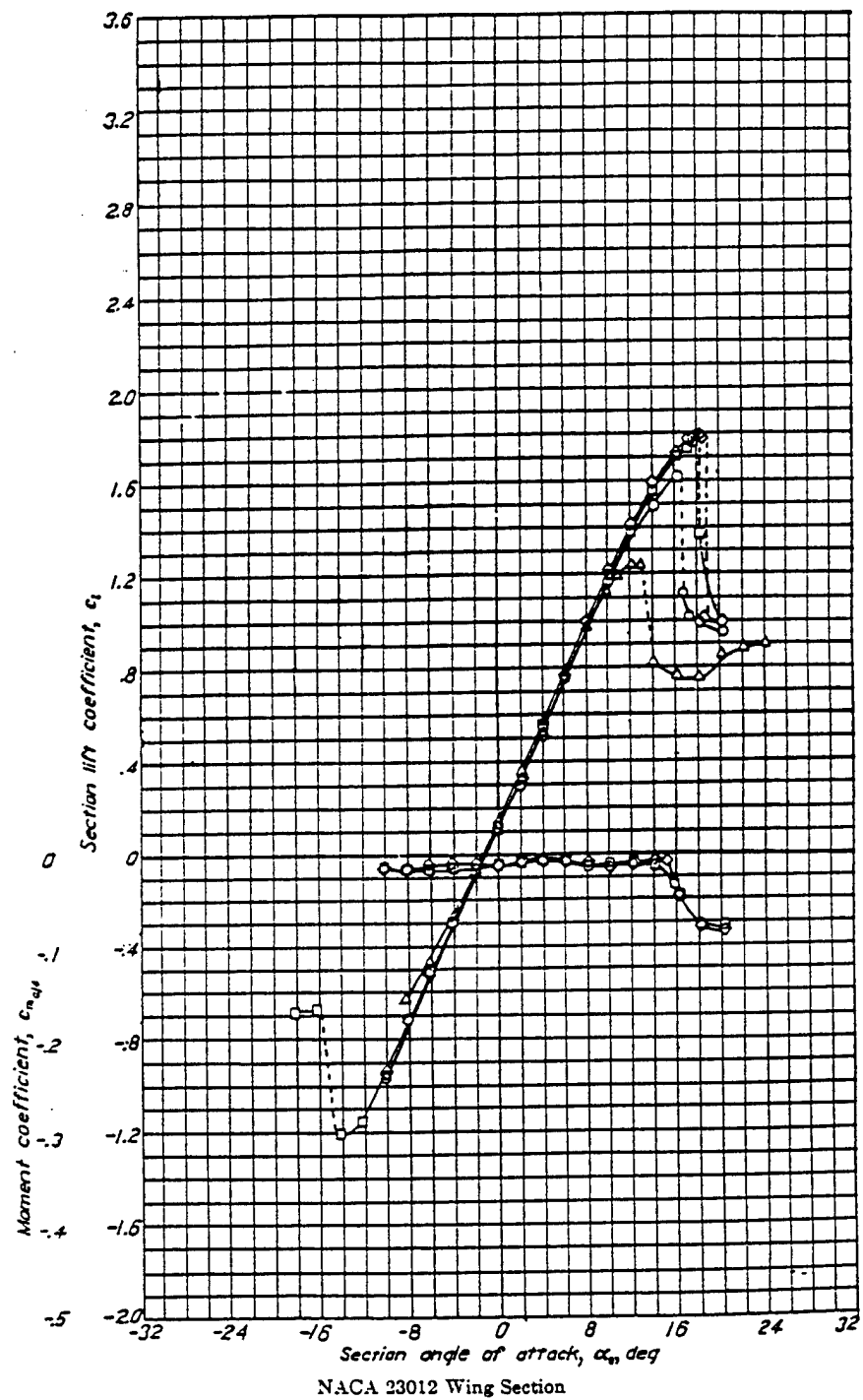
# APPENDIX IV

## NACA 23012 WING SECTION



NACA 23012 Wing Section (Continued)





---

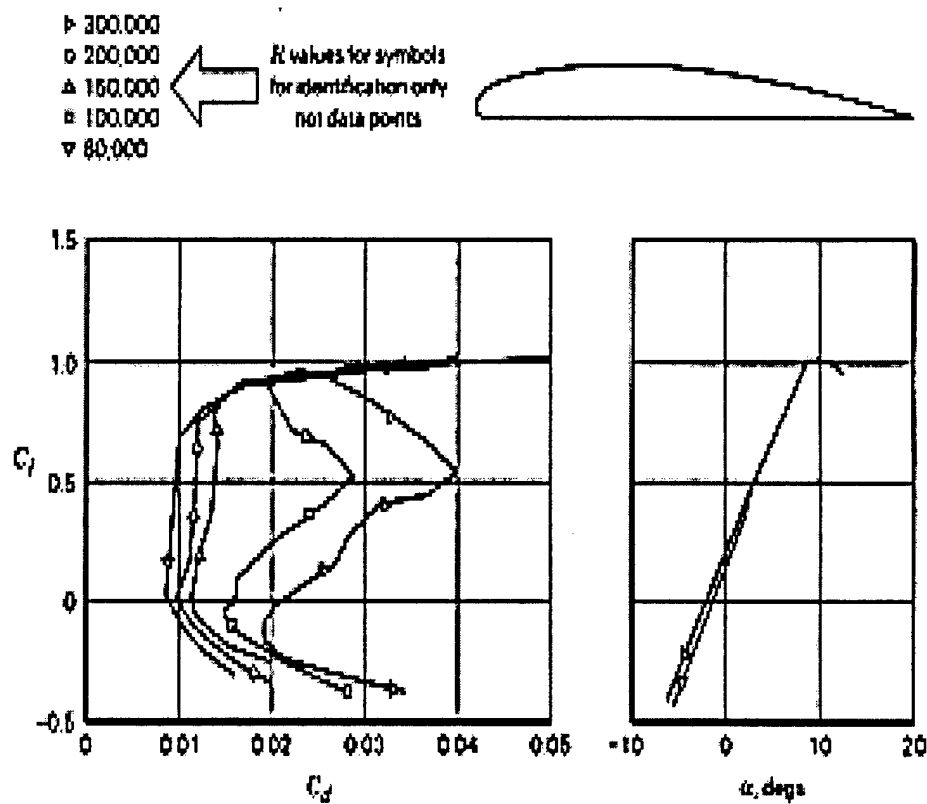


---

APPENDIX  
V

---

LOW SPEED AIRFOIL (E374) CHARACTERISTICS



Test results for the E374 airfoil.

## APPENDIX

### VI

#### CALCULATION OF CENTER OF GRAVITY LOCATION

#### Constants

<u>Components</u>	<u>Weights (lb)</u>	<u>Lengths to CG from Engine Mount (in)</u>	<u>Moment of each Component (lb in)</u>
Cone&prop	0.10	-1.000	-0.1
Motor	0.68	1.750	1.19
Controller	0.16	4.000	0.64
Battery Pack	2.50	7.147	17.8675
Weights	7.50	13.600	102
Battery (control)	0.20	20.625	4.125
Receiver	0.11	21.250	2.3375
Servo1	0.08	22.875	1.83
Servo 2	0.08	22.875	1.83
Switch	0.02	24.125	0.4825
Fuselage	0.70	12.000	8.4
Wing	2.00	12.900	25.8
Boom&rods	0.36	30.200	10.872
Empannage	0.40	40.000	16
<b>Totals</b>	<b>14.89</b>		<b>193.2745</b>

#### Equations

Find total moment about Engine Mount

$$M_{AboutEngineMount} = \sum FL$$

$$M_{AboutEngineMount} = 193.2745 \text{ lb in}$$

Location of the Centroid from Engine Mount

$$\bar{x} = \frac{\sum FL}{W_T}$$

$$W_T = 14.89 \text{ lb}$$

$$\bar{x} = 12.98 \text{ in}$$

# APPENDIX VII

## MOTOR STATIC ANALYSIS

### Static Analysis - Eddy Bee

Motor: Aveox 1406/4Y; 1500 RPM/V; 0.06 Ohms; 1.2A idle.

Battery: Sanyo 2000SCR; 15 to 19 cells; 2000mAh; 0.004 Ohms/cell.

Speed Control: Astro 211; 0.002 Ohms.

Drive System: Aveox/Robbe 3.7:1 Gearbox; 11x7 to 11x13 geared 3.7:1.

Airframe: Eddy Bee; 702sq.in; 241.5 to 249.7oz; 49.5 to 51.2oz/sq.ft; Cd=0.063; Cl=0.7; Clmax=1.24.

Filter: 50A max, 75A max (ESC).

NC	Gear Ratio	Diam (in)	Pitch (in)	Weight (oz)	Amps	Volts	Input (W)	Output (W)	Loss (W)	Effic (%)	InPLd (W/lb)	OutPLd (W/lb)	Prop RPM	Thrust (oz)	PSPd (MPH)	Time (m:s)
15	3.70	11.0	7.0	241.5	11.3	17.3	194.8	167.3	27.6	85.9	12.9	11.1	6740	33.9	44.7	10:39
15	3.70	11.0	8.0	241.5	12.5	17.2	215.2	186.0	29.1	86.5	14.3	12.3	6679	38.0	50.6	9:36
15	3.70	11.0	9.0	241.5	13.7	17.2	234.6	203.8	30.8	86.9	15.5	13.5	6621	42.0	56.4	8:46
15	3.70	11.0	10.0	241.5	14.8	17.1	253.3	220.7	32.6	87.1	16.8	14.6	6564	45.9	62.2	8:05
15	3.70	11.0	11.0	241.5	15.9	17.0	271.2	236.7	34.5	87.3	18.0	15.7	6509	49.6	67.8	7:32
15	3.70	11.0	12.0	241.5	17.0	16.9	288.4	251.9	36.5	87.3	19.1	16.7	6455	53.2	73.4	7:03
15	3.70	11.0	13.0	241.5	18.1	16.9	304.9	266.4	38.5	87.4	20.2	17.6	6404	56.8	78.3	6:39
16	3.70	11.0	7.0	243.6	12.5	18.4	229.8	199.3	30.5	86.7	15.1	13.1	7145	38.1	47.4	9:36
16	3.70	11.0	8.0	243.6	13.9	18.3	253.6	221.1	32.5	87.2	16.7	14.5	7075	42.6	53.6	8:39
16	3.70	11.0	9.0	243.6	15.2	18.2	276.3	241.7	34.6	87.5	18.1	15.9	7008	47.1	59.7	7:54
16	3.70	11.0	10.0	243.6	16.5	18.1	298.0	261.2	36.8	87.7	19.6	17.2	6943	51.3	65.8	7:18
16	3.70	11.0	11.0	243.6	17.7	18.0	318.8	279.7	39.1	87.7	20.9	18.4	6881	55.5	71.7	6:47
16	3.70	11.0	12.0	243.6	18.9	18.0	338.6	297.1	41.5	87.7	22.2	19.5	6820	59.4	77.5	6:22
16	3.70	11.0	13.0	243.6	20.0	17.9	357.7	313.7	44.0	87.7	23.5	20.6	6762	63.3	83.2	6:00
17	3.70	11.0	7.0	245.6	13.8	19.4	268.2	234.4	33.8	87.4	17.5	15.3	7543	42.4	50.0	8:42
17	3.70	11.0	8.0	245.6	15.3	19.3	295.7	259.6	36.1	87.8	19.3	16.9	7464	47.5	56.5	7:51
17	3.70	11.0	9.0	245.6	16.7	19.2	321.9	283.2	38.7	88.0	21.0	18.4	7388	52.3	63.0	7:10
17	3.70	11.0	10.0	245.6	18.1	19.1	346.8	305.4	41.4	88.1	22.6	19.9	7315	57.0	69.3	6:37
17	3.70	11.0	11.0	245.6	19.5	19.0	370.5	326.4	44.2	88.1	24.1	21.3	7244	61.5	75.5	6:10
17	3.70	11.0	12.0	245.6	20.8	18.9	393.2	346.1	47.1	88.0	25.6	22.5	7177	65.8	81.6	5:47
17	3.70	11.0	13.0	245.6	22.0	18.9	414.9	364.8	50.1	87.9	27.0	23.8	7111	70.0	87.5	5:27
18	3.70	11.0	7.0	247.7	15.1	20.5	310.1	272.8	37.2	88.0	20.0	17.6	7934	46.9	52.6	7:56
18	3.70	11.0	8.0	247.7	16.9	20.4	341.6	301.5	40.1	88.3	22.1	19.5	7845	52.4	59.4	7:09
18	3.70	11.0	9.0	247.7	18.3	20.2	371.4	328.2	43.2	88.4	24.0	21.2	7760	57.7	66.1	6:32
18	3.70	11.0	10.0	247.7	19.9	20.1	399.6	353.3	46.4	88.4	25.8	22.8	7678	62.8	72.7	6:03
18	3.70	11.0	11.0	247.7	21.3	20.0	426.5	376.9	49.7	88.3	27.5	24.3	7600	67.6	79.2	5:38
18	3.70	11.0	12.0	247.7	22.7	19.9	452.0	398.9	53.2	88.2	29.2	25.8	7524	72.3	85.5	5:17
18	3.70	11.0	13.0	247.7	24.0	19.8	476.4	419.7	56.7	88.1	30.8	27.1	7451	76.9	91.7	5:00
19	3.70	11.0	7.0	249.7	16.5	21.5	355.5	314.5	41.0	88.5	22.8	20.1	8319	51.6	55.1	7:16
19	3.70	11.0	8.0	249.7	18.3	21.4	391.1	346.7	44.4	88.6	25.1	22.2	8219	57.6	62.3	6:33
19	3.70	11.0	9.0	249.7	20.0	21.2	424.7	376.7	48.0	88.7	27.2	24.1	8125	63.3	69.2	6:00
19	3.70	11.0	10.0	249.7	21.6	21.1	456.4	404.6	51.8	88.6	29.2	25.9	8034	68.7	76.1	5:33
19	3.70	11.0	11.0	249.7	23.2	21.0	486.5	430.9	55.7	88.5	31.2	27.6	7947	74.0	82.8	5:11
19	3.70	11.0	12.0	249.7	24.7	20.9	515.0	455.2	59.8	88.4	33.0	29.2	7863	79.0	89.4	4:52
19	3.70	11.0	13.0	249.7	26.1	20.8	542.1	478.2	63.9	88.2	34.7	30.6	7783	83.8	95.8	4:36

## APPENDIX VIII

### MOTOR PERFORMANCE

## In-Flight Analysis - Eddy Bee at 87% Throttle

Motor: Aveox 1406/4Y; 1500 RPM/V; 0.06 Ohms; 1.2A idle.

Battery: Sanyo 2000SCR; 17 cells; 2000mAh; 0.004 Ohms/cell.

Speed Control: Astro 211; 0.002 Ohms.

Drive System: Aveox/Robbe 3.7:1 Gearbox; 14x9 geared 3.7:1.

Airframe: Eddy Bee; 702sq.in; 245.6oz; 50.4oz/sq.ft; Cd=0.063; Cl=0.7; Clmax=1.24.

Filter: 50A max, 75A max (ESC).

Stats: 27 W/lb in; 23 W/lb out; 32 MPH stall; 42 MPH level @ 87% (12:06); 127ft/min @ 2.6°; -266ft/min @ -5.5°.

AirSpd (MPH)	EPitch (in)	Drag (oz)	Lift (oz)	Amps	Volts	Input (W)	Output (W)	Loss (W)	Effic (%)	Prop RPM	Thrust (oz)	PSPd (MPH)	Time (m:s)
0.0	9.00	0.0	0.0	26.4	15.9	419.4	360.5	58.9	86.0	5805	66.6	49.5	4:33
1.0	8.82	0.0	0.1	26.0	15.9	414.5	356.6	57.9	86.0	5824	65.7	48.6	4:37
2.0	8.64	0.1	0.6	25.7	16.0	409.5	352.7	56.8	86.1	5842	64.7	47.8	4:40
3.0	8.46	0.1	1.3	25.3	16.0	404.5	348.7	55.8	86.2	5861	63.8	47.0	4:44
4.0	8.28	0.2	2.2	25.0	16.0	399.4	344.6	54.8	86.3	5879	62.8	46.1	4:48
5.0	8.10	0.3	3.5	24.6	16.0	394.3	340.5	53.8	86.4	5898	61.9	45.3	4:53
6.0	7.93	0.5	5.0	24.2	16.1	389.2	336.4	52.8	86.4	5917	60.9	44.4	4:57
7.0	7.75	0.6	6.8	23.9	16.1	384.0	332.2	51.8	86.5	5936	60.0	43.6	5:01
8.0	7.58	0.8	8.9	23.5	16.1	378.7	327.9	50.8	86.6	5955	59.0	42.8	5:06
9.0	7.41	1.0	11.3	23.2	16.1	373.4	323.6	49.9	86.6	5975	58.1	41.9	5:11
10.0	7.24	1.3	14.0	22.8	16.2	368.1	319.2	48.9	86.7	5994	57.1	41.1	5:16
11.0	7.07	1.5	16.9	22.4	16.2	362.7	314.8	48.0	86.8	6014	56.1	40.3	5:21
12.0	6.90	1.8	20.1	22.0	16.2	357.3	310.2	47.0	86.8	6033	55.1	39.4	5:27
13.0	6.73	2.1	23.6	21.7	16.2	351.8	305.7	46.1	86.9	6053	54.1	38.6	5:32
14.0	6.57	2.5	27.4	21.3	16.3	346.2	301.1	45.2	86.9	6073	53.2	37.8	5:38
15.0	6.40	2.8	31.4	20.9	16.3	340.7	296.4	44.3	87.0	6093	52.2	36.9	5:44
16.0	6.24	3.2	35.7	20.5	16.3	335.0	291.6	43.4	87.0	6113	51.1	36.1	5:51
17.0	6.07	3.6	40.3	20.2	16.3	329.3	286.8	42.5	87.1	6133	50.1	35.3	5:57
18.0	5.91	4.1	45.2	19.8	16.4	323.6	281.9	41.7	87.1	6153	49.1	34.4	6:04
19.0	5.75	4.5	50.4	19.4	16.4	317.8	277.0	40.8	87.2	6173	48.1	33.6	6:11
20.0	5.59	5.0	55.8	19.0	16.4	312.0	272.0	40.0	87.2	6194	47.1	32.8	6:19
21.0	5.43	5.5	61.5	18.6	16.4	306.1	266.9	39.2	87.2	6214	46.0	32.0	6:27
22.0	5.27	6.1	67.5	18.2	16.5	300.1	261.7	38.4	87.2	6235	45.0	31.1	6:35
23.0	5.12	6.6	73.8	17.8	16.5	294.1	256.5	37.6	87.2	6256	44.0	30.3	6:44
24.0	4.96	7.2	80.4	17.4	16.5	288.1	251.2	36.8	87.2	6277	42.9	29.5	6:53
25.0	4.81	7.9	87.2	17.0	16.6	281.9	245.9	36.0	87.2	6298	41.9	28.7	7:03
26.0	4.65	8.5	94.3	16.6	16.6	275.8	240.5	35.3	87.2	6319	40.8	27.9	7:13
27.0	4.50	9.2	101.7	16.2	16.6	269.5	235.0	34.6	87.2	6340	39.7	27.0	7:24
28.0	4.35	9.8	109.4	15.8	16.6	263.2	229.4	33.8	87.1	6361	38.7	26.2	7:35
29.0	4.20	10.6	117.4	15.4	16.7	256.9	223.8	33.1	87.1	6383	37.6	25.4	7:47
30.0	4.05	11.3	125.6	15.0	16.7	250.5	218.0	32.5	87.0	6404	36.5	24.6	8:00
31.0	3.91	12.1	134.1	14.6	16.7	244.0	212.2	31.8	87.0	6426	35.4	23.8	8:13
32.0	3.76	12.9	142.9	14.2	16.8	237.5	206.4	31.1	86.9	6448	34.3	23.0	8:28
33.0	3.61	13.7	152.0	13.8	16.8	230.9	200.4	30.5	86.8	6470	33.2	22.1	8:43
34.0	3.47	14.5	161.3	13.3	16.8	224.3	194.4	29.9	86.7	6492	32.1	21.3	9:00
35.0	3.33	15.4	171.0	12.9	16.8	217.6	188.3	29.3	86.5	6514	31.0	20.5	9:17

36.0	3.18	16.3	180.9	12.5	16.9	210.8	182.1	28.7	86.4	6537	29.9	19.7	9:36
37.0	3.04	17.2	191.1	12.1	16.9	204.0	175.8	28.2	86.2	6559	28.7	18.9	9:57
38.0	2.90	18.1	201.5	11.6	16.9	197.1	169.5	27.6	86.0	6582	27.6	18.1	10:19
39.0	2.76	19.1	212.3	11.2	17.0	190.1	163.1	27.1	85.8	6604	26.5	17.3	10:42
40.0	2.63	20.1	223.3	10.8	17.0	183.1	156.5	26.6	85.5	6627	25.3	16.5	11:08
41.0	2.49	21.1	234.6	10.3	17.0	176.0	149.9	26.1	85.2	6650	24.2	15.7	11:36
42.0	2.35	22.2	246.2	9.9	17.1	168.9	143.2	25.6	84.8	6673	23.0	14.9	12:07
43.0	2.22	23.2	258.0	9.5	17.1	161.7	136.5	25.2	84.4	6696	21.8	14.1	12:41
44.0	2.09	24.3	270.2	9.0	17.1	154.4	129.6	24.8	84.0	6720	20.7	13.3	13:18
45.0	1.95	25.4	282.6	8.6	17.1	147.0	122.6	24.4	83.4	6743	19.5	12.5	14:00
46.0	1.82	26.6	295.3	8.1	17.2	139.6	115.6	24.0	82.8	6767	18.3	11.7	14:46
47.0	1.69	27.7	308.3	7.7	17.2	132.1	108.4	23.6	82.1	6791	17.1	10.9	15:38
48.0	1.56	28.9	321.5	7.2	17.2	124.5	101.2	23.3	81.3	6815	15.9	10.1	16:37
49.0	1.43	30.2	335.1	6.8	17.3	116.9	93.9	23.0	80.3	6839	14.7	9.3	17:44
50.0	1.31	31.4	348.9	6.3	17.3	109.2	86.5	22.7	79.2	6863	13.5	8.5	19:01
51.0	1.18	32.7	363.0	5.8	17.3	101.4	78.9	22.4	77.9	6887	12.3	7.7	20:31
52.0	1.06	34.0	377.4	5.4	17.4	93.5	71.3	22.2	76.3	6911	11.1	6.9	22:17
53.0	0.93	35.3	392.0	4.9	17.4	85.6	63.6	22.0	74.3	6936	9.8	6.1	24:24
54.0	1.66	36.6	406.9	9.5	19.7	187.8	159.4	28.4	84.9	7769	22.0	12.2	12:37
55.0	1.55	38.0	422.2	9.0	19.8	178.2	150.3	28.0	84.3	7795	20.7	11.4	13:19
56.0	1.44	39.4	437.7	8.5	19.8	168.6	141.1	27.5	83.7	7822	19.3	10.7	14:06
57.0	1.33	40.8	453.4	8.0	19.8	158.8	131.7	27.1	83.0	7848	18.0	9.9	14:59
58.0	1.22	42.3	469.5	7.5	19.9	149.0	122.3	26.7	82.1	7875	16.6	9.1	16:01
59.0	1.12	43.7	485.8	7.0	19.9	139.1	112.7	26.3	81.1	7902	15.3	8.4	17:11
60.0	1.01	45.2	502.4	6.5	19.9	129.0	103.1	26.0	79.9	7929	13.9	7.6	18:33
61.0	0.90	46.7	519.3	6.0	20.0	118.9	93.3	25.7	78.4	7957	12.6	6.8	20:10
62.0	0.80	48.3	536.5	5.4	20.0	108.8	83.3	25.4	76.6	7984	11.2	6.0	22:05
63.0	0.70	49.9	553.9	4.9	20.1	98.5	73.3	25.2	74.4	8012	9.8	5.3	24:27
64.0	0.59	51.4	571.6	4.4	20.1	88.1	63.1	24.9	71.7	8039	8.4	4.5	27:22
65.0	0.49	53.1	589.6	3.9	20.1	77.6	52.8	24.8	68.1	8067	7.0	3.8	31:07
66.0	0.39	54.7	607.9	3.3	20.2	67.0	42.4	24.6	63.3	8095	5.6	3.0	36:06
67.0	0.29	56.4	626.5	2.8	20.2	56.4	31.9	24.5	56.5	8123	4.2	2.2	43:00
68.0	0.19	58.1	645.3	2.3	20.2	45.6	21.2	24.4	46.4	8151	2.8	1.5	53:14
69.0	0.09	59.8	664.4	1.7	20.3	34.8	10.4	24.4	29.9	8180	1.4	0.7	70:00

# In-Flight Analysis - Eddy Bee

Motor: Aveox 1406/4Y; 1500 RPM/V; 0.06 Ohms; 1.2A idle.

Battery: Sanyo 2000SCR; 17 cells; 2000mAh; 0.004 Ohms/cell.

Speed Control: Astro 211; 0.002 Ohms.

Drive System: Aveox/Robbe 3.7:1 Gearbox; 14x9 geared 3.7:1.

Airframe: Eddy Bee; 702sq.in; 245.6oz; 50.4oz/sq.ft; Cd=0.063; Cl=0.7; Clmax=1.24.

Filter: 50A max, 75A max (ESC).

Stats: 39 W/lb in; 33 W/lb out; 32 MPH stall; 42 MPH level @ 87% (12:06); 300ft/min @ 6.2°; -266ft/min @ -5.5°.

AirSpd (MPH)	EPitch (in)	Drag (oz)	Lift (oz)	Amps	Volts	Input (W)	Output (W)	Loss (W)	Effic (%)	Prop RPM	Thrust (oz)	PSPd (MPH)	Time (m:s)
0.0	9.00	0.0	0.0	33.0	18.1	597.7	512.8	84.8	85.8	6529	84.2	55.6	3:38
1.0	8.84	0.0	0.1	32.7	18.1	591.7	508.3	83.4	85.9	6549	83.2	54.8	3:40
2.0	8.68	0.1	0.6	32.3	18.1	585.6	503.7	82.0	86.0	6569	82.2	54.0	3:43
3.0	8.52	0.1	1.3	31.9	18.2	579.6	499.0	80.6	86.1	6589	81.2	53.2	3:46
4.0	8.36	0.2	2.2	31.5	18.2	573.4	494.3	79.2	86.2	6609	80.2	52.3	3:48
5.0	8.20	0.3	3.5	31.1	18.2	567.2	489.5	77.8	86.3	6630	79.2	51.5	3:51
6.0	8.05	0.5	5.0	30.7	18.2	561.0	484.6	76.4	86.4	6650	78.1	50.7	3:54
7.0	7.89	0.6	6.8	30.4	18.3	554.7	479.7	75.0	86.5	6671	77.1	49.9	3:57
8.0	7.74	0.8	8.9	30.0	18.3	548.3	474.7	73.7	86.6	6691	76.1	49.0	4:00
9.0	7.58	1.0	11.3	29.6	18.3	541.9	469.6	72.3	86.7	6712	75.0	48.2	4:04
10.0	7.43	1.3	14.0	29.2	18.4	535.5	464.5	71.0	86.7	6733	74.0	47.4	4:07
11.0	7.28	1.5	16.9	28.8	18.4	528.9	459.3	69.6	86.8	6754	72.9	46.6	4:10
12.0	7.13	1.8	20.1	28.4	18.4	522.4	454.0	68.3	86.9	6775	71.8	45.7	4:14
13.0	6.98	2.1	23.6	28.0	18.4	515.7	448.7	67.0	87.0	6796	70.8	44.9	4:17
14.0	6.83	2.5	27.4	27.6	18.5	509.1	443.3	65.8	87.1	6818	69.7	44.1	4:21
15.0	6.68	2.8	31.4	27.2	18.5	502.3	437.8	64.5	87.2	6839	68.6	43.3	4:25
16.0	6.54	3.2	35.7	26.7	18.5	495.5	432.3	63.2	87.2	6861	67.6	42.5	4:29
17.0	6.39	3.6	40.3	26.3	18.6	488.6	426.7	62.0	87.3	6882	66.5	41.7	4:33
18.0	6.25	4.1	45.2	25.9	18.6	481.7	421.0	60.7	87.4	6904	65.4	40.8	4:38
19.0	6.10	4.5	50.4	25.5	18.6	474.7	415.2	59.5	87.5	6926	64.3	40.0	4:42
20.0	5.96	5.0	55.8	25.1	18.6	467.7	409.4	58.3	87.5	6948	63.2	39.2	4:47
21.0	5.82	5.5	61.5	24.7	18.7	460.6	403.5	57.1	87.6	6970	62.1	38.4	4:52
22.0	5.68	6.1	67.5	24.2	18.7	453.4	397.5	56.0	87.7	6993	60.9	37.6	4:57
23.0	5.54	6.6	73.8	23.8	18.7	446.2	391.4	54.8	87.7	7015	59.8	36.8	5:02
24.0	5.40	7.2	80.4	23.4	18.8	438.9	385.3	53.7	87.8	7037	58.7	36.0	5:08
25.0	5.26	7.9	87.2	23.0	18.8	431.6	379.0	52.5	87.8	7060	57.6	35.2	5:14
26.0	5.12	8.5	94.3	22.5	18.8	424.2	372.7	51.4	87.9	7083	56.4	34.4	5:20
27.0	4.99	9.2	101.7	22.1	18.9	416.7	366.3	50.3	87.9	7105	55.3	33.6	5:26
28.0	4.85	9.8	109.4	21.7	18.9	409.1	359.9	49.3	88.0	7128	54.1	32.8	5:32
29.0	4.72	10.6	117.4	21.2	18.9	401.5	353.3	48.2	88.0	7151	53.0	32.0	5:39
30.0	4.58	11.3	125.6	20.8	18.9	393.9	346.7	47.2	88.0	7175	51.8	31.1	5:46
31.0	4.45	12.1	134.1	20.3	19.0	386.1	340.0	46.1	88.0	7198	50.6	30.3	5:54
32.0	4.32	12.9	142.9	19.9	19.0	378.3	333.2	45.1	88.1	7221	49.5	29.5	6:02
33.0	4.19	13.7	152.0	19.5	19.0	370.4	326.3	44.2	88.1	7245	48.3	28.7	6:10
34.0	4.06	14.5	161.3	19.0	19.1	362.5	319.3	43.2	88.1	7269	47.1	27.9	6:19
35.0	3.93	15.4	171.0	18.6	19.1	354.4	312.2	42.2	88.1	7292	45.9	27.2	6:28
36.0	3.80	16.3	180.9	18.1	19.1	346.4	305.0	41.3	88.1	7316	44.7	26.4	6:38
37.0	3.68	17.2	191.1	17.6	19.2	338.2	297.8	40.4	88.1	7340	43.5	25.6	6:48
38.0	3.55	18.1	201.5	17.2	19.2	330.0	290.4	39.5	88.0	7364	42.3	24.8	6:59
39.0	3.43	19.1	212.3	16.7	19.2	321.6	283.0	38.7	88.0	7389	41.1	24.0	7:10
40.0	3.30	20.1	223.3	16.3	19.3	313.3	275.5	37.8	87.9	7413	39.9	23.2	7:23
41.0	3.18	21.1	234.6	15.8	19.3	304.8	267.8	37.0	87.9	7438	38.6	22.4	7:36
42.0	3.06	22.2	246.2	15.3	19.3	296.3	260.1	36.2	87.8	7462	37.4	21.6	7:50
43.0	2.94	23.2	258.0	14.9	19.4	287.7	252.3	35.4	87.7	7487	36.1	20.8	8:05
44.0	2.81	24.3	270.2	14.4	19.4	279.0	244.3	34.7	87.6	7512	34.9	20.0	8:20
45.0	2.70	25.4	282.6	13.9	19.4	270.2	236.3	33.9	87.4	7537	33.6	19.2	8:38
46.0	2.58	26.6	295.3	13.4	19.5	261.4	228.2	33.2	87.3	7562	32.3	18.5	8:56
47.0	2.46	27.7	308.3	13.0	19.5	252.5	220.0	32.5	87.1	7588	31.1	17.7	9:16
48.0	2.34	28.9	321.5	12.5	19.5	243.5	211.6	31.9	86.9	7613	29.8	16.9	9:37

49.0	2.23	30.2	335.1	12.0	19.6	234.4	203.2	31.2	86.7	7639	28.5	16.1	10:01
50.0	2.11	31.4	348.9	11.5	19.6	225.3	194.6	30.6	86.4	7664	27.2	15.3	10:26
51.0	2.00	32.7	363.0	11.0	19.6	216.0	186.0	30.0	86.1	7690	25.9	14.5	10:54
52.0	1.88	34.0	377.4	10.5	19.7	206.7	177.2	29.5	85.7	7716	24.6	13.8	11:25
53.0	1.77	35.3	392.0	10.0	19.7	197.3	168.4	28.9	85.3	7742	23.3	13.0	11:59
54.0	0.81	36.6	406.9	4.4	17.4	77.6	55.8	21.8	71.9	6961	8.6	5.3	26:58
55.0	0.69	38.0	422.2	4.0	17.5	69.5	47.9	21.6	68.9	6985	7.3	4.5	30:10
56.0	0.56	39.4	437.7	3.5	17.5	61.3	39.8	21.5	65.0	7010	6.1	3.8	34:15
57.0	0.44	40.8	453.4	3.0	17.5	53.1	31.7	21.4	59.7	7036	4.8	3.0	39:38
58.0	0.33	42.3	469.5	2.5	17.6	44.8	23.5	21.3	52.5	7061	3.6	2.2	47:05
59.0	0.21	43.7	485.8	2.1	17.6	36.4	15.2	21.2	41.6	7086	2.3	1.4	58:03
60.0	0.09	45.2	502.4	1.6	17.6	27.9	6.7	21.2	24.0	7112	1.0	0.6	75:50



# APPENDIX IX

## PERFORMANCE CALCULATIONS

Type: Motor & Battery

### Dimensions:

Span:	1.5 ft
Root Chord:	1.5 ft
Tip Chord:	0.5 ft
Taper Ratio:	0.5
Mean Chord (geometrical):	0.75 ft
Mean Chord (dynamical):	0.788 ft
Wing Area:	4.875 ft <sup>2</sup>
Wing Aspect Ratio:	8.67
Wing Loading:	3.03 lb/ft <sup>2</sup>
Total Area Loading (incl. stab.):	2.52 lb/ft <sup>2</sup>
Length of Fuselage:	1.5 ft
Height of Fuselage:	1.5 ft
Width of Fuselage:	1.5 ft
Stab. Lever Distance:	1.5 ft
Parasitic Drag Area:	0.1056 ft <sup>2</sup>
Stab. Span:	1.5 ft
Stab. mean Chord:	0.5 ft
Stab. Area:	0.975 ft <sup>2</sup>
Stab. Aspect Ratio:	2.31
Vert. Stab Area/Vertical Tail Area)	0.4875 ft <sup>2</sup>
Fin Height:	1.16 ft
Fin Mean chord:	0.42 ft
Rudder Area:	0.195 ft <sup>2</sup>
Elevators area if used:	0.2535 ft <sup>2</sup>
ENGINE LOCATION	1.625 ft
Nose length:	1 ft
Fin offset from wing L E	0.6 ft
Aerodynamic Center	1.1875 ft

### Weights:

Wing:	1 lb
Fuselage:	1 lb
Stabilator:	1 lb
Battery Pack:	1 lb
Undercarriage:	1 lb
Motor (with Gear and Prop.):	1 lb
Payload:	1 lb
RC-Equipment:	1 lb
Total Weight:	14.748 lb

(Maximum) 2.5

(Maximum) 7.5

### How to use this spreadsheet:

Before changing any variables in the purple cells, make a safety copy from this file

SI dimensions must be used, otherwise the values will not calculate correctly.

For different profiles than indicated, you may change the factor 1.2 under Cd. For a 12% thick airfoil (like Clark Y) it should be 1.5.

The power values listed are the ones required by the plane. To get the values for your drive you must divide these values by the efficiency of your drive, usually around 0.6 - 0.7

1 ft/sec = 0.7 mph

from prop driver

Wing TE to stab LE 1 ft

Wing profile: NACA 23012

Velocity	Dynamic Pressure	Wing	RE-No.	RE-No. corrected	C <sub>l,0</sub>	C <sub>l</sub>	C <sub>D</sub>	Glideangle	Resistance Thrust	Resistance Thrust
ft/sec	q(lb/ft <sup>2</sup> )	C <sub>L</sub>						C <sub>L</sub> /C <sub>D</sub>	T(lb)	T(ounces)
0	0.00	0.00	0	0.00000	0.00500	0.00000	0	0.00	0.00	0.00
15	0.27	11.31	75.178	2.40000	0.00500	4.94798	7.353	1.54	9.59	153.37
20	0.48	6.36	100.237	0.18000	0.00500	1.56557	1.751	3.64	4.06	64.91
30	1.07	2.83	150.355	0.12000	0.00500	0.30925	0.434	6.51	2.26	36.23
35	1.46	2.08	175.414	0.06000	0.00500	0.16692	0.232	8.96	1.65	26.34
40	1.90	1.59	200.474	0.02400	0.00500	0.09785	0.127	12.54	1.18	18.81
45	2.41	1.26	225.533	0.02520	0.00500	0.06109	0.091	13.77	1.07	17.14
60	4.28	0.71	300.710	0.00900	0.00500	0.01933	0.033	21.22	0.70	11.12
75	6.69	0.45	375.888	0.00816	0.00500	0.00792	0.021	21.47	0.69	10.99
90	9.63	0.31	451.065	0.00804	0.00500	0.00382	0.017	18.64	0.79	12.66
105	13.10	0.23	526.243	0.00744	0.00500	0.00206	0.015	15.92	0.93	14.82

Loadfactor	CL	ft/sec
3.1 g	0.5	125.62
4 g	0.6	130.27
5.9 g	0.7	146.47

### Wing Dimensions

Chord c	1.000000	ft
Wing Span b	1.000000	ft
e (for elliptic wing)	0.500000	
Wing Area S	4.875	ft <sup>2</sup>
Aspect Ratio	8.666667	

### Airfoil Data

Thickness  
Max. Camber located at feet from L.E

**Maximum Weight of Aircraft** 1000 lb

Since dealing with a finite wing, need to obtain slope. The wing slope,  $\alpha_0$  can be obtained from any two points the linear curve. Also we can assume that the Reynolds Number will not be higher than  $5 \times 10^6$

	Angle of Attack	Coefficient of Cl	cd(at zero lift)
Alpha1			
Alpha2			
Alpha at zero			
a:(per degree)	0.106		
a	0.085834		

$C_{Lmax}$	1.24
------------	------

Angle of Attack of Wing	CL	CD
0	0.1287513	0.00685451
1	0.2145855	0.00837363
2	0.30041969	0.01065232
3	0.38625389	0.01369058
4	0.47208809	0.01748839
5	0.55792229	0.02204577
6	0.64375649	0.02736271
7	0.72959068	0.03343922
8	0.81542488	0.04027529
9	0.90125908	0.04787092
10	0.98709328	0.05622611
11	1.07292748	0.06534087
12	1.15876168	0.07521519
13	1.24459587	0.08584907
14	1.33043007	0.09724252
15	1.41626427	0.10939553
16	1.50209847	0.1223081
17	1.58793267	0.13598024
18	1.67376686	0.15041194

**Performance:**

Star Velocity, $V$	5.45 m/s
Planet Velocity, $V_p$	55.86 m/s
Star Flight Velocity	66.54 m/s
Star Turn Radius	8.481 m

1. *Chlorophyll a* and *Chlorophyll b* contents were determined by spectrophotometry using the method of Lichtenthaler and Whaley (1987).

Time	8.00
Speed during lift	0.00
Lift-off Distance	167.88
Payload Fraction	5.33557

APPENDIX

X

SPECIFIC FUSELAGE MATERIAL COST ESTIMATIONS

**Fiberglass only**

Catlg #	Part name	Material	Amount/Qnty	Qnty	Cost / item	Cost
<b>FibreGlast Developments Corp</b>						
1094-B	Bi-directional E-Glass	9 oz Fiberglass	3 yards	1	19.95	19.95
543-A	Style 7781 E-Glass	9 oz Fiberglass	1 yard	1	12.95	12.95
2000-A	System 2000 Epoxy Resin	Epoxy resin	1 quart	1	24.95	24.95
2120-A	2120 Epoxy Hardener	Epoxy Hardener	1/2 pint	1	9.95	9.95
1016-A	Parting Wax	Mold Wax	24 oz.	1	8.95	8.95
13-A	PVA Release Film	Mold Release Mat.	1 quart	1	8.95	8.95
577-B	Polyethelene Bagging Film	Vacume Bagging	3 yards	1	6.95	6.95
579-B	Breather/Bleeder	Molding Mat.	3 yards	1	16.95	16.95
582-B	Nylon Release Peel Ply	Molding Mat.	3 yards	1	29.95	29.95
891-A	Vacume Connector	Vacume Connector	1 connector	1	4.95	4.95
893-A	Vacume Tubing	1/2" Plastic Tubing	1 foot	8	0.95	7.60
581-A	Sealant Tape	Vacume Bag Sealer	25 feet	1	6.95	6.95
591-A	Quart Starter Kit	Gloves,brushes,etc	various	1	9.95	9.95
588-A	Quart Mixing Kit	Cups,sticks,etc	various	1	4.95	4.95
					Sub Total	\$173.95
<b>Hechingers Hardware</b>						
5041611	9x11 Ultra Fine Abrasive 660	Sandpaper	4 sheets	1	3.41	3.41
5093513	Alum Oxide Abrasive Pack	Sandpaper	20 sheets	1	5.79	5.79
4046207	Flannel Cloths	Buffing Cloths	6 sheets	1	4.99	4.99
5993225	Paint Pail	Mixing Cup	1 cup	2	0.33	0.66
5429915	PVC Pipe	4" Dia Pipe	5 feet	1	6.79	6.79
					Sub Total	\$21.64
					Total Cost	\$195.59

## Kevlar & Fiberglass

Catlg #	Part name	Material	Amount/Qnty	Qnty	Cost / item	Cost
<b>FibreGlast Developments Corp</b>						
545-B	5HS Kevlar Second Quality	5 oz Kevlar	1 yards	1	16.95	16.95
543-A	Style 7781 E-Glass	9 oz Fiberglass	1 yard	1	12.95	12.95
2000-A	System 2000 Epoxy Resin	Epoxy resin	1 quart	1	24.95	24.95
2120-A	2120 Epoxy Hardener	Epoxy Hardener	1/2 pint	1	9.95	9.95
1016-A	Parting Wax	Mold Wax	24 oz.	1	8.95	8.95
13-A	PVA Release Film	Mold Release Mat.	1 quart	1	8.95	8.95
577-B	Polyethelene Bagging Film	Vacume Bagging	3 yards	1	6.95	6.95
579-B	Breather/Bleeder	Molding Mat.	3 yards	1	16.95	16.95
582-B	Nylon Release Peel Ply	Molding Mat.	3 yards	1	29.95	29.95
891-A	Vacume Connector	Vacume Connector	1 connector	1	4.95	4.95
893-A	Vacume Tubing	1/2" Plastic Tubing	1 foot	8	0.95	7.60
581-A	Sealant Tape	Vacume Bag Sealer	25 feet	1	6.95	6.95
591-A	Quart Starter Kit	Gloves,brushes,etc	various	1	9.95	9.95
588-A	Quart Mixing Kit	Cups,sticks,etc	various	1	4.95	4.95
Sub Total						\$170.95

### **Hechingers Hardware**

5041611	9x11 Ultra Fine Abrasive 660	Sandpaper	4 sheets	1	3.41	3.41
5093513	Alum Oxide Abrasive Pack	Sandpaper	20 sheets	1	5.79	5.79
4046207	Flannel Cloths	Buffing Cloths	6 sheets	1	4.99	4.99
5993225	Paint Pail	Mixing Cup	1 cup	2	0.33	0.66
5429915	PVC Pipe	4" Dia Pipe	5 feet	1	6.79	6.79
Sub Total						\$21.64

**Total Cost      \$192.59**

## Graphite & Fiberglass

Catlg #	Part name	Material	Amount/Qnty	Qnty	Cost / item	Cost
<b><u>FibreGlast Developments Corp</u></b>						
1069-A	3K 2x2 Twill Weave	5.7 oz Graphite	1 yard	1	59.95	59.95
1094-A	Bidirectional E-Glass	9 oz Fiberglass	1 yard	1	9.95	9.95
2000-A	System 2000 Epoxy Resin	Epoxy resin	1 quart	1	24.95	24.95
2120-A	2120 Epoxy Hardener	Epoxy Hardener	1/2 pint	1	9.95	9.95
1016-A	Parting Wax	Mold Wax	24 oz.	1	8.95	8.95
13-A	PVA Release Film	Mold Release Mat.	1 quart	1	8.95	8.95
577-B	Polyethelene Bagging Film	Vacume Bagging	3 yards	1	6.95	6.95
579-B	Breather/Bleeder	Molding Mat.	3 yards	1	16.95	16.95
582-B	Nylon Release Peel Ply	Molding Mat.	3 yards	1	29.95	29.95
891-A	Vacume Connector	Vacume Connector	1 connector	1	4.95	4.95
893-A	Vacume Tubing	1/2" Plastic Tubing	1 foot	8	0.95	7.60
581-A	Sealant Tape	Vacume Bag Sealer	25 feet	1	6.95	6.95
591-A	Quart Starter Kit	Gloves,brushes,etc	various	1	9.95	9.95
Sub Total						\$206.00
<b><u>Hechingers Hardware</u></b>						
5041611	9x11 Ultra Fine Abrasive 660	Sandpaper	4 sheets	1	3.41	3.41
5093513	Alum Oxide Abrasive Pack	Sandpaper	20 sheets	1	5.79	5.79
4046207	Flannel Cloths	Buffing Cloths	6 sheets	1	4.99	4.99
5993225	Paint Pail	Mixing Cup	1 cup	2	0.33	0.66
5429915	PVC Pipe	4" Dia Pipe	5 feet	1	6.79	6.79
Sub Total						\$21.64
Total Cost						\$227.64

## Balsa only

Catlg #	Part name	Material	Amount/Qnty	Qnty	Cost / item	Cost
<b>Tower Hobbies</b>						
TOWR1360	1/8 x 4 x 36 balsa sheet	outer fuselage	8 sheets	2	7.49	14.98
TOWR1905	1/6 x 6 x 12 plywood	inner fuselage	1 sheet	4	1.49	5.96
TOWR1855	1 x 3 x 30 balsa block	bottom front	1 block	1	2.59	2.59
TOWR1910	1/8 x 6 x 12 plywood	bulkheads	1 sheet	2	1.79	3.58
TOWR1655	3/8 x 3/8 x 36 triangle	reinforcements	8 sticks	2	2.99	5.98
HCAR3600	Bullet CA glue	adhesive	2oz.	3	7.99	23.97
HCAR3650	Bullet CA+ glue	slow adhesive	2oz.	2	7.99	15.98
HCAR3750	Activator Spray	accelerator	2oz.	2	4.79	9.58
XACR2180	X-Acto knife set	cutting tools	1 set	1	15.59	15.59
HCAR5100	Steel T-pins 1"	temp.fasteners	100/box	1	2.09	2.09
Sub Total						\$100.30

## Hechingers Hardware

5041611	9x11 Ultra Fine Abrasive 660	Sandpaper	4 sheets	1	3.41	3.41
Sub Total						\$3.41
Total Cost						\$103.71

# **PROPOSAL FOR THE DESIGN OF AN UNMANNED AIR VEHICLE**

## **ADDENDUM PHASE: PART SEVEN**

*Prepared for Gregory Page*

*Submitted 13 April 1998*

*by the Syracuse University Chapter of the American Institute of Aeronautics and Astronautics*

### *Design Team Members:*

*Kevin Bendowski*

*Kevin Bishop*

*Nick Borer*

*Marc Brock*

*Jarrold Cafaro*

*Arun Chawan*

*Garvin Forrester*

*Tom Jones*

*Dr. Hiroshi Higuchi, Advisor*

## TABLE OF CONTENTS

<b>7. Lessons Learned</b>	<b>1</b>
7.1 Aircraft Design Challenges	1
7.1.1 Tail Boom	1
7.1.2 Landing Gear Configuration	1
7.1.3 Front Motor Cowling	1
7.2 Cost Estimate	2
7.3 Cost Reduction Techniques	3
 <b>List of Tables and Figures</b>	
Table VII-I. <i>Estimated Cost</i>	2
Table VII-I. <i>Actual Cost</i>	2



## **7. LESSONS LEARNED**

### **7.1 Aircraft Design Changes**

Since its completion, some changes have been implemented into the original design proposed. These are believed to be necessary or desirable based on technical and budget considerations. These alterations are not trade-offs, but instead decisions made after careful analysis.

#### **7.1.1 Tail Boom**

The first change takes place at the rear of the fuselage, to the boom that connects the main body (where the avionics and payload are housed) to the empennage. Originally, this was going to be made from eight pieces of balsa wood, which were to run from the rear of the composite main body to the empennage.

This configuration will be replaced with a lightweight yet durable section of 1.5 inch PVC pipe. This section of PVC pipe will be connected to the main body of the fuselage through two plywood bulkheads at the rear of the graphite main body. The empennage will pass through slots cut into the pipe, and everything will be fastened with epoxy. This will save on some weight, while easing the manufacturing process. Also, no covering will be needed for the PVC pipe, saving a little on overall cost.

#### **7.1.2 Landing Gear Configuration**

The original design called for a tricycle type landing gear configuration, with the nose gear attached to the front "firewall" bulkhead (at the rear of the motor) and controlled via an extension of the rudder servo. The main gear would pass through the fuselage and into a bulkhead aft of the wing saddle. While this would make the aircraft easier to land, it would be a bit difficult to design and link, and would cause more drag.

This has been waived in favor of a taildragger configuration, with a smaller tail wheel attached directly to the rudder. The main gear will be moved forward to a bulkhead forward of the wing saddle. This saves on weight and drag, and is easier to manufacture. Also, the special accessories required to affix a nose gear to an aircraft will not be needed.

#### **7.1.3 Front Motor Cowling**

Finally, the front cowling design was changed. Initially, the design report proposed to cut and sand down four rectangular pieces of balsa to a more aerodynamic shape. This would involve quite a bit of time and patience, and there would be difficulty involved in getting an exact fit between the pieces.

The remedy was found in a bottle – a two-liter plastic soda bottle, to be exact. The bottle will be trimmed and fastened to the front of the main body with balsa scraps and small wood screws (so it can be removed later for access). The soda bottle proved to be about four inches in diameter, so the fit will be very close. The save in design time and hassle is great, at very little in cost.

#### **7.1.4 Projections for Next Year**

This year's entry so far has met all expectations that were entered at the beginning of the year. While there still is more testing and manufacturing to be completed, the design team is nonetheless happy about this revelation. However, this does not mean that there is not room for improvement next year. More experimental techniques will probably be integrated into next year's entry.

Some of these techniques could include a radical change in wing design. So far, the team's two entries (last year's and this year's) have been straight, high wing monoplanes. Winglets could be added to the wingtips to decrease the vortices encountered there, thus increasing the available lift. A more efficient low speed airfoil could be found, or even designed by team members. Other control surfaces, such as flaps, may be integrated as well. Finally, the wing could be composed of advanced materials, as opposed to the wood that gives its shape now.

The fuselage may need to be radically altered to make way for a mid- or low-wing monoplane, if deemed necessary. A pusher prop or ducted fan may be used for propulsion, further increasing the need for

a change in the design of the body. Retractable landing gear, while requiring heavier equipment to operate, may be desirable to reduce drag, and the fuselage would have to change for that as well.

Some of these changes have already been proposed. Next year's entry from Syracuse will probably have winglets, a custom airfoil, and more control surfaces. This aircraft will most likely have more accessories and will be better suited for its mission since more funds can be used for the aircraft and not its components (radio, receiver, charger, etc.). Only time will tell for sure.

## 7.2 Cost Estimate

Component	Estimated Cost
Motor & Speed Controller	350
Radio & Receiver	250
Battery Pack	300
Battery Charger	150
Materials	-
- balsa/glue	100
- composite	200
Accessories	100
- covering materials	-
- propellers	-
- landing gear	-
- control rods/horns	-
Other	50
<b>Estimated Total</b>	<b>1500</b>

Table VII-I. *Estimated Cost*

Component	Manufacturer	List Price
Motor & Speed Controller	Aveox	339.44
Radio & Receiver	Futaba	231.05
Battery Pack	Trinity	319.96
Battery Charger	AstroFlight	154.99
Materials		-
- balsa/glue	Tower Hobbies	52.21
- composite	Fibre Glast	227.64
Accessories	Tower Hobbies	107.82
- covering materials		-
- propellers		-
- landing gear		-
- control rods/horns		-
Other		-
- printing	Kinko's	60
- shipping	USPS	20
- battery pack assembly	S.U. Chemistry Dept.	20
<b>Actual Total</b>		<b>1533.11</b>

Table VII-II. *Actual Cost*

The actual cost of the project closely matched the estimated value. The prices for the most costly components could easily be guessed due to readily available manufacturers' catalogs, and the valuable experience gained from team members who also participated in the previous year's competition. The budget overflow was due to unexpected expenses such as printing and shipping. The unanticipated costs will be useful for future cost estimations.

### 7.3 Cost Reduction Techniques

The manufacturing of the aircraft on a limited budget required some cost saving techniques. The area where the most attention to cost cutting was on the design and manufacture of the fuselage. For one, the mold was not custom made. Instead, a four-inch diameter piece of PVC (polyvinyl chloride) pipe provided the basic shape needed. The pipe was cut in half, and the two halves used as the molds for the fuselage. The PVC pipe was an inexpensive alternative to other methods of creating molds such as the use of RTV (Room Temperature Vulcanizing) rubber.

This molding process involved creating a vacuum to remove the excess epoxy from the matrix while the epoxy cured. For this process, plastic vacuum bags were needed to enclose the mold and graphite. While some vacuum bags were purchased, not enough were on hand for the entire process. Instead of purchasing more bags, it was decided that some could be made. This was achieved by utilizing excess window insulation sheets, which were of the same grade as the vacuum bags. This proved to be well suited for sealing the molds. These sheets of plastic were cut to size and sealed with duct tape, at virtually no cost to the group.

An oven was needed to place the vacuum-sealed molds in while they cured. Instead of purchasing a curing oven, one was improvised by placing a space heater inside a steel cabinet. The space heater was able to bring the temperature inside the cabinet up above one hundred degrees Fahrenheit. This method was very effective, and the entire curing oven came at no cost to the team.

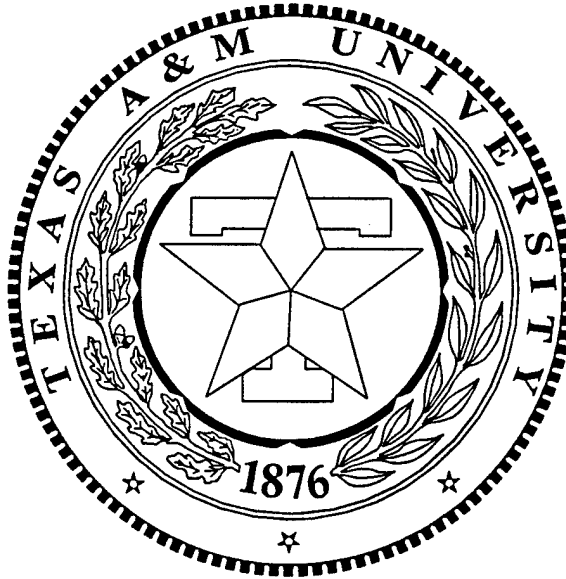
The materials for the fuselage were carefully calculated, so none would be wasted. A precise amount of graphite was ordered, with a little excess to account for rounding and cutting errors. In addition, the amounts of epoxy and resin that were used during the molding process were carefully monitored, so little would be wasted.

The last aspect of the fuselage included an inexpensive way of constructing a cowling for the aircraft. Molding the graphite into a conical shape in the PVC pipe would prove to be quite difficult, so improvisation prevailed again. It was decided that using the top half of a two-liter soft drink bottle would be the easiest and cheapest thing to do, and would provide the right shape. Since the bottle would be a non-load-bearing member, the strength of the material was not a great consideration, and its very low cost was augmented by the fact that the team members could also relieve their thirst in its manufacture.

The most important cost saving technique for the wing was in the use of materials. The wing used was made from balsa wood, a very inexpensive and readily available material. It is cheap to manufacture and easy to repair, which fit all the necessary criteria.

Some investments for future competitions were made with the electronic equipment purchased. The radio transmitter, batteries, and battery charger are all things that can be reused in the future. Since these items needed to be purchased this year, it was the general consensus not to go "cheap" on them. Between these three items, about seven hundred dollars was spent, almost half of our budget. This amount may seem like quite a bit, however, by carrying over this equipment for use on future planes, this team is saving each group to come seven hundred dollars. Hence, we resisted the urge to buy the cheapest electronics needed, and instead invested in quality equipment.

AIAA Student Design/Build/Fly  
Competition  
The Texas Tall Boy



Proposal Phase

Designed and developed by:

Robert "Rip" Rippey III

M. Shea Parks

Kendrah S. Smith

David Sellmeyer

Texas A&M University, College Station, Texas

March 16, 1998

# Table of Contents

	Page
Table of Contents	i
1. Executive Summary	1
1.1. Major development areas	1
1.2. Design tools overview	2
2. Management Summary	2
2.1. Architecture and assignment areas of the design team	2
2.2. Management structures and timing	3
3. Conceptual Design	3
3.1. Figures of merit	3
3.2. Alternative concepts investigated	4
3.3. Design parameters investigated	5
4. Preliminary Design	5
4.1. Figures of merit	5
4.2. Design parameter and sizing trades	6
4.2.1. <i>Flying weight</i>	6
4.2.2. <i>Aspect ratio</i>	6
4.2.3. <i>Handling qualities</i>	6
4.2.4. <i>Landing gear</i>	7
4.2.5. <i>Propulsion cooling</i>	7
4.2.6. <i>Aircraft disassembly</i>	8
4.2.7. <i>Component access</i>	9
4.3. Analytic methods	9
4.4. Minimum configuration and vehicle sizing	10
4.5. Key features which distinguish the final configuration	11
5. Detailed Design	11
5.1. Final design	11
5.2. Innovative techniques	13
5.3. Cost reductions	14
5.4. New configuration ideas	14
6. Manufacturing Plan	14
6.1. Figures of merit	14
6.2. Manufacturing processes for final design	15
6.2.1. <i>Manufacturing plan</i>	15
6.2.2. <i>Wing construction</i>	15
6.2.3. <i>Tail surface construction</i>	16
6.2.4. <i>Fuselage construction</i>	17
6.2.5. <i>Landing gear construction</i>	17
6.3. Alternative manufacturing processes investigated	17
6.4. Analytic methods used	18
6.5. Manufacturing timing	18
6.6. Key features	18
References	20

**Appendix A**

Preliminary and Detailed Performance Development Calculations

**Appendix B**

Stability and Control Calculations

**Appendix C**

ElectriCalc Data

**Appendix D**

Wing Airfoil Analysis Data

**Appendix E**

Wind Tunnel Propulsion Test Data

**Appendix F**

Design Parameters for the Aggie Flyer

**Appendix G**

Design Parameters for the Texas Tall Boy

**Appendix H**

Landing Gear Layup

**Appendix I**

Drawing Package for the Texas Tall Boy

**Appendix J**

Scheduled and Actual Timing of Major Events

**Appendix K**

Component Weight Breakdown

# 1. Executive Summary

## 1.1. Major development areas

Designated the Texas Tall Boy (TTB), the 1997-1998 entry from Texas A&M University began as a second-generation aircraft with its origins in the 1996-1997 entry, the Aggie Flyer. After the team considered the rule changes for this year's contest, most notably the air race style competition imposed by the new time limit, it was observed that the Aggie Flyer could easily be modified to perform better under the new rules. With that in mind, the team derived the Texas Tall Boy from the Aggie Flyer by making slight changes to sizing, configuration, and structure.

Initially though, many design changes and alternative configurations were investigated in the conceptual design stage in order to be verify that the TTB would perform best if based on the Aggie Flyer. Included in this list of possible configurations was the consideration of a flying wing, a canard configuration, tandem wings, and eventually variable geometry.

In first considering a flying wing aircraft, it was decided that working around the stability and control issues that accompanied a flying wing concept was beyond the scope of the project, and so that concept was abandoned. Similarly, the second alternative of a canard configuration was rejected because the team was not as familiar with the design of such an unconventional layout. For the third option, a tandem wing aircraft was investigated, but was later discarded because the additional induced drag of a second wing would have cost precious speed. Finally, the team considered an airplane with variable geometry since wing sweep could be changed to the optimal position for each flight phase. This idea was later ruled out due to the figures of merit governing the conceptual design phase.

Throughout this conceptual design phase, tools used to guide the design included computer programs and other electronic tools, but most influential was the team's experience with the previous DBF competition. After considering all possible alternatives, the team settled on a conventional aircraft layout similar to that of the Aggie Flyer. Since the team wanted to optimize the propulsion system and airframe size to produce an airplane that would complete as many laps around the race course as possible in the given time limit, it was decided that the TTB could be designed to have a lower profile than its predecessor.

By using the previous design entry, many aspects of the new design were refined and improved while allowing the positive aspects of the original design survive. Subsequently, the considered changes to the design included reducing the frontal area of the fuselage while retaining much of the same layout of internal components. The final airplane configuration resembled a more refined and sleek derivative of the Aggie Flyer.

During the preliminary design phase, the team began to use computational tools. For estimating initial thrust and endurance performance, the different power systems and airplane configurations were related using the ElectriCalc software by SLK Electronics. In order to manipulate different performance and handling qualities, an Excel tool was developed which used the standard methods outlined in *Airplane Design, Part I: Preliminary Sizing of Airplanes* by Roskam. Much of the information obtained during this phase was

further refined through decisions based on the figures of merit identified/developed during the competition and the conceptual design.

### *1.2. Design tools overview*

During the preliminary design phase more computational tools were used. For determining initial thrust and endurance estimates relating many different power system configurations, the software ElectriCalc by SLK Electronics was used. In order to manipulate different performance and handling qualities, a personally developed general computing program in Microsoft Excel was set up using the standard methods outlined by *Airplane Design, Part I: Preliminary Sizing of Airplanes* by Roskam. Much of the information obtained during this phase was further refined through decisions based on the figures of merit yielded by the competition and the conceptual design. These calculations are shown in Appendix A: Preliminary and Detailed Performance Development Calculations.

The detailed design allowed more use of computation methods for developing the design of the TTB. For the determination of the airfoil section and the 3-D to 2-D needs of the aircraft, computer programming was needed. An airfoil analysis software, PANZ, was used with information produced from the preliminary design. This allowed more insight on the interaction of many different airfoils with the general needs of the aircraft.

The general design programming used previously in the preliminary design for the performance and handling qualities was further refined for the detail design. This programming allowed easy access to make modifications and manipulate final concepts without starting from scratch. Also, for specific performance areas such as stability and control and handling qualities, further Matlab programming was developed using methods from small perturbation stability and control analysis. The primary source of this information was derived from the methods in *Flight Stability and Automatic Control* by Nelson.

## **2. Management Summary**

### *2.1. Architecture and assignment areas of the design team*

The assignment areas of the design team were divided among the four team members, Rip, Shea, Kendrah, and Dave. Robert "Rip" Rippey III, a senior Aerospace Engineering major, was the team leader. He monitored the budget and ordered materials and parts for the airplane. Because of Rip's ten years of R/C experience and position as team leader in the previous AIAA Design/Build/Fly (DBF) competition, the team designated him pilot, airframe constructor, and materials coordinator. Rip also researched and selected a cooling system for the propulsion system. Rip and Shea collaborated during the conceptual, preliminary, and detailed design phases of the TTB.

M. Shea Parks, also a senior Aerospace Engineering major, chose the airfoil and design for the Texas Tall Boy based on graphs, charts, and calculations from his and Rip's research and their previous DBF experience. Because of Shea's two years of wind tunnel experience, he was chosen to conduct tests on various motor/battery/propeller combinations for final



component selection. In addition, Shea compiled the bulk of the drawings for the completed aircraft.

Kendrah Smith, a freshman Math major with previous experience in an aerospace engineering related project, assisted Shea with the motor/battery/propeller testing and the drawing package. Also, Kendrah arranged preliminary data for the airfoil selection and motor/battery/propeller combinations. Furthermore, she assisted Dave in obtaining real time performance data during flight testing of the TTB.

Dave Sellmeyer, a junior Aerospace Engineering major, brought knowledge gained from his experience with an unmanned aerial vehicle (UAV) company, construction of composite structures, and radio control (R/C) modeling to the team. For this reason, he constructed the composite main landing gear for the TTB. In addition, Dave tested and modified several composite landing gears previous to selecting the final construction lay-up. Finally, Dave obtained performance measurements during the flight testing of the aircraft.

## *2.2. Management structures and timing*

The overall design and development of the TTB was regulated by a series of management structures. Configuration and design control rarely presented a problem due to the overall methodology and objectives of the design team. Once a major aspect of the design and development was finally decided upon, little deviation from the concept was incorporated.

Design task schedule control, primarily governed by the team leader, was developed as a guide for the design team. This allowed the team to continuously evaluate the state of events and advancements in the competition development. Located in Appendix J: Scheduled and Actual Timing of Major Events, are a milestone chart and table of all major events focused on for the entire development of the TTB. The preliminary scheduled event completion dates and the actual event completion dates are represented. In many of the production phases of the design the team did not meet the projected dates. However, all phases were completed with marginal time to allow intermediate alterations and refinements.

# 3. Conceptual Design

## *3.1. Figures of merit*

The figures of merit considered during the conceptual design phase were an optimized propulsion system, the projected speed of the aircraft, and the final flying weight of the aircraft. The team wanted to have an aircraft that would be considerably faster than the previous airplane. Initially, the airplane was to have a cruising speed of 100 ft/sec. Such increased speeds involved looking at lowering the drag and increasing the wing loading of the previous generation design. The weight of the aircraft needed to be reduced in every way possible for the best performance. More importantly, a propulsion system would be required to provide enough thrust for a climb-and-glide strategy similar to that used in the 1996-1997 competition; however, the run time would have to be balanced to complete the laps within the seven minutes of flying.

The final ranking of the figures of merit were established and evaluated with the aid of the design and development programming methods of *Airplane Design, Part I: Preliminary Sizing of Airplanes* by Roskam, and the power combinations yielded from the ElectriCalc software. They are listed below in order of importance:

- Optimized propulsion system
- Projected speed of the aircraft
- Final flying weight

### *3.2. Alternative concepts investigated*

The basis of the conceptual design started with the Texas A&M University AIAA (DBF) entry from the 1996-1997 competition. Since this airplane was optimized for range by using high speed, it was considered a derivative of the previous generation aircraft. The Aggie Flyer was by far the lightest and fastest airplane at the 1996-1997 competition. Using the method of evolving the previous design based on past experience proved to be the primary method of conceptual design.

Although the team derived a second-generation aircraft, many alternative concepts were investigated in order to try to improve the overall design of the Aggie Flyer. Concepts investigated initiated with the examination of the wing configuration. The previous competition entry was a conventional fixed wing aircraft, which utilized a single carbon fiber and balsa wood spar assembly. An array of ideas such as a flying wing, tandem wing, variable geometry wing, and canard configurations were debated.

The flying wing, tandem wing, and canard configurations were rejected due to the stability and control challenges and all around impracticality that was represented through initial wing concept research. Variable geometry was debated with slightly more detail. It was recognized that, with a variable geometry wing, the design aircraft might be able to deliver an improved performance at different phases of the competition flight course when compared to a conventional wing. However, this concept also proved to be impractical due to the amount of mechanical structure that would be needed in order to be effective. The amount of extra mechanics and weight was simply not worth the performance tradeoffs. The end result of the conceptual stage was to remain with a conventional fixed wing and stabilizer design.

The single wing spar concept was also further investigated. The previous design proved to be effective in many of the design target areas and mission features, however, some of the figures of merit such as easy transportation and disassembly (which will be discussed in later sections), were not maximized to their full potential. Therefore, modular wings and joined carbon tubing spars were investigated.

The empennage concepts of the Aggie Flyer were investigated. The truss (non-airfoil) concept was used previously with performance and handling results that could be improved.

Therefore, when developing the TTB, airfoiled vertical and horizontal tail sections were researched and debated in order to push the previous design to more efficient states of performance. Specifically, the incorporation of an airfoil into the tail surfaces was to help keep airflow attached to the surface, resulting in more effective control surfaces.

### *3.3. Design parameters investigated*

Once initial alternatives in the configuration were investigated and decided upon, the design parameters were established. Early in the design process, the team watched video footage of the flights made by the Aggie Flyer to determine the time of flight and average flight speed. First, the aircraft had a relatively high wing loading (for this size airplane) of 30.0 oz/ft<sup>2</sup>. Second, flight strategy consisted of using full power only for half of the upwind leg of the course and a power-off glide for the rest of the course. These two features produced flight averaging eight minutes, including takeoff, landing, and the two 360-degree turns, as required by the competition rules. At most, eleven laps at a speed of approximately 80 ft/sec around the course were completed during any of the flights made by the Aggie Flyer during the competition. A list of the design parameters of this aircraft is given in Appendix F.

## **4. Preliminary Design**

### *4.1. Figures of merit*

Ranked in the order of importance, the figures of merit that governed this phase of the design process were:

- Transportation of the aircraft
- Structural component accommodation
- Payload and propulsion system access
- Simplicity of design
- Propulsion system cooling
- Final flying weight
- Total drag
- Aesthetics

## *4.2. Design parameter and sizing trades*

### **4.2.1. Flying weight**

The basis of the preliminary design started with establishing the major design parameters and sizing trades. The mission requirements focused greatly around the payload fraction and the influence of systems component weight. The mandated 7.5 pound steel payload and an optimized total performance weight of 16 pounds (256 oz.) were the first parameters established. This total weight was derived from estimations of systems components (motor, batteries, radio equipment, etc.), airframe structure, landing gear, and all other components from the previous design. Overall weight and its effects on range and performance became the key issues in deriving the other design parameters and sizes.

Once the preliminary total performance weight was derived, the wing efficiency was examined. By using the weight parameters in addition with the pilot control skills, research results from the previous design, and preliminary calculations a wing loading range of 2 lbs/ft<sup>2</sup> (32 oz/ ft<sup>2</sup>) to 2.30 lbs/ ft<sup>2</sup> (36.8 oz/ ft<sup>2</sup>) was incorporated. After debate and examination it was decided that to better accommodate a more efficient design the wing loading should be established at 2.25 lbs/ft<sup>2</sup> (36.0oz/ ft<sup>2</sup>), thus yielding a wing area of 7.11 ft<sup>2</sup>.

### **4.2.2. Aspect ratio**

The next parameter derived was the aspect ratio. The Aggie Flyer had an extremely efficient aspect ratio of 10.0, which proved to also be a feasible sizing tradeoff for the TTB. Also incorporated into the wing efficiency was the design parameter of the airfoil performance and thickness. An airfoil needed to be selected that could perform with efficient aerodynamic characteristics and be able to accommodate the necessary internal wing control devices and allow for the overall structural rigidity. The aerodynamic qualities demanded a relatively thin airfoil due to the sizing trades of speed versus drag. However, the systems accommodations required slightly thicker families of airfoils.

### **4.2.3. Handling qualities**

The all around performance and handling qualities of the TTB were also major design parameters inspected. These parameters primarily focused upon keeping drag coefficients reduced while allowing the lifting and velocity potentials to be maximized efficiently based upon energy and power available from the power combination. This method yielded great scrutiny over the power combination and the trades of performance, which was aided in using the previous design as solid reference.

Stability and ease of pilot control presented some problems in the previous design. Therefore, focus was placed on improving some of the aspects of these problems. One case in the Aggie Flyer design was that the wing was incorporated with an incidence angle in relation to the fuselage centerline that caused the fuselage to cruise at trim with an angle of attack. Although preliminary calculations showed a positive result, the actual model proved to have less than desirable handling in certain maneuvers. As a result, the Texas Tall Boy incorporated an incidence angle of 2 degrees relative to the thrust line.

#### 4.2.4. Landing gear

Another design parameter was the focus of the most practical and efficient type of landing gear. The landing gear for the TTB needed to have minimal static deflection while the aircraft was fully loaded in order to keep the wheels somewhat aligned during takeoff and landing roll. If the gear could not keep the axles aligned properly, a ground loop could occur, resulting in damage to the aircraft.

Large dynamic deflection (25%-40% deflection relative to the length of the landing gear) due to landing could be acceptable for the purpose of allowing the landing gear to absorb landing loads without transferring too much force into the fuselage structure.

As mentioned for figures of merit, overall aircraft weight and total drag were important factors in determining the landing gear configuration. The fewest wheels and accompanying structure would result in the lightest and cleanest landing gear configuration. However, at least three wheels were desired to maintain longitudinal stability on the ground (without relying on wing skids) and smooth steering. Ultimately, if all ground contact points were wheels, rather than skids, the takeoff acceleration would be higher, and the ground roll would be shorter. The propulsion system should not waste any of its limited energy in getting the aircraft off the ground.

Tricycle and tailwheel landing gear were left to choose from. From experience, it was known that the tricycle gear was more stable on the ground, while the tailwheel configuration could have more problems with ground loops.

Going back to the low-weight figure of merit, the team decided that appropriately-sized wheels and accompanying structure for a tailwheel landing gear would be about 25% lighter than that for a tricycle gear. The tailwheel landing gear was chosen for the competition aircraft.

Structurally, the main gear would be required to take lateral loads presented in the case of a ground loop at landing speeds (to be determined in the detailed design phase). Also, the tail wheel and accompanying structure would need to be able to withstand side loads; however, experience showed that vertical loads on the tail wheel would be minimal.

Retractable landing gear was considered, but two of the figures of merit overrode the one in favor. Although retractable gear would reduce the drag of the aircraft in flight, the mechanical complexity and the weight of the additional structure required for such an operation rendered this feature nearly profitless for the aircraft.

#### 4.2.5. Propulsion cooling

Cooling for the propulsion system was mandatory. The electronic speed control for the motor was the most critical component to be cooled since overheating could cause damage to the circuitry. The propulsion battery pack and motor needed adequate cooling for maximum power output, as stated by the manufacturers of the items.

Since overall drag on the aircraft was a figure of merit during the preliminary design phase, the cooling system would be required to have the lowest drag possible. The tradeoff for this figure of merit was pressure recovery in the cooling system. Research and development of air intake geometry by NACA produced a low-drag flush inlet with up to 92% pressure recovery for subsonic speeds. Published data detailing the geometry of the NACA flush inlets was found in *Aircraft Design: A Conceptual Approach* by Raymer.

The single inlet was placed on the bottom of the fuselage, immediately behind the plane of the propeller. This area was determined to be a high-pressure area for all desired flight conditions. Motor cooling was provided by such a forward location of the inlet. Intake air would then flow past the heat sink side of the speed control (the side of the speed control with the electronic components was mounted to the bottom of the "ducting" that maintained airflow only where desired through the bottom of the aircraft).

The propulsion battery was offset from the sides of the fuselage (as opposed to a tight, high-contact fit inside the fuselage) in order to provide quicker heat radiation. The rails that would raise the battery pack from the bottom of the fuselage would serve as the last stage of the ducting before the air exited the aircraft.

As explained previously the wing incidence relative to the fuselage centerline was set such that the fuselage centerline has no angle of attack when cruising. The fuselage bottom was shaped relative to the centerline to provide a low-pressure area aft of the propulsion battery for the cooling air to exit. A NACA flush inlet was reversed and installed in this area. The area of the outlet was 56% larger than that of the inlet in order to prevent stagnation in the cooling duct. The entire cooling system is detailed in Appendix I: Drawing Package for the Texas Tall Boy.

#### 4.2.6. Aircraft disassembly

One of the figures of merit governed the disassembly of the aircraft. The team desired to be able to transport the airplane in a small, two-door car. With a wingspan of 101 inches already determined, the airplane could not fit in the car with a single-piece wing. For simplicity, the wing separated into only two pieces. This disassembly resulted in three components, namely the fuselage, which was 55 inches long, and the two wing panels, which were 49.5 inches long, each.

The two wing panels joined by means of a 12-inch-long  $\frac{1}{2}$ " O.D. pulltruded (referring to the manufacturing process) carbon fiber tube that remained fixed in the fuselage. Two 8-32 bolts attached the wings by threading into the two overlapping secondary hardwood joiners that were fixed in the wing panels.

Not only did the removable wings provide disassembly for easy transportation, but this feature also allowed the steel payload to be installed and removed. The 7.5 pounds of steel were shaped as two rectangular blocks that secured in the fuselage and extended nonstructurally into the wing panels.

#### 4.2.7. Component access

For component access, three hatches were built into the aircraft. One hatch was on the upper side of the fuselage, just ahead of the wing leading edge. It extended to the fuselage centerline (rather than a panel just on the top of the fuselage) to provide easy access to the speed control and the battery-motor connection. Although aesthetics were relatively unimportant compared to some of the other figures of merit, this forward hatch doubled as a "canopy" that would be seen on larger, manned aircraft.

Propulsion battery access was provided by means of the second hatch. This large (eight-inch-long), removable panel served as the floor of the fuselage, immediately aft of the main landing gear. The receiver and receiver battery pack could also be accessed when this panel was removed.

Finally, a small panel was located on the bottom of the fuselage for access to the rudder and elevator servos. All of the hatches can be seen in the Drawing Package for the Texas Tall Boy (Appendix I).

#### 4.3. Analytic methods

Several computational methods were utilized during the preliminary design phase. The primary method was to use basic computational programming software such as Microsoft Excel to develop and organize the preliminary configuration, sizing, and performance parameters. The method of developing this parts of this programming were the computational and sizing estimates in, *Airplane Design, Part I: Preliminary Sizing of Airplanes* by Roskam and *Model Aircraft Aerodynamics* by Simons. The performance computational portions of the programming were based upon the methods dictated in *Fundamentals of Aerodynamics*, by Anderson and *Introduction to Flight* by Anderson. Appendix A, Preliminary and Detailed Performance Development Calculations, details these preliminary results using many different parameter choices.

Another computational analysis method used in the preliminary design phase was the ElectriCalc power system evaluation software by SLK Electronics. This software allowed the design team to evaluate many different combinations for the propulsion and power system before having to make any decisions or purchases on any components. The ElectriCalc software was used in the previous year's competition design development and was proven to be an effective tool for systems selection. Appendix C, ElectriCalc Data, shows output and results of the software for some of the initial combinations examined. As a comparison to a small selection of the combinations researched the Aggie Flyer's results are displayed.

The information most importantly examined was the overall thrust output at full throttle and the propulsion battery total power depletion time. These parameters were maximized for efficiency, and the other yielded information was used as secondary screening factors.

A non-computational analytic method was the development of a low-speed wind tunnel test in order to screen power system combinations. Basis for the development of the testing came from methods described in *Low-Speed Wind Tunnel Testing*, by Rae and Pope. Many

different components had been purchased or borrowed from other modelers to see the real time effects of different components. A full detail of the wind tunnel test and its results is located in Appendix E: Wind Tunnel Propulsions Test Data.

To aid in the preliminary airfoil selection for the wing, an airfoil analysis software named PANZ was used. PANZ is software written and developed by Dr. Tom Pollock, Professor, Aerospace Engineering Department, Texas A&M University. This software uses the actual shape and design of a prescribed airfoil and analyzes the 2-dimensional performance characteristics based on the design flight conditions. This 2-D information is returned and matched to the optimized conditions and design parameters desired.

Displayed in Appendix D, Airfoil Analysis Data, are the 2-D coefficients of lift curves of several different airfoil possibilities examined. Also included are coefficient of lift curves for PANZ calculated data and widely published data for selected airfoils. The publications used were the *Comprehensive Reference Guide to Airfoil Sections for Light Aircraft*, by Aviation Publications, and *New Airfoils for R/C Sailplanes*, by Selig and Gopalathnam. By plotting the curves for the R.A.F. 32 airfoil used in the Aggie Flyer and those of the most efficient possible airfoils (SA7035 and SA7038), the proficiency and accuracy of the PANZ software is shown with positive results.

#### *4.4. Minimum configuration and vehicle sizing*

The minimum configuration and vehicle sizing developed during the preliminary design phase is divided into many parameters. Beginning with the weight breakdown, a total weight of 16 pounds was based upon approximate airframe, propulsion system, control system choices. This weight and corresponding wing loading yielded a conventional wing (area: 7.11 ft<sup>2</sup> and span: 8.63 ft), empennage (vertical tail volume: 0.496 ft<sup>3</sup> and horizontal tail volume: 0.66 ft<sup>3</sup>), and control surface (aileron: 5.0%, rudder 12.0%, and elevator: 20.0%) sizing is located in Appendix A.

The fuselage sizing was established with the initial payload, systems components, wing, and empennage placement. The fuselage was initially designed to be 2.5 in. wide and 3 inches deep at the maximum (center of gravity) cross section. The length from firewall to trailing edge was at a minimum 4 ft.

The payload was placed at the estimated center of gravity, laying into the wings from the fuselage. The propulsion and control systems were laid out down the centerline axis of the fuselage. The overall static margin due to all components was estimated to be 14.0%.

The wing airfoil performance developed to make the preliminary selections required maximum 2-D coefficients of lift during cruise, take off and landing of 0.132 and 0.113. However, the maximum coefficients of drag 0.045 were 0.033, respectively. The vertical and horizontal tail airfoil requirements, which needed to provide a clean and attached flow, were established with a 8% - 12% symmetrical airfoil. This information is also held in Appendix A.



#### *4.5. Key features which distinguish the final configuration*

The Texas Tall Boy incorporated several key features which distinguished it from typical model aircraft. First, over ninety percent of the airframe and empennage is built with lightweight balsa wood. This construction practice yielded an extremely light airframe of only three pounds. In order to offset any losses of strength caused by this application, high strength carbon fiber was used as a spar cap (detailed in the section titled "Manufacturing Plan"). A set of wound carbon tubes were embedded between balsa stock to form the spar box in each wing with unidirectional carbon adhered to the outer surfaces of the spars. A pulltruded carbon fiber tube was used to join the two wing halves together. In addition to strengthening the wing, this design allows for easy transportation to the flying site.

Further weight reductions were realized without costing strength through the use of composite materials in the landing gear. Carbon roving was layered around a balsa core to form the main landing gear strut. In combining the carbon strut with low profile molded-resin wheels, a six-ounce weight savings resulted over traditional aluminum strut/rubber wheels. Bending tests indicated that the composite landing gear yielded one third as much as the aluminum gear when subjected to normal landing loads.

Another feature found in the Texas Tall Boy was the incorporation of NACA cooling scoops into the fuselage design. Since the main battery required a large surrounding air mass to prevent overheating, cooling scoops were used to provide a continuous supply of air over the lower surface of the battery. This feature allowed the overall dimensions of battery compartment to remain small, thus reducing the fuselage profile drag and increasing the airplane's speed and efficiency.

As a signature by the builder of the TTB, a long dorsal fin introduced a distinctive sweeping vertical stabilizer ending in a sharply pointed rudder. This added a sleek look to the aircraft, which when combined with the other key features, allowed it to be distinguished from other aircraft on the flight line.

### **5. Detailed Design**

#### *5.1. Final design*

Final performance information such as the takeoff, landing, thrust, and handling qualities are highlighted in Appendix A. In summary, the TTB has a takeoff coefficient of lift of 0.139, at a velocity of 80.4 ft/s, yielding a rolling distance of 76.2 ft. The landing coefficient of lift is 0.118, at a velocity of 87.1 ft/s, and a rolling distance of 187 ft. The values of maximum velocity and minimum glide sink are 88.0 ft/s and 73.3 ft/s. The overall drag polars are; zero lift drag: 0.043, clean: 0.046, and total takeoff configuration: 0.067. The G-loading capability on a maximum bank angle of 53 degrees is 1.9. And a maximum G-loading in a sudden pull-up at a stall angle of 10 degrees is 1.79.

The endurance requirements of the TTB were fulfilled by identifying important mission objectives, optimizing the flight strategy, and incorporating results reduced from the wind tunnel test into the design of the propulsion system. The resulting performance of the

engine/battery combination turned out to be highly efficient, yielding a total battery endurance of approximately 3½ minutes, which included a 20-second takeoff phase. With this endurance, a 4½-minute power-off glide was possible in order to satisfy the mission requirements of a 7-minute maximum on-course flight time.

Using small perturbation theory as described in *Flight Stability and Automatic Control*, some simple stability and control analyses were done in order to check the modal characteristics of the Texas Tall Boy. Matlab was used to perform the calculations as shown in Appendix B. The determination of the modal characteristics was important since the aircraft was required to complete the course without stability augmentation. Of particular interest was the period and damping ratio of the phugoid mode. With a period of 9.30 seconds and a relatively low damping ratio of 0.042, the altitude oscillations caused by the phugoid mode would yield challenging landings. Since the phugoid damping ratio was inversely proportional to the lift to drag ratio of the aircraft, altitude variations during the low landing speeds could be reduced by increasing drag and/or reducing lift during the landing approach. Raising the ailerons, to simulate spoilers, could achieve this goal, but only flight testing would confirm the effectiveness.

The rest of the modes had stable roots, showing that the aircraft would be able to maneuver around the course within the skills of the pilot. Lateral/directional stability was ensured by the damping ratio of 0.071 and period of 1.70 seconds presented with the dutch roll mode.

The team selected the components for the plane according to the figures of merit for the detailed design. Analysis data from ElectriCalc and research of electric propulsion systems led the team to choose the Aveox 1412/2Y coupled with a 3.7:1 inline gearbox. The Aveox M60 speed control (for 14-32 cells) was chosen because of size and weight reduction and ease in programming compared to its predecessor (used in the Aggie Flyer during 1996-97 DBF competition). To keep the propulsion battery pack under the 2.5-pound limit, nineteen 2000 mAh cells were used. ElectriCalc data confirmed these cells as having the highest capacity of any cells commercially available.

To reduce the drag while gliding with the climb-and-glide strategy, a folding propeller was used. The ElectriCalc data showed that a 15-inch propeller with a 9.5-inch pitch would result in high thrust (125 oz.) with moderate run times (2.6 minutes). The data for this combination is shown in Appendix C. Specifically, a Graupner carbon fiber propeller with these specifications was used because of its weight difference compared to a heavier, injection-molded nylon propeller.

All components of the propulsion system are shown in Appendix I: Drawing Package for the Texas Tall Boy.

Control was provided by a Futaba 8-channel PCM radio system. The transmitter provided mixing required for the separate aileron servos, allowing them to work together as flaps. Rather than using a 500 mAh receiver battery pack (common for this size airplane), the team chose to use a 250 mAh pack to reduce the overall weight of the aircraft (by 1.2 oz).

Standard ball-bearing servos were used for the rudder and elevator, but smaller, lighter servos were used for the ailerons due to the limited room inside the wing panels. The aileron servos also had ball bearings, but their metal gears (as opposed to plastic gears) and coreless motors set them apart from the rudder and elevator servos. Ball bearings around the output shaft on a servo reduce the slop. This is important since any slop in control linkages can allow aeroelasticity to become a problem, resulting in flutter. Coreless servos were desired for the ailerons because of their quick response and accurate control response. Metal gears ensured that the gear teeth would not skip under high-load conditions such as a fast roll rate.

Control system component locations are shown in the Drawing package for the Texas Tall Boy (Appendix I).

Weights of the control and propulsion components are given in Appendix K. The total weight of the unloaded aircraft was seven pounds. With the payload weighing seven pounds 8 ounces, this gave a payload fraction of 51.7%.

### *5.2. Innovative techniques*

Though a modular wing design is no longer considered an innovative design in model airplanes, the way in which it was accomplished deserves special attention. In most modular wing model airplanes, the wing is primarily constructed from foam, which easily accommodates a tube/joiner design. In the case of the TTB, nearly 95 percent of the wing was constructed in the traditional wood framework style.

In almost every case, a design such as this would rely on a standard spar-box configuration. However, the TTB built upon this old design by adding new configuration ideas found in modern foam-core wings. A wound carbon fiber tube was located in between the top and bottom spars of the box and was secured to the shear webs by adding triangular balsa stock to each side of the tube. For added strength, the tube and spars were then wrapped with kevlar ribbon.

Once the wings were completed, they were joined at the fuselage by a single pulltruded carbon fiber rod. A secondary joiner was added directly forward of the carbon joiner and consisted of overlapping hardwood members extending from each wing. The two halves of the secondary joiner were then secured by metal bolts driven through the top surface of the fuselage.

Other composite construction found its place in the landing gear design (detailed in the "Manufacturing Plan"). The elliptical shape could more easily be produced by molding unidirectional carbon fiber than by bending aluminum, for example. The fact that this landing gear configuration was fixed, rather than retractable, also let the team stay away from costly retraction components.

In choosing a construction material, weight became the key element essential to reducing the total weight of the new assembly. Carbon fiber roving was chosen as the primary structural element with the secondary material being balsa wood. The carbon provided a superior strength to weight ratio for the purpose of absorbing transverse loads, while the balsa provided enough crush strength to resist the lay-up process.

### 5.3. Cost reductions

Looking into the systems architecture of the aircraft, the analysis tools used greatly reduced the overall cost of the design process. For example, the ElectriCalc data (shown in Appendix C) allowed us to analyze several motor/battery/propeller combinations without having to purchase and test all of the equipment.

Cost reduction for the detailed design rested ultimately on the fuselage. The fuselage was simple enough in design that it could easily be constructed of wood (common for aircraft of this size) rather than expensive composites required for a more complex fuselage design. However, if this aircraft were to be produced in larger quantities, it would be desirable to have a single mold to lay up many composite fuselages, regardless of the shape.

### 5.4. New configuration ideas

New configuration ideas for the Texas Tall Boy allowed the wing to be divided into halves for convenient transportation. Wound carbon tubes in the wing panels served to connect the wing panels and to distribute loads to the wing spar. A pultruded carbon rod served as the primary structural element in the spar assembly.

In an attempt to improve the ground handling qualities of the TTb over its predecessor, the Aggie Flyer, a new landing gear was designed. Of the issues considered for change, overall stiffness was foremost on the list with total weight coming in a close second. The new design called for a single-piece strut formed to an elliptical shape instead of the previous straight-legged strut. This shape was chosen to reduce the internal moments of the structure near the fuselage.

## 6. Manufacturing Plan

### 6.1. Figures of merit

The manufacturing process and selection of materials used to produce the airframe revolved around several figures of merit. The first and foremost element of the manufacturing process centered on selecting the materials. Since the design of the TTb originated from the concept of a lightweight airframe, the weight of the materials involved was considered premium. Second in the hierarchy was the level of skill and sophistication of machinery required to produce various parts of the airplane. Since direct access to expensive and complex manufacturing machinery as well as the knowledge of how to use such machinery was limited, it was important to select processes that could be carried out using common shop equipment, such as band saws and drill presses.

After considering these issues, the third figure of merit taken into account was the time required to complete each process. Because the schedule set forth by the team's management structure allowed for only a small production window in December and early January, each process needed to span a short time frame. Such short production times were illustrated in the production of the landing gear, where the total time required to produce and to test a landing gear strut was only three and a half days. Beyond these considerations,

availability and cost did not seriously enter the picture when determining the manufacturing process, as funding and supplying of materials was provided almost exclusively by Texas A&M University.

Below the figures of merit governing the manufacturing plan are listed below in order of importance:

- Selection of light-weight materials
- Level of skill required to produce components
- Time required to construct components

## *6.2. Manufacturing processes for final design*

### **6.2.1. Manufacturing plan**

All components of the aircraft were built simultaneously for efficiency. Completion of each assembly was followed by integration with the major assembly and alignment with the other components.

Throughout the construction process, epoxy and carpenter's wood glue were used exclusively due to their easy application characteristics and reputations for consistently good joints.

### **6.2.2. Wing construction**

The basic structure of the wing panels was formed by 3/32" balsa ribs connected by two 1/4" x 3/8" balsa spars located at 25% chord. One-sixteenth-inch balsa was used as shear webbing between the top and bottom spars to complete a box spar for the wing.

To satisfy the structural requirement of having the fully loaded aircraft picked up by its wingtips, 3/8" unidirectional carbon fiber was applied as spar caps. The carbon fiber was applied symmetrically (top and bottom) as follows. Two layers were applied over the full span of each panel. One layer spanned the inboard 50% of each wing panel. A physical test using this identical spar structure showed that the spar alone, without any additional structure (such as leading edge sheeting) satisfied the structural requirement for an aircraft weighing 16 pounds (the estimate for the Aggie Flyer). To reduce the discontinuity effects of having two full-span layers and the 50%-span layer as spar caps for the new aircraft, an additional strip of carbon fiber was applied, symmetrically top and bottom, spanning the inboard 75% of each panel. This also added a higher safety factor for the overall structural integrity of the wing.

Knowing the fragility of balsa, the team realized that it would not be feasible to have sharp balsa trailing edges using just 1/16" balsa sheeting. For this reason, 3/8"-wide strips of 1/64" 3-ply birch plywood were glued between the top and bottom trailing edge pieces. When sanded, this produced a sharp, durable trailing edge.

The 1/16" balsa leading edge sheeting completed the D-tube structure of the wing panels, yielding high torsional rigidity in the wing.

Cap strips made of 3/8"-wide strips of 1/16" balsa were cemented to the ribs in the wing. These provided more surface area for the covering material to adhere to. This was important since the wing panels relied on the high tensile strength of the covering material to provide more structural rigidity.

Ailerons were cut from the trailing edge and hinged to a false spar installed along the cut in each wing panel. The hinge line was at the top surface of the wing. The resulting gaps in the bottom surface of the wing were sealed by plastic strips anchored along the hingeline on the wing.

One servo was used for each aileron to simplify linkage for the two wing panels. Since the wing panels separated at the fuselage, only a wire from each servo had to be plugged into the receiver to make the ailerons operational. Alternatively, a single servo could have been mounted in the fuselage, requiring aileron linkage to be assembled every time the wing panels were installed.

Separate servos also allowed mixing functions for the control surfaces on the wings. For example, the surfaces could move independently as ailerons or together as flaps by means of electronic mixing provided by the transmitter.

A 2-56 threaded pushrod coupled with a control horn mounted on each aileron provided control from the servo.

The carbon fiber joiner tube in the fuselage joined the wing panels by inserting into a 17"-long 1/2" I.D. graphite tube mounted in each wing panel. These tubes were epoxied to the shear webbing on the aft side of the box spar. Triangle stock completed the joint between the tube and the shear webbing. The entire box spar, wing graphite tube, and triangle stock were wrapped with 1/8"-wide kevlar ribbon to prevent any separation of the wing joining components. The wraps were spaced about 1/2" apart along the full span of the tube in order to distribute the load evenly to the main wing spar.

#### **6.2.3. Tail surface construction**

Since the horizontal and vertical stabilizers had airfoil sections (as opposed to flat surfaces), they were built up, similar to the wing. Construction of the tail surfaces started with a 3/32" balsa spar laminated with a single layer of unidirectional carbon fiber on each side. Placed such that the long dimension of the cross section was normal to the chord of the ribs, each spar extended the full length of its respective stabilizer. The 3/32" balsa ribs for each surface slid onto the spar and were aligned via a construction jig. One-quarter-inch square balsa was used for the leading edges of the stabilizers.

The roots of the stabilizers were sheeted with 1/16" balsa to provide solid mounting surfaces for the fuselage. Torsional rigidity was also increased from the root sheeting.

Construction of the rudder and elevators were similar to the ailerons in that the trailing edge had 3/8" strips of 1/64" 3-ply birch plywood between the 1/16" balsa sheeting. The elevator was hinged at the upper surface and sealed on the bottom, similar to the ailerons. Rudder hinges were put along the centerline of the cross section.

In order to take the loads presented by the built-in tailwheel, the rudder was built up with two layers of 1/32" 3-ply birch plywood on the inside of the sheeting and two layers of 2-oz. fiberglass cloth on the outside.

#### 6.2.4. Fuselage construction

The fuselage construction began with 3/32" balsa slab sides doubled with 1/32" 3-ply birch plywood from the firewall to the location of the wing root trailing edge. Additional doubling was used around the wing joiner and payload openings. One-eighth-inch balsa was applied cross-grain to the top and bottom of the fuselage to provide torsional rigidity to the semi-monocoque fuselage structure. This was the lightest way to build the fuselage since it eliminated the need for any internal structure, such as bulkheads and stringers.

One-eighth-inch light ply was used for the propulsion battery access hatch on the bottom of the fuselage. Immediately forward of this hatch was the landing gear block, made from 1/8" 5-ply birch plywood. The same material was used to make the firewall for the single electric motor.

#### 6.2.5. Landing gear construction

Composite construction was used exclusively for the fabrication of the main landing gear. Several layers of unidirectional carbon fiber were surrounded a 1/16" balsa core. The resin-laden lay-up was vacuum bagged over a blue foam template to form its elliptical shape. Appendix B shows the lay-up of the carbon fiber layers. Vinyl sheets placed around the lay-up allowed the landing gear to cure with a smooth finish.

Simple drop tests with the expected weight of the fully loaded aircraft (16 pounds) attached to a board determined the properties of heavier and lighter lay-ups.

Four 1/4 x 20 nylon bolts attached the final main landing gear to the fuselage. Nylon bolts were used in order to allow the gear to detach without damaging the fuselage in the event of a rough landing.

Solid 2-56 pushrods ran from the elevator and rudder to the respective servos. Two supports along the length of the pushrods were installed to keep the pushrods from bowing while in compression.

### 6.3. *Alternative manufacturing processes investigated*

Alternative manufacturing processes were investigated to optimize the construction efficiency of the aircraft. First of all, an all-balsa and plywood structure was considered. The team members were quite familiar with the construction techniques involving wood. However, this method of fabrication was avoided on the wing in particular. In order to satisfy the structural requirement of having the fully loaded aircraft supported by its wingtips, a relatively massive wooden spar would be required.

Bulkhead fuselage construction involves using a series of bulkhead throughout the fuselage to support the sheeting on the airframe. The team considered this method of fabrication but realized that it was not necessary since a light and simple tube structure could be achieved with two slab sides and top and bottom sheeting.

A molded composite fuselage was also examined. Since only two aircraft were to be built, the team members did not want to take the time to produce a mold. Also, molded fiberglass fuselages of similar size (compared to some competition radio controlled sailplanes in production) were 10% - 20% heavier than built-up balsa and plywood structures.

Composite wing panels and tail surfaces were considered for their inherent structural integrity. However, the team members lacked experience with forming carbon or fiberglass around such thin foam cores that would form the basis of the wing panels and tail surfaces.

Foam wing panels and tail surfaces could simply be sheeted with thin balsa. Such construction methods could reduce building time by an estimated 60%, but even these components with low-density white foam cores are substantially heavier than their built-up counterparts.

A completely aluminum main landing gear was considered for this aircraft. Comparison to the aluminum landing gear from the Aggie Flyer showed that the composite gear (with comparable stiffness) was 65% lighter.

#### *6.4. Analytic methods used*

Having decided on of using a two-piece wing for transportation reasons, the team put a lot of emphasis on the integrity of the joining structure. Knowing that the spar structure within the wing panels was sufficient from data acquired for the Aggie Flyer's main wing spar, a ½" O.D. carbon fiber tube, identical to the wing panel joiner, was tested for strength. A three-point test was conducted such that the two supports were 5.75 inches apart. Fracture of the outer fibers occurred with a load of 650 pounds applied to the middle. Simple calculations showed that the aircraft could weigh up to 43.6 pounds with the current wing panel joiner and still satisfy the structural requirements.

#### *6.5. Manufacturing timing*

The manufacturing of the first prototype of the TTB began on November 20, 1997 and was completed on January 1, 1998. Approximately 425 hours was spent on the construction. Displayed in Appendix J, Scheduled and Actual Timing of Major Events, is a manufacturing milestone completion chart.

#### *6.6. Key features*

Some innovative techniques were introduced during the manufacturing process to accommodate the elements of the detailed design. For example, the tailwheel was embedded inside the rudder by using an 8-32 bolt as the axle and the control horn attachment. The rudder was built up as described in the manufacturing process to handle the loads presented by control actuation and steering.

In order to yield the cleanest configuration, the control linkages for the elevator were concealed inside the vertical stabilizer. Access to the clevis and elevator control horn was provided by a cutout in the base of the vertical stabilizer that was later sealed by covering material.



Another innovation used to reduce the drag even further involved installing the receiver switch inside the fuselage. The switch was toggled by means of a small hole on each side of the fuselage through which a pin could be inserted.

In producing the landing gear, the layup shown in Appendix H was formed over a male mold made from blue foam. It was then vacuum-bagged under 15 psi for 12 hours. After curing, the landing gear was trimmed of excess material and smoothed to a low-drag profile.

## References

1. Roskam, Jan, *Airplane Design, Part I: Preliminary Sizing of Airplanes*, Roskam Aviation and Engineering, Ottawa, Kansas, 1990.
2. Anderson, John D., Jr., *Fundamentals of Aerodynamics*, Second Edition, McGraw-Hill, Inc., New York, 1991.
3. Rae, W.H. and Pope, A., *Low-Speed Wind Tunnel Testing*, 2nd Edition, Wiley and Sons, New York, 1984.
4. Raymer, Daniel P., *Aircraft Design: A Conceptual Approach*, American Institute of Aeronautics and Astronautics, Education Series, Jan. 1985.
5. Anderson, John D., Jr., *Introduction to Flight*, Third Edition, McGraw-Hill, Inc., New York, 1989.
6. *Comprehensive Reference Guide to Airfoil Sections for Light Aircraft*, Aviation Publications, Appleton, Wisconsin, 1982.
7. Nelson, Robert C., *Flight Stability and Automatic Control*, McGraw-Hill, Inc., New York, 1989.
8. Selig, Michael, S., and Ashok Gopalarathnam, *New Airfoils for R/C Sailplanes*, World Wide Web Site, [http://amber.aae.uiuc.edu/~m-selig/uiuc\\_lsar/saAirfoils.html](http://amber.aae.uiuc.edu/~m-selig/uiuc_lsar/saAirfoils.html), 1997.
9. Simons, Martin, *Model Aircraft Aerodynamics*, Model and Allied Publications, Watford, 1978.

## Appendix A

*Preliminary and Detailed Performance Development Calculations*

## Nomenclature for Preliminary and Detailed Performance Development Calculations

Symbol	Description
ALPHA, $\alpha$	Aircraft angle of attack
ARht, ARHtail	Horizontal tail aspect ratio
ARvt, ARVtail	Vertical tail aspect ratio
ARw, ARwing	Wing aspect ratio
B	Wing reference span
Bh	Horizontal tail reference span
bv	Vertical tail reference span
CD, CD	Drag force coefficient
CD <sub>0</sub>	Zero lift drag polar
CD <sub>clean</sub>	Clean aircraft drag polar
CD <sub>to</sub>	Clean drag polar at takeoff
CD <sub>ld</sub>	Clean drag polar at landing
CD <sub>lg</sub>	Clean drag polar with landing gear attached
CL, CL <sub>3D</sub>	3-D Lift force coefficient
CL, CL <sub>2D</sub>	2-D Lift force coefficient
CL <sub>mean</sub>	3-D Averaged powered cruise lift coefficient
CL <sub>mean</sub>	2-D Averaged powered cruise lift coefficient
CL <sub>minsnk</sub>	3-D minimum sink/gliding lift coefficient
CL <sub>minsnk</sub>	2-D minimum sink/gliding lift coefficient
CL <sub>to</sub>	3-D Coefficient of lift at takeoff
CL <sub>to</sub>	2-D Coefficient of lift at takeoff
CL <sub>ld</sub>	3-D Coefficient of lift at landing
CL <sub>ld</sub>	2-D Coefficient of lift at landing
C <sub>mean</sub> , C <sub>bar</sub>	Mean Aerodynamic chord
C <sub>r</sub>	Wing root chord
C <sub>t</sub>	Wing tip chord
CN, CN	Normal force coefficient
CPM, C <sub>m</sub>	Pitching moment coefficient
CRM, C <sub>l</sub>	Rolling moment coefficient
CY, CY	Side force coefficient
CYM, C <sub>n</sub>	Yawing moment coefficient
DELTA, $\delta$	Downwash correction factor
DPDL, dp/dl	Test section longitudinal static pressure gradient (psf/ft)
DRAG	Drag force (lbs)
EOR	End of run wind off balance check point
ESBS, $\epsilon$ SBsupport	Solid blockage correction factor due to support system
F	Drag polar parasite area
HMC	Vertical moment transfer distance (ft)
HPC	Vertical pivot point transfer distance (ft)
L/D	Lift force to drag force ratio

$\Lambda$	Wing taper ratio
$\Lambda_h$	Horizontal tail taper ratio
$\Lambda_v$	Vertical tail taper ratio
M	Mach number
$\mu$	Wing sweep angle
$\mu$	Air viscosity (lbs-sec/ft <sup>2</sup> )
N/A	Normal force to axial force ratio
$\phi$	Model roll angle (deg.)
PM	Pitching moment (ft-lbs)
$\psi$	Model yaw angle (deg.)
PT	Data point number
Q, q	Dynamic pressure (psf)
QCORR	Dynamic pressure correction option flag
Re No, Re	Reynolds number
$\rho$	Air density (slugs/ft <sup>3</sup> or lbs-sec <sup>2</sup> /ft <sup>4</sup> )
RK1, K1	Wing blockage correction factor
RK3, K3	Body blockage correction factor
RL	Reynolds number reference length (ft)
RM	Rolling moment
S	Wing reference area
SIDE	Side force (lbs)
SOR	Start of run wind off balance check point
ST, Stail	Horizontal tail platform area (ft <sup>2</sup> )
Sw	Drag polar parasite wetted area
TAU1B, $\tau_{1body}$	Body blockage correction factor
TAU1W, $\tau_{1wing}$	Wing blockage correction factor
TAU2T, $\tau_{2tail}$	Horizontal tail streamline curvature correction factor
TAU2W, $\tau_{2wing}$	Wing streamline curvature correction factor
TEMP	Test section temperature (°F)
THETA, $\theta$	Maskell dynamic pressure correction constant
TMAX, $t_{max}$	Maximum body thickness (ft)
UMC	Longitudinal moment transfer distance (ft)
UPC	Longitudinal pivot point transfer distance (ft)
VCr	Vertical tail root chord
VCt	Vertical tail tip chord
WL	Wing loading
Wto	Total takeoff and performance weight
X	Horizontal 2-D geometric wing coordinate
Xmean	Mean aerodynamic center horizontal coordinate
Y	Vertical 2-D geometric wing coordinate
Ymean	Mean aerodynamic center vertical coordinate
YM	Yawing moment (ft-lbs)

## *Preliminary and Detailed Performance Development Calculations*

### Configuration Estimates

\*All final values listed in bold face

Total Weight, Wto		Wing Loading, WL		Aspect Ratio, AR	
14.00	Wto	1.80	Wto/S	7.00	B <sup>2</sup> /S
14.50	lb	1.90	lb/ft <sup>2</sup>	8.00	
15.00		2.00		8.50	
15.50		2.10		9.00	
16.00		2.25		9.25	
16.50		2.30		9.50	
17.00		2.35		10.00	
18.00		2.40		11.00	

### Wing Area, S (ft<sup>2</sup>)

	WL							
Wto	1.80	1.90	2.00	2.10	2.25	2.30	2.35	2.40
14.00	7.78	7.37	7.00	6.67	6.22	6.09	5.96	5.83
14.50	8.06	7.63	7.25	6.90	6.44	6.30	6.17	6.04
15.00	8.33	7.89	7.50	7.14	6.67	6.52	6.38	6.25
15.50	8.61	8.16	7.75	7.38	6.89	6.74	6.60	6.46
16.00	8.89	8.42	8.00	7.62	7.11	6.96	6.81	6.67
16.50	9.17	8.68	8.25	7.86	7.33	7.17	7.02	6.88
17.00	9.44	8.95	8.50	8.10	7.56	7.39	7.23	7.08
18.00	10.00	9.47	9.00	8.57	8.00	7.83	7.66	7.50
S1 =		6.89	S2 =	7.11				

# Wing Span, B (ft)

# Taper Ratio, Lambda

AR	S1	S2			0.40
7.00	6.94	7.05			0.45    Lambda = 0.45
8.00	7.42	7.54			0.50
8.50	7.65	7.77			0.55
9.00	7.87	8.00	B1 =	7.87	0.60
9.25	7.98	8.11	B2 =	8.43	0.65
9.50	8.09	8.22			
10.00	8.30	8.43			Sweep Angle, Mu
11.00	8.71	8.84			Mu =            0.0

# Mean Aerodynamic, Tip and Root Chords, Cmean, Ct, and Cr

Cmean =	0.84	ft	Cmean = S/B
	10.12	in	
Ct =	0.52	ft	Ct = S / ((B/2) x (1+Lamda / Lambda))
	6.28	in	
Cr =	1.16	ft	Cr = S / ((B/2) x (1+Lambda))
	13.96	in	

### Tail Sizing Vertical Tail, V and Horizontal Tail, H

$x_h = \begin{matrix} 2.50 & \text{ft} \\ 30.00 & \text{in} \end{matrix}$ 
 $x_v = \begin{matrix} 2.29 & \text{ft} \\ 27.48 & \text{in} \end{matrix}$ 
 $Ar_h = 4.50$   
 $Ar_v = 1.20$

### Horizontal Tail Volume, Area and Span, $V_h$ , $sh$ , and $b_h$

$V_h = 0.66$ 
 $sh = \begin{matrix} 1.06 & \text{ft}^2 \\ 152.01 & \text{ft}^2 \end{matrix}$ 
 $sh = V_h * S * c_{mean} / x_h$

$b_h = \begin{matrix} 2.18 & \text{ft} \\ 26.15 & \text{in} \end{matrix}$ 
 $b_h = (Ar_h * sh)^{1/2}$

### Horizontal Mean Aerodynamic, Tip and Root Chords, $H_{cmean}$ , $H_{Ct}$ , and $H_{Cr}$

$C_{mean} = \begin{matrix} 0.48 & \text{ft} \\ 5.81 & \text{in} \end{matrix}$ 
 $H_{cmean} = sh / b_h$ 
 $Lambda_h = 0.65$   
 $Mu_{1/4Chord} = 7 \text{ Degrees}$

$C_t = \begin{matrix} 0.47 & \text{ft} \\ 5.63 & \text{in} \end{matrix}$ 
 $H_{Ct} = sh / ((b_h / 2) * (1 + Lambda_h / Lambda_h))$

$C_r = \begin{matrix} 0.72 & \text{ft} \\ 8.63 & \text{in} \end{matrix}$ 
 $H_{Cr} = sh / ((b_h / 2) * (1 + Lambda_h))$

### Vertical Tail Volume, Area and Span, $V_v$ , $sv$ , $b_v$ $sv = V_v * s * b / x_v$

$V_v = 0.0496$ 
 $sv = \begin{matrix} 0.49 & \text{ft}^2 \\ 70.93 & \text{in}^2 \end{matrix}$

$b_v = \begin{matrix} 0.77 & \text{ft} \\ 9.23 & \text{in} \end{matrix}$ 
 $b_h = (Ar_v * sv)^{1/2}$



Vertical Mean Aerodynamic, Tip and Root Chords, VCmean, VCt, and VCr

$$\begin{array}{llll} \text{VCmean} = & 0.64 & \text{ft} & \text{VCmean} = \text{sv}/\text{bv} \\ & 7.69 & \text{in} & \text{Lambdav} = 0.33 \end{array}$$

$$\text{VCt} = 0.32 \quad \text{ft} \quad \text{VCt} = \text{sv}/((\text{bv}/2) \times (1 + \text{Lambdav}/\text{Lambdav}))$$

$$\begin{array}{llll} \text{VCr} = & 1.50 & \text{ft}^3 & \text{VCr} = \text{sv}/((\text{bv}/2) \times (1 + \text{Lambdav})) \\ & 17.96 & \text{in}^3 & \end{array}$$

Cart Coord, Y	Y/(B/2), 2Y/B	Chord(Y), cy
0.00	0.00	13.96
0.25	0.06	13.50
0.50	0.12	13.05
0.75	0.18	12.59
1.00	0.24	12.14
1.25	0.30	11.68
1.50	0.36	11.23
1.75	0.42	10.77
2.00	0.47	10.32
2.25	0.53	9.86
2.50	0.59	9.40
2.75	0.65	8.95
3.00	0.71	8.49
3.25	0.77	8.04
3.50	0.83	7.58
3.75	0.89	7.13
4.00	0.95	6.67
4.22	1.00	6.28

#### Preliminary Lifting Performance

Time of Flight, Tf		Lap Distance, Lap	
7.00	min	700.00	ft
420.00	sec		

Total Flight Distance, Dt    Dt = Lap x Laps Completed

#### Cruise and Soar Velocities, Vcmax and Vcminsink

Vcmax		Vcminsink		Vcmax = Dt / Tf or timed
m/h	ft/s	m/h	ft/s	Atmospheric Density, rho
40.00	58.67	30.00	44.00	rho <sub>sl</sub> = 378 slugs/ft <sup>3</sup>
45.00	66.00	35.00	51.33	
50.00	73.33	40.00	58.67	rho <sub>wk</sub> = 227 slug/ft <sup>3</sup>
55.00	80.67	45.00	66.00	
60.00	88.00	50.00	73.33	
65.00	95.33	55.00	80.67	

**Stall Velocity, V<sub>stall</sub>**

m/h	ft/s
67	98.27

**Take Off Velocity, V<sub>to</sub>**

ft/s
80.40

**Landing Velocity, V<sub>ld</sub>**

ft/s
87.10

**Takeoff Roll**

fts
76.20

**Landing Roll**

ft
187.00

**Cr, Soar, Toff, and Ld Velocity Coefficient of Lift, CL**

CL <sub>mean</sub>	L <sub>mnsnk</sub>	CL <sub>to</sub>	CL <sub>ld</sub>	CL = (2 x W <sub>to</sub> ) / (rho x V <sub>c</sub> <sup>2</sup> x S)
0.244	0.352	0.136	0.116	

**C and S Airfoil Coefficient of Lift, Cl**

Cl <sub>mean</sub>	Cl <sub>mnsnk</sub>	Cl <sub>to</sub>	Cl <sub>ld</sub>
--------------------	---------------------	------------------	------------------

$$Cl = 4 / \pi \times CL \times S / B \times (1 - (2Y/B)^2)^{1/2}$$

**Preliminary Drag Polar Coefficient Data****Parasite Wetted Area, S<sub>w</sub> (ft<sup>2</sup>)**

51.16	ft <sup>2</sup>	S <sub>w</sub> = 10 <sup>A</sup> (C + (D x Log <sub>10</sub> W <sub>to</sub> ))
		F = 10 <sup>A</sup> (A + (B x log <sub>10</sub> S <sub>w</sub> ))

**Parasite Area, F (ft<sup>2</sup>)**

0.307	ft <sup>2</sup>
-------	-----------------

A =	-2.2218
B =	1.0000
C =	1.0892
D =	0.5147

W <sub>to</sub>	16.00
-----------------	-------

**Zero Lift Drag Polar, C<sub>Do</sub>**

$$C_{Do} = F / S$$

C <sub>Do</sub> =	0.043
-------------------	-------

**Clean Aircraft Drag Polar, C<sub>Dclean</sub>**

C <sub>Dclean</sub> =	0.04546	C <sub>Dclean</sub> = C <sub>Do</sub> + (CL <sup>2</sup> / Pi * AR * e)
-----------------------	---------	---

### Drag Poles for Other Configurations

	Delta CDo	Efficiency Factor, e
Clean		0.83
Take Off Flaps	0.016	0.78
Landing Flaps	0.068	0.73
Landing Gear	0.021	—

### Clean with Landing Gear Drag Polar, Cdolg

$$\begin{aligned} CD_{to} &= 0.061 & CD_{clean} &= (CDo + \delta) + (CL^2 / \pi * AR * e) \\ CD_{ld} &= 0.114 \\ CD_{lg} &= 0.066 \end{aligned}$$

## Appendix B

### *Stability and Control Calculations*

## Nomenclature for Longitudinal Stability Calculations

Symbol	Description
M	Mach number, using a temperature of 75°F
V	Velocity (ft/s)
U <sub>o</sub>	Velocity (ft/s)
W	Weight (lbs)
g	gravity (ft/s <sup>2</sup> )
m	mass (slugs)
S	Surface area of the wing (ft <sup>2</sup> )
b	Wingspan (ft)
AR <sub>w</sub>	Aspect ratio of the wing
C <sub>bar</sub>	Mean aerodynamic chord (ft)
L <sub>t</sub>	Distance from aircraft C.G. to horizontal tail quarter chord
S <sub>t</sub>	Surface area of the horizontal tail (ft <sup>2</sup> )
AR <sub>t</sub>	Aspect ratio of the horizontal tail
S <sub>e</sub>	Surface area of the elevator (ft <sup>2</sup> )
X <sub>cg</sub>	Location of the aircraft C.G. w.r.t. the mean aerodynamic chord leading edge (ft)
X <sub>ac</sub>	Location of the wing aerodynamic center with respect to the MAC leading edge(ft)
CL <sub>w2D</sub>	2-D wing lift curve slope
CL <sub>at2D</sub>	2-D horizontal tail lift curve slope
CD <sub>u</sub>	Drag coefficient due to compressibility effects
C <sub>mu</sub>	Moment coefficient due to compressibility effects
C <sub>maFuse</sub>	Moment coefficient contribution from the fuselage
Sweep <sub>w</sub>	Sweep of the wing quarter chord (degrees)
Sweep <sub>t</sub>	Sweep of the horizontal tail quarter chord (degrees)
Beta	Interpolation variable used to determine CL <sub>w3D</sub> and CL <sub>at3D</sub>
kw	Interpolation variable used to determine CL <sub>w3D</sub>
kt	Interpolation variable used to determine CL <sub>at3D</sub>
CL <sub>w3D</sub>	3-D wing lift curve slope
CL <sub>at3D</sub>	3-D horizontal tail lift curve slope
eta	Efficiency factor of the horizontal tail
V <sub>h</sub>	Horizontal tail volume (ft <sup>3</sup> )
rho	Density of air at 1500 ft (altitude of contest site) (slug/ft <sup>3</sup> )
Q	Dynamic pressure (lb/ft <sup>2</sup> )
CD <sub>o</sub>	Reference drag coefficient
I <sub>y</sub>	Moment of inertia about the y-axis of the aircraft (slug-ft <sup>2</sup> )
tau	Flap-effectiveness parameter
X <sub>delE</sub>	Force in x-direction produced by elevator deflection (lbs)
DeDa	Change in downwash due to a change in angle of attack
CL <sub>alpha</sub>	Aircraft lift curve slope
C <sub>malpha</sub>	Aircraft moment curve slope

$C_{D\alpha}$	Aircraft drag curve slope
$C_{Lu}$	Lift coefficient due to compressibility effects
$C_{Xu}$	X-force coefficient due to compressibility effects
$C_{L\dot{\alpha}}$	Aircraft unsteady lift curve slope
$C_{m\dot{\alpha}}$	Aircraft unsteady moment curve slope
$C_{Lq}$	Aircraft lift curve slope with respect to pitch rate
$C_{mq}$	Aircraft moment curve slope with respect to pitch rate
$C_{L\delta E}$	Elevator lift coefficient
$C_{m\delta E}$	Elevator moment coefficient
$\alpha_W$	Wing angle of attack (radians)
$i_w$	Wing incidence angle relative to fuselage centerline (radians)
$i_t$	Horizontal tail incidence angle relative to fuselage centerline (radians)
$C_{L0}$	Reference wing lift coefficient
$\epsilon_0$	Reference downwash angle (radians)
$C_{L0}$	Reference aircraft lift coefficient
$L_\alpha$	Aircraft lift as a function of angle of attack (lbs)
$M_\alpha$	Aircraft moment as a function of angle of attack (ft-lbs)
$L_u$	Aircraft lift due to compressibility effects (lbs)
$L_{\dot{\alpha}}$	Unsteady aircraft lift (lbs)
$M_{\dot{\alpha}}$	Unsteady aircraft moment (ft-lbs)
$L_q$	Aircraft lift as a function of pitch rate (lbs)
$M_q$	Aircraft moment as a function of pitch rate (ft-lbs)
$L_{\delta E}$	Elevator lift (lbs)
$M_{\delta E}$	Elevator moment (ft-lbs)
$X_u$	Force in x-direction due to compressibility effects (lbs)
$Z_u$	Force in z-direction due to compressibility effects (lbs)
$M_u$	Moment due to compressibility effects (ft-lbs)
$M_{\dot{w}}$	Moment due to vertical acceleration (ft-lbs)
$X_{\dot{w}}$	Force in x-direction due to vertical velocity (lbs)
$Z_{\dot{w}}$	Force in z-direction due to vertical velocity (lbs)
$M_{\dot{w}}$	Moment due to vertical velocity (ft-lbs)
$Z_{\delta E}$	Force in z-direction due to elevator deflection (lbs)
$\Omega_{SP}$	Natural frequency of the short period oscillations (Hz)
$DR_{SP}$	Damping ratio for the short period mode oscillations
$T_{half\_SP}$	Time for the amplitude of the short period mode oscillations to half (sec)
$T_{SP}$	Period of the short period mode oscillations (sec)
$N_{half\_SP}$	Number of oscillations for the amplitude of the short period mode oscillations to half
$\Omega_{Phugoid}$	Natural frequency of the phugoid mode oscillations (Hz)
$DR_{Phugoid}$	Damping ratio for the phugoid mode oscillations
$T_{half\_Phugoid}$	Time for the amplitude of the phugoid mode oscillations to half (sec)
$T_{Phugoid}$	Period of the phugoid mode oscillations (sec)
$N_{half\_Phugoid}$	Number of oscillations for the amplitude of the phugoid mode oscillations to half

### Additional Comments

The orthogonal coordinate system used has the x-axis extending forward through the nose of the aircraft, the y-axis going through the right-hand side, and the z-axis pointing through the bottom of the aircraft.

All stability derivatives and coefficients were derived assuming level flight with small perturbations only.



## *Longitudinal Stability Calculations*

### Code written for Matlab

```
M = 0.0781
V = 88
Uo = V
W = 16.0
g = 32.174
m = W / g
S = 7.11
b = 8.43
ARw = 10.0
Cbar = 0.84
Lt = 2.29
St = 1.06
ARt = 4.50
Se = 0.212
Xcg = 0.35 * Cbar
Xac = 0.25 * Cbar
CLaw2D = 5.80
CLat2D = 6.14
CDu = 0
Cmu = 0.05
CmaFuse = .5
Sweepw = 0.0
Sweept = 7.0
Beta = sqrt(1 - M^2)
kw = CLaw2D / (2 * 3.1416)
kt = CLat2D / (2 * 3.1416)
CLaw3D = 2 * 3.141 * ARw / (2 + sqrt(ARw^2 * Beta^2 / kw^2 * (1 + (tan(Sweepw/57.3))^2 / Beta^2) + 4))
CLat3D = 2 * 3.141 * ARt / (2 + sqrt(ARt^2 * Beta^2 / kt^2 * (1 + (tan(Sweept/57.3))^2 / Beta^2) + 4))
eta = 1
Vh = St / S * Lt / Cbar
rho = 0.00227
Q = .5 * rho * V^2
CDo = 0.025
Iy = .8
tau = 0.4
XdelE = 0

DeDa = 2*CLaw3D / (3.1416*ARw)

% Coefficients
CLalpha = CLaw3D + eta * St / S * CLat3D * (1 - DeDa)
Cmalpha = CLaw3D * (Xcg - Xac) / Cbar + CmaFuse - eta * Vh * CLat3D * (1 - DeDa)
CDalpha = 0.04 * CLalpha
CLalphadot = 2 * eta * CLat3D * Vh * DeDa
Cmalphadot = -2 * eta * CLat3D * Vh * Lt / Cbar * DeDa
CLq = 2 * eta * CLat3D * Vh + CLaw3D * (.5 + 2 * (Xac - Xcg) / Cbar)
Cmq = -2.2 * eta * CLat3D * Vh * Lt / Cbar
CLdelE = St / S * eta * CLat3D * tau
CmdelE = - eta * Vh * CLat3D * tau
alphaW = 2.0*3.1416/180
iw = alphaW
it = 0.0
```

```

CLOW = CLaw3D*alphaW
epsilonO = 2*CLOW/(3.1416*ARw)
CLO = eta * (S/St) * CLat3D * (iw + it - epsilonO)
CLU = M^2 / (1 - M^2) * CLO
CXu = -CDu

% Dimensional counterparts
Lalpha = (CLalpha + CDO) * Q * S / m
Malpha = Cmalphat * Q * S * Cbar / Iy
Lu = (CLU + 2 * CLO) * Q * S / (m * Uo)
Lalphadot = CLalphadot * Cbar * Q * S / (2 * Uo * m)
Malphadot = Cmalphadot * Q * S * Cbar^2 / (2 * Uo * Iy)
Lq = CLq * Q * S * Cbar / (2 * Uo * m)
Mq = Cmqt * Q * S * Cbar^2 / (2 * Uo * Iy)
LdelE = CLdelE * Q * S / m
MdelE = CmdelE * Q * S * Cbar / Iy

% Additional Stuff for the A and B matrices (Longitudinal Equations of Motion)
Xu = - (CDu) * Q * S / (m * Uo)
Zu = - Lu
Mu = Cmu * Q * S * Cbar / (Uo * Iy)
Mwdot = Malphadot / Uo
Xw = - (CDalpha - CLO) * Q * S / (m * Uo)
Zw = - (CLalpha + CDO) * Q * S / (m * Uo)
Mw = Cmalphat * Q * S * Cbar / (Uo * Iy)
ZdelE = - CLdelE * Q * S / m

% A and B matrices
A = [Xu Xw 0 -g; Zu Zw Uo 0; Mu+Mwdot*Zu Mw+Mwdot*Zw Mq+Mwdot*Uo 0; 0 0 1 0]

B = [XdelE 0; ZdelE 0; MdelE+Mwdot*ZdelE 0; 0 0]

% eigenvectors and eigenvalues
[vec,eval] = eig(A)
fac = diag(1./[Uo Uo (2*Uo)/Cbar 1]);
vec = fac * vec;
vec = vec * diag(1./vec(4,:))

% for the short period
Omega_SP = norm(eval(1,1))
DR_SP = abs(real(eval(1,1)))/Omega_SP
Thalf_SP = 0.69 / abs(real(eval(1,1)))
T_SP = 2 * pi / abs(imag(eval(1,1)))
Nhalf_SP = Thalf_SP / T_SP

% for the phugoid
Omega_Phugoid = norm(eval(3,3))
DR_Phugoid = abs(real(eval(3,3)))/Omega_Phugoid
Thalf_Phugoid = 0.69 / abs(real(eval(3,3)))
T_Phugoid = 2 * pi / abs(imag(eval(3,3)))
Nhalf_Phugoid = Thalf_Phugoid / T_Phugoid

```

## Matlab Output

M = 0.0781	Beta = 0.9969	it = 0
V = 88	CLaw3D = 4.8384	Clow = 0.1689
Uo = 88	CLat3D = 4.0158	epsilonO = 0.0108
W = 16	eta = 1	CLo = 0.6506
g = 32.1740	Vh = 0.4064	CLu = 0.0040
m = 0.4973	rho = 0.0023	CXu = 0
S = 7.1100	Q = 8.7894	Lalpha = 663.2226
b = 8.4300	CDo = 0.0250	Malpha = -9.5531
ARw = 10	Iy = 0.8000	Lu = 1.8639
Cbar = 0.8400	tau = 0.4000	Lalphadot = 0.6031
Lt = 2.2900	XdelE = 0	Malphadot = -0.8585
St = 1.0600	DeDa = 0.3080	Lq = 2.8284
ARt = 4.5000	CLalpha = 5.2527	Mq = -3.0657
Se = 0.2120	Cmalpha = -0.1456	LdelE = 30.0943
Xcg = 0.2940	CDalpha = 0.2101	MdelE = -42.8396
Xac = 0.2100	CLalphadot = 1.0055	Xu = 0
CLaw2D = 5.8000	Cmalphadot = -2.7411	Zu = -1.8639
CLat2D = 6.1400	CLq = 4.7159	Mu = 0.0373
CDu = 0	Cmq = -9.7891	Mwdot = -0.0098
Cmu = 0.0500	CldelE = 0.2395	Xw = 0.6291
CmaFuse = 0.5000	CmdelE = -0.6529	Zw = -7.5366
Sweepw = 0	alphaW = 0.0349	Mw = -0.1086
Sweept = 7	iw = 0.0349	ZdelE = -30.0943

## Matrix A

0	0.6291	0	-32.1740
-1.8639	-7.5366	88.0000	0
0.0555	-0.0350	-3.9242	0
0	0	1.0000	0

## Matrix B

0	0
-30.0943	0
-42.5460	0
0	0

## Matrix evec

-0.0135 + 0.1217i	-0.0135 - 0.1217i	-0.7083 + 0.7005i	-0.7083 - 0.7005i
-0.1446 - 0.9817i	-0.1446 + 0.9817i	0.0709 - 0.0431i	0.0709 + 0.0431i
0.0072 - 0.0188i	0.0072 + 0.0188i	-0.0086 + 0.0117i	-0.0086 - 0.0117i
-0.0017 + 0.0030i	-0.0017 - 0.0030i	0.0167 + 0.0134i	0.0167 - 0.0134i

### Matrix eval

$$\begin{bmatrix} -5.7590 + 0.9310i & 0 & 0 & 0 \\ 0 & -5.7590 - 0.9310i & 0 & 0 \\ 0 & 0 & 0.0286 + 0.6754i & 0 \\ 0 & 0 & 0 & 0.0286 - 0.6754i \end{bmatrix}$$

### Matrix evec

$$\begin{bmatrix} 0.3695 - 0.1626i & 0.3695 + 0.1626i & -0.0608 + 0.5248i & -0.0608 - 0.5248i \\ -2.5611 + 2.0356i & -2.5611 - 2.0356i & 0.0151 - 0.0414i & 0.0151 + 0.0414i \\ -0.0275 + 0.0044i & -0.0275 - 0.0044i & 0.0001 + 0.0032i & 0.0001 - 0.0032i \\ 1.0000 + 0.0000i & 1.0000 - 0.0000i & 1.0000 + 0.0000i & 1.0000 - 0.0000i \end{bmatrix}$$

### Modal Characteristics

$$\Omega_{SP} = 5.8338$$

$$DR_{SP} = 0.9872$$

$$Th_{SP} = 0.1198$$

$$T_{SP} = 6.7489$$

$$N_{half\_SP} = 0.0178$$

$$\Omega_{Phugoid} = 0.6760$$

$$DR_{Phugoid} = 0.0423$$

$$Th_{Phugoid} = 24.1150$$

$$T_{Phugoid} = 9.3035$$

$$N_{half\_Phugoid} = 2.5921$$

## Nomenclature for Lateral/Directional Stability Calculations

Symbol	Description
$U_o$	Velocity (ft/s)
$M$	Mach number, using a temperature of 75°F
$\rho$	Density of air at 1500 ft (altitude of contest site) (slug/ft <sup>3</sup> )
$S$	Surface area of the wing (ft <sup>2</sup> )
$W$	Weight (lbs)
$g$	gravity (ft/s <sup>2</sup> )
$m$	mass (slugs)
$I_x$	Moment of inertia about the x-axis of the aircraft (slug-ft <sup>2</sup> )
$I_z$	Moment of inertia about the z-axis of the aircraft (slug-ft <sup>2</sup> )
$AR_w$	Aspect ratio of the wing
$AR_v$	Aspect ratio of the vertical tail
$Cl_{w2D}$	2-D wing lift curve slope
$Cl_{vt2D}$	2-D vertical tail lift curve slope
$\eta_v$	Efficiency factor of the vertical tail
$S_v$	Surface area of the vertical tail (ft <sup>2</sup> )
$d\sigma_{\beta}$	Change in sidewash due to change in angle of sideslip
$Z_v$	Distance from fuselage centerline to vertical tail aerodynamic center
$L_v$	Distance from aircraft center of gravity to vertical tail quarter chord
$b$	Wingspan (ft)
$\bar{c}$	Mean aerodynamic chord (ft)
$V_v$	Vertical tail volume (ft <sup>3</sup> )
$Q$	Dynamic pressure (lb/ft <sup>2</sup> )
$\text{volume}_{\text{fuse}}$	Volume of the fuselage (ft <sup>3</sup> )
$\text{width}_{\text{fuse}}$	Average width of the fuselage (ft)
$H_{\text{wingroot}}$	Height of the fuselage at the wing root (ft)
$C_{\beta_{\text{fuse}}}$	Weathercock effect due to the fuselage
$C_l_o$	Reference aircraft lift coefficient
$\text{Sweep}_w$	Sweep of the wing quarter chord (degrees)
$\text{Sweep}_v$	Sweep of the vertical tail quarter chord (degrees)
$\beta$	Interpolation variable used to determine $Cl_{w3D}$ and $Cl_{vt3D}$
$k_w$	Interpolation variable used to determine $Cl_{w3D}$
$k_t$	Interpolation variable used to determine $Cl_{vt3D}$
$C_{y\beta_{\text{tail}}}$	Side force coefficient due to sideslip caused by the vertical tail
$C_{y\beta}$	Side force coefficient due to sideslip
$C_{y\dot{p}}$	Side force coefficient due to roll rate
$C_{y\dot{r}}$	Side force coefficient due to yaw rate
$C_{l\beta}$	Dihedral effect coefficient
$C_{l\dot{p}}$	Damping coefficient in roll
$C_{l\dot{r}}$	Rolling moment coefficient due to yaw

Cn <sub>beta</sub>	Weathercock effect coefficient
C <sub>np</sub>	Yawing moment coefficient due to roll
C <sub>nr</sub>	Damping coefficient in yaw
Y <sub>beta</sub>	Side force due to sideslip (lbs)
Y <sub>p</sub>	Side force due to roll rate (lbs)
Y <sub>r</sub>	Side force due to yaw rate (lbs)
L <sub>beta</sub>	Dihedral effect (ft-lbs)
L <sub>p</sub>	Damping in roll (ft-lbs)
L <sub>r</sub>	Rolling moment due to yaw (ft-lbs)
N <sub>beta</sub>	Weathercock effect (ft-lbs)
N <sub>p</sub>	Yawing moment due to roll (ft-lbs)
N <sub>r</sub>	Damping in yaw (ft-lbs)
Omega <sub>roll</sub>	Natural frequency of the roll mode oscillations (Hz)
Thalf <sub>roll</sub>	Time for the amplitude of the roll mode oscillations to half (sec)
Omega <sub>spiral</sub>	Natural frequency of the spiral mode oscillations (Hz)
Thalf <sub>roll</sub>	Time for the amplitude of the spiral mode oscillations to half (sec)
Omega <sub>DR</sub>	Natural frequency of the dutch roll mode oscillations (Hz)
DR <sub>DR</sub>	Damping ratio for the dutch roll mode oscillations
Thalf <sub>DR</sub>	Time for the amplitude of the dutch roll mode oscillations to half (sec)
T <sub>DR</sub>	Period of the dutch roll mode oscillations (sec)
Nhalf <sub>DR</sub>	Number of oscillations for the amplitude of the dutch roll mode oscillations to half

### Additional Comments

The orthogonal coordinate system used has the x-axis extending forward through the nose of the aircraft, the y-axis going through the right-hand side, and the z-axis pointing through the bottom of the aircraft.

All stability derivatives and coefficients were derived assuming level flight with small perturbations only.

## *Lateral/Directional Stability Calculations*

### Code written for Matlab

```
Uo = 88
M = 0.0781
rho = 0.00227
S = 7.11
W = 16.0
g = 32.174
m = W / g
Ix = 15
Iz = 16
ARw = 10.0
ARvt = 1.2
Claw2D = 5.80
Clavt2D = 6.14
etaV = 1
Sv = 0.49
dsigmadbeta = 0.3
Zv = 0.375
Lv = 2.5
b = 8.43
Cbar = 0.84
Vv = (Sv/S) * Lv/Cbar
rho = 0.00227
Q = 0.5 * rho * Uo^2

%Fuselage stuff
volumefuse = (2.375*3*36)/12^3
widthfuse = 2.375/12
Hatwingroot = 3/12

Cnbetafuse = -1.3*volumefuse*Hatwingroot/(S*b*widthfuse)
Clo = W / (Q*S)
Sweepw = 0.0
Sweepvt = 41
Beta = sqrt(1 - M^2)
kw = Claw2D / (2 * 3.1416)
kt = Clavt2D / (2 * 3.1416)
ClalphaW = 2 * 3.141 * ARw / (2 + sqrt(ARw^2 * Beta^2 / kw^2 * (1 + (tan(Sweepw/57.3))^2 / Beta^2) + 4))
ClalphaV = 2 * 3.141 * ARvt / (2 + sqrt(ARvt^2 * Beta^2 / kt^2 * (1 + (tan(Sweepvt/57.3))^2 / Beta^2) + 4))
Cybetatail = ClalphaV
Q = .5 * rho * Uo^2

% Stability Coefficients

Cybeta = - etaV * (Sv/S) * ClalphaV * (1 + dsigmadbeta)
Cyp = - 2 * etaV * (Sv/S) * ClalphaV * (Zv/b)
Cyr = 2 * etaV * Vv * ClalphaV
Clbeta = 0.0
Clp = - ClalphaW / 12 * (1 + 3 * Sweepw) / (1 + Sweepw) - 2 * etaV * (Sv/S) * (Zv/b)^2 * ClalphaV
Clr = Clo / 4 - 2 * (Lv/b) * (Zv/b) * Cybetatail
Cnbeta = Cnbetafuse + etaV * Vv * ClalphaV * (1 + dsigmadbeta)
Cnp = - Clo / 8 + 2 * etaV * Vv * ClalphaV * (Zv/b)
```

$$C_{nr} = -2 * \eta V * V_v * (L_v/b) * C_{\alpha V}$$

% Directional Derivatives

$$\begin{aligned} Y_{\beta} &= Q * S * C_{y\beta} / m \\ Y_p &= Q * S * b * C_{yp} / (2 * m * U_0) \\ Y_r &= Q * S * b * C_{yr} / (2 * m * U_0) \\ L_{\beta} &= Q * S * b * C_{l\beta} / I_x \\ L_p &= Q * S * b^2 * C_{lp} / (2 * I_x * U_0) \\ L_r &= Q * S * b^2 * C_{lr} / (2 * I_x * U_0) \\ N_{\beta} &= Q * S * b * C_{n\beta} / I_z \\ N_p &= Q * S * b^2 * C_{np} / (2 * I_z * U_0) \\ N_r &= Q * S * b^2 * C_{nr} / (2 * I_z * U_0) \end{aligned}$$

% Set up the matrix for the lateral/directional equations of motion

$$A = [Y_{\beta}/U_0 \quad Y_p/U_0 \quad -(1-Y_r/U_0)g/U_0; L_{\beta} \quad L_p \quad L_r \quad 0; N_{\beta} \quad N_p \quad N_r \quad 0 \quad 0 \quad 1 \quad 0 \quad 0]$$

$$[evec, eval] = eig(A)$$

% Roll mode

$$\begin{aligned} \Omega_{roll} &= \text{norm}(eval(3,3)) \\ \text{Thalf}_{roll} &= 0.69 / \text{abs}(\text{real}(eval(3,3))) \end{aligned}$$

% Spiral mode

$$\begin{aligned} \Omega_{spiral} &= \text{norm}(eval(4,4)) \\ \text{Thalf}_{spiral} &= 0.69 / \text{abs}(\text{real}(eval(4,4))) \end{aligned}$$

% Dutch roll mode

$$\begin{aligned} \Omega_{DR} &= \text{norm}(eval(1,1)) \\ DR\_DR &= \text{abs}(\text{real}(eval(1,1))) / \Omega_{DR} \\ \text{Thalf}_{DR} &= 0.69 / \text{abs}(\text{real}(eval(1,1))) \\ T_{DR} &= 2 * \pi / \text{abs}(\text{imag}(eval(1,1))) \\ N_{half\_DR} &= \text{Thalf}_{DR} / T_{DR} \end{aligned}$$



## Matlab Output

Uo = 88	Cbar = 0.8400	Cybeta = -0.1476
M = 0.0781	Vv = 0.2051	Cyp = -0.0101
rho = 0.0023	rho = 0.0023	Cyr = 0.6757
S = 7.1100	Q = 8.7894	Clbeta = 0
W = 16	volumefuse = 0.1484	Clp = -0.4036
g = 32.1740	widthfuse = 0.1979	Clr = 0.0205
m = 0.4973	Hatwingroot = 0.2500	Cnbeta = 0.4352
Ix = 15	Cnbetafuse = -0.0041	Cnp = -0.0019
Iz = 16	Clo = 0.2560	Cnr = -0.2004
ARw = 10	Sweepw = 0	Ybeta = -18.5455
ARvt = 1.2000	Sweepvt = 41	Yp = -0.0608
Claw2D = 5.8000	Beta = 0.9969	Yr = 4.0672
Clavt2D = 6.1400	kw = 0.9231	Lbeta = 0
etaV = 1	kt = 0.9772	Lp = -0.6790
Sv = 0.4900	ClalphaW = 4.8384	Lr = 0.0346
dsigmadbeta = 0.3000	ClalphaV = 1.6472	Nbeta = 14.3279
Zv = 0.3750	Cybetatail = 1.6472	Np = -0.0031
Lv = 2.5000	Q = 8.7894	Nr = -0.3160
b = 8.4300		

## Matrix A

-0.2107	-0.0007	-0.9538	0.3656
0	-0.6790	0.0346	0
14.3279	-0.0031	-0.3160	0
0	1.0000	0	0

## Matrix evec

-0.2476 + 0.0340i	-0.2476 - 0.0340i	0.0080	-0.0083
0.0090 - 0.0001i	0.0090 + 0.0001i	0.5465	-0.0176
0.1181 + 0.9610i	0.1181 - 0.9610i	-0.2965	-0.3561
-0.0002 - 0.0024i	-0.0002 + 0.0024i	-0.7832	-0.9342

## Matrix eval

-0.2635 + 3.6981i	0	0	0
0	-0.2635 - 3.6981i	0	0
0	0	-0.6978	0
0	0	0	0.0189

### Modal Characteristics

$\Omega_{\text{roll}} = 0.6978$

$T_{\text{half\_roll}} = 0.9889$

$\Omega_{\text{spiral}} = 0.0189$

$T_{\text{half\_spiral}} = 36.5516$

$\Omega_{\text{DR}} = 3.7075$

$T_{\text{DR}} = 0.0711$

$T_{\text{half\_DR}} = 2.6191$

$T_{\text{DR}} = 1.6990$

$N_{\text{half\_DR}} = 1.5415$

### *Summary of Stability Calculations*

Mode	Natural Frequency (rad/s)	Damping Ratio	Time to Half (s)	Period (s)
Short Period	5.83	0.987	0.12	6.75
Phugoid	0.68	0.042	24.12	9.30
Roll	0.70	N/A*	0.99	N/A*
Spiral	0.02	N/A*	36.55	N/A*
Dutch Roll	3.71	0.071	2.62	1.70

\* N/A since the roll mode and spiral mode are non-oscillatory.

## Appendix C

*ElectriCalc Data*

## ElectriCalc Data

The information displayed below was the actual output produced by ElectriCalc for various aircraft power combinations.

### Setup and Combination

	Aggie Flyer 1996-97 Design	Texas Tall Boy Combination 1	Texas Tall Boy Combination 2	Texas Tall Boy Combination 3	Texas Tall Boy Combination 4
Motor	1412/2Y	1412/2Y	1412/3Y	1412/3Y	Max15-13Y
Motor Manufacturer	Aveox	Aveox	Aveox	Aveox	MaxCim
Gearing	3.7	3.7	3.7	3.7	3.7
Motor KRPM	22.9	24.9	17.0	18.8	17.0
Motor Power (Watts)	990.0	880.0	834.0	680.0	1020.0
Motor Current (amps)	59.5	49.5	45.0	34.4	62.8
Motor Voltage (volts)	16.6	17.8	18.5	19.8	16.2
Propeller Type	Carbon folder	Carbon folder	Carbon folder	Carbon folder	Carbon folder
Propeller Diameter (inches)	15.0	15.0	18.0	18.0	18.0
Propeller Pitch (inches)	13.6	9.5	8.0	8.0	8.0
Propellor Yoke Pitch (degrees)	5.0	0.0	5.0	0.0	5.0
Pitch Speed (ft/sec)	80.0	60.0	56.0	38.0	56.0
Propeller KRPM	6.2	6.7	4.6	5.1	4.6
Propeller Power (Watts)	859.0	767.0	691.0	576.0	689.0
Battery Current (amps)	59.5	49.0	45.0	34.4	62.2
Battery Milli-amp hours	1950.0	2200.0	2200.0	2200.0	2200.0
Battery Duration Time (minutes)	1.9	2.6	2.8	3.6	2.0
Cell Type	N-1700SCRC	N-2000CR	N-2000CR	N-2000CR	N-2000CR
Cell Count	19.0	19.0	19.0	19.0	19.0
Cell Voltage (volts)	1.3	1.3	1.3	1.3	1.3
Cell Resistance (milli-ohms)	5.5	5.3	5.3	5.3	5.3
% Throttle	100.0	99.0	100.0	100.0	99.0
% System Efficiency	61.0	66.0	65.0	70.0	47.0
% Motor Efficiency	89.0	90.0	85.0	87.0	70.0
Watts/Pound	62.0	55.0	52.0	43.0	64.0
Thrust (ounces)	123.0	125.0	125.0	106.0	125.0

## Appendix D

### *Wing Airfoil Analysis Data*

## Wing Airfoil Analysis Data

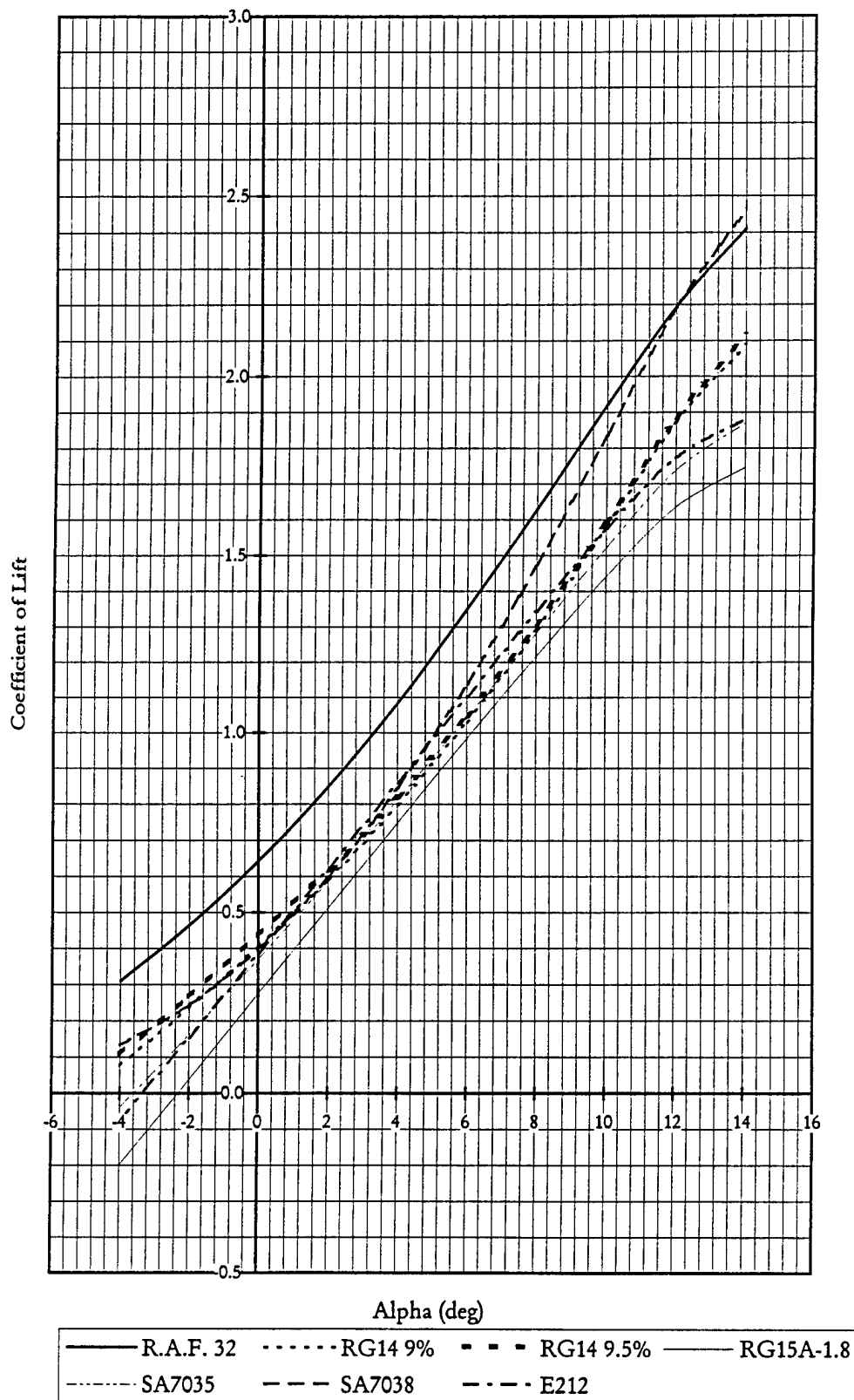
### Calculated Cl vs. Alpha Values Using PANZ

Alpha	RAF32	SA7038	SA7035	Airfoil			
				E212	RG14 9%	RG14 9.5%	15A-1.8/11
-4	0.311	0.133	-0.039	-0.074	0.078	0.109	-0.199
-2	0.465	0.244	0.162	0.154	0.237	0.268	0.038
0	0.643	0.399	0.370	0.386	0.406	0.436	0.275
2	0.849	0.599	0.586	0.621	0.592	0.618	0.512
4	1.084	0.845	0.811	0.860	0.798	0.820	0.748
6	1.351	1.138	1.043	1.102	1.031	1.048	0.984
8	1.629	1.472	1.282	1.343	1.292	1.306	1.217
10	1.921	1.835	1.521	1.575	1.580	1.592	1.440
12	2.196	2.192	1.737	1.772	1.873	1.886	1.634
14	2.411	2.463	1.871	1.881	2.089	2.114	1.746

### Published Cl vs. Alpha Values

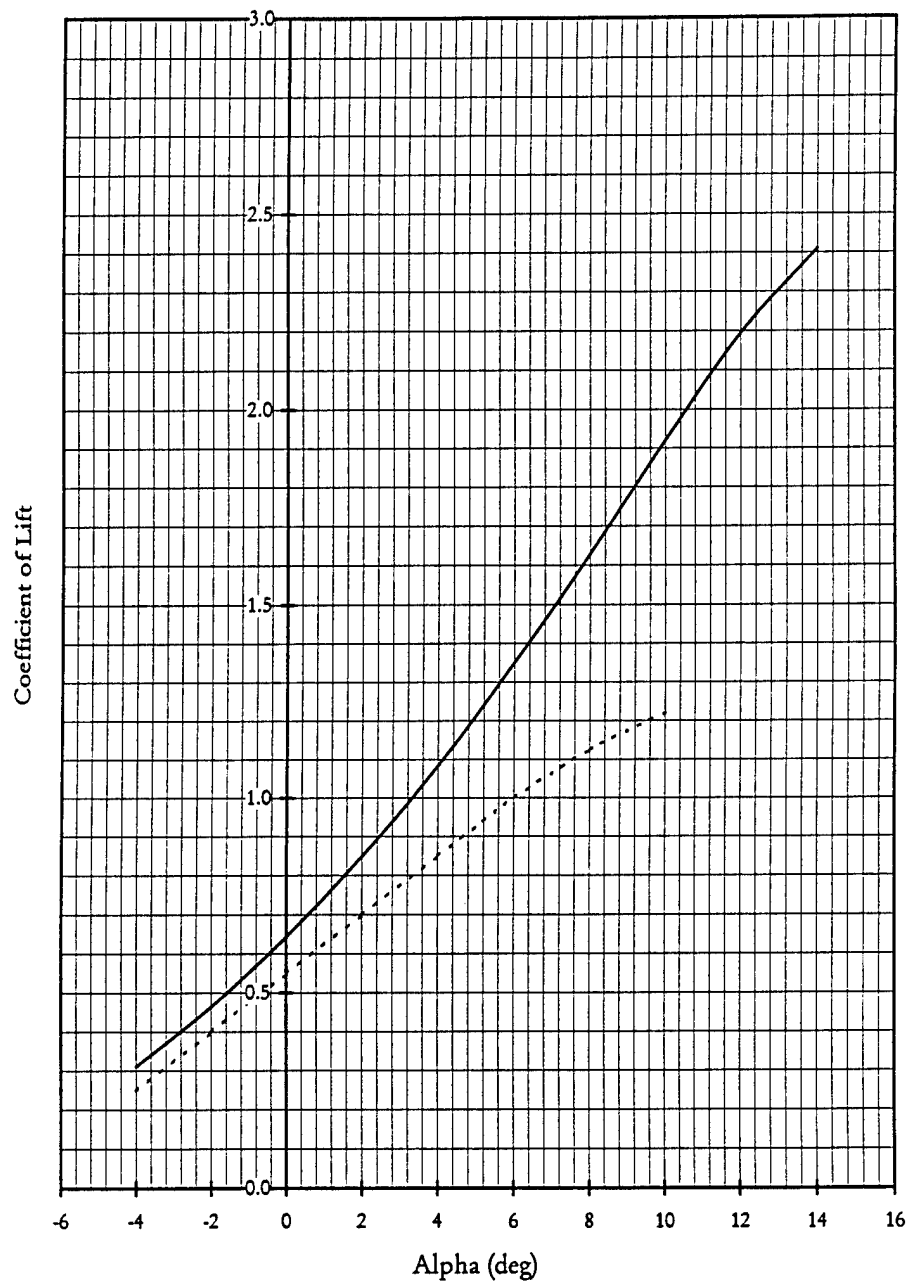
Alpha	RAF32	Airfoil	
		SA7038	SA7035
-4	0.249	—	—
-2	0.400	0.200	0.120
0	0.550	0.400	0.300
2	0.700	0.625	0.560
4	0.850	0.800	0.750
6	1.000	1.030	0.900
8	1.125	1.210	1.120
10	1.220	1.300	1.250

# Calculated Cl vs. Alpha for Various Airfoils





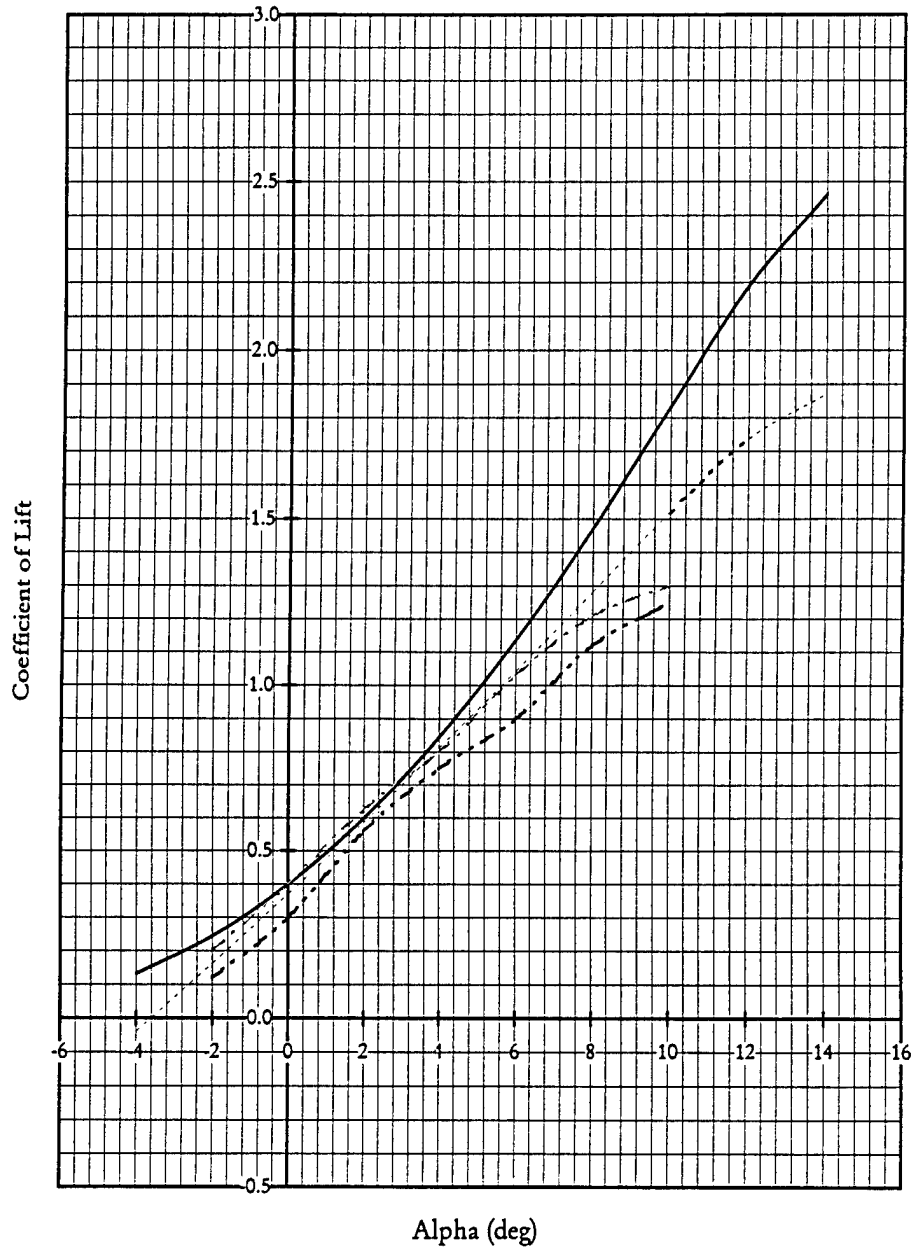
# Published and Calculated Cl vs. Alpha for the R.A.F. 32\*



— R.A.F. 32 Calc    - - - - - R.A.F. 32 Pub.

\*Airfoil used on the Aggie Flyer

# Published and Calculated Cl vs. Alpha for the SA7035 and the SA7038\*



..... SA7035 Calc. — SA7038 Calc. - - - SA7035 Pub. - . - . SA7038 Pub.

\*Airfoil used on the Texas Tall Boy

## Appendix E

### *Wind Tunnel Propulsion Test Data*

## *Wind Tunnel Propulsion Test Data*

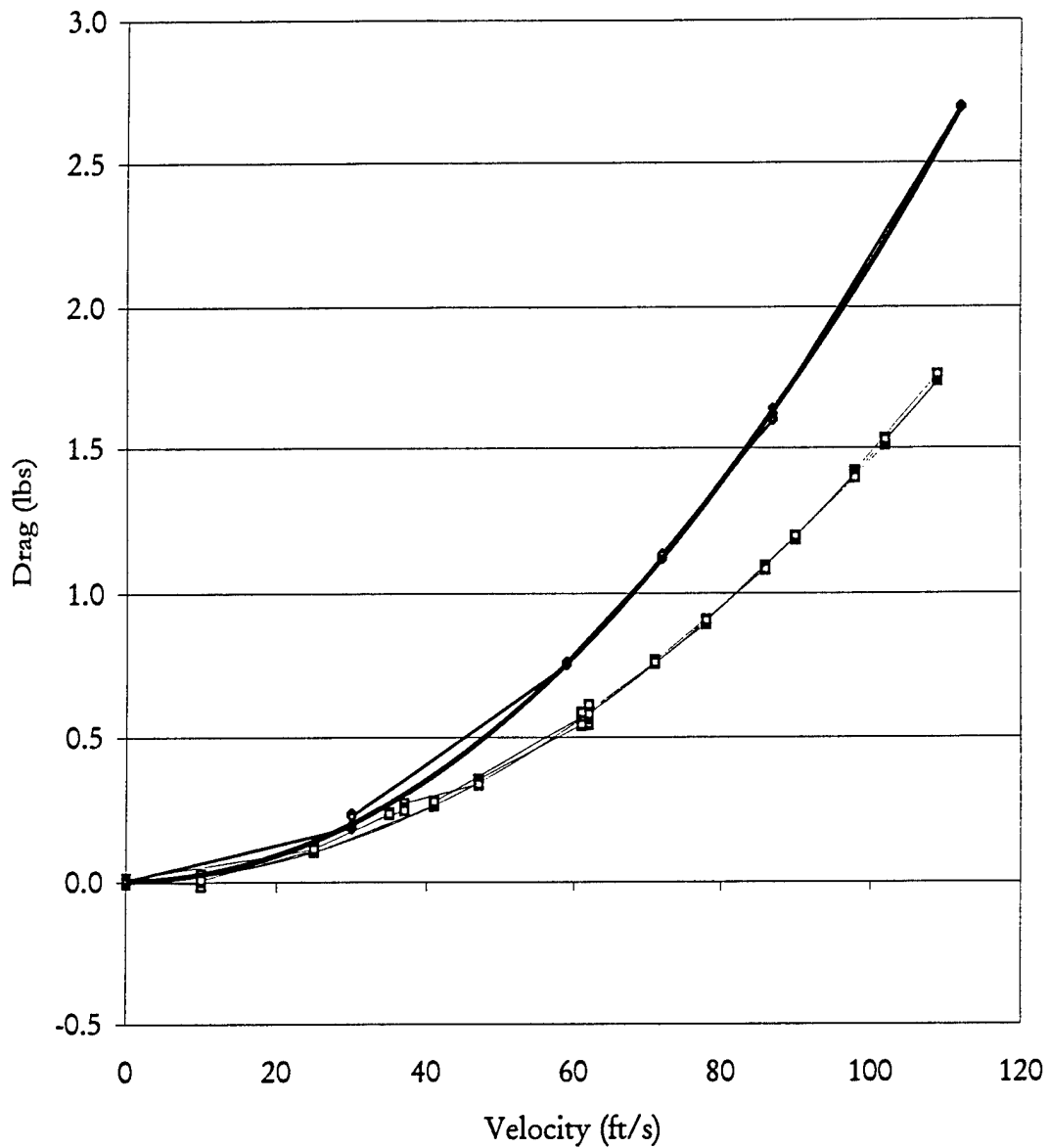
A low speed wind tunnel test was developed in order to help determine the most efficient motor/battery/propeller combination for the Texas Tall Boy. The testing facility was a 3 ft. by 5 ft. closed system wind tunnel located at the Department of Aerospace Engineering, Texas A&M University. The setup and data reduction procedures are methods taken from *Low-Speed Wind Tunnel Testing*, by Rae and Pope.

The primary focus of the test was to aid in answering the efficient drag and thrust design parameters set for by the mission requirements and overall needs of the TTB airframe design. Force and moment data was obtained using an external balance and data acquisition system developed at TAMU. The information collected allowed the values of raw force to be reduced and modified for use in endurance calculations and estimates for both the preliminary and detailed design of the TTB.

The reduced and refined information displayed below was obtained by testing a variety of types of components primarily broken up into two major combinations. Combination 1 consisted of the power system from the Aggie Flyer, and combination 2 consisted of highly researched purchased or borrowed components.

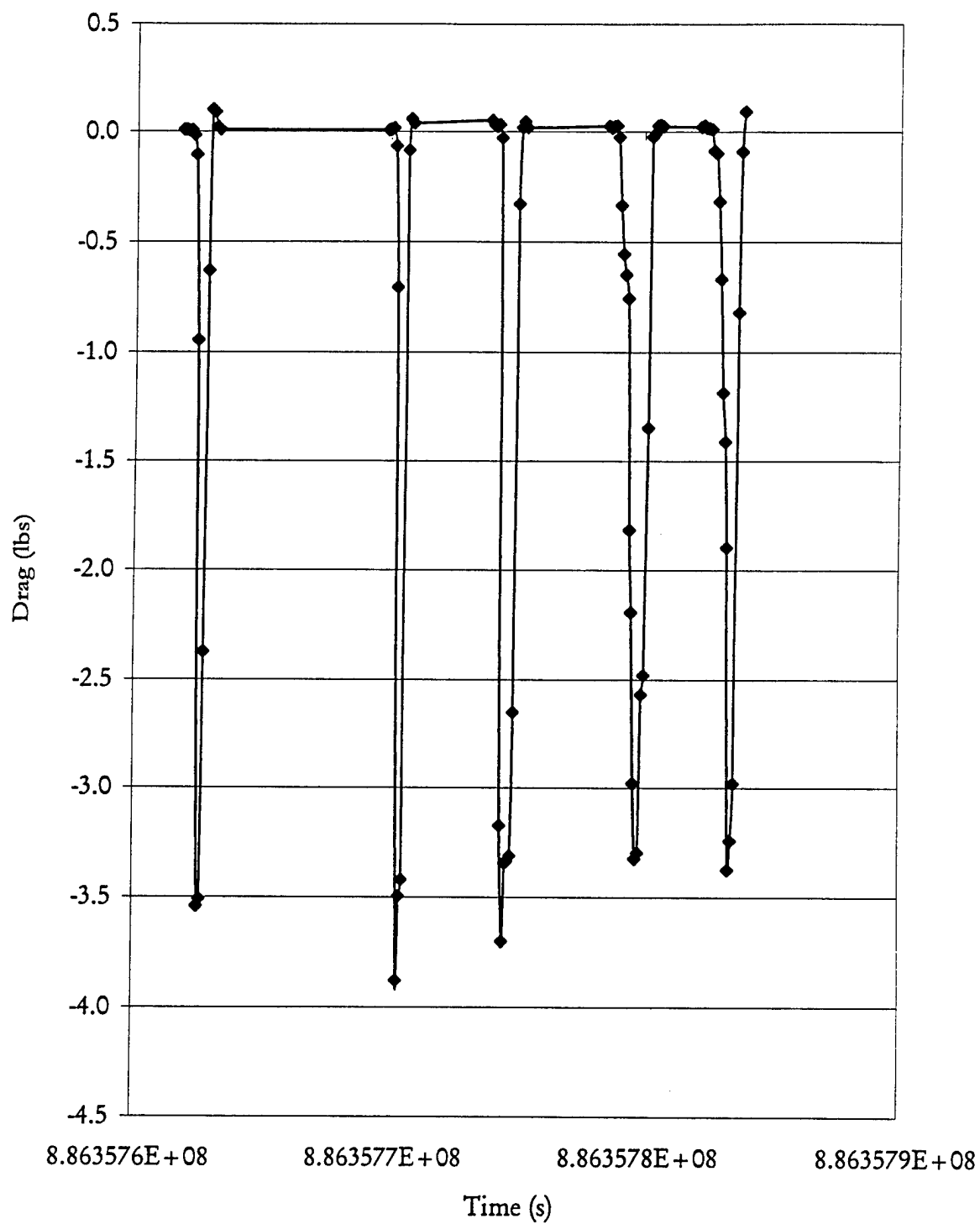
The test data began with a series of wind-on tare velocity sweeps in order to determine the drag effects of the power combination testing mount and motor-off propeller effects. This mount housed any of the combinations of motors, controller, batteries, and propellers. Then, selected motor combinations were tested at set wind tunnel velocities offering a range of estimated flight conditions. Appendix E, Wind Tunnel Propulsion Test Data, contains the examples of major test information used for further analysis of the TTB power system.

## Wind-on Tares for the Testing Mount and Propeller



—□— Mount Only —○— Prop/Spinner — Poly. (Mount Only) — Poly. (Prop/Spinner)

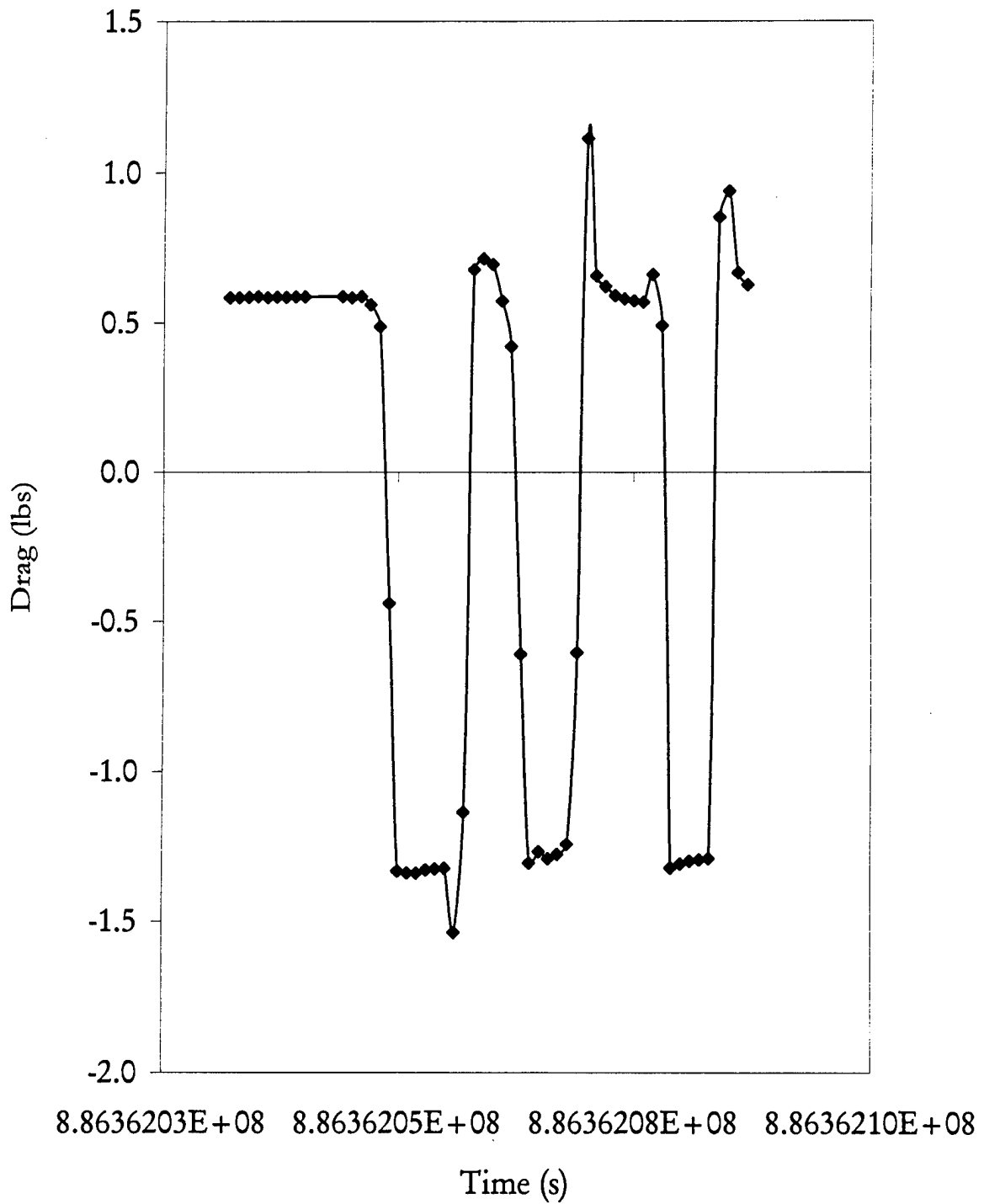
1412/3Y Power Combination Throttle Bursts  
at Wind Tunnel Speed of 0 ft/sec



## Bursts (ft/s)

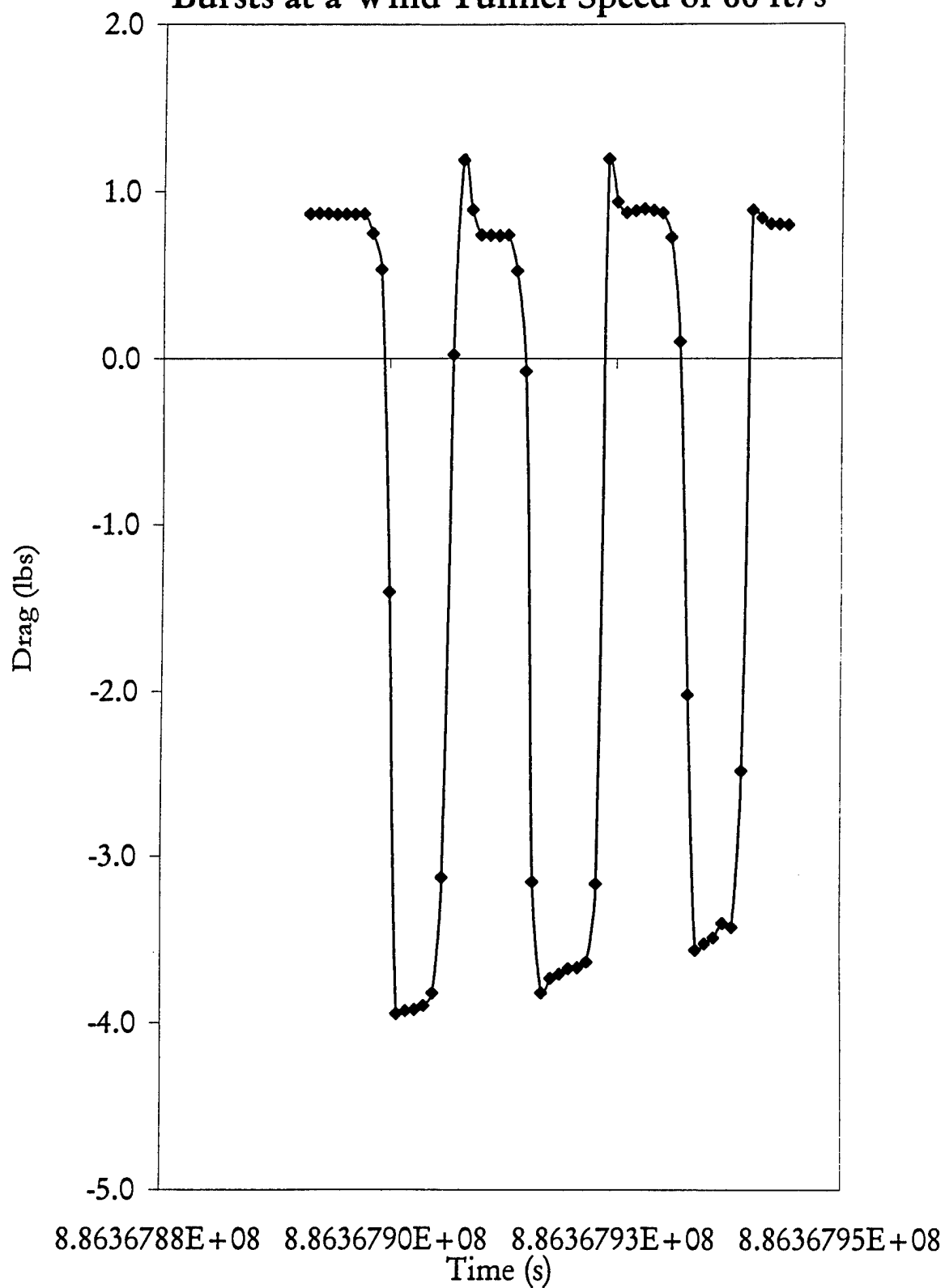


1412/3Y Power Combination Throttle  
Bursts at Wind Tunnel Speed of 56 ft/s

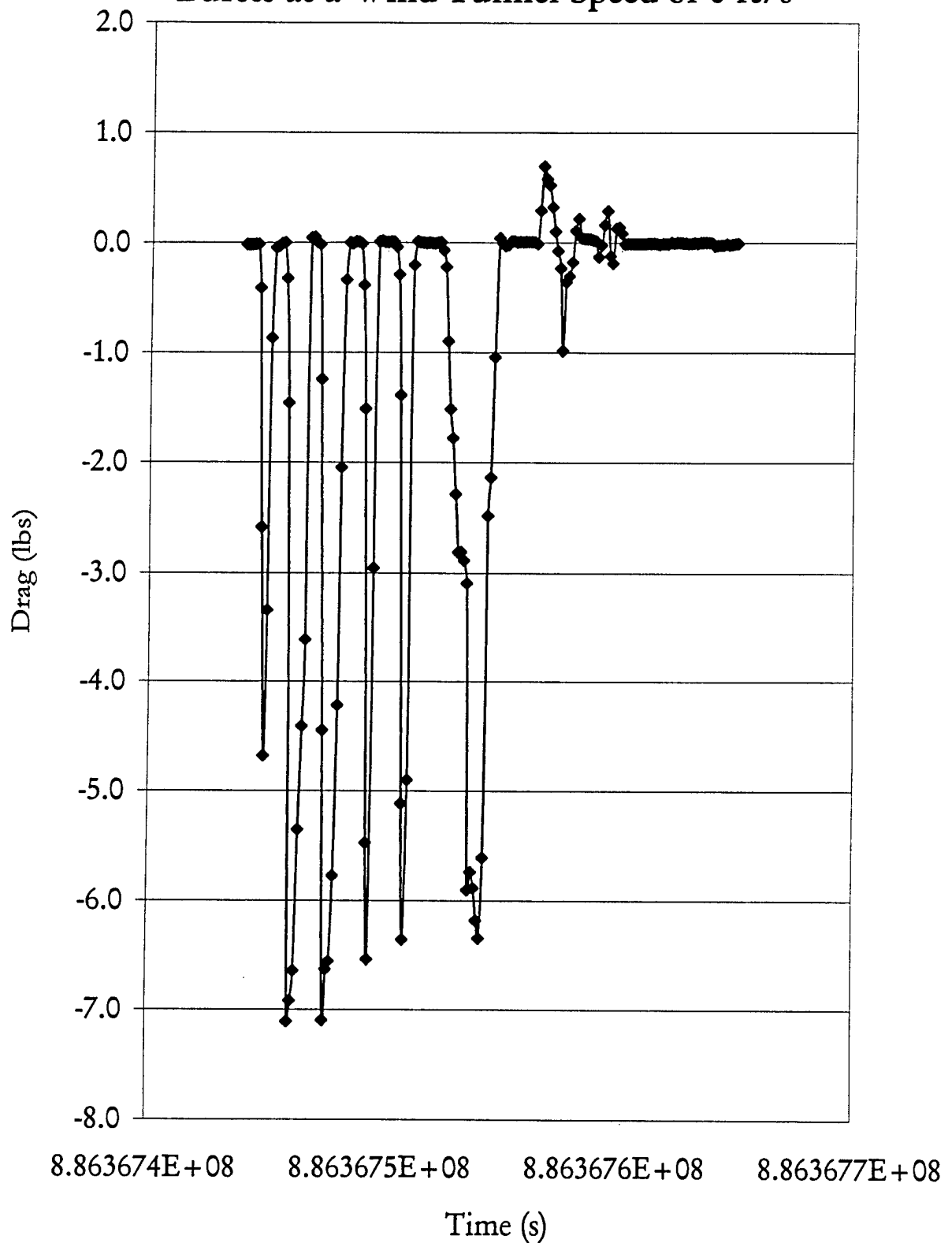




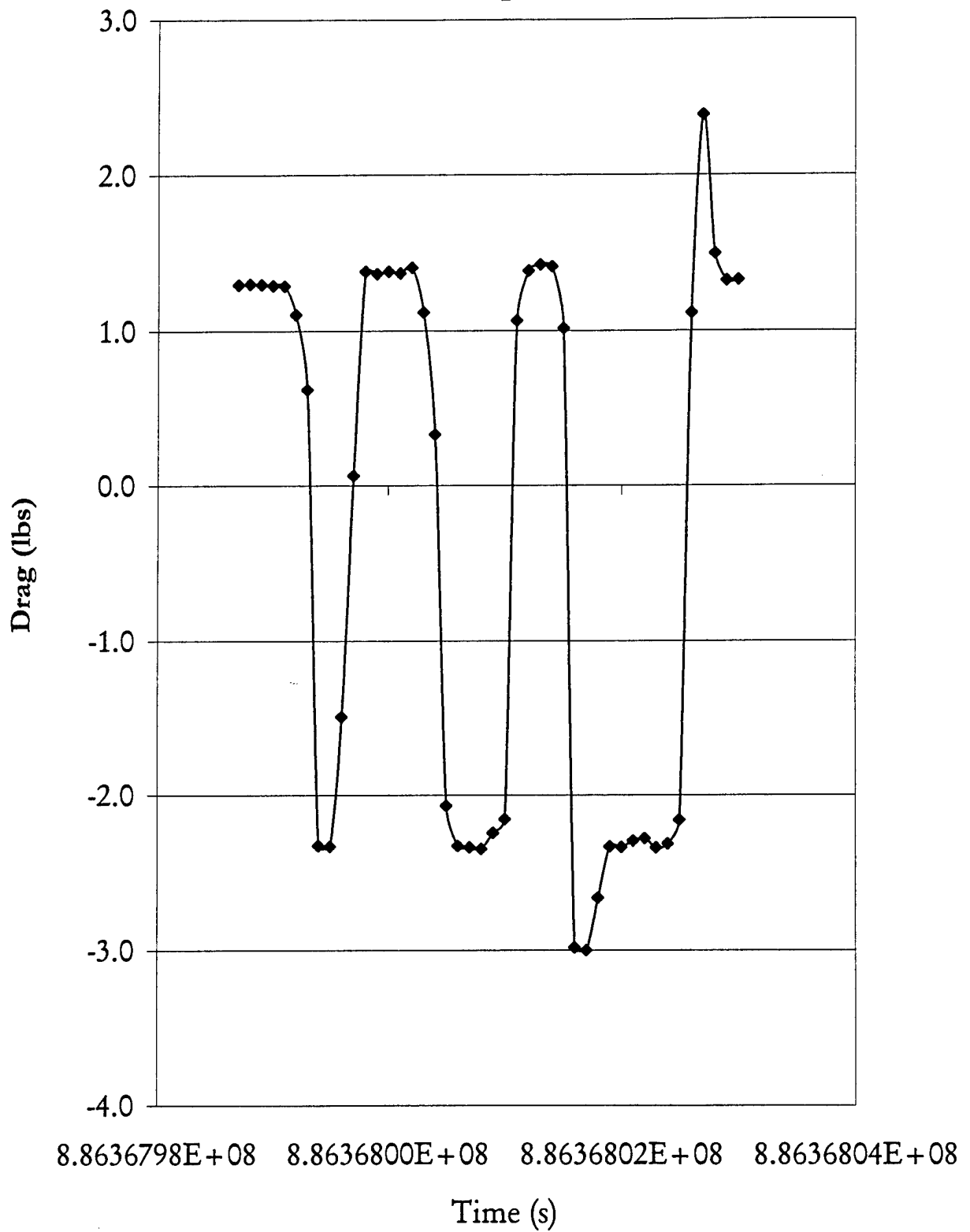
1412/2Y Power Combination Throttle  
Bursts at a Wind Tunnel Speed of 66 ft/s



1412/2Y Power Combination Throttle  
Bursts at a Wind Tunnel Speed of 0 ft/s



1412/2Y Power Combination Throttle Bursts at  
a Wind Tunnel Speed of 84 ft/s



## Appendix F

*Design Parameters for the Aggie Flyer*

## *Design Parameters for the Aggie Flyer*

### Geometry

#### Wing

Wingspan:	107.3 inches
Wing area:	1152.0 square inches
Aspect ratio:	10.0
Taper ratio:	0.45
Airfoil:	R.A.F. 32, 12.9% thickness
Sweep:	0 degrees at 30% chord
Dihedral:	None

#### Horizontal Tail

Span:	28.5 inches
Area:	169.2 square inches
Aspect ratio:	4.80
Taper ratio:	0.667
Airfoil:	Flat

#### Vertical Tail

Height:	9.875 inches
Area:	82.1 square inches
Aspect ratio:	1.19
Taper ratio:	0.415
Airfoil:	Flat

#### Tail Moment Arms (from mean aerodynamic leading edge)

To horizontal tail aerodynamic center:	30.0 inches
To vertical tail aerodynamic center:	27.0 inches

#### Wing Incidence (relative to thrust line)

0 degrees

### Propulsion Systems

Motor:	Aveox 1412/2Y
Motor Speed Controller:	Aveox F5HV
Power Battery Cells/Pack:	RC1700 SCR (19 cells)
Propeller/Yoke Combination:	Aeronaut 15 inch x 9.5 inch/5°

### Aircraft Takeoff Weight

15 pounds, 1 ounce

## Appendix G

*Design Parameters for the Texas Tall Boy*

## *Design Parameters for the Texas Tall Boy*

### Geometry

#### Wing

Wingspan: 101.2 inches  
Wing area: 1024.0 square inches  
Aspect ratio: 10.0  
Taper ratio: 0.45  
Airfoil: Selig SA7038, 9.2% thickness  
Sweep: 0 degrees at 25% chord  
Dihedral: None

#### Horizontal Tail

Span: 26.15 inches  
Area: 152.0 square inches  
Aspect ratio: 4.50  
Taper ratio: 0.65  
Airfoil: NACA 0010

#### Vertical Tail

Height: 9.23 inches  
Area: 70.9 square inches  
Aspect ratio: 1.20  
Taper ratio: 0.33  
Airfoil: NACA 0008

#### Tail Moment Arms (from mean aerodynamic leading edge)

To horizontal tail aerodynamic center: 30.0 inches  
To vertical tail aerodynamic center: 36.0 inches

#### Wing Incidence (relative to thrust line)

2 degrees

### Propulsion Systems

Motor: Aveox 1412/2Y  
Motor Speed Controller: Aveox M60  
Power Battery Cells/Pack: RC2000 SCR (19 cells)  
Propeller/Yoke Combination: Graupner 15 inch x 9.5 inch/0°

### Aircraft Takeoff Weight

14 pounds, 8 ounces

## Appendix H

### *Landing Gear Layup*



Angles are given relative to the forward edge of the landing gear.

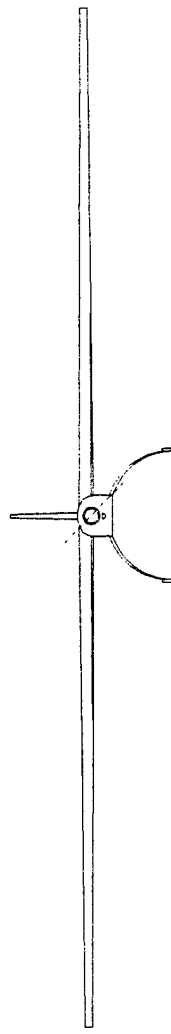
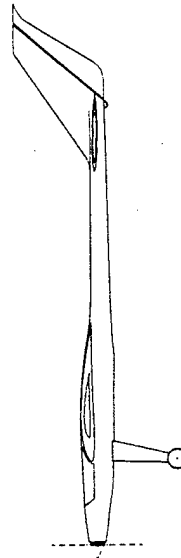
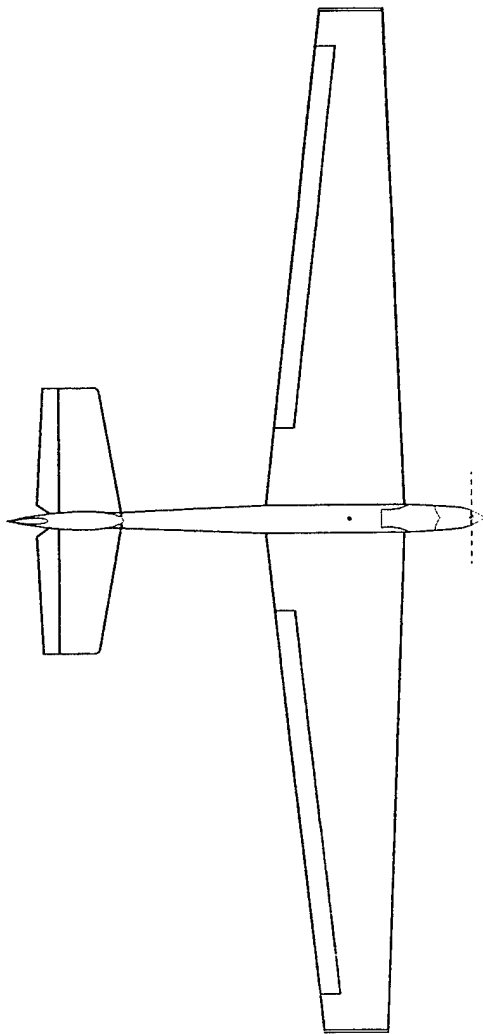
[illegible]

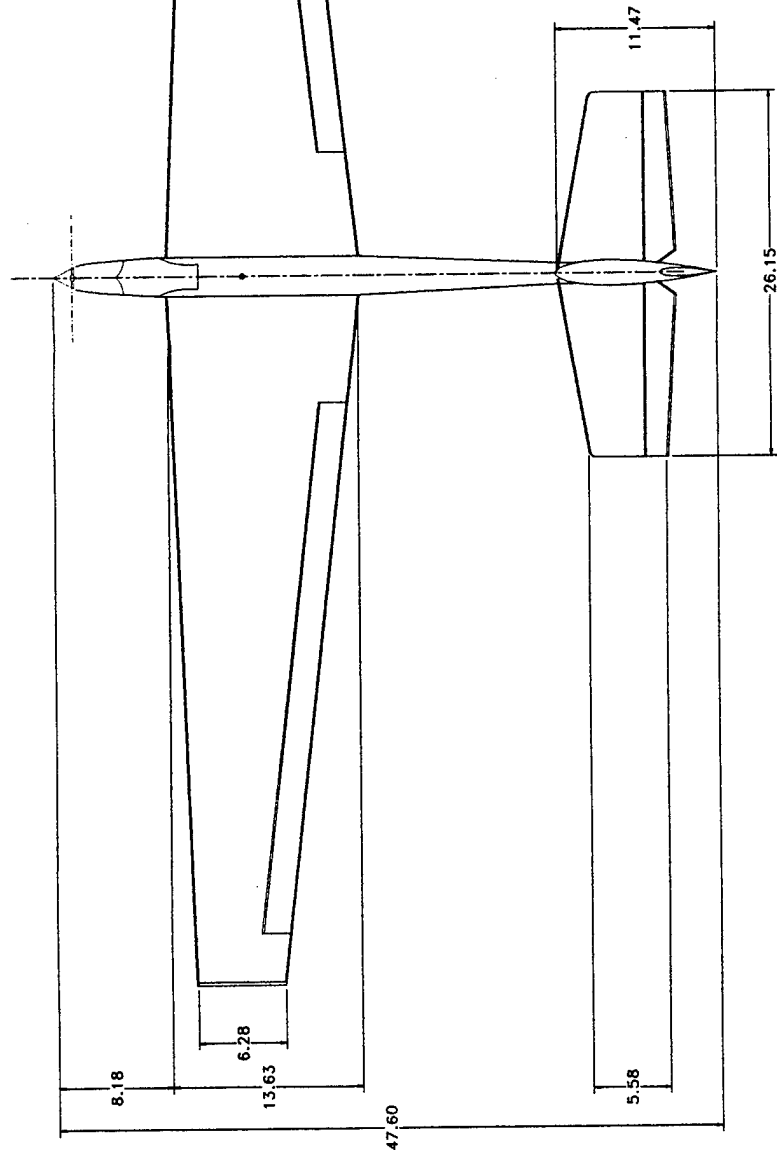
H-1

## Appendix I

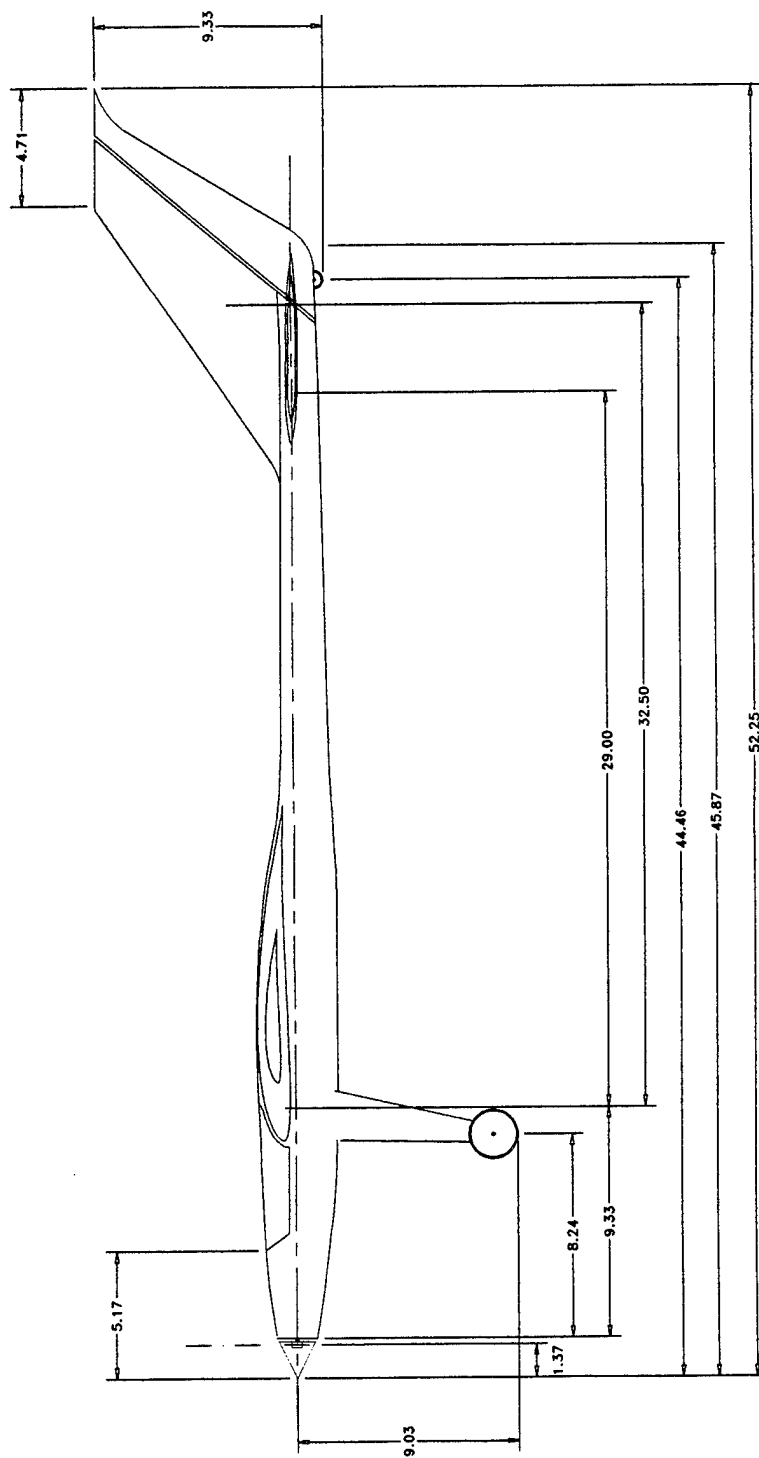
*Drawing Package for the Texas Tall Boy*

1997-1998 AIAA  
Design/Build/Fly  
Competition Design  
Texas Tail Boy





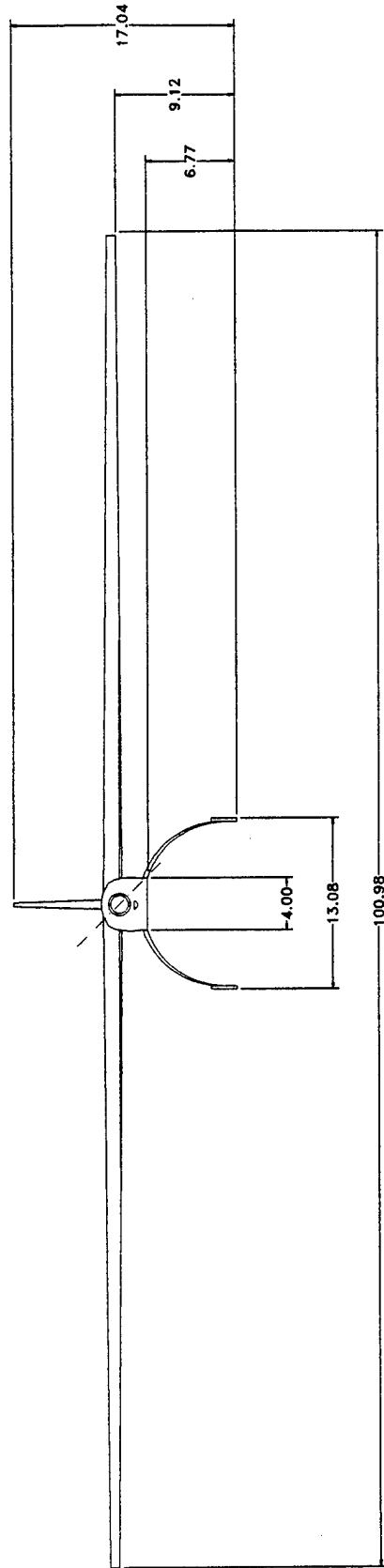
Texas Tall Boy  
Dimensioned Top View  
All Dimensions are in Inches

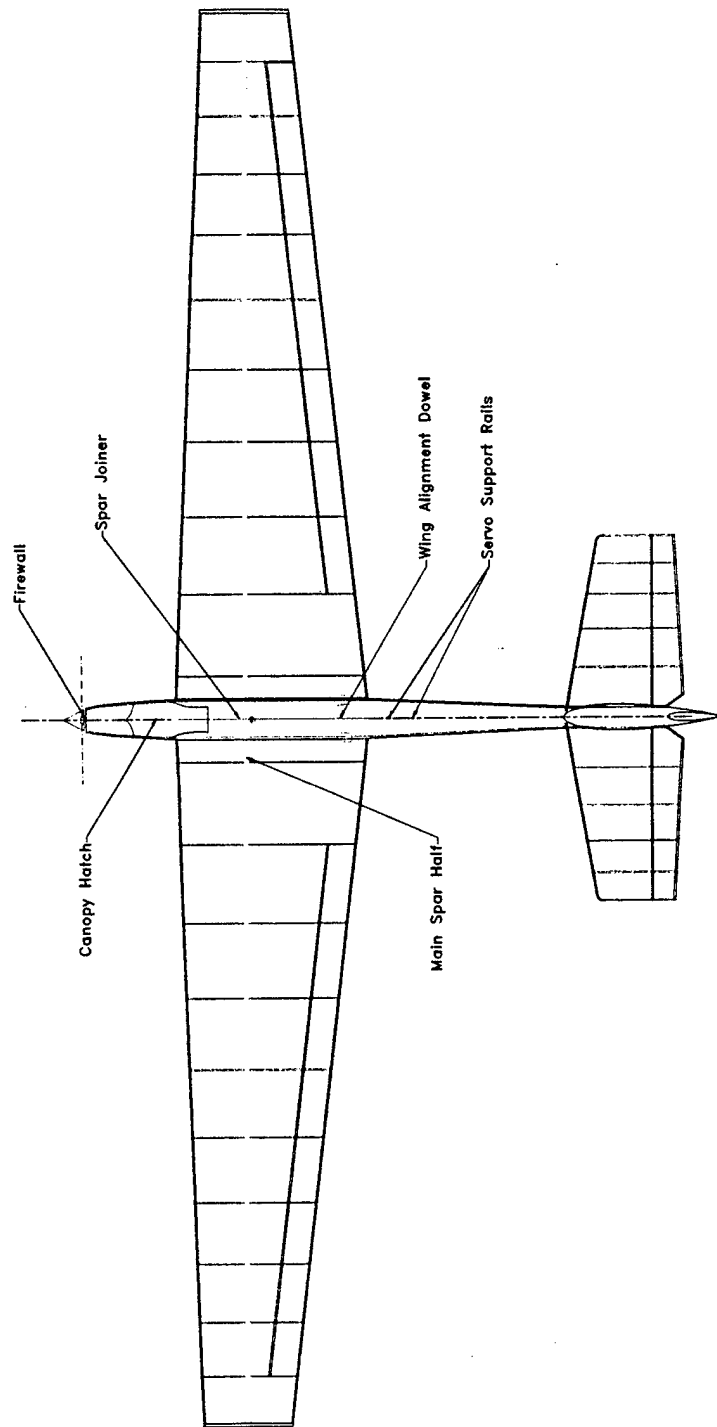


Texas Tall Boy  
Dimensioned Side View

# Texas Tall Boy Dimensioned Front View

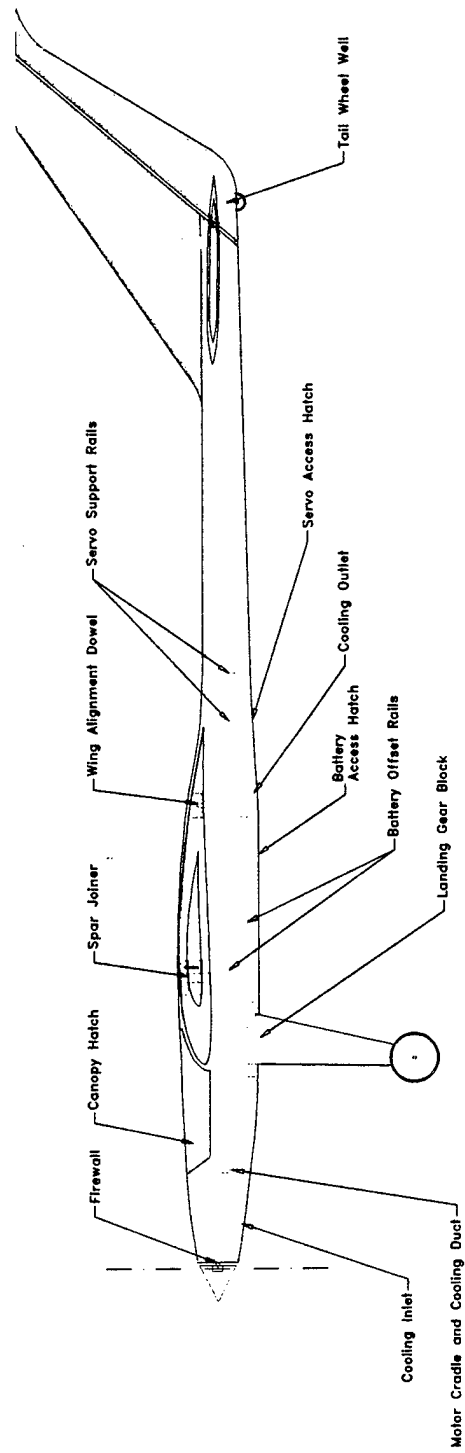
All Dimensions are in Inches





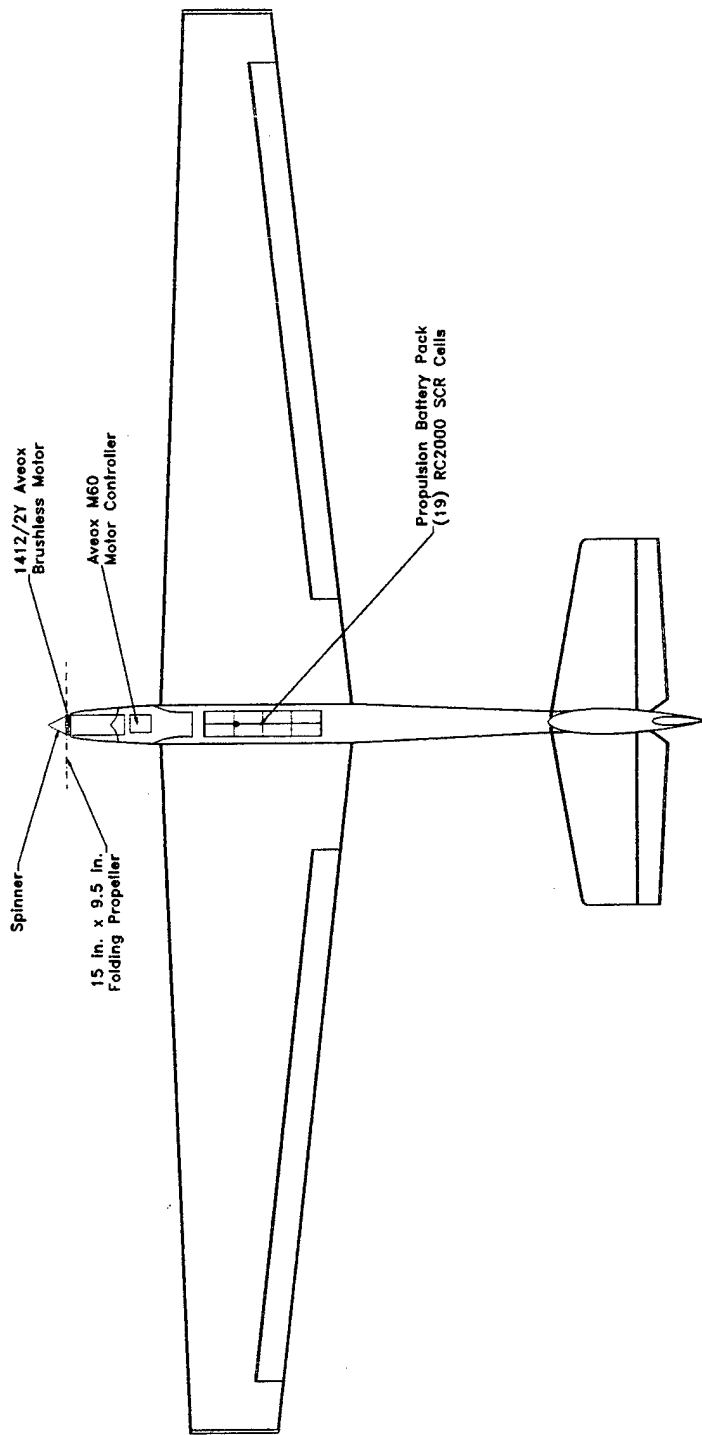
# Texas Tall Boy Internal Structure Top View

All Dimensions are in Inches

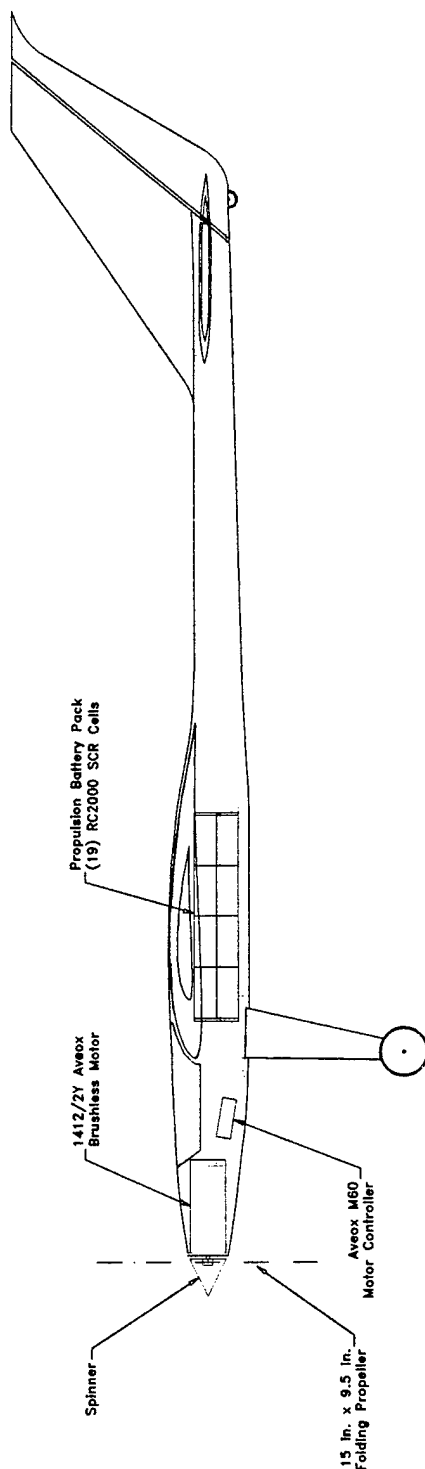


Texas Tall Boy Fuselage  
 Internal Structure Side View

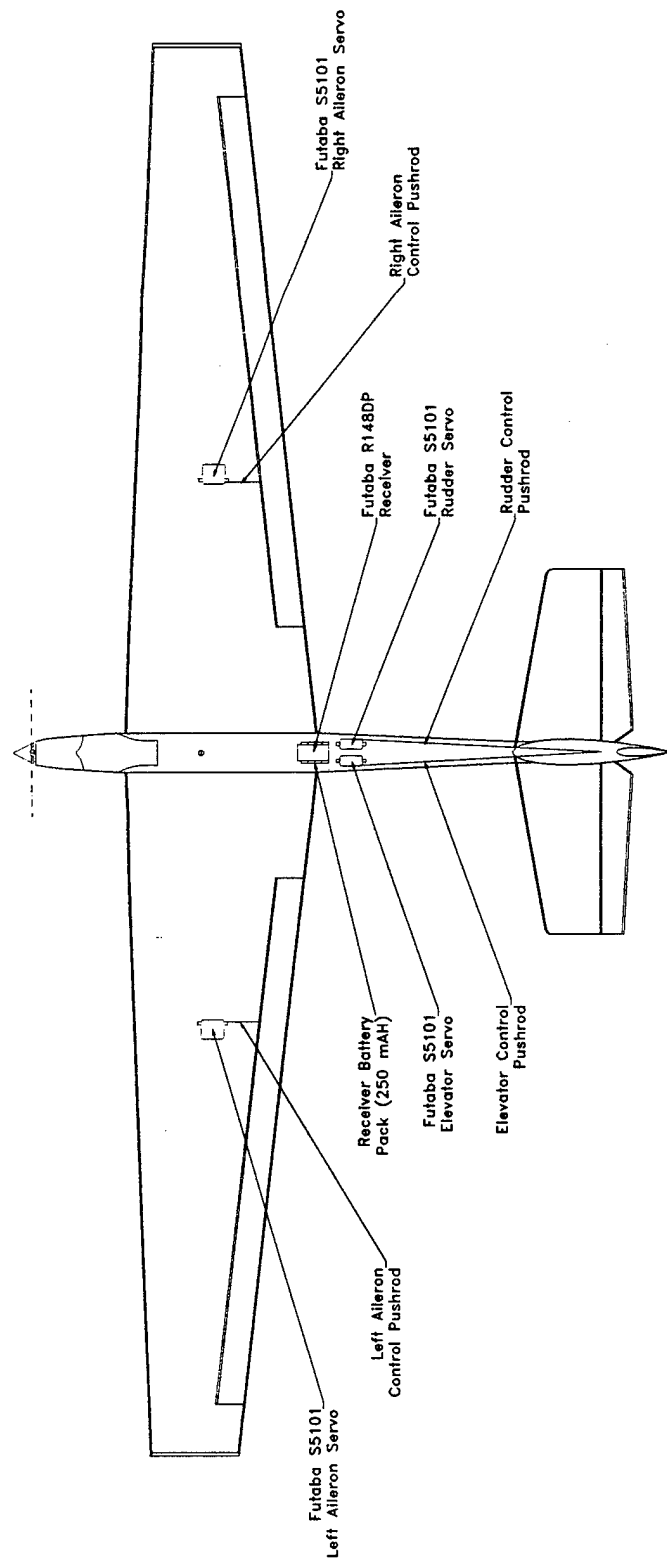




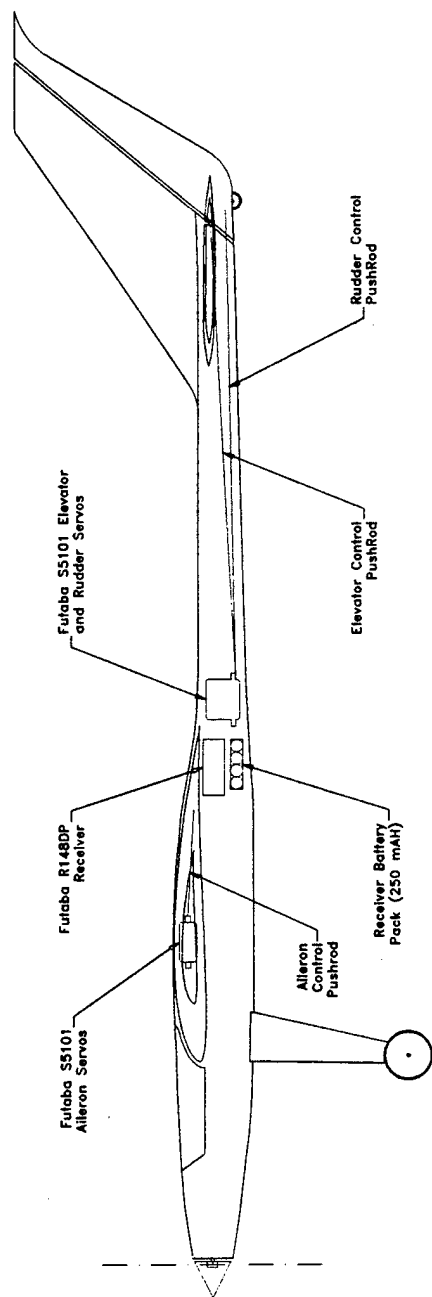
Texas Tall Boy  
Propulsion System  
Top View



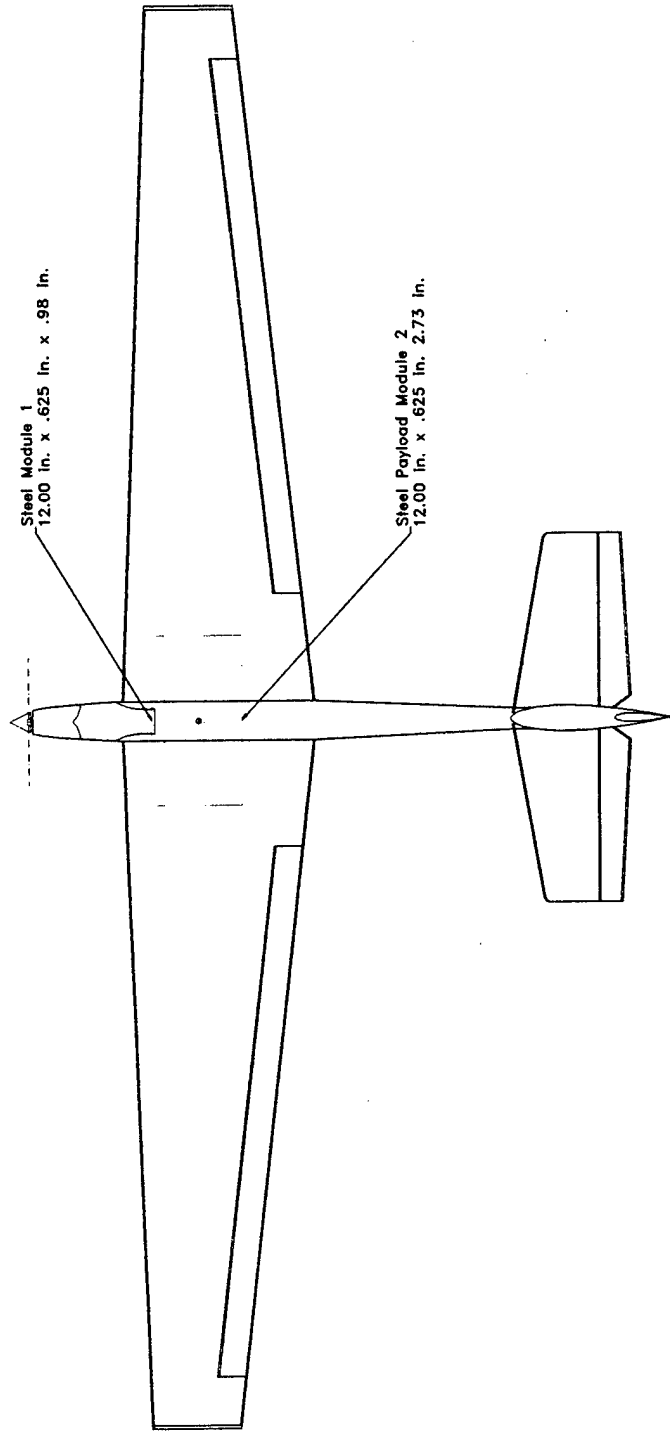
Texas Tall Boy Propulsion  
System Side View



Texas Tall Boy Control  
System Top View



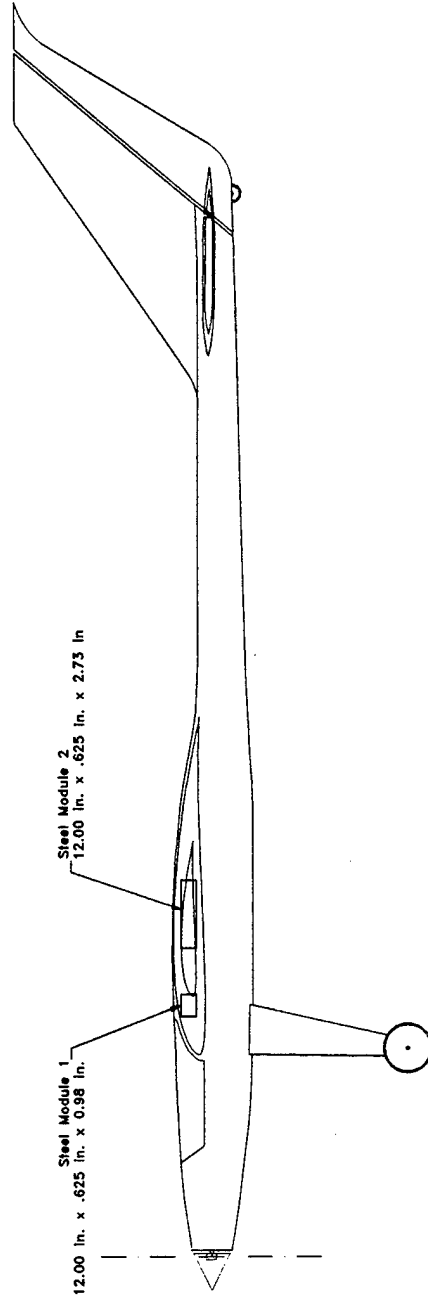
Texas Tall Boy Control  
System Side View



Steel Module 1  
12.00 in. x .625 in. x .98 in.

Steel Payload Module 2  
12.00 in. x .625 in. x 2.73 in.

Texas Tall Boy  
Payload Module  
Location Top View

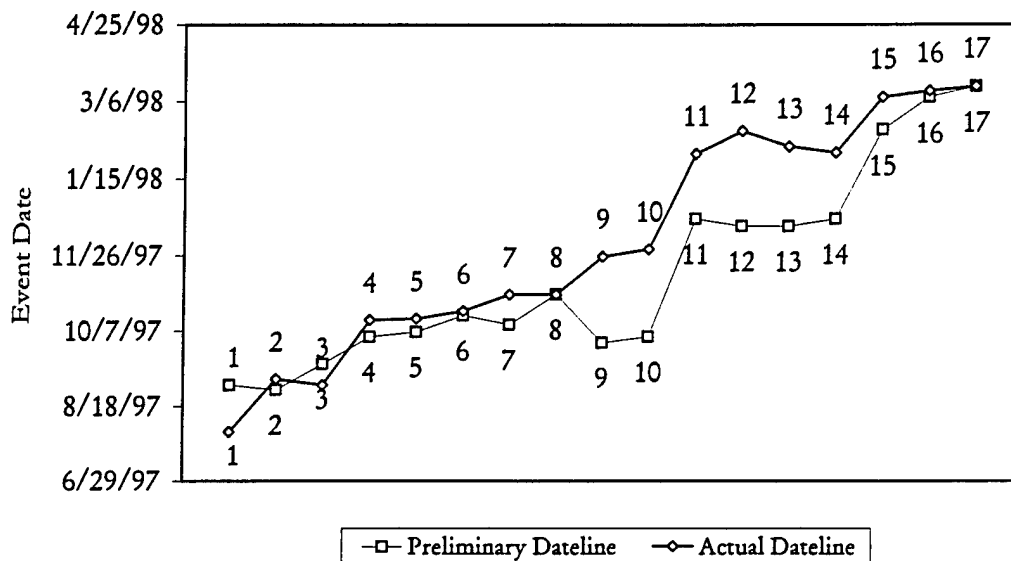


Texas Tall Boy Payload  
Module Location Side View

## Appendix J

### *Scheduled and Actual Timing of Major Events*

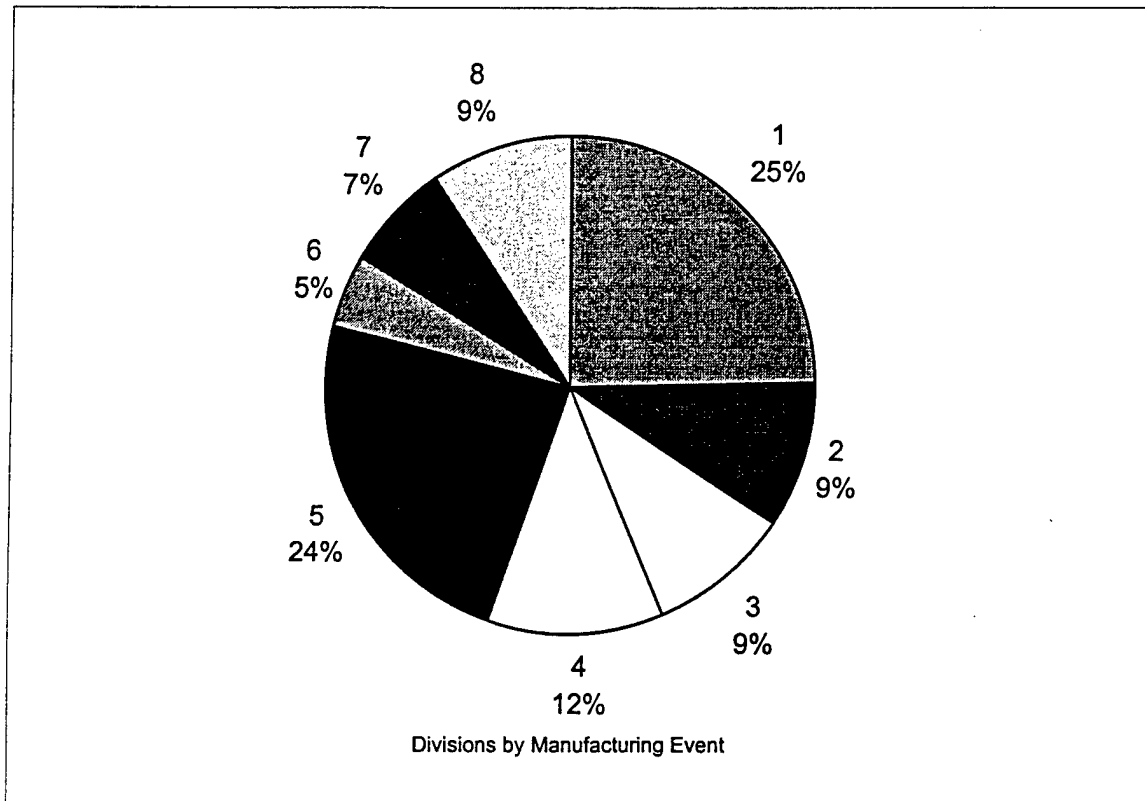
# Design and Development Milestone Completion Chart for the Texas Tall Boy



Event and Number	Scheduled Dates	Actual Dates
1 Conceptual Design Stage	9/1/97	8/1/97
2 Determine faculty advisor (Dr. Valasek)	8/29/97	9/5/97
3 Preliminary Design Stage	9/15/97	9/1/97
4 Submit list of materials for first model to faculty advisor	10/3/97	10/14/97
5 Order materials for first model	10/6/97	10/15/97
6 Send Notice of Intent to Compete, 1997-98 Contest Year	10/17/97	10/20/97
7 Wing Spar Testing	10/11/97	10/31/97
8 DUE DATE - Notice of Intent to Compete	10/31/97	10/31/97
9 Detailed Design Stage	9/29/97	11/25/97
10 General drawings of first model ready	10/3/97	11/30/97
11 Aircraft Construction	12/20/97	1/31/98
12 Research of Power Systems	12/15/97	2/15/98
13 Power System Testing	12/15/97	2/5/98
14 First flight of first model	12/20/97	2/1/98
15 Proposal Phase of written report preparation	2/16/98	3/9/98
16 Send in 5 copies of Proposal Phase of written report	3/9/98	3/13/98
17 DUE DATE - Proposal Phase of written report	3/16/98	3/16/98
18 First flight of second model	3/14/98	—
19 Determine changes for second model	1/12/98	—
20 Submit list of materials for second model to faculty advisor	1/16/98	—
21 Order materials for second model	1/19/98	—
22 Have general drawings of second model ready	1/26/98	—
23 Start construction of second model	1/26/98	—



**Manufacturing Milestone Completion  
Chart for the Texas Tall Boy**



<u>Event and Number</u>	<u>Starting Date</u>	<u>Completion Date</u>	<u>Estimated Time Yields (hours)</u>
1 Wing Panels	11/20/97	12/28/97	105
2 Landing Gear Construction	12/18/97	12/23/97	40
3 Empennage Surfaces Without Control Surfaces	12/23/97	12/28/97	40
4 Control Surfaces	12/29/97	1/11/98	50
5 Fuselage	1/5/98	1/11/98	100
6 Final Assembly - Component Joining	1/12/98	1/18/98	20
7 Entire Airframe Covering	1/19/98	1/25/98	30
8 Installation of propulsion, control and radio systems	1/26/98	1/30/98	40
Complete Aircraft Construction	11/20/97	1/30/98	<u>Total = 425</u>

## Appendix K

### *Component Weight Breakdown*

## *Systems Architecture*

### **Propulsion System**

Aveox 1412/2Y motor:	10.6 oz
Aveox M60 speed control:	1.5 oz
Propulsion battery pack:	39.5 oz

### **Control System**

Futaba R148DP receiver:	1.1 oz
Receiver battery pack:	2.0 oz
Futaba S5101 servo (elevator):	1.5 oz
Futaba S5101 servo (rudder):	1.5 oz
Futaba S9602 servo (aileron):	1.1 oz
Futaba S9602 servo (aileron):	1.1 oz

### **Airframe**

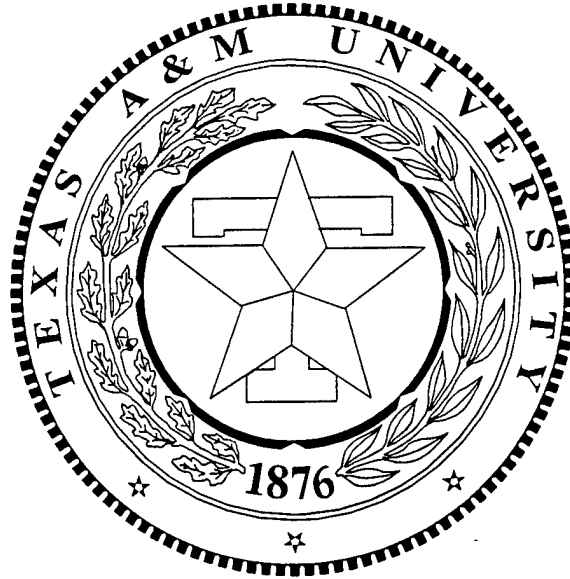
Fuselage with tail surfaces:	8.4 oz
Fuselage hatches and access panels:	2.2 oz
Wing joiner:	1.2 oz
Right wing panel:	8.3 oz
Left wing panel:	8.3 oz
Right aileron:	1.2 oz
Left aileron:	1.2 oz
Elevator:	0.8 oz
Rudder:	0.4 oz
Landing gear:	3.4 oz
Main wheels:	1.2 oz
Tail wheel:	0.2 oz

### **Total\* (without payload)**

7 pounds, 0 ounces

\*The total weight of the aircraft includes the covering material and miscellaneous hardware.

AIAA Student Design/Build/Fly  
Competition  
The Texas Tall Boy



Addendum Phase

Designed and developed by:

Robert "Rip" Rippey III

M. Shea Parks

Kendrah S. Smith

David Sellmeyer

Texas A&M University, College Station, Texas

April 13, 1998

# Table of Contents

	Page
Table of Contents	<u>i</u>
7. Lessons Learned	<u>21</u>
7.1. Final Contest Aircraft vs. Proposal Design	21
7.2. Areas of Improvement	21
7.2.1. <i>Changes in the Aircraft Structure</i>	21
7.2.2. <i>Changes in the Landing Gear Design</i>	21
7.2.3. <i>Changes in the Manufacturing Process</i>	22
7.3. Manufacturing and Component Price Lists	22
Appendix L	
Manufacturing and Component Price Lists	

## 7. Lessons Learned

### *7.1. Final Contest Aircraft vs. Proposal Design*

Experience from the 1996-1997 AIAA Design/Build/Fly Competition allowed the team to produce an aircraft that was identical to the Proposal design aircraft. Since the Texas Tall Boy was a derivative of the Aggie Flyer, the aircraft construction proceeded smoothly according to what the team had planned.

### *7.2. Areas of Improvement*

There were some areas of the Texas Tall Boy design and competition aircraft that could be improved in order to develop a next generation aircraft. After a period of flight testing, two primary types of possible alterations were discovered. They were changes in the structural design and sizing as well as improvements in the manufacturing process.

#### **7.2.1. Changes in the Aircraft Structure**

There were only a few changes that could be made for the TTB in terms of all around sizing and structural design. There was not any need for changes concerning the wing configuration. It was still felt that the most efficient configuration for the AIAA DBF competition was a conventional fixed wing aircraft. However, flight testing showed that directional control decreased substantially with low airspeeds. With the Texas Tall Boy fully loaded, the stall speed was high enough that this was not a problem. At low airspeeds, the unloaded aircraft would occasionally lose directional control and enter a short-lived spin.

The Texas Tall Boy flew well at its design weight, but the sizing of the vertical tail could be altered in order to improve the stability and handling qualities of the aircraft while flying without the payload. Through a great deal of flight time and pilot familiarization, it was decided that a larger vertical tail would be more desirable when flying without the full payload.

Such simple modifications of the airframe would require no additional time to incorporate into a next-generation design of the TTB. The actual size of the vertical tail has not been fully determined, but the amount of time that it would take for the development of the size change would be minimal. The majority of time would be in the research and investigation of the sizing, as opposed to the additional amount of manufacturing time required. The new design process would not be any more time intensive than the process allotted previously for the construction of TTB. Monetary costs of the development would also be minimal. This is due to the idea that the same materials and methods of construction would be used for any changes.

### 7.2.2. Changes in the Landing Gear Design

A derivative of the Texas Tall Boy would also have an improved landing gear. The ten degrees of camber built into the main gear proved to be too much since it put excessive loads on the wheels during landing. It was estimated that with less than five degrees camber, the wheels would be subjected to loads closer to the plane of the wheel. This amount of camber would also be enough to prevent ground loops on landing.

### 7.2.3. Changes in the Manufacturing Process

Changes in the manufacturing process are also minimal. Since the primary constructor of the TTB was highly skilled and had knowledge of the most efficient building methods, little was examined for improvement. The only improvement in the manufacturing process would involve the installation of the carbon joiner tube in the wing. The initial wing construction used a method of placing the joiner tube directly behind the shear webbing connecting the top and bottom spars. It was learned that a simpler structure could be used to accommodate the joiner tube. This alteration would be to add the spar joiner tube between the top and bottom spars before the shear webbing is applied. There would be no additional cost involved in implementing this modification, while the time used for incorporating the joiner would actually be reduced.

## 7.3. *Manufacturing and Component Price Lists*

Lists of components and their prices are given in Appendix L. The items are separated according to the airframe, propulsion system, control system, and ground support. Of these, the propulsion system was the most costly area of the Texas Tall Boy. This was due to the fact that the TTB incorporated technology that is relatively new and expensive. The design utilized both a brushless motor and a microprocessor speed controller.

Since this was the second time that Texas A&M University entered the AIAA Design/Build/Fly competition, the Texas Tall Boy was able to incorporate many of the components used in the previous years Aggie Flyer. For example, some of the components used in the 1996-1997 competition for the propulsion system, control system, and ground support were also used for the 1997-1998 competition. These items are marked in the appropriate tables of Appendix L.

The total cost for the Texas Tall Boy came to \$ 2030.57. However, excluding the reused components, the additional cost in order to produce the TTB was only \$ 913.07.

## Appendix L

### *Manufacturing and Component Price Lists*



---

## Airframe

---

Component	Cost (each)
Wood for airframe	\$ 35.00
Wing spar joiner	\$ 20.00
Kennedy Composites	
Wing spar joiner tubes (2)	\$ 20.00
Kennedy Composites	
Wheels	\$ 6.95
Performance Specialties speed wheels	
Covering material (4 rolls, 6 feet each)	\$ 11.99
TopFlite Monokote	
Adhesives	\$ 20.00
Miscellaneous hardware	\$ 20.00
(hinges, control horns, clevises, screws, etc.)	
Subtotal	\$ 189.91

---

---

## Propulsion System

---

Component	Cost (each)
<b>Motor*</b>	\$ 184.76
Aveox 1412/2Y Brushless Motor	
<b>Speed control</b>	\$ 219.96
Aveox M60	
<b>Gearbox*</b>	\$ 116.95
Robbe 3.7:1 Planeta gearbox	
<b>Battery pack</b>	\$ 181.05
New Creations NC19N2000	
<b>Propeller/Spinner</b>	\$ 61.51
Graupner 15 x 9.5 carbon folder	
<b>Propeller yoke</b>	\$ 9.72
<b>Subtotal</b>	<b>\$ 773.95</b>

---

\*reused from the 1996-1997 AIAA DBF competition

---

## Control System

---

Component	Cost (each)
<b>Radio*</b>	\$ 439.99
Futaba 8UAP 8 channel PCM	
<b>Aileron servos (2)</b>	\$ 89.99
Futaba S9203 coreless, ball-bearing	
<b>Elevator and rudder Servos (2)*</b>	\$ 54.99
Futaba S5101 ball-bearing	
<b>Receiver battery pack</b>	\$ 16.99
Futaba 250 mAh	
<b>Subtotal</b>	<b>\$ 746.94</b>

---

\*reused from the 1996-1997 AIAA DBF competition

---

## Ground Support

---

Component	Cost (each)
Propulsion battery charger*	\$ 164.95
Astro 112D Digital Charger 1-36 cell	
Source for propulsion battery charger*	\$ 42.93
Heavy Duty Marine Battery	
Source battery charger*	\$ 57.94
Digital ammeter	\$ 53.95
Subtotal	\$ 319.77

---

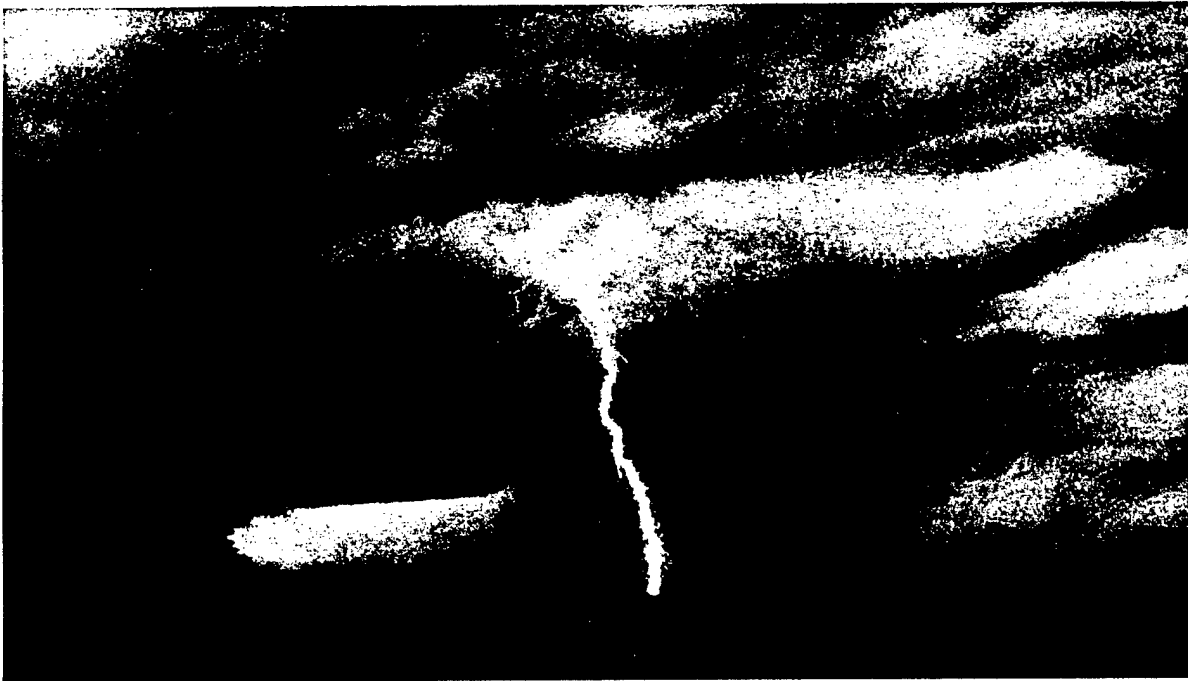
\*reused from the 1996-1997 AIAA DBF competition

Total Cost	
Category	Subtotals
Airframe	\$ 189.91
Propulsion System	\$ 773.95
Control System	\$ 746.94
Ground Support	\$ 319.77
Total	\$ 2030.57

# Cessna/ONR Student Design/Build/Fly Competition

## Longhorn Lightning Aircraft Design Proposal

16 March 1998



*Submitted to:*

AIAA Design/Build/Fly Contest

Gregory S. Page / Bldg. 210  
Kaman Sciences Corporation  
2560 Huntington Avenue  
Alexandria, VA 22303

*Submitted by:*

*Longhorn Lightning  
Design Team*

Roman Aguilera III  
Kristi Crutchfield  
Robin Kinsey  
David Magerstadt  
Greg Maroney

The University of Texas at Austin  
Austin, Texas

# Table of Contents

1. Executive Summary.....	1
2. Management Summary.....	3
3. Conceptual Design.....	4
4. Preliminary Design.....	7
Wing.....	9
Fuselage.....	10
Propulsion.....	11
5. Detail Design.....	12
6. Manufacturing Plan.....	16
7. References.....	18
8. Drawing Package.....	19
3-View Drawing.....	19
System Component Layout.....	20
Milestone Chart.....	21

## Executive Summary

The 1998 AIAA Student Design/Build/Fly Competition consists of teams of students from different universities designing, building, and flying an aircraft. The design teams then have a flyoff at a national competition held in Wichita, Kansas, at the end of April. The competition is to have their aircraft carry a 7.5lb payload and takeoff in three hundred feet while clearing a six foot obstacle. Then the aircraft while still carrying the payload will fly as many laps as possible within seven minutes over a course designated by two pylons spaced seven hundred feet apart. The design team from The University of Texas at Austin will develop a competitive aircraft design and to aid in the process will set the following design stages: conceptual design, preliminary design, and detailed design.

In the conceptual design stage, a tailless aircraft design was chosen over a conventional tailed aircraft and canard aircraft. This decision was made to chose this design due to the low drag design created by the combination of low surface area, low weight, and low interference drag due to the absence of a tail. The winglets on the tailless aircraft reduce drag and provide directional stability. The tailless aircraft also incorporated functional efficiency (one component of the aircraft accomplishing more than one function). For instance, the wing was designed to provide lift and stability for the aircraft. The decision to mount the motor in a pusher configuration was made during the conceptual phase. The pusher design was chosen over a tractor design in that the pusher configuration adds to stability due to the propeller will act as a vertical tail.



Additionally a pusher design reduces the propeller wake interaction with the airframe which thereby reduces the skin friction drag.

The preliminary design consisted of sizing the aircraft to maximize performance. The aircraft needs to be designed to carry the payload while minimizing drag. Due to the tailless design, the batteries and payload were mounted in the "loading box" within the fuselage. The motor and receiver were mounted behind the loading box. While researching propellers, a variable pitch propeller was chosen over conventional propellers because it gave better overall performance characteristics and the mounting procedure was the same. Fixed landing gear was chosen over retractable landing gear because of its ease of installation, lightweight, and simplicity. The main landing gear is mounted to the wings in a tricycle configuration.

During the detailed design phase, the construction materials were chosen for the aircraft. The wing is comprised of 1lb density polystyrene foam and it is covered with a thin balsa sheeting for added strength. The equations of motion for flight in a vertical plane were used to calculate endurance, range, and takeoff distance. Performance characteristics (i.e. stall and max speeds, lift and drag coefficients, and thrust available) were calculated using LinAir [1] and Electro Flight Design 1.01 (EFD) [2]. These software packages were used in the preliminary and detail design phase.

Electro Flight Design 1.01 (EFD) is a software package that calculates run time, speed, drag, battery efficiency, and propeller efficiency. Using EFD the pitch and diameter of the propeller was determined that gave the highest speed and run time. Combining the results from EFD and LinAir gave the first glimpses of the performance and shape of the aircraft for the preliminary design.

## Management Summary

The University of Texas at Austin Longhorn Lightning design team is comprised of the following five members: Roman Aguilera III, Kristi Crutchfield, Robin Kinsey, David Magerstadt, and Greg Moroney. As team leader, Roman is responsible for ensuring that all deadlines are met and for maintaining a communication link between the team members and the sponsors and advisors. After establishing a conceptual aircraft design, the required tasks were distributed among the team members. Greg and Kristi were responsible for the propulsion systems of the aircraft. The structural design aspects of the plane were divided among David, Roman, and Robin. David developed the wing, Roman designed the fuselage, and Robin configured the landing gear. Weekly team meetings were held at 3 P.M. on Mondays to discuss updates on changes or developments concerning the project. Additional meetings were held when necessary.

The team is sponsored by Rhinehart and Associates and is advised by Dr. Phillip Varghese. Chris Boultinghouse, who is a member of the Academy of Model Aeronautics (AMA), will pilot the Longhorn Lightning airplane.

To insure timely completion of the project, all milestones and/or tasks have been compiled into a schedule of work, shown in the drawing package. This schedule illustrates both completed tasks and tasks yet to be completed. The team leader is able to use this work schedule to remind team members of upcoming deadlines.

# Conceptual Design

During the conceptual design phase the design parameter considered was the aircraft configuration. Under this design parameter there were three alternative concepts:

- Conventional
- Canard
- Tailless

These alternatives represent the three major aircraft configurations. The mission profile for the 1998 contest states that each aircraft shall:

- Carry a 7.5lb steel payload
- Takeoff and clear a 6ft obstacle in 300ft
- Perform 2 opposite direction  $360^0$  turns
- Fly a maximum number of laps around the designated course in 7 minutes
- Land within the marked 300ft landing area

The figures of merit (FOM) which were selected to support this mission profile in order of importance are:

- Low drag at low Reynolds number-

This will maximize the airspeed for a given thrust

- Low weight-

This will maximize acceleration on takeoff and reduces drag.

- Functional efficiency-

The aircraft components will perform more than one task improving efficiency, simplicity, and systems reliability

These FOMs were used to evaluate the alternative aircraft configurations and arrive at a final configuration. The three aircraft configurations were ranked from one to three in each of the FOMs, with one being the best. The final ranking was calculated by adding the individual FOM rankings. The aircraft configuration chosen was the one with the lowest final ranking number.

Table 1. Aircraft configuration's ranking by FOMs

	Tailless	Conventional	Canard
Low drag at low Reynolds number	1	2	3
Low weight	1	3	2
Functional efficiency	1	2	3
Final Ranking	3	7	8

The tailless design has the lowest drag at the low Reynolds numbers encountered in model flight because it has the least surface area devoted to non-lift-producing tasks, such as supporting the tail or the canard surfaces. This feature of tailless aircraft also contributes to its high ranking in the other two figures of merit as well. Because the tailless design wastes little structure on non-lifting components, it has the lowest weight of all the concepts considered. Additionally, because the tailless design uses most of its components for more than one task, it has the highest functional efficiency of the three designs considered. For instance, the wing supports the aircraft and provides the stability for flight. The wing also supports the fins at the tips, providing directional stability. The fuselage carries the payload and houses the propulsion system as well as supporting the landing gear.

# Preliminary Design

## Wing

After the tailless design was selected for the project, the next job was to size the wing, fuselage and vertical fins. The known weights of the components were summed and then the airframe weight was estimated in order to develop a preliminary takeoff weight for sizing calculations. The weight estimates were as follows,

•	Payload	= 7.5 lb
•	Battery	= 2.5 lb
•	Electronics	= 0.5 lb
•	Motor/Propeller	= 1.0 lb
•	Airframe (25% of GTW)	= 4.0 lb
<hr/> <b>Total Weight</b>		<b>= 15 lb</b>

Once the preliminary takeoff weight was estimated, the wing sizing process could begin. The initial wing size was based on a rule of thumb wing loading of  $23\text{oz/ft}^2$ . Using this value gave a wing area of  $10.4\text{ft}^2$ . The wing span was initially set at 8ft, giving an aspect ratio of 6.75. To provide directional stability, fins were used at the tip of each wing. In addition to providing directional stability, the fins act to reduce vortex drag at the wing tips. The fin area =  $0.5\text{ft}^2$  and the fin span = 1.0ft with the dihedral angle =  $90^\circ$ . The fin size was determined using the tail volume coefficient of another tailless glider model. The sweep was initially set at  $20^\circ$ , the taper at 0.8, and the twist was

established using the equation for wing twist in **Tailless Aircraft in Theory and Practice** [4].

Once the preliminary dimensions of the wing were established, the initial configuration was tested using the PC-based software LinAir. LinAir was used to calculate the performance parameters  $C_L$ ,  $C_D$ ,  $C_M$ , and the efficiency factor  $e$  for the configuration over a range of angles of attack. The performance parameters were then inserted into a spreadsheet program developed to calculate the total drag and the L/D ratio for the entire aircraft. Wings with fins only were tested in LinAir and the effects of the fuselage and landing gear were accounted for using the equivalent parasite area method as described in Introduction to Airplane Flight Mechanics by Dr. David G. Hull [3].

To determine the wing size for the final configuration, many preliminary configurations were tested. Wing spans of 6, 8, and 10ft were tested using wing areas of 6, 8, and 10ft<sup>2</sup> for a total of 9 configurations in the first round of testing. The wing sweep and fin size was held constant during the preliminary round of testing. The results at  $V = 45$  mph showed that the performance improved as the wing loading and aspect ratio were increased. Once the trend of higher wing loading and aspect ratio for lower drag was established, the aspect ratio was limited to 8 and the wing loading was fixed at 30oz/ft<sup>2</sup>. The aspect ratio limit was imposed for structural reasons and the wing loading limit was determined by the takeoff requirements. In the final round of testing the sweep and taper ratio were varied while the aspect ratio and wing loading were held fixed. No improvement was found by changing either the sweep or taper so they were fixed at the original values. After the main parameters of span, area, taper, and sweep for the wing

were established, the fin size and the twist were recalculated for the final configuration.

The accuracy of the method is estimated at 5%.

The final configuration for the wing with fins is as follows,

#### **The Wing:**

Span	= 93in
Area	= 1080in <sup>2</sup>
Taper	= 0.8
Sweep of the quarter chord line	= 20°
Washout	= 6° linear
Dihedral	= 0°

#### **The Fin:**

Span	= 10in
Area	= 66.7in <sup>2</sup>
Taper	= 0.5
Sweep of the quarter chord line	= 25°
Washout	= 0°
Dihedral	= 90°



## Fuselage

The fuselage was designed utilizing the original FOMs. The design parameters chosen to be optimized to support the FOMs are the following, listed in order of importance:

- Center of gravity location-

The fuselage was designed to minimize CG movement when the 7.5lb payload was added or removed. This is very important for stability in tailless aircraft designs.

- Total surface area and cross sectional area-

This was minimized to reduce parasite drag and fuselage weight. Additionally, the designed would be streamlined further enhancing the designs ability to reduce drag.

To begin the optimization process, all components contained in the fuselage were given estimated weights and dimensions which were obtained through research. Different configurations of these components were investigated and center of gravity locations were calculated for these configurations. Once this was completed, using the equivalent parasite area method, the coefficient of drag for each fuselage design being investigated was calculated. The accuracy of this process is expected to be within ten percent. The final configuration design is a 30in cylindrical tube design which houses a "loading box". This loading box will contain the 2.5 lb battery pack and the 7.5lb payload. These two components will be velcroed in this loading box. This will allow the battery pack to be

moved to an optimum location when the payload is removed. By having this feature, the CG location can actually be kept at the same location with and without the payload.

### Propulsion

The figure of merit selected for this system was to maximize the thrust for eight minutes. Eight minutes was used to account for the time consumed during takeoff, the two initial 360° turns, the seven minute timed lap portion, and for landing. The design parameters for this system were chosen to be and were deemed to be equally important, are as follows:

- Propeller
- Gearing
- Motor
- Battery pack

These design parameters are the major components of the propulsion system thereby making them important design parameters. Different combinations of battery size, motors, gearing, and propellers were investigated. Over 500 combinations were investigated. To aid in the optimization process, Electric Model Aircraft Performance was used. This program allows the specific input of all the design parameters and outputs the performance. The accuracy is estimated to be within 5%. The final configuration for the propulsion system is a Maxcim NEO-13Y, Maxcim 35A-21 controller, a 1:3.7 gear ratio, Sanyo 2000 nicad cells, and a 12in propeller. In researching the components, an

automatic variable pitch propeller was discovered and due to the enhanced performance it brought was incorporated into the aircraft design.

## Detail Design

Using kinematics and dynamics, the equations of motion for flight in a vertical plane were derived and utilized in analyzing the aircraft's performance in the following areas: takeoff, range, and endurance. The following equations were specifically used:

$$\frac{dX}{dt} = V \cos \gamma$$

$$\frac{dh}{dt} = V \sin \gamma$$

$$\frac{dV}{dt} = \left(\frac{g}{W}\right)[T \cos(\alpha + \epsilon_0) - D - W \sin \gamma]$$

Where  $V$  is the velocity of the aircraft

$X$  is the position of the aircraft's center of gravity

$\gamma$  is the aircraft's flight path angle

$h$  is the aircraft's altitude

$W$  is the aircraft weight

$T$  is the aircraft thrust

$\alpha$  is the aircraft's angle of attack

$\epsilon_0$  is the thrust vector when  $\alpha$  is zero

$D$  is the aircraft's drag

Additionally, kinematics and dynamics were used to derive the equations of motion for turning flight. These equations were used to analyze the aircrafts handling qualities such as turning capabilities. The equations of motion used are:

$$\frac{d\chi}{dt} = \frac{gL \sin \mu}{WV}$$

$$W = L \cos \mu$$

Where  $\chi$  is the aircraft's heading angle

$L$  is the aircraft's lift

$\mu$  is the aircraft's bank angle

Using these equations along with LinAir and Electro Flight Design, the aircraft's predicted performance has been tabulated in Table 2.

Table 2. Results of Performace Calculations

Aircraft performance analyzed	Expected performance
Takeoff run	180 ft
Lap speed	3960 ft/min
Laps completed in seven minutes	17
Turn radius at lap speed	108 ft
G load capability	3.75
Range	6 miles

Endurance	13 minutes
Landing distance	90 ft
Payload fraction	50%

All the major internal aircraft components that will be used are detailed in Table 3. The propulsion components were selected from the iterative process in finding the best combination of propeller, gear ratio, motor, and battery pack to produce the maximum thrust for eight minutes.

The radio control system was selected by finding a high performance system that offered expandability and the option to program set flight configurations. The aircraft will be designed with the elevon as the only control surfaces. This sets the number of servos used to four: one for the motor, one for the nose wheel, and one for the left and right elevon. The two elevons will control the aircraft about its lateral, longitudinal, and vertical axes.

The landing gear will be a tricycle gear with the main landing gear wheels mounted on the wings. Initially a retractable landing gear system was thought to be preferred. However, upon researching, the weight of a retractable gear was much greater than the fixed landing gear and retractable landing gears offered much additional complexities than a fixed landing gear.

The drawing package contains a 3-view drawing of the aircraft and details all the important dimensions. Additionally, there is a component layout of all aircraft systems.

Table 3. Component Selection

Component	Manufacturer	Weight	Dimensions
Propeller	Kress Jets	2.4 oz	12" diameter
Motor	MaxCim 35A-25NB	7.5 oz	1.37" diameter 3" length
Controller	Sanyo 2000	3.0 oz	2.31" length 1.5" width 0.8" thick
Battery	Airtronics Stylus PCM	40 oz	10" length 2" width 2" height
Receiver	Airtronics Stylus PCM	2.0 oz	3" length 2" width 0.5" width
Servos	Airtronics 94732 Contest Servos	1.8 oz each	2.1" length 0.8" width 1.7" height
Payload	Steel (0.283 lbs./in <sup>2</sup> )	120 oz	12" length 1.5" width 1.5" height

## Manufacturing Plan

The wings were cut from blocks of expanded polystyrene foam using a hot-wire bow guided by templates pinned to the ends of the blocks. Grooves were cut on the top and bottom of the wing cores to accept wooden spar caps and a polycarbonate sheet was wrapped around and bonded to the leading edge extending to the 30% chord line on top and bottom. After the wing halves are joined, the spar caps are installed, and the sheeting is attached, the wing was covered with a self-adhesive polymer film to provide strength and toughness. The flight control surfaces were cut from the completed wing sections and the servos and control rods were installed. The wing tip fins were manufactured in the same manner as the wings and then installed on the tips of the wings.

The fuselage pod consists of a wooden deck attached to the top of the wing that supports the payload, batteries, motor and radio equipment. The nose landing gear is also mounted on the fuselage pod deck. The fuselage pod deck is enclosed within a lightweight foam fairing to provide streamlining.

The other manufacturing processes considered include composite wing skins and balsa sheeting over foam. These were rejected because they either require vacuum bagging to bond them to the foam or they increase the cost or both. The resulting structure would require more time and care to build than was available and would be more difficult to repair as well.

The materials selected for building the batteries are: Sanyo 2000 battery cells, gold plated battery connectors, 14 gauge wire, 2 in 1 epoxy, solder at a 60-40 lead to tin

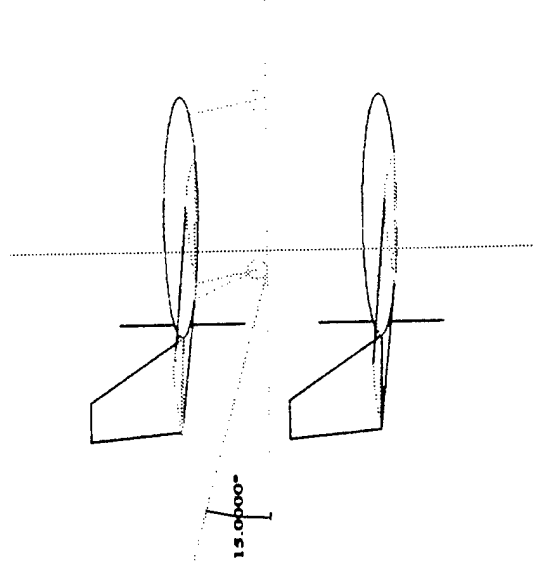
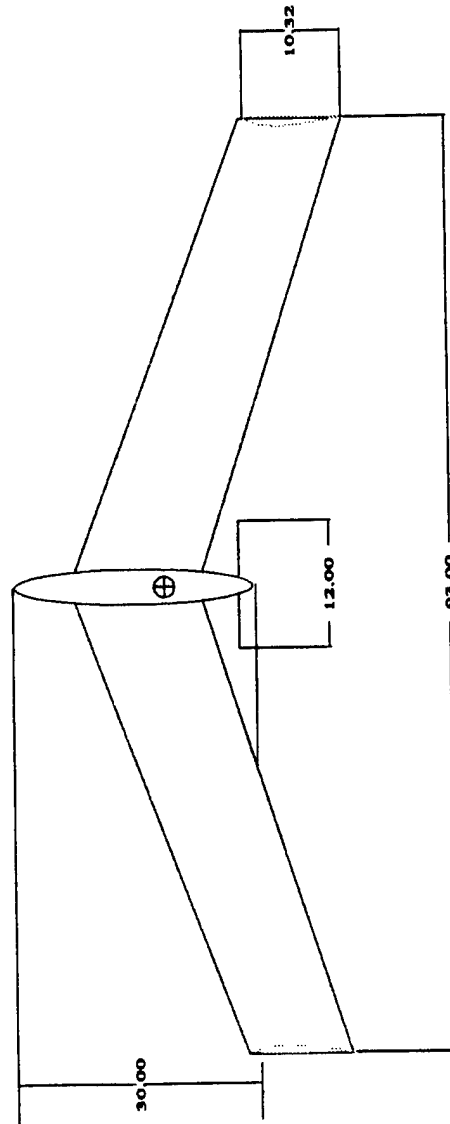
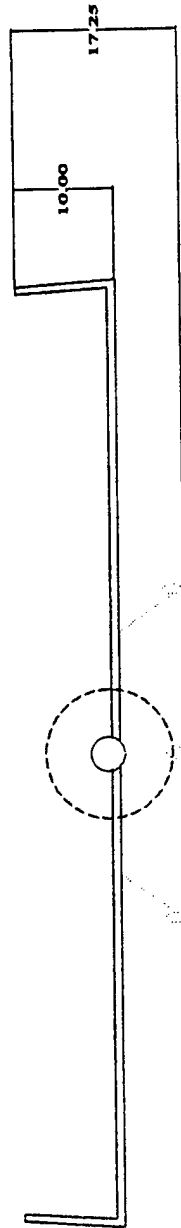
ratio, clear shrink wrap, and Litespeed battery clamps. The batteries were built by soldering the connectors to the cells in such a configuration that layered one row of cells on top of another, and wiring the lead from the batteries to the battery clamps. The alternative manufacturing process that was considered was to have the batteries built by an outside source. This option was not pursued due to the lack of control on the dimensions of the assembled battery pack. The FOMs that were considered in building the batteries were cell availability and cost, ease of manufacture, and storage capacity per cell. The cost limited the cells from low to medium cost due to the number of cells required. The number of cells needed also affected the availability of the cells in such a way that they could be acquired quickly and in large amounts. The storage capacity per cell is very important because this FOM determines how long the aircraft will run and what speed the aircraft will run. The cells had to be relatively simple to manufacture since a team member would be building and shaping the battery pack.



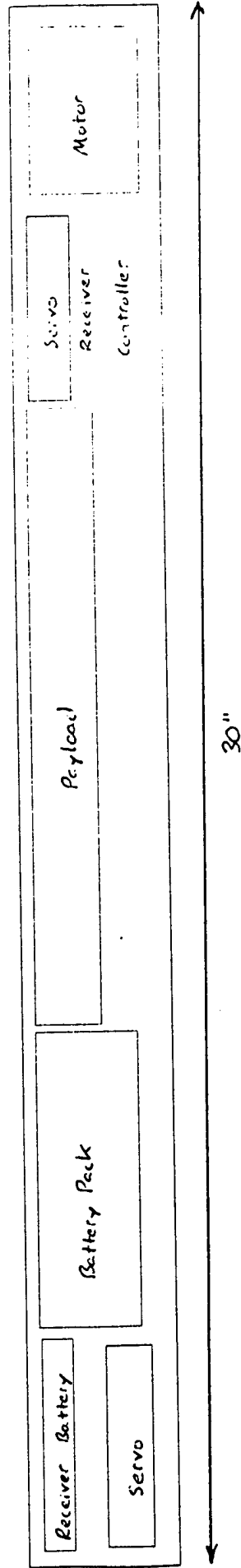
## References

1. LinAir. Desktop Aeronautics. Stanford, CA, 1987-1992.
2. Electro Flight Design. John S. Kress and Robert S. Kress, 1993.
3. Hull, David G. *Introduction to Flight Dynamics*, Ginny's Printing, Austin, Tx, 1998.
4. Nickel, Karl. And Wolfahart, Michael. *Tailless Aircraft and Theory In Practice*,  
AIAA Educational Series, 1992.

3 View Drawing Units : Inches
Cr : 12.90 in.
Ct : 10.32 in.



# Component Layout



Task Name	Planned Start	Duration in	Planned Finish	1997						
				Nov	Dec	1998 Jan	Feb	Mar	Apr	May
1st General Meeting	<u>11/7/97</u>	0	<u>11/7/97</u>	■						
Conceptual Design	<u>11/7/97</u>	11	<u>11/24/97</u>	←■						
Team Organization	<u>11/24/97</u>	0	<u>11/24/97</u>	■						
Preliminary Design	<u>11/24/97</u>	20	<u>12/22/97</u>	←■						
Detailed Design	<u>1/5/98</u>	25	<u>2/9/98</u>			←■				
Gathering of Materials	<u>2/7/98</u>	19	<u>3/6/98</u>				←■			
Airplane Construction	<u>2/27/98</u>	10	<u>3/13/98</u>					→■		
Report Preparation	<u>2/27/98</u>	10	<u>3/13/98</u>					→■		

**CESSNA DESIGN/BUILD/FLY STUDENT COMPETITION**

**Design Report-ADDENDUM PHASE**

**The University of Texas at Austin**

**Entry name: Longhorn Lightning**

**April 7,1998**

## Design Report-ADDENDUM PHASE

Since the Proposal Phase of the CESSNA Student Design/Build/Fly Competition was sent in for The University of Texas at Austin, changes have been made in the proposed aircraft design. Either by testing or through calculations, these changes were made to optimize the performance of our aircraft. Although most changes were minor, they play an intricate part in the final design.

The proposed parameters for the fin were as follows:

Span	=10in.
Area	=66.7in <sup>2</sup>
Taper	=0.5
Sweep of the quarter chord line	=25°
Washout	=0°
Dihedral	=90°

Now, after further calculations and testing, only two of the parameters have been altered for the final design and they are as follows:

Span	=9in.
Area	=54in <sup>2</sup>

These modifications were implemented to improve the performance characteristics of the aircraft.

The change we have made to the fuselage is our greatest change. The preliminary design was proposed to be a 30 inch long cylindrical tube design. Taking into account the moment of inertia, a change was implemented to the fuselage, changing it to a three dimensional, horizontally aligned "airfoil pod shape" that is 24 inches long. This houses the "loading box." By changing the fuselage design, the components could be arranged in a more compact configuration. The payload was cut in half and placed side by side (6" long, 3" wide, 1.5" high), and the batteries were stacked in two rows and in three columns

(6" long, 3" wide, 1.75" high). In the preliminary design, the payload was 12 inches long, 1.5 inches wide, and 1.5 inches high. These altered dimensions were found to utilize our fuselage space better. The materials used for the fuselage are wood, EPS foam, and fiberglass with epoxy. We wanted to ensure structural strength with the addition of the fiberglass and epoxy to the preliminary design.

The wing spars are reinforced by connecting them in the middle with segments of fir wood. The spars are swept back at 20° with the wings. The wings are covered with a structural skin from the front spar to the trailing edge that consists of fiberglass and epoxy to ensure stability of the wings with the addition of the spars.

The last additional change that was made concerns the location of the landing gear. The main landing gear is no longer mounted to the wings and is now mounted to the fuselage. That makes all three parts of the tricycle gear now mounted to the fuselage. This change was made because of the simpler installation, and it also provides greater clearance needed to prevent the rear propeller from hitting the ground.

In our assessment of all the costs, the actual costs did not exceed expected costs. We, as a group, hypothesized that the total costs would not exceed \$2000.00 after the first part of the components were ordered. As will be shown in the table of "Manufacturers List Price", the total cost for this project is \$1837.89.

There are three areas that have been identified for the second generation design: landing gear type, material selection, and fuselage aerodynamics.

A retractable landing gear that is light would enhance the performance of the aircraft. Current landing gears on the market weigh much more than fixed landing gear.

More time invested into researching simple and light retractable landing gear to select a better retractable landing gear would give this aircraft better performance. The estimated cost is expected to be \$150 with a six hour time to implement.

Lighter and stronger composite materials will be used in the second generation aircraft design. The current materials used were selected based on cost, availability, and ease in manufacturing. With the experience gained in the design and fabrication of this first generation aircraft, steps can now be taken to add the latest technology in materials. Estimated cost is \$400 with a twelve hour time to implement.

Lastly, more time will be devoted to research and the design of the fuselage shape and integration with the wing. The fuselage will be designed for a specific speed and optimized to reduce drag. There is no additional cost and time associated with the implementation of this enhancement.



## Manufacturers List Price

<u>Component</u>	<u>Manufacturer</u>	<u>Price</u>
<b><u>PROPULSION</u></b>		
Propeller	Kress Jets	\$49.95
( w/ automatic controller)	Kress Jets	\$69.95
<hr/>		
Motor	MaxCim 35A-25NB	\$422.00
( w/ Controller)		
<hr/>		
Battery Pack	Sanyo 2000	40 cells @ \$8.95 ea
<hr/>		
Battery Charger	Astroflight	\$149.99
<hr/>		
<b><u>FLIGHT CONTROL SYSTEMS</u></b>		
{	Battery	Airtronics Stylus PCM
	Receiver	Airtronics Stylus PCM
	Servos	Airtronics 94732 contest servos
<hr/>		
<b><u>MISCELLANEOUS</u></b>		
Payload	Steel (0.283 lbs./in <sup>2</sup> )	\$8.00
<hr/>		
Wood	Fir Pine Balsa	\$30.00
<hr/>		
Fiberglass		\$20.00
<hr/>		
Epoxy		\$15.00
<hr/>		
Foam		\$20.00
<hr/>		
<b>TOTAL</b>		<b>\$1837.89</b>

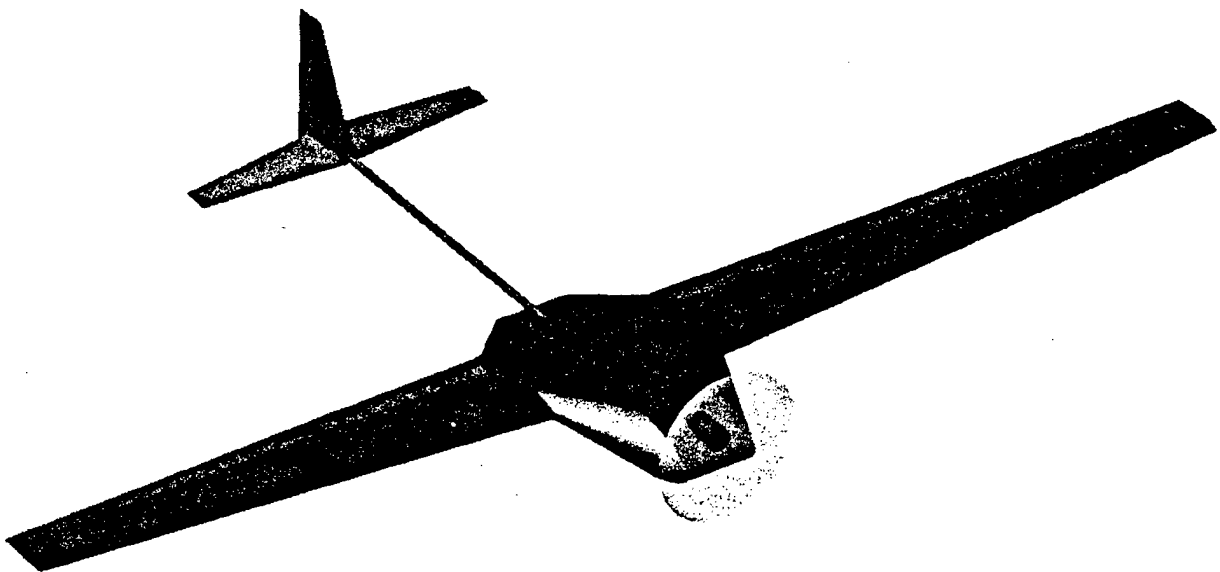
---

**1997/1998 AIAA Foundation/Cessna Aircraft/ONR  
Student Design/Build/& Fly Competition**

---

**Design Report**

---



**Utah State University**

**March 9, 1998**

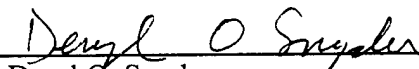
March 9, 1998

To Whom It May Concern:

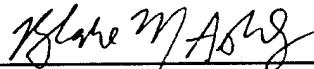
We feel it is necessary to mention that the Detail Design section of our report may appear too long because of the many figures and tables. However, we removed all the figures and tables and verified that this section does indeed meet the five page limitation. Also, we have included appendices to provide completeness to our report. Appendices A and B serve to further clarify some of the mathematical models used in our analysis. Appendices C, D, and E are computer drawings of our design that fit more naturally in appendices than in the body of the report.

Thank you for your part in making this competition a positive learning experience for all involved. We look forward to the competition on April 25.

Sincerely,



Deryl O. Snyder  
Team Leader  
Utah State University



Blake M. Ashby  
Lead Writer  
Utah State University

# Table of Contents

<b>Executive Summary</b>	<b>1</b>
<b>Management Summary</b>	<b>3</b>
<b>Conceptual Design</b>	<b>5</b>
<b>Alternative Concepts</b>	<b>5</b>
Tail vs. Canard Configuration	5
High vs. Low Wing	6
Conventional Tail vs. V-tail	6
One-Motor vs. Two-Motors	6
Brushless vs. Brush Motor	6
Payload in Fuselage vs. Payload in Wing	6
Center of Gravity In Front Of vs. Behind Wing Quarter-Chord	7
Cylindrical Fuselage vs. Airfoil-Shaped Fuselage	7
Composite vs. Spruce Wood Beams in Wing	7
Landing Gear—Tail-Dragger vs. Nose-Wheel	7
Airspeed Controller vs. No Airspeed Controller	8
Tapered vs. Rectangular Wing	8
<b>Figures of Merit Summary</b>	<b>8</b>
<b>Preliminary Design</b>	<b>10</b>
<b>Analytical Methods and Tools</b>	<b>10</b>
“Airplane” Program	10
“Params” Program	10
“Mpeff” Program	11
“Wind” Program	12
“Analyse an Airfoil” Program	12
<b>Design Parameter and Sizing Selection</b>	<b>12</b>
Flight Speed	12
Reducing Planform Area	14
<b>Summary of Key Features</b>	<b>16</b>
Wing	16
Fuselage	17
Tail Surfaces	17
Landing Gear	17
Power Plant	17
Airspeed Controller	17
<b>Detail Design</b>	<b>18</b>
<b>Final Performance Data</b>	<b>18</b>
Takeoff Performance	18
Handling Qualities	19
Range and Endurance	21
G-load Capability	22
Payload Fraction	23
Other Performance Plots	24
<b>Power Plant Component Selection</b>	<b>28</b>
<b>Airspeed Controller Interfacing</b>	<b>29</b>

Airborne Controls _____	29
Ground Station _____	31
<b>Drawing Package _____</b>	<b>31</b>
<b><i>Manufacturing Plan _____</i></b>	<b><i>32</i></b>
<b>Wing Construction _____</b>	<b>32</b>
Beam _____	32
Foam Core _____	32
Balsa/Monokote Sheeting _____	33
Control Surfaces _____	33
<b>Fuselage Construction _____</b>	<b>33</b>
Frame _____	33
Hatches _____	34
Motor Mount _____	34
Beam to Tail _____	34
Landing Gear _____	34
<b>Tail Construction _____</b>	<b>35</b>
<b>Cost of Designed Airplane _____</b>	<b>35</b>
<b>Manufacturing Milestone Chart _____</b>	<b>37</b>
<b>References _____</b>	<b>37</b>
<b><i>Appendix A—Equations Relating to Power Plant _____</i></b>	<b><i>38</i></b>
<b><i>Appendix B—Takeoff Analysis _____</i></b>	<b><i>40</i></b>
<b><i>Appendix C—Detailed Drawing Package of Final Design _____</i></b>	<b><i>42</i></b>
<b><i>Appendix D—Alternate Fuselage Construction Technique _____</i></b>	<b><i>49</i></b>
<b><i>Appendix E—Alternate Wing Construction Technique _____</i></b>	<b><i>52</i></b>
<b><i>Appendix F—Schematics for Velocity Controller _____</i></b>	<b><i>54</i></b>

## Executive Summary

A design team consisting of students at Utah State University have designed, analyzed, and are building an airplane that will compete in the 1997/98 Cessna/ONR Student Design/Build/Fly Competition sponsored by AIAA in Wichita, Kansas on April 25, 1998. This design consisted of developing an unmanned, electric-powered, radio-controlled airplane that will complete the most number of laps possible around a specified course in a seven-minute time limit. The airplane is powered by 2.5 pounds of NiCad batteries and must carry a 7.5 pound steel payload.

The general designs first investigated for the airplane were a tail configuration and a canard configuration. The tail configuration was selected over the canard because of concerns about stability and construction. High wing and low wing configurations were investigated as well. A high wing design was selected because less dihedral was required to provide roll stability. A wing with less dihedral is more efficient and also easier to construct. The location of the center of gravity of the airplane was analyzed. An airplane with the center of gravity in front of the quarter chord of the wing will be more stable. However, this arrangement has a lower lift-to-drag ratio because the tail needs to generate more negative lift to keep the plane balanced. It was decided to put the center of gravity behind the quarter chord of the wing to minimize the negative lift from the tail. Finally, T-tail and V-tail configurations were considered. The T-tail was selected because of concerns about complexities involved with the design and construction of a V-tail.

Different conceptual designs for the power plant of the airplane were considered. Some thought was given to using two motors instead of just one for the airplane. The single motor arrangement was selected because of design simplicity and construction costs. Also, brushless and brush motors were investigated. From a performance standpoint, the brushless motors are noticeably better, but the design team is more familiar with the brush motors. Also, the brushless motors and speed controls are substantially more expensive than the brush motors and speed controls. Therefore, a single brush motor system was selected because the slight improvement in performance could not justify the extra cost of the brushless motor system.

Several different designs for the structural components of the airplane have been investigated. The placement of the payload was analyzed. Some benefit came from placing the payload in the wings, particularly for large wingspans. As the size of the wings was decreased because of increased desired airspeeds, those benefits became less distinct, so the steel was placed in the fuselage. A cylindrical fuselage design was investigated as well as an airfoil-shaped fuselage. The airfoil-shaped fuselage was selected because it is lower in drag, lighter in weight, and less expensive to build. The composition of the structural beam for the wing support was also studied. Alternatives considered were box beams of spruce wood or carbon fiber composites. The spruce wood beam was slightly lighter, but allowed for excessive deflection when loaded. The composite beam was chosen because it provided the necessary strength and stiffness for the wing.

The evolution of the structural design of the airplane was closely tied to the evolution of the aerodynamic analysis of the airplane. Initially, the wing of the airplane had a large planform area and a high aspect ratio, which required a long, very strong beam to support the airplane. As the designed airspeed of the airplane increased and the planform area of the wing decreased, the necessary strength of the beam also decreased. However, the analysis showed that increasing the g load capability of the airplane would increase the number of laps possible. This caused the strength requirements of the beam to increase once again. Also, a tapered wing was chosen over a rectangular wing because of enhanced aerodynamic efficiency and increased strength at the wing root.

Numerous design tools and analytical methods were used at each step of the design process. Most of these methods involved the use of computer programs that were either already available or were developed by the team members. The first program used is the "Airplane" program, an aircraft design package developed at Utah State University. This program was used to iteratively modify the various parameters of the airplane at each step in the design process. "Airplane" was also used to ensure that the design had proper handling characteristics by making sure the aerodynamic moments about the center of gravity in all three directions stayed within acceptable boundaries.

The second program, "Params", is a computer program the design team wrote in FORTRAN. This program was used throughout the design process to help evaluate the effects various design changes had upon the airplane's performance. Using "Params", plots can easily be generated that describe various performance parameters as a function of airspeed including lift-to-drag ratio, thrust available and required, power available and required, minimum turning radius, rate of climb, throttle setting required, and energy consumption. "Params" can also be used to perform a thorough takeoff analysis and predict the number of laps the airplane design can complete in the seven-minute time limit.

The third program, "Mpeff" (for Motor/Propeller efficiency), was also written in FORTRAN by the design team to assist in the selection of appropriate combinations for the electric motor, speed control, battery pack, and propeller. This program uses input parameters generated by "Params" that describe the aerodynamic characteristics of the airplane, along with the pertinent specifications of the motors, speed controls, battery pack set-ups, and propellers. "Mpeff" automatically evaluates each possible combination and, after eliminating those that prevent takeoff in the specified 300 feet, determines which combinations provide the best overall efficiency over a range of airspeeds.

The fourth program, "Wind", was developed by the design team to determine the effects of wind on the airplane's performance. This program will be used at the competition to help the pilot know the optimum airspeeds for the wind conditions at the time of flight.

The final program, "Analyse an Airfoil", was used to help the design team select a suitable airfoil shape for the wing. This program was written by Martin Hepperle and posted on the Internet. The chosen airfoil was verified to perform well at low Reynolds numbers using this program. Also, the lift slope, maximum lift coefficient, and stall angle of the airfoil were determined, which were used in other areas of the analysis of the airplane design.

One of the most important decisions that had to be made was the designed airspeed of the airplane. Every airplane has an optimal airspeed at which drag is minimized and the lift-to-drag (L/D) ratio is maximized. Initially, the airplane was designed to fly at 30 mph. Using the tools described previously, it was determined that the time would expire much sooner than the available battery power at this airspeed. Therefore, the planform area of the airplane needed to be significantly decreased in order to increase the designed airspeed. Ideally, the team would have liked to design the airplane with a minimum drag airspeed of approximately 70 mph. However, structural limitations imposed by the need to carry the 7.5 pound payload made this task nearly impossible. Ultimately, the airplane was designed with a minimum drag airspeed of 53 mph, but will actually fly closer to 70 mph in order to use the available energy in the time allotted. Finally, a velocity controller was designed for the airplane. This will allow the airplane to maximize the number of laps completed in the competition by ensuring the airplane always flies at the most efficient airspeed for the existing wind conditions.

## Management Summary

In order to successfully involve 30 team members in the design, it was decided early on that the team would be sub-divided into three main groups, each emphasizing a different aspect of a successful design. One group emphasized computer iteration and theoretical optimization of the aerodynamic design, another designed an electronic airspeed controller, and the final group attempted to form a better theoretical model for the battery/motor/propeller combination through experimentation. Table 1 on the following page shows how each team member was (or will be) involved in each aspect of the airplane design, construction and testing. A rating of '5' indicates maximum involvement and a rating of '0' indicates no involvement.

The entire team has had weekly meetings with the faculty advisor, Dr. W.F. Phillips to document progress and share design information. One day each month was designated as a day for each of the groups to present new information learned during their research into the aircraft design. This presentation served to ensure each group was on schedule as well as keep the other teams up to date on the progress of the design. Figure 1 is a summary milestone chart for the project, and shows when the major tasks in the design have been and will be completed.

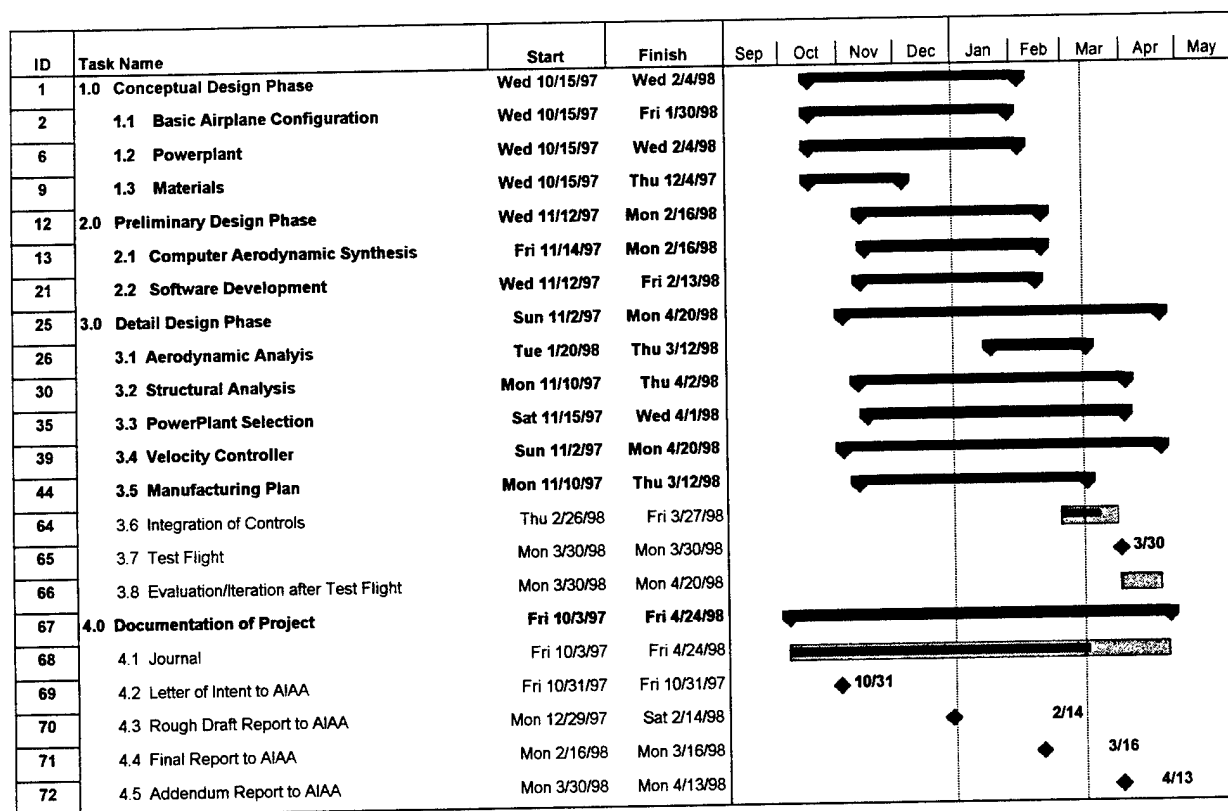


Figure 1—Design Management Timeline



Table 1—Team member contributions

	Corey Gravelle	Piotr Was	Harold Boman	Trayford	Mark Goodsell	Suart Thompson	Kara Palkki	Mike Watson	Duane Garbe	David Kent	Karl Johnson	Blake Ashby	Shelly Barlow	Greg Neilson	Deryl Snyder	Chris Wright	Under Classmen
1.0 Conceptual Design Phase	5	5	5	5	5	5	5	5	5	5	5	5	5	5	5	5	2
1.1 Basic Airplane Configuration	5	5	5	2	2	5	5	5	5	5	5	5	5	3	5	5	2
1.2 Powerplant	4	4	4	2	2	4	4	4	4	4	4	5	4	2	4	4	2
1.3 Materials	4	4	4	5	5	4	5	5	5	4	4	4	4	5	4	4	2
2.0 Preliminary Design Phase	5	5	5	5	5	5	5	5	5	5	5	5	5	5	5	5	2
2.1 Computer Aerodynamic Synthesis	5	5	4	0	0	5	4	4	5	0	5	2	0	5	4	2	
2.1.1 Design Parameter/Sizing selection	4	4	4	0	0	4	5	5	5	0	5	3	1	5	4	2	
2.1.2 Structural Design																	
2.1.2.1 Wing	4	4	4	5	5	4	5	4	4	0	3	4	5	4	5	2	
2.1.2.2 Fuselage	4	4	4	5	5	4	5	4	5	1	3	4	4	5	5	2	
2.1.2.3 Tail	4	4	4	5	5	5	5	5	5	0	3	4	5	3	4	2	
2.2 Software Development																	
2.2.1 Params Program	0	0	0	0	0	0	0	0	0	0	0	0	0	5	0	0	0
2.2.2 Mpeff Program	0	0	0	0	0	0	0	0	0	0	0	5	0	0	4	0	0
2.2.3 Wind Program	0	0	0	0	0	5	0	0	0	0	0	0	0	0	0	0	0
3.0 Detail Design Phase	5	5	5	5	5	5	5	5	5	3	5	5	5	5	5	5	3
3.1 Aerodynamic Analysis																	
3.1.1 Take off Performance	2	3	2	0	0	1	2	3	2	0	5	1	2	5	1	0	
3.1.2 Range and Endurance	2	3	2	0	0	5	2	3	2	0	5	2	2	5	2	0	
3.1.3 Stability	4	5	4	0	0	5	4	4	4	0	5	4	3	3	4	3	
3.2 Structural Analysis	5	5	5	5	5	5	5	5	5	0	5	5	5	5	5	2	
3.2.1 Composites	1	1	1	1	1	4	5	5	5	0	1	4	5	3	3	2	
3.2.2 Woods (Balsa-spruce)	2	2	5	5	5	2	3	2	2	0	2	3	2	2	3	3	
3.3 PowerPlant Selection																	
3.3.1 Motor/Prop Testing	5	5	5	0	0	1	1	1	1	1	1	1	1	1	1	1	2
3.3.2 Computer Performance	5	5	5	0	0	4	5	5	5	0	5	1	1	4	1	2	
3.3.3 Battery Configuration	4	4	5	2	2	3	4	5	4	1	3	2	3	3	3	0	
3.4 Velocity Controller																	
3.4.1 Design of electronics	0	0	0	0	0	3	3	3	3	5	0	0	0	0	0	0	0
3.4.2 Sensor Calibration	0	0	0	0	0	3	3	3	3	5	0	0	0	0	0	0	0
3.4.3 Integration	1	1	1	1	1	5	4	4	4	3	1	1	1	1	1	0	
3.5 Manufacturing Plan	5	5	5	5	5	5	5	5	5	5	5	5	5	5	5	3	
3.5.1 Material Testing	3	3	3	3	3	3	4	5	4	2	1	5	3	1	5	2	
3.5.1.1 Foam	1	1	1	1	1	4	5	5	5	0	1	5	3	1	5	3	
3.5.1.2 Composite	1	1	1	1	1	4	5	5	5	0	1	4	3	1	3	0	
3.5.1.3 Wood	3	3	3	5	5	3	3	3	3	0	1	3	3	1	3	2	
3.5.2 Wing Construction	3	3	3	5	5	4	5	4	5	0	1	5	3	2	5	2	
3.5.3 Fuselage Construction	3	3	3	5	5	4	5	4	5	0	1	5	4	2	5	2	
3.5.4 Tail Construction	3	3	3	5	5	4	5	4	5	0	1	5	4	1	5	2	
3.6 Integration of Controls	3	3	3	5	5	3	5	4	4	2	1	5	4	1	5	2	
3.7 Evaluation/Iteration after Test Flight	5	5	5	5	5	5	5	5	5	5	5	5	5	5	5	2	
3.8 Documentation of Project	5	5	5	5	5	5	5	5	5	5	5	5	5	5	5	3	
3.8.1 Journal	5	5	5	5	5	5	5	5	5	5	5	5	5	5	5	0	
3.8.2 Letter of Intent to AIAA	1	1	1	1	1	1	1	1	1	1	1	1	1	1	1	0	
3.8.3 Rough Draft Report for AIAA	5	3	3	1	1	3	4	3	5	0	5	3	4	4	3	0	
3.8.4 Final Report to AIAA	2	1	1	1	1	2	1	1	2	2	5	1	4	5	1	0	
3.8.5 Addendum Report to AIAA	3	5	4	2	1	2	5	4	3	1	5	1	2	5	3	0	

scale of 0-5 indicating level of involvement \*\* blocked sections indicate major focus for particular team members

## Conceptual Design

A number of alternative concepts were investigated in the conceptual design process. The various design tradeoffs are discussed and evaluated below based on numerous design criteria or figures of merit (FOM). These include a high lift-to-drag (L/D) ratio, proper stability, maneuverability, sufficient power, high power-plant efficiencies, cost, ease of construction, weight, team members' experience, strength, and wing deflection.

### Alternative Concepts

#### Tail vs. Canard Configuration

One of the first design decisions made was whether to build an airplane with a traditional wing/tail configuration or with a canard/wing configuration. Designs for both configurations were developed on the computer using the "Airplane" program developed at Utah State University (see Figure 2 and Figure 3). Initially, it appeared that the canard configuration could achieve a slightly higher L/D. However, in order to achieve this, significant sweep was placed in the wings to keep the center of gravity closer to the main wings. The center of gravity needs to be located near the wings because the airplane must be lifted from its wing tips at the competition. A swept wing introduces greater challenges in construction than a non-swept wing would. Moreover, team members felt more comfortable designing and building a traditional wing/tail configuration than a canard configuration. Overall, the need to easily achieve proper stability, center of gravity location, and ease of manufacture outweighed the slight advantage in L/D ratio causing the team to select the wing/tail configuration.

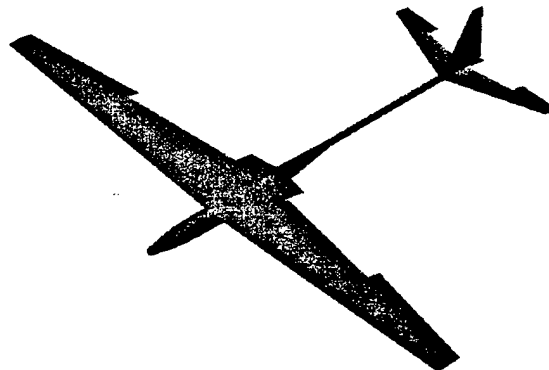


Figure 2—Conceptual Tail Configuration

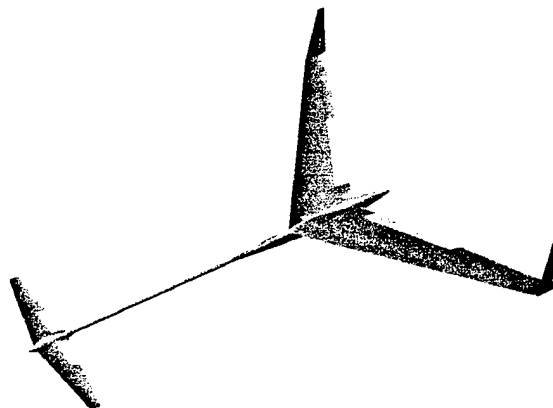


Figure 3—Conceptual Canard Configuration

## High vs. Low Wing

The team investigated the advantages and disadvantages of a design with a high wing versus a low wing. In terms of performance (L/D), there was no perceived benefit of one configuration over the other. However, the high wing design makes it easier to achieve sufficient roll stability and therefore requires that less dihedral be designed into the wing. The reason for this is that the airflow around the fuselage creates a stabilizing roll moment for a high wing and a destabilizing roll moment for a low wing. A wing with less dihedral is a more efficient lifting surface because the lifting force vector is closer to vertical. Also, a low-dihedral wing simplifies construction. Therefore, the team decided to design for a high wing configuration.

## Conventional Tail vs. V-tail

Some consideration was given to using a V-type tail in place of the conventional horizontal and vertical tail surfaces. The justification for this was to reduce drag because there would only be two surfaces instead of three (left and right horizontal tail and vertical tail). This type of configuration introduces other complications with ensuring stability, the design of control surfaces, and construction. The team members felt more comfortable with the conventional configuration and the reduction in drag by the V-tail was not significant enough, so the conventional tail was selected.

## One-Motor vs. Two-Motors

Higher power-plant efficiencies in steady-level flight is the justification for using two motors instead of one. Motors run more efficiently at higher throttle settings. However, a design that requires the motor operate near full throttle just to sustain steady-level flight would not have enough power to lift-off in the required 300 feet runway. Therefore, a more powerful motor could be used to takeoff, and once the desired altitude is achieved, the power could be switched to a second motor which is more efficient at the flying speed. This setup would use the available battery power more efficiently. However, this type of setup is significantly more complicated to design and build. Also, the cost and weight needed for the motors would be twice as much. The design team determined that the small increase in efficiency does not outweigh the extra cost, weight, and design difficulty necessary to implement it, so the single motor system was selected.

## Brushless vs. Brush Motor

Another significant decision in this design process was whether to use a brushless or a brush motor for propulsion. Brushless motors generally perform more efficiently than brush motors. Brushless motors have lower internal resistance and lower frictional losses than brush motors and therefore run cooler at higher currents. Cooler running motors are more efficient because the resistance of the copper in the motors increases with temperature. Another positive attribute of brushless motors is that there is less radio noise generated that can interfere with the remote control. In addition, the weight of the brushless motor selected for our design is slightly less than the brush motor that meets our design requirements.

The main drawback to the brushless motor systems is they cost approximately twice as much as a suitable brush motor system. Also, the lack of experience with the new brushless motors caused the team to question how reliable they are compared with the brush motors that have been used for years. Although the brushless motors perform more efficiently, the team could not justify the extra expense for one extra lap (see Figure 17 and Figure 18). Therefore, the brush motor system was selected.

## Payload in Fuselage vs. Payload in Wing

Another consideration investigated was where to place the 7.5 pound steel payload. An alternative to placing the steel in the fuselage is placing the steel inside the wing. The main benefit of this is the load from the steel would no longer be concentrated at the center of the wing, but would be distributed over a wider area, decreasing the necessary strength of the beam in the wing. One drawback to this design is that the steel in the wings would increase the rolling moment of inertia of the airplane. This would require the

aileron be made larger in order effectively control the airplane. Calculations about how far the steel would need to extend from the fuselage into the wing were made assuming the steel would be placed inside the tapered box beams that run the length of the wing. As the wing area was decreased as discussed in the Preliminary Design section, placing the payload inside the tapered box beams became less and less feasible. Therefore, the design team finally elected to place the payload in the fuselage.

### **Center of Gravity In Front Of vs. Behind Wing Quarter-Chord**

A plane with the center of gravity ahead of the quarter-chord of the wing will always be stable in pitch. In general, the horizontal tail generates negative lift to balance the airplane in flight. If the center of gravity is ahead of the quarter-chord of the main wing, the horizontal tail must generate more negative lift than if the center of gravity is behind the quarter-chord. Therefore, an airplane with the center of gravity located further back will have a higher overall lift-to-drag ratio for the airplane. Ensuring pitch stability with this configuration is only slightly more difficult. Since it is easy enough to design a stable airplane with the center of gravity behind the quarter-chord of the main wing, the design team decided to do so in order to increase the L/D ratio of the airplane.

### **Cylindrical Fuselage vs. Airfoil-Shaped Fuselage**

The two main fuselage configurations considered are the cylindrical fuselage and the airfoil-shaped fuselage. The cylindrical fuselage design is more conventional and therefore easier to design and adds more flexibility to the location of the internal components. Drawings of our alternate fuselage design are shown in Appendix D. The second approach investigated was an innovative airfoil wing/fuselage design. In this design, the fuselage would be simply an enlargement in the center of the wing and would still maintain an airfoil shape (though non-cambered). The fuselage would be constructed just like the wing with a foam core surrounded by a balsa and Monokote sheeting. Hatches would be constructed in the top and bottom of the fuselage and the various components would be attached inside of the Styrofoam. This design is a little more complicated to develop, but it provides great benefits in terms of reduced drag, weight, and cost over the cylindrical fuselage design.

### **Composite vs. Spruce Wood Beams in Wing**

The conceptual design of the wing required a beam structural member in the wing. Several different beams were analyzed including beams composed of aluminum, various kinds of wood, and composite fiber materials. These beams were analyzed with a variety of cross-sectional shapes from circular and square solid beams to I-beams and box beams. These beams went through an initial screening based on weight, deflection, and ultimate strength. The aluminum beams were eliminated because of weight.

The beams that looked promising were a box beam that had a very thin airplane modelers plywood as a webbing that held either spruce or carbon fiber composite spars as far as possible away from the neutral axis. Both beam designs were constructed and tested. The spruce beam had a slightly lower weight but a greater deflection and lower ultimate strength than the carbon fiber beam. A large deflection in the main beam would transfer a large portion of the load to the foam core and balsa sheeting of the wing. Since the foam core and balsa sheeting of the wing itself can not support the deflection generated with the spruce beam, the carbon fiber composite beam was selected despite its slightly larger weight.

### **Landing Gear—Tail-Dragger vs. Nose-Wheel**

The two concepts investigated concerning the landing gear were the “tail-dragger” and “nose-wheel” configurations. The “nose-wheel” configuration consists of the traditional two wheel landing gear located behind the center of gravity and a wheel placed towards the nose of the plane. The “tail-dragger” has the same two-wheel landing gear placed in front of the center of gravity with a small wheel attached to the rudder. The “tail-dragger” setup requires less weight and develops less drag in flight than the “nose-wheel”

configuration. Also, construction of the "tail-dragger" is less complicated because steering is achieved by simply attaching the tail-wheel to the rudder, requiring no additional servo linkages. Therefore, the "tail-dragger landing gear was chosen.

In addition, the possibility of using retractable landing gear to reduce the drag in flight was investigated. However, the design team decided against using retractable landing gear, because they would add significant weight and cost to the final design.

### **Airspeed Controller vs. No Airspeed Controller**

The results of the analyses indicate there is a particular airspeed at which the airplane should fly to obtain the maximum range. Even a skilled pilot cannot gauge precisely at what airspeed the plane is flying, so using an airspeed controller will provide the ability to validate the optimal design. In order for the plane to travel a maximum distance in a given period of time, the effects of wind speed and direction must be taken into consideration and compensated for, which can also be accomplished using an airspeed controller. The disadvantages of such a system include the increased weight, cost, and design complexity. However, this team possesses the experience to design such a system. Also, the tremendous increase in efficiency due to flying at the proper airspeed clearly justifies the extra weight and cost. Therefore, the team elected to design and build an airspeed controller for the airplane.

### **Tapered vs. Rectangular Wing**

A tapered wing provides benefits in terms of aerodynamic efficiency over a rectangular shaped wing. Also, for a given wing area, a tapered wing allows for a larger root chord. This is important because the maximum moment occurs at the root and that is where the maximum strength must be. However, too much taper makes the wing tips small which increases the probability of wing tip stall. A rectangular wing is easier to build, but less efficient. All things considered, the team decided to design for a tapered wing. The specifics regarding the team's selection of the taper ratio are detailed in the Preliminary Design section.

### **Figures of Merit Summary**

Table 1 gives subjective quantitative values for each of the figures of merit (FOM) for competing concepts. Each figure of merit was rated from '1' to '3' with '3' being best. Values of '0' were given when the figure of merit did not apply. The chosen design concept is shown in bold.

Table 2—Final Ranking Chart for Alternative Concepts

	High L/D	Stability/Maneuverability	Sufficient Power	Power-plant efficiency	Cost	Manufacturability	Weight	Team Experience	Strength	Deflection	Total Score
<b>Wing/Tail</b>	<b>2</b>	<b>2</b>	<b>0</b>	<b>0</b>	<b>0</b>	<b>3</b>	<b>0</b>	<b>3</b>	<b>0</b>	<b>0</b>	<b>10</b>
Canard/Wing	3	1	0	0	0	1	0	1	0	0	6
<b>High Wing</b>	<b>1</b>	<b>3</b>	<b>0</b>	<b>0</b>	<b>0</b>	<b>2</b>	<b>0</b>	<b>0</b>	<b>0</b>	<b>0</b>	<b>6</b>
Low Wing	0	1	0	0	0	1	0	0	0	0	2
<b>V-Tail</b>	<b>2</b>	<b>0</b>	<b>0</b>	<b>0</b>	<b>0</b>	<b>1</b>	<b>0</b>	<b>1</b>	<b>0</b>	<b>0</b>	<b>4</b>
<b>T-Tail</b>	<b>1</b>	<b>0</b>	<b>0</b>	<b>0</b>	<b>0</b>	<b>2</b>	<b>0</b>	<b>2</b>	<b>0</b>	<b>0</b>	<b>5</b>
<b>1 motor</b>	<b>0</b>	<b>0</b>	<b>2</b>	<b>2</b>	<b>3</b>	<b>3</b>	<b>2</b>	<b>3</b>	<b>0</b>	<b>0</b>	<b>15</b>
2 motors	0	0	3	3	1	1	1	1	0	0	10
<b>Brushless motor</b>	<b>0</b>	<b>0</b>	<b>3</b>	<b>3</b>	<b>1</b>	<b>0</b>	<b>2</b>	<b>1</b>	<b>0</b>	<b>0</b>	<b>10</b>
<b>Brush motor</b>	<b>0</b>	<b>0</b>	<b>2</b>	<b>2</b>	<b>3</b>	<b>0</b>	<b>1</b>	<b>3</b>	<b>0</b>	<b>0</b>	<b>11</b>
<b>Steel in wings</b>	<b>0</b>	<b>1</b>	<b>0</b>	<b>0</b>	<b>0</b>	<b>1</b>	<b>0</b>	<b>1</b>	<b>0</b>	<b>0</b>	<b>3</b>
<b>Steel in fuselage</b>	<b>0</b>	<b>2</b>	<b>0</b>	<b>0</b>	<b>0</b>	<b>3</b>	<b>0</b>	<b>2</b>	<b>0</b>	<b>0</b>	<b>7</b>
<b>CG behind 1/4-chord</b>	<b>3</b>	<b>1</b>	<b>0</b>	<b>0</b>	<b>0</b>	<b>0</b>	<b>0</b>	<b>0</b>	<b>0</b>	<b>0</b>	<b>4</b>
CG in front of 1/4-chord	1	2	0	0	0	0	0	0	0	0	3
<b>Cylindrical fuselage</b>	<b>1</b>	<b>0</b>	<b>0</b>	<b>0</b>	<b>1</b>	<b>2</b>	<b>1</b>	<b>0</b>	<b>0</b>	<b>0</b>	<b>5</b>
<b>Airfoil-shaped fuselage</b>	<b>2</b>	<b>0</b>	<b>0</b>	<b>0</b>	<b>2</b>	<b>1</b>	<b>2</b>	<b>0</b>	<b>0</b>	<b>0</b>	<b>7</b>
<b>Composite wing beam</b>	<b>0</b>	<b>0</b>	<b>0</b>	<b>0</b>	<b>1</b>	<b>1</b>	<b>2</b>	<b>2</b>	<b>3</b>	<b>3</b>	<b>12</b>
Spruce wing beam	0	0	0	0	2	2	3	2	1	1	11
<b>Tail-Dragger</b>	<b>2</b>	<b>1</b>	<b>0</b>	<b>0</b>	<b>0</b>	<b>2</b>	<b>2</b>	<b>0</b>	<b>0</b>	<b>0</b>	<b>7</b>
Nose-Wheel	1	2	0	0	0	1	1	0	0	0	5
<b>Velocity Controller</b>	<b>3</b>	<b>0</b>	<b>0</b>	<b>3</b>	<b>1</b>	<b>1</b>	<b>1</b>	<b>0</b>	<b>0</b>	<b>0</b>	<b>9</b>
No Velocity Controller	1	0	0	1	2	2	2	0	0	0	8
<b>Tapered Wing</b>	<b>3</b>	<b>0</b>	<b>0</b>	<b>0</b>	<b>0</b>	<b>1</b>	<b>0</b>	<b>0</b>	<b>2</b>	<b>2</b>	<b>8</b>
Rectangular Wing	2	0	0	0	0	2	0	0	1	1	6

## Preliminary Design

### *Analytical Methods and Tools*

A number of analytical methods were used at each step of the design process. Most of these methods involved the use of computer programs that are detailed below.

#### **“Airplane” Program**

The “Airplane” program is an aircraft design software package developed at Utah State University. It uses Prandtl’s lifting line theory to predict the induced drag and the downwash of all the elements on each other. Boundary layer theory is used to predict the parasitic drag on all the components. “Airplane” also accesses another program called “Airfoil” that uses potential flow panel methods to determine the characteristics of the chosen airfoil for the lifting surfaces.

This program was used to iteratively modify the major parameters of the airplane design. At each step, the user can see how the design looks and study the aerodynamic and stability characteristics of the design. This program proved to be the major tool in sizing the various components and exploring various design tradeoffs. There are some limitations to this software that made it difficult to accurately model the design. For example, the program does not take into account landing gear and the fuselage can only be represented by circular, oval, or polygonal shapes.

#### **“Params” Program**

“Params” is a program developed by the design team to assist in the performance determination of the airplane at each step of the design process. “Params” uses data files of the lift and drag coefficients at varying angles of attack generated by the “Airplane” program. A  $C_L$  vs.  $C_D$  curve is generated and the constant coefficients  $C_{D0}$ ,  $C_{DL0}$ , and  $e$  are calculated with a least squares fit for the following 2nd-order relation:

$$C_D = C_{D0} + C_{DL0}C_L + \frac{C_L^2}{\pi eAR} \quad (1)$$

where  $C_{D0}$  is the drag coefficient at zero lift,  $C_{DL0}$  is the drag slope at zero lift, and  $e$ , is the Oswald efficiency factor. These three coefficients effectively describe the lift versus drag characteristics of the airplane and are used throughout the programs “Params”, “Mpeff”, and “Wind” for the various analyses.

To account for the effects of the landing gear neglected by the “Airplane” program, a typical landing gear was tested in the wind tunnel at Utah State University. The drag coefficient was determined and added to the  $C_{D0}$  term for the analysis.

Numerous parameters can be studied as a function of airspeed for the particular airplane design with the many plots “Params” easily generates. The performance plots menu from “Params” is shown in Figure 4. Some specific plots for the final airplane design are included in the Detail Design section.

In addition, given the appropriate motor, speed control, propeller, and battery pack parameters, “Params” performs a detailed take-off analysis using a fourth-order Runge-Kutta method. The final and maybe most important analysis “Params” performs uses information from the energy consumption, minimum turning radius, and take-off analyses to generate a plot of the maximum number of laps the airplane can complete as a function of airspeed.

Performance Plot Options:

0. Return to Main Options
1. Lift-to-drag ratio
2. Thrust Required
3. Power Required
4. Minimum turning radius
5. Motor/prop efficiency (at thrust required for airspeed)
6. Thrust available (different air densities)
7. Thrust available (different throttle settings)
8. Thrust available with thrust required (different throttle settings)
9. Power available (different air densities)
10. Power available (different throttle settings)
11. Power available with power required (different throttle settings)
12. Rate of climb (different air densities)
13. Rate of climb (different throttle settings)
14. Throttle setting required for steady, level flight
15. Energy consumption rate at steady level flight
16. Energy consumed per lap using minimum turning radius
17. Energy consumed per lap (varying turning radii)

-->

Figure 4 -- Performance Plots menu of "Params" program.

### "Mpeff" Program

A detailed analysis of the power plant of the airplane was performed in order to select appropriate combinations for the electric motor, speed controller, battery pack, and propeller. "Mpeff", a program developed by the design team, was used extensively in this process. This program uses equations relating the various components derived from the simple schematic shown in Figure 5.

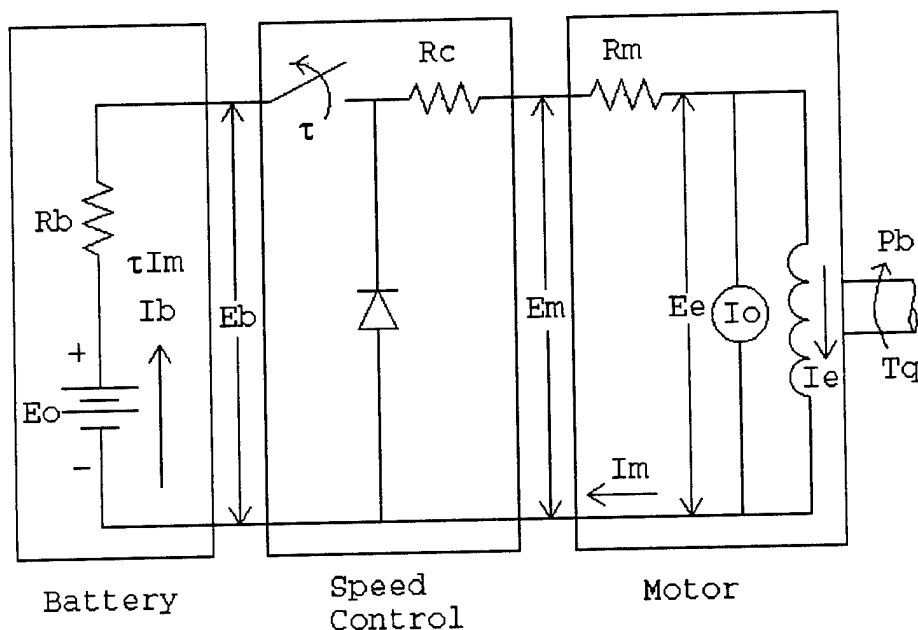


Figure 5--Schematic of Motor/Speed Control/Battery System



The power required to turn the propeller shaft and the thrust delivered by the propeller were calculated according to equations developed from limited empirical data gathered from *Electric Motor Handbook* written by Robert J. Boucher of Astroflight, Inc. These equations relate the propeller performance to its pitch and diameter. All the equations that "Mpeff" uses to describe this model are detailed in Appendix A.

### "Wind" Program

The "Wind" program was developed to determine the effects of a head wind or crosswind on the airplane's performance. This program will be used at the competition to help the pilot know the optimum airspeed for the current wind conditions. Figure 6 shows the output capabilities of the program.

<p>Menu of Plot Options:</p> <ol style="list-style-type: none"> <li>1. Airspeed/Thrust</li> <li>2. Airspeed/Throttle</li> <li>3. Airspeed/Power Consumption</li> <li>4. Airspeed/Specific Range</li> <li>5. Airspeed/Specific Range/Wind speed</li> <li>6. Airspeed/Specific Range/Ground speed</li> </ol>
--

Figure 6—Menu of Plot Options of "Wind Program"

### "Analyse an Airfoil" Program

The "Analyse an Airfoil" program was written by Martin Hepperle and posted on the Internet at <http://beadec1.ea.bs.dlr.de/Airfoils/calcfail.htm>. This program uses a second-order vortex panel method to calculate the velocity profile of the airfoil and uses an integral boundary layer method to compute the drag over the airfoil. With this program, the characteristics of the chosen airfoil were studied to make sure it performs well at low Reynolds numbers (~400,000) and provides sufficient lift. Specifically, it calculates and plots the lift, drag, and quarter-chord moment coefficients as a function of angle of attack. From this, the lift slope, maximum lift coefficient and stall angle of the airfoil can be determined. This program was used to analyze some common airfoils and the results corresponded very well with the experimental data published in *Theory of Wing Sections* by Abbott and Von Doenhoff.

## Design Parameter and Sizing Selection

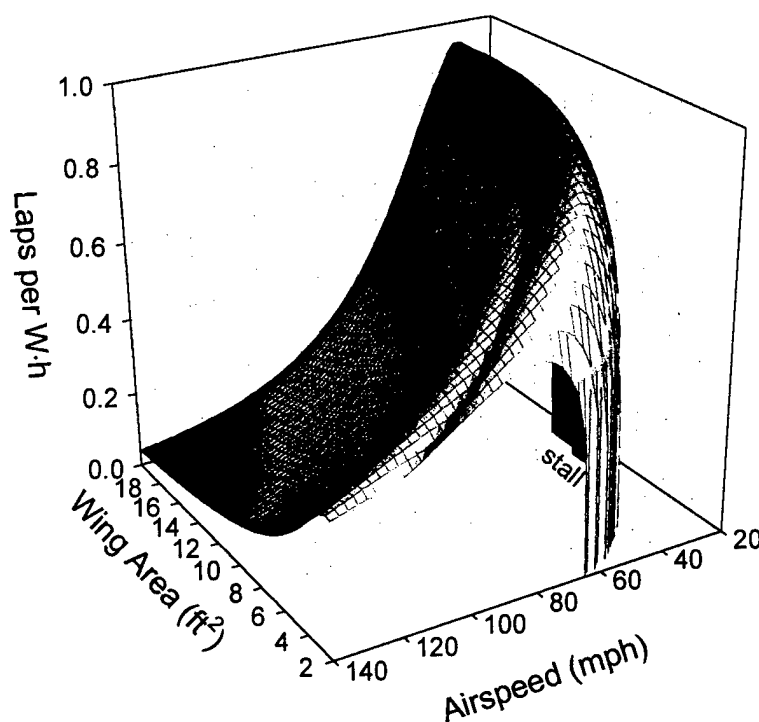
### Flight Speed

One of the most critical decisions for this design was the selection of the best velocity to fly the airplane. Initially, it was decided to fly at a speed low enough to allow for ease of landing and small turning radii. Also, the airplane should fly fast enough to get good efficiencies with the power plant. Based only on intuition, the airplane was initially designed to fly at 30 mph. For a given airplane design, there is an optimum airspeed that maximizes the lift-to-drag ratio and minimizes the thrust required. This airspeed is referred to as the minimum drag airspeed,  $V_{MD}$ , or the best L/D airspeed. The  $V_{MD}$  and the drag at this airspeed can be closely approximated as follows:

$$V_{MD} = \frac{\sqrt{2}}{\sqrt[4]{\pi e A R C_{D0}}} \sqrt{\frac{W/S}{\rho}} \quad D_{min} = 2 \sqrt{\frac{C_{D0}}{\pi e A R}} W \quad (2), (3)$$

Equation (2) indicates that the terms that can be varied to adjust the minimum drag airspeed are the Oswald efficiency factor,  $e$ , the aspect ratio,  $AR$ , the weight,  $W$ , and the planform area,  $S$ . The air density,  $\rho$ , obviously cannot be controlled.  $V_{MD}$  can be increased by decreasing the Oswald efficiency factor and the aspect ratio. However, as is shown equation (3), decreasing those parameters would in turn increase the drag which is undesirable. Also, it is counterproductive to design an airplane for anything other than minimum weight, so the only parameter that can really be adjusted to increase the minimum drag velocity is the wing planform area.

The effects of varying wing planform area and airspeed were studied to discover if there is an optimum planform area and airspeed for a given design. The results of this analysis are shown below in Figure 7. This plot takes into consideration the course geometry, assuming the plane takes all turns at the minimum possible turning radius, and includes the variation of motor/prop efficiency with airspeed. From this plot, it is seen for a given planform area there is a corresponding optimal velocity which maximizes the number of possible laps. The shallow valley that becomes apparent at low planform areas is due to the transition between stall-limited and load-limited turns. Clearly, it is desirable to fly near the optimum airspeed to minimize the energy consumed per lap.



**Figure 7—Number of Laps per W-h as a function of Airspeed and Planform Area**

The next concern was how the seven-minute time limit affects the choice of airspeed. Using the energy consumption analysis capabilities of "Params", Figure 8 was generated. The airplane would clearly run out of time before it would run out of battery power if flown at 30 mph. The airplane needed to be designed to fly efficiently at a much higher airspeed. From the time limited curve it can be seen that, even if the airplane had infinite energy, there is a limit to the number of laps that could be completed in seven minutes. This maximum is due to the increasing minimum turning radius with increasing airspeed. At airspeeds above this maximum, any benefit of increased velocity is counteracted by an increase in distance around the course.

It can be seen from the plot that the airplane should fly at least 70 mph to complete the maximum number of laps in seven minutes. The planform area for the airplane designed to fly at 30 mph was about  $11 \text{ ft}^2$ . Thus, this value had to be reduced significantly to raise the minimum drag airspeed to an acceptable level and shift the energy limited curve to the right.

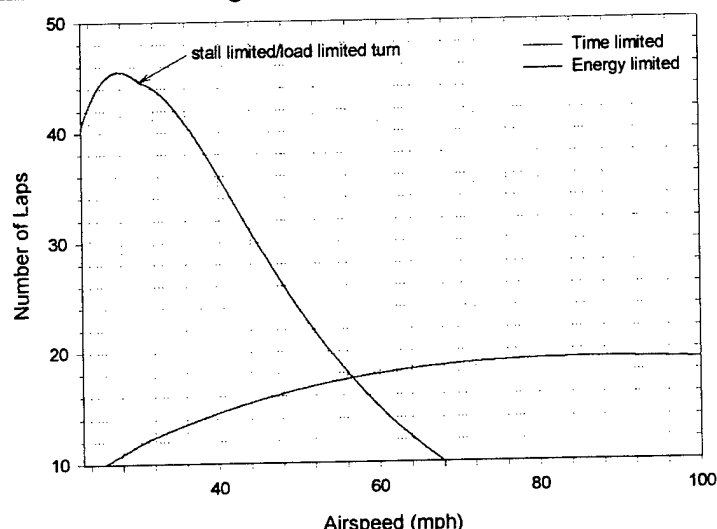


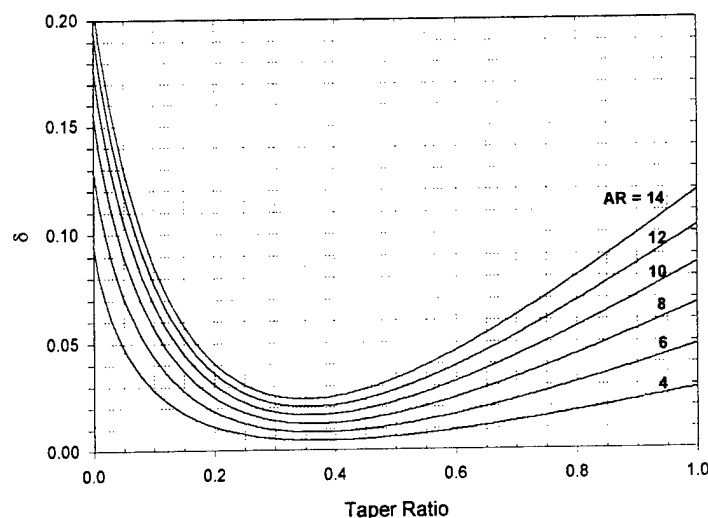
Figure 8—Maximum Number of Laps For Early Airplane Design

### Reducing Planform Area

Many structural and manufacturing difficulties developed while reducing the wing area. To raise the minimum drag airspeed to 70 mph, the planform area would need to be reduced to approximately  $1.85 \text{ ft}^2$ . This is not realistic for a number of reasons. An airplane with that planform area that can lift a 7.5 pound payload would be difficult, if not impossible, to design and build. The smallest the design team felt comfortable with was a wing area of  $3.0 \text{ ft}^2$ . This corresponds to a  $V_{MD}$  of about 53 mph which is much closer to the desired flight speed of 70 mph.

Many design tradeoffs had to be made in reducing the planform area. The initial design called for an aspect ratio of about 18 which would increase the  $L/D$  ratio of the airplane. In order to keep this aspect ratio, the mean chord length of the wing needed to be reduced to 4.9 in. The design team felt that this was too small to manufacture the precise dimensions of the airfoil. Therefore, the minimum mean chord length was set at 6 in. This meant the aspect ratio of the main wing became 12.0 with a wing span of 6 feet. This resulted in some reductions in the  $L/D$  ratio, but not enough to decrease the airplane's predicted performance by even one lap.

Another parameter examined was the wing's taper ratio. According to calculations performed by the famous English aerodynamicist, Herman Gauert, a tapered wing is most efficient with a taper ratio of approximately 0.35 as shown in Figure 9 (Anderson). The lower the induced drag factor  $\delta$  is, the more efficient the wing is. The initial design had a taper ratio of 0.35. However, maintaining this taper ratio required that the wing tip chord length be 3.1 in. Once again, the inability to manufacture a precise airfoil that small and the concern of wing tip stall in flight caused the design team to alter the taper ratio. A satisfactory compromise was achieved by setting the taper ratio at 0.5 which caused the wing tip chord length to be 4.0 in. and the wing root chord length to be 8.0 in. This taper ratio also provides structural benefits over an untapered wing by increasing the size of the root chord where the bending moment is maximum. Once again, the effects of this compromise were studied with the "Params" program, and still the airplane design's predicted number of laps did not decrease by going with a less efficient taper ratio.



**Figure 9—Induced Drag Factor  $\delta$  vs. Taper Ratio**

The location and size of the tail surfaces were determined using the “Airplane” program. The horizontal tail surface must be positioned and sized so that the airplane has no pitching moment about the center of gravity in flight. This moment is kept at zero by trimming the elevators in flight. In general, the further the tail is from the wing, the smaller it can be. The vertical tail surface was sized to be large enough to maintain yaw stability, but also as small as possible to reduce drag.

Finally, the airfoil was selected to provide the airplane with the proper performance characteristics. This design is a low Reynolds number application ( $\sim 500,000$  at the wing root and  $\sim 250,000$  at the wing tip) and therefore an airfoil that performs well at these Reynolds numbers was selected. The empirical data of the Wortman FX63B airfoil indicates good performance at low Reynolds numbers. However, the designed lift coefficient at zero angle of attack for this airfoil is approximately 1.17. This airplane design does not need such a heavily cambered airfoil, so this airfoil was modified using a program at Utah State University called “Airfoil”. The necessary lift coefficient at zero angle of attack to fly at 70 mph (103 ft/sec) and support the estimated weight of the airplane of 16 pounds was calculated with the following equation:

$$C_L = \frac{W}{\frac{1}{2} \rho V^2 S} = \frac{16 \text{ lb}}{\frac{1}{2} (0.002289 \text{ slug / ft}^3) (103 \text{ ft / sec})^2 (3.0 \text{ ft})} = 0.44 \quad (4)$$

The thickness and camber distribution of the airfoil were maintained, and the maximum camber was altered so the designed lift coefficient at zero angle of attack was reduced to 0.52. This caused the lift coefficient of the whole airplane to be reduced to about 0.44 at zero angle of attack. A plot of the lift coefficient versus angle of attack is shown in Figure 10. This airfoil has a maximum lift coefficient of 1.53 with no flaps and 1.90 with 25% of the chord flaps deflected just 5 degrees. A plot of this airfoil is shown in Figure 11.

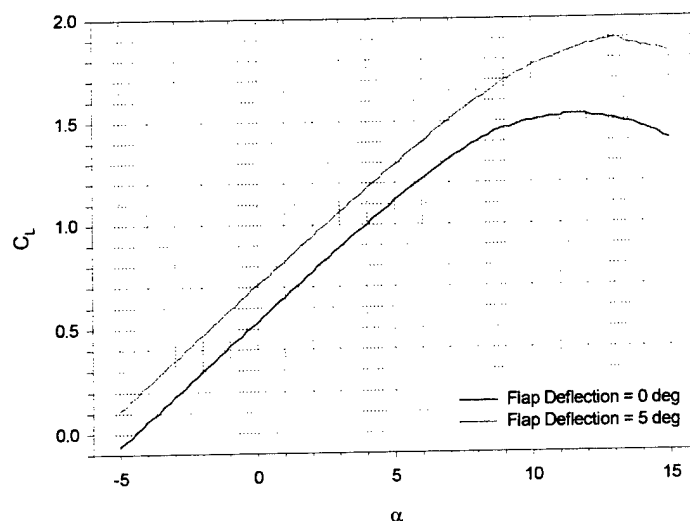


Figure 10— $C_L$  vs. Angle of Attack for Wing Airfoil

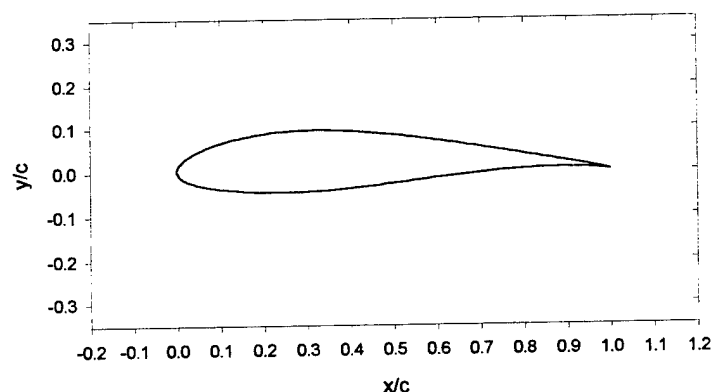


Figure 11—Modified Wartman FX63B Airfoil Shape

## Summary of Key Features

### Wing

The primary structural component of the wing is a tapered box beam that extends from wing tip to wing tip with the thickest portion of the taper located in the center of the fuselage. Attached to the beam is a Styrofoam core which provides the overall shape and size of the wing. A thin sheeting of balsa wood is used to protect the Styrofoam core and provide a smooth contact surface for the Monokote. The purpose of the Monokote cover is to seal all imperfections on the surface of the wing and help maintain laminar flow.

The airplane has a high wing design with a taper ratio of 0.50. This taper ratio provides improved aerodynamic and structural characteristics over the non-tapered wing. The wing has a planform area of 3.0 ft<sup>2</sup> with an aspect ratio of 12.0. The analysis indicated the airplane should be designed for a small planform area to increase the minimum drag airspeed. The minimum drag airspeed for this design is 53 mph, but the actual flight speed for the competition will be around 70 mph in order to maximize the number of laps. The airfoil selected for the wing is a modified Wartman FX63B with a designed lift coefficient of 0.52 at zero angle of attack. Flaps will be used with the wing to allow for easier takeoff and landing.

## **Fuselage**

Probably the most innovative aspect of this airplane is the fuselage design. The fuselage consists of a Styrofoam core in the shape of a symmetric airfoil which tapers outward to match up with the cambered airfoil of the wing. Two 3/32 inch plywood bulkheads will extend forward from the wing's box beam and will provide the necessary support for the landing gear and the components. The steel payload and the avionics components including the batteries, receiver, servos, speed controller, and the motor will rest on or be attached to a structure supported by the bulkheads as shown in the drawing 6 in Appendix C. The entire fuselage will be sheeted with balsa wood and covered with Monokote.

## **Tail Surfaces**

A carbon fiber tube will extend from the wing's box beam near the center of the fuselage to the tail of the airplane and attach to the horizontal and vertical tail surfaces. The tail surfaces will also be constructed out of a symmetric airfoil-shaped Styrofoam core covered with balsa sheeting and Monokote. However, no support beams will be used, because the loads on these surfaces are not near the loads on the wings. The horizontal surface will be an all-flying tail which eliminates the need to construct elevator surfaces.

## **Landing Gear**

The landing gear configuration will consist of standard Hallco-brand Temper-Lock landing gear attached to the fuselage in front of the center of gravity and a small wheel placed on the rudder. This wheel will provide greater steering capabilities at slower speeds on the runway. To minimize the drag, typical racing wheels will be used on the landing gear.

## **Power Plant**

A conventional brush motor system has been selected for this design despite the possible improved efficiency from using a brushless motor. The brushless motor system will only improve performance by one lap, but costs nearly twice as much.

## **Airspeed Controller**

The maximum range of any airplane design is significantly affected by flying at the proper airspeed. Even the most experienced pilot can not accurately gage the airspeed by just watching the airplane fly. Therefore, an airspeed controller system has been designed that will measure the airspeed and allow the pilot to adjust the speed to fly at optimum efficiency.

## Detail Design

### Final Performance Data

#### Takeoff Performance

One of the main constraints of this design problem is the takeoff distance. The airplane must start from rest, takeoff, and clear a six-foot-high barrier within 300 feet. The governing equation is simply Newton's second law including thrust, drag, and rolling friction forces. This second-order differential equation was numerically integrated until the lift equaled the weight, as shown in Figure 12, using a fourth-order Runge-Kutta method as detailed in Appendix B. The thrust, drag, and rolling friction forces are plotted as a function of velocity in Figure 13.

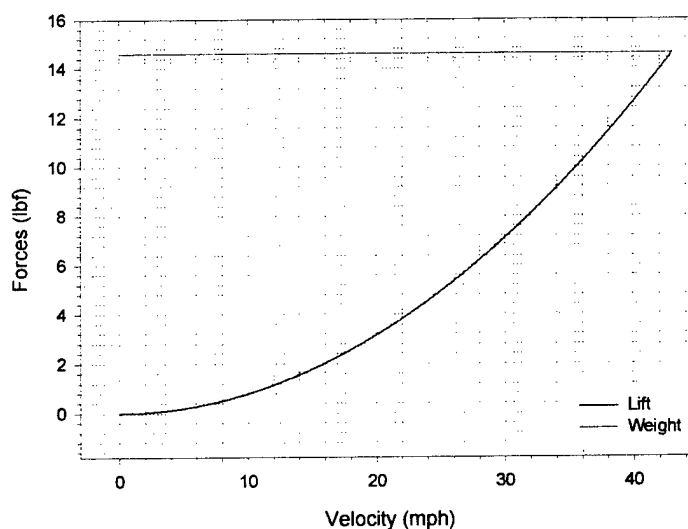


Figure 12--Lift Force and Weight vs. Velocity

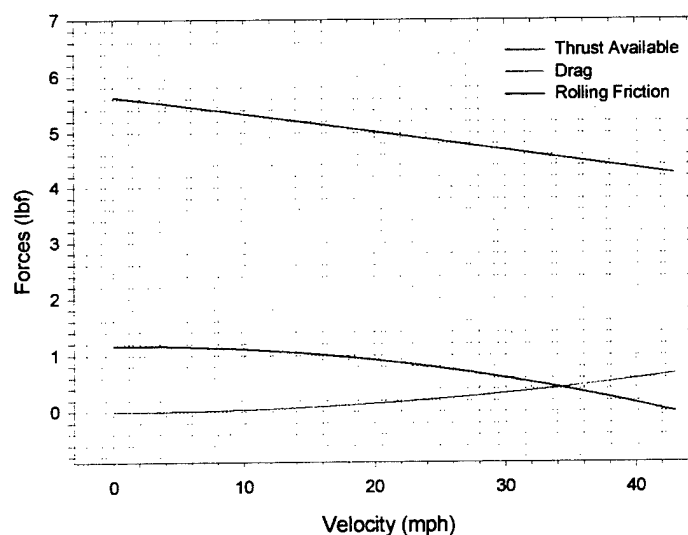


Figure 13--Thrust, Drag, and Rolling Friction Forces vs. Velocity

After finding the distance until the airplane lifts off the ground, the rate of climb was calculated. The remaining distance needed to clear the ribbon was determined using the rate of climb. The values calculated

from this analysis are included in the power plant component selection section later. The analysis indicates that the airplane will just takeoff within the 300 feet without the use of flaps, but will easily takeoff with the use of flaps.

### Handling Qualities

The airplane's handling qualities are measured by its stability characteristics in pitch, yaw, and roll and by how well the control surfaces are able to maneuver the airplane.

### Stability Characteristics

The three restoring moments about the center of gravity cause the airplane to return to equilibrium after it has been disturbed by an outside force. To determine whether or not an airplane is stable in these three directions, the slope of the moment with respect to angle of attack or sideslip angle must be analyzed. The stability characteristics for this design are summarized in Table 3.

Also, the degree of pitch stability is measured by the stick fixed static margin, which is defined as the distance between the airplane's neutral point and center of gravity divided by the mean chord length of the wing. This value is then converted to a percentage.

$$\frac{X_{NP} - X_{CG}}{\bar{c}} \times 100 = S.M.\% \quad (5)$$

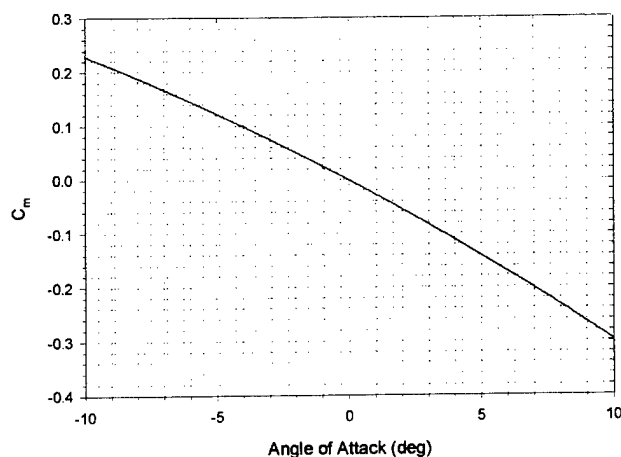
The static margin for any airplane should be at least 10%. For this airplane, it is 25.0%

**Table 3—Stability Characteristics**

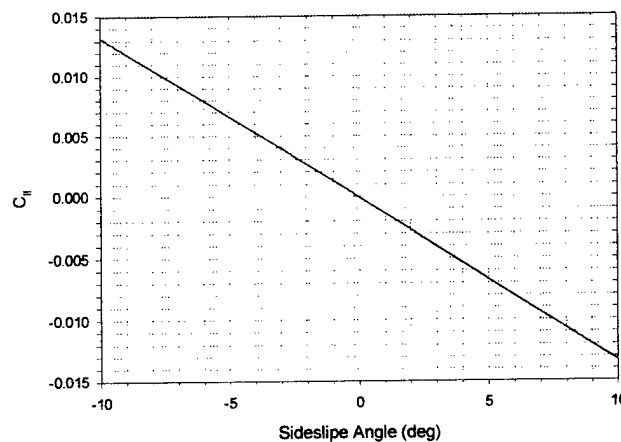
Stability Characteristic	Requirement for slope of moment coefficient	Good Range (deg <sup>-1</sup> )	Upper Limit (deg <sup>-1</sup> )	Actual Value (deg <sup>-1</sup> )
Pitch	$\frac{dC_m}{d\alpha} < 0$	—	—	-0.0263
Roll	$\frac{dC_{ll}}{d\beta} < 0$	-0.001 to -0.002	-0.004	-0.00133
Yaw	$\frac{dC_{ln}}{d\beta} > 0$	0.0015 to 0.0020	—	0.00185

The pitching moment coefficient as a function of angle of attack is shown in Figure 14 and the rolling and yaw moment coefficients as a function of sideslip angle for the design are shown in Figure 14 and Figure 15.

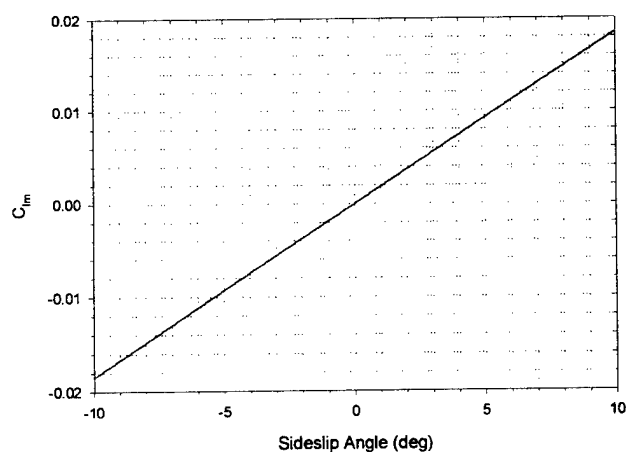




**Figure 14—Pitching Moment vs. Angle of Attack**



**Figure 15—Rolling Moment Coefficient vs. Sideslip Angle**



**Figure 16—Yawing Moment Coefficient vs. Sideslip Angle**

### **Control Surface Sizing**

The ailerons were initially sized using the “rules of thumb” from *Design & Build your own R/C Aircraft*. The book indicates that the ailerons should be 12% of the wing area. Since this airplane design has a large

load of steel that increases the moment of inertia, 16% of the total wing area will be ailerons. The “Airplane” program was used to calculate how much deflection would be necessary for ailerons of this size. According to Perkins and Hage, for general aviation aircraft, the dimensionless roll rate should be greater than 0.07 for adequate roll control as shown in the equation 6 (Perkins and Hage):

$$\frac{\omega_{roll} b}{2V_a} \geq 0.07 \quad (6)$$

where  $\omega$  is the roll rate,  $b$  is the wing span, and  $V_a$  is the airspeed. For this design, the ailerons must be deflected 17.5 degrees to produce a dimensionless roll rate of 0.07.

The “rules of thumb” indicate that the rudder should be 30% to 50% of the vertical fin area. The book recommends 30% be used if the airplane has a high wing. However, the rudder was sized at 40% to compensate for the extra control needed to counteract the 7.5 pound payload. The airplane will have a all-flying tail and, therefore, the elevator sizing is not relevant to this design.

### Range and Endurance

The range, in terms of number of laps the airplane can complete, is calculated with “Params”. As long as the other necessary design requirements are met, the maximum number of laps is the most important design parameter. The design team used this performance determination as a tool for making decisions throughout the process. Depending on the speed the airplane flies, the range can be limited by the seven-minute time constraint or by available energy in the battery.

This analysis deducts the energy consumed in takeoff, reaching the flying altitude, and completing the first lap with the two 360 degree turns from the total available battery energy. The remaining energy is then used to calculate the number of possible laps as airspeed is varied.

The maximum number of laps for the airplane design using the Aveox brushless motor with a 9x10 propeller is shown in Figure 17. The airplane will run out of time before battery power if flown at airspeeds less than 80 mph and will run out of battery power before time for airspeeds faster than that. The airplane should be able to complete 22 laps if flown between 76 and 81 mph.

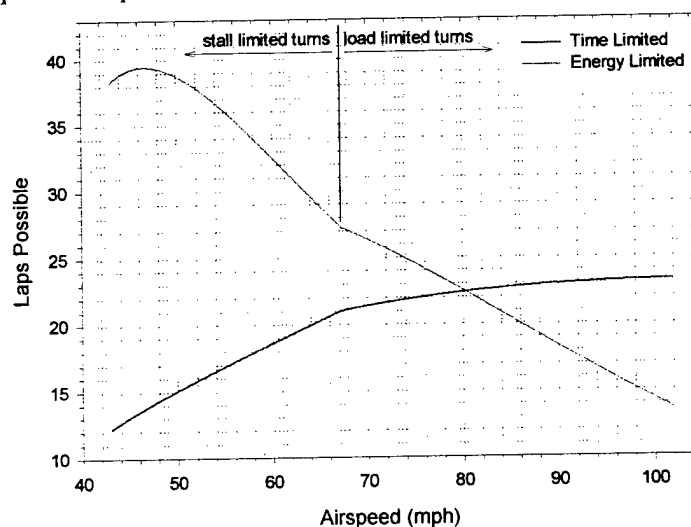


Figure 17—Maximum Number of Laps for Final Design Using Brushless Motor

The maximum number of laps for the airplane design using the Astroflight brush motor with a 10x11 propeller is shown in Figure 18. The design is time limited up to about 71 mph and energy limited at speeds higher than that. If the plane flies between 67 and 75 mph, it should be able to complete 21 laps.

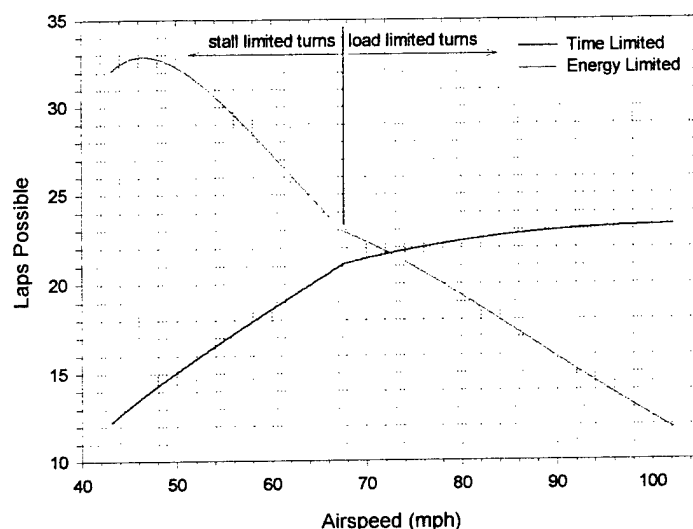


Figure 18—Maximum Number of Laps for Final Design Using Brush Motor

### G-load Capability

The competition rules state that before flying in the competition the airplane must be able to be lifted by its wing tips without failure simulating a 2.5g load case. Therefore, at minimum, the plane must be able to withstand a 2.5g maneuver. However, as is shown by the plot in Figure 19, by increasing the positive load limit, the airplane can increase the number of laps it can complete in the time limit.

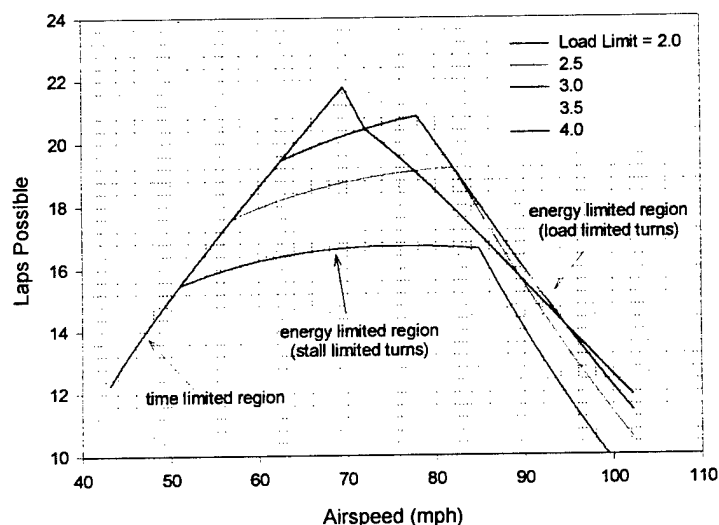
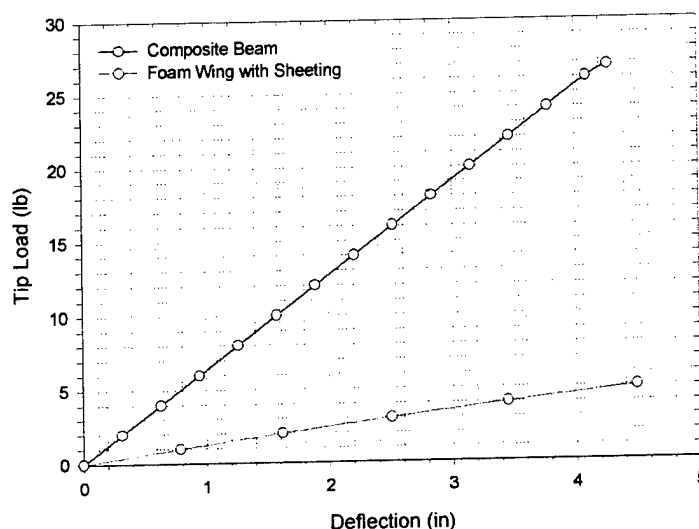


Figure 19—Maximum Number of Laps Varying the Positive Load Limit

The calculations for this plot were made assuming the airplane is turning at its minimum possible turning radius. Up to a certain airspeed, the minimum possible turning radius is limited by wing stall and above that airspeed, it is limited by the positive load limit of the airplane. By increasing the strength of the wing, the airplane can spend less time and distance on the turns and therefore increase the number of completed

laps in seven minutes. As is seen by the plot, increasing the positive load limit beyond 3.5g gives little to no benefit. This is because the minimum turning radius is stall-limited before it is strength-limited. Therefore, this airplane was designed to withstand a 3.5g load case.



**Figure 20—Load-Deflection Curve for Wing**

The tapered box beam in the wing is the primary structural member that must withstand the 3.5g load. To test for this strength, a full scale tapered beam that measures half the span of the wing was constructed. Also, a Styrofoam wing covered with balsa wood and Monokote sheeting without an internal beam was constructed to determine the deflections that the sheeting could withstand without buckling. The root end of the wing and the root end of the beam were fixed in a cantilevered arrangement and a load was applied to the free end. An analysis of a simply supported beam indicates that a 3.5g load can be simulated if 87.5% of the total weight of the airplane is applied to each wing tip. Using a conservative weight of 16 lb. it was determined that each wing would have to support 14 lb. In Figure 20, a plot of the tip load versus the deflection indicates that within the safe deflection of the sheeting, the beam itself will have a safety factor of about 2.5. When the strength of the sheeting is added, the safety factor is nearly three.

### **Payload Fraction**

At this stage of the design process the weight of the plane is estimated to be 14.77 pounds, which is less than the original estimate of 16 pounds. This makes the weight of the payload to the total weight ratio .508 or 50.8%. The weight of the payload to the dry weight of the airplane 1.032 or 103.2%. Therefore, the payload is over half of the total weight of the aircraft. A more detailed weight analysis is shown in Table 4.

Table 4—Weight Summary

<b><u>Airframe Structure:</u></b>	
Fuselage	0.92 lb.
Landing Gear	0.6 lb.
Tail	0.32 lb.
Tail Tube	0.08 lb.
Wings	0.85 lb.
<b><u>Subtotal:</u></b>	<b><u>2.77 lb.</u></b>
<b><u>Internal Components and Payload:</u></b>	
Motor	0.75 lb.
Motor Batteries	2.5 lb.
Motor Speed Control	0.06 lb.
Propeller & Spinner	0.18 lb.
Push Rods	0.06 lb.
Receiver & Servo Package	0.8 lb.
Steel Payload	7.5 lb.
Velocity Controller & Pitot Tube	0.15 lb.
<b><u>Subtotal:</u></b>	<b><u>12 lb.</u></b>
<b><u>Total:</u></b>	<b><u>14.77 lb.</u></b>

### Other Performance Plots

Using "Params" a number of other performance predictions can be made. The lift-to-drag ratio is plotted vs. airspeed for three different altitudes in Figure 21. Note that the maximum for L/D occurs at the minimum drag velocity of 53 mph at Wichita's altitude, as is expected.

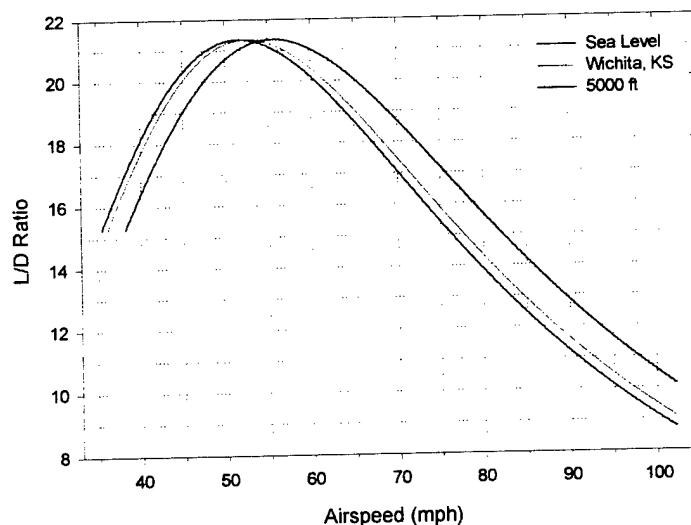
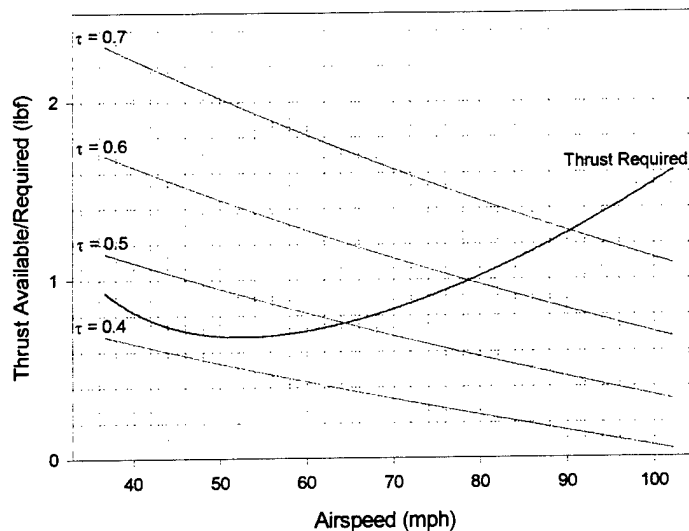


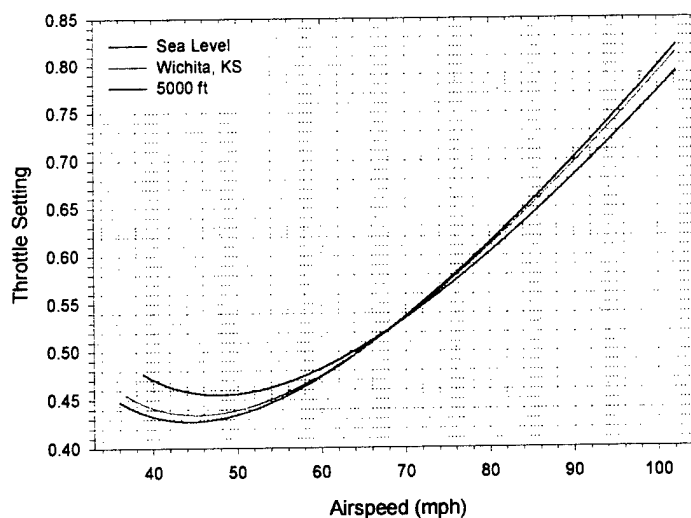
Figure 21—L/D ratio vs. Airspeed

Figure 22 shows the thrust required and the thrust available using the brush motor with 10x11 propeller for throttle settings of 0.4, 0.5, 0.6, and 0.7 as a function of airspeed. The airplane will fly at the airspeed corresponding to the intersection of the thrust required and thrust available curves for a given throttle setting.



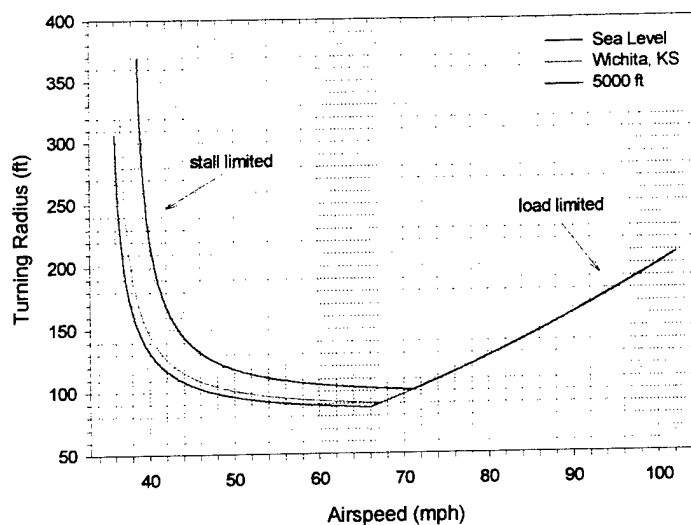
**Figure 22—Thrust Available and Thrust Required**

The throttle setting required for steady, level flight using the brush motor and 10x11 propeller is plotted for varying airspeeds for three different altitudes in Figure 23. Flying at 70 mph will require a throttle setting of about 0.535.



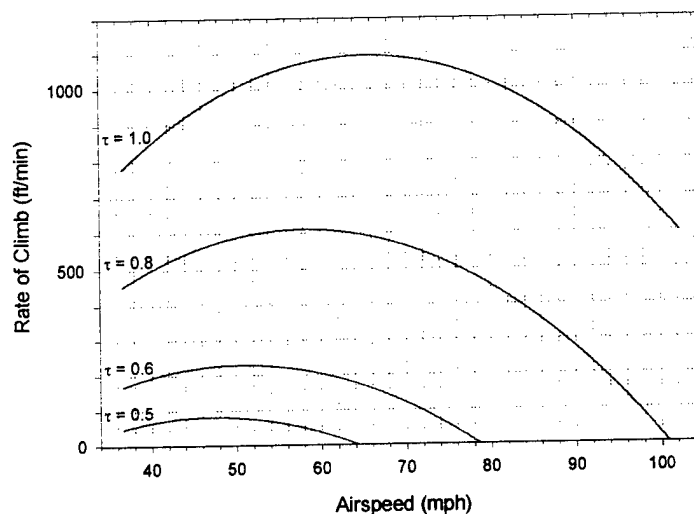
**Figure 23—Required Throttle Setting for Steady, Level Flight**

The minimum turning radius for this design is shown in Figure 24 as a function of airspeed for three different altitudes using a positive load limit of 3.5. For the left-hand section of each curve, the turning radius is limited by wing stall. For the right-hand section of each curve, the turning radius is limited by the strength or positive load limit of the airplane.



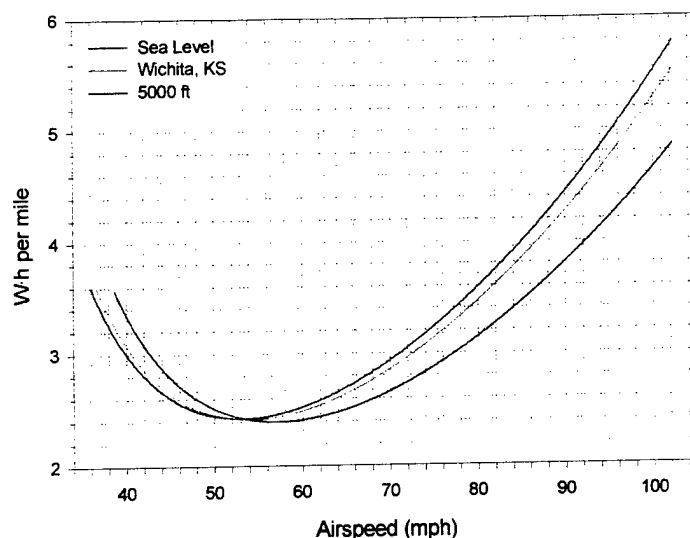
**Figure 24—Minimum Turning Radius vs. Airspeed**

The rate of climb at Wichita's altitude for various throttle settings using the brush motor is shown in Figure 25.



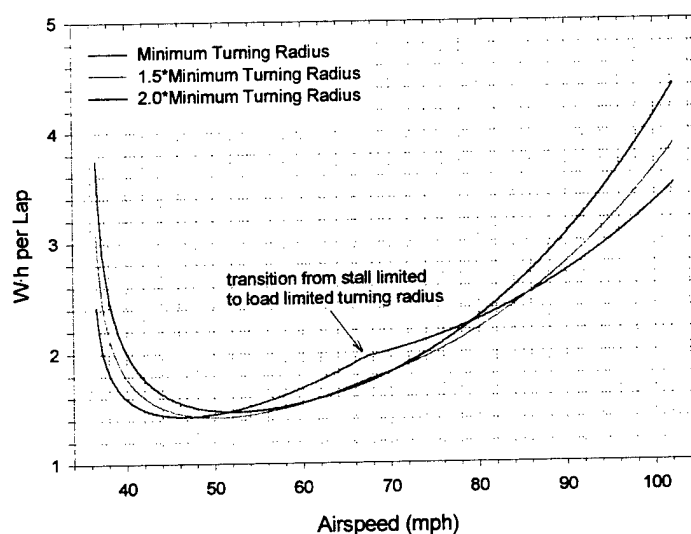
**Figure 25—Rate of Climb vs. Airspeed**

The energy consumption rate in steady, level flight for three different altitudes is shown in Figure 26. The minimum occurs at an airspeed slightly higher than the minimum drag airspeed. This is due to the fact that the power plant efficiency increases with airspeed.



**Figure 26—Energy Consumption Rate vs. Airspeed**

A more useful plot, the energy consumption per lap, is shown in Figure 27. Note that it is not always most efficient to take turns at the minimum turning radius. This is because for sharper turning radii, the wings must generate more lift. This extra lift causes a significant increase in the induced drag. Also, the most efficient airspeed is less than the minimum drag airspeed. This is due to the fact that the turning radius increases with velocity and therefore more energy is required to travel the extra distance necessary for higher airspeeds on the turns.



**Figure 27—Energy Consumption Per Lap vs. Airspeed**

The “Wind” program allowed the team to analyze the effects of a head wind, tail wind, or crosswind on the specific range or optimum airspeed. Figure 28 is a plot of the specific range of this design as a function of airspeed and headwind over the range of wind speeds permissible at the competition.



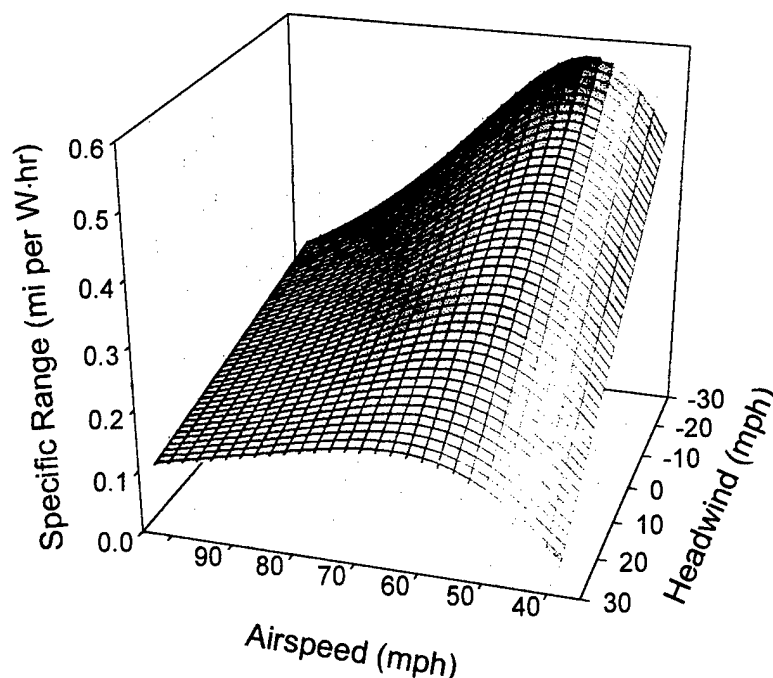


Figure 28—Specific Range vs. Airspeed and Wind Conditions

### **Power Plant Component Selection**

The “Mpeff” program was used to determine the most efficient motor, propeller, and battery pack combinations for the design. The “Mpeff” program uses information generated by the “Airplane” program about the design’s aerodynamic characteristics and automatically studies the efficiencies of every reasonable motor/propeller combination for a range of airspeeds. The power plant combinations investigated included 24 Aveox brushless motors and 10 Astroflight brush motors using every reasonable propeller from 4 to 16 inches in diameter.

“Mpeff” helped the team determine that a battery pack of about 20 cells is necessary to provide enough power for takeoff. However, exceeding this number of cells by too much requires the motors and speed controls run outside of their safe operating ranges. The battery pack selected includes 19 1.2V Sanyo RC-2300 NiCad cells with a capacity of 2300 mAh per cell. This battery pack will provide 52.44 Watt-hours of energy. The calculations demonstrated that this 22.8 Volt battery pack would provide the needed power for takeoff. Many other battery pack configurations were investigated, but this chosen combination provided the most energy in 2.5 pounds for battery packs with approximately 20 cells.

The “Mpeff” program was used to narrow the selection of power plant combinations. Both a combination using an Aveox brushless motor and speed control and a combination using an Astroflight brush motor was determined that meet the design requirements for this airplane. The cost of the brushless motor and speed control is \$368. The cost of the brush motor and speed control is just over half that at \$190. The performance of both systems was evaluated and as shown in Figures 11 and 12, the airplane can complete 22 laps with the brushless combination and 21 laps with the brush motor combination. The design team did not feel that one extra lap could justify the extra \$178, so the brush motor system was chosen.

“Mpeff” performs a rough take-off analysis and eliminates the combinations that do not provide sufficient power for take-off. The overall efficiencies of the remaining motor, speed control, propeller, and battery pack combinations were studied over a range of airspeeds and “Mpeff” determined the motor/propeller

combinations that provide the best efficiencies. In addition, the current levels of the remaining possible combinations were examined to make sure the maximum current limitations specified by the manufacturer are not exceeded.

The best combinations, as determined by "Mpeff," were then run through the more thorough takeoff analysis in "Params" to make sure that they can actually lift off in the required distance. The best Astroflight motor for this airplane is the 625G motor with a 1.63:1 gear ratio with a 10x11 propeller which gives an overall efficiency of 58.1%. This motor/propeller combination can takeoff in 260 feet without flaps and in 210 feet with flaps deflected at 5 degrees. The maximum current for this combination is 40.5 amps which is slightly above the maximum current rating of 35 amps for this motor. However, the current will only exceed this limit briefly during takeoff, so there should not be any problem. The motor current during steady flight at 70 mph is only 16.4 amps. The best speed controller for this motor and battery pack is Astroflight's model 210. This has a maximum current rating of 45 amps and can handle up to 19 NiCad cells. This motor will also work well with 10x12, 11x11, and 11x12 propellers. The power plant efficiencies for this combination with all four propellers are shown in Figure 29.

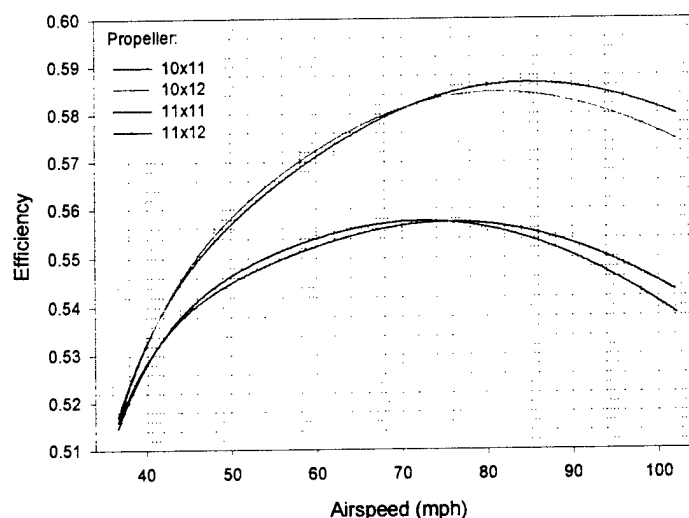


Figure 29—Power Plant Efficiency vs. Airspeed for four propellers

## Airspeed Controller Interfacing

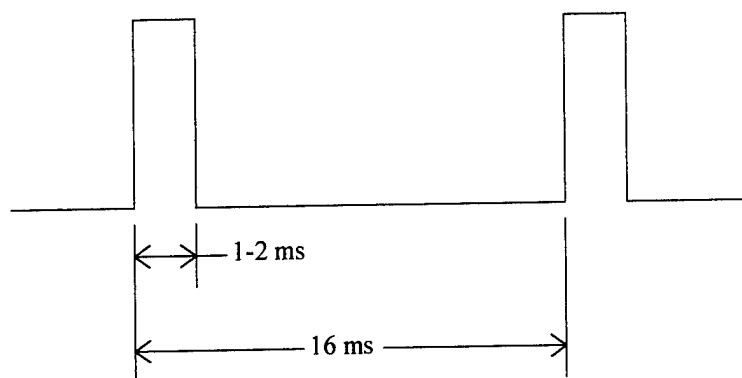
The design decided upon after several iterations can be separated into two components: airborne controls and the ground station.

### Airborne Controls

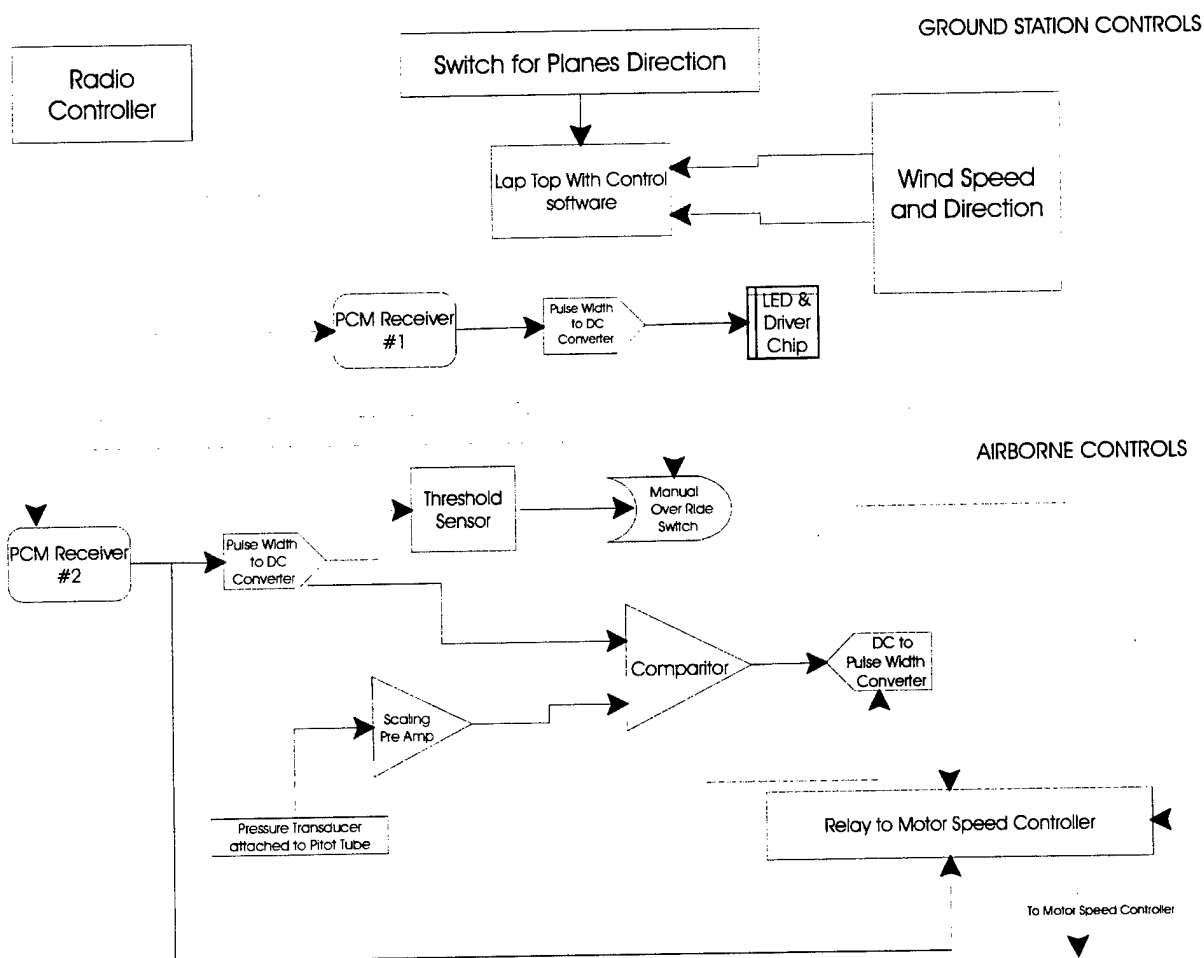
**Pitot tube pressure transducer:** The pitot tube is mounted on the tip of the wing, well outside of the propeller wash, sampling both the stagnation and static pressure. These values are fed to a pressure transducer that interprets the pressure difference between the two flows as an airspeed for the airplane. This is done using Bernoulli's principle for fluid flow.

**Circuitry for Velocity Controlled Flight (VCF):** The key to understanding how the airspeed controller works is how the PCM receiver interprets the signal sent by the radio controller. The signal is a simple square wave that repeats itself every 16 ms. The Spike lasts from 1 to 2 ms as shown in Figure 30. A throttle setting of 0% is indicated by a spike 1 ms long and throttle of 100% is indicated by a spike 2 ms long. Other throttle settings are just linear functions of these values. Once this signal is received, it is redirected in two directions. (See Figure 31). The first path is used as a timing or triggering signal for other chips. The second is passed through a pulse width signal to a volts DC converter, which allows

the signal to be interpreted by a comparator (OP-Amp) chip as a desired airspeed. The comparator checks this value against the measured airspeed input from the pitot tube pressure transducer sensor. The output is in volts DC, representing a needed motor speed. This voltage is then converted back into a pulse width signal and feed into a solid state relay which decides between this signal or one of two override signals.



**Figure 30--PCM Signal Diagram**



**Figure 31--Velocity Controller Flow Chart**

## Ground Station

Laptop computer with control software: The computer software collects input from the wind monitor. Then based on the planes parasitic and induced drag coefficients, the "wind" program, developed by the team, compares ground speed to airspeed and returns what the needed airspeed should be to maximize the airplane's specific range.

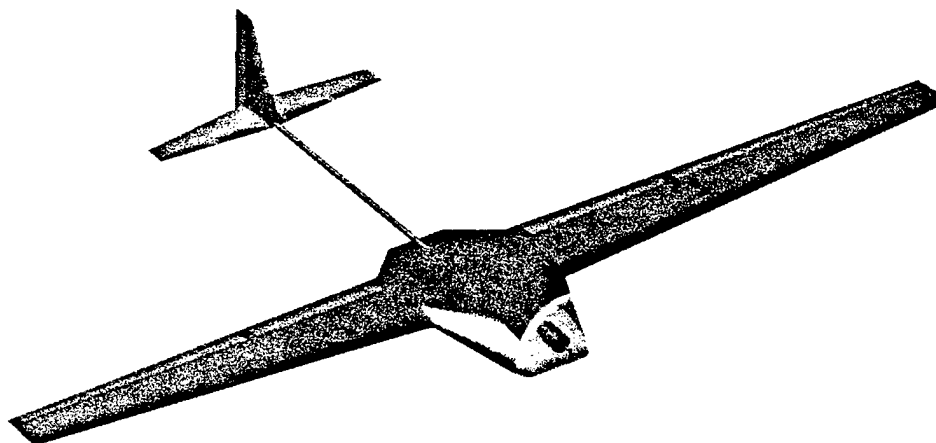
Wind direction and speed monitor: This equipment is on loan from Campbell Scientific of Logan, Utah. This sensor samples current wind conditions and communicates them to the lap top software. The ability to sample existing wind conditions gives the airplane the capacity to dynamically adjust its airspeed for maximum specific range.

Standard Radio Controller: Throttle settings between 5% and 95% will be the input for the VCF on board the airplane. It will be interpreted as a desired airspeed. The switch on the controller, reserved for retractable landing gear, will be used to arm and manually override the system.

Circuitry for manual over-ride switch (MOS): Between 0-5% and 95-100% throttle, a threshold sensor detects a spike of 1 or 2 ms, and tells the relay to select this original signal. Otherwise, the modified signal will be selected. An OR gate is placed after the threshold sensor, where it will tell the relay to always select the unadapted signal if the MOS switch is off. If the switch is on it will tell the relay to select the modified signal added to the restrictions that were previously stated.

LED read out of selected airspeed: A PCM receiver is used to intercept the current throttle position and relays the signal to a pulse width to volts DC converter chip which translates the received signal into the input required for an LED driver and display chip. This read out can then be visually compared to the value calculated by computer software as the airplanes maximum specific range airspeed.

## Drawing Package



**Figure 32—The Airplane**

The airplane design was modeled using the SDRC Ideas software package. This program was chosen because it allowed creation of a true 3D model which could be used for fuselage layout as well as center of gravity and moment of inertia analyses. Figure 32 shows a picture of the completed airplane design. Detailed drawings of the airplane's overall dimensions and fuselage component layout are contained in Appendix C.

## Manufacturing Plan

### Wing Construction

#### Beam

The manufacturing process for the carbon fiber composite box beam in the wing began with the laying up of the fiber composite laminates. Unidirectional pre-preg carbon fiber material was selected for the construction of the beam. The pre-preg material and the facilities to lay up the carbon fiber sheet are readily available at Utah State University, which made possible the construction and use of the fiber composite material. A large sheet of the carbon fiber composite material was laid up and the carbon fiber runners for the beam were cut to exact dimensions. The laminae were laid up as shown in Figure 33, with orientations calculated to oppose the stresses that the beam will experience. The majority of the plies are oriented in the longitudinal direction to compensate for the large bending moment on the wing. The composite sheet was laid up with an effort to maintain cleanliness and was then vacuum packed to remove voids in the material. Both of these efforts helped to increase the strength of the fiber composite material. After the composite was laid up, it was cured in a large oven.

0°
0°
90°
0°
45°
-45°
0°
90°
0°
0°

**Figure 33 – Orientation of Pre-preg Composite Laminae**

Using a circular saw and a blade designed to cut ceramic materials, the composite sheet was cut into one-half inch wide strips. These strips were then cut to the proper lengths for the construction of the beam for the wing. The best adhesive found to attach the composite material to the aircraft plywood webbing is epoxy. Jet Instant glue, which is popular among modelers, was also tried but it did not perform well with the composite runners and was hard to work with. The difficulties encountered with the construction of the first prototype box beam demonstrated the value of using a jig. The box beam was not completely square and when the beam was tested, there was significant twist. A wood jig was designed, constructed, and placed inside the beam while it was being assembled to ensure good tolerances. The jig was wrapped in wax paper to allow the jig to be removed after the adhesive finished curing. The epoxy used with the composite beam needs an extended amount of time to cure. To hold the components of the beam in place while the epoxy cured, elastic bands were wrapped around the beam.

At the center of the beam, a balsa wood member will be constructed to fill the hollow box portion of the beam located in the fuselage. This will create a solid section to attach the fuselage beam to the wing beam.

#### Foam Core

Surrounding the beam in the wing is a foam core that gives the wing its airfoil shape. An alternative construction technique was investigated that used balsa wood airfoil shaped ribs covered by Monokote, as

shown in Appendix E. The balsa rib concept was eliminated because of the irregular surface that the ribs create in the Monokote. The irregular surface would degrade the aerodynamic performance of the wing.

A low density polystyrene was selected to minimize weight. The foam for the wings was cut using a hot wire cutter according to the following sequence. First, an outline of the planform area of the wing was cut from the Styrofoam. Then, a one-half inch portion was cut out of the Styrofoam to allow room for the main support beam. Next, the flaps and ailerons were cut out and left in the main foam block. Finally, the airfoil shape was cut out using airfoil templates attached to the Styrofoam. This procedure allowed for clean and accurate cuts on all portions of the wing. The scrap Styrofoam pieces that surrounded the cutout airfoil shape were saved for future use.

The airfoil templates for the Styrofoam were originally cut from scrap pieces of balsa and plywood. This proved to be insufficient for several reasons. First the wood templates were difficult to construct to high tolerances. This was a particular problem as the size of the airfoils decreased, particularly at the wing tips. The wood was not an ideal surface to run the wire cutter along because the wire hangs up on the wood causing a poor surface finish on the Styrofoam. To counter these problems, aluminum airfoil templates were machined using a CNC mill which achieved excellent tolerances and gave a smooth surface for the wire to run across.

After the Styrofoam was cut to the proper shape, it was attached to the beam and made ready for application of balsa sheeting and Monokote. The construction of the plane has been completed to this point. The remaining procedures are detailed as follows.

### **Balsa/Monokote Sheeting**

The sheeting on the wing is primarily to create a smooth surface which will allow the airflow to remain laminar as long as possible. Secondary purposes of the sheeting include protecting the Styrofoam and adding strength to the wing.

The sheeting that will be used is 1/32-inch thick balsa. The sheeting will be wrapped around the wing with the grain of the balsa lined up with the longitudinal direction of the leading edge of the wing. 3M Spray Adhesive will be used to attach the balsa to the Styrofoam and beam assembly. To hold the balsa securely in place while the adhesive sets up, the scrap pieces of Styrofoam saved from the airfoil cutting process will be fastened around the balsa wood and wing assembly. Monokote will be applied to the balsa wood sheeting using a custom sealing iron to create a smooth, aerodynamic surface.

### **Control Surfaces**

The control surfaces will be made of a foam core with balsa sheeting and Monokote covering similar to the wing. The foam core will be the section of foam cut out from the wing as mentioned previously. It will then be sheeted with 1/32 inch balsa, and covered with Monokote. The control surfaces will then be placed back into position and will be hinged to the wing. The control surface hinges will be attached to a plywood airfoil section that extends from the wing beam to the trailing edge of the wing on each side of the control surface. The servos for the ailerons will be in each wing and push rods will run to the aileron to control it. The servo for the flaps will be inside the fuselage and the push rods will be directed to the flaps through the wing.

## ***Fuselage Construction***

### **Frame**

Due to the ease of construction and the cost of materials, the fuselage will be constructed similarly to the wing. The fuselage will be uniquely shaped and constructed to increase the aerodynamic performance. The

shape of the fuselage will be a symmetric airfoil which transitions smoothly on both sides to the cambered airfoil used for the wing. Following the same hot wire method outlined in the wing section, the fuselage will be cut out of foam and glued with 3M Spray Adhesive to the wing beam. The electronic components and payload will be carried in a section defined by two airfoil-shaped bulkheads placed five inches apart inside the fuselage as shown in the drawing 6 in Appendix C. These bulkheads will be cut from 3/32 inch aircraft plywood and will be the main support structure for all of the components. Wooden dowel stretchers extend between the two bulkheads providing a shelf-like structure to which the majority of components will be attached. Most of the components will be attached by conventional means. However, the motor batteries will be attached with Velcro to allow the batteries to be moved easily to adjust the center of gravity location.

### **Hatches**

The fuselage will have a hatches that open from the top and bottom to provide access to the payload and electronic components of the plane. The hatches will be cut out of the foam and coated with balsa. They will then be placed in the proper position in the fuselage. The entire fuselage will then be coated in Monokote. The Monokote will be cut along the sides and back of the hatches. This will leave one side for a hinge. When the hatches are closed they will be taped down along the cut portion of Monokote.

### **Motor Mount**

The motor mount will be attached to the bulkheads in the fuselage. The motor will be connected to the bulkheads by thin carbon fiber composite tubes. There are two spars that run up next to the motor and the motor will be connected to the spars using two hose clamps. The composite tubes were tested to determine their material properties. Using these material properties, an analysis on the motor mount was done which indicated that the stresses within the composite tubes would be well within safe limits. Perhaps more importantly, the deflection that the motor mount will experience as a result of the thrust force will be extremely small. This will ensure that the direction of thrust will remain constant in relation to the orientation of the airplane. Overall, this design is light-weight, simple to construct, inexpensive, and allows motors of various dimensions to be used.

### **Beam to Tail**

To connect the tail to the fuselage, there is a 0.505-inch composite tube that will run from the beam in the wing to the tail of the plane. The tube will mount directly to the beam running through the wings using a PVC bracket centered in the fuselage. The tube will run back to the tail which will be 26 inches from the beam. The vertical and horizontal surfaces of the tail will attach to the tube with an aluminum mounting bracket. The composite tube is the ideal selection because it is light, strong, and will allow the push rods from the servos in the fuselage to run inside of the tube to the tail control surfaces. Additionally, the composite tubes are readily available for only seven dollars from a kite hobby shop.

### **Landing Gear**

The main landing gear selected was Halco-brand Temper-Lock Landing Gear model HALQ2130. The maximum airplane weight for this landing gear as specified by the manufacturer is 10.0 pounds. This design exceeds that by nearly five pounds, so the landing gear was modeled using SDRC Ideas and a finite element analysis was performed. The analysis showed that the stresses incurred during a moderate landing are well below the yield strength of the heat-treated aluminum alloy landing gear. The weight limitations specified by the manufacturer obviously include a safety factor and are designed to withstand a lifetime of hard landings. The landing gear for this application only needs to withstand a few weeks of testing and the competition. To improve the aerodynamic properties of the landing gear the leading and trailing edges will be ground to a more streamlined shape. A small tail-dragger wheel will be attached to the rudder of the

airplane. The small wheel was selected over a wire since the wheel will allow easier maneuverability on the ground.

### ***Tail Construction***

Based on the information and experience gained during the analysis and construction of the wing, both the horizontal and vertical tail surfaces will have a foam core covered with 1/32 inch balsa sheeting and Monokote. Because the loads on these surfaces are not as high as those placed on the wing, these surfaces will not have a main support beam.

The horizontal surface will be all flying, with a pivot point located at its quarter-chord. This type of surface was chosen primarily for its ease of construction, reduction in weight, and low material cost. A push rod will run from a servo in the fuselage to a lever arm on a wooden dowel that will provide the torque needed to move the surface. The dowel transfers the torque to a rectangular piece of balsa wood glued into the foam of the horizontal surface. The dowel pivots in an aluminum bracket that will be attached to the fuselage-to-tail tube. Bearings and lubrication will be used to allow the dowel to rotate smoothly without binding.

The vertical surface will attach to the fuselage-to-tail tube with an aluminum bracket. A 90° triangle will be used to ensure the proper alignment between the horizontal and vertical surface. The control surface will be constructed the same manner as the wing control surfaces. The servo for the rudder will be inside the fuselage and a push rod will run from the fuselage through the composite tube to the rudder. Monokote will act as a hinge and will attach the rudder to the vertical stabilizer.

### ***Cost of Designed Airplane***

Considerable consideration was given to reducing the cost of the airplane throughout the design process. As much as possible, the design team tried to develop a low-cost design in terms of materials used and manufacturing processes. A detailed breakdown of the costs of the individual components in the final design is shown in Table 5. All costs are based on manufacturer's suggested retail prices (MSRP).



Table 5--Manufacturing Cost Analysis

<b><u>Airframe Structure:</u></b>		<b><u>MSRP</u></b>
Aircraft Plywood 1/32"		16.00
Aircraft Plywood 3/32"		10.95
Balsa Wood Sheeting 1/32"		17.50
Balsa Wood Supports		3.50
Carbon Fiber Prepreg		25.95
Carbon Fiber Tail Tube		7.00
Hard Wood Dowels 3/16" & 1/4"		0.75
Hinges		1.50
Landing Gear Mount		9.00
Monokote		36.00
Motor Support Clamps		0.80
Plastic Bolts & Nuts 3/8"		4.00
Scotch Tape		1.29
Styrofoam		15.75
Tail Gear		3.00
Tail Tube Support Bracket		1.89
Tail Tube Support Clamps		0.80
Wheels & Collars		2.00
Wing Tip Skids		0.59
	<b><u>Subtotal:</u></b>	<b><u>158.27</u></b>
<b><u>Internal Components and Payload:</u></b>		
Motor		125.00
Motor Batteries		150.00
Propeller & Spinner		11.20
Push Rods		2.75
Radio & Receiver Package		350.00
Speed Controller		65.00
Steel Payload		3.83
	<b><u>Subtotal:</u></b>	<b><u>707.78</u></b>
<b><u>Construction Supplies:</u></b>		
Aluminum Templates		1.95
Balsa Filler		3.89
Epoxy		9.95
Glue Accelerant		5.29
Masking Tape		0.79
Rubber Bands		1.98
Spray Glue		4.11
Wood Glue		10.49
Wood Jigs		5.00
	<b><u>Subtotal:</u></b>	<b><u>43.45</u></b>
	<b><u>Total:</u></b>	<b><u>\$909.50</u></b>

## Manufacturing Milestone Chart

The schedules event timings are detailed below in Figure 34.

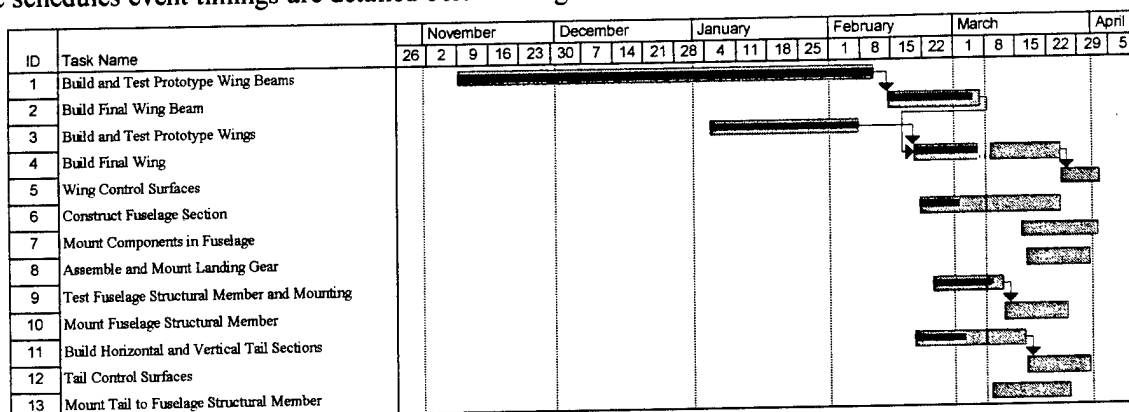


Figure 34—Manufacturing Milestone Chart

## References

Abbott, Ira H. and Von Doenhoff, Albert E., *Theory of Wing Sections Including a Summary of Airfoil Data*, Dover Publications, Inc., New York, 1959.

Anderson, John D. Jr., *Fundamentals of Aerodynamics*, 2<sup>nd</sup> Ed., McGraw-Hill, Inc., New York, 1991.

Boucher, Robert J., *Electric Motor Handbook*, Astroflight, Inc.

Perkins and Hage, *Airplane Performance Stability and Control*, Wiley, 1949.

Smith, Kenneth L. *Design & Build your own R/C Aircraft*, Robson House Hobby Supplies, Edmonton, Alberta, Canada, 1984.

## Appendix A--Equations Relating to Power Plant

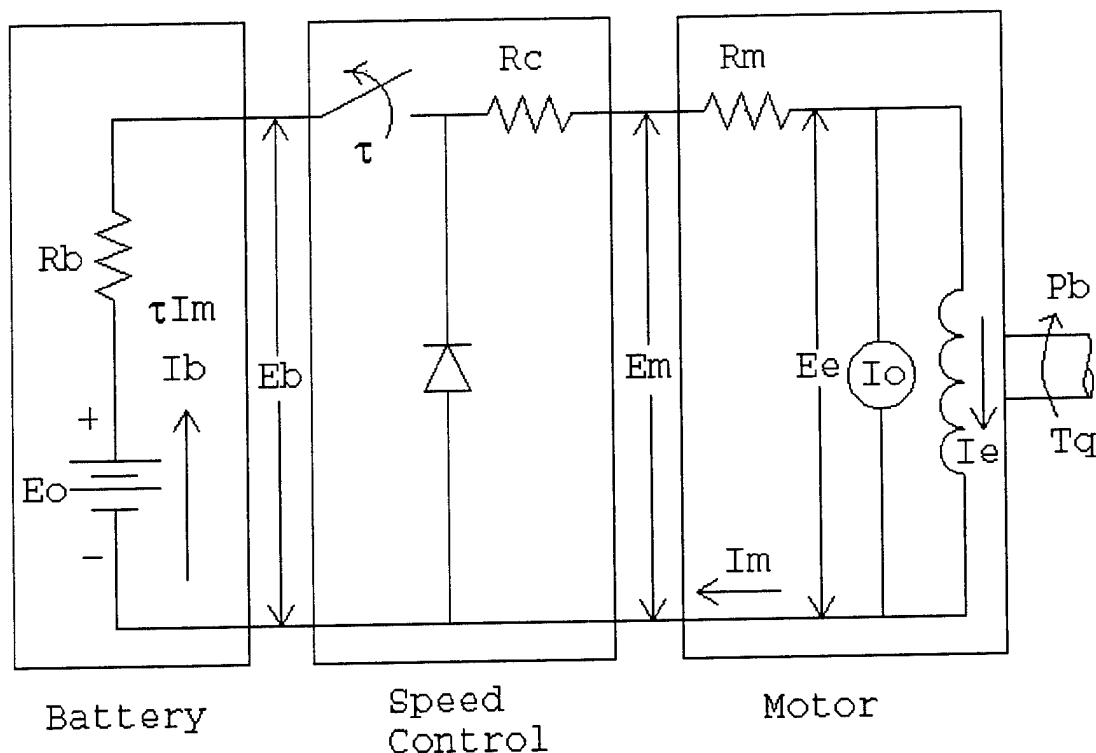


Figure 35--Schematic of Motor/Speed Control/Battery System

The following mathematical relationships for the motor, speed control, and battery are utilized in the "Mpeff" program. Voltage and Current values in equations are labeled on schematic above.

### Motor:

Shaft rotational speed (rpm):

$$n = \frac{K_v}{G_r} (E_m - I_m R_m)$$

Output torque of motor shaft (ft-lbf):

$$T_q = \frac{7.0432 G_r}{K_v} (I_m - I_o)$$

where:

$K_v$  = motor voltage constant  
(rpm/volt)

$G_r$  = gear ratio of the motor

$R_m$  = internal resistance of the motor

### Speed Control:

$$I_b = \tau I_m$$

$$E_m = \eta_s \tau E_b - I_m R_c$$

Speed control efficiency:

$$\eta_s = 1 - 0.078(1 - \tau)$$

where:

$\tau$  = throttle setting (0 to 1)

### Battery Pack:

$$E_b = E_o - R_b I_m$$

where:

$R_b$  = internal resistance of the battery pack

The power required to turn the propeller shaft and the thrust delivered by the propeller were calculated according the equations that follow. These equations relate the propeller performance to its pitch and diameter. They were developed from limited empirical data gathered from *Electric Motor Handbook* written by Robert J. Boucher of Astroflight, Inc.

**Propeller:**

Thrust available:

$$T_A = C_T \rho n^2 d^4$$

Break power required:

$$P_b = C_p \rho n^3 d^5$$

Torque required:

$$T_q = \frac{C_p}{2\pi} \rho n^2 d^5$$

Propeller efficiency:

$$\eta_p = \frac{T_A V_a}{P_b}$$

Advance ratio:

$$J = \frac{V_a}{nd}$$

Thrust Coefficient:

$$C_T = C_{T_o} - C_{TJ} J$$

Power Coefficient:

$$C_p = C_{p_o} + C_{p_i}$$

$$C_{T_o} = \begin{cases} 0.4077 \frac{p}{d} - 0.36625 \left( \frac{p}{d} \right)^2; \frac{p}{d} \leq 0.40 \\ 0.0586 + 0.1147 \frac{p}{d}; \frac{p}{d} \geq 0.40 \end{cases}$$

$$C_{TJ} = \begin{cases} 0.524185 - 1.72181 \frac{p}{d} + 1.78940 \left( \frac{p}{d} \right)^2; \frac{p}{d} \leq 0.46 \\ 0.142503 - 0.0760669 \frac{p}{d} + 0.0154988 \left( \frac{p}{d} \right)^2; \frac{p}{d} \geq 0.46 \end{cases}$$

$$C_{p_o} = 0.00868 + 0.00450 \left( \frac{p}{d} \right)^2 + 0.01643 \left( \frac{p}{d} - J \right)^2$$

$$C_{p_i} = \frac{1}{2} C_T \left( J + \sqrt{J^2 + \frac{8}{\pi} C_T} \right)$$

where:

 $\rho$  = air density $p$  = propeller pitch $d$  = propeller diameter $V_a$  = airspeed

## Appendix B—Takeoff Analysis

The governing equation for the takeoff analysis is simply Newton's second law. This equation is represented by the following pair of first order differential equations for the velocity,  $V_a$ , and distance traveled,  $x$ :

$$\frac{dV_a}{dt} = \frac{g}{W}(T_a - D - F_r) \quad \frac{dx}{dt} = V_a$$

where  $g$  is the gravitational constant,  $W$  is the weight,  $T_a$  is the thrust available,  $D$  is the drag, and  $F_r$  is the rolling friction force.

The thrust available,  $T_a$ , as a function of velocity for this airplane using the Astroflight 625G motor with a 10x11 propeller is shown in Figure 36 below. A polynomial expression for  $T_a$  was generated from a least squares fit of this plot.

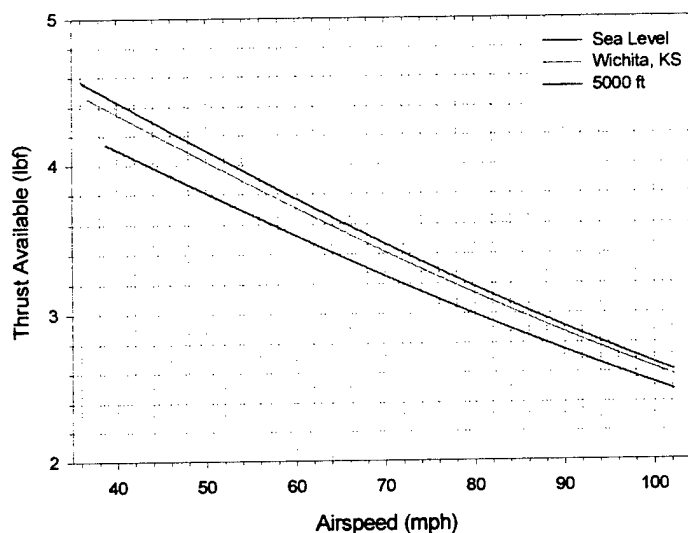


Figure 36—Thrust Available vs. Airspeed

The induced drag on the airplane during takeoff is reduced because the trailing vortices interact with the ground. An empirical correlation factor is included and the relationship for drag is:

$$D = \frac{1}{2} \rho V_a^2 S \left( C_{D0} + \frac{(16h/b)^2}{1 + (16h/b)^2} \left( C_{DL0} C_L + \frac{C_L^2}{\pi e AR} \right) \right)$$

where  $h$  is the height of the wing above the ground and  $b$  is the wingspan.

The rolling friction force is calculated according to:

$$F_r = \mu_r (W - L) = \mu_r \left( W - \frac{1}{2} \rho V_a^2 S C_L \right)$$

where  $\mu_r$  is the coefficient of rolling friction. The design team performed experiments on a surface similar to a typical runway with a typical landing gear apparatus and determined that this coefficient is approximately 0.08.

The lift coefficient was assumed to be reasonably constant and it was assigned a value of 70% of the maximum lift coefficient at stall. The chosen airfoil has a maximum lift coefficient of 1.53 with no flap deflection and 1.90 with only 5 degrees flap deflection. The liftoff velocity,  $V_{LO}$ , is the airspeed that the lift just equals the weight for this value of the lift coefficient.

$$V_{LO} = \frac{\sqrt{2}}{\sqrt{0.7C_{L_{max}}}} \sqrt{\frac{W}{S} \rho}$$

"Params" performs a fourth-order Runge-Kutta integration using the pair of first order, ordinary differential equations for velocity and distance shown above. Using the initial conditions of  $V_a(0)=0$  and  $x(0)=0$ , these two equations were numerically integrated until the velocity equals the lift-off velocity calculated above. From this point, the rate of climb was calculated from the following equation using the lift-off velocity:

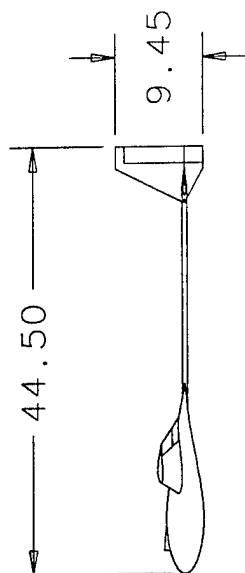
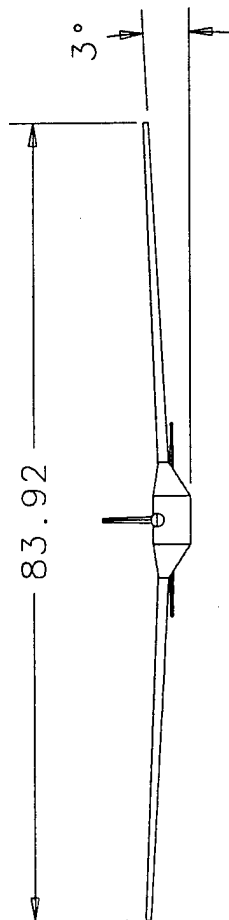
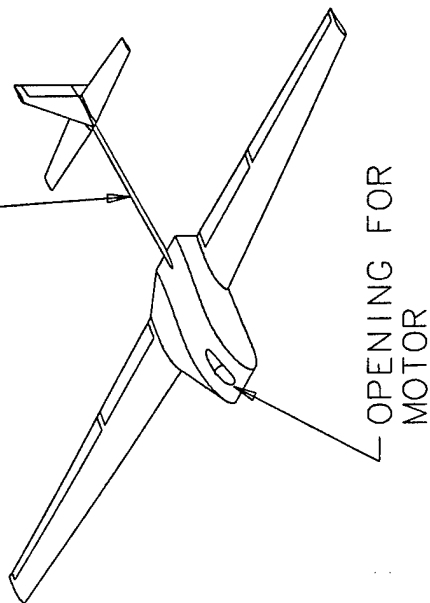
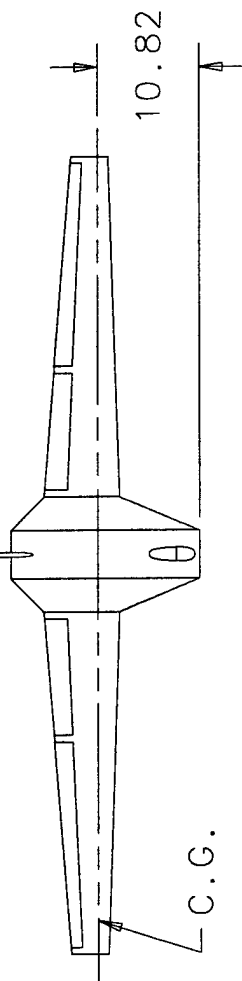
$$R / C = V_a \frac{T_a - T_R}{W}$$

The time needed to climb six feet was calculated from the rate of climb and multiplied by the horizontal component of velocity, giving the distance needed to clear the ribbon. This distance was added to the liftoff-distance calculated above to give the total distance required to takeoff and clear the six-foot ribbon.



## **Appendix C—Detailed Drawing Package of Final Design**

0.5050D X 0.4171D X  
29.20 LEN  
CARBON FIBER TUBE



ORGANIZATION

Utah State University

TITLE

USU-2 AIRPLANE

SIZE

A

DATE

02/28/98

DRAWN BY

D. Snyder

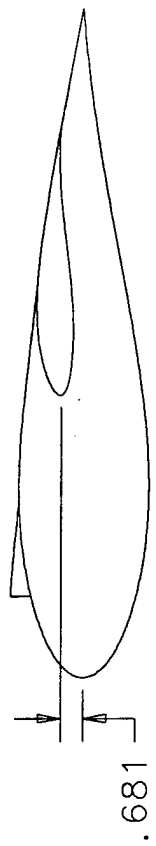
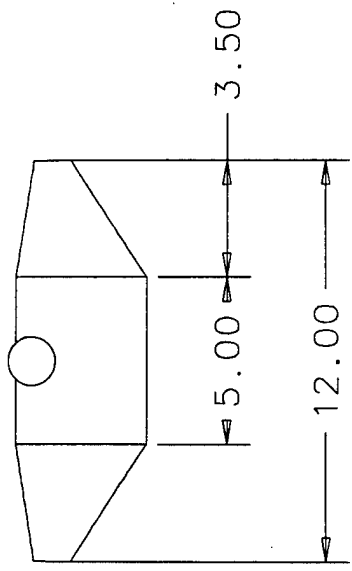
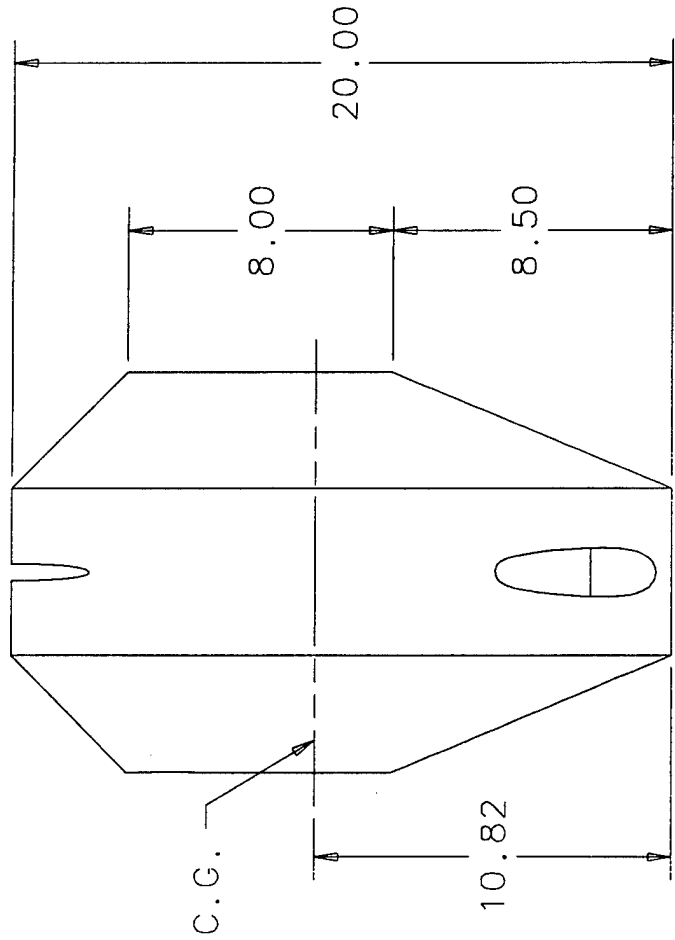
SCALE

0.050

SHEET

1 OF 6





ORGANIZATION

Utah State University

TITLE

FUSELAGE

SIZE

A

DATE

02/28/98

DRAWN BY

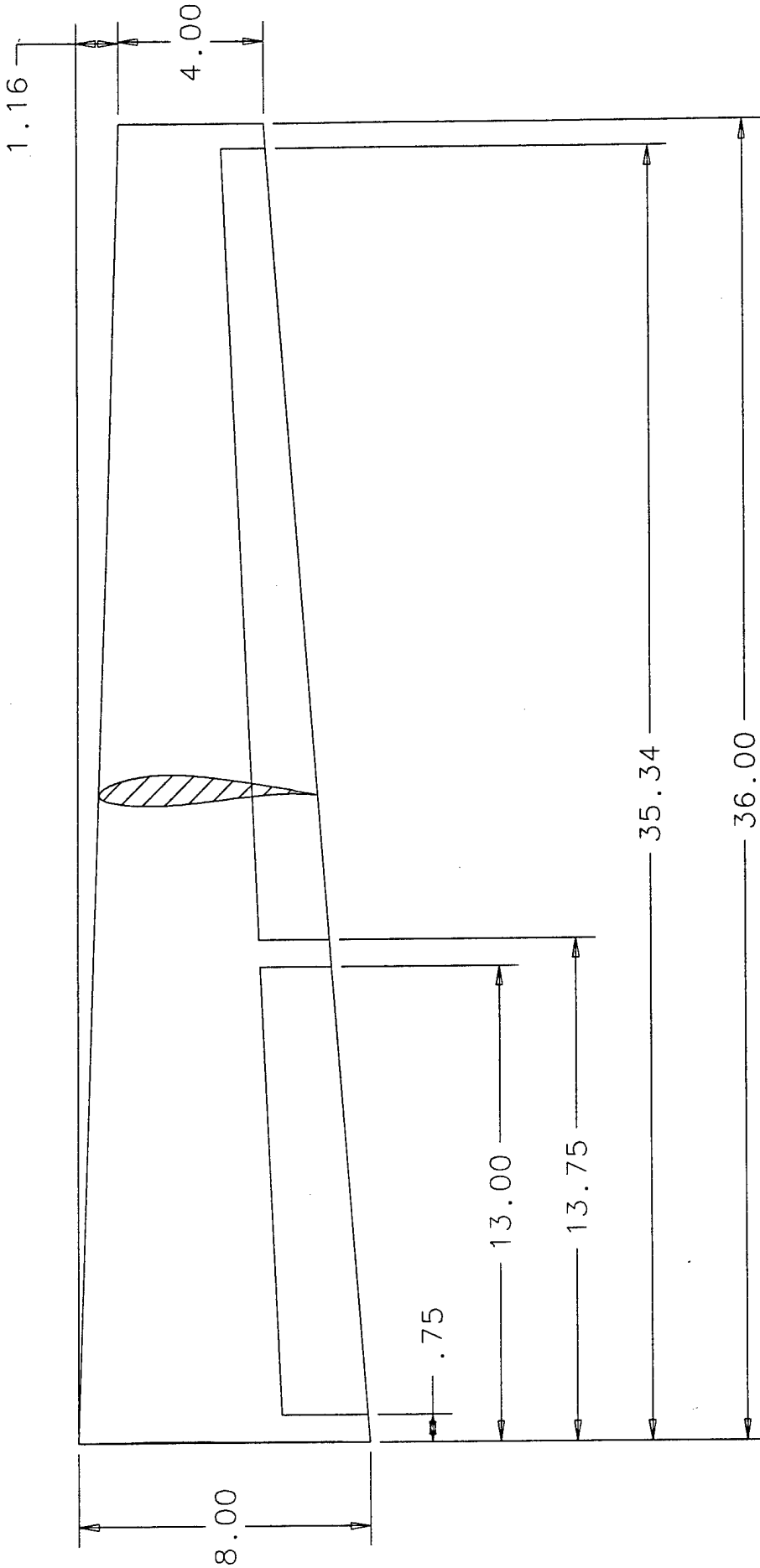
D. Snyder

SCALE

0.175

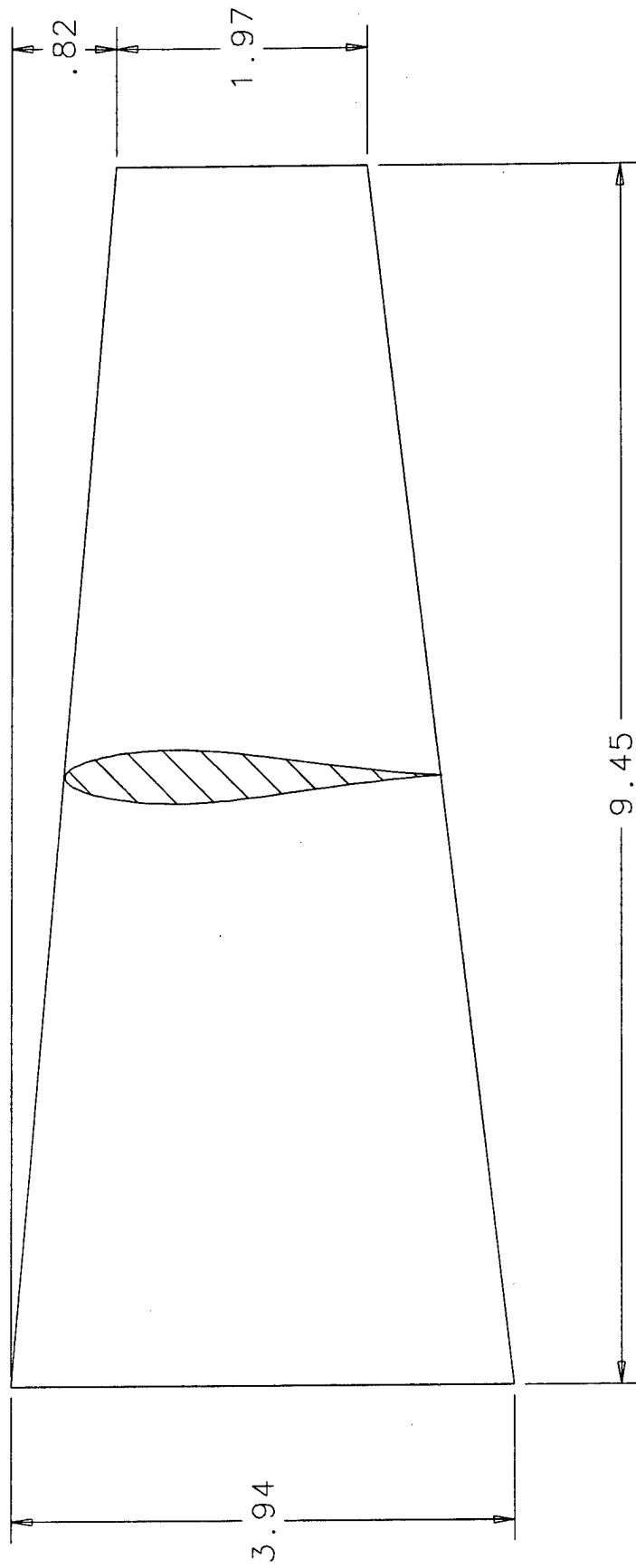
SHEET

2 OF 6



FLAP ANDAILERON  
WIDTH = 30% OF CHORD

ORGANIZATION			
Utah State University			
TITLE			
Wing			
SIZE	DATE	DRAWN BY	
A	02/28/98	D. Snyder	
SCALE		SHEET	3 OF 6
0.230			



ALL-FLYING TAIL:  
ENTIRE SURFACE PIVOTS AS ELEVATOR

ORGANIZATION

Utah State University

TITLE

HORIZONTAL TAIL

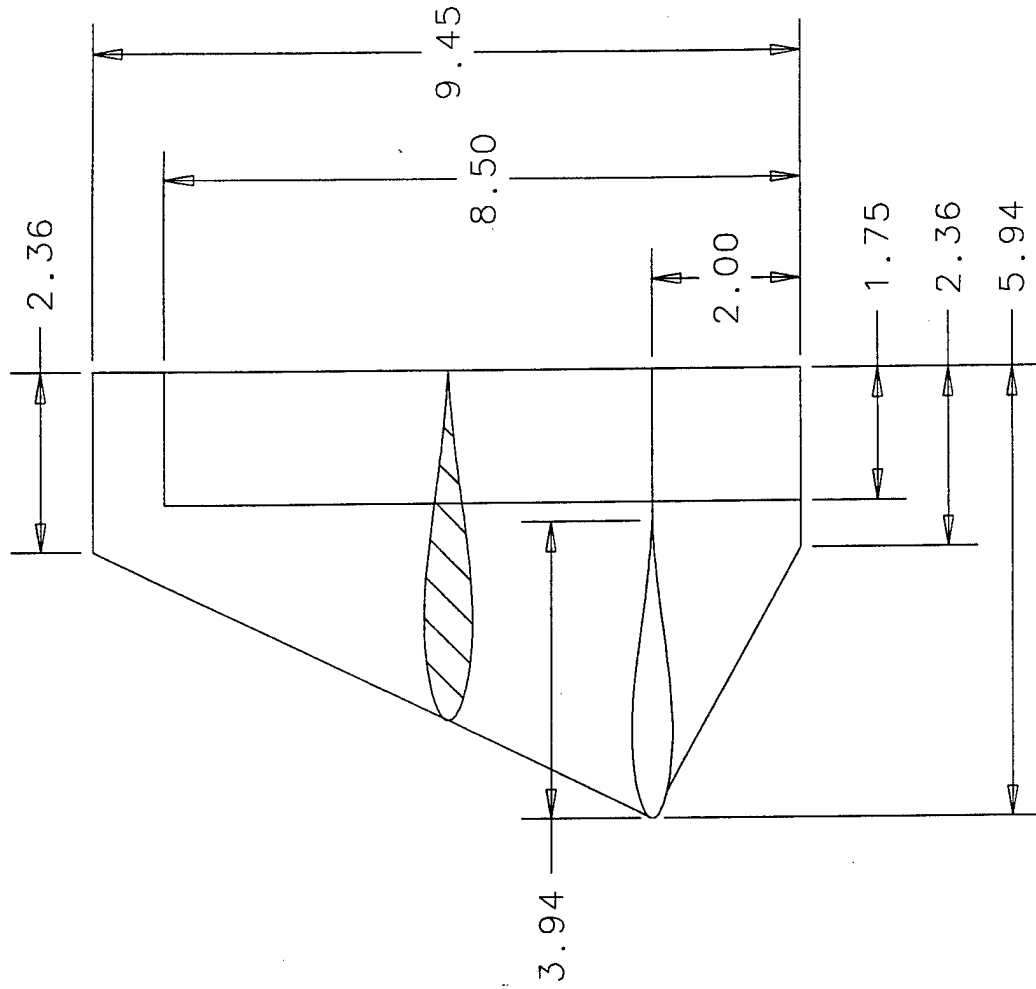
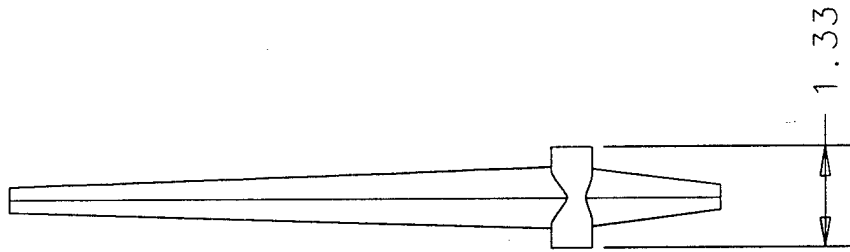
SIZE  
A

DATE  
02/28/98

DRAWN BY  
D. Snyder

SCALE  
0.750

SHEET  
4 OF 6



ORGANIZATION

Utah State University

TITLE

Vertical Tail

SIZE

A

DATE

02/28/98

DRAWN BY

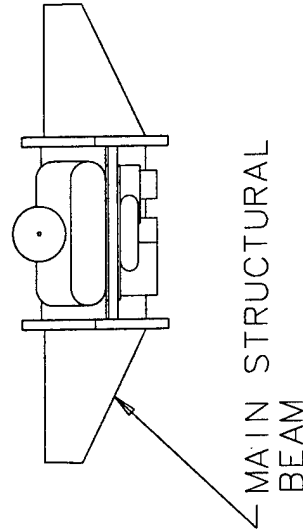
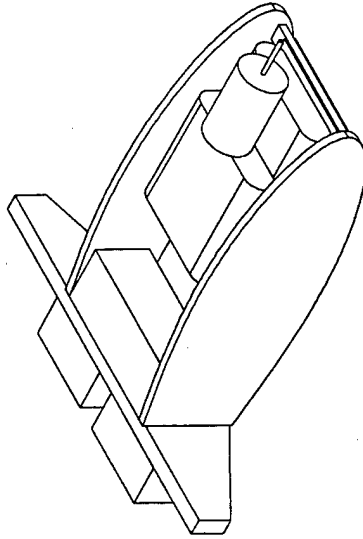
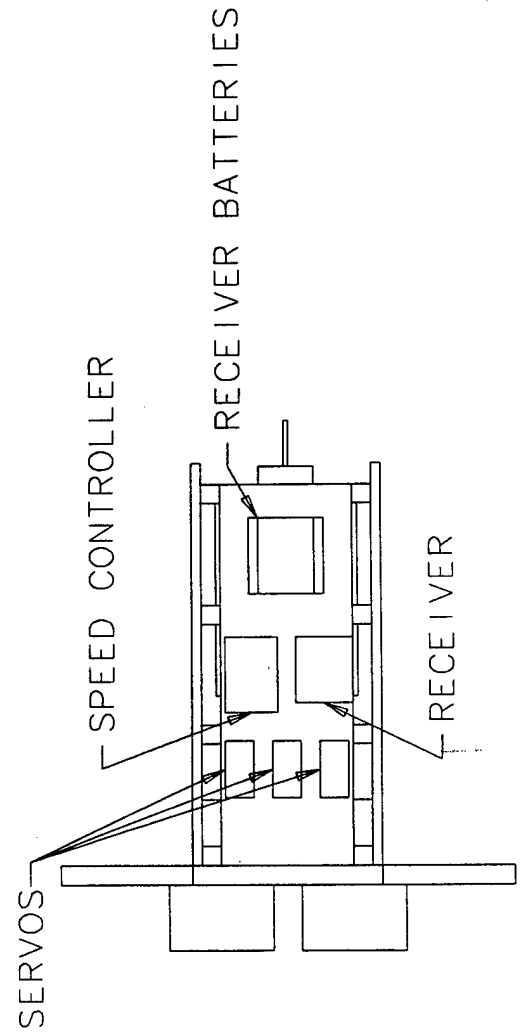
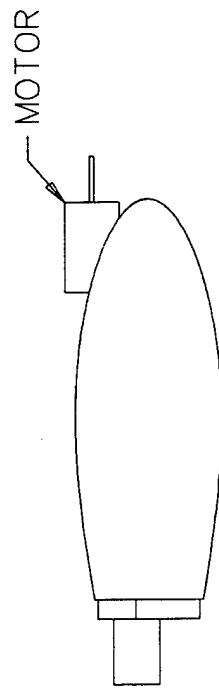
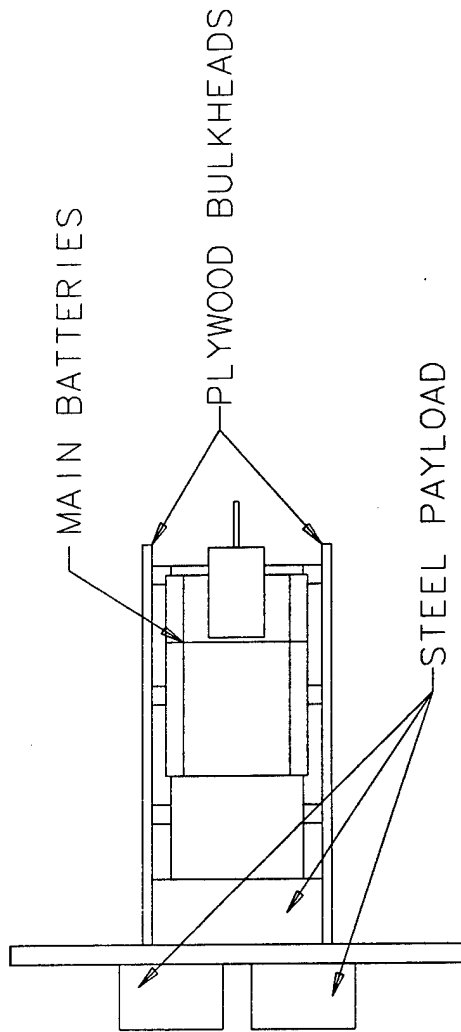
D. Snyder

SCALE

0.400

SHEET

5 OF 6



ORGANIZATION

Utah State University

TITLE

FUSELAGE INTERIOR

SIZE

A

DATE

02/28/98

DRAWN BY

D. Snyder

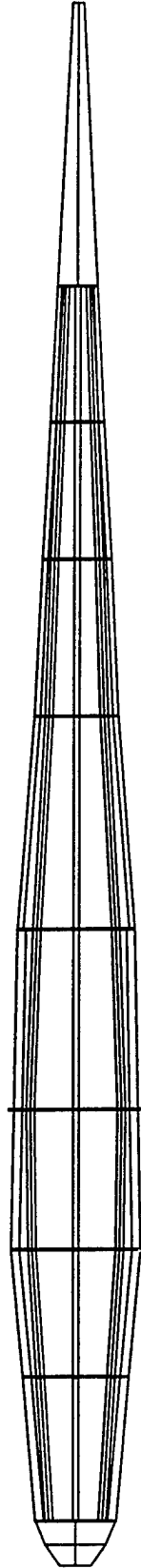
SCALE

0.200

SHEET

6 OF 6

## **Appendix D—Alternate Fuselage Construction Technique**



ORGANIZATION

Utah State University

TITLE

Alternate Fuselage

SIZE

A

DATE

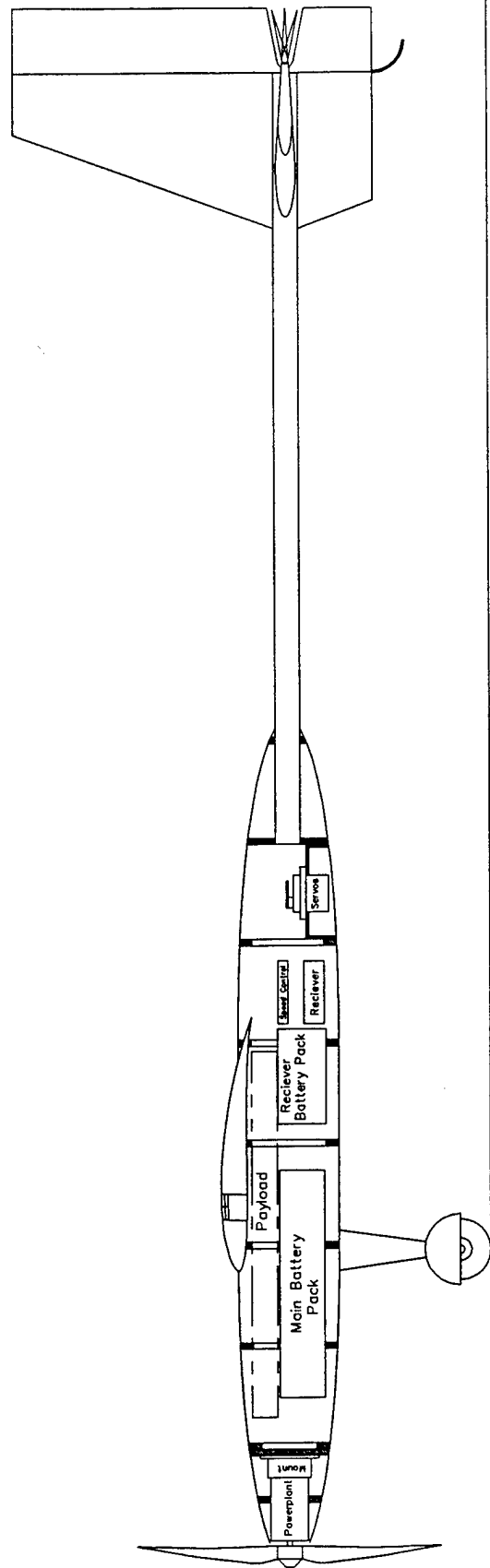
3/10/98

DRAWN BY

S. Thompson

SCALE

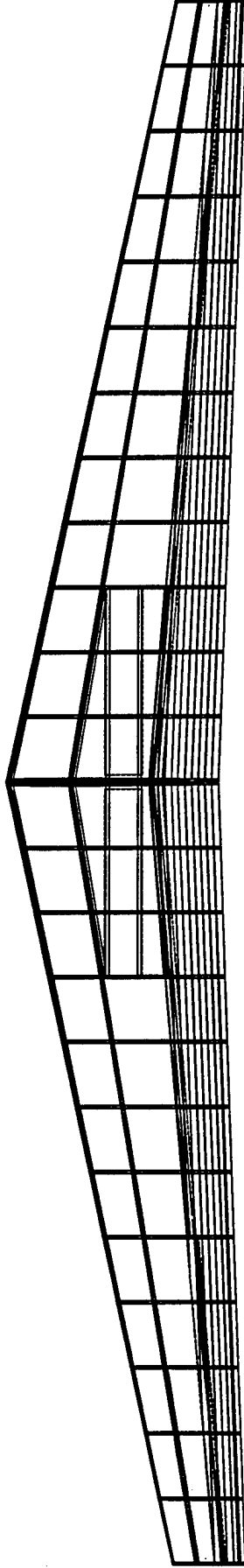
SHEET



ORGANIZATION		Utah State University	
TITLE		COMPONENT CONFIGURATION	
SIZE	DATE	DRAWN BY	
A	2/5/98	M. WATSON	
SCALE		1=10	SHEET 3 OF 3

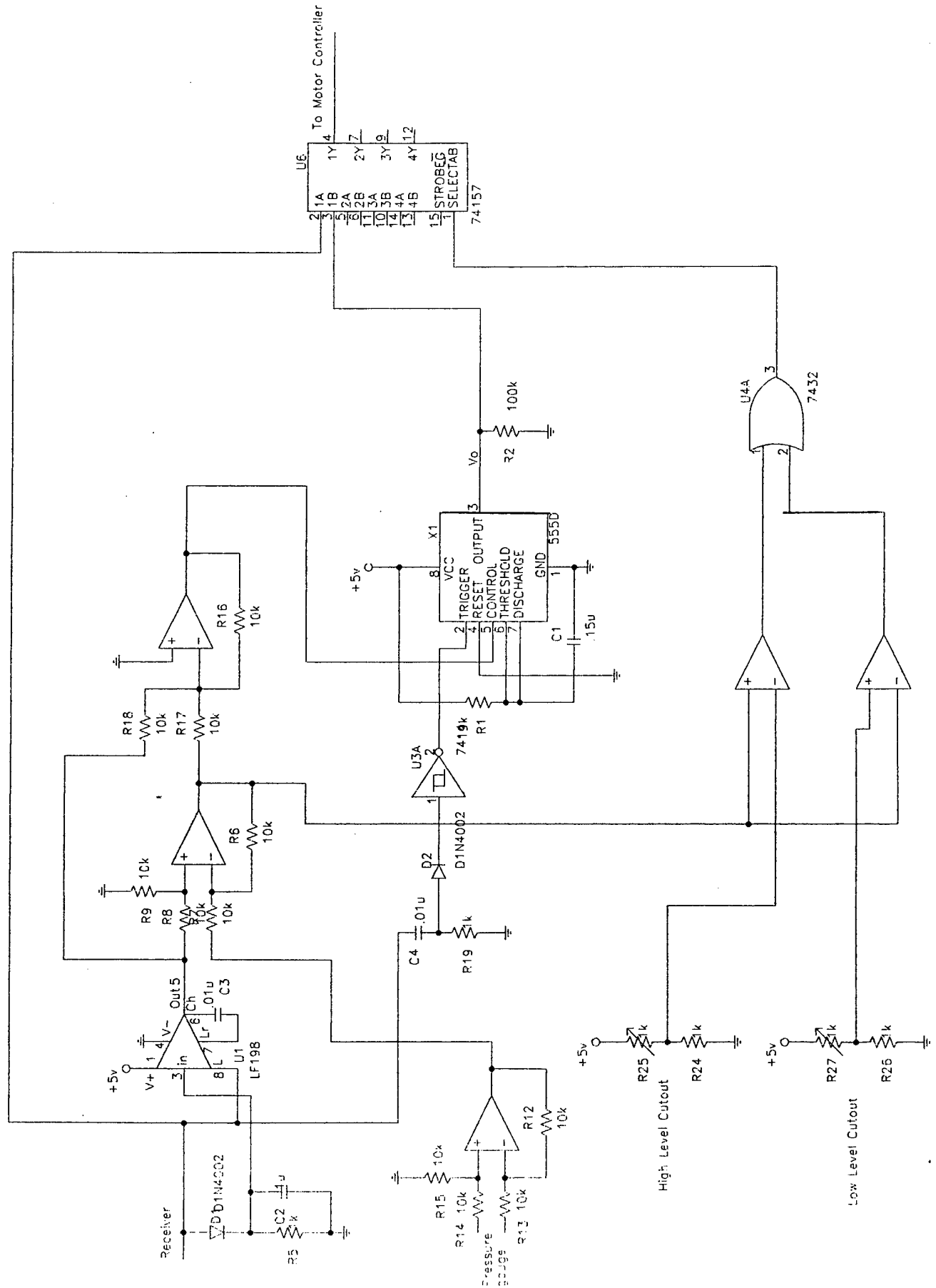


## **Appendix E—Alternate Wing Construction Technique**



ORGANIZATION			
Utah State University			
TITLE			
Alternate Wing			
SIZE	DATE	DRAWN BY	
A	3/10/98	S. Thompson	
SCALE		SHEET	

## **Appendix F—Schematics for Velocity Controller**



---

**1997/1998 AIAA Foundation/Cessna Aircraft/ONR  
Student Design/Build/& Fly Competition**

---

**Design Report--Addendum Phase**

---

**Utah State University**

**April 10, 1998**

# Table of Contents

<b><i>Lessons Learned</i></b>	<b><i>1</i></b>
<b>Differences in Final Contest Aircraft</b>	<b>1</b>
Internal Component Layout	1
Propeller Selection	1
Wind Analysis	3
Cost Summary	6
Time to Implement Changes	8
<b>Areas for Improvement in Next Design</b>	<b>8</b>
Tail Boom Design	8
Main Support Beam in Wing	8
Easy Modifications	8
Battery Pack	8

## Lessons Learned

### *Differences in Final Contest Aircraft*

For the most part, the design team stayed with the airplane design configuration as described in the proposal phase of the Design Report. However, some minor modifications in the fuselage layout were made as needed during the actual construction of the aircraft. Also, some additional analyses and tests were performed that altered the airplane's performance predictions. Specifically, analysis and testing was performed to assist in the selection of the correct propeller and flight speed in varying wind conditions.

### Internal Component Layout

Probably the most significant changes made involved the internal layout of the various components in the fuselage. Before the airplane was actually constructed, the weight of different articles could only be estimated. With these estimations, the layout of the fuselage was developed. Table 1 shows the weight analysis of the completed airplane. (The previous weight analysis is shown in Table 4 on page 24 of the proposal phase of the Design Report). None of the components' weights were heavier than estimated, but the actual weight of the horizontal and vertical tail surfaces was 0.20 pounds lighter. This was a positive development as the total weight of the airplane was reduced to 14.57 pounds as shown. However, this had a significant effect upon the location of the airplane's center of gravity. As a result, modifications were made in the location of the internal components to position the center of gravity properly.

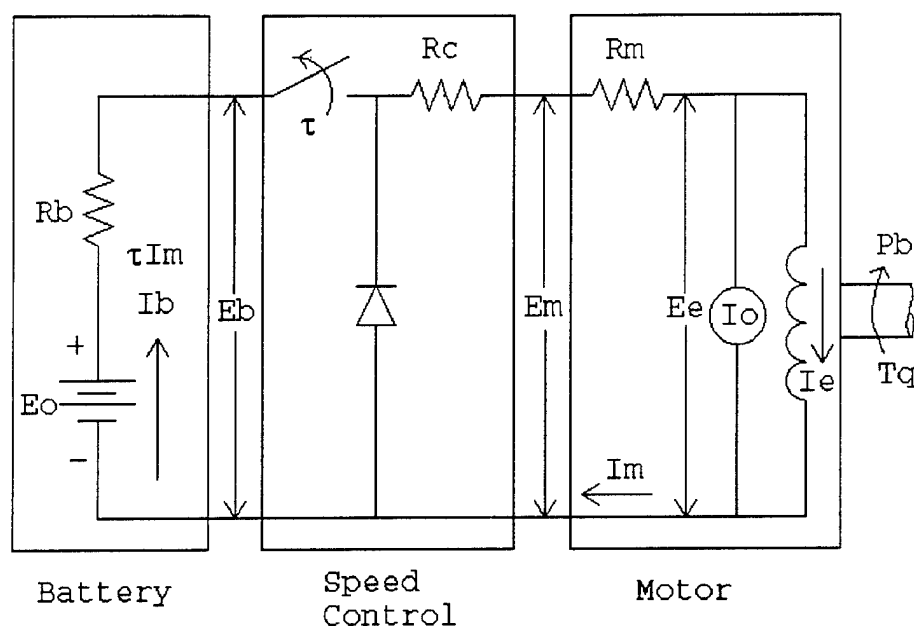
**Table 1—Weight Summary**

<b><u>Airframe Structure:</u></b>	
Fuselage	0.92 lb.
Landing Gear	0.6 lb.
Tail	0.12 lb.
Tail Tube	0.08 lb.
Wings	0.85 lb.
<b><u>Subtotal:</u></b>	<b><u>2.57 lb.</u></b>
<b><u>Internal Components and Payload:</u></b>	
Motor	0.75 lb.
Motor Batteries	2.5 lb.
Motor Speed Control	0.06 lb.
Propeller & Spinner	0.18 lb.
Push Rods	0.06 lb.
Receiver & Servo Package	0.8 lb.
Steel Payload	7.5 lb.
Velocity Controller & Pitot Tube	0.15 lb.
<b><u>Subtotal:</u></b>	<b><u>12 lb.</u></b>
<b><u>Total:</u></b>	<b><u>14.57 lb.</u></b>

### Propeller Selection

As detailed in the proposal phase of the Design Report, the final selection of the electric motor, speed controller, battery pack, and propeller was made with the help of "Mpeff", a program developed by the design team. In general, the design team feels that the mathematical model used to describe the motor,

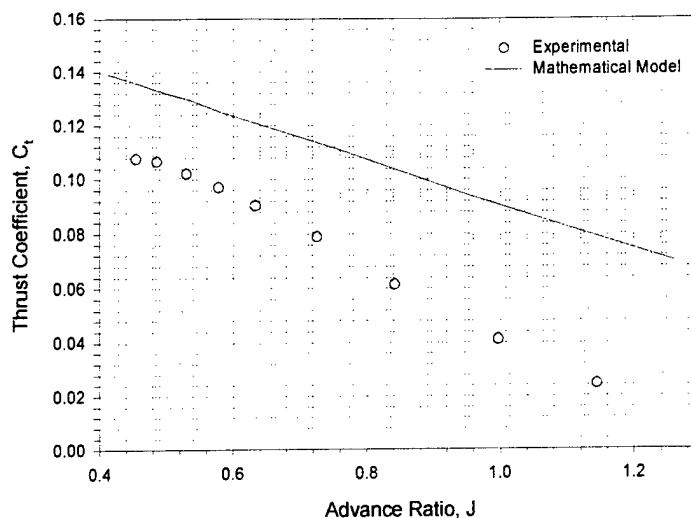
speed controller, and battery pack, as shown in Figure 1 (also see Appendix A of the proposal phase), has been well tested and closely predicts the combined performance of these elements of the power plant. However, since the mathematical equations used to describe the performance of the propeller in this program were derived from very limited information gathered from one source, the design team suspected that the performance results predicted by "Mpeff" were not correct.



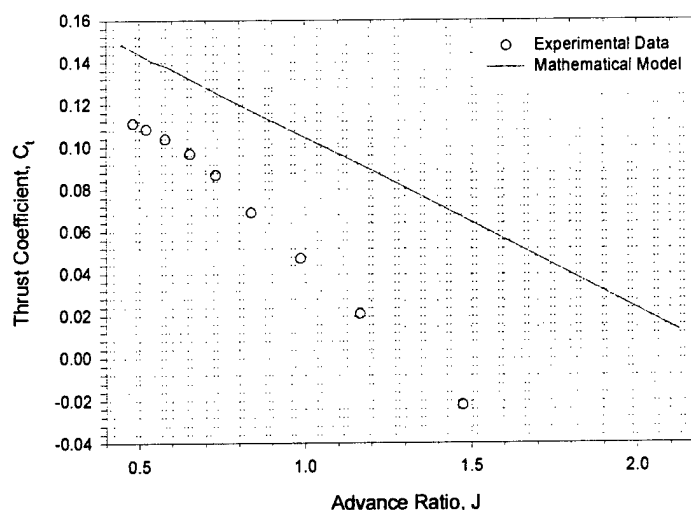
**Figure 1—Schematic of Motor/Speed Control/Battery System**

The design team felt it was necessary to compare the predicted propeller characteristics calculated by "Mpeff" with experimental data. Several propellers were tested in a low speed wind tunnel with the use of a single motor and a direct voltage source. Two plots comparing the experimental data collected during this test with the results of "Mpeff" are shown in Figure 2 and Figure 3. From these two plots, it can be seen that the "Mpeff" program predicts a higher thrust output than the actual thrust output measured experimentally. The difference between the thrust output results was significant enough to warrant a change in the power plant design by increasing the size of the propeller. Initial flight tests indicate that a 12x12 propeller will be sufficient to allow take off in the required distance. Further study of the experimental data will help the design team correct the mathematical equations that describe the propeller performance and update the "Mpeff" program so that it more closely approximates the experimental data.





**Figure 2 – Thrust Coefficient versus Advance Ratio for 11x11 Propeller at an Airspeed of 35.5 MPH**



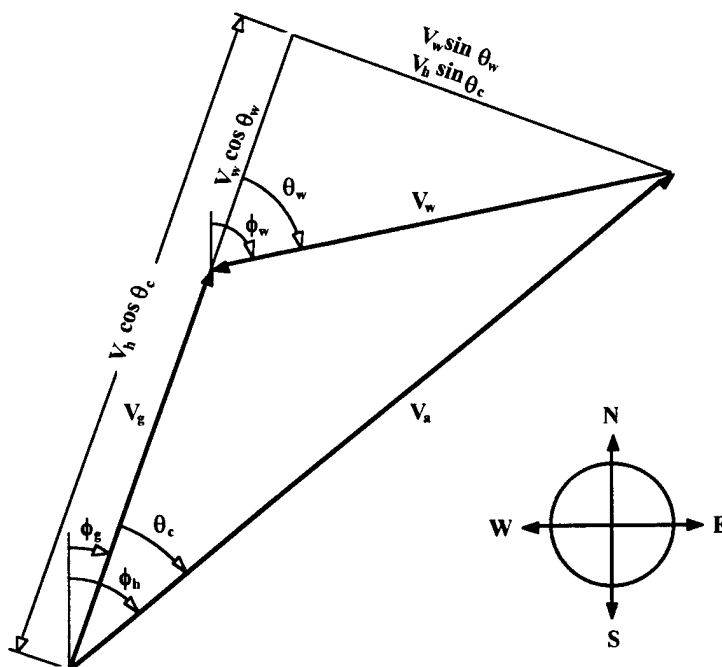
**Figure 3 – Thrust Coefficient versus Advance Ratio for 11x12 Propeller at an Airspeed of 35.5 MPH**

## Wind Analysis

As explained in the design report, an electronic airspeed controller will be used to ensure that the aircraft is flown at its optimum airspeed. Part of this system is a laptop computer running software that calculates the desired airspeed as a function of wind speed. The program, as explained in the design report, calculates the maximum range airspeed as a function of headwind in steady, level flight. The optimum airspeed is different for the upwind leg than for the downwind leg, so it was planned that the airspeed would be adjusted accordingly. However, it was found that this was too much for the pilot to have to do and still safely fly the airplane. So, new software has been developed that calculates the optimum constant airspeed for the entire course as a function of wind direction and speed.

The first step in developing the model was to relate the ground speed to the airspeed and wind speed and direction; Figure 4 shows this relation. From the figure, it is seen that if the aircraft is flying directly into a

headwind, the ground speed will be less than the airspeed by an amount equal to the speed of the wind. If the aircraft is flying directly with a tailwind, the ground speed will be equal to the sum of the airspeed and the wind speed. A crosswind also effects the ground speed of the aircraft because in order to maintain a specified ground track over the ground, the pilot must "crab" into the wind at an angle to the desired line of flight. When flying in a direct crosswind, only one component of the airspeed contributes to the ground speed, the other must balance the crosswind to keep the aircraft from drifting off track.



**Figure 4 – The relationship between ground speed, airspeed, and wind speed**

Using Figure 4, it can be shown that the ground speed,  $V_g$ , is given as

$$V_g = \sqrt{V_a^2 - V_{cw}^2} - V_{hw}$$

where  $V_a$  is the airspeed,  $V_{cw}$  is the crosswind component, and  $V_{hw}$  is the headwind component.

While the aircraft is in a turn, the wind will cause the entire "turning curve" to move. The amount that this curve is shifted,  $X_{hw}$  or  $X_{cw}$ , is simply the wind speed multiplied by the time in the turn, or

$$X_{hw} = \left( \frac{\pi R}{V_a} \right) \cdot V_{hw} \qquad X_{cw} = \left( \frac{\pi R}{V_a} \right) \cdot V_{cw}$$

where  $R$  is the turning radius.

Taking these relations and the course geometry into account, the total time to complete a lap as a function of airspeed, headwind speed, and crosswind speed can be expressed as

$$t = \left( \frac{2L_s}{V_a} \right) \left( \frac{V_a \sqrt{V_a^2 - V_{cw}^2}}{V_a^2 - V_{hw}^2 - V_{cw}^2} \right) + \left( \frac{2\pi R}{V_a} \right) \left( \frac{V_a^2 + V_{cw}^2 \sqrt{V_a^2 - V_{hw}^2}}{V_a^2 - V_{hw}^2 - V_{cw}^2} \right)$$

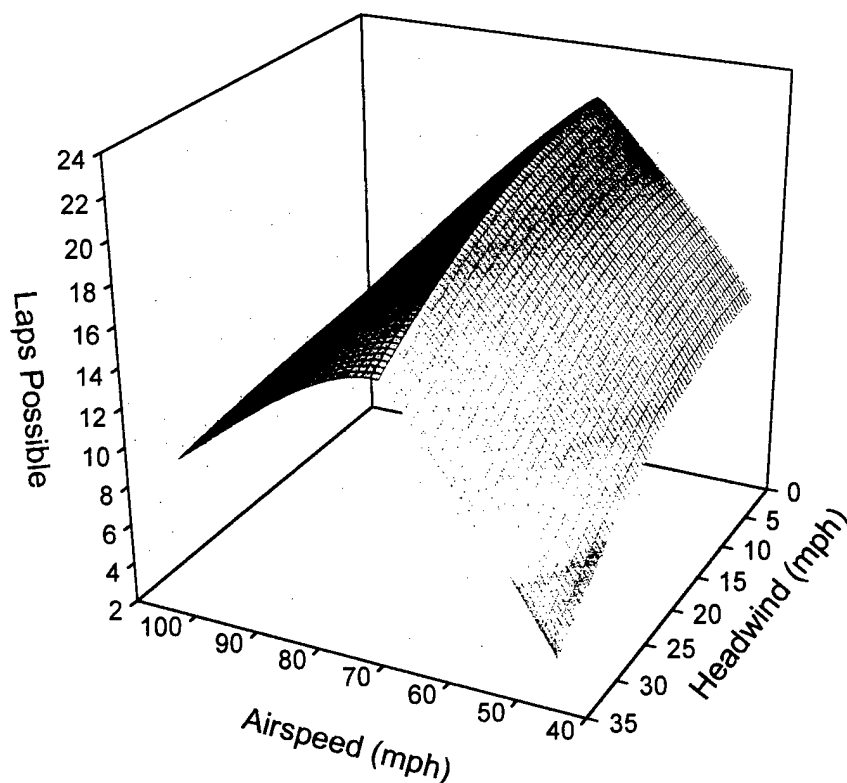
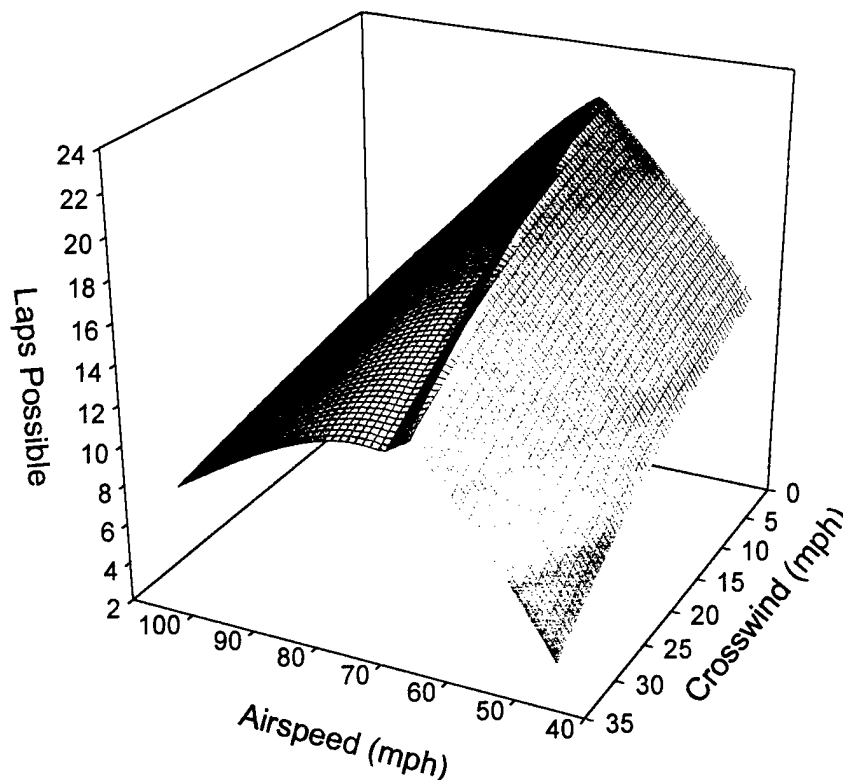


Figure 5—Maximum Number of Laps Varying Headwind



**Figure 6--Maximum Number of Laps Varying Crosswind**

Figure 5 and Figure 6 show the maximum number of laps that can be completed for different magnitudes of headwind and crosswind. The maximum number of laps are calculated from a strictly time-limited approach, and from an energy-limited approach which takes into account the aircraft drag characteristics, battery capacity, and power-plant energy consumption parameters. From these plots, two major characteristics can be seen:

- 1) The cross wind has larger effect on the optimum airspeed than the headwind
- 2) The optimum airspeed decreases with larger wind speeds

Decreasing the airspeed in a wind may seem counterintuitive. In fact, both the energy limited optimum airspeed and the time limited optimum airspeed increase with wind speed. However, for this design the optimum always occurs at the intersection of the time limited curve and the energy limited curve, and this intersection moves to lower airspeeds with higher wind speeds.

The design team feels that this new method of calculating the optimum airspeed is an improvement because the pilot will no longer have to worry about adjusting the airspeed for each leg of the course.

### **Cost Summary**

A summary of the manufacturers list prices of the various items used in the construction of the final design is shown in Table 2. (This is modified from Table 5 on page 36 in the proposal phase of the Design Report). The items shown in red were higher than estimated and the items shown in blue were lower than estimated. The cost of the airframe structure was estimated at \$158.27, but actually was \$174.68. The internal components and payload turned out to cost \$697.23, over \$10 less than the estimated \$707.68. The

cost of construction supplies cost \$75.16, over \$30 more than the expected \$43.45. In all, the final airplane design cost \$947.07, which was almost \$40 more than the \$909.50 cost indicated in the proposal phase.

**Table 2--Design Cost Summary**

<b><u>Airframe Structure:</u></b>	<b><u>MSRP</u></b>
Aircraft Plywood 1/32"	16.00
Aircraft Plywood 3/32"	10.95
Balsa Wood Sheeting 1/32"	37.50
Balsa Wood Supports	3.50
Carbon Fiber Prepreg	25.95
Carbon Fiber Tail Tube	7.00
Hard Wood Dowels 3/16" & 1/4"	0.75
Hinges	1.50
Landing Gear Mount	1.00
Monokote	36.00
Motor Support Clamps	0.80
Plastic Bolts & Nuts 3/8"	4.00
Scotch Tape	1.29
Styrofoam	15.75
Tail Gear	3.00
Tail Tube Support Bracket	1.89
Tail Tube Support Clamps	0.80
Wheels & Collars	7.00
<b><u>Subtotal:</u></b>	<b><u>174.68</u></b>
<b><u>Internal Components and Payload:</u></b>	
Motor	125.00
Motor Batteries	115.15
Propeller & Spinner	30.00
Push Rods	8.25
Radio & Receiver Package	350.00
Speed Controller	65.00
Steel Payload	3.83
<b><u>Subtotal:</u></b>	<b><u>697.23</u></b>
<b><u>Construction Supplies:</u></b>	
Aluminum Templates	1.95
Balsa Filler	10.89
Epoxy	15.95
Glue Accelerant	5.29
Masking Tape	0.79
Rubber Bands	1.98
Spray Glue	12.33
Wood Glue	20.98
Wood Jigs	5.00
<b><u>Subtotal:</u></b>	<b><u>75.16</u></b>
<b><u>Total:</u></b>	<b><u>\$947.07</u></b>

## **Time to Implement Changes**

The manufacturing plan was developed to easily accommodate necessary design changes. As the manufacturing process progressed, the problems were identified and resolved "on the fly". As is typical for this type of project, the actual time required to construct the airplane exceeded the time expected. Therefore, the airplane's completion date was extended by approximately one week due to the modifications previously mentioned.

## ***Areas for Improvement in Next Design***

### **Tail Boom Design**

During initial flight tests, a few problems with interference between the radio and receiver while the motor is running were discovered. It was found that the interference was worse when the antenna was placed near the carbon fiber in the main support beam of the wing and the carbon fiber tail boom. Therefore, a possible remedy to this problem is to use a different material for the tail boom so the antenna can be run through it.

In addition, the carbon fiber tube used for the tail boom was designed to resist bending, but was not designed to resist torsion. This allows the tail section to twist about the main axis when rudder is applied in flight. This does not significantly affect the airplane's performance, but a future version would be improved by using a tail boom designed to better resist torsion.

### **Main Support Beam in Wing**

As is documented in the proposal phase of the Design Report, the main support beam in the wing was designed to withstand a 3.5g load. The beam was tested for strength and it was discovered that the beam can withstand that loading with a safety factor of three. Therefore, the main beam could be made smaller and lighter in a future version of the wing. The size of the beam in the current design caused some difficulties in maintaining the proper airfoil shape in the wing sections. Thus, reducing the beam size would also provide benefits in the aerodynamic performance.

### **Easy Modifications**

One definite improvement for a future design is to allow for easier access, modification, and repair of the various components of the airplane. Some items are permanently built into the structure, so in order to access them, parts of the airplane would have to be disassembled.

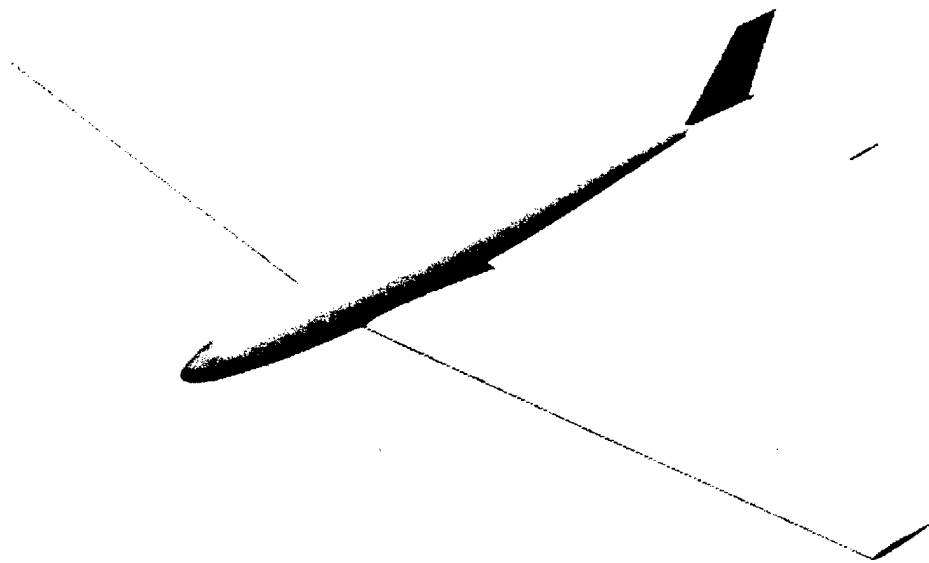
### **Battery Pack**

When the 19-cell battery pack was ordered from the manufacturer, it was clearly stated by the design team that the finished weight was to be less than 2.5 pounds. Upon inspection of the delivered product, it was found that the manufacturer had cut a few corners in order to meet this weight requirement. Most noticeably, the connectors between the individual cells are too small, causing excess internal losses and generating much heat. To prevent this from occurring in a future iteration, the design team would find a battery pack manufacturer here at the university so that closer control could be maintained over the manufacturing process.

# **Virginia Tech Team**

## **1998 Design/Build/Fly Competition**

### **Proposal**



March 16, 1998

## EXECUTIVE SUMMARY

---

The Virginia Tech team proudly presents Hokie Bird III in response to the Request for Proposals for the 1998 AIAA/Cessna/ONR Design/Build/Fly Competition. A drawing of the proposed aircraft is shown in Figure 1. The aircraft is a conventional design, with a single tractor propulsion system and an aft mounted empennage.

The management structure of the team was informal in nature, which allowed maximum flexibility in the distribution of tasks. Participation in the project was strictly voluntary, and no class credit was received for work on the project. This ensures that all team members are motivated by the project rather than requirements.

The conceptual design of the aircraft was selected through a set of quantitative and qualitative criteria. The conventional configuration was chosen because it was determined to be the most competitive design over a broad range of issues. Other arrangements considered were a flying wing, canard, displaced tail, inverted gull wing, and a pod mounted motor design.

Preliminary sizing was accomplished through the use of the RACE spreadsheet written specifically for this competition. The spreadsheet used component weight calculations, propulsion system calculations, and aerodynamic calculations to converge to the preferred configuration arrangement. Takeoff performance was calculated, and trajectory optimization was done to improve the efficiency of competition flights.

Propellers which might work in the design were identified through the use of computer codes written for the competition. A test matrix of various gear ratios, propeller pitches, propeller diameters, and motors systems has been established. Preliminary wind tunnel tests of the propulsion system have been conducted in the Virginia Tech Open Jet Wind Tunnel. Subsequent tests will be used to finalize the selection of the propeller and motor system. Data will be compiled to ensure the propellers will produce sufficient thrust to meet the take off and cruise requirements of our design. The most promising combinations will then be flight-tested to see if the predicted performance is realized.

Beam theory analysis was used to design the wing spar for expected flight loads and the loads imposed by the static ground test. A retractable taildragger landing gear system was chosen for Hokie Bird III to reduce drag in flight. This system was designed to keep the weight penalty associated with retractable gear to a minimum. Tail surfaces were sized conservatively to ensure good stability and control of the aircraft. A low wing design allows the payload to be carried over the CG while using the wing support structure to bear these loads. The motor is located near the center of the fuselage to minimize the pitching moment associated with thrust changes.

The design phase of the project encompassed roughly the first half of the fall semester. Other design tasks, such as the propulsion system testing, are still ongoing. Construction of the aircraft began immediately following the freezing of the final configuration. The construction process undertaken by both experienced students and those with no prior construction experience. Training inexperienced members is the most time consuming task of the project. Inter-group communication and staying on schedule were considered extremely important.

The aircraft fuselage is constructed of molded carbon fiber composites. The wing uses a foam core sheeted with balsa wood, with a spruce box spar. Tail surfaces are foam cores sheeted with



hardwood laminate. Fuselage and tail surfaces will be painted, while the wings will be covered with Monokote.

Test flying is scheduled to begin at least a month before the competition. Test flights of Hokie Bird III are expected to be the most productive area of refinement. A near complete lack of prior flight testing and experience prevented the 1997 competition team from capitalizing on improvements in several inefficiencies in the aircraft. The development period for propeller, motor, and aerodynamic refinement will require at least a month to complete. The success of our design on competition will hinge on the improvements made as real world experience dictates.

The team concept, coupled with a multiple point attack on our design criteria will help to ensure a competitive design in competition. Theoretical modeling, controlled tests in wind tunnels coupled with full scale flight tests should allow the Hokie Bird III to be one of the most highly refined designs in the field.

## MANAGEMENT SUMMARY

A team consisting of freshmen, sophomores, juniors, and seniors was formed at the beginning of the 1997-98 school year. This team set the goal of having a flying aircraft at least one month ahead of the competition date. The successful interaction between all team members is vital to the success or failure of Hokie Bird III.

The varied composition of the team and relatively small size of between six and sixteen members allowed a relaxed management structure. All members of the team were involved with the major configuration decisions. This process quickly eliminated from consideration all configurations that would have been difficult to fly or manufacture. After the final configuration was chosen all members agreed to forgo any major changes unless experience dictated otherwise. All team members are working on the construction of several aircraft components. The management structure consists of one team leader who makes sure all deadlines are met and who is responsible for finding a way to make up time if a delay occurs. Figure 2 illustrates how the main divisions of the team relate to one another. All members are participating in aircraft construction. The other tasks are the main responsibility of the individuals listed.

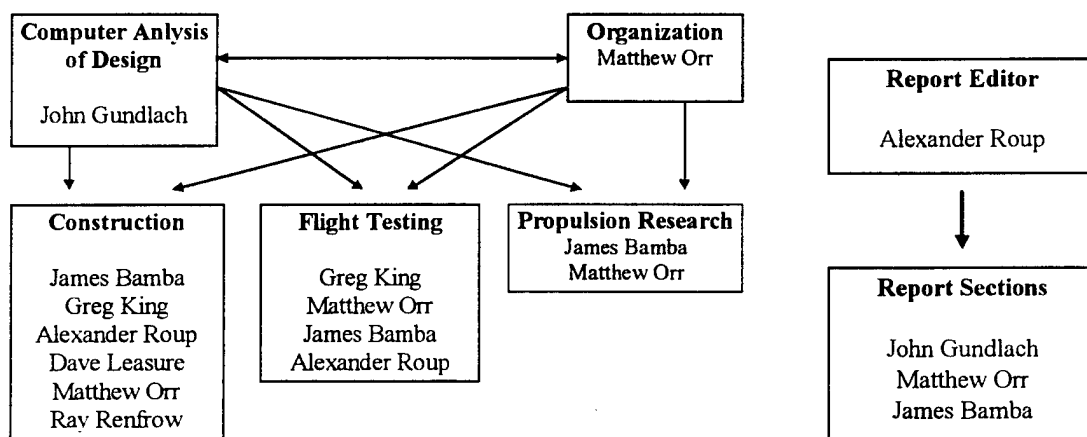
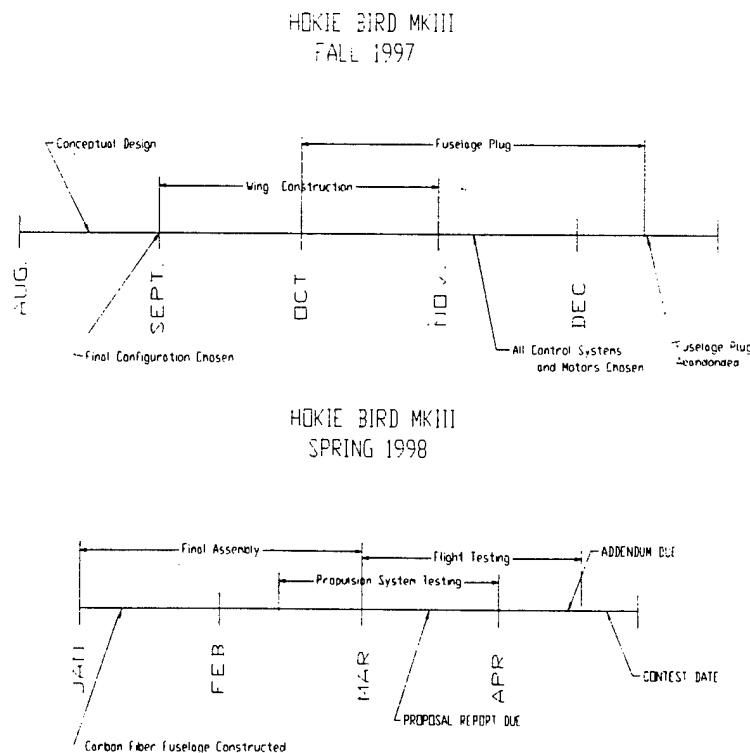


Figure 2--Management Structure

The project timeline is shown in Figure 3. The schedule detailed in the timeline has been updated to show when events occurred. When the fuselage plug was not finished in time to meet the deadline at the end of the first semester an alternative fuselage mold was obtained. This change put the construction back on schedule in relation to the original timeline formed at the inception of the project. The budget of the project is provided from our sponsor Allied Signal and through the Aerospace and Ocean Engineering Department at Virginia Tech. Our team manager consults with the faculty advisor whenever any major problems arise. This keeps the project on track toward the scheduled milestones. The perspective of a non-participant in the project is often refreshing because it can lead to the consideration of options not considered by the team.

A disciplined approach has been applied to construction. The airframe is complex and its construction requires much of the time available to complete. Full team meetings every Monday night and frequent email messages have allowed the team members to discuss topics in a timely manner and keep all members informed of the tasks that need to be performed over the coming weeks and months. One of the few problems encountered to date is the lack of knowledge of basic construction techniques by the students involved with the project. Training of new members takes time but is essential to the future success of the project. The more experienced members of the team have often paired off to guide others through both the design and construction processes that were new to them



**Figure 3—Milestone Chart**

## CONCEPTUAL DESIGN

---

Lessons learned from the 1997 AIAA Student Design/Build/Fly competition design process and flight testing of the 1997 competition entry, Hokie Bird II, resulted in an accelerated conceptual design process this year. Conventional, flying wing, displaced tail, and canard configurations were revisited to see if any advantage could be gained from changing the layout given the modified requirements. For various reasons the conventional configuration was selected once again.

A conventional configuration offers a high lift to drag ratio ( $L/D$ ), high endurance parameter ( $C_L^{3/2}/C_D$ ), is easily controllable, and allows more options for component arrangements. Also, this configuration offers the largest database of successful aircraft to help guide the design, and the pilot has the highest comfort level with this type. This design will be used as a benchmark for the other alternatives. The three versions of a conventional configuration are a conventional arrangement of wing/fuselage/tail, an inverted gull wing, and a low fuselage with a pod motor mount.

The flying wing is the simplest design to manufacture. However, the maximum attainable lift coefficient is much lower than that of a conventional design, which causes increased take-off and landing distances. Also, trim restrictions make the use of flaps impractical. Yaw control is difficult without the use of winglets, and if winglets are used, the design may as well be changed to a displaced tail. The lift to drag ratio for a flying wing is typically lower than that of a conventional design, and the lift to drag ratio is the main parameter for constant power range performance. At higher airspeeds the total drag of the flying wing could be lower due to a smaller frontal and surface area, resulting in a greater endurance. However, a high lift coefficient is required in the turns and the payload requirements make the  $L/D$  and endurance parameter stronger driving factors than minimum drag at higher speeds, thus making a flying wing the least desirable alternative from a performance standpoint. Also, due to the short coupling of the control surfaces, the extra expense of a gyro might be necessary to maintain stability.

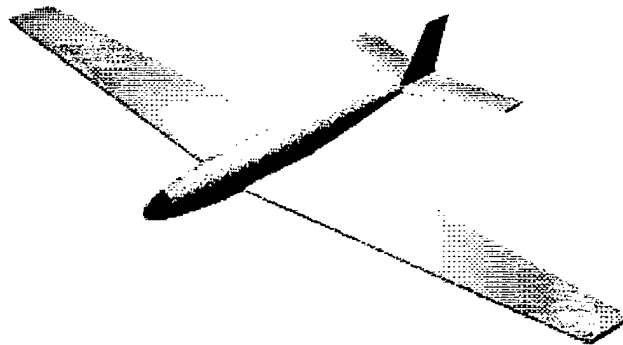
A canard configuration offers great aesthetics and, if designed properly, is incapable of conventional stall. However, the canard has a lower lift to drag ratio than a conventional design, a lower maximum lift coefficient, and offers no reductions in complexity. There is no compelling reason to select a canard layout.

The displaced tail design, shown in Figure 4, offers the simplicity of a flying wing with the aerodynamic efficiency close to a conventional design. However, the torsional strength requirements of this configuration lead to a heavy wing structure. The fuselage frontal area would be similar to the conventional design. Unlike the conventional design, the short tail moment arm leads to large tail surfaces. Tricycle landing gear is necessary because of the short fuselage and would be heavier than a tailwheel arrangement. Though an aesthetically pleasing configuration, it does not offer significant advantages over a conventional design for the 1998 competition.



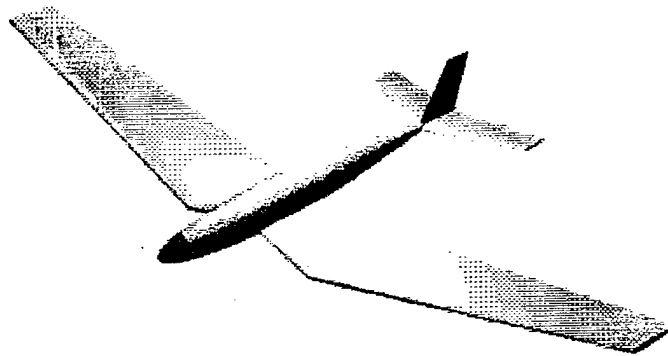
**Figure 4—Displaced Tail Configuration**

The conventional wing/fuselage/tail configuration, shown in Figure 5, has several benefits, thus making it a popular selection for the majority of aircraft designs. Some of the most notable strengths of this configuration are its simplicity of construction, relative predictability of handling qualities, and ease of analysis. The thrust line is very close to or at the centerline of the aircraft, making effects of changing power settings on aircraft trim very small.



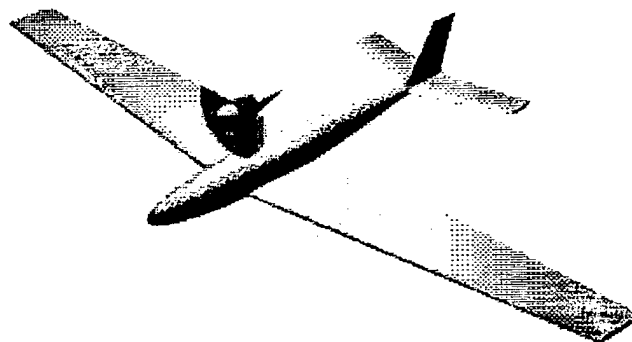
**Figure 5—Conventional Configuration**

The inverted gull wing configuration, shown in Figure 6, is a conventional configuration with the inboard wing panel having a sharp anhedral that abruptly changes to dihedral after the landing gear. The benefit of this configuration over a straight wing with protruding landing gear is that the landing gear length is greatly reduced, which may improve the combined aerodynamic efficiency of the wing/landing gear combination. It is also less susceptible to mechanical failure, less complex, and possibly lighter than a retractable gear system. The drawbacks of this design include increased structural weight and complexity of manufacture.



**Figure 6—Inverted Gull Wing Configuration**

The low fuselage with a pod motor mount, shown in Figure 7, is essentially a conventional design with a low, glider-like, fuselage with wheels protruding from its underside, with a motor pod above the fuselage. The benefits of this design include decreased landing gear weight and drag, and reduced take-off distance due to a strong ground effect associated with the low wing. Unfortunately, this significantly larger ground effect will increase floating on landing, and the wings will not be allowed to travel through a safe roll angle range without striking the tips on the ground. The aft portion of the fuselage would need to be angled upward to allow for rotation, unless a constant lift coefficient take off were allowed. This constant angle take-off and landing would result in a high take-off speed and landing speed. An angled tail boom would result in a fuselage drag increase. The vertical distance between the thrust line and the center of drag will necessitate thrust dependent trim changes, resulting in a larger horizontal stabilizer that produces more drag.



**Figure 7—Pod Motor Mount Configuration**

The conceptual design decision criteria are listed in Table 1. The conventional configuration was chosen for reasons of efficiency, manufacturability, and operational reliability.

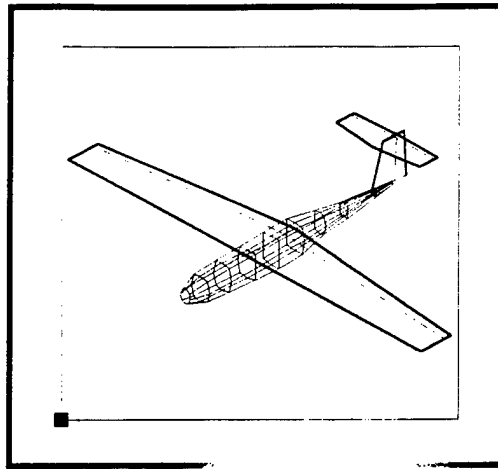
	Maximum Value	Conventional	Inverted Gull Wing	Pod Motor Mount	Displaced Tail
<b>Figure of Merit</b>					
Simplicity of Construction	20	20	10	15	18
Uniqueness	10	4	10	6	10
Expected Efficiency					
Due to Wing Configuration	15	15	10	15	15
Due to Powerplant/Propeller Configuration	15	15	15	12	12
Due to Landing Gear Configuration	15	10	13	13	8
Due to Empennage Configuration	15	15	15	15	13
Landing/Takeoff Performance and Reliability	10	10	10	6	10
<b>Total</b>	<b>100</b>	<b>89</b>	<b>83</b>	<b>82</b>	<b>86</b>

**Table 1—Conceptual Design Selection Criteria**

## PRELIMINARY DESIGN

Design work for both preliminary and final design phases was done in the RACE spreadsheet, written in Microsoft Excel. All aerodynamic and electric propulsion performance calculations, as well as weight estimation, layout, and sizing were written in Excel as a second generation of the ELEC Fortran program used to design Hokie Bird II for the 1997 competition. Microsoft Excel was selected as the most appropriate software for the design tool because Excel allows faster coding than with a programming language, the outputs can be easily seen, and an optimizer is available.

RACE uses the graphics of MeasureC, an Envision Designs program that determines aircraft stability and displays an aircraft image as a graph. MeasureC requires a large number of aircraft dimensions to perform the analysis or show the aircraft graph and can be overly cumbersome to manipulate. Although this program is useful for many applications, it is not diverse enough for the UAV design effort. RACE has an interface between the user and graphing portion of MeasureC that uses convenient parameters such as aspect ratio, taper ratio, and tail volume coefficients rather than XYZ coordinates. Figure 8 is an example of the graphical output of RACE.



**Figure 8—Graphical Output of the RACE Code**

There are two options for determining the wing area, span, and aspect ratio. The first option requires the root chord and wing span as inputs, and then the wing area and aspect ratio will be calculated. The second option requires the entry of wing area and either the wing span or desired aspect ratio, and outputs are either wing aspect ratio or the wing span, respectively. Both alternatives allow wings of up to six panels, each of which can have sweep, taper, dihedral, and a designated percentage of the total span.

The weight build-up and center of gravity section sums the component weights and longitudinal locations to determine the total weight and center of gravity of the vehicle. To find the weight of a balsa-covered foam core wing the volume and surface area must be determined. The product of the wing volume and the foam density gives the foam weight; the product of wing surface area, balsa weight per unit area, and epoxy mass fraction yields the skin weight. The sum of the skin, foam and spar is the total wing weight. Determining the weight of the spar was considerably more challenging. The program described later in the spar design section was used to design numerous spars from sets of systematic manipulations of several variables such as wing span,  $b$ , aspect ratio,  $AR$ , taper ratio,  $\lambda$ , airfoil thickness to chord ratio,  $t/c$ , take-off weight,  $W_{TO}$ , and maximum load factor,  $n$ . A regression analysis was performed to derive the following function to estimate the weight of a spruce box beam spar based on a baseline of similar specifications to the final design:

$$W_{spar} = 0.0000034(b)^{1.1959}(AR)^{.6794}(\lambda)^{.2421}(t/c)^{.6164}(n * W_{TO})^{.8686} \quad (1)$$

The weight estimation does not include the weight nor the strength of the carbon fiber cap strips used in the competition airframe, as they are there only for an extra factor of safety. Since the spar weight is a function of the take-off weight and the take-off weight is dependent upon the spar weight, the take-off weight had to be solved iteratively. Horizontal and vertical stabilizer weights were estimated in a similar manner except no spar was present. The fuselage weight was estimated by:

$$W_{fuse} = Const * W_{wing} * \frac{L_f}{b} \quad (2)$$

where  $L_f$  is the fuselage length, and the constant is approximately 1.0 based on similar models. Weights of components such as the motor, speed control, servos, batteries, and numerous other items were added, as was the product of the weight and the distance from a reference. The locations of the components were then adjusted until the actual center of gravity corresponded to the desired location found through the stability analysis.

The performance section outputs the  $L/D$ ,  $C_L^{3/2}/C_D$ , drag, velocity,  $C_L$  of the wing,  $C_L$  of the horizontal stabilizer, and whether or not any part of the wing has stalled. The user or solver program inputs the angle of attack of the wing at the main user interface. Prandtl linear lifting line theory is then used to determine the lift distribution, the 3-D lift coefficient, and the stall condition of the wing. The wing is considered to be stalled if any local lift coefficient exceeds the maximum section lift coefficient of the selected airfoil. The horizontal stabilizer 3-D lift coefficient is found from static stability requirements. These two lift coefficients are normalized on associated areas and combined to determine the total lift coefficient for the entire aircraft and the level flight velocity. The profile drag coefficients for the wing and tail sections were found by interpolating between lift coefficients and Reynolds numbers. Several section drag coefficients were found for the wing along the span based on the 2-D lift coefficients determined from Prandtl lifting line theory. The fuselage drag coefficient was based on methods found in Hoerner's *Fluid Dynamic Drag*<sup>1</sup>.

The propulsion section outputs the endurance; propulsion efficiencies; and both the currents and voltages of the battery, speed control, and motor. Inputs are the propeller pitch, diameter, and solidity; resistance and maximum currents of each component; and motor RPM/volt and no-load current. Coefficient of power and coefficient of thrust versus advance ratio data is available for three separate propellers. Two have the same pitch/diameter ratio and two have the same solidity, with one overlapping data set. The selected propeller's data is found by interpolating its pitch/diameter ratio and solidity with that of the reference propellers. Given the flight speed and required thrust from the performance section, the propeller RPM, power absorbed and efficiency are found. A quadratic equation including terms such as RPM/volt, motor no-load current, and various resistances is then solved to find the battery current. Once the battery current is known, the voltages and currents of all the components can be found. The total power from the battery at the given flight condition is

$$P_{batt} = I_{batt} V_{batt} + I_{batt}^2 R_{batt} \quad (3)$$

The total energy of the battery is

$$E_{batt} = AH * V_{batt} \quad (4)$$

where AH is the battery capacity in Amp-hours. The endurance of the battery discharge at a steady rate is modeled as:

$$T = \frac{E_{batt}}{P_{batt}} * \%SOC \quad (5)$$

where %SOC is an approximation of the useable percentage of the initial battery state of charge. If a battery is expected to be discharged at high currents, the %SOC will be lower than for lower current due to resistance losses.



The electric propulsion system analysis involves the propeller, gearbox, motor, speed control, and batteries. Two scenarios must be evaluated, one for maximum power output, and one for less than maximum power output. For the first scenario, a current limit exists for either the motor, speed control, or battery system, and determines the maximum power that can be produced.

The electric propulsion system has to be a combination of commercially available batteries, motors, speed controls, gear boxes, and propellers. Because designing specialized parts for this system is against the contest rules, a true optimization is not possible. Instead, a trial and error method in which combinations of discreet electric propulsion system elements must be implemented.

### **Takeoff Performance**

Take-off performance analysis involves the thrust produced by the propeller as the aircraft speeds up, decrease in rolling resistance as the aircraft produces lift, and changing drag coefficient as the Reynolds number increases. The take-off velocity is assumed to be 1.3 times the stall speed, and for simplicity, the take-off roll is assumed to occur at a constant lift coefficient associated with take-off speed. The climb past the 6-foot obstacle is also assumed to occur at the same lift coefficient.

### **Trajectory Optimization**

The objective of trajectory optimization is to attain the maximum speed possible while staying aloft for seven minutes after the initial turn demonstration. The course consists of two parts: straight and level flight, and the turning flight. The aircraft is assumed to fly at the same velocity in turns as in straight and level flight and without changing altitude as a worse case scenario. Competition flight profiles will likely involve some vertical maneuvering to slow the aircraft before initiating turns, but flight tests will determine the fastest turning method. Even so, a conservative analysis is preferred so errors will lead to higher speeds rather than lower. The bank angle,  $\phi$ , and the angle of attack are variables used to find the best turn radius that meets the criterion, and usually results in a lift coefficient close to stall. If the radius is made too small, the aircraft will require excessive power to maintain level flight. If the radius is too large, the power requirements will be lower but the turning time will be too great, resulting in a high energy loss. The bank angle resulting in minimum energy loss is 45 degrees, but the aircraft must pull bank angles around 60 degrees in order to turn as quickly as possible.

Level flight velocities roughly corresponded to that of maximum L/D, but usually slightly faster. At first glance this competition appears to be a pylon race for overweight models where minimum drag is the most significant factor, but upon closer inspection the payload capacity requirements and limited energy drive the design closer towards a range optimized aircraft where L/D is the most significant parameter. Use of the cambered SD7032 section is a result of necessity of a high L/D.

## **DETAIL DESIGN**

---

### **Aerodynamic Analysis**

The RACE software was used for some aspects of the detail design stages. The same procedures described in the previous section were used to evaluate the final configuration.

The Selig Donovan SD 7032 and modified SD 7032 airfoils were selected for the wing of Hokie Bird III<sup>2</sup>. This airfoil and its modified derivative were two candidates among over 50 sections for which data was readily available. Data from each airfoil was used in the performance program and the SD 7032 yielded the best compromise for speed, endurance, and take-off distance. Airfoils with a large trailing edge cusp such as the Wortman FX63-137 were not selected because construction would prove to be significantly more difficult than with lower-cambered sections, and because the such sections did not yield the highest performance. A SD 7032 with the thickness modified to 15% was used at the root to house the retractable landing gear. A standard SD 7032 is incorporated from midspan to the tip.

### **Propulsion Testing Introduction**

Wind tunnel tests are being conducted in the Virginia Tech Open Jet Wind Tunnel to find the optimum combination of propeller and motor at flight airspeed. Wind tunnel testing will be safer than flight testing, because reducing the amount of flight time will reduce the probability of a crash in the testing phase of the project. Also, the efficiency of the power system can be tested while the rest of the plane is still being built. Testing the reliability of the motor is also a desired to avoid any problems with electric motors such as those that were encountered in the 1997 competition. Preliminary tests of the motor systems have already been performed. Further tests are planned before a final propulsion system is chosen.

Hokie Bird III will require the maximum available power for takeoff and climb, but it must be able to fly at partial throttle to finish the expected nine-minute flight time. During a competition flight, the aircraft will climb, make 360 degree left and right hand turns, and then fly through the course at the maximum velocity maintainable for seven minutes. Estimating the maximum velocity for nine minutes is essential for obtaining the maximum number of laps within the allowed time limit.

### **Propulsion Testing Apparatus**

The endurance and speed requirements of this design dictate a need for a propeller which can provide a reasonable range, while providing the maximum thrust available. The nine-minute endurance was agreed upon by the members of the team as a reasonable allowance for climb and the two required turns. This will allow an ample margin of power to complete the maximum number of laps the conditions allow.

Several propeller configurations were considered in the initial design. One, two, three, and four bladed props made up the field from which the final configuration was chosen. Ground clearance and availability problems quickly eliminated the single bladed propeller from consideration as it would have been approximately twenty inches in radius to run efficiently with the motors available. Three and four bladed props would provide adequate ground clearance but

the lack of suitable choices precluded their use. They could offer slightly higher climb rates but efficiency would have suffered. The blades are spaced 90 or 120 degrees apart and the wakes might have caused some problems. Two blade propellers are chosen as they have the fewest compromises, and below 1000 ft/sec they are superior<sup>3</sup>. Table 2 lists the selection criteria for propeller types.

Figure of Merit	Maximum Value	Single Bladed Propeller	Two Bladed Propeller	Three Bladed Propeller	Four Bladed Propeller
Availability	30	0	30	20	11
Ground Clearance	20	5	12	17	20
Expected Efficiency	30	30	25	21	16
Balancing Ease	5	3	5	4	1
Minimum Cost	15	-	15	11	8
Total	100		87	73	56

**Table 2—Propeller Selection Criteria**

The propellers selected for testing consist of several APC C-2 props with various pitches and diameters. Also, one folding prop designed for gliders, the 14X8.5 Aeronaut Glas, which is thinner and has a wider cord, will be tested. The pitch, diameter, and airspeed will affect the overall thrust put out by the propeller. This force consists of the useful thrust perpendicular to the propeller and drag that prevents the propeller from spinning<sup>4</sup>. Since the propellers tested are not variable pitch only one engine speed can be used for a given power<sup>5</sup>. This dictates that the propellers and motors used must be closely matched in performance. Thin airfoil folding propellers as well as thicker airfoil APC props were chosen for the testing.

The motors being tested consist of the Aveox 1412-3Y and the Maxcim MaxNEO-13Y. The Aveox was used in Hokie Bird II for the 1997 competition. The Aveox has fixed timing. This forces the user to set the timing for either maximum power or maximum endurance. This compromise is not acceptable in this year's competition as both speed and endurance are required to be competitive. The Maxcim has been chosen for bulk of the propeller testing. The timing of the motor is adjusted for optimum efficiency by the controller. The controller allows for a linear throttle response and is efficient at lower throttle settings.

Since wind tunnel time is limited, a test platform with all of the components of the power system mounted on it was constructed to allow quick set up. The test platform was built from plywood and measured 4"x4"x18". The test platform was mounted on a strain gauge pedestal balance that measured force on the thrust axis.

The Virginia Tech Open-Jet Wind Tunnel was used for all propeller tests. The test section of the tunnel is 3 feet in diameter, 3 feet long, and is open to the surrounding room. The flow speed is variable from 0 to 67 m/s and is measured by a Meriam Micromanometer model 34FB2 connected to a 3 mm diameter pitot-static probe mounted at the front of the test section. The manometer has an accuracy of  $\pm 0.01$  inches of water. The temperature inside the wind tunnel is measured using a digital thermometer with an accuracy of  $\pm 0.1$  degrees Celsius. Ambient pressure is measured with a Mechanism Ltd. Mk. 2 precision aneroid barometer.

## Propulsion Test Procedure

The wind tunnel dynamic pressures will be varied from 0 inches of water to 2 inches of water or velocities from 0 to 66 miles per hour. The range of propellers and motors will be narrowed down to the most promising combinations after preliminary tests to make the most use out of the given testing time.

The propulsion system will be powered by both the NiCad battery packs chosen for the competition and a DC power supply. The power supply will be used for testing the efficiency of the propulsion system, because many data points can be taken without having to recharge the battery packs. The NiCad packs will be used for testing the endurance of the propulsion system.

## Data Acquisition

The efficiency of the propulsion system will be calculated as thrust power divided by electrical power in. The data to be obtained includes thrust at full throttle for nine minutes, maximum static thrust, thrust at cruise, endurance, current, and voltage. The electrical current from the power supply is measured with an ammeter in series with the power supply. The power supply voltage is measured with a voltmeter. The strain gauge balance measures the thrust and drag of the system. A photocell attached to a tachometer is mounted to the test platform behind the prop to measure rpm. A flashlight is mounted outside of the wind tunnel facing the photocell to provide sufficient light for the photocell to work correctly. All of the data is read directly into a computer using Labview software and a data acquisition card for fast processing.

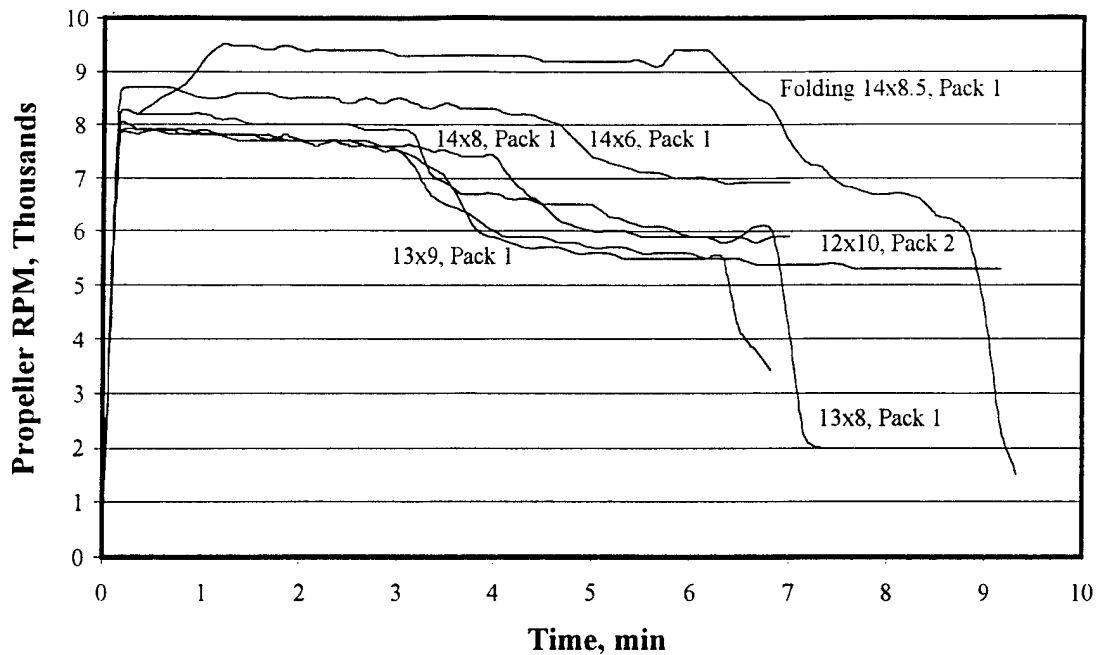
## Preliminary Results

The results of the static thrust tests for each prop are shown in Table 3. The engine used was the Aveox 1412-3Y with a gear ratio of 2.73:1.

Propeller	APC 14X6	Folding Aeronaut 14X8.5	APC 13X9	APC 13X8	APC 12X10
Static Thrust, lbs	7.96	7.32	7.2	6.8	5.48
Power Supply Voltage	23.9	24.0	23.9	23.9	24.0

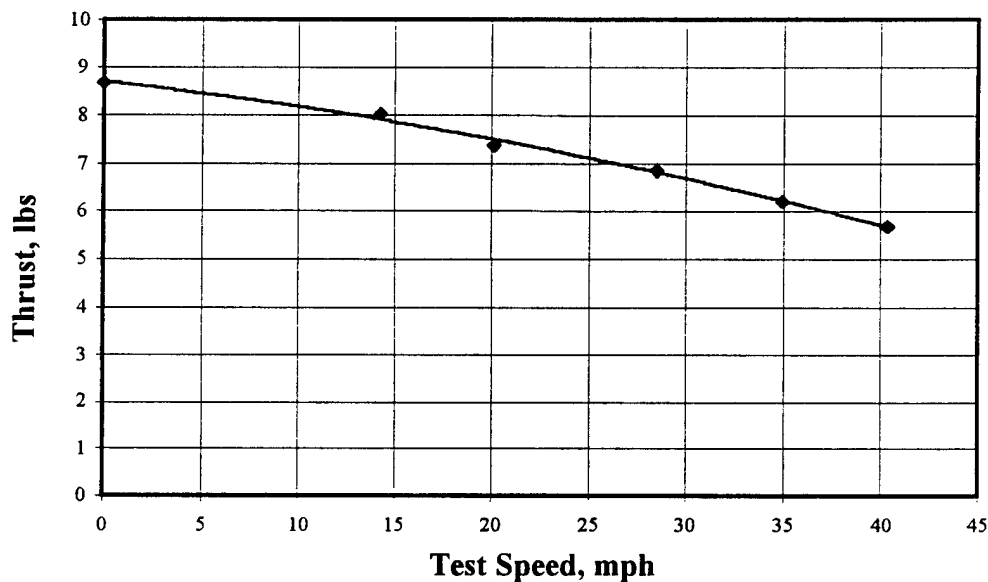
**Table 3—Static Thrust Tests with Aveox Motor**

In preliminary tests, consisting of static tests and tests at two inches of water, the folding prop was found to have a much higher rpm over a longer time period than all of the other props. It was not known how much thrust was being produced until balance measurements could be made. These tests at a velocity of 2 inches of water are shown in Figure 9.



**Figure 9—2" H<sub>2</sub>O Test Time History**

Sample data of thrust with respect to velocity is shown in Figure 10, with the drag of the test platform removed.



**Figure 10—Maxcim Motor, Folding 14x8.5 Aeronaut Propeller**

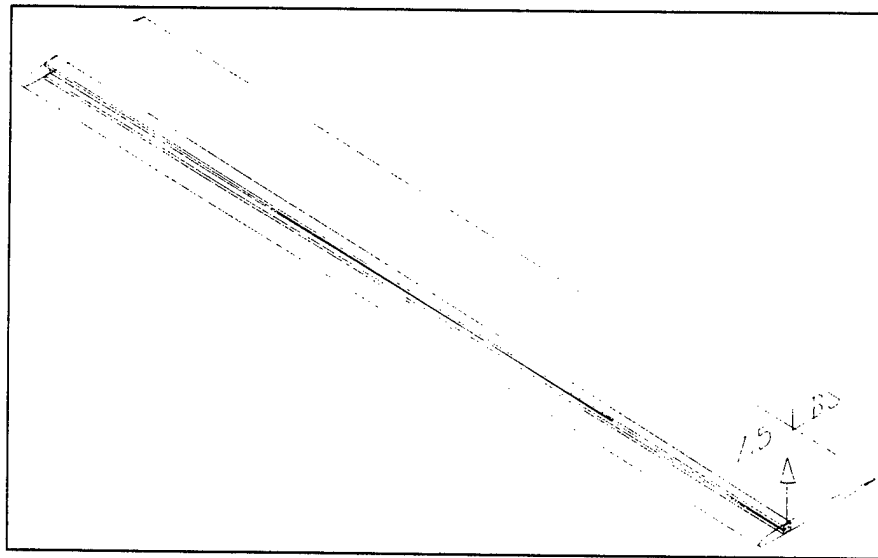
### Wing Spar Design

In order to ensure structural stability of the aircraft, a wing spar design and analysis procedure was conducted. The wing spar is essentially a box beam made of spruce. Due to the availability of spruce sheets, cost considerations, time constraints, and complexity factors, the

flange and webs of the beam have a constant thickness of readily available wood. A 3/16 inch thick sheet was spliced, cut, and glued into a beam. Material properties for the spruce were found in a table from *Beer and Johnston*<sup>5</sup>. Failure criteria were 5.6 ksi in compression, 8.6 ksi in tension, and 1.12 ksi in shear, and a Young's Modulus of  $1.5 \times 10^6$  psi was used. The primary design constraint of the beam is normal yield stress in compression; this value was used to determine failure of the wing under loading. The wing was assumed to be rigid in torsion. The wing skin (balsa) was assumed to carry all torsional loads to simplify the analysis. Von Mises' stresses were thus ignored. This is a reasonable assumption since the skin forms a closed torsion tube. The box beam was designed to carry all the bending loads that may be incurred on the plane during flight and ground static testing.

The most critical design point was the wing root. In order to minimize the weight of the beam, a tapered design was used. The thicknesses of the webs and flanges were kept constant, but the height of the beam was varied. Since the thickness of the airfoil is 1.375 inch at the root and 0.65 inches at the tip, this is a necessary design criterion. The spar will be located at the wing quarter chord to minimize torsional effects due to non-centric loading.

Two modes were considered for failure. The first is the mission requirement that the plane be supported at the wingtips and still be allowed to carry the fully loaded aircraft weight of 15 lbs as shown in Figure 11.



**Figure 11—Wing Spar Location**

The bending moment along the wing spar in this loaded condition is a linear relationship. Shear stresses along the wing span are equal to the tip load along the entire span. The design condition is the normal stress when the spar fails under compressive yielding. This condition was analyzed using beam theory and a factor of safety using the given design is 1.5.

The next failure criterion was cruise flight. An elliptical lift distribution was assumed along the span of the wing. The tapered beam was then analyzed along the span to check for failure criteria. The maximum normal stress was found to be located at the wing root as expected.

An important consideration is the weight of the spruce wing spar member. If a specific weight of 0.015 lbs/in is used and the dimensions of the box spar are kept constant over the entire wing span (no taper), the weight of the spruce spar is 0.851 lbs. This design is relatively simple and adequately meets mission requirements. For additional stiffness, water-jet cut carbon fiber laminate strips of 0.007" thickness were added to the top and bottom of the spar.

### **Landing Gear System**

The landing gear system chosen for Hokie Bird III was a taildragger configuration with retractable mains and a tailwheel buried in the rudder. A taildragger configuration was chosen because the total system weight would be less than a tricycle configuration. Also, the rudder mounted tailwheel enables ground steering without the need for a separate steering servo. Because the tailwheel is recessed into the rudder, drag is reduced considerably. A Spring-Air pneumatic retraction system was installed on the main landing gear to reduce drag. The retraction system is powered by compressed air located in an air reservoir in the fuselage. Pneumatic lines are run through a valve mechanism and out to the retraction pistons in the wings. The gear retract inward to the fuselage centerline. In case of pressure loss, the gear is forced to the down position by a spring to avoid damage from a belly landing. The longitudinal and lateral position of the main gear was determined by a method presented in *Pazmany*<sup>6</sup>.

### **Empennage Sizing**

The tail surfaces were sized to meet a tail volume specification. The desired tail volumes were determined from statistical data from other model aircraft and general aviation aircraft. The final tail volume coefficients were 0.55 for the horizontal stabilizer and 0.04 for the vertical stabilizer. These surfaces were sized conservatively to ensure positive control of the aircraft, because it is believed the aircraft may be difficult to fly because of its high wing loading and low power loading.

## **MANUFACTURING PLAN**

---

Constructing the aircraft designed presents an interesting challenge. Only a few members of the team have previous experience with the construction techniques used. This necessitated the manufacturing of the plane to be as easy as possible while still being able to attain the required performance. Techniques described in *Lambie* relating to the uses of different composite materials and glues were applied to the project<sup>7</sup>. Another valuable source of information on vacuum bagging is Alexander's "Composite Construction" article published in the November issue of *Sport Aviation* in 1997<sup>8</sup>. These sources, were invaluable references to teach new team members the basics of working with various materials.

### **Fuselage Construction**

The intent of the fuselage design was to offer high strength with minimum weight and drag. After considering the ease of construction and the strength to weight of a built-up balsa structure and a molded composite fuselage, the molded composite fuselage was chosen. The advantages of the molded construction outweighed the possibility of a lighter wood structure. A molded part is much quicker to make and assemble once the molds are made. If a mishap occurs in flight testing,

a new fuselage could be fabricated in a matter of days and alignment could be assured. The internal volume of a molded fuselage will be greater than that of a comparable wood structure, as the sides of the structure are thinner and fewer bulkheads are required to stiffen the structure and carry the loads from the payload and the wing.

An electric planer was purchased and construction of a pine plug was begun in October 1997. The initial form of the fuselage had been carved out of the pine block by the end of the semester. The intention was initially to have the plug finished and the molds laid up by the end of the fall semester. It was decided at this point to look for an alternative fuselage mold.

The required length and internal volume are the main constraints in the selection of a fuselage and it was quickly determined that there was no commercially available substitute currently in production. The cost of having a custom plug and molds made would have been too expensive and the control of quality and tight dimensional tolerances would have been required. A search for a suitable mold was initiated and went on for the better part of a month. The mold for a low frontal area fuselage of the required length was acquired with the intention of modifying the fuselage to meet the requirements of the design. This mold is not the ideal solution to our design, but it has the fewest compromises of all the options available. Table 4 lists the criteria used to select the fuselage construction method.

Figure of Merit	Maximum Value	Wood	Fiberglass	Carbon Fiber	Kevlar
Simplicity of Construction	20	11	20	14	7
Internal Volume	30	15	24	28	29
Weight	30	24	22	28	26
Strength/Durability	20	13	12	15	17
<b>Total</b>	<b>100</b>	<b>63</b>	<b>78</b>	<b>85</b>	<b>79</b>

**Table 4—Fuselage Construction Selection Criteria**

After looking through the materials available it is decided that the fuselage will be laid up by hand in the molds using 4.8oz bi-directional carbon fiber. Durability of the fuselage is an important issue for our design as Hokie Bird II suffered a failure in the landing gear attachment structure due to an excessive load on landing. This year that should not be a problem as the landing gear retracts into the wing. The carbon is both lighter and stronger than fiberglass of similar thickness. Kevlar was also considered as was used for the fuselage of last year's design. However, Kevlar requires special tools to cut properly and was eliminated from consideration this year due to problems with compatibility with other fabrics. Two layers of the carbon cloth were laid over a single layer of 1.5 oz fiberglass cloth except in the vertical fin where the anticipated loads did not require the additional strength and weight. The fiberglass creates a smooth surface finish as the weave is tighter than the carbon cloth.

The mold is first cleaned with alcohol and then an airbrush is used to spray a parting agent evenly onto the surface. This parting agent allows the finished part to be removed from the mold with no damage to the mold or part by keeping the epoxy from adhering to the surface. The epoxy used in the lay up is West Systems 105 used in concert with the 205 hardener to provide a working time of approximately two hours in the mold. Care must be taken to remove all excess



epoxy from the lay-up as the excess adds little strength and quite a bit of weight. The fuselage is laid up in two separate halves, as the mold is split down the middle. This arrangement allows the workers to make sure the cloth fits into the mold properly and that the parts can be removed from the molds. We chose to use female molds, as the surface finish is superior to that from a male mold. Also, the parting agent can make the internal structure difficult to attach to a part created from a male mold.

After the left and right halves of the fuselage are fully cured the parts are carefully removed from the mold. Any excess cloth is trimmed and the mating edges are sanded even with the edges of the mold by hand. Narrow strips of 2.5oz fiberglass cloth are cut which run from the nose to tail of the fuselage on both the top and bottom. The parts are then returned to the molds and the two halves are bolted together using pre-drilled holes to ensure the alignment of the fuselage stays true. The fiberglass strips are then applied to the inside seams using the same West Systems 105 epoxy resin with a hardener that allows a 30 minute working time. The joined fuselage is allowed to cure overnight. The molds are removed from the fuselage and the fuselage shell is structurally complete. The seams are filled with a mixture of micro-balloons and epoxy mixed to the consistency of peanut butter. This mixture strengthens the seam while allowing a very easy medium to sand and shape.

A piece of Dow Blueboard foam is used to create a hatch. The foam is shaped using a special tool similar to a cheese grater which allows a great deal of control of the finished product. The hatch will be used to allow extraction of the payload without requiring removal of the wing. Attaching the pneumatic lines for the gear retraction mechanisms and connecting the servo wires in the wing will also necessitate the hole in the structure.

A battery compartment is in the lower section of the fuselage. It is part of a cooling system designed to keep the motor controller, batteries, and engine cool through the use of a forced air system. A specially designed intake, baffles, and correctly sized exit will allow greater efficiency of the motor system. The extra weight of the structure should be alleviated by the increased efficiency of the power system due to the decrease in resistance of electrical components with a decrease in their temperature in flight. This assembly will be reinforced to act as a landing skid in the event that our landing gear fails. For the 1997 competition, our design inadvertently used the motor controller as a landing skid, which turned out to be a costly learning experience.

### **Wing Construction**

Drawings for the wing templates were generated with the Compufoil Professional Series computer program. This program has a large airfoil database, including the Selig SD 7032 airfoil coordinates. Compufoil accounts for the thickness of the wing sheeting and the loss of foam due to the cutting procedure and corrects the drawings accordingly. A template for the upper surface and lower surface of each airfoil is created as the templates are level with the bottom of the cutting table to provide the correct twist in the wing and ensure accuracy when the foam core is cut. The templates are constructed by adhering the printouts from Compufoil to Formica using 3M Formula 77 contact adhesive. The templates are cut out on a band saw and then sanded carefully to their final shape.

A Tekoa Feather Cut foam cutting system is used to cut wing cores from Dow pink insulation foam. This foam was chosen for its small cell size and light weight. The more

commonly used white foam has a larger cell size and is very fragile until the skins have been applied. Ni-chrome wire is used on the foam cutting bow, as it maintains its shape well and resists sagging better than most other wires commonly used for foam cutting, such as steel. This wire is put in tension on a bow to compensate for its expansion when heated. The heated wire is pulled through the foam block by a system of weights and pulleys while riding over the Formica templates. The speed of the wire across the templates has a great influence over the surface finish of the core and several attempts are usually required when learning how to cut foam core wings. The shucks or beds from the cores will be used in the attachment of the skins and must be saved. Any imperfections in the foam cores were filled with lightweight vinyl spackling compound and then sanded smooth.

The spar is constructed of aircraft quality spruce obtained from Aircraft Spruce and Specialty Company. The spar is constructed of two  $\frac{1}{2}$ " wide by  $\frac{1}{8}$ " deep pieces of spruce that run continuously from tip to tip. This was done to simplify the structure and eliminate the need for reinforcement that would be necessary if there is to be a break in the structure. The two pieces are separated by  $\frac{1}{32}$ " plywood shear members. The spar is doubled in thickness where the landing gear attaches to absorb landing loads with an extra measure of safety. Construction of the spar used a jig for alignment. West Systems epoxy is used again due to its ease of use and good bonding capability. The spar is then sanded and carbon fiber cap strips are added to help further reinforce the spar. The additional reinforcement should not be necessary but erring on the side of safety carries a only a small weight penalty.

A section is cut out of the cores where the spars are to be affixed. This is done using a hot wire foam cutter and precise measurements. After the excess foam has been removed the pieces of the core are glued to the spar. The next step in the construction process of the wing is to provide a structure to mount the retractable landing gear in the wing. Two plywood half ribs  $\frac{1}{8}$ " thick are used to mount the  $\frac{1}{2}$ " plywood rails used as attachment points for the retracts. Cut-outs are made to house the wheels in the wing and the structure is filled and sanded to provide a smooth surface for attaching the sheeting. Balsa blocks are attached to the leading edge of the wing and sanded to shape. At this time the holes for the two flap servos and two aileron servos are cut out using a piece of sheet metal heated with a propane torch. Channels are then cut in the lower surface of the wing using a cheap soldering iron. The iron is guided along a metal straight edge to provide an even cut and a model airplane wheel collar is used to control the depth of the channel. The extensions to connect the receiver and the servos are then laid in the channels and a thin layer of filler is spread over them with a squeegee to maintain the profile of the wing.

The sheeting type of the wing was changed during the construction. Obechi was originally the material of choice, as it comes in large sheets and need not be joined together from multiple pieces like balsa. The skin has been changed to  $\frac{3}{32}$ " balsa, as obechi is so thin any sanding would compromise the structure and it is brittle and easily shattered. Our spar deflects a bit when proof loaded and the obechi cracked in tests while the balsa simply bent. The top and bottom balsa sheets are created by joining several sheets together. All joints are cut at angles to maximize the gluing surface and help create a stronger structure. The skins are then sanded and then set aside for attachment to the wing.

Epoxy is spread over the sheeting and a strip of 1.5 ounce fiberglass cloth 4 inches wide is affixed to the trailing edge of the wing. The fiberglass stiffens the control surfaced to provide positive control and minimize the chance of flex and flutter. This assembly is then placed inside a

vacuum bag and surrounded with bleeder cloth to make sure all the air was evacuated. Vacuum bagging is a process in which a composite lay-up is inserted into a sealed enclosure and a pump is used to evacuate air to a differential pressure of at least 16 inches of Mercury (Hg). This creates suction on the part inside, effectively giving a uniform force over the entire surface. Excess epoxy then flows away from the part and ensures an even epoxy distribution.

Once removed from the bag, the excess sheeting is removed and the wing is sanded. Fit check templates are to be used to ensure the integrity of the airfoil at several stations along the wing. The leading edge is shaped in a similar manner. The servos are attached to plywood plates that screw into mounting blocks in the wing. This provides a low drag and simple means of flight control actuation. The control surfaces are attached to the wing and faced with balsa wood. The flaps and ailerons will have similar design. The flaps will work in concert at low velocities. Balsa blocks or a winglet will be added to the tip of the wing to provide an aesthetically pleasing surface.

### **Tail Surfaces**

The horizontal tail and rudder of this aircraft are manufactured out of foam cores in a manner similar to the wings. Templates are created and cores are cut with a hot wire. The vertical stabilizer is molded into the fuselage and is therefore constructed out of carbon fiber. The fin uses only a single layer of carbon above the attachment point for the horizontal tail, as the anticipated loads are quite small in comparison to the rest of the fuselage structure.

The horizontal tail is sheeted with a one-millimeter thick hardwood veneer called obechii. This provides a good surface to finish and also allows the airfoils on the tails to be very precise. The core is sanded, sheeted, and bagged. After removing the stabilizer from the bag the excess material is again trimmed and the surface is sanded to shape by hand. The goal is to create a strong, light, and accurate surface.

Elevators will be cut out of the horizontal tail after it is attached to the fuselage. They will be faced with balsa and hinged in the same way as the surfaces on the wing. The rudder is constructed of obechii over a foam core faced with balsa. The unique feature of the rudder is that the tail-wheel is buried inside to provide a low drag means of controlling the aircraft on the ground. The fuselage is closed at the rear with the vertical stabilizer with a hard balsa post. Model aircraft hinges are used to provide a strong attachment for the rudder to this post, which should be able to survive most landings that this aircraft will experience.

### **Final Assembly**

Assembly of all the individual components marks the first stage in the final assembly of the aircraft. The wing, tail, servos, motor, batteries, controller, landing gear, receiver, and payload must be integrated into the basic structure of the aircraft to provide a flying airframe. The horizontal tail will be permanently attached to the fuselage. The wing will be removable to facilitate shipment to and from the competition site.

The templates for the wing are used to trace the outline of the airfoil on the fuselage at the required two-degree angle of attack for cruise. A Dremel Tool using a fiberglass reinforced cut-off wheel is used to cut the profile of the wing out of the fuselage. The angle of the wing is set with respect to the centerline of the fuselage, which coincides with the thrust line of the motor.

One quarter inch thick plywood is glassed into the fuselage to serve as a mount for the wing. It should be structurally sufficient for mild accelerations when inverted but is not designed for aerobatics when the plane is flown with the 7.5 pound payload.

A fillet is constructed by bolting the wing to the fuselage with wax paper covering the wing so the fillet will remain attached to only the fuselage. A mixture of West Systems filler, micro-balloons and West Systems epoxy is shaped by hand using surgical gloves to the desired fillet shape. The wing is then removed and the fillet sanded to its final shape by hand. The fillet serves to distribute the load from the fuselage into the wing over a larger area and avoids the high stress concentration that would result without it. It is also intended to reduce the intersection drag between the fuselage in wing.

The horizontal tail halves are glassed together. The fuselage is cut at the tail attachment location using the templates and the halves are lined up with the wing. Several measurements are taken to assure alignment and the tail is glassed in place using 2 oz. fiberglass cloth. A fillet is constructed between the fuselage and the horizontal tail using the same filler as used on the wing fillets. Two servos will be used to independently control the two elevator halves. This was done so that if one side fails, there will be a good chance of landing the aircraft safely. The servos will be located in the aft fuselage in a compartment.

All of the propulsion system is located in the front of the plane to balance the aircraft and keep the wires short to minimize the resistance of the system. The air reservoir for the retractable landing gear is located in the rear of the fuselage along with the rudder servo, retract servo, receiver, and battery. This allows the payload to be positioned near the center of mass of the aircraft. All of the systems and hardware are purchased from the supply available to model aircraft enthusiasts as this allows for the rapid location of replacement parts and gives the option of many different suppliers. This also helps to keep the cost of the project within reason.

## **Finishing**

The fuselage, horizontal tail, and rudder assemblies are to be painted when finished. The paint must be selected so that the added weight is minimal. It is not necessary for the performance of the aircraft but it will improve the looks and bring out pride in the team members. The looks of the aircraft are important but sacrificing performance is to be avoided at all costs. The best paint commonly available is the K&B Manufacturing Ultra-Poxy paint. It provides an easy way to paint the plane with the minimum possible addition of weight.

The key to a successful paint job lies in the surface preparation before the paint is applied to the aircraft. Lightweight automotive primer will be sprayed on the fuselage and tail with an airbrush run from a compressor. This will then be sanded almost completely off, filling pinholes and leaving a smooth surface. Any major imperfections will be filled with lightweight filler and sanded smooth. When a satisfactory finish has been obtained, all dust and debris will be removed from the surface with the use of tack cloths. The surface will then be sprayed with a white base coat. Striping will be added and the plane will be clear coated after the stripes have been lightly sanded by hand to blend the edges into the base surface. If the combined weight of these materials is too great in future tests, this procedure will be modified.

The wing will be covered with Monokote. This is a plastic hobby grade covering that has a heat activated adhesive on one side. It is ironed down and then shrunk tight with a heat gun to

cover the wood. This provides a smooth surface with a minimal weight penalty. The covering will be used to hinge the control surfaces on the wing to avoid gaps, which would cause unwanted aerodynamic effects.

Once the aircraft is finished cosmetically, all of the systems will be installed for the final time and an extensive ground test, flight testing, and development program will be conducted.

## APPENDIX A—REFERENCES

---

- <sup>1</sup> Hoerner, S.F., *Fluid Dynamic Drag*, Hoerner Fluid Dynamics, Vancouver, 1965.
- <sup>2</sup> Selig, M. S. et. al. *Summary of Low-Speed Airfoil Data*. Virginia Beach, Va.: SoarTech Publications, 1995.
- <sup>3</sup> Falk, K, *Aircraft Propeller Handbook*. New York: The Ronald Press Company, Copyright 1942.
- <sup>4</sup> McMahon, P, *Aircraft Propulsion*. New York: Pittman, Copyright 1979.
- <sup>5</sup> Beer, F. and Johnston, E., *Mechanics of Materials, 2<sup>nd</sup> Edition*. New York: McGraw-Hill, Inc. 1992.
- <sup>6</sup> Pazmany, L., *Light Airplane Design*. San Diego, Ca.: L. Pazmany, 1963.
- <sup>7</sup> Lambie, J., *Composite Construction for Homebuilt Aircraft, 2<sup>nd</sup> Edition*. Hummelstown: Markowski International. 1995
- <sup>8</sup> Alexander, R. "Composite Construction," *Sport Aviation* November, 1997

S=745.5 in<sup>2</sup>  
Weight=18 lbs

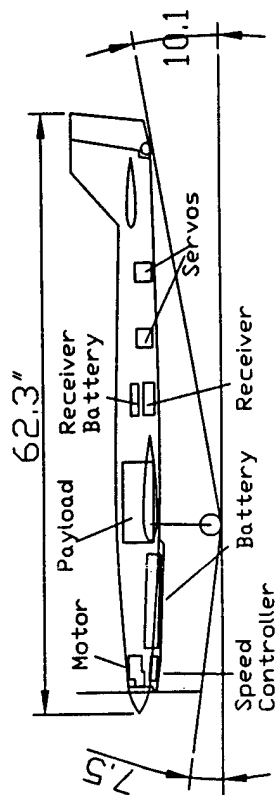
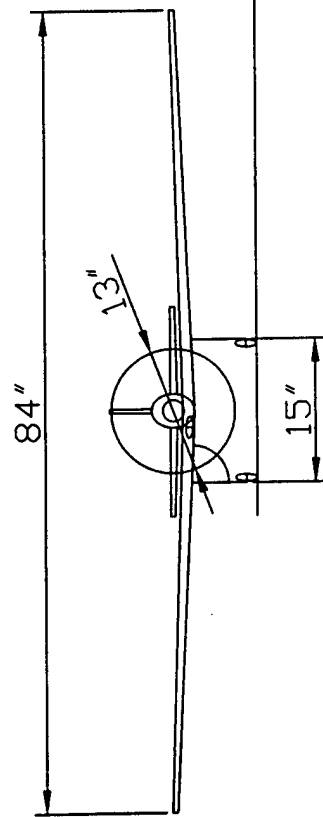
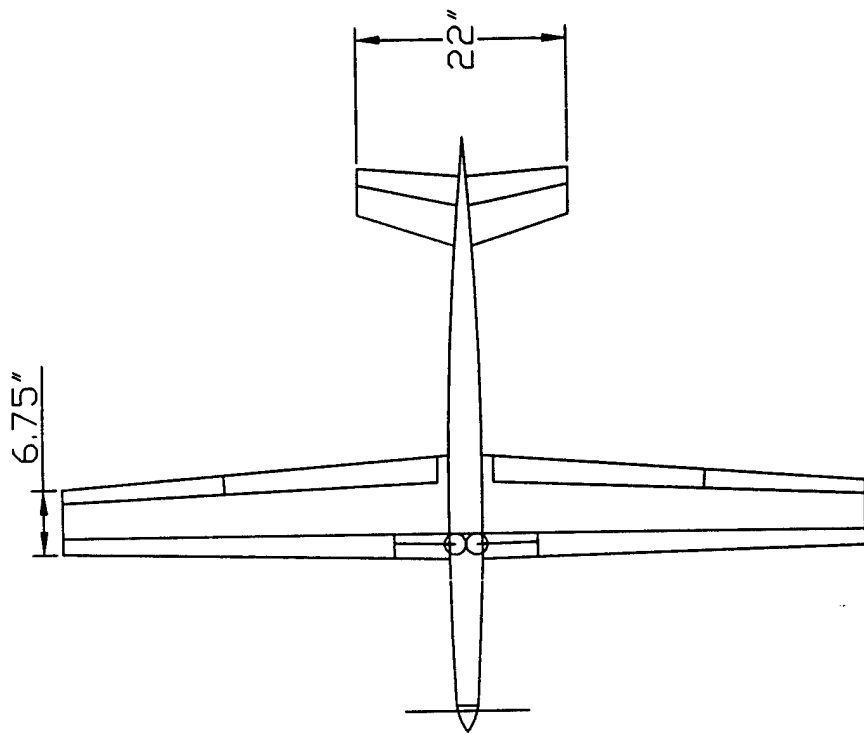


Figure 1

Virginia Tech  
Hokie Bird III

## **TEAM MEMBERS**

---

<b>Seniors</b>	<b>Juniors</b>	<b>Sophomores</b>
John Gundlach	Greg King	Matt Orr
Alexander Roup	Ray Renfrow	James Bamba
	Dave Leasure	



## **TABLE OF CONTENTS**

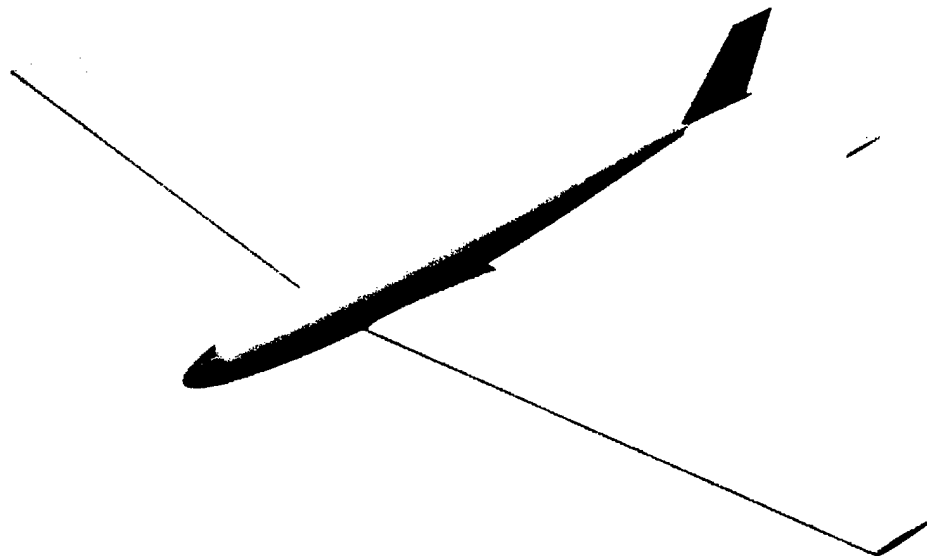
---

<b>Executive Summary</b>	<b>1</b>
<b>Management Summary</b>	<b>2</b>
<b>Conceptual Design</b>	<b>4</b>
<b>Preliminary Design</b>	<b>7</b>
<b>Detail Design</b>	<b>11</b>
<b>Manufacturing Plan</b>	<b>16</b>
<b>References</b>	<b>A</b>

# **Virginia Tech Team**

## **1998 Design/Build/Fly Competition**

### **Addendum Report**



April 13, 1998

## **ADDENDUM REPORT**

---

The Virginia Tech team has successfully attained the majority of goals set for the manufacture and development of our entry in the AIAA/Cessna/ONR design build fly competition for the 1997-98 academic year.

The first flight of the Hokie Bird III took place on April 7, within two and a half weeks of the estimated date. The flight was successful in all respects and did not uncover any design flaws. No improvements to the configuration design are foreseen for a next-generation aircraft, other than tailoring the design to the requirements of the competition. The slippage was attributed to the part time nature of the project. Estimating the time available of the team members could be done with greater accuracy if the project were to be assigned class credit. Because grades were not assigned for participation in the project, team members were often unable to prioritize work on the project ahead of other class work. Construction time requirements could be reduced in future years by using as many off-the-shelf components as available. These could include the fuselage being modified from a kit or ARF model instead of constructed from scratch by the team.

The construction processes used on this plane were derived from two previous aircraft and are well suited to a design to be built by students in a very limited time span. The same construction methods would therefore be used for a next generation design. An all molded wing with carbon skins could have had a much more accurate airfoil than the wing that was constructed. The greater accuracy might have given an advantage in the competition, but the additional construction time required would have been excessive and would have reduced the time available for equally important tasks. The molds for the wing would only be used for the construction of one wing, and the materials cost would be greater than the project budget would tolerate.

The dimensions and aircraft layout match those presented in the Proposal Phase nearly exactly. The major design decisions that have been made since that time are the wing tip design, the selection of a motor and speed control combination, and the selection of a color scheme.

The team considered several wing tip designs. A rounded tip was selected to satisfy the requirements for a strong tip and one that would not greatly increase the weight of the wing. Ease of manufacture and aesthetics were also factors in the decision.

Wind tunnel propulsion tests have convinced the team to use the MaxCim motor system with a propeller to be determined through flight-testing. The wind tunnel tests indicated several propellers that merit further testing. A major problem in the flight test planning has been the selection of a suitable site for flight test. A field of sufficient size to allow a full range of the tests has not been located. These flight tests are believed to be instrumental to success in competition. Flight tests will be required to be completed at least a week before the competition to allow the packaging and shipment of the model via UPS or FedEx.

The color scheme chosen is a simple red and white scheme, which minimizes the amount of finishing materials used and saves weight. Only one stripe on each wing tip minimizes tripping of the flow over the wing due to joints in the covering material. Use of the Virginia Tech school

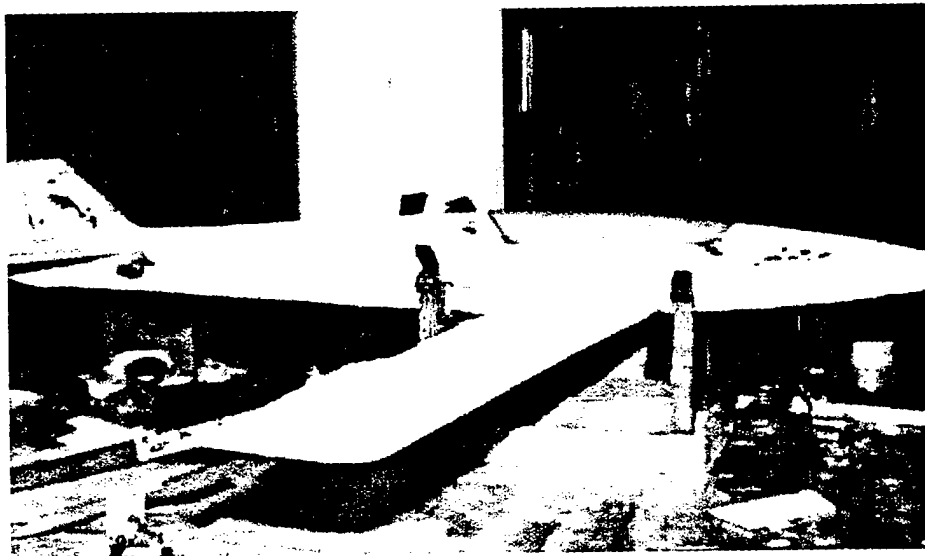
colors might have been more appropriate, but would have resulted in visibility compromises that would be unacceptable for a competition aircraft.

The use of retractable landing gear is a design decision that may not yield the expected benefits. Retraction tests indicated that the flex of the landing gear legs and reliability of the system could compromise the aircraft. The gear doors, which were designed to reduce the drag of the gear when retracted, were determined to be too complex to use on the aircraft. The increment in drag of the open wheel wells could be higher than a carefully faired fixed landing gear. A fixed landing gear system would also reduce the possibility of mechanical failure resulting in a gear up landing. For these reasons, a backup fixed gear modification is being investigated in case a gear failure should occur.

The component cost breakdown of Hokie Bird III is listed in Table 1. The total aircraft cost was calculated to be \$4293. Aircraft component costs were agreed well with the expected values used in design evaluations. The majority of costs were in the incurred propulsion system and the electronics, which was expected. The propulsion system costs were fixed by the requirements of the desired performance. The electronics costs were dictated by the desired control surface mixing combinations for landing approach and high load factor turns. The radio system is also planned for use in future aircraft, therefore distributing the cost over several projects.

Future designs may use more prefabricated airframe components, which may increase the airframe cost. However, future aircraft will not require a new radio system, which will greatly reduce the project cost. The total project cost of a next generation aircraft will be approximately \$2700, or about \$1600 less than Hokie Bird III. The most significant changes to a future project would be in the group structure, such as receiving class credit for participation. These changes would have a large benefit to the project without requiring any increase in cost.

A photograph of the aircraft during construction is included in Figure 1. Since the photograph was taken, the wing and horizontal stabilizers have been covered with Monokote, and the fuselage has been fully primed.



**Figure 1—Hokie Bird III Fully Assembled**

**Table 1--Aircraft Component Price List**

All costs include taxes and shipping

**Fuselage**

Mold	\$150.00
Carbon Fiber	\$35.00
Fiberglass	\$16.50
Epoxy	\$8.00
Plywood	\$10.00
Balsa	\$3.50
CA	\$5.00
Microballoons	\$6.00
Foam	\$5.00
<b>Subtotal</b>	<b>\$239.00</b>

**Wing**

Balsa	\$45.00
Spruce	\$50.00
Plywood	\$30.00
Monokote	\$28.00
Foam	\$25.00
Epoxy	\$7.00
Fiberglass	\$5.00
Hinge Tape	\$5.00
Lightweight Filler	\$5.00
<b>Subtotal</b>	<b>\$200.00</b>

**Empennage**

Obeche	\$5.00
Balsa	\$5.00
Monokote	\$7.00
Foam	\$4.00
Epoxy	\$3.00
Fiberglass	\$2.00
Lightweight Filler	\$1.00
<b>Subtotal</b>	<b>\$27.00</b>

**Propulsion System**

Motor and Controller	\$409.00
Batteries	\$430.00
Propellers	\$100.00
<b>Subtotal</b>	<b>\$939.00</b>

**Landing Gear System \$130.00**

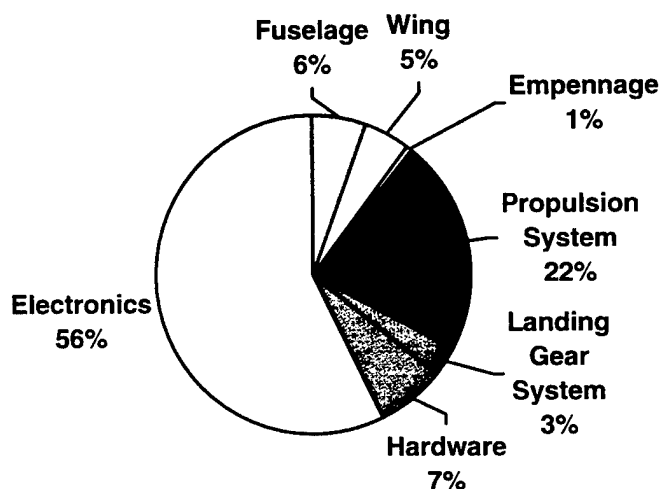
**Hardware \$300.00**

**Electronics**

Futaba 9ZHS	\$1,800.00
Mini-Servos	\$458.00
Miscellaneous	\$200.00
<b>Subtotal</b>	<b>\$2,458.00</b>

**Total Aircraft Cost \$4,293.00**

**Component Cost Percentages**





# Table of Contents

<u>Section or Figure</u>	<u>Page</u>
List of Members, Officers, and Advisors	1
Executive Summary	2
Management Summary	4
Milestone Chart, Figure 1	5
Conceptual Design	6
Ranking Chart, Figure 2	9
Prototype Pictures, Figure 3	10
Powered Sailplane, Figure 4	11
Delta Wing, Figure 5	12
Pylon Racer, Figure 6	13
Canard, Figure 7	14
Flying Wing, Figure 8	15
Preliminary Design	16
Detailed Design	20
Battery Comparison, Figure 9	25
Landing Gear, Figure 10	26
Materials Strength, Figures 11a-11c	27
Propulsion Assembly, Figure 12	30
CG Location, Figure 13	31
Manufacturing Plan	32
Manufacturing Milestone Cart, Figure 14	37
Milling Pictures, Figure 15	38
Shell Lay-up, Figure 16	39
Joggle Joint and Hatch Layout, Figure 17	40
Manufacturing Samples, Figure 18	41
Bibliography	42
Acknowledgements	43
Drawing Package Table of Contents	45

1997/98 WSU AIAA Members

Member	Position or Office	Class
David Darrow Jr.	President	Senior
Kevin Koller	Vice President	Junior
Ken Beahm	Business Manager	Junior
Amir Qureshi	Center Section Manager	Junior
Aaron Allina	Wing Manager	Sophomore
John Maguire	Report Manager	Senior
Josh Lavalleur	Webmaster	Freshman
Barry Ells Jr.		Junior
Mark Fuller		Senior
Jeramy Sutliff		Junior
Bill Johns	Technical Advisor	Professor
Walter Grantham	Administrative Advisor	Professor



## Executive Summary

Development on the conceptual design for the WSU Flight Team's 1997/1998 Unmanned Aerial Vehicle began at the conclusion of last year's competition. As the group began to reorganize itself, a clear design path began to make itself known. The initial five designs considered were a pylon racer platform, a delta wing, a flying wing, a canard platform, and a conventional powered sailplane. It was unanimously decided that an ambitious design, such as a flying wing would best fit the constraints of this year's competition. However, designing a stable and controllable flying wing would require an entire year of testing and design revision. The designing of the 1997/1998 WSU CougarAIR Flying Wing began in early September.

The first problem faced by the design team was the lack of a large enough wind tunnel that was student accessible. Without proper testing it would be difficult to know when the optimum design had been found or what problems a current design had. Two possible solutions to this problem arose: a car-mounted wind tunnel, or extensive unpowered and powered flight testing. The car-mounted wind tunnel concept consisted of mounting a specially made stinger, or lift and drag measurement device, to the roof of a car, attaching the test model, and then accelerating to anticipated flight speed to make measurements. This idea was discarded because of high costs involved in purchasing proper data acquisition and analysis software and unavoidable errors that are introduced with non laminar air and bumps in the driving surface. The alternate path was followed: extensive powered and unpowered flight testing would provide enough qualitative data on the flight characteristics of the aircraft to effectively identify problems.

As the flying wing began to take shape, key design elements, such as airfoil shape, balance and stability, wing sweep, and control surfaces were investigated. The most critical element of the plane to emerge was its pitch stability. The tailless flying wing is traditionally unstable in pitch and is typically balanced by computer. By sweeping the wings back as far as possible and placing elevons at the wing tips we hoped to provide a large enough pitching moment to stabilize the plane and provide adequate control authority. The use of an airfoil specially designed for tailless aircraft with a slight recurve on the trailing edge was used to further increase stability. By the end of October, a design had emerged that we hoped would provide the low drag, high lift, and stability that was required to earn a winning flight score.

This design was turned into a foam model and flown. The issue of pitch stability had been resolved as the plane flew for over 100 yards in straight and level flight with no control inputs. In steeply banked turns, however, the plane exhibited little lateral stability.

The success of the foam model exhibited the characteristics that would make it a viable option for the competition plane and full-scale design work commenced. The first set of negative polyurethane foam molds were milled in the beginning of December with the intention of molding a composite center section and attaching various wing panels,

such as wings with winglets or anhedral, to solve the lateral stability problem.

Negative molding proved to be a very good concept, but was much more difficult to implement than expected. The molds were designed and milled with little problem, but complications arose when it came time to finish them and pull parts out. Numerous attempts were made with different release agents and waxes before a good part was produced. The winning combination used epoxy-based primer to finish the molds, overlaid with four layers of a mold release wax and a thin coat of polyvinyl alcohol (PVA). This combination ultimately provided a part with a smooth, undamaged surface that was suitable for use without further surface finishing. However, because of the complexity and time involved in constructing the composite center section, another foam center section was made simultaneously so that flight testing could be resumed.

Another set of unpowered flight tests was carried out using the new foam center section and two different types of wings. It was found that a flat wing, no dihedral, with winglets provided lateral stability in highly banked turns. At the time of submission of this report, wings with anhedral have not been tested.

Powered flight is the next goal, and for that to happen many of the components that are only in design have to come together. Development of the internal structure and location of flight hardware has become the primary focus at this point. The final composite skin lay-ups are being manufactured, and methods of creating low drag hatches and control surfaces are being refined. Work is continuing on optimizing battery and motor configuration and location. Landing gear has been purchased, but it was decided that they were far too heavy, so work is underway on re-machining key components out of lighter materials, including titanium and carbon fiber/epoxy composite. The goal is to have a month of flight testing before the contest with the final configuration.

For further design analysis, a solid CAD model created using Pro/ENGINEER will be imported into Fluent for computational fluid flow analysis. The goal of this will be to identify trouble spots in the airflow across the surface that are not evident in flight testing. Then, once the design has been tested, the molds for the competition version of the aircraft will be milled.

Overall the project turned from application of class principles to innovation for solving complex problems. The flying wing shape itself is not a highly documented design and certainly not in our configuration. The composite lay-up techniques we are using are non-traditional to this scale of aircraft as well, and have required a significant amount of research and experiment. The majority of the information about these techniques was gathered from telephone conversations with specialized companies and people who had applied the process in different applications. The goal of the group was to produce a technically advanced, highly efficient, and reliable aircraft. The dedication, initiative and creativity of the all group members has lent itself excellently to achieving this goal.

## Management Summary

Choice of a management style for the 1997-98 WSU AIAA Flight Team was based on the need to divide the work among different groups according expected tasks. The goal of this management structure was equal involvement of everyone in the design and construction of the airplane. It was decided that different groups would be formed to take on the specific tasks for each phase of the design process and when those tasks were accomplished, the group would dissolve and the members would be reassigned.

Management was initially broken into a president, vice president, and five design group leaders who oversaw their respective design groups. A design leader headed each group and they were in charge of brainstorming and reporting progress or problems. The five design groups consisted of Aerodynamics, Structures, Propulsion, Landing Gear/Winglets, and Manufacturing. Once the preliminary design was finished, design data was compiled and preliminary manufacturing began in December 1997.

With the bulk of the design completed, the WSU AIAA Flight Team was reorganized to better use the available labor. The five design groups were disbanded and two manufacturing groups, Center Section and Wings, were created as well as a Public Relations and a Report group. The executive management was enhanced with the addition of a Business Manager to over see the business affairs of the project and manage the Public Relations Group. The management structure of the new manufacturing groups was similar to that of the initial design groups. This amounted to a total of six managerial positions controlling the direction of the project. This combination has proved extremely effective in keeping the project on track and focused.

AIAA Management Table	
Fall 1997 Semester	
President	Dave Darrow
Vice President/Design Manager	Kevin Koller
Aerodynamics Group Manager	Kevin Koller
Structural Group Manager	Ken Beahm
Landing Gear/Winglets Group Manager	Ken Beahm
Manufacturing Group Manager	Kevin Koller
Spring 1998 Semester	
President	Dave Darrow
Vice President/Design Manager	Kevin Koller
Business Manager	Ken Beahm
Center Section Manager	Amir Qureshi
Wing Manager	Aaron Allina
Report Managers	John Maguire

## 1997-98 WSU AIAA Milestone Chart

Event	Planned Completion Date	Actual Completion Date
Establish First Group Managers	9/11/97	9/11/97
Calculations	9/18/97	9/18/97
Choose Conceptual Design	9/25/97	9/22/97
Determination of Final Design Path	10/1/98	9/26/97
Determine Airfoil Shape	10/1/97	9/29/97
Preliminary CAD Design	10/6/97	9/30/97
Intermediate CAD Design	10/10/97	10/9/97
Begin Construction of Prototype Models	10/24/97	10/14/97
Determine Manufacturing Method	10/15/98	10/16/97
Glide Testing of Preliminary Design	11/23/97	11/23/97
Choose Motor, Gearing, Propeller	1/12/98	12/17/97
Reorganize Groups/Managers	1/15/98	1/22/98
Composites Testing	2/14/98	2/7/98
Center Section Mold Manufacture	1/30/98	2/28/98
Battery Testing	2/12/98	2/28/98
Pro E solid Model	3/8/98	3/8/98
Finalize Wing Design	2/21/98	
Finish/Submit Report	3/11/98	3/12/98
Fluent Fluid Flow Analysis	3/14/98	
Mechanical Assembly	3/20/98	
Electrical Assembly	3/20/98	
Powered Testing of Preliminary Design	3/21/98	
Center Section Assembly	3/21/98	
Wing Mold Construction	3/27/98	
Final Mold Manufacture	3/28/98	
Complete Construction of Final Design	4/4/98	
Submit Addendum Report	4/8/98	
Powered Flight Testing	4/18/98	
Competition	4/25/98	

## Conceptual Design Phase

Design alternatives for this year's contest entry were investigated for the first time in early September 1997. The first phase of these initial discussions were directed toward what the design considerations should be for this year's contest entry. With the time limit addition to this year's contest, not only efficiency but also high speed would be needed to develop a winning flight score. Initial design ideas included a pylon racer platform, a delta wing, a flying wing, a canard platform, and a powered sailplane.

The parameters used to screen these designs were primarily related to flight performance criteria. The cost and time required to implement the design were also factored into the design choice but to a lesser extent. A design that would perform the best would be chosen, then cost and time factors could be improved through the use of innovative manufacturing techniques. The design parameters used were: drag, lifting ability, stability, and maneuverability.

The largest portion of the flight score is based on the number of laps completed in 7 minutes; the more laps completed, the higher the score received. To accomplish this the aircraft must have a high cruise speed. For the analysis of which aircraft platform to choose, it was assumed that the same, optimum propulsion system would be used in any design. Therefore, if the amount of thrust is constant, it does not need to be factored into the relative speed of each design. Since thrust is a constant, the only other way to increase speed is to reduce drag. Thus, the drag on the aircraft was the parameter assigned the highest weighting. Since the design must be able to lift a 7.5 pound payload, the parameter given the next highest weighting was the lifting ability. Further, to have a safe aircraft and decrease the chance of a crash, stability is important. Finally, maneuverability is important so that the aircraft is able to make tight turns. This allows the maximum portion of the flight path to be spent traveling directly between turn judges. It also allows for greater freedom in determining the most efficient method of flying the plane. The importance of each parameter was discussed and weighted as follows: low drag 50%, high lifting ability 25%, high stability 15%, and adequate maneuverability 10%.

### Drag analysis

The drag coefficient ( $C_D$ ) can be theoretically determined for most wing shapes, but accurately determining a  $C_D$  for the entire aircraft that may include various fuselage shapes is difficult. This is typically done with wind tunnel testing or the use of computational fluid dynamics (CFD). At the conceptual design phase we determined that this level of accuracy was not required and that the major differences in drag for the five conceptual designs could be arrived at more quickly. ElectriCalc software was used to evaluate a  $C_D$  for each design. This software is in wide use for designing electrically powered model aircraft due to the wide range of design information that is calculated and the accuracy of the results. Design parameters for the aircraft that we built for last year's competition were input into the program to test the accuracy of the software against real performance data for that aircraft. The output values for maximum speed, climb rate, and motor run time all had less than 10% error. A  $C_D$  value for last year's plane was never calculated by a CFD analysis or wind tunnel tests, but since the values that could be measured were reasonably accurate, it was assumed that the value for  $C_D$  would have the same relative accuracy. The design parameters that are input into ElectriCalc include: aircraft configuration (sailplane, pylon racer, etc.), airfoil type (flat bottom, semi symmetrical, full symmetrical), amount of streamlining for the design, wing thickness, and landing gear type (retractable in the up position was selected for all designs). Given these parameters, ElectriCalc output an estimation of the drag coefficient for each aircraft. To assign a drag score for each

design the drag coefficients were normalized and then subtracted from 1 so the design with the greatest  $C_D$  is assigned a score of zero for this section.

**Powered sailplane** - this design has an average  $C_D$  due to its large tail and sleek fuselage.  $C_D = 0.041$ , normalized  $C_D = 0.732$ , score = 0.268, weighted score = 0.134

**Pylon racer** - this design has a high  $C_D$  due to its inefficient low aspect ratio wings.  $C_D = 0.050$ , normalized  $C_D = 0.893$ , score = 0.107, weighted score = 0.0535

**Canard** - virtually the same  $C_D$  as the powered sailplane due to similar dimensions but a rearrangement of stabilizer position.  $C_D = 0.040$ , normalized  $C_D = 0.714$ , score = 0.286, weighted score = 0.143

**Delta wing** - highest  $C_D$  due to the need for a thicker airfoil to create the required lift with this inefficient wing shape.  $C_D = 0.056$ , normalized  $C_D = 1$ , score = 0, weighted score = 0

**Flying wing** - the lowest  $C_D$  of all these design options. This is due to the lack of a tail or fuselage and the efficiency of its moderately high aspect ratio wing.  $C_D = 0.035$ , normalized  $C_D = 0.625$ , score = 0.375, weighted score = 0.1875

#### Analysis of lifting ability

The coefficient of lift ( $C_L$ ) for an aircraft maintaining a constant altitude is given by the following equation:

$$C_L = [(C_D - C_{DP})\pi(b^2/S)e]^{1/2}$$

Where:  $C_{DP}$  = coefficient of profile drag,  $b$  = wing span,  $S$  = wing area, and  $e$  = efficiency factor. Wing span, wing area, coefficient of drag are known for each conceptual design, but values for  $C_{DP}$  and  $e$  were approximated with criteria outlined in various aerodynamics texts (see Bibliography on page 42). To assign a score for lifting ability to each design the lift coefficients were normalized so the design with the greatest  $C_L$  is assigned a score of one for this section.

**Powered sailplane** - decrease in lifting ability by the large rear tail required to produce negative lift that counteracts the large positive pitching moment of the high aspect ratio wing.  $e = 0.9$ ,  $b = 12$  ft.,  $C_{DP} = 0.023$ ,  $S = 1400$  in<sup>2</sup>,  $C_L = 0.794$ , normalized  $C_L = 0.962$ , weighted score = 0.241

**Pylon racer** - lifting ability is moderately decreased by the small rear tail that must produce negative lift to counteract the small positive pitching moment of the low aspect ratio wing.  $e = 0.8$ ,  $b = 8$  ft.,  $C_{DP} = 0.025$ ,  $S = 1150$  in<sup>2</sup>,  $C_L = 0.710$ , normalized  $C_L = 0.861$ , weighted score = 0.215

**Canard** - moderate increase in lifting ability by the medium size front stabilizer required to produce the lift that counteracts the large positive pitching moment of the high aspect ratio wing.  $e = 0.87$ ,  $b = 10$  ft.,  $C_{DP} = 0.022$ ,  $S = 1100$  in<sup>2</sup>,  $C_L = 0.803$ , normalized  $C_L = 0.973$ , weighted score = 0.243

**Delta wing** - A tail causes no lifting influence for this aircraft because a low moment airfoil is used that does not require a tail.  $e = 0.82$ ,  $b = 5$  ft.,  $C_{DP} = 0.019$ ,  $S = 1300$  in<sup>2</sup>,  $C_L = 0.719$ , normalized  $C_L = 0.872$ , weighted score = 0.218

**Flying wing** - A tail causes no lifting influence for this aircraft because a low moment airfoil is used that does not require a tail.  $e = 0.96$ ,  $b = 10$  ft.,  $C_{DP} = 0.015$ ,  $S = 1250$  in<sup>2</sup>,  $C_L = 0.825$ , normalized  $C_L = 1$ , weighted score = 0.25

### Stability analysis

The stability section lends itself to an empirical analysis method. Elements of high stability receive a high score, those with low stability receive a low score. Scores for each design will be out of 10 points possible. These scores will then be normalized and weighted as in previous sections.

**Conventional powered sailplane** - most stable due to long moment arms from the center of gravity to all control surfaces for good control authority and a high rotational moment of inertia in all directions. Also the drag on the rear tail pulls the aircraft back into strait and level flight after control inputs are neutralized. points = 10, normalized points = 1, weighted score = 0.150

**Pylon racer** - less stable due to its compact low aspect ratio design resulting in low rotational moment of inertia in all directions and short moment arms from the center of gravity to all control surfaces. points = 4, normalized points = 0.40, weighted score = 0.060

**Canard** - less stable than either the powered sailplane or the pylon racer due to the horizontal stabilizer being far in front of the center of gravity. When the plane turns the drag on the horizontal stabilizer tries to push it behind the wing, which if not properly stabilized by control inputs, could throw the plane into a spin. points = 2, normalized points = 0.20, weighted score = 0.030

**Delta wing** - Between the pylon racer and canard. Its low aspect ratio design results in low rotational moment of inertia in all directions and short moment arms from the center of gravity to all control surfaces. It doesn't have the stabilizing effect of a rear tail or the destabilizing effect of a forward tail. points = 3, normalized points = 0.30, weighted score = 0.045

**Flying wing** - Between the conventional powered sailplane and the pylon racer. It has long moment arms from the center of gravity to all control surfaces for good control authority and a high rotational moment of inertia in all directions but does not have the stabilizing effect of a rear tail. points = 7, normalized points = 0.70, weighted score = 0.105

### Maneuverability analysis

In general the parameters that increase the stability of an aircraft decrease its maneuverability. Thus the points and normalized points assigned for stability of the designs will be reversed for maneuverability but weighted scores will change.

**Powered Sailplane** - points = 2, normalized points = 0.20, weighted score = 0.02

**Pylon racer** - points = 4, normalized points = 0.40, weighted score = 0.04

**Canard** - points = 10, normalized points = 1, weighted score = 0.1

**Delta wing** - points = 7, normalized points = 0.70, weighted score = 0.07

**Flying wing** - points = 3, normalized points = 0.30, weighted score = 0.03

\*\*\*\* The ranking chart for this section is figure 2 on page 9 \*\*\*\*

Figure 2 Conceptual Design Ranking

Design	Weighted Drag Score	Weighted Lifting Score	Weighted Stability Score	Weighted Maneuverability Score	Total Score
Powered Sailplane	0.134	0.241	0.150	0.020	0.545
Pylon Racer	0.054	0.215	0.060	0.040	0.369
Canard	0.143	0.243	0.030	0.100	0.516
Delta Wing	0.000	0.218	0.045	0.070	0.333
Flying Wing	<b>0.188</b>	<b>0.250</b>	<b>0.105</b>	<b>0.030</b>	<b>0.573</b>

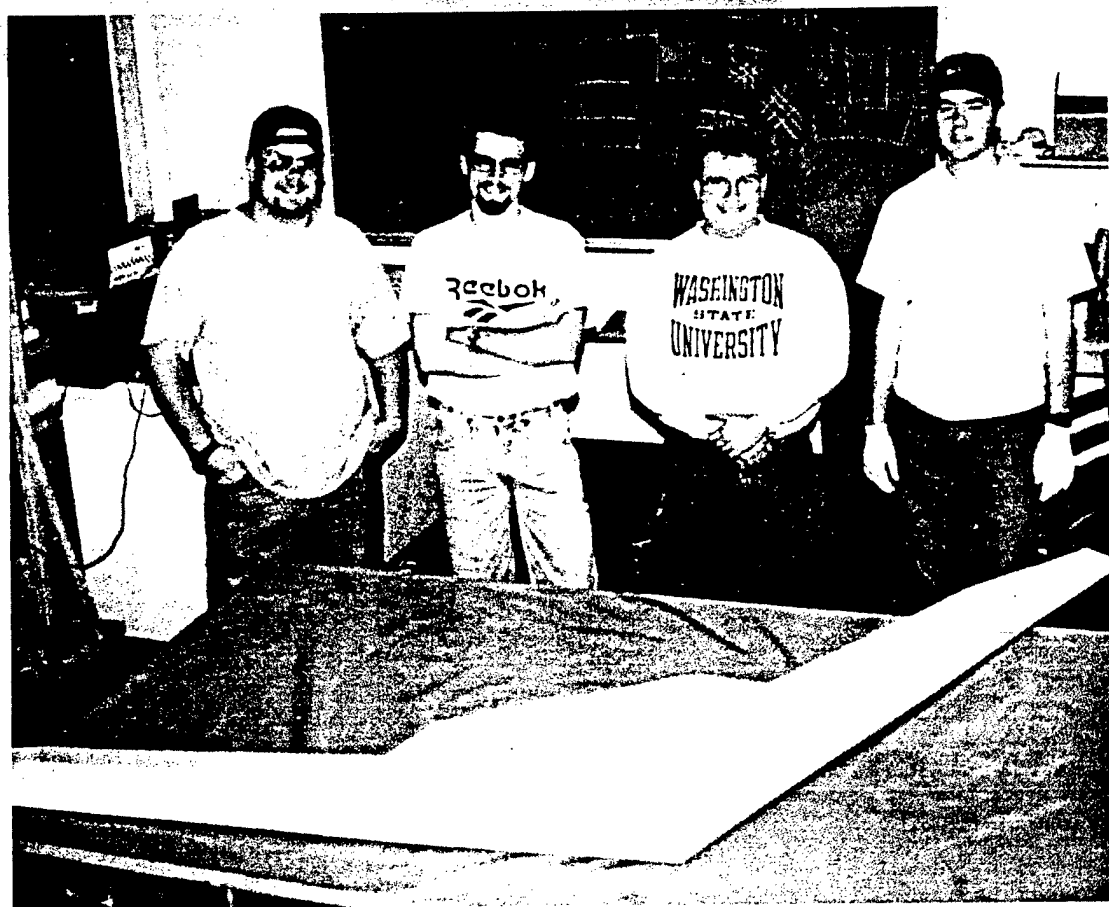


Flight testing  
of a prototype

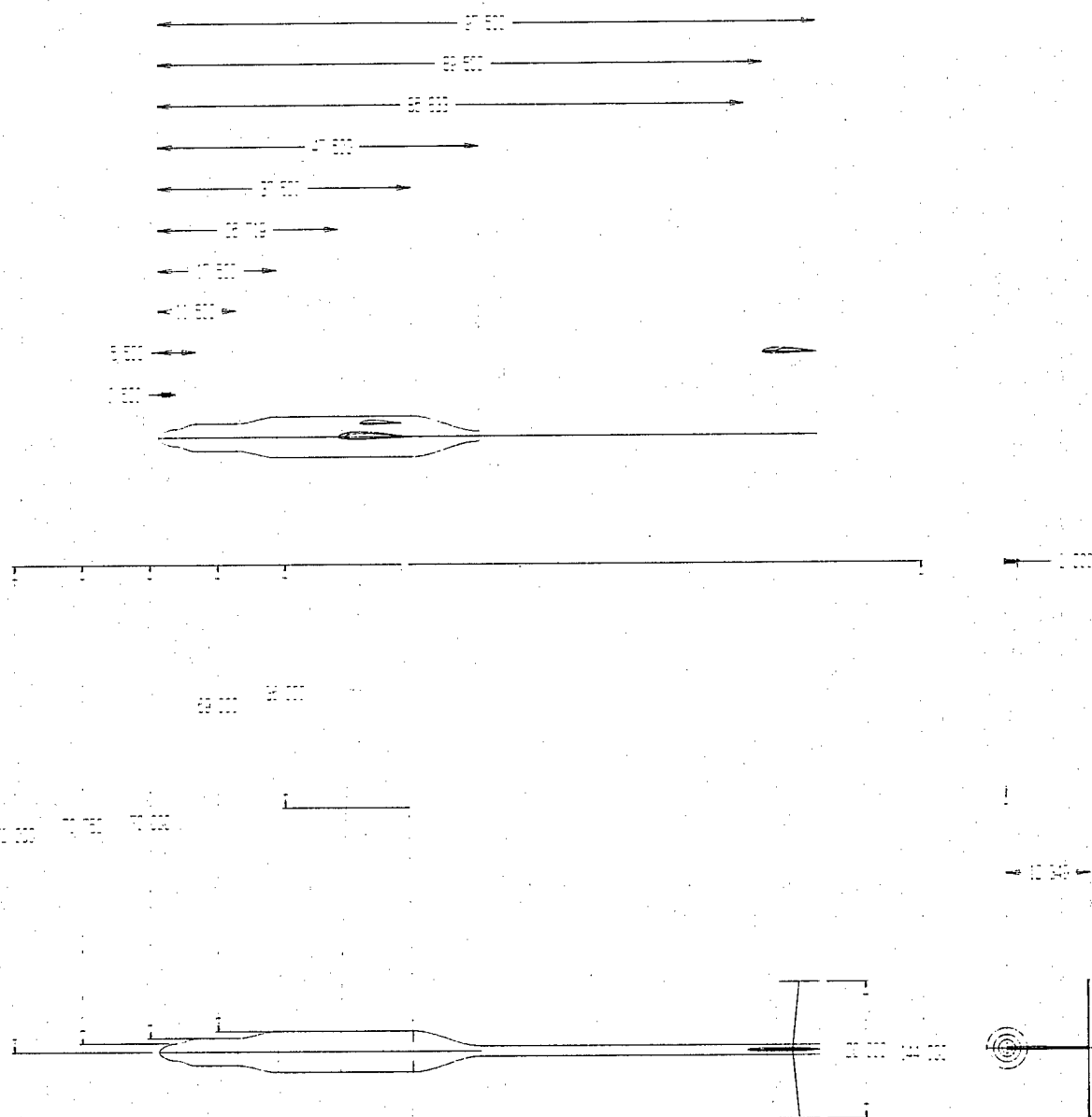


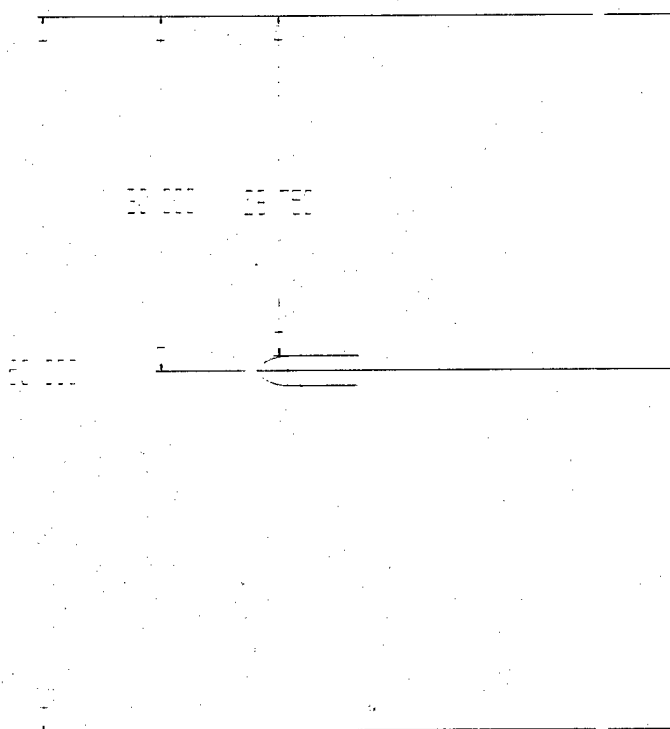
Prototype design  
in flight

Unfinished  
prototype foam core  
with AIAA team  
members

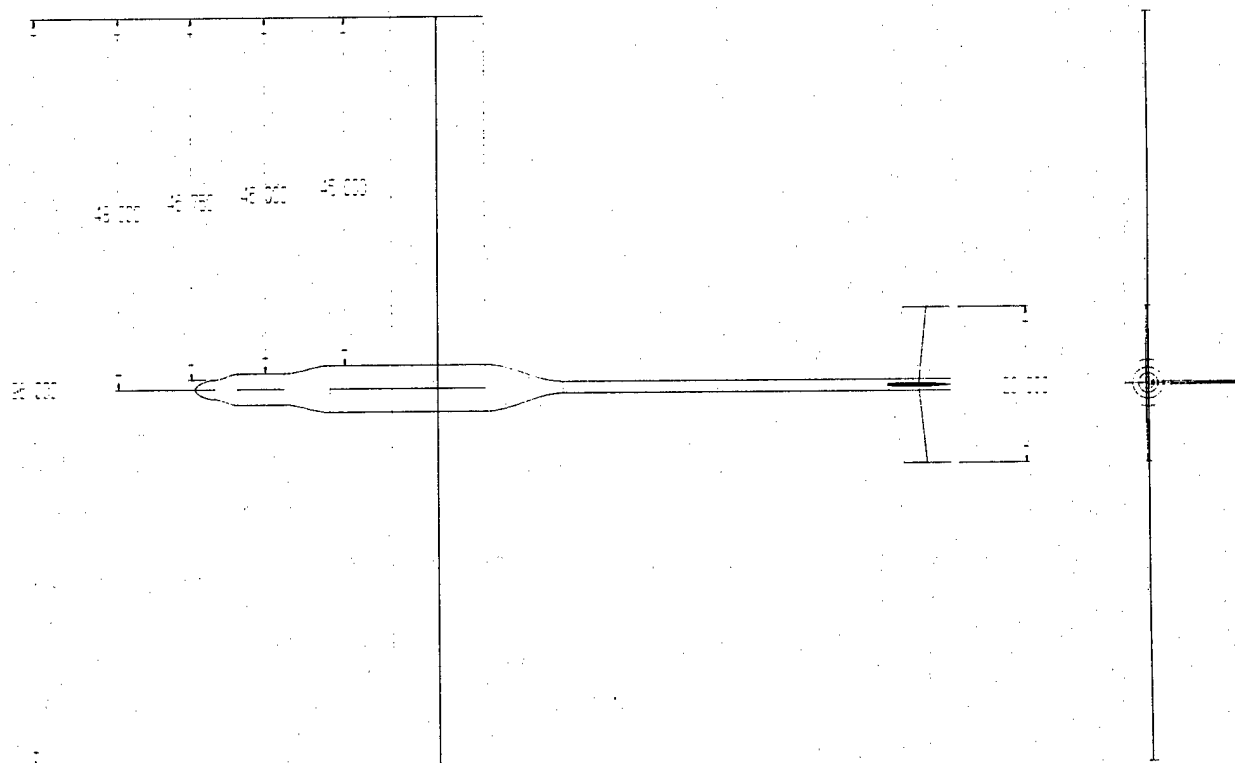
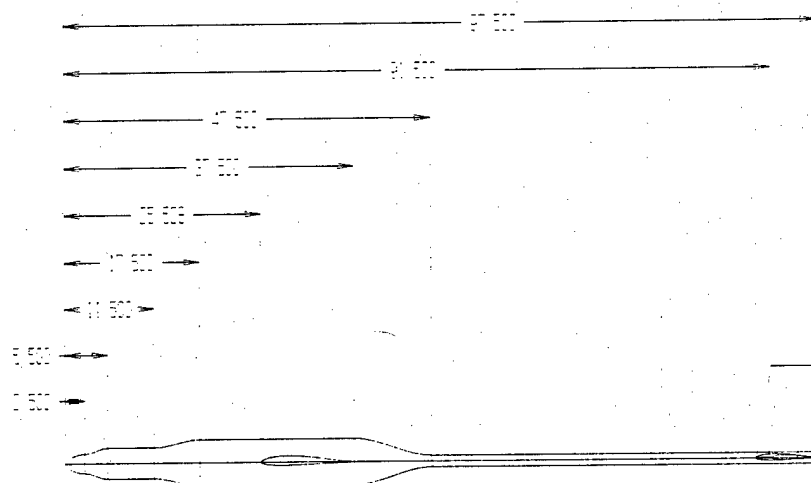


# Flowchart of the process

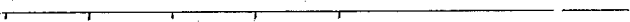
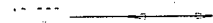
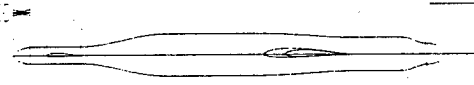
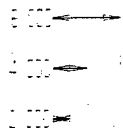
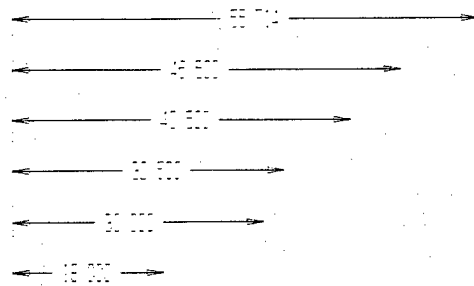




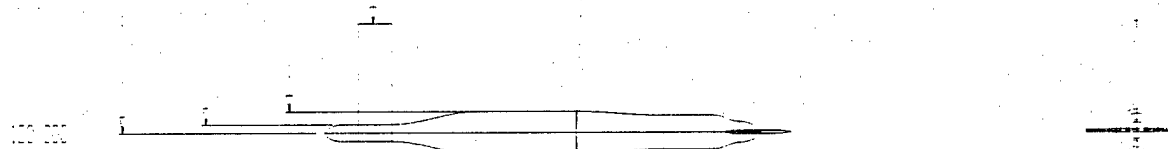
7-01-1967

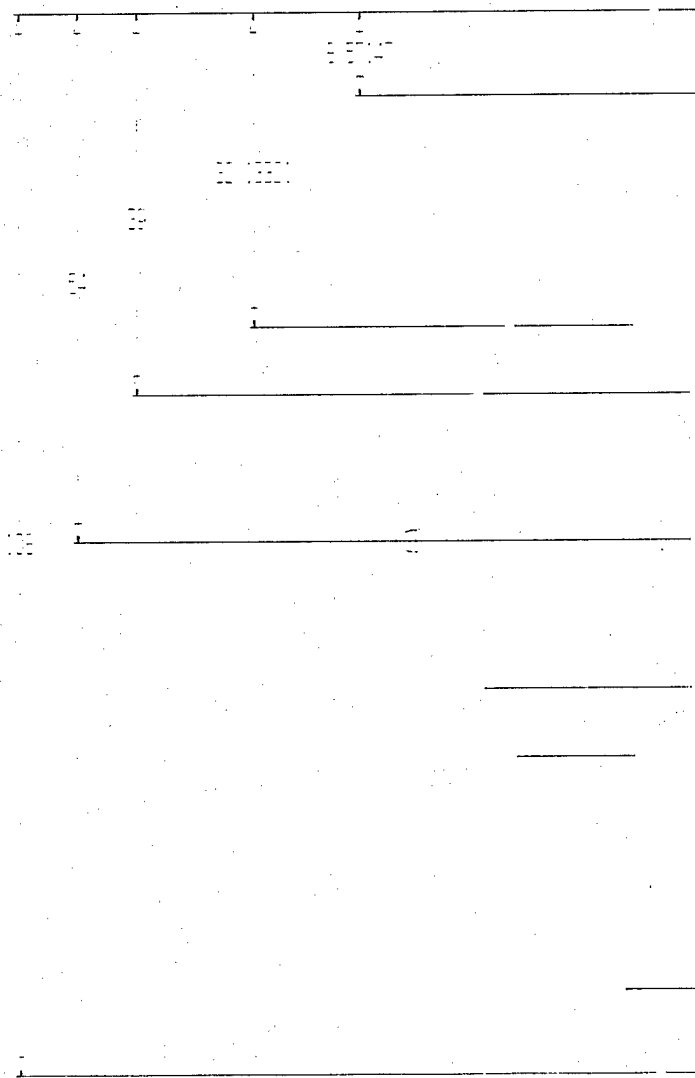
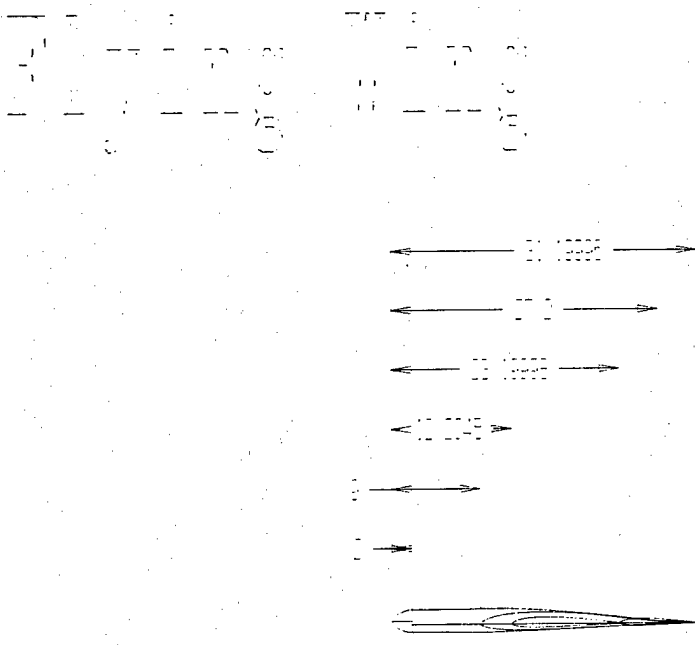


3  
 3 7 3 7 3  
 3 7 3 7 3



61 000 59 000 57 000 47 000





## Preliminary Design

### Design Highlights:

Once the flying wing shape had been established, initial design concentrated on the basic aspects of balance and control. A flying wing requires a low moment airfoil in order to compensate for the lack of a tail. The MH 62 airfoil had a low pitching moment, enough space to accommodate all the internal parts and was specifically designed to work with flying wing platforms. With the airfoil chosen, initial design work was concentrated on how to position internal parts and maintain an acceptable location for the center of gravity (CG).

In all of the initial designs flight hardware placement forced the CG too far forward to maintain balance without lessening the amount of wing sweep added for pitch stability. The easiest way to cure this instability was to extend the center section back six inches in order to allow flight hardware to be moved back. This extension did not significantly change the position of the center of lift (CL) and with proper positioning of flight hardware would lead to a balanced plane.

The next issue was propulsion configuration and location. A baseline motor, the Aveox 1415 was chosen with a 3.7:1 gear reduction and a 26 cell battery pack consisting of Sanyo 1700 mAh cells. Our propeller range was left open, but a maximum diameter of 18 inches was set to allow for ground clearance. These decisions were based on computer simulations done in ElectriCalc. The assumption was made that a tractor configuration would provide greater airflow over the wing during the takeoff and thus shorten the required run. Also the tractor configuration allowed for less distortion of the overall shape of the plane since the propeller cowling would be in the front where the airfoil was already thick. The motor, however had to be placed as far aft as possible to maintain the CG at the current position.

Placement of the motor further back meant a long drive shaft would be required to transfer power from the motor to the propeller. The motor, gear reduction, drive shaft, and all other hardware associated with the transfer of power to the propeller will be housed in a single cylinder. This propulsion containment cylinder (PCC) is removable to allow easy access for maintenance of the motor and speed control. In addition, the propulsion tube provides increased cooling of the motor and speed control by focusing airflow generated by inlet ducts and an inline fan across them.

The batteries, one of the largest and heaviest components, needed to be placed far aft in order to maintain the CG location. The diameter of sub-C or larger cells would not permit placement far enough aft, however, A-size cells allowed movement of the battery packs back almost one inch, enough to balance the plane. Their position in back of the propulsion tube will allow diversion of air used for motor cooling to also cool the batteries before being vented. In order to increase the cell count, the batteries were arranged to require less wiring between packs and less shrink-wrap around the cells.

Retractable style landing gear were chosen in order to eliminate drag associated with fixed gear. Commercially available landing gear were purchased for use in initial powered flight testing, however to reduce total plane weight, redesign with lighter materials is planned for the final configuration. In order to take full advantage of all the benefits of retractable landing gear, they will be completely enclosed in the aircraft during flight. A tricycle landing gear configuration was designed with the front wheel steerable.

To make the flying wing design stable, the wings are swept back to allow the elevator control surfaces on the wingtips to be placed as far back as possible. Sweeping the wings also caused the CG to move back. As much sweep as possible was desired for controllability, but not so much that the plane would be thrown out of balance. Wing sweep also causes a torsional load along the span of the wings. To solve this problem materials for the wing skin were chosen and oriented provide extremely high stiffness and resist any torsional deflection at the wingtips.

Pitch and roll will be controlled by a system of elevators and ailerons. The optimal location for elevators is as far back as possible. The optimal location for ailerons is as far to the sides as possible. For this design these positions correspond to the same area of the wing. Therefore, aileron and elevator inputs are mixed together in one set of control surfaces called elevons. Flaps are on the inboard sections of the wings to increase lift during takeoff and landing.

Once the preliminary shape of the plane was fixed, structural considerations were investigated. To allow for the lightest possible wing sections the skin of the wing carries almost all of the loading. To prevent buckling of the wings foam spacers are placed between the skins. The weight of the center section and gear forces will be transferred to the rest of the airframe through a rib and spar system. The spars allow easy attachment of internal components and provide a structural connection from the wings to the center section.

#### Visualization:

The drawings made ranged from crude sketches on cardboard to solid models in Pro/ENGINEER v.18.0. The drawings provided a concise means of sharing information without misinterpretation. The most extensive work was done in CADKey 97, where parts were drawn and fitted in the aircraft. The drawings not only helped with making sure dimensions were accurate, but they also allowed the plane to be seen in its final form before it was constructed. Problem areas on the surface could be quickly identified and corrected before costly and wasteful mistakes were made. Once a semi-final platform was decided upon, the drawings were converted into computer numerical control (CNC) code needed for milling the components. Once milled, the molds served as templates to organize internal components and visualize where reinforcement may be needed in the final design .

Through the use of a Fused Deposition Modeling (FDM) rapid prototyping



machine, a 14<sup>th</sup> scale model was made. This allowed us to have a small physical model to use as a visual aid for communicating design ideas. This was also made to investigate the possibilities of using the rapid prototype system to create wind tunnel models to test future aircraft.

Eventually solid CAD models will be created using Pro/ENGINEER and then imported into Fluent, a computational fluid dynamics (CFD) program. This will allow us to see where pressures buildups may cause adverse effects in the flying model. Models will be tested at several angles of attack to compare the differences. The simplicity of the flying wing design allows us to focus on maintaining clear airflow over the entire wing surface. We wanted to keep a highly efficient wing, so turbulence created by surfaces not associated with the lift of the aircraft will be minimized to allow undisturbed airflow over the airfoil.

#### Prototyping:

After a preliminary design was drawn the next step was prototyping. The purpose of the first stage of prototyping was to verify that the design would maintain stability and be controllable in flight. With all the unknown aspects of a flying wing design it was deemed necessary to construct and fly a test version of the aircraft before a commitment was made to this design. Flight tests included the consideration of various configurations of wing shapes, sweeps, and airfoil thickness in order to find an optimum configuration.

The models built in the first stage of prototyping were constructed by cutting airfoil shapes out of two-inch extruded polystyrene insulating foam with a hot-wire. A one-half scale model was built and glide tested. This model showed that flight was possible with this design. Once the feasibility of the airfoil was proven, production of a full-scale model commenced. The model was cut from the same foam as the half-scale model, and covered with a layer of Monokote, a heat shrink covering, to provide a smooth airfoil surface. Servos and radio gear were then added and elevon control surfaces were cut into the outer wing panels. After the aircraft was balanced, ballast was added at the center of gravity to increase wing loading to a flyable amount. The design proved to be quite stable in straight, level flight and shallow turns, but in a steep bank it became difficult to control.

Since the model had proven itself controllable in flight, the decision was made to continue with design and construction. Research was continued in the area of lateral stability. A higher sweep angle was decided upon to increase pitch stability as well. A finalized center section mold was designed and milled with the intention of keeping a constant center section design while allowing the wing panels to be changed.

The center section skin was constructed using carbon fiber paper and S-glass with an internal spar structure. The wings were made of fiberglass coated polystyrene foam with a balsa wood trailing edge. The variations in wing design included one with dihedral, one with anhedral, and one with a flat profile for the outer wing. The purpose of these different shapes is to test possible solutions to the control difficulties experienced

during the initial full-scale glide test. These models are currently being flown and modifications will be made to the design to try and determine the best final wing shape.

#### Lessons learned from flight-testing:

The first flight test model was flown simply to prove that the design would fly. It was a simple, unpowered foam model with composite tape reinforcement. Two elevon control surfaces were added at the wingtips for roll and pitch control connected to servos and a radio. Steel ballast was required to get the wing loading up high enough (18 oz/ft<sup>2</sup>) so it wouldn't get blown around like a leaf if a gust of wind was encountered.

The first Monokote model was then launched off a steep hill into the wind for preliminary testing. It exhibited excellent stability in straight and level flight; it was so good that no control inputs were required to keep it on heading or at the correct pitch. The first model however did not bank well. Once past a bank of about 30 degrees, it became unrecoverable. The bank continued to increase despite control inputs and the aircraft crashed.

Analysis of the design showed that five degrees of dihedral was causing an unbalanced rolling force on the wing tip because of its increased speed and lift relative to the other wing. As the turn progressed this force became greater and greater until the plane became uncontrollable, leading to a crash.

A second model was built with the sole intention of testing different wing configurations. It was a center section with detachable outer wing sections. This allowed us to test multiple wing configurations around a common center section. The second test aircraft was flown, this time with great success. It had similar weight and wing area to the first model, but with no dihedral and winglets added at the wing tips. This configuration proved so far superior to the previous configuration that the flight time went from under one minute unpowered to over twenty minutes unpowered. The only complaint about the aircraft was that it was a little sluggish in its responses. It was also neutrally stable, with no tendency to return itself to straight and level flight, but no tendency to become unstable when left alone.

The prototype model also demonstrated stability over a wide range of CG locations. Balance problems do not seem to be a problem in this design. It was noticed that the aircraft became more sluggish in its pitch response as the CG was moved forward which may also be adjusted in the final model to obtain the desired handling characteristics. The increased speed of the powered model combined with more care to tolerances and smooth flow over the airfoils should add to the controllability of the final model.

## Detailed Design

### Take-Off Performance

Flight testing of a final contest version of our design has not been done at the writing of this report. Take off performance is hard to estimate due to the number of variables involved i.e., ground effect, how many pounds of thrust, rolling resistance, drag with landing gear down, wing loading and final flight weight.

Approximately 3.25 lb. of thrust will be available for the duration of the take off, final flight weight will be approximately 17 lbs., wing loading will be approximately 32 oz. / ft.<sup>2</sup>, assuming a semi-smooth paved strip, rolling resistance with our landing gear will be less than ¼ pound. Observed unpowered flight tests of prototypes demonstrated an air speed of 30 - 40 miles per hour. This suggests a low drag airframe for which the allotted thrust should be adequate. Lowered landing gear will induce an estimated 20% increase in drag. These factors equate to a high take-off speed and a long take-off roll.

### Handling qualities

The handling qualities for the flying wing design were developed through an extensive flight test program. Several different prototypes were constructed out of polystyrene foam. Each prototype tested had a new aerodynamic configuration, i.e. wing sweep, control surface placement, airfoil percent thickness, winglet design, dihedral/anedral, etc. Notes were taken on the performance characteristics of each design and analyzed to determine whether the design handled better or worse than previous prototypes. This test was repeated until all design parameters were finalized.

The handling capabilities of the final design are very similar to those of a traditional aircraft with a tail. The design is very stable in pitch and roll and has a gentle stall. It is quite responsive to roll inputs and has an average response to pitch inputs. Aerobatic maneuvers are somewhat limited due to the lack of a rudder but the aircraft turns quickly and that is all that is needed for this contest.

### G-load capability

G-load capability is yet to be determined, and will be addressed in the addendum to this report. G-load capability will be determined using destructive test methods conducted on a competition version of the airframe. The test will consist of loading a competition airframe with a measured load until structural failure occurs. Finite Element Analysis (FEA) of the airframe was explored, but abandoned due to the extensive resources required by this method of testing for a design of our type. An accurate FEA would include: the multiple fiber plies and their orientation in the skin; complex composite beams and ribs; and the strength of the glue joints between the beams, ribs, and skin.

### Range and endurance

We designed the plane to fly with an effective course cruise speed of 50 miles per hour, and a maximum speed of 55-60 miles per hour. At maximum thrust the batteries last 8.17 minutes, which gives a maximum range of 6.81 miles at a speed of 50 miles per hour. This value does not include the time and energy required for a take off. The average take off time is estimated to be 11.5 seconds (0.160 miles) which would reduce the maximum range to 6.65 miles. The two flat turns to prove maneuverability will be performed directly following the take off and should take up 1400 ft. Landing requires another half of a lap, or 750 ft. The range available for laps around the course is then reduced to 6.24 miles, which equates to 7.49 minutes of flight time. We are limited to 7 minutes of time for lap counting, which equates to 5.89 miles traveled on the course. The course for the contest has 700 ft. legs and assuming that a tight turn with an arc length of 50 ft is done at the end of each leg, that equals 1500 feet per lap. This gives a theoretical lap count of 20.

### Payload fraction

Aircraft take off weight is estimated to be 17 lb., the steel payload weighs 7.5 lb.

$$\text{Payload fraction} = \text{payload weight} / \text{total weight} = 7.5 / 17 = 0.441$$

### Component Selection:

#### Motor

A brushless design was chosen due to the efficiency gained by eliminating the drag induced by brushes interacting with the armature of the motor. The selection of an Aveox brushless motor allowed the reuse of a compatible speed controller purchased for the 1996/1997 competition attempt. For this reason Aveox was selected as the motor supplier. A 1400 series motor was chosen due to the fact that it was the lightest and most efficient available, while still meeting the power requirements of our design.

#### Batteries

The power system of the aircraft was probably the most critical system to design correctly. A poorly designed system could have a large effect on total run-time, speed and energy wasted. An efficient motor and battery combination would provide higher top speeds and larger lap counts. Aveox brush less motors are widely considered the most efficient and reliable electric motors of this scale available. They also are made in sizes varying from a total power output of less than 100 watts to several thousand watts. A properly sized battery can deliver between 40 and 50 Watt hours if the battery is discharged slowly to .1 V per cell. At the currents that are necessary for high speed flight and discharge of the battery in the time allotted, the capacity drops to 37 to 41 Watt hours. Under most flight conditions the cells will only be run down to .9 V per cell because power output drops to levels at which the plane can no longer maintain level flight. Cell counts were limited by the available speed control's maximum voltage and the 2.5 lb. weight limit. The optimal cell count seemed to be close to the maximum voltage accepted by the speed control (32 cells). Only one viable pack option existed in

this range, the Sanyo 1400series. The internal resistance at our currents ended up causing the generation of too much heat for safe battery operation. Other options were explored in the 22-26 cell range with the Sanyo 1700 and 1800 series cells. The 1800's seemed to have the power density, high voltage and low internal resistance required for an efficient system. Each cell was individually tested for properties and then they were assembled into flight ready packs. The 1700's had a higher energy density and total voltage than the 1800's, but also a much higher internal resistance. Tests showed that the resistance was enough to lower average cell voltage to a 1.05 V/cell over the run-time with a fairly constant decline in power over the duration of the test. The 1700's were able to provide an average of 39.81 Watt hours during a 7C discharge rate. (A 7C discharge rate is a discharge equal to 7 times the rated cell capacity in Amp hours.) The 1800's are designed for higher currents than the 1700's and have a lower internal resistance as well as a higher capacity per cell. The cell count was down by 3 cells from the 1700's so the capacity was offset by a lower voltage. The 1800's during testing maintained an average of 1.15 V/cell for the duration of the test. These cells also had much less of a tendency to drop off in voltage until the end of the test, meaning they would provide more power at the end of the flight. They had a total capacity of 40.89 Watt hours at a 7C discharge rate. Tests also showed that if the battery maintained temperatures between 100 and 140 degrees F, they were able to provide a slightly higher voltage at the current levels expected for the competition.

Now that values for currents were known, a motor could be selected. Projected maximum power input was between 350 and 400 watts, so a motor was chosen to fit this range. The Aveox 1412 series seemed to provide power in the range that was necessary. The winding on the motor would determine the speed at which the motor would turn given a voltage. Lower RPM's would require a larger propeller to draw the same power from the motor. Higher RPM's would require smaller propellers or a gear reduction to draw the same power. A large propeller would provide higher efficiency than a smaller propeller so the motor was also picked according to the propeller sizes available. Initial calculations were performed in ElectriCalc to determine motor and propeller sizing. It calculated an Aveox 1412 with a 3.7:1 gear reduction and an APC propeller would provide very high efficiency, high top speed, and run for more than eight minutes with the batteries that had been selected. In actual tests, it was determined that ElectriCalc numbers were high. The voltage drop and a lower total useable capacity due to the .9 volt per cell cutoff were not taken into account by the program. The battery pack however, did run for an adequate amount of time and runtime could be lengthened if the throttle was pulled back, although this results in a slight motor efficiency loss.

### Landing gear

Due to the nature of aerodynamic drag, which increases with the square of velocity, the elimination of all protrusions was imperative to increasing the speed of the aircraft. For this reason retractable landing gear was selected instead of streamlined fixed gear. The selection of retractable landing gear over a fixed landing gear increased the weight of the aircraft. This weight penalty was reduced by replacing structural components of the retracts with high specific modulus materials like titanium and carbon fiber/epoxy

laminates. This resulted in a 40% weight reduction of the landing gear units.

### Propeller

An APC propeller was chosen for its high efficiency and wide range of available pitch sizes. The high efficiency of this propeller is due to the thin profile and Fiberglass construction. This allows the propeller to resist deformation in high speed / high thrust situations. Pitch sizes up to 16 were readily available and are well suited for the combination of the flying wing airframe and the Aveox motor that are being used.

### Servos

Standard servos are used on the large flap surfaces and to steer the nose gear which are high-load applications in this aircraft. Mini servos are used on the outer elevons where the airfoil cross section is too small for a standard servo and the loads are less. A mini servo is also used to actuate the control valve for the pneumatic power system of the retractable landing gear.

### Wheels

The hubs are made of nylon and were manufactured on a lathe. Six small holes were drilled in each hub to decrease weight while still retaining the required stiffness and strength. The outer tire is made from high density foam rubber that is glued onto the hub with epoxy. An oil-filled ball bearing is inserted into the hub and provides a virtually frictionless rotation about the axle. This minimizes rolling resistance which results in a shorter take-off roll.

### Systems architecture

All systems in the aircraft were designed or re-manufactured for minimal weight and maximum reliability. Drag reductions were given higher priority over weight reductions as demonstrated with the choice of retractable landing gear. All systems were also designed to be highly serviceable with large hatches and fasteners that are easily removable (see Figure 17, page 40). Consideration was paid to the proven reliability of components and in some cases reliability was proven through our own testing programs. Components were modeled on the computer to check for tolerances and clearances before decisions on placement were made. Attention was also paid to the placement and isolation from the electric fields produced by the motor for sensitive electronics like the radio receiver.

### Innovative configurations

A removable propulsion tube was designed into the structure of the plane allowing unhindered access to the entire propulsion system. The retractable landing gear were offset at a 20° angle, moving wheels to the thickest portion of the center section. This allowed the use of a larger tire size, further reducing rolling resistance. A thrust bearing

on the titanium propeller drive shaft transfers thrust loads to the airframe, rather than the motor.

#### Innovative manufacturing processes

Hatches are constructed by laying up a section of cloth in the mold that is slightly larger than the desired hatch size, in the exact hatch location. Once cured, this composite part is trimmed to exact size and coated with polyvinyl alcohol (PVA) release agent. This coated hatch is then placed back in the mold and a wet lay-up for the skin is constructed on top of the hatch. This forms a relief in the outer skin which will be filled by the hatch. This construction technique generates an opening in the surface of the airframe with high tolerances. This will decrease the aerodynamic drag induced by the edges of the hatch.

Airframe production cost was reduced by constructing the outer shell of the aircraft from just two composite pieces (top and bottom) that are joined with epoxy adhesive (see Figure 18, page 41). This increases strength, and decreases weight, cost, and complexity through the elimination of fasteners. Production cost is reduced further through a negative mold technique. Multiple copies of the aircraft are required for testing manufacturing techniques, structural integrity, and flight performance. Although the cost of negative molds is greater initially, the cost per part decreases as production levels increase. The quality and quantity of parts produced by one set of negative molds makes them the preferred manufacturing method.

# Battery Comparison

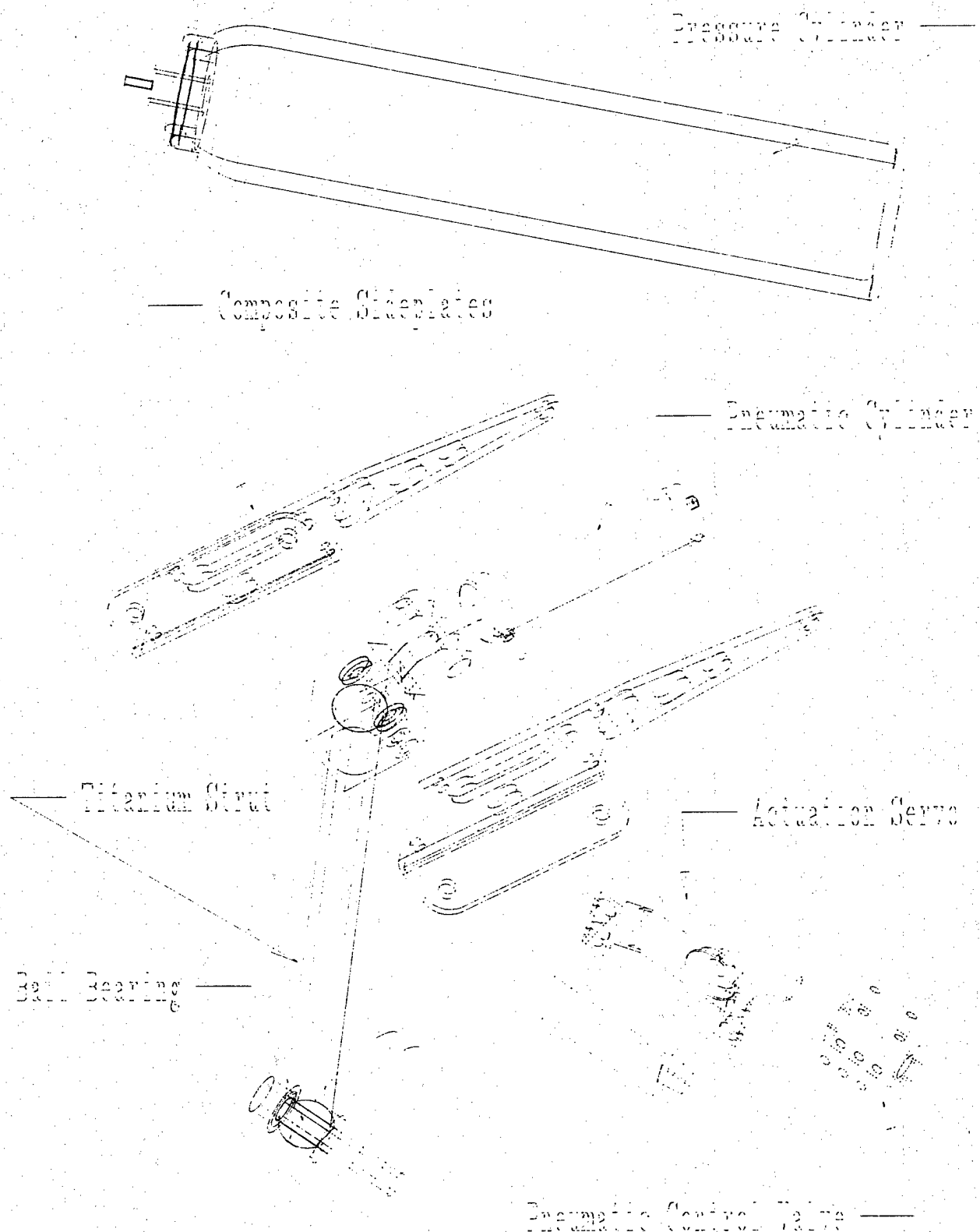
## Figure 9

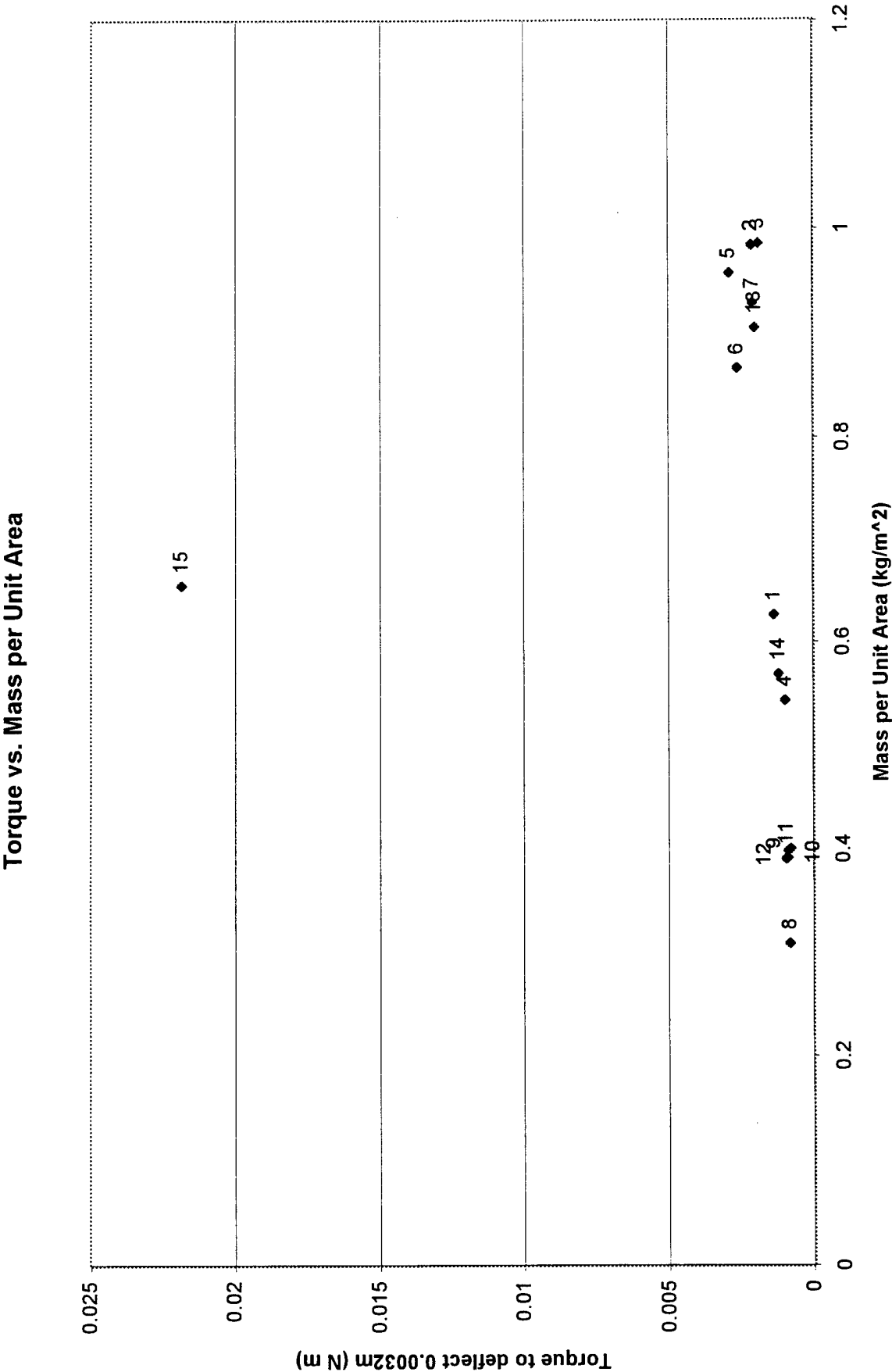
Packaging Wt. factor = 1.05  
Cell Interconnect power factor = .98

Cap. Rating (A-h)	Cell #	Cell Wt. (g)	Stabil. 1C Cap. (A-h)	7C rate Current (A)	7C rate Cap. (A-h)	7C rate Energy (W-h)	Run time @7C (min)	Max # of cells	Total Energy to 1.0V per cell (W-h)
2.3	1	58.58	2.156	16.10	1.736	1.916	6.47	18	37.49
	2	59.12	2.345		1.984	2.203	7.39		
	3	58.93	2.344		1.951	2.158	7.27		
	4	58.85	2.322		1.844	2.045	6.87		
	5	58.75	2.273		1.969	2.194	7.34		
	6	59.10	2.295		1.897	2.103	7.07		
Typicals:		58.91	2.309		1.915	2.125	7.14		
1.25	7	42.19	1.257	8.75	1.144	1.323	7.84	25	32.11
	8	42.16	1.228		1.109	1.279	7.60		
	9	42.47	1.256		1.139	1.313	7.81		
	10	42.57	1.240		1.105	1.272	7.58		
	11	42.48	1.263		1.148	1.329	7.87		
	12	42.55	1.271		1.149	1.328	7.88		
Typicals:		42.42	1.254		1.135	1.311	7.78		
1.9	13	55.76	1.955	13.30	1.756	2.004	7.92	19	37.08
	14	55.62	1.888		1.692	1.921	7.63		
	15	55.47	1.932		1.741	1.988	7.85		
	16	56.07	1.954		1.740	1.976	7.85		
	17	55.36	1.938		1.750	1.998	7.89		
	18	55.70	1.966		1.771	2.015	7.99		
Typicals:		55.64	1.945		1.747	1.992	7.88		
1.8	19	47.46	1.844	12.60	1.681	1.909	8.00	22	40.89
	20	47.85	1.883		1.687	1.904	8.03		
	21	47.84	1.849		1.695	1.932	8.07		
	22	47.89	1.827		1.682	1.904	8.01		
	23	47.81	1.783		1.610	1.818	7.67		
	24	47.20	1.835		1.655	1.869	7.88		
Typicals:		47.74	1.839		1.676	1.897	7.98		
1.7	25	42.88		11.90	1.494	1.645	7.53	25	39.81
	26	43.13			1.474	1.621	7.43		
	27	42.82			1.495	1.646	7.54		
	28	42.99			1.459	1.607	7.36		
	29	43.40			1.456	1.597	7.34		
	30	42.81			1.474	1.626	7.43		
Typicals:		42.96			1.475	1.625	7.44		

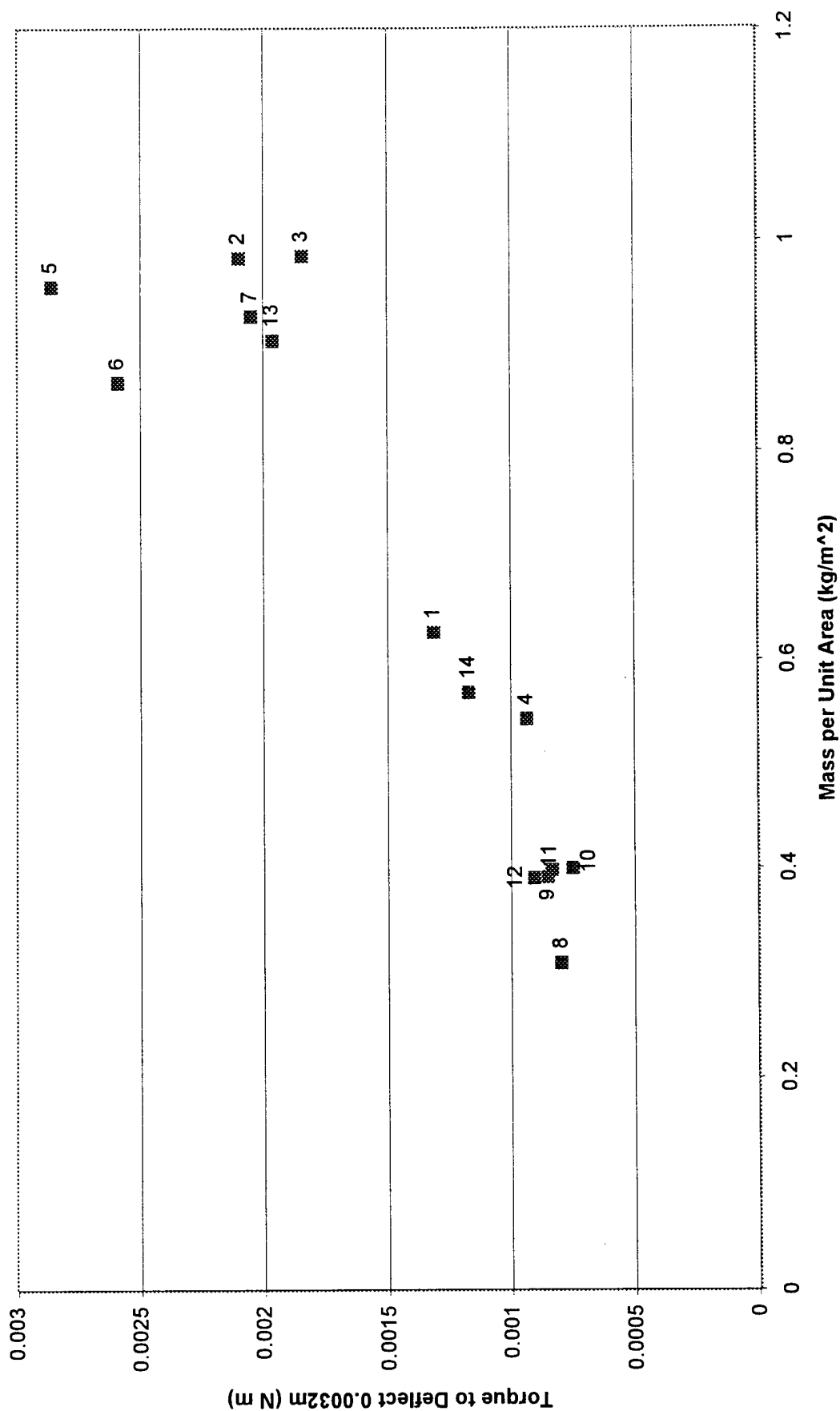


# Landing Gear





Torque vs. Mass per Unit Area  
(Test # 15 not included)

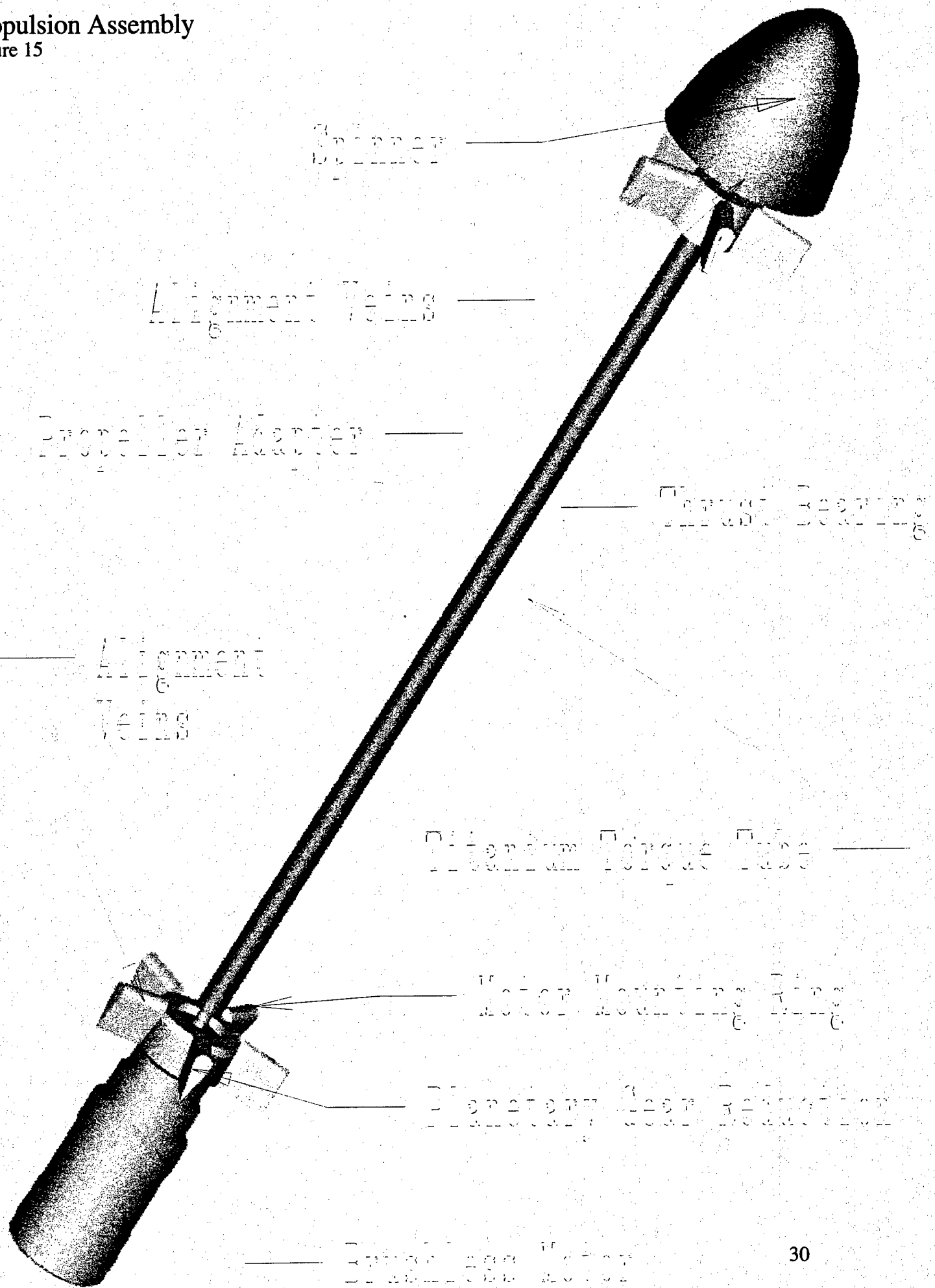


# Materials Strength

Figure 11c

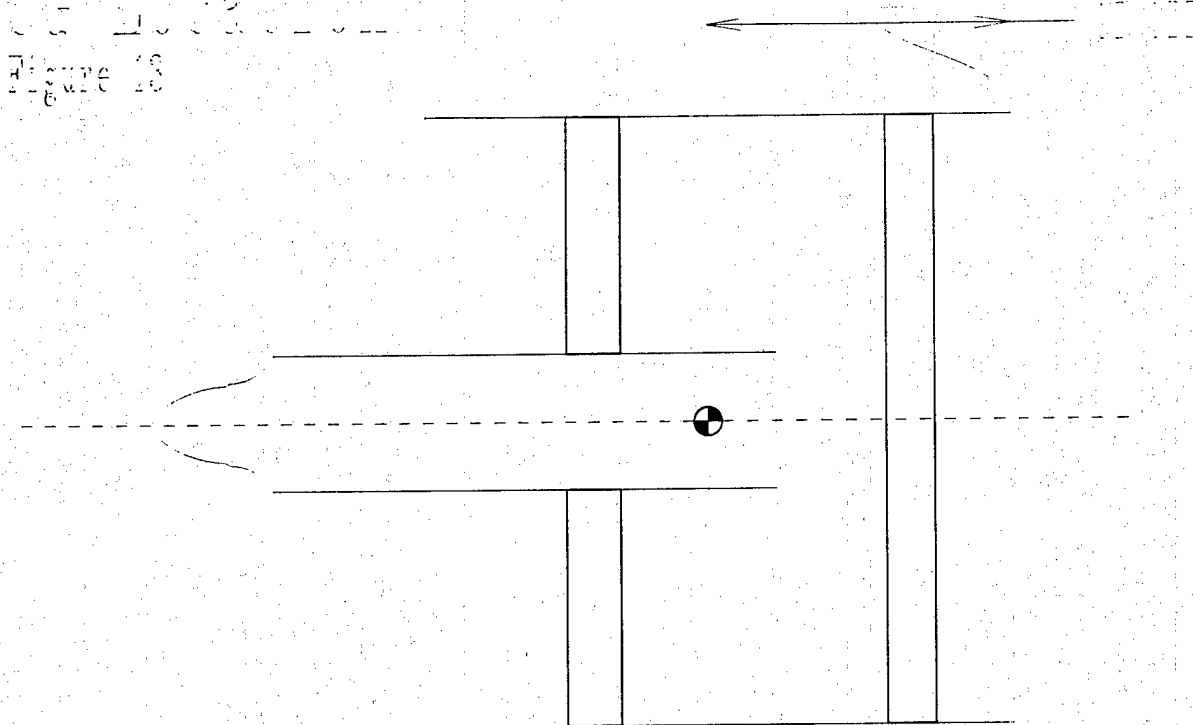
Materials Selection Chart					
Test #	Test Piece	Test Piece Mass (kg)	Surface Area (m <sup>2</sup> )	Mass per unit area (kg/m <sup>2</sup> )	Torque (N m)
1	Glass w/ 2 balsa strips	0.00351	0.0056	0.626785714	0.63 0.0013119
2	4 layer carbon 5.4 oz	0.00561	0.0057	0.984210526	0.7135 0.0020968
3	2 glass layer w/ solid balsa	0.00493	0.005	0.986	1.834 0.00184264
4	1 layer 5.4 oz carbon 1 glass	0.0025	0.0046	0.543478261	0.049 0.0009344
5	2 layer glass w/ solid foam	0.00766	0.008	0.9575	1.431 0.00286301
6	2 layer glass w/ foam + holes	0.00693	0.008	0.86625	1.813 0.00259016
7	2 layer glass w/ foam X's	0.00548	0.0059	0.928813559	0.481 0.00204821
8	1 layer 2.9 oz carbon	0.00213	0.0069	0.308695652	0.024 0.00079611
9	2 layer glass	0.00227	0.0058	0.39137931	0.013 0.00084844
10	1 layer 5.4 oz carbon + paper	0.002	0.005	0.4	0.017 0.00074752
11	2 layer glass	0.00223	0.0056	0.398214286	0.017 0.00083349
12	1 layer glass / 2.9 oz carbon	0.00242	0.0062	0.390322581	0.037 0.0009045
13	4 layer glass	0.00525	0.0058	0.905172414	0.11 0.00196225
14	2 layer 5.4 oz carbon	0.00313	0.0055	0.569090909	0.073 0.00116987
15	S-glass w/ foam & carb. paper	0.01948	0.0297	0.655892256	0.00167 0.02184259

# Propulsion Assembly Figure 15



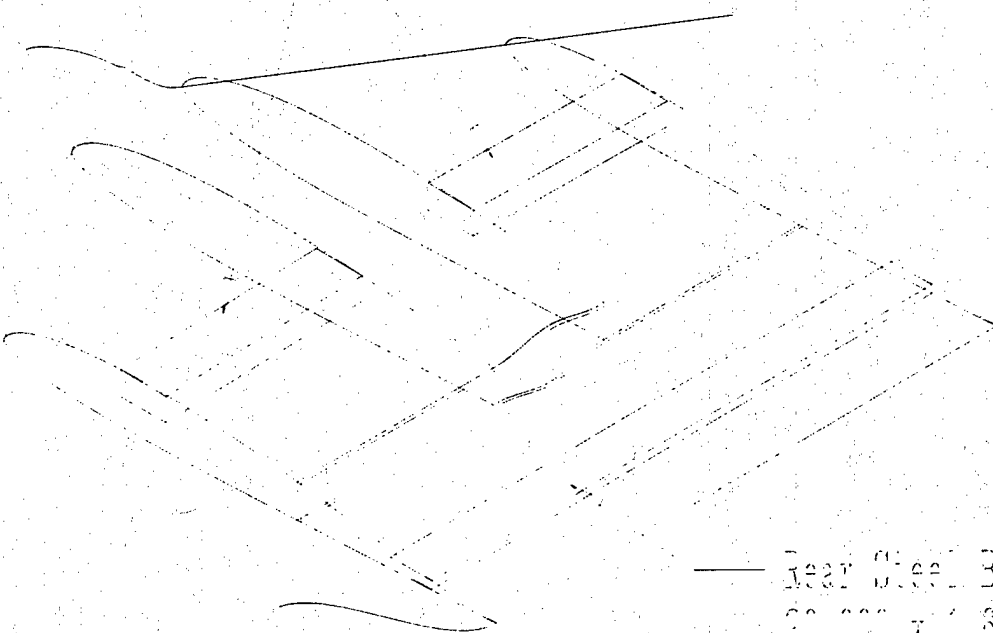
7.737 x 1.830 x 0.640

Figure 18



Forward Steel Blocks

7.737 x 1.830 x 0.640 (x2)



Rear Steel Block

4.000 x 1.830 x 0.640

## Manufacturing Plan

The decision of what manufacturing process to use for this year's design was developed concurrently with other design issues. The ability to manufacture the shape and outer form of the aircraft as well as the required internal structure was as important a design parameter as the functionality of the design. This reduced final design rework when it came time to finally start manufacturing aircraft.

The figures of merit used to evaluate each manufacturing process were surface finish of parts produced, tolerance and accuracy available, cost, and skill level required to implement. The surface finish of the parts that are exposed to the flow of air around the aircraft must be uniform, without pits or protrusions that will disrupt the boundary layer. This will help keep the boundary layer thin and laminar over most of the airfoil, reducing drag and increasing the maximum speed of the aircraft. Increasing speed is a major goal of this project, therefore surface finish is assigned a weighting of 30%. Increasing the tolerance and accuracy available to parts created with a particular manufacturing process decreases the number of parts that are scrapped from not meeting quality control standards. These standards are high for this project since the aircraft is pushing the limits of reducing drag and weight, thus tolerance and accuracy is assigned a weighting of 30%. Cost reduction was evaluated for initial setup, project cost to create prototypes and contest model, and a per unit cost if the design was put into commercial production. Overall cost reduction was assigned a weighting of 25%. The skill level to implement the manufacturing plan was assigned the lowest weighting. Through good engineering and construction practice even the most difficult methods can be broken down into manageable steps. Skill level was assigned a weighting of 15%.

Manufacturing processes that were investigated were:

- Negative molding with fiber reinforced polymeric composite layup
- Positive molding with fiber reinforced polymeric composite layup
- Wood construction with polymeric composite reinforcement

### Wood construction

This manufacturing process involves generating templates for each part on the aircraft. If the design is created in a CAD environment, each part can be isolated and printed out on a laser or inkjet printer to create a disposable template. Templates for parts that are larger than an 8 ½ x 11 piece of paper can be created by sectioning the drawing and printing out one section at a time. These sections are then aligned and taped together. Permanent templates of formica or metal can then be created from the disposable templates. Once templates are constructed, each part of the aircraft structure is cut out using them.

**Cost – low** - The process of constructing templates is inexpensive but very time

consuming. Cutting out the parts is also a long and tedious process.

**Accuracy - variable** – it depends on the skill and diligence of the craftsman.

**Surface finish – variable** - with proper sanding and many coats of primer it is good. The problem is the time involved with this finish and the added weight. Heat shrink covering can be applied, this method saves weight but sags in an open structure and bubbles up in a fully sheeted structure decreasing the accuracy of the aircraft.

**Skill required to implement – high** - good results can not be achieved without adequate experience in cutting, sanding, and shaping. This typically requires building two full models.

#### Positive molding with composite layup

The CAD model of the aircraft is imported into computer aided manufacturing (CAM) software to generate CNC machine tool paths. A CNC mill is then used to cut a disposable positive mold “plug” in the shape of the aircraft. The plug is then sanded smooth and treated with release agents. Usually a mold release wax is coupled with poly vinyl alcohol (PVA). The fiber reinforced polymer composite is then layed up over the plug. Typically the composite is fiberglass/epoxy or carbon fiber/epoxy. Light vacuum bagging can be done to improve surface finish as long as it is not powerful enough to deform the plug. The next step is to fill and sand the surface to an acceptable finish and then apply paint if required. The plug is removed from the cured composite part by cutting hatches in the surface and cutting out the disposable material. Sometimes the plug is desolved by chemical treatment.

**Cost – high** – CNC machining must be used to keep accuracy within acceptable levels with this method. The machining process must be repeated for each aircraft since the mold is disposable. Machining time is dependent on the size and complexity of the aircraft but at approximately \$50 per hour it adds up fast. The cost to build five aircraft for testing and competing would be enormous with this method.

**Accuracy – moderately high** – The CNC machining ensures high dimensional accuracy of the mold plug but often the low density of a disposable mold material deforms under vacuum bagging.

**Surface finish – moderate** – If the vacuum bagging is done correctly and the mold does not deform, little filling and sanding is required to achieve a good finish. The vacuum bagging process is very tricky; too little vacuum and air bubbles may be left in the composite decreasing strength, too much and the plug deforms. The difficulty in establishing the correct vacuum often leads to less than perfect parts and gives this category a moderate rating.

**Skill required to implement – variable** – it is high if the CNC coding and machining is



done by the designer. Mastering a CAM software package is involved and running a CNC mill requires a thorough knowledge of machining to create accurate parts. Skill requirements are lower if these items are contracted out; but the cost increases.

#### Negative molding with composite layup

Negative molding is similar to positive molding in that CNC machining is utilized to create the molds but in this case the accuracy of this machining defines the outer surface of the aircraft instead of the inner surface. Following machining, tool paths are leveled, painted with epoxy primer, and wet sanded to an ultra-smooth finish. The surface of the mold defines the surface of the part in this case. For this reason it is advantageous to get the surface of a negative mold pristine; but this only has to be done once since the molds can be used over and over to make a high number of aircraft before needing repair.

**Cost – variable** – the initial cost to create the molds is high compared to creating one model from wood construction, however if multiple aircraft are needed, the cost per part goes down for every successive plane built. If time is viewed as money, the time to build a wood aircraft is greater than the time to create a composite one with this technique making negative molding more cost effective

**Accuracy – high** – CNC machining gives the molded surface a high degree of accuracy and since the mold is permanent it can be created from stronger, more durable materials making it impervious to the stresses of vacuum bagging.

**Surface finish – high** – The priming and sanding of the molds only has to be done once and then multiple aircraft can be constructed without sanding. For this reason negative molds are usually given a high surface finish that translates to a smooth aircraft surface.

**Skill required to implement – variable** – as with positive molding; if CNC coding and machining is contracted out the only skills required are block sanding, spraying primer, and waxing. If the CNC work is done by the designer, a learning curve must be traveled in that area before accurate results can be accomplished.

#### Summary

If only one aircraft is being produced, the manufacturing process of choice is wood. The cost will be the lowest of the three methods which were explored in this report and the time required will be approximately the same. With practice, this method can produce accuracy approaching that of negative molds but surface finish is not as good.

If multiple aircraft are in the production plan, the manufacturing process of choice is negative molding. The high accuracy and excellent surface finish, quick construction time, and low per part cost makes this method excel above all others.

If the part to be manufactured has a very complex shape that would require several negative molds to produce it, or for applications like tubing and conduits where the surface finish of the inside is more important than the outside, positive molding is the way to go.

Each one of these manufacturing processes have advantages and disadvantages. For the design build fly competition WSU AIAA chose negative molding for its high accuracy and excellent surface finish while keeping overall cost down for our prospective need of five aircraft (3 testing, 1 contest, 1 back up in case of crash).

### Specifics on implementation

WSU AIAA used polyurethane closed cell foam as a mold material for several reasons: it is isotropic (no grain as in wood), it is dimensionally stable over a wide temperature range, it is chemically stable for use with various epoxies and primers, it is easily machined with high feed rates that cut down on machining time and cost, and it is available in several different densities. A density of 18 lbs/ft<sup>3</sup> was used for our molds which had the best compromise of machining speed and resistance to deformation under vacuum bagging stresses.

A stressed skin design was used in the construction of our aircraft in order to reduce weight. High specific strength materials were used to further decrease weight while maintaining adequate strength. S-glass is the main constituent of the load carrying skin. This material was selected for good specific strength, low electrical conductivity to reduce radio interference, and low cost as compared to carbon fiber. The choice of all materials was arrived at through a testing program. Testing was conducted on small samples, approximately 25 square inches in area, which involved different materials and material orientations. Since all of the material combinations that were tested had theoretical strengths that would be adequate for structural support, the objective of these tests was to determine the maximum stiffness that could be achieved with the lightest combination of these materials. The testing apparatus was set up to measure the amount of force required to deflect each test section a measured amount given a known moment arm. The deflection amount was 0.125 inch based on an acceptable deformation of the aircraft skin given no internal reinforcement. Data from these tests was then used to determine an average stiffness for each test combination. Next, using the measured mass of each specimen and its surface area, stiffness versus mass per unit area was plotted. This graph (see figure 11 on page 27) allowed the elimination of combinations of materials that had inferior stiffness or higher mass per unit area than other composites. These tests also allowed the determination of the optimum matrix volume fraction and fiber orientation for each section.

The optimum stiffness and weight were achieved using a composite composed of a layer of bi-directional weave S-glass and 1/4 inch thick polyurethane foam hexagons between two layers of carbon fiber paper all in a matrix of Shell Epon 828 epoxy resin.

The reason this particular composite has the highest specific stiffness of those tested is that the foam hexagons form a series of miniature beams which increase the material's resistance to bending and torsion. The hexagon pattern was not used in more than one aircraft because it provides more stiffness than is required by flight loads and it took too much time to manufacture.

For ease of manufacture and adequate structural stiffness, a composite fabricated from one layer of fiberglass paper and one layer of 3.6 ounce S-glass fiberglass in a Shell Epon 828 epoxy matrix is used. The fiberglass paper has a random fiber orientation that provides equal strength in all directions as well as a smooth surface finish that reduces drag. The 3.6 ounce S-glass has a bidirectional weave and contributes most of the structural strength in the shell of the aircraft.

Once the two halves of the outer shell are molded, they are joined to form the shell of the aircraft. At the leading edge a stepped joggle-joint (see figure 17 on page 44) was used, then laminated with the same epoxy resin used in the skin lay-up. The joggle joint helps ensure an accurate alignment between the two halves, which allows for the same degree of dimensional accuracy in the assembly as is used in making the individual parts. The mechanical interlocking of this joint design also adds to the strength of the aircraft structure. A lap joint is used to join the halves at the trailing edge. For the center section of the aircraft a series of internal ribs and spars also distribute the high loads produced by wing bending and landing gear impact. The ribs and spars are constructed of 1/8 inch thick polyurethane foam covered with a layer of 5.4 ounce carbon fiber saturated with epoxy. The internal structure is joined to the shell using epoxy fillet joints with microballoon particulate reinforcement. The ribs used in the internal structure of the outer wing panels are reinforced with carbon fiber because it was determined that these ribs would not be subjected to the high loads experienced by the center section ribs.

The final design of the aircraft uses retractable, pneumatic landing gear. During the manufacturing of the shell and internal structure of the plane, it was decided that with the current aircraft design, the commercially available landing gear provided a higher safety factor than is necessary. The significant weight of the landing gear could be reduced by remanufacturing several of the parts using high specific modulus materials. Many of the major steel components were replaced with machined titanium parts (shaft and pivots). Titanium tubing replaced the original steel tubing for gear legs. The shock absorbing springs were removed because the titanium shafts were much more flexible than their steel counterparts. Finally, the aluminum side plates were replaced with carbon fiber/epoxy laminates.

Figure 14

Negative Mold Manufacturing Milestones				



Generating CNC Center Section mold tool path with MasterCAM.

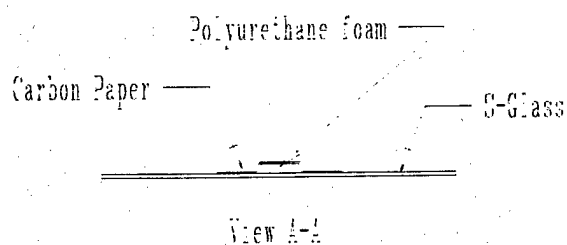


Manufacturing Center Section mold on a 3 axis CNC mill.



Carbon Fiber Composite Prototype during the lay-up process in the female molds.

# Shell Layer Diagram



Kevlar 3.0 oz 90x90  
(bottom shell only)

Kevlar 3.0 oz 90x90  
(bottom shell only)

Carbon 2.9 oz  
45x45 to vertical

S-Glass 3.6 oz satin  
45x45 to wing direction

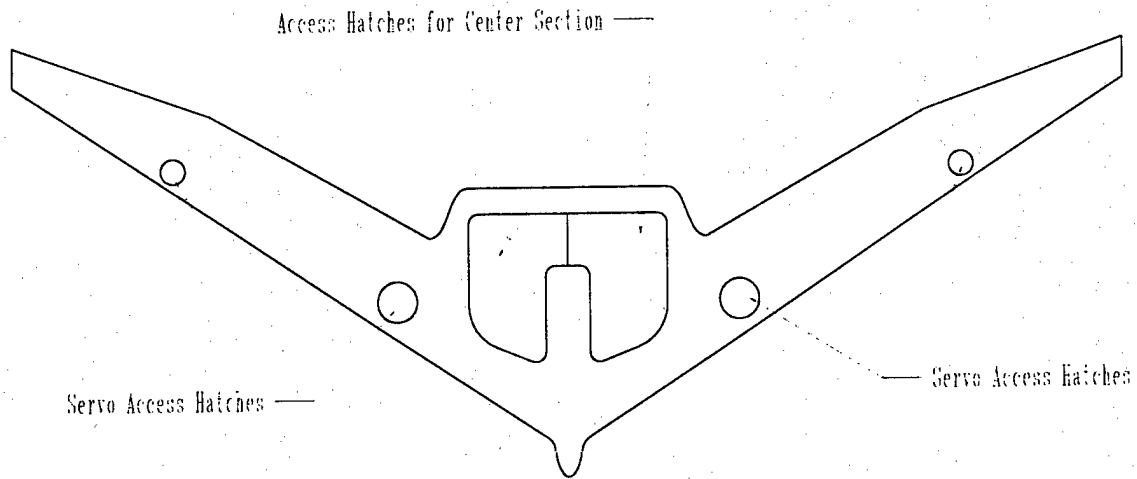
Kevlar 3.0 oz 90x90  
(bottom shell only)

S-Glass 3.6 oz satin  
45x45 to wing direction

S-Glass 3.6 oz satin  
90x90 to vertical

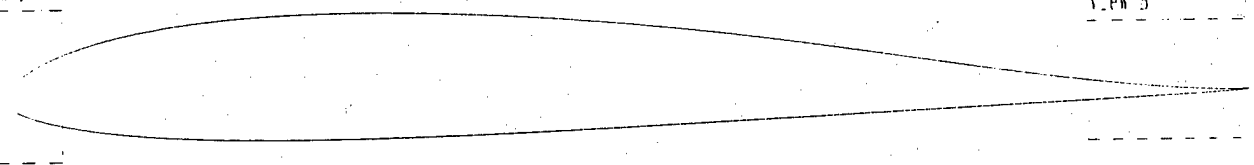
3.125" x 0.375" polyurethane foam strips  
capped with 2 layers of 0.75 oz  
carbon paper

# Hatch Layout



View A

View B



Leading Edge Joint

Trailing Edge Joint

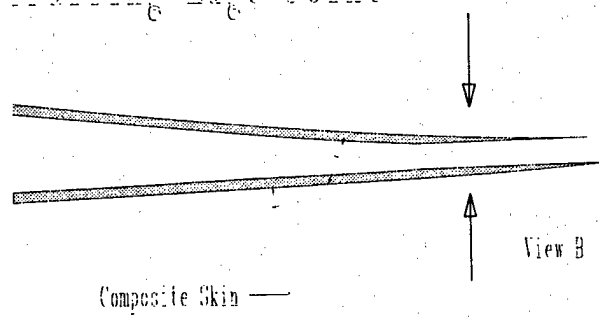
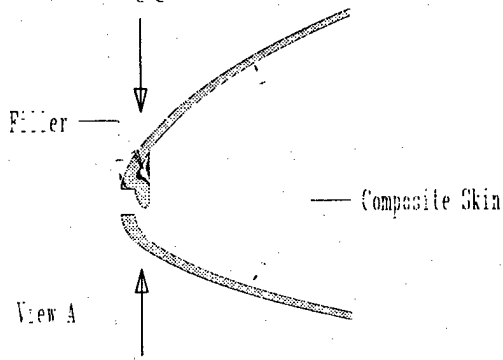
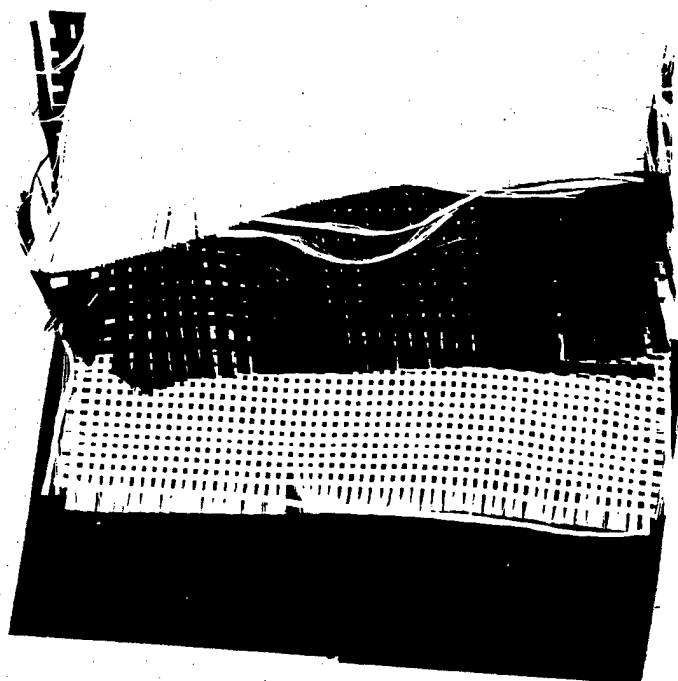


FIGURE 15

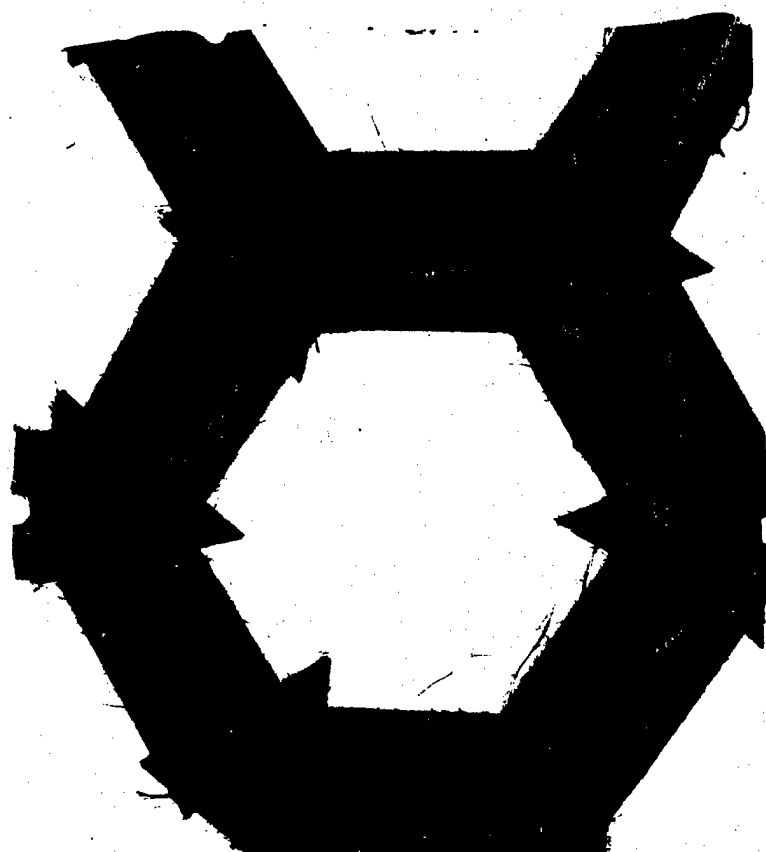
90° x 90° S-GLASS

45° x 45° S-GLASS



SKIN STIFFENING  
BY USING FOAM  
RUNNERS

90° x 90° CARBON



5.4 OZ S-GLASS (CROWFOOT WEAVE)  
5.4 OZ CARBON FIBER, PLAIN  
3.6 OZ S-GLASS, PLAIN  
0.75 OZ CARBON PAPER

LAST-A-FOAM 18 LBS/FT<sup>3</sup>  
POLYURETHANE FOAM

SKIN STIFFENING BY USING A HEXAGONAL  
FOAM PATTERN, S-GLASS, AND CARBON  
PAPER



## Bibliography

Bertin, John J. et al. Aerodynamics for Engineers.

Englewood Cliffs, NJ: Prentice-Hall, Inc. , 1979

Corning, Gerald. Super Sonic & Subsonic Airplane Design.

Ann Arbor, MI: Braun-Brumfield Press, 1960

Dwinnell, James H. Principles of Aerodynamics.

New York, NY: McGraw-Hill Book Company, Inc. , 1949.

Lennon, Andy. Basics of R/C Model Aircraft Design.

Wilton, CT: Air Age, Inc. , 1996.

## Acknowledgments

During the design and manufacture of this years plane, numerous financial and knowledge hurdles to overcome. We decided early on to take on an ambitious, challenging project this year and we feel that we have met that goal. Along the way we ran into things we either lacked the money to purchase or knowledge to completely understand with out outside help. We looked to professors and peers as well as into industry for help. We would like to thank the following individuals and companies for their time and donations for the benefit of our project.

Hobbytoun USA

Sanyo

Shell Chemical

General Plastics

Molen Company

Robart Manufacturing

Idall Technical Papers, Inc.

Brad Strangeways  
Vice President, Symmetry Resources

Dr. Clayton T. Crowe, Professor  
Department of Mechanical and Materials Engineering  
Washington State University

Dr. Walter J. Grantham, Professor  
Department of Mechanical and Materials Engineering  
Washington State University

Dr. William E. Johns, Associate Professor  
Department of Mechanical and Materials Engineering  
Washington State University

Dr. Amit Bandyopadhyay, Assistant Professor  
Department of Mechanical and Materials Engineering  
Washington State University

Dr. Lloyd V. Smith, Assistant Professor  
Department of Mechanical and Materials Engineering  
Washington State University

Dr. Stephen D. Antolovich, Professor and Director  
Department of Mechanical and Materials Engineering  
Washington State University

John Christensen, Graduate Student  
Department of Mechanical and Materials Engineering  
Washington State University

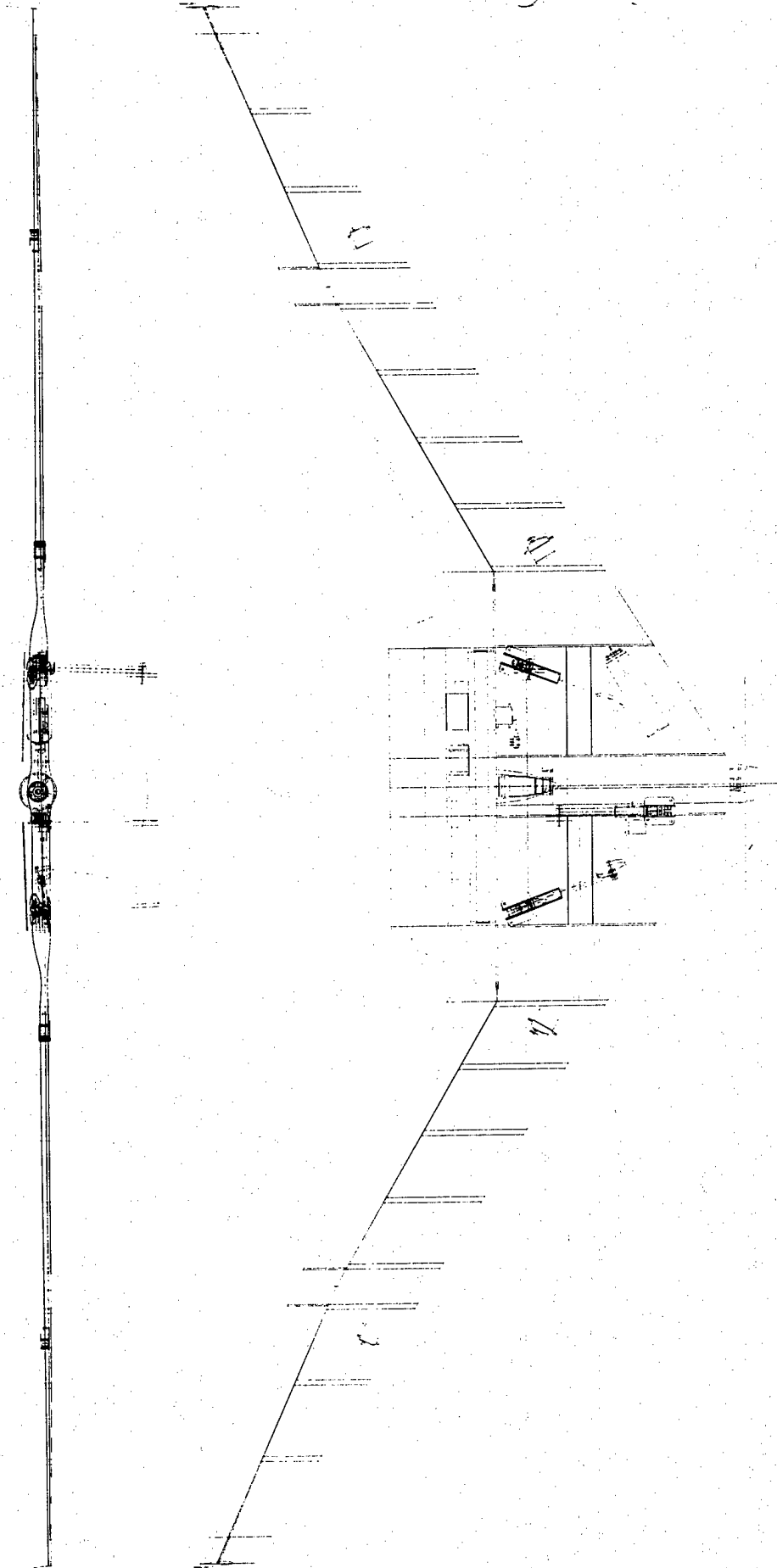
Kapil Pant, Graduate Student  
Department of Mechanical and Materials Engineering  
Washington State University

We would also like to acknowledge the Department of Mechanical and Materials Engineering at Washington State University, without whom this project would have never made it off the ground. Their funding support is the backbone of this project and for that we thank them.

## Drawing Package Table of Contents

<u>Section or Figure</u>	<u>Page</u>
Complete Systems Drawings	
Three View	CS-1
Isometric	CS-2
Mechanical Systems Drawings	
Three View	MS-1
Isometric	MS-2
Structural Drawings	
Three View	S-1
Isometric	S-2
Electrical Systems Drawings	
Three View	ES-1
Isometric	ES-2
Major Dimensions Drawing	D-1

**Preceding Page Blank**



11/99/1998 ASAA DBF Compet  
 11/99/1998 ASAA DBF Compet

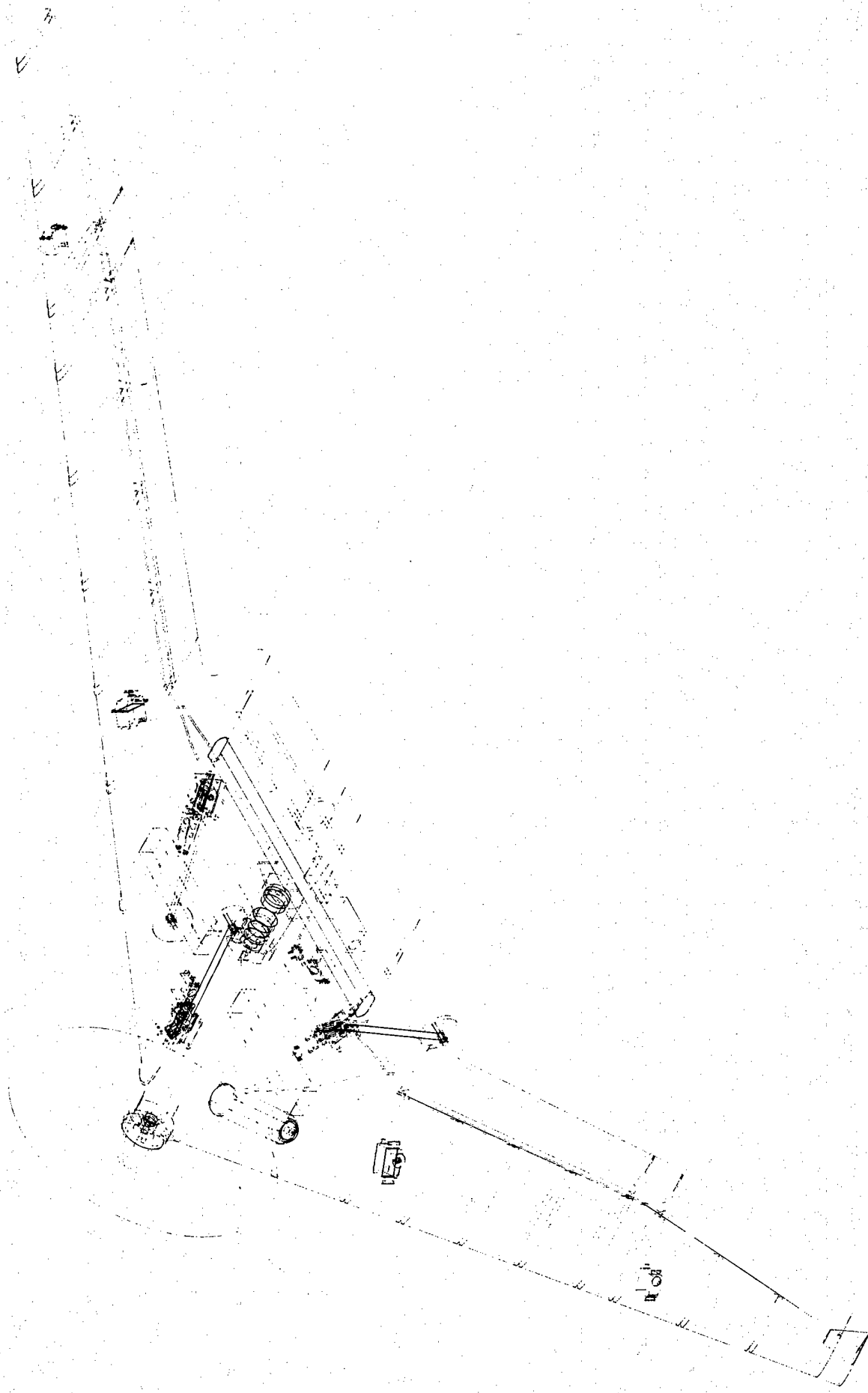
Drawn By 11/99/1998 ASAA DBF Compet

Date 11/99/1998 ASAA DBF Compet

View 11/99/1998 ASAA DBF Compet

Part 11/99/1998 ASAA DBF Compet

Part 11/99/1998 ASAA DBF Compet



Part Complete Systems Drawing

View

Isometric

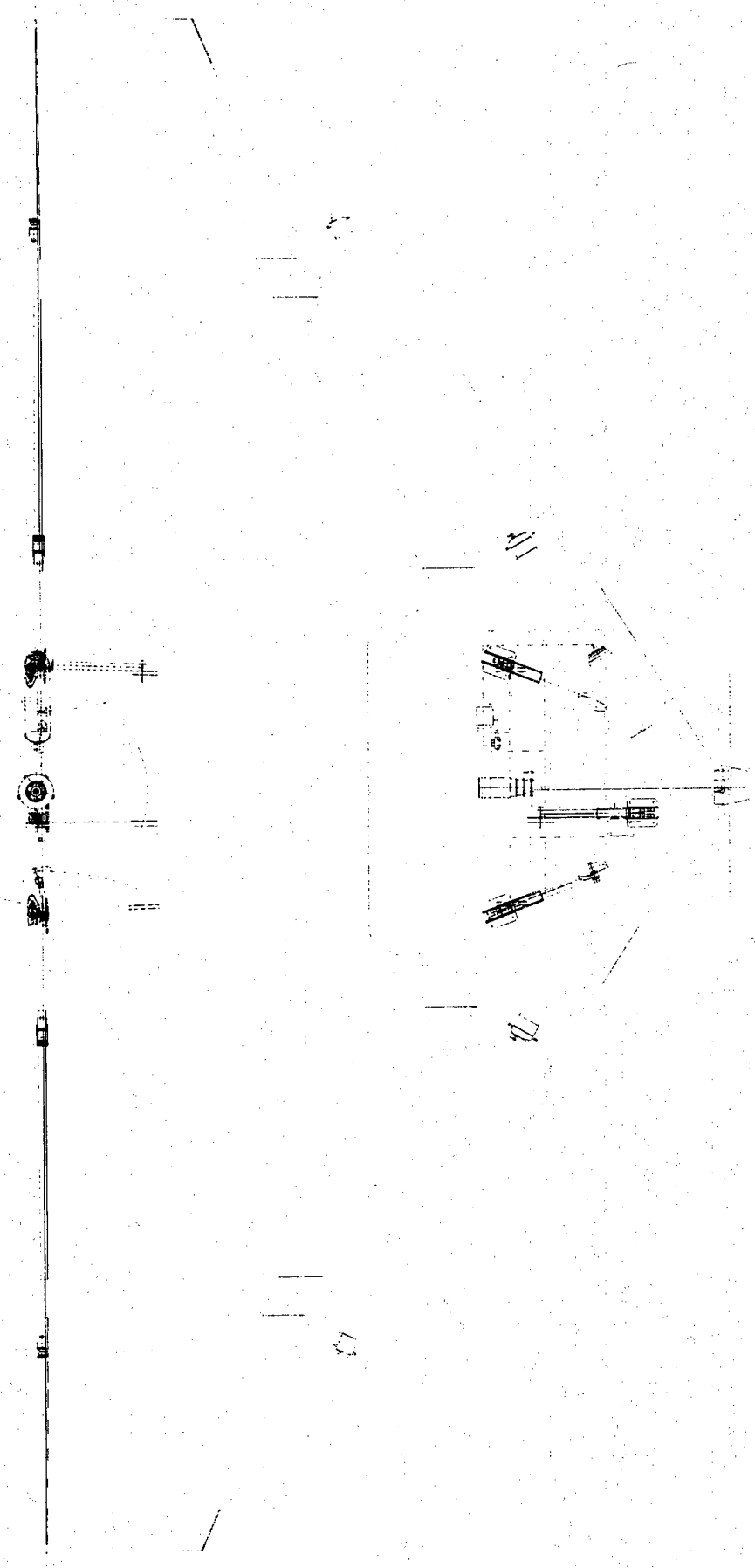
Date

3-9-98

Drawn By

Kevin Volney

1997-1998 AIAA DIF Competitor  
Washington State University



1997-1998 AIAA BPP Compa  
 tion State Exer

Drawn By  
 Date

Date

View

Part Mechanical Components Drawing

Propeller 1/16" Dia 1

Rear Landing Gear offset at 30 degrees from centerline to allow for larger wheel diameter

VIEW A

Elevons

Flaprons

Pressure Cylinder for Pneumatic Retractable Landing Gear

Standard Servo

Standard Servo for Aileron Gear Steering

Air Inlet Slot

Thrust Bearing

Front Steerable Gear

VIEW A

Gear Actuation Servo

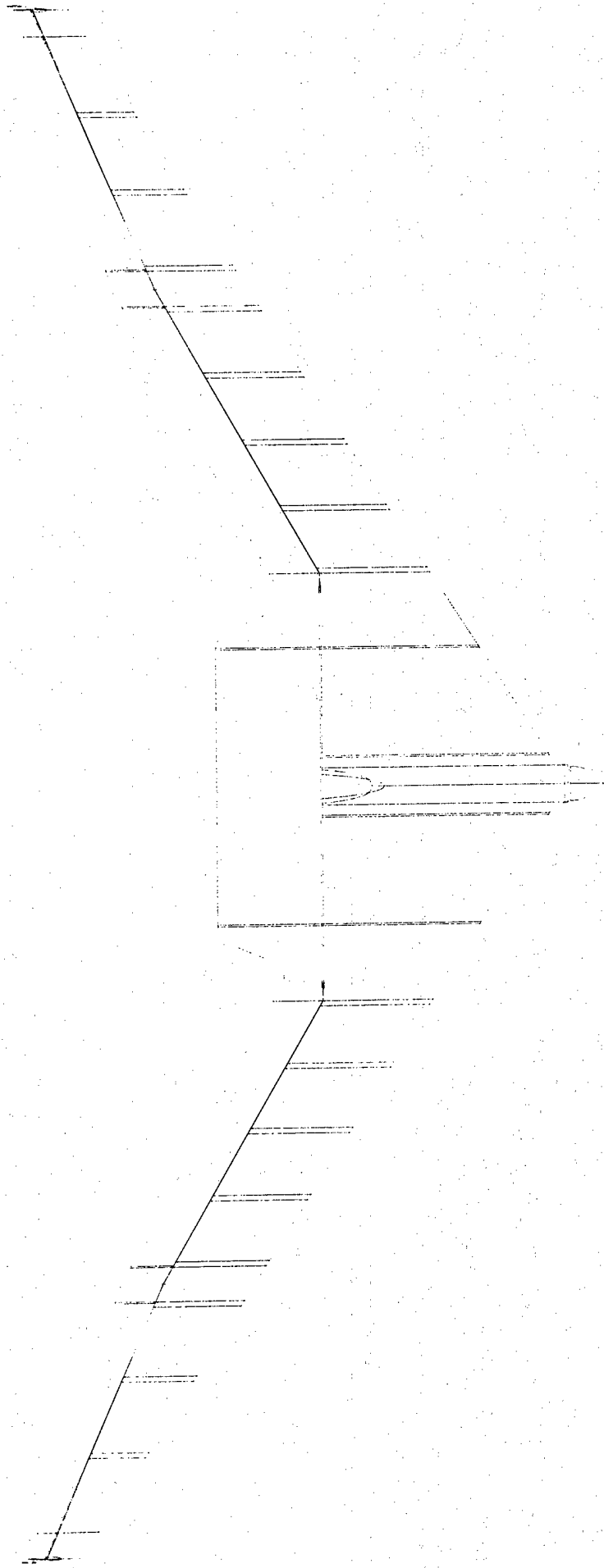
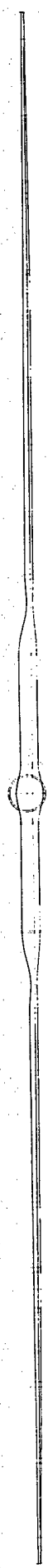
Titanium Drive Shaft

Mini Servo for Gear Valve Actuation

Pneumatic Gear Control

Mini Servo





1997-1998 AIAA DDP Comp  
 1000 State Hwy

Draw By: [Name]  
 Date: [Date]

View: [View]  
 Date: [Date]

Part: [Part]  
 Drawing: [Drawing]

Part: [Part]  
 Drawing: [Drawing]

Preparation Tube (Carbon Cloth, 15x15)

Main Ribs:  
(1 layer of 5.1 oz s-glass  
on 125" foam)

Low density foam spacers (No fiber)

Main Spar (2 layers of 5.1 oz s-glass on 125" foam)

Wing Spar (1 layer of 5.1 oz s-glass at 15x15  
and one layer of 3.0 oz s-glass at 90x90)

Part Structure Drawing

View

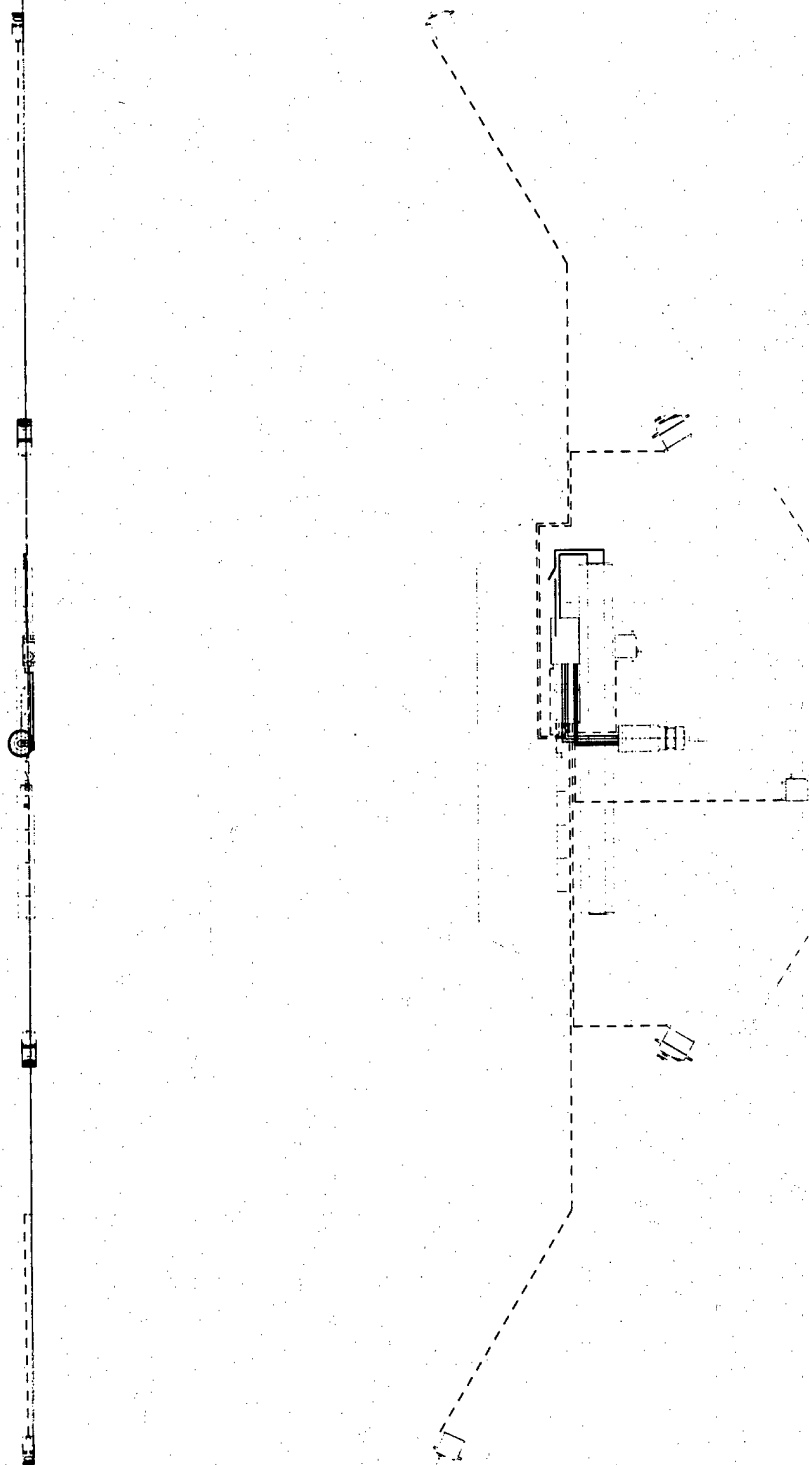
Location

Date 8-9-98

Drawn By

Y. C. Y. Y.

1997-1998 AIAA DIF Compet  
Washington State Univ.



Mini Servo (ELEV Channel)

Standard Servo (AUX1 Channel)

Standard Servo (RUD Channel)

Mini Servo (AUX1 Channel)

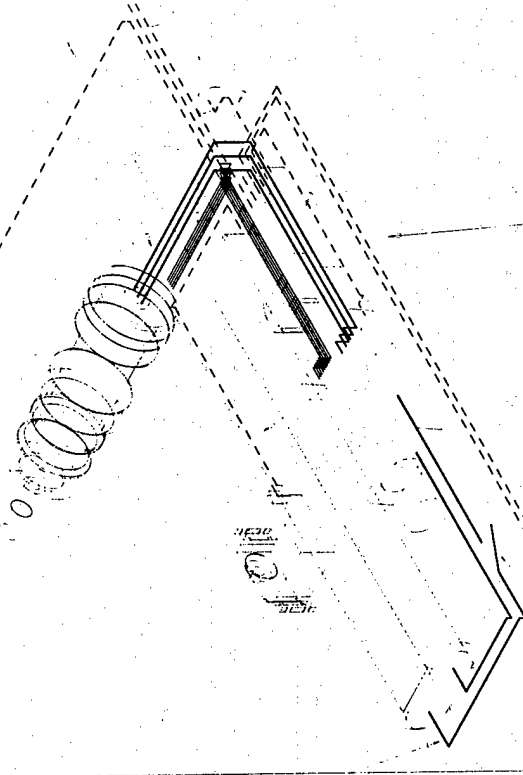
Standard Servo (AUX2 Channel)

Sanyo Sub-C Battery Pack

Receiver Battery Pack

Electronic Speed Control (THRO Channel)

View



Main Power Switch

Servo Signal Wires

1997/1998 ATAA DBF Compe  
Washington State Univer

Drawn By

Date 7.3.08

View

Part 01241101 07010000 00000000

View A-A

Airfoil Data Points

1	0.0000	0.0000	1	0.0000	0.0000
2	0.0000	0.0000	2	0.0000	0.0000
3	0.0000	0.0000	3	0.0000	0.0000
4	0.0000	0.0000	4	0.0000	0.0000
5	0.0000	0.0000	5	0.0000	0.0000
6	0.0000	0.0000	6	0.0000	0.0000
7	0.0000	0.0000	7	0.0000	0.0000
8	0.0000	0.0000	8	0.0000	0.0000
9	0.0000	0.0000	9	0.0000	0.0000
10	0.0000	0.0000	10	0.0000	0.0000
11	0.0000	0.0000	11	0.0000	0.0000
12	0.0000	0.0000	12	0.0000	0.0000
13	0.0000	0.0000	13	0.0000	0.0000
14	0.0000	0.0000	14	0.0000	0.0000
15	0.0000	0.0000	15	0.0000	0.0000
16	0.0000	0.0000	16	0.0000	0.0000
17	0.0000	0.0000	17	0.0000	0.0000
18	0.0000	0.0000	18	0.0000	0.0000
19	0.0000	0.0000	19	0.0000	0.0000
20	0.0000	0.0000	20	0.0000	0.0000

Wing Airfoil

•All 6.0

1997-1998 AIAA BDF Canceled  
Wing Airfoil Data

Drawn By

Date

View

Part

Wing Airfoil

Wing Airfoil

Wing Airfoil

Wing Airfoil

Wing Airfoil

Wing Airfoil

Wing Airfoil

Wing Airfoil



## Addendum

### Design Deviations

As unpowered flight testing came to a conclusion and powered flight testing began some minor changes were implemented. The center of gravity of the final design was adjusted rearward in order to let internal components remain in positions that did not change the overall surface of the plane. If the CG had been left where it was, some components would have had to been moved to positions that no longer allowed for the part to fit 100% inside the plane and bubbles in the skin would have been required. This was accomplished by changing the wing sweep from  $33^{\circ}$  to  $30^{\circ}$  and by extending the chord of the center section by one inch. This allowed the movement of the CG back by almost a full inch in relation to the CL thus making the balance of the aircraft much less of a concern. The reduced sweep however will result in a small loss of pitch control. Controllability during takeoff and landing was by far the issue that required the implementation of the most design changes. The prototype design proved to be difficult to control as it neared the end of the takeoff run or on final approach with a crosswind. As the aircraft would lift into the air, the nose wheel, providing steering, would lift off the ground resulting in a loss of directional control with either the option of a cut in power to regain control or a crash. To solve this problem a rudder was added to the nose gear that enhances yaw control on the runway during the takeoff roll and during landing. The rudder affixed to the nose gear prevents retraction, so the nose gear of the final design is fixed. The winglets were also enlarged slightly for the final design to decrease sideslip and cause the plane to be more stable in yaw.

### Lessons Learned

#### Manufacturing:

The entire manufacturing process was a learning experience for the group this year. The method chosen for manufacture, female mold composite lay-up using a vacuum bag compression, was completely new to most of the members. Much consultation with faculty and manufacturing engineers was necessary to solve problems with the molds and their implementation. Prototype manufacturing showed that the surface finish on the molds is not as important as the preparation of the surface with proper release agents. More time was spent finishing the original prototype molds than was spent investigating which release agents work best for this application and how they work together with the epoxy, waxes, and primers. It was also discovered that different primer types layered over each other were not as durable as several layers of a specific primer. Some release agents were not compatible with some primers and after a great deal of experimentation a combination that worked consistently and provided satisfactory results was found.

The entire aircraft was designed using CADKey 97, a vector based 3-D drawing package. This allowed for relatively rapid changes to the design and also offered a greater flexibility in the surface configurations that were possible as compared to a solid modeling package such as Pro/ENGINEER. It allowed for easy transportation to our manufacturing software, but not to analysis software. Since the drawings were not in a defined solid form, many of the analysis tools were not able to work with our files. Computational Fluid Dynamics software such as Fluent could not interpret our file types. In the end it became too time intensive and required

more processing power than was available so the CFD aspect of the project was shelved. Other manufacturing problems were encountered after CNC code was generated. We found that to insure proper alignment of the molds, the code had to be generated from a certain set of parameters. These related everything from the position of the drawing in the computer to the setup of the tools on the milling machine. Once these details were worked out, machining went smoothly. We did find that the limited travel of the CNC machinery available to us caused the molds to be segmented into six pieces each, increasing chance of error during final assembly of the molds. Precautions were taken to minimize this error.

#### Prototype Testing:

The most important thing learned from prototype testing was that the earlier a program can be started the better. Even with thorough planning, problems were uncovered in flight testing that were not anticipated in the design process. Problems encountered during prototype testing include landing gear design, controllability, as well as scheduling. The prototype designs demonstrated less than acceptable control, both on the ground and in the air. In the beginning the landing gear and wheels caused problems because the hard rubber wheels were not appropriate for the runway surface and tracking down the runway was difficult. The strength of the landing gear mounts then became a problem when high stress was encountered during extreme maneuvers on the ground and fatigue caused by the rough runway. Angle of attack and yaw control problems surfaced when takeoff speed was approached. If the angle of attack was too low on takeoff, the elevators could not provide enough control to rotate the plane and if the angle was too high it would rotate prematurely. The proposed schedule for the preliminary design and final design stages of the project changed from the original plan due to the duration of time the female mold manufacturing process required. It took longer to finish and test the preliminary design, so less testing of the final design could be performed.

#### Management:

The group reorganized at the beginning of spring semester, 1998 because the design groups formed in the fall didn't have goals that could be reached until near the end of the project. Short term, realistic design goals proved to promote better progress of the project. The design goals for the spring were attainable within a few weeks, so more people were willing to work hard to meet those goals. These new design groups also allowed more individual responsibility to be exercised on minor design decisions, which increased morale and aided progress.

#### Future Project Improvements

##### Design Improvements:

To improve this year's airplane design for future competition, several design improvements are possible. First, yaw stability could be further improved by integrating clamshell drag rudders or winglet control surfaces into the design. Either clamshell drag rudders or winglet control surfaces would allow the elimination of the rudder on the nose gear thereby permitting nose gear retraction, decreasing drag and increasing top speed. Next, the entire



airframe could be reduced in weight by performing an accurate finite element analysis and designing skin thickness and internal structural strength to meet those guidelines. Wind tunnel testing could also be both performed and simulated. Aerodynamic characteristics could be tested in a wind tunnel with a physical model, or they could be tested using computational fluid flow analysis. Finally, more contact with engineers working in aircraft design and composites manufacturing would allow many more improvements by applying their knowledge to improve the design.

#### Manufacturing:

The molding process, being the most important part of the manufacture of this aircraft is one of the few areas where significant improvement could be made. Changing to a denser and more durable mold material, such as aluminum, could be made. A mold constructed from this material would be more robust and easily transportable. Furthermore, it would not require as much surface preparation, such as sanding and filling the micro holes left in the foam, which could speed design change time considerably and add to accuracy. A more dense material would also produce a superior surface finish because a finer tool path could be used. Larger mold sections could also ease problems with mold construction by removing joints and by maintaining a flat, level mold. One improvement that could be made to the composite lay-up process would be to use prepreg carbon fiber or fiberglass to speed part production. This would require use of an autoclave to cure the composites which is currently unavailable to us.

Design Change	Time to implement (in man hours)
Yaw stability	100-150
Finite element analysis	150-300
Wind Tunnel Testing	50-75 per model
Contact with experts	-100 (would probably save time in the long run)
Remanufacture of Aluminum molds	175-250
Prepreg lay-up	-10-20

#### Cost Comparison

The total monetary cost of the project far exceeded the projected costs made at the beginning of the year. Despite this, the budget given to us by the department was not overrun due in large part to donations. The overall emphasis of the project was to create a highly efficient, easily reproducible aircraft with the technology that we had available to us. In accomplishing this large expenditures were made but the cost per copy of the aircraft itself is still relatively low. Many of the donations received were parts of the highest quality, so if we had to buy them ourselves we would not have chosen that particular part, but since it was free, we did not turn it down. As many items from last year as possible were also used to keep costs under control. The expected cost of the plane as a separate entity was very close to what was predicted and relatively low. The following table shows the total costs of producing one aircraft.

## Cost Comparison

### Mechanical Components

Motor:	Aveox 1412 5Y	\$209.00
Landing Gear:	Robart Retractable	\$340.00
Propellers:	APC 16x16	\$12.00
Servos:	JR Mini-Standard	\$120.00
Misc. Hardware:		\$50.00
Propulsion Assembly:		\$35.00
Wheels:		\$40.00
<b>Total:</b>		<b>\$806.00</b>

### Materials

S-Glass:	5.4 oz Crow Foot Weave	\$30.00
Carbon Fiber:	5.1 oz Plain Weave	\$80.00
	2.5 in Braided Sleeve	\$30.00
Kevlar:	4.0 oz Plain Weave	\$15.00
Foam:	18 lb/ft <sup>3</sup> Polyurethane	\$20.00
Epoxy:	Shell 862 and Hardener	\$80.00
<b>Total:</b>		<b>\$255.00</b>

### Electrical

Batteries:	Sanyo 1800 mAh 23 cell	\$280.00
Speed Control:	Aveox 3-Phase	\$240.00
Receiver:	JR 9-Channel PCM	\$120.00
Receiver Battery Pack:		\$25.00
Misc. Electrical:		\$50.00
Charger:		\$180.00
Transmitter:		\$290.00
<b>Total:</b>		<b>\$1185.00</b>

### Cost of Manufacture

CNC Mill Time:	\$1200.00
Polyurethane Mold Foam:	\$500.00
Epoxy Primer:	\$80.00
Fillers:	\$30.00
Finishing Materials:	\$25.00
Release Agents:	\$25.00
Vacuum Bagging:	\$70.00
<b>Total:</b>	<b>\$1930.00</b>

### Cost of Prototyping

Composites:	\$150.00
Extruded Polystyrene:	\$130.00
Servos:	\$60.00
Hot Wire Apparatus:	\$210.00
Balsa:	\$25.00
Adhesives:	\$60.00
Covering:	\$40.00
Misc. Hardware:	\$30.00
<b>Total:</b>	<b>\$705.00</b>

**Grand Total:** **\$4881.00**



WEST VIRGINIA UNIVERSITY

PROPOSAL PHASE REPORT

"RAPTOR"

Second Annual AIAA Student  
Design/Build/Fly Competition

Wichita Kansas

1997-1998 Contest Year

16 March 1998

***Mechanical and Aerospace  
Engineering Department***

College of Engineering and Mineral Resources  
West Virginia University • Morgantown, WV 26506-6106

**WEST VIRGINIA UNIVERSITY FINAL DESIGN REPORT  
"RAPTOR"**

**Second Annual AIAA Student Design/Build/Fly Competition  
Wichita, Kansas  
1997-1998 Contest Year  
16 March 1998**

**Department of Mechanical and Aerospace Engineering  
West Virginia University  
Morgantown, West Virginia**

## ACKNOWLEDGEMENTS

At this time the project team would like to thank all persons and corporations who through financial support and material donations made this year's contest entry a success.

We would like to thank our corporate sponsor, Aurora Flight Sciences of West Virginia, for its financial support, composite material donations, and composite construction techniques. The team also owes its thanks to the Department of Mechanical and Aerospace Engineering for its financial contributions, the space to build the contest entry and its predecessors, and finally for the use of the low speed wind tunnel. The project team extends its gratitude to the Morgantown Municipal Airport for the use of runway 28 for the purpose of flight testing.

Finally, the success of this project is largely due to the guidance and support of Dr. John Loth, Dr. Ever Barbero, and John Craig who's contribution to this team was outstanding.

Team West Virginia would finally like to thank AIAA and Cessna for hosting this years competition.

## TABLE OF CONTENTS

	<u>Page No.</u>
I Executive Summary	1.
II Management Summary	3.
II.a Organization	3.
II.b Management Structures	3.
II.c Milestones	3.
III Conceptual Design	5.
III.a Mission Specifications and Figures of Merit	5.
III.b Alternative Concepts Investigated	5.
III.c Primary Design Parameters	7.
III.d Analysis Tools	7.
III.e Final Configuration	7.
IV Preliminary Design	9.
IV.a Design Parameters for Sizing Study	9.
IV.a.i Airfoil Research	9.
IV.a.ii Wing Sizing Study	9.
IV.a.iii Tail Sizing Study	10.
IV.b Analysis Tools	11.
IV.b.i Propulsion System Testing	11.
IV.b.ii Structural Testing	11.
V Detail Design	17.
V.a Performance Characteristics	17.
V.a.i Takeoff Performance	17.
V.a.ii Handling Qualities	18.
V.a.iii Maximum G Load Capability	18.
V.a.iv Range and Endurance Capability	19.
V.a.v Payload Fraction and Weight Analysis	19.
V.b Component Selection and Systems Architecture	19.
V.c Drawing Package	20.

## TABLE OF CONTENTS (continued)

	<u>Page No.</u>
VI Manufacturing Plan	29.
VI.a Manufacturing Processes Selected	29.
VI.b Fuselage Manufacturing Processes Investigated	30.
VI.c Wing Manufacturing Processes Investigated	30.
VI.d Tail and Tail Boom Manufacturing Processes Investigated	31.
VI.e Analytical Methods	31.
VI.f Manufacturing Milestones	32.
 VII Lessons Learned	
(not included at this time)	
 References	
(not included at this time)	

## I. EXECUTIVE SUMMARY

This report represents the effort by the WVU AIAA student design/build/fly competition project team and is the result of over a year of development ranging from building materials and construction methods to the detailed design of the "Raptor". The design process described in this report was the product of extensive aerodynamic research, research of composite construction materials and techniques, structural testing of composite materials, software analysis and wind tunnel testing of the propulsion system, flight testing of the prototype "Javelin", and analytical modeling using several software packages and aircraft design books.

The design process began with lessons learned from the 1996-1997 competition. The team learned that the drag and the propulsion of the aircraft were the most critical factors, even more so than the reduction of weight of its various components. The lessons learned last year coupled with this year's change in rules gave way to several different configurations for the final aircraft. All configurations were designed with the reduction of drag (i.e. increase of the maximum velocity) as the foremost criteria followed closely by reduction of weight. A total of three different configurations for the final design, two low winged aircraft and one high winged aircraft were analyzed. The analysis of the conceptual designs indicated that the low winged aircraft would have better handling qualities while the velocities of the low and high winged aircraft seemed to be equal.

Emphasis was placed on the development of a standardized fuselage with a streamline aerodynamic shape that would be able to hold the internal components of the aircraft including the radio, battery, motor and speed controller, the tail surface actuators, and the payload. The fuselage was also developed using advanced composite molding techniques. Emphasis was also placed on the design of the wing taking into account the dihedral for lateral stability, high aspect ratio, high Oswald Efficiency Factor, and the volume required for retractable landing gear. The last major area of the design development was the propulsion system of the aircraft. Software, wind tunnel testing, and flight testing were used to find the best overall propeller to use and to optimize the energy use of the battery.

The prototype aircraft "Javelin" was a low winged "V-tail" aircraft with fixed main landing gear and a steerable tail wheel. Unfortunately the team realized that the prototype was too slow for the competition as the goal for this year was essentially maximum velocity. Flight testing of the "Javelin" yielded a maximum velocity of about 50 mph even though it was designed for just over 40 mph. This inconsistency gave way to the design of the "Raptor". Designed for over 50 mph, this aircraft features a reduced wing area and retractable main landing gear.



The success of this year's entry into the second annual AIAA Student Design/Build/Fly Competition is largely due to the hard work of the team and excellent management of time and resources. Team West Virginia is honored to enter the "Raptor" into this years competition.

## II. MANAGEMENT SUMMARY

### II.a Organization

The organization was divided into five groups with each student having primary responsibilities to one of these groups. Depending on time, skill and interest, the student also was active in a secondary group. In some special cases, the students were working in three different groups to meet a short term objective. The organization is shown below with students in their primary groups.

Group: **Design/Analysis/Report**  
Members: Steve Dick, Group Head  
Joe Ferguson  
Ed Wen

Group: **Wind Tunnel**  
Members: Bryan Shoemaker, Group Head  
Tom Scarberry

Group: **Construction/Drawing**  
Members: Bill Carenbauer, Group Head  
Adam Ensminger  
Kevin Ford  
Bongani Malinga  
Andy Williams

Group: **Flight Test**  
Members: Pete Cooke, Group Head  
Michael Benkert  
Joe Giordano  
Brandon Richards

Group: **Finance/Procurement/Trip**  
Members: Ed Wen, Group Head  
Veeter Jones

Faculty: **Dr. John Loth**

### II.b Management Structures


Each student was asked to work at least three hours a week and to turn in an index card that reported what activity was performed and how much time was spent. In order to keep the personnel appraised of the program's status, they met once a week to give debriefs on their progress to each other and to discuss the next week's objectives. In addition, the Group Heads met separately to coordinate activities between the groups and to discuss issues with the faculty.

Drawings of the aircraft were first sketched on paper and later input into AutoCAD R14. From these drawings, one could see the status of the airplane and the construction group could use it for reference. In general, the construction group worked from hand sketched drawings since it would be unacceptable to wait for the drawings to be generated in AutoCAD.




















































### II.c Milestones

The milestones for the "Javelin" and "Raptor" programs are shown in Table II.i.

Table II.i Milestones for Javelin and Raptor programs

Planned = 

Actual = 

Milestone	Jun	Jul	Aug	Sep	Oct	Nov	Dec	Jan	Feb	Mar	Apr
<b>Design/Analysis/Report</b>											
• Concept Design											
											
• Prelim. Design Javelin											
											
• Prelim. Design Raptor											
											
• Detail Design Raptor											
											
• Report Preparation											
											
<b>Wind Tunnel Group</b>											
• Wind Tunnel Set-Up											
											
• Prop/Motor/Bat Testing											
											
<b>Construction Group</b>											
• Develop Manu. Methods											
											
• Javelin Construction											
											
• Raptor Construction											
											
<b>Flight Test Group</b>											
• Fly 7 min, 7.5lbs (Javelin)											
											
• Fly 7 min, 7.5lbs (Raptor)											
											
<b>Finance/Procurement/Trip</b>											
• Fund Raising											
											
• Airplane/Hotel/Trans											
											

### **III. CONCEPTUAL DESIGN**

#### **III.a Mission Specifications and Figures of Merit**

In order to begin the conceptual design phase, the following mission specifications were derived from the 1997/1998 contest rules and regulations.

- Fly the maximum number of laps around a 700 ft. course in 7 minutes.
- Carry a 7.5 lb. steel payload
- Land and take-off within a 300 ft. runway length while clearing a 6 ft. obstacle at the end of the take-off run.
- Propulsion to be provided by a 2.5 lb. Ni-Cad battery.
- Execute a complete right and left-hand turn before entering the timed 7 minute phase in order to exhibit satisfactory handling qualities.

Using these mission specifications, the Figures of Merit (FOM) used for screening possible configurations of primary components were found. These FOM's were arranged in order of importance and are as follows:

- Maximum velocity (i.e. lowest drag). This FOM reflects the maximum number of laps in seven minutes.
- Large thrust-to-weight ratio to provide adequate acceleration on the runway. This FOM reflects the 300 ft. runway length restriction as well as the 6 ft. obstacle at the end of the runway.
- Maximize energy management.
- Satisfactory but low static margin stability. This FOM reflects maneuverability and performance while minimizing pilot effort.
- Practical and low cost manufacturing processes.
- Ease of carrying and removing payload.

#### **III.b Alternative Concepts Investigated**

Several different configurations were considered for each of the major aircraft components. The first aircraft component considered was the wing planform and its vertical

location on the fuselage. (The horizontal location was fixed according to center of gravity requirements.) The two vertical wing locations considered were high-wing and low-wing. The criteria used to evaluate the two vertical wing locations were dynamic stability, performance characteristics (i.e. maneuverability), complexity of design and fabrication, and landing gear configuration. Open loop stability laws dictate that the more dynamically stable an aircraft is, the less maneuverable it is. This parameter would indicate that a low wing aircraft would be more favorable. Unfortunately, a low wing aircraft is more complex to fabricate due to the necessary wing dihedral for minimum stability. A drawback to a high winged aircraft is the additional height requirement for the landing gear to retract into the wing.

The landing gear configuration is another major conceptual area of interest. The two landing gear configurations considered were fixed and retractable. Fixed landing gear offer better flexibility with regard to their location and are generally stronger and more durable. These attributes come at a cost of a significantly increased coefficient of drag for the aircraft. On the other hand, retractable landing gear come with a penalty of being less durable and more complex to build and maintain. In the positive sense, retractable landing gear greatly diminish the effects of drag in flight as they only have drag considerations during take off and landing, not during climb and cruise conditions, where the majority of the flight takes place.

Another major conceptual design consideration was the tail arrangement. The three different tail arrangements considered were the conventional tail, the "T-tail", and the "V-tail." The conventional tail is the easiest of the three to manufacture and is structurally the strongest. However, it is the least aerodynamically efficient. In addition, the horizontal tail must be somewhat larger than the others in order to counteract the effects of the downwash from the main wing. The "T-tail" arrangement compensates for this downwash effect by raising the horizontal tail above the downwash wake. It also allows for a smaller vertical tail area as an end-plate effect is created. This arrangement is structurally more heavier than a conventional design. The final tail arrangement considered was the "V-tail." Of the three, the "V-tail" is the most aerodynamically efficient. This is due to the fact that it has the smallest drag coefficient, which is a factor of the amount of wetted area present. However, this arrangement is the most complex design to implement. The two reasons for this are the dihedral angle that must be determined and implemented and the required actuator mixing for the elevator and rudder movements.

### **III.c Primary Design Parameters**

In the conceptual design of the aircraft, all of the primary design parameters were centered around the wing planform. These included the effects of the aspect ratio on the induced drag, taper ratio on Oswald efficiency factor, and the cruise velocity on wing area. The aspect ratio is inversely proportional to the induced drag coefficient of the aircraft. Therefore, the larger the aspect ratio the smaller the induced drag coefficient. The taper ratio is also inversely proportional to the Oswald efficiency factor to a certain degree. A taper ratio of .45 recovers most of the span-wise efficiency in the Oswald efficiency factor. The relationship between the wing area and the cruise velocity was also investigated. It is proven that by holding all parameters constant in the general equation for lift of an aircraft except the velocity and the wing area, the required wing area decreases as the cruise velocity increases. All of these factors were varied during the preliminary design of the aircraft.

### **III.d Analysis Tools**

Two major analysis tools were utilized in the conceptual design stage. The first tool used was a commercially distributed software package to calculate energy usage, durability, power available, thrust available, and efficiencies of the motor and the propeller. The outputs of the software were later correlated by actual wind tunnel test data. Another tool used at this stage was a preliminary aircraft numeric model for simple lift and drag calculations. This tool was derived from existing text books and experience of various aircraft drag components. These tools proved to be vital to the overall conceptual design of the competition aircraft.

### **III.e Final Configuration**

When considering the importance of the FOM's, a relative scale or "Weighting Factor" ranging from 1-10 was determined as seen in Table III.i. A higher number is given to the more important characteristic and a lower number to the less important characteristic. Once these "Weighting Factors" are known, a ranking scale ranging from 1-5 was developed as seen in Table III.ii. This table shows the desirable characteristics for each FOM. The "Weighting Factor" and the ranking were combined in Table III.iii in order to determine the most desirable configuration for the overall competition design.

As can be seen in Table III.iii the totals for each option for each of the three major aircraft components are listed. The final configuration has the highest number in each category. The configuration of the "Javelin" and later the "Raptor" is a low winged "V tail" aircraft with retractable landing gear (only the "Raptor" has retractable landing gear).

Table III.i Weighting Factor for Figures of Merit

Figure of Merit	Weighting Factor
Maneuverability	6
Cost Effectiveness	3
Simplicity of Manufacture	2
Drag	10
Weight	7

Table III.ii Numeric Rating of Figures of Merit

Figure of Merit	Ranking		
	1, 2	3	4, 5
Maneuverability	Low	Average	High
Cost Effectiveness	High	Average	Low
Simplicity of Manufacture	Complex	Average	Simple
Drag	High	Average	Low
Weight	Heavy	Average	Light

Table III.iii Final Configuration

Figure of Merit	Configuration						
	Vertical Wing Location		Landing Gear		Tail		
	Low Wing	High Wing	Fixed Gear	Retractable Gear	Conventional	"T tail"	"V tail"
Maneuverability	5 (x 6)	2 (x 6)	NA	NA	3 (x 6)	5 (x 6)	4 (x 6)
Cost Effectiveness	4 (x 3)	5 (x 3)	5 (x 3)	3 (x 3)	3 (x 3)	3 (x 3)	4 (x 3)
Simplicity of Manufacture	3 (x 2)	5 (x 2)	5 (x 2)	2 (x 2)	5 (x 2)	4 (x 2)	3 (x 2)
Drag	5 (x10)	4 (x10)	1 (x10)	5 (x10)	3 (x10)	4 (x10)	5 (x10)
Weight	5 (x7)	4 (x7)	5 (x7)	4 (x7)	2 (x7)	3 (x7)	5 (x7)
<b>Total</b>	<b>133</b>	<b>105</b>	<b>70</b>	<b>91</b>	<b>81</b>	<b>108</b>	<b>127</b>

## IV. PRELIMINARY DESIGN

### IV.a Design Parameter for Sizing Studies

#### IV.a.i Airfoil Research and Selection

Throughout the process of the conceptual design and into the preliminary design, extensive research of many different airfoils was conducted. To narrow the choices of airfoils down to the final airfoil selected the candidates were screened extensively against the following parameters:

- designed for the aircraft's operating Reynolds number
- high  $C_L$  vs.  $\alpha$  slope
- wide but low value "drag bucket"
- wide range of  $\alpha$  at the airfoil's optimum  $C_L/C_D$  for maximum velocity
- availability of experimental data and x-y coordinate points of the airfoil

The first airfoil selected from the study was the Clark Y airfoil. This airfoil was the selection for the prototype aircraft "Javelin." Continuing the research and after consulting with the top radio controlled aircraft people in the country, a better airfoil was found after the "Javelin" was built. This airfoil was the RG-15. Wind tunnel tested at the University of Illinois Urbana-Champaign, this airfoil offered better characteristics than the Clark Y and was later incorporated in the design and construction of the competition aircraft "Raptor."

The numeric data on the RG-15 airfoil is shown in Figure IV.i. For the RG-15 airfoil the best angle of attack for maximum velocity was found to be  $2^\circ$ . This gave rise to the  $2^\circ$  angle of incidence on the "Raptor". Therefore, at cruise, the thrust line would be perfectly level. The lift coefficient was found to be .45 at cruise conditions and the parasite drag coefficient was .008. A key feature of this airfoil was the almost linear change of the drag verses the lift from a lift coefficient value of .45 to a value of .85, as seen in Figure IV.ii. This region corresponds to the best lift to drag ratio for maximum velocity. Figure IV.iii shows the best lift to drag for maximum range which is different than the best lift to drag for maximum velocity.

#### IV.a.ii Wing Sizing Study

As previously stated, an increase of the cruise velocity results in a decrease of the required



wing area, assuming the other variables in the general equation for lift are kept constant. This relationship is shown numerically in Table IV.i. Initial estimates of the overall drag of the "Javelin" combined with the available thrust provided by the propulsion system limited the maximum velocity of the "Javelin" to just over 40 mph. This combined with the lift coefficient of the Clark Y airfoil used on the "Javelin" required the prototype aircraft to have no less than 7.5 ft<sup>2</sup> of wing area. Table IV.i shows the lift coefficient of the RG-15 airfoil used in the construction of "Raptor". Flight Testing of the "Javelin" proved that the first estimates of the drag of the aircraft were too high as the aircraft exceeded 50 mph. Consequently, the "Raptor" was designed for over 50 mph and combined with the improved lift coefficient of the RG-15 airfoil the required wing area dropped from 7.5 ft<sup>2</sup> on the "Javelin" to 6 ft<sup>2</sup> on the "Raptor."

The root chord of the "Raptor" was determined to be no less than 15 in. This was determined by the geometric thickness of the wing profile required to allow the retraction of the main landing gear. It was also determined that a taper ratio of .4 would recover the most span wise loading efficiency in the Oswald efficiency factor, this parameter results in a tip chord length of 6 in. The taper ratio parameter also produced the desired high aspect ratio for the wing, which for the "Raptor" was 7.9 and wing span of approximately 6.9 ft. Optimization for the span wise loading efficiency revealed that geometrically defined sweep angle be split between the leading edge and the trailing edge. This is to say that the leading edge sweep angle is equal to the trailing edge sweep angle or a zero degree sweep angle at the 50% chord.

#### **IV.a.iii Tail Sizing Study**

The size of the "V tail" for both the "Javelin" and the "Raptor" was accomplished from longitudinal stability. The static margin or the difference between the center of gravity and the aerodynamic center of the aircraft was optimized and found to be .25. This value was a compromise between a higher value for minimum pilot effort and a lower value for extreme maneuverability and performance. High maneuverability and minimum pilot effort are both components of the overall required "good flight handling qualities."

The value of .25 for the static margin could have been accomplished by either lengthening the tail boom or by increasing the wetted tail area. In keeping with the design strategy of minimum drag, the tail boom was lengthened and the wetted tail area was reduced, to a certain extent, to reduce the overall drag. The longitudinal stability criteria coupled with the length of the tail boom gave rise to the required projected horizontal tail area which is different than the actual wetted area of the "V tail" surfaces. The experience of the design team and the pilot's experience

resulted in 30 degrees of dihedral of the "V tail" surfaces. Therefore, with the dihedral and the horizontal projected area known, geometry was utilized to find the true wetted tail area and the dimensions of the "V tail" surfaces.

#### **IV.b Analysis Tools**

##### **IV.b.i Propulsion System Testing**

The analysis of the propulsion system was focused on finding the best propeller to use for the available power of the motor and battery combination. The motor and the battery were found not to affect the maximum thrust of the system significantly, only the energy consumption or how long the available energy would last. Several different propellers were tested with varying diameters, pitch, chord thickness, and manufacturer. The maximum static thrust for each of the propellers tested is documented in Table IV.ii and Figure IV.iv. The thrust as a function of velocity is shown in Figure IV.v.

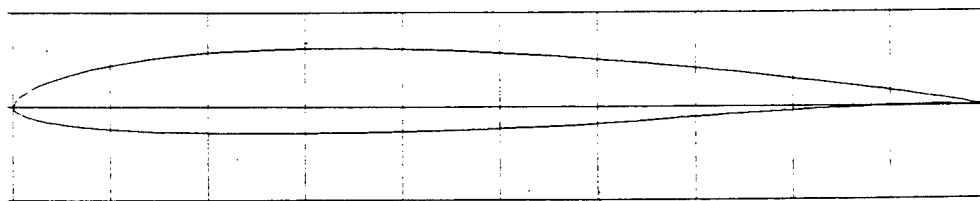
The results of the propulsion system testing indicated that the best propeller to use is the APC 15-10. This propeller is 15 in. in diameter and has a pitch of 10 in.

As previously stated the motor and the battery used had very little influence on the maximum thrust of the propulsion system. The brand of the motor, speed controller, and the battery does, however, greatly influence the energy consumption and therefore the longevity of the battery at any given consumption rate or throttle setting. Research and then testing in the wind tunnel found that the best motor to use was the MaxCim MaxNEO-13Y motor with the Maxu35A-25NB speed controller. Both these products are commercially available and were installed in both the "Javelin" and later in the "Raptor". The competition battery pack was composed of 19 RC-2000 cells yielding 2.5 lbs in weight, 23 volts DC, and 2200 mah.

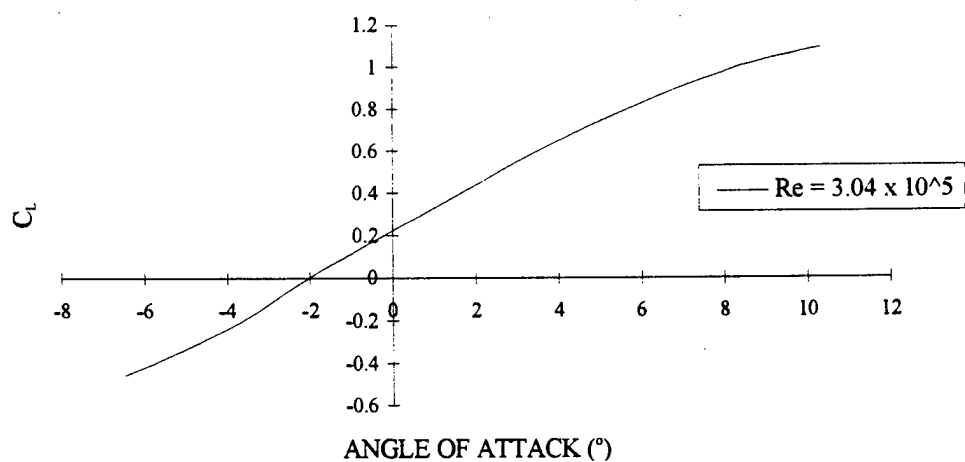
##### **IV.b.ii Structural Testing**

Structural testing for both the "Javelin" and the "Raptor" wing structures was conducted. The test specimens were 4 in. long, 2 in. wide, and .75 in thick, these specimens were simply supported and subjected to a bending load. The specimen cross sections varied between blue construction Styrofoam and white packing Styrofoam with balsa wood laminate on either side of the Styrofoam. The results of the testing procedure indicated that for reasons of time, money, strength, and weight considerations, the wings should be made from the blue Styrofoam laminated with balsa sheeting. This results are discussed more extensively in the

manufacturing process and plan section of this report.



LIFT COEFFICIENT vs. ANGLE OF ATTACK FOR RG15(B)



DRAG COEFFICIENT vs. ANGLE OF ATTACK FOR RG15(B)

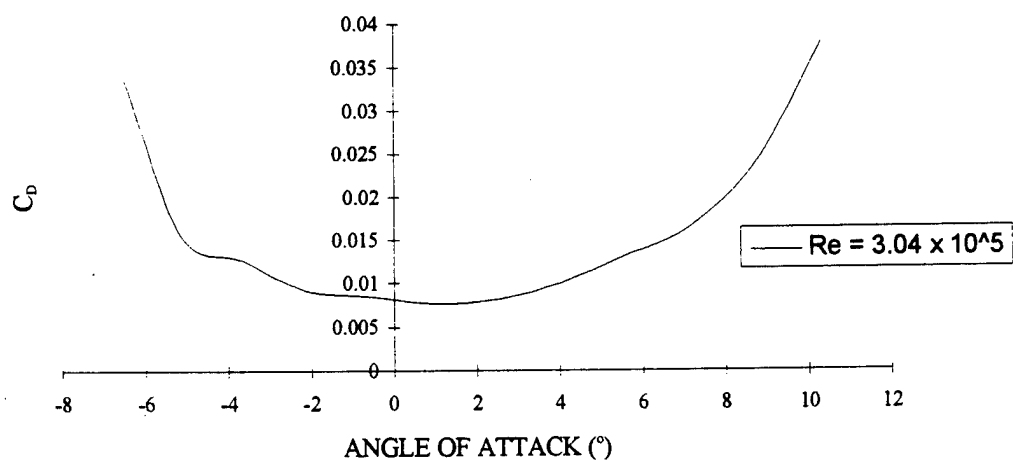


Figure IV.i RG-15 General Characteristics

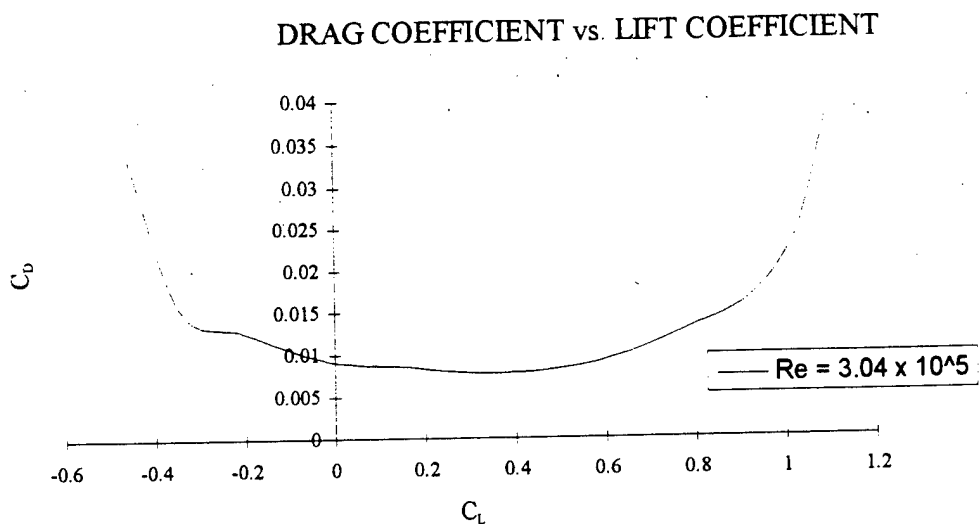


Figure IV.ii Calculation of Best Lift to Drag Ratio for Maximum Velocity

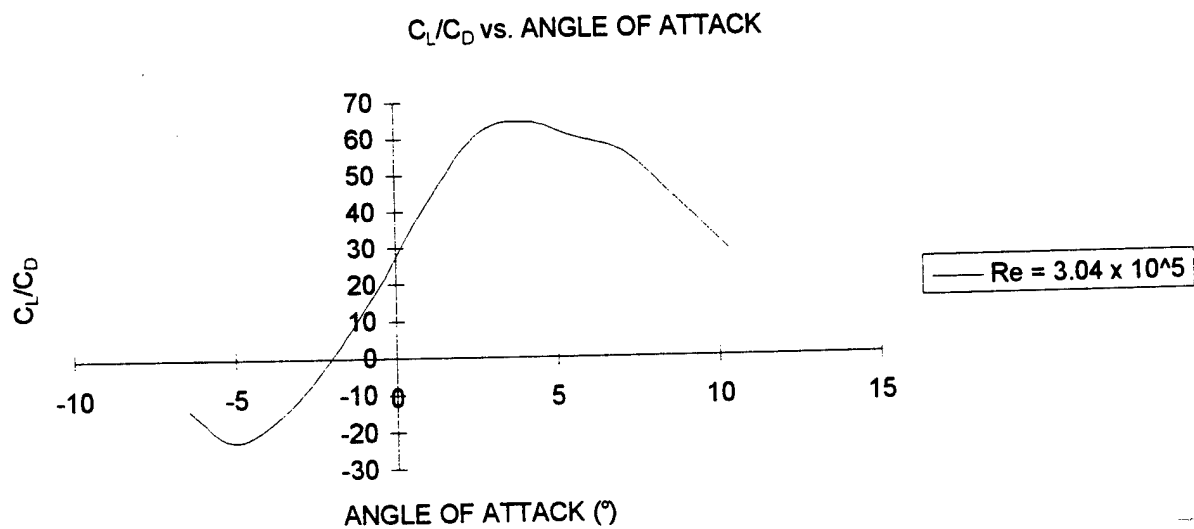


Figure IV.iii Best Lift to Drag Ratio for Maximum Range

Table IV.i Relationship Between Cruise Velocity and Required Wing Area

WEIGHT = 17 lb  
 AIR DENSITY = 0.002377 slug/ft<sup>3</sup>  
 ROOT CHORD = 15 in  
 1.25 ft  
 TAPER RATIO = 0.4  
 TIP CHORD = 6 in  
 0.5 ft

VELOCITY (mph)	VELOCITY (ft/s)	C <sub>L</sub> @ CRUISE 2° INCIDENCE	WING AREA (ft <sup>2</sup> ) REQUIRED @ CRUISE
20	29.33	0.45	36.94
21	30.80	0.45	33.51
22	32.27	0.45	30.53
23	33.73	0.45	27.93
24	35.20	0.45	25.65
25	36.67	0.45	23.64
26	38.13	0.45	21.86
27	39.60	0.45	20.27
28	41.07	0.45	18.85
29	42.53	0.45	17.57
30	44.00	0.45	16.42
31	45.47	0.45	15.38
32	46.93	0.45	14.43
33	48.40	0.45	13.57
34	49.87	0.45	12.78
35	51.33	0.45	12.06
36	52.80	0.45	11.40
37	54.27	0.45	10.79
38	55.73	0.45	10.23
39	57.20	0.45	9.72
40	58.67	0.45	9.24
41	60.13	0.45	8.79
42	61.60	0.45	8.38
43	63.07	0.45	7.99
44	64.53	0.45	7.63
45	66.00	0.45	7.30
46	67.47	0.45	6.98
47	68.93	0.45	6.69
48	70.40	0.45	6.41
49	71.87	0.45	6.15
50	73.33	0.45	5.91
51	74.80	0.45	5.68
52	76.27	0.45	5.46
53	77.73	0.45	5.26
54	79.20	0.45	5.07
55	80.67	0.45	4.88
56	82.13	0.45	4.71
57	83.60	0.45	4.55
58	85.07	0.45	4.39
59	86.53	0.45	4.24
60	88.00	0.45	4.10

Table IV.ii Static Thrust Values for Various Propellers

Performed By: Tom Scarberry and Bryan Shoemaker

Date Performed: 3/3/98

Current(amps): 23

Voltage(volts): 26.5

Prop Type	Volts	Thrust(lb)
Master Airsrew 13x8	1.81	9.69
Top Flite 15x8	1.78	9.53
APC 15x10	2.15	11.52
APC 15x12	1.98	10.61
APC 15x13 Narrow	1.58	8.45

$$\text{Thrust} = 5.3636 \times \text{Volts} - 0.0144$$

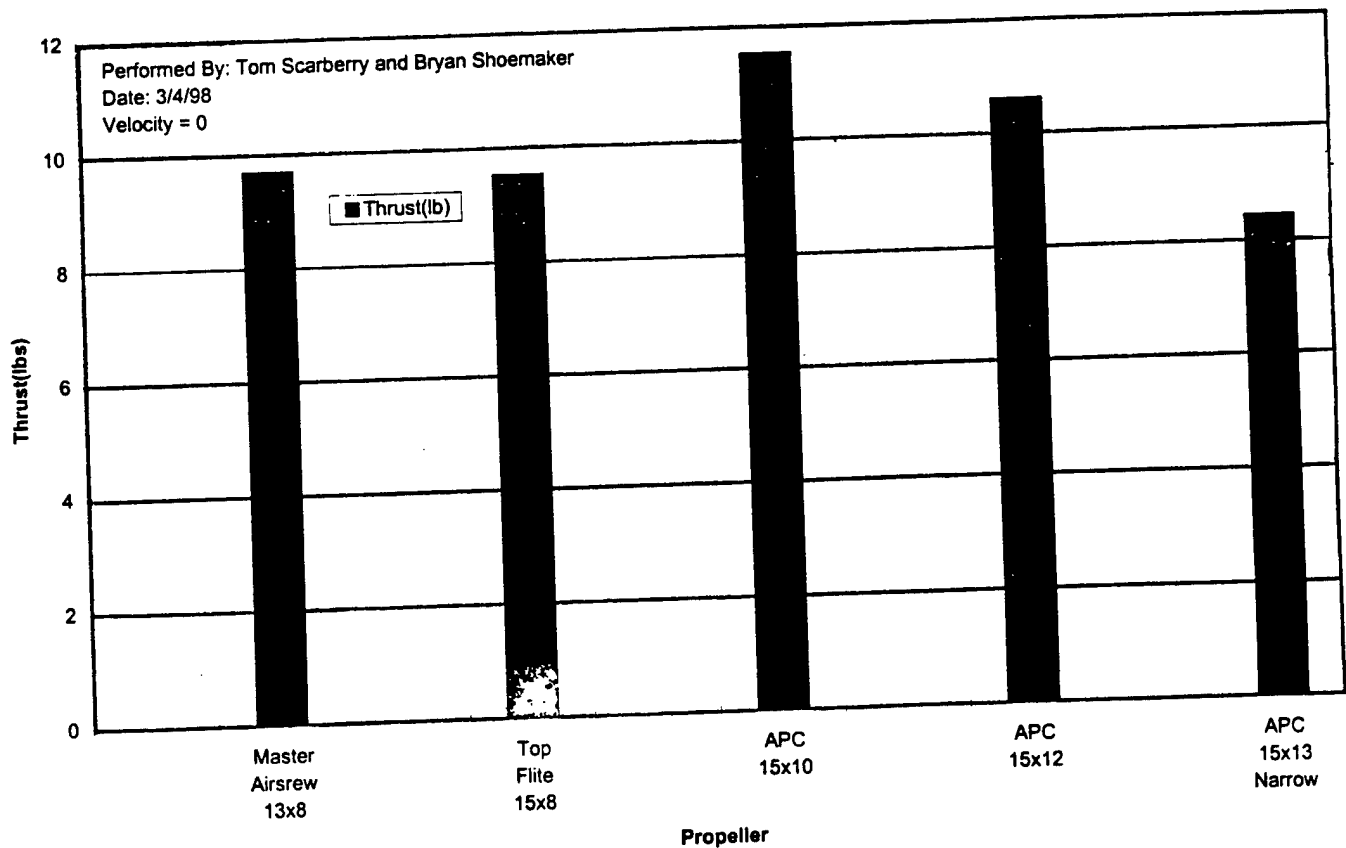
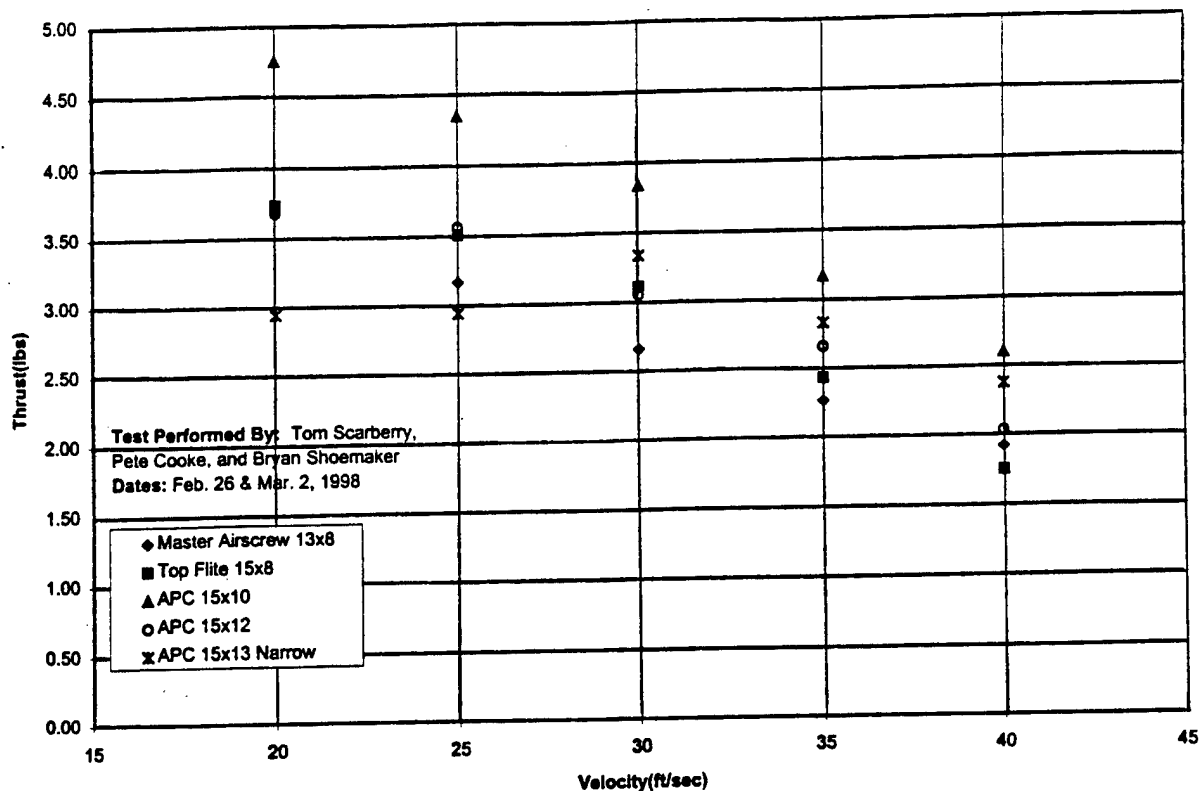
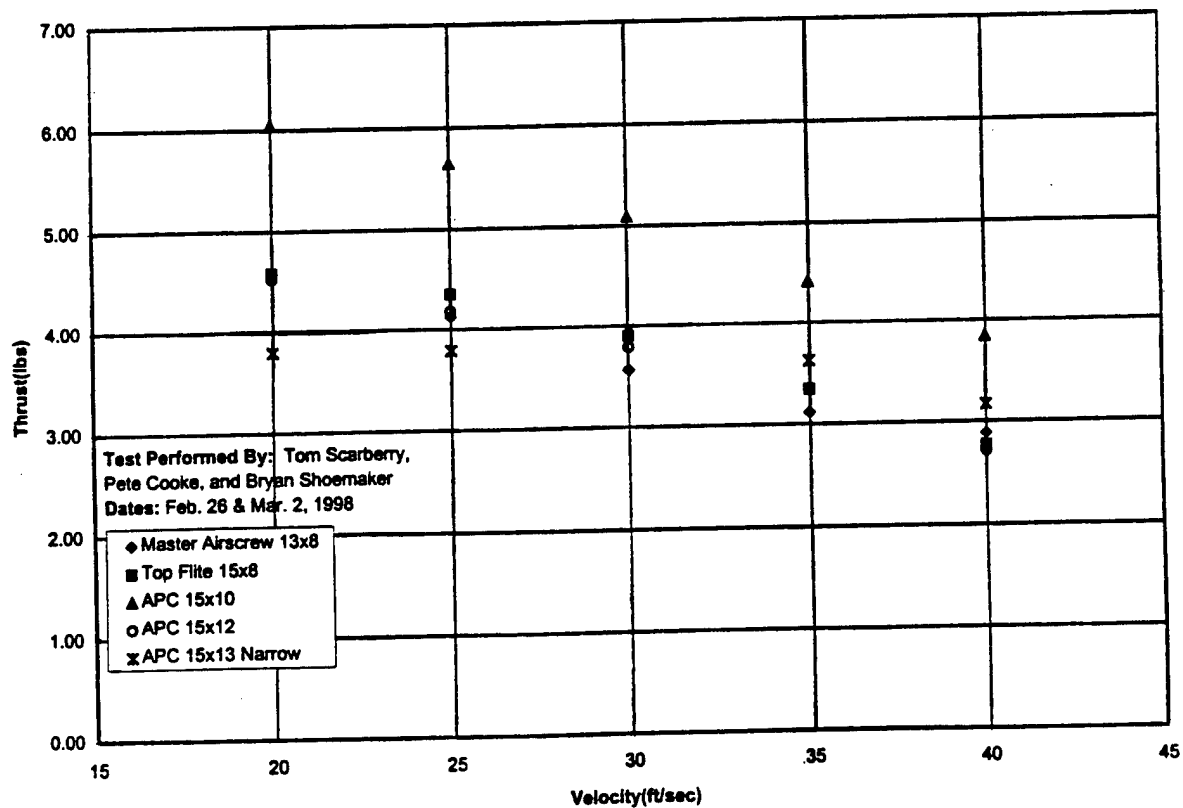


Figure IV.iv Static Thrust Test for Various Propellers



*Flight Test Thrust versus Velocity for 300 Watts*



*Flight Test Thrust versus Velocity for 400 Watts*

Figure IV.v Thrust as a Function of Velocity

## V. DETAIL DESIGN

### V.a Performance Characteristics

#### V.a.i Takeoff Performance

Takeoff performance of an aircraft is of vital consideration when designing an aircraft. The "Javelin" had 7.5 ft<sup>2</sup> of wing area, this was designed for cruise conditions. Fortunately, because the aircraft was somewhat slower than the "Raptor" and it had a larger wing area than the "Raptor", the runway takeoff speed was not too excessive (i.e. the runway takeoff speed was less than 30 mph). Thus it was determined that flaps on the "Javelin" to increase the camber of the wing profile were unnecessary. Due to the reduced wing area of the "Raptor" of only 6 ft<sup>2</sup> and the designed higher cruise velocity, it was determined that the "Raptor" needed flaps to achieve slower runway takeoff and landing speeds. Texts on the theory of high lift devices were utilized to design and analyze the competing flap designs. The analysis was based upon screening of designs based upon the following Figures of Merit (FOM).

- Effective increase of the lift coefficient of the profile (i.e. increase of the airfoil's camber)
- Drag coefficient increase of the profile due to both the parasitic drag and the drag increase due to the increase of lift
- Complexity of construction of the flaps

Most of the existing flap designs were eliminated due to the complexity and the manufacturing processes that were available. The two remaining designs were of the plain flap and the split flap design. However, extensive analysis of the split flaps revealed that the increase of the drag coefficient was too excessive, therefore the split flap design was eliminated even though it was less complex to build. The "Raptor" has plain flaps on the trailing edge of the wing on either side of the fuselage, in total, extending over 60% of the wing span. The flaps are also at a constant 20% of the chord length, that is to say that they taper with the taper ratio of the wing planform. Construction of the flaps in this way is more complex than a constant width of the flaps, however it was felt that the aerodynamic benefits far outweighed the increase of construction complexity. The increase of the camber of the profile combined with the increase of the angle of attack at takeoff conditions allowed the "Raptor" to achieve takeoff speeds of less than 30 mph.

The theoretical performance of "Raptor" as it accelerates down the runway is shown in



Table V.i. The last column of Table V.i is the distance down the runway as functions of time and velocity, while the last row shows the values of the runway length, time, and velocity for the minimum runway distance required for takeoff (i.e. the value of the lift exceeds the aircraft weight). For energy consumption reasons the pilot will takeoff at a lower throttle setting and a larger rotation speed thereby maximizing the use of the available runway.

#### **V.a.ii Handling Qualities**

The handling qualities of the aircraft were evaluated with flight testing. The "Javelin" had excellent handling qualities in takeoff performance, climbing, and turning and banking conditions. The only deficiency of the prototype aircraft's handling qualities was in landing. While the aircraft still handled well, the overall landing speed was too high and it glided too well making it extremely difficult for the pilot to land in the marked runway. This deficiency coupled with the takeoff analysis caused the "Raptor" to be equipped with flaps. The flaps in the landing condition lower the landing speed and help to slow the aircraft down more rapidly.

#### **V.a.iii Maximum G-Load Capability**

A program was written to analyze the moments and stresses at critical points. Since the carbon tube spar extends 8 in. into each wing, the analysis of the transfer of load from the spar into the balsa laminate is very complex and would require time-consuming finite element modeling. Instead, a conservative assumption was made that the wing was only composed of the balsa sheeted laminate. Separately, the carbon fiber spar was analyzed with the same bending moments to arrive at the G-Load for the spar.

G-Load capability of the aircraft was calculated using the strength values obtained from the structural testing performed on 1/16" balsa sheeted laminates (see Manufacturing Plan) and material properties data obtained from the carbon tube manufacturer. Figure V.i shows the results of the analysis. The critical point occurs at the wing root and failure occurs at +9.51G and -10.5G loading. For the carbon spar, failure occurs at +15.2G and -15.2G loading.

Given that there are stress concentrations at the transition from the spar to the laminate wing, a further conservative factor of .5 was applied to all ultimate stresses. The result was that the maximum G-load capability is approximately +/- 5Gs. Based on typical gust loads factors of -1.5 to 3.0G, this aircraft appears flight worthy. Also this aircraft would be capable of 75-80 degree turns as was its predecessor, "Javelin."

#### **V.a.iv Range and Endurance Capability**

With the cruise velocity of the "Raptor" over 50 mph, the aircraft was determined to be able to complete about 15 laps in the time slot allowed (7 minutes). This analysis is based upon numerical computations and the propulsion analysis software. This analysis also assumes that 10% of the energy of the battery was consumed on takeoff and climb of the aircraft and on the required left and right hand turns.

#### **V.a.v Payload Fraction and Weight Analysis**

The payload fraction appears in Table V.ii. The final weight for "Javelin" was 1.1 pounds over the predicted weight. This is attributed to the weight of stiffening the mechanical mixer system in the fuselage and to the materials used in the wing. "Raptor" is expected to take advantage of reduced wing area to reduce wing weight and computerized mixer to reduce fuselage weight. The retractable landing gear, however, expected to be heavier than the fixed landing gear of the "Javelin."

#### **V.b Component Selection and Systems Architecture**

The components selected appear in Table V.iii. As was mentioned in previous sections, the MaxCim motor and speed controller system was judged as most efficient, even though competitor Aveox and Kontronik make excellent brushed motors. Based on the propulsion software, a gear ratio of 4.5:1 yielded the best range performance. The highest commercially available ratio was 4.28:1 so it was chosen. The industry seems to be in fair agreement that the highest energy density Ni-Cad battery available is the Sanyo RC2000 cell.

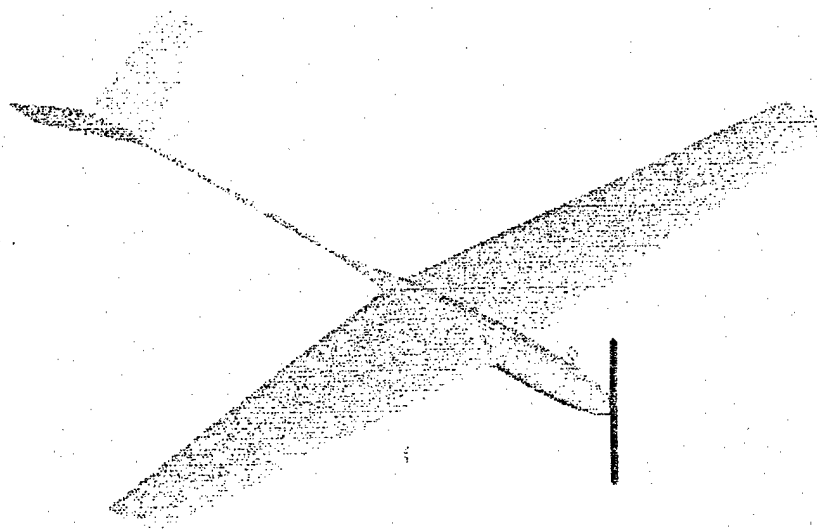
Based on inputs from the pilot for more precise response, High Torque Ball Bearing Servos and steel push rods were used for the tail surfaces instead of general duty servos and plastic tube pushrods as used in 1996/1997's competition.

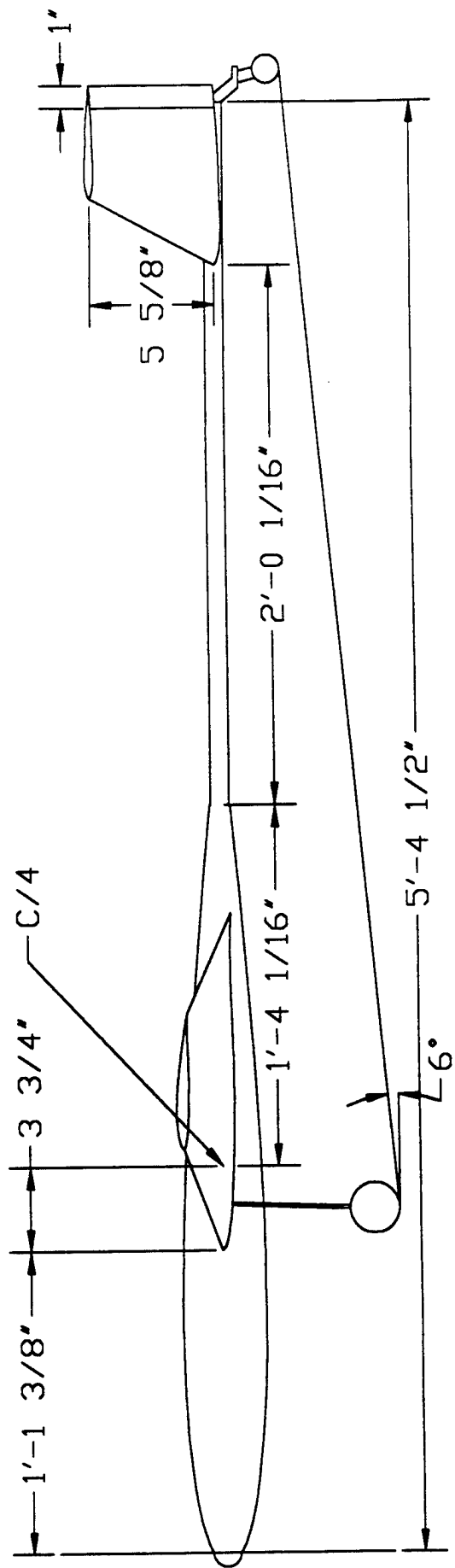
In terms of system architecture, the main improvement of "Javelin" over "Raptor" is the use of a computerized radio. "Javelin" used a mechanical mixer for the V-tail which added extra weight and high complexity to the fuselage. With the Airtronics Stylus 8 computerized radio, V-Tail and Flaperon mixing is all handled off the airplane.

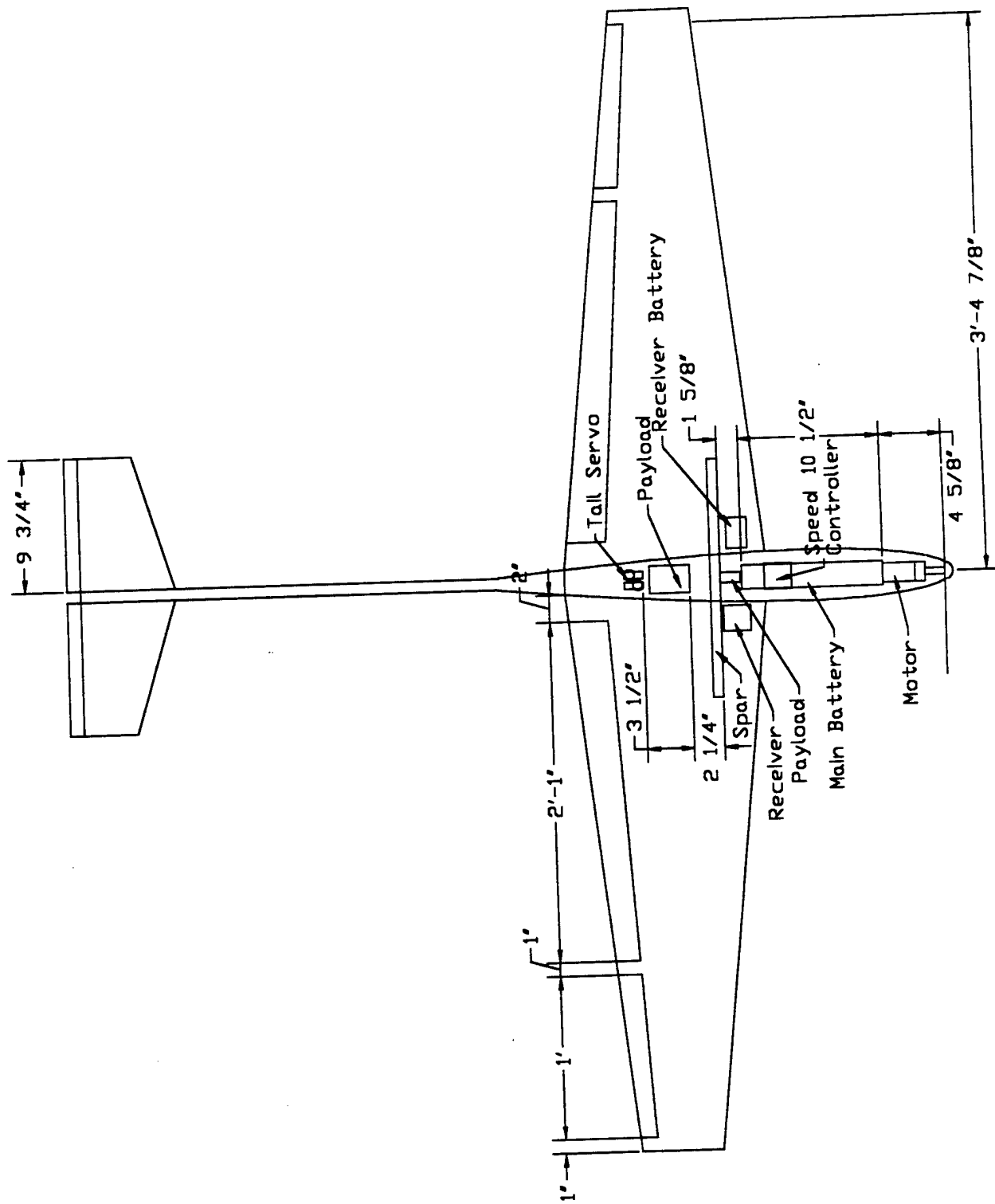
Finally, the receiver and receiver battery were located in the wing for both "Javelin" and

"Raptor." This greatly improved the space available within the fuselage for components and balancing the aircraft.

**V.c Drawing Package**







Item	Wing	V-Tail (Actual Surface)	Horiz-Tail (Proj. into X-Y plane)	Vertical-Tail (Proj. into Y-Z plane)
Area [ft <sup>2</sup> ]	598	1.02	0.88	0.25
Span [in]	82.00	22.50	19.49	5.63
Aspect Ratio	7.81	3.46	3.00	0.87
Mean Aero. Chord [in]	11.14	6.62	6.62	6.62
Taper Ratio	0.40	0.63	0.63	0.63
Airfoil	RG-15	NACA 0009	-	-
Root Chord [in]	15.00	8.00	8.00	8.00
Tip Chord [in]	6.00	5.00	5.00	5.00
Sweep @ 50% Chord [deg]	0.00	7.60	8.60	8.60
Dihedral [deg]	2.50	30.00	30.00	30.00
Root Chord Incidence [deg]	2.00	0.00	0.00	0.00
Ailerons [% chord, % span]	20, 29	-	-	-
Flaps [% chord, % span]	20, 71	-	-	-
Elevator [% chord, % chord]	-	19.30	-	-

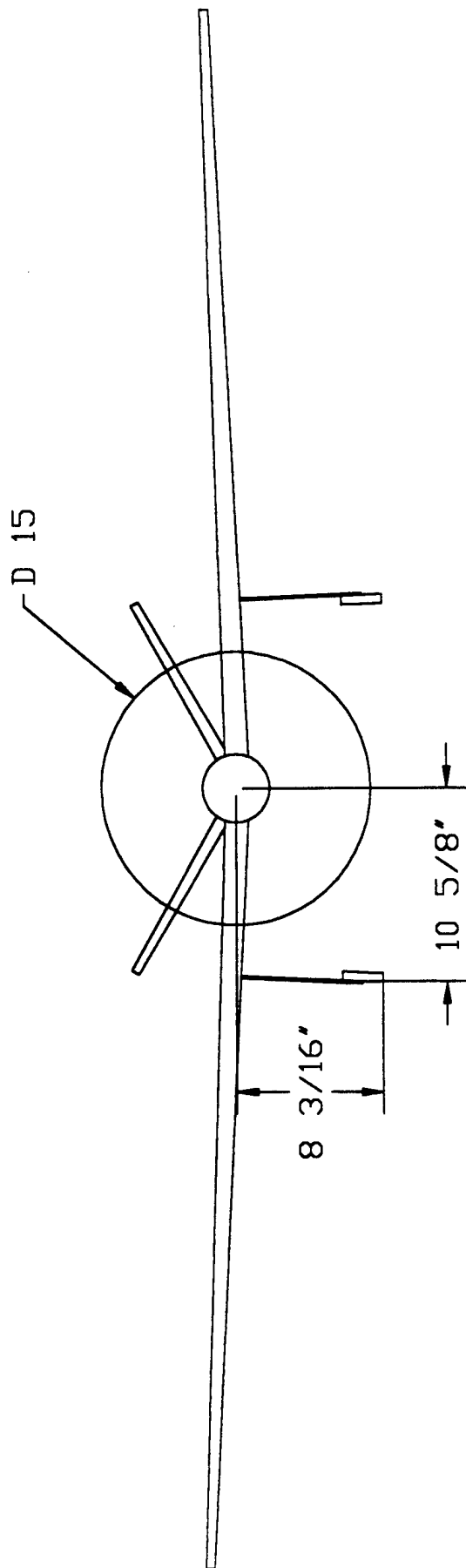


Table V.i Takeoff Analysis at Maximum Throttle Setting

WEIGHT = 17 lb  
 AIR DENSITY = 0.002377 slug/ft<sup>3</sup>  
 SWALD EFFICIENCY = 0.95  
 ASPECT RATIO = 7.84  
 WING AREA = 6 ft<sup>2</sup>  
 C<sub>Do</sub> @ a=7° = 0.018  
 ΔC<sub>Do</sub> = 0.036  
 C<sub>L</sub> @ 15°, 2c, a=7° = 2.2  
 C<sub>Do</sub> FUS. & TAIL = 0.0455  
 C<sub>D</sub> = 0.30635  
 RICTION CONSTANT 0.02

VELOCITY (mph)	VELOCITY (ft/s)	THRUST (lbf)	DRAG (lbf)	Wc (lbf)	LIFT (lbf)	S (ft)	ACCELERATION (ft/s <sup>2</sup> ) DOWN RUNWAY	Δ TIME (s)	TIME (s)	DISTANCE (ft) DOWN RUNWAY
0	0.00	8.20	0.00	17.00	0.00	0.00	14.89	0.00	0.00	0.00
1	1.47	8.04	0.00	17.00	0.03	0.07	14.57	0.10	0.10	0.07
2	2.93	7.88	0.02	17.00	0.13	0.30	14.25	0.10	0.20	0.30
3	4.40	7.72	0.04	17.00	0.30	0.70	13.90	0.11	0.31	0.66
4	5.87	7.55	0.08	17.00	0.54	1.27	13.54	0.11	0.42	1.18
5	7.33	7.39	0.12	17.00	0.84	2.04	13.17	0.11	0.53	1.84
6	8.80	7.23	0.17	17.00	1.21	3.03	12.78	0.11	0.64	2.65
7	10.27	7.07	0.23	17.00	1.65	4.26	12.38	0.12	0.76	3.59
8	11.73	6.91	0.30	17.00	2.16	5.76	11.96	0.12	0.88	4.68
9	13.20	6.75	0.38	17.00	2.73	7.56	11.52	0.13	1.01	5.90
10	14.67	6.59	0.47	17.00	3.37	9.72	11.07	0.13	1.14	7.25
11	16.13	6.43	0.57	17.00	4.08	12.27	10.60	0.14	1.28	8.73
12	17.60	6.26	0.68	17.00	4.86	15.30	10.12	0.14	1.43	10.32
13	19.07	6.10	0.79	17.00	5.70	18.88	9.63	0.15	1.58	12.02
14	20.53	5.94	0.92	17.00	6.61	23.13	9.12	0.16	1.74	13.81
15	22.00	5.78	1.06	17.00	7.59	28.18	8.59	0.17	1.91	15.69
16	23.47	5.62	1.20	17.00	8.64	34.22	8.05	0.18	2.09	17.64
17	24.93	5.46	1.36	17.00	9.75	41.50	7.49	0.20	2.29	19.64
18	26.40	5.30	1.52	17.00	10.93	50.38	6.92	0.21	2.50	21.65
19	27.87	5.13	1.70	17.00	12.18	61.34	6.33	0.23	2.73	23.65
20	29.33	4.97	1.88	17.00	13.50	75.12	5.73	0.26	2.99	25.59
21	30.80	4.81	2.07	17.00	14.88	92.84	5.11	0.29	3.28	27.43
22	32.27	4.65	2.27	17.00	16.33	116.31	4.48	0.33	3.60	29.07
23	33.73	4.49	2.49	17.00	17.85	148.67	3.83	0.38	3.99	30.43



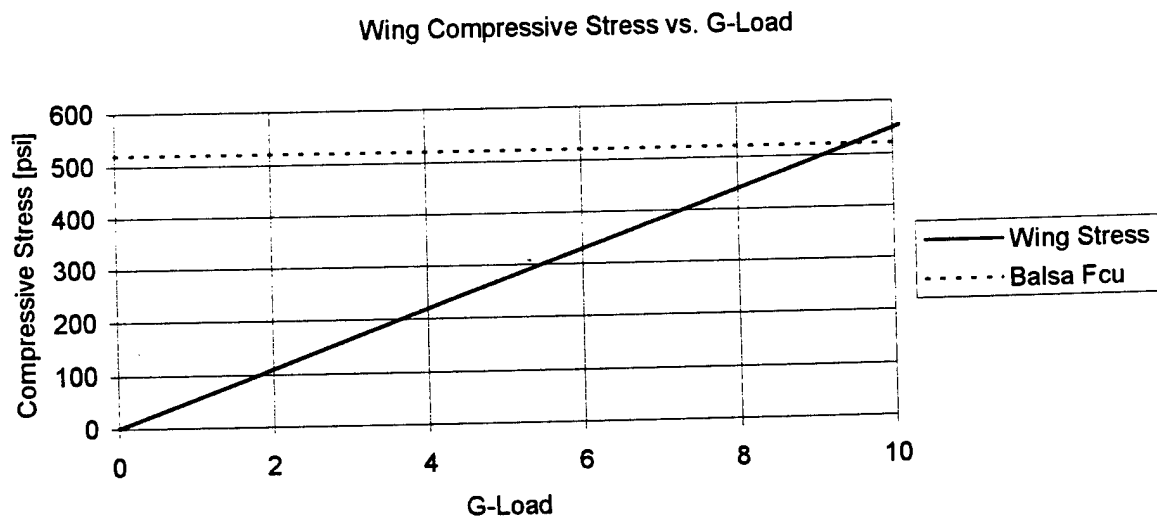
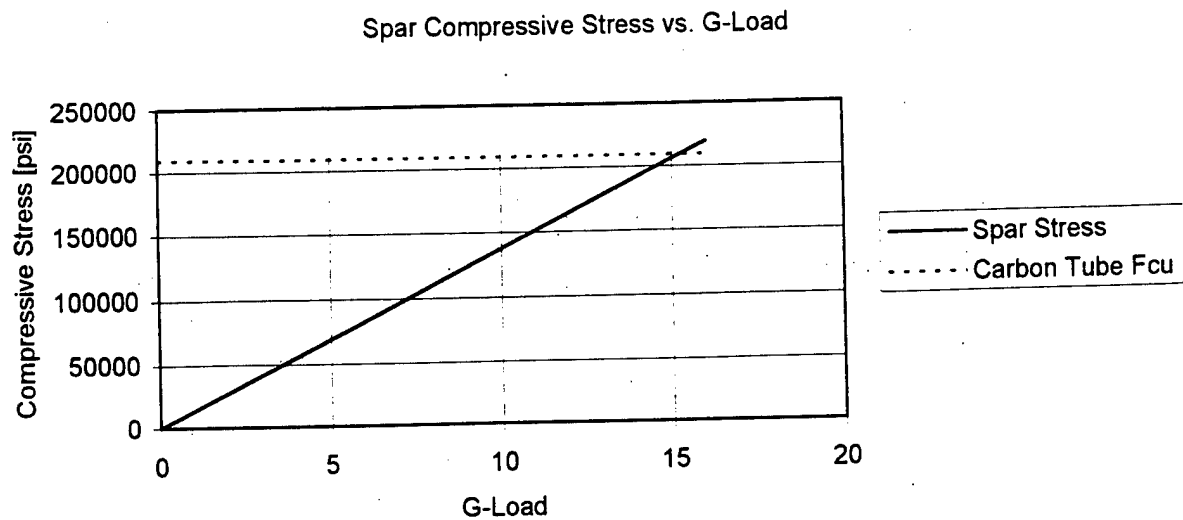


Figure V.i Maximum G-Load for Spar and Wing

Table V.ii Weight Analysis

## Javelin Weight Analysis

	#	Unit Weight [oz]	Predicted Weight [oz]	Actual Weight [oz]
<b>Fixed Wt. Items</b>				
Propeller	1	3.25	3.25	3.25
Motor/Spinner	1	10.00	10.00	10.00
Speed Controller	1	3.50	3.50	3.50
Battery	1	39.50	39.50	39.50
Receiver	1	1.70	1.70	1.70
Rec Battery	1	3.20	3.20	3.20
Servo	4	1.20	4.80	4.80
Control Rods/Wires	2	0.50	1.00	1.00
Payload	1	120.00	120.00	120.00
Sub-Total			186.95	186.95
% of Total			73%	68%

<b>Variable Weight Items</b>	Predicted Weight [oz]	Actual Weight [oz]
Left Wing	16	22.30
Right Wing	16	20.80
Fuselage	12	17.60
Main Gear	12	11.50
Tail	5	5.60
Spar	3	4.00
Tail Boom	3	3.60
Tail Gear	2	1.25
Sub-Total	69	86.65
% of Total	27%	32%

	Predicted	Actual
Total Weight [oz]	255.95	273.60
Total Weight [lb]	16.00	17.10
Payload Fraction		44%

## Raptor Weight Analysis

	#	Unit Weight [oz]	Predicted Weight [oz]
<b>Fixed Wt. Items</b>			
Propeller	1	3.25	3.25
Motor/Spinner	1	10.00	10.00
Speed Controller	1	3.50	3.50
Battery	1	39.50	39.50
Receiver	1	1.70	1.70
Rec Battery	1	3.20	3.20
Servo	6	1.20	7.20
Control Rods/Wires	4	0.75	3.00
Payload	1	120.00	120.00
Sub-Total			191.35
% of Total			72%

<b>Variable Weight Items</b>	Predicted Weight [oz]
Left Wing	16
Right Wing	16
Fuselage	12
Main Gear	16
Tail	5
Spar	3
Tail Boom	3
Tail Gear	2
Sub-Total	73
% of Total	28%

	Predicted
Total Weight [oz]	264.35
Total Weight [lb]	16.52
Payload Fraction	45%

Table V.iii Component Selection

Component	Make	Model
Propeller	APC	15x10; Pattern
Motor	MaxCim	MaxNEO-13Y
Speed Controller	MaxCim	Maxu35A-25NB
Gearbox	MEC	Super Box, 4.28:1
Battery	Sanyo	RC-2000, 2200 mAh
Radio/Receiver	Airtronics	Stylus-8
Rec. Battery	Sanyo	600 mAh
Servo	Airtronics	94141, High Torque BB Micro Servo

## VI. MANUFACTURING PLAN

There are a variety of manufacturing processes and materials available to suit the load conditions on the aircraft. The processes chosen were a result of evaluating the following Figures of Merit (FOM):

- Strength/Weight - Strength to weight ratio of component produced from this process. Higher score means higher ratio. FOM weighting = 0.40.
- Time - Time required to complete this process. FOM weighting = 0.30.
- Cost - Costs of materials, tooling required to use this process. FOM weighting = 0.10.
- Strategic Benefit - potential for future benefits from investment made in developing this process. FOM weighting = 0.10.
- Accuracy - qualitative measure of how closely manufactured component will represent the designed component with this process. FOM weighting = 0.05.
- Durability/Repair - resistance of component to damage (i.e. shipping, handling) and ease of repair when made with this process. FOM weighting = 0.05.

### VI.a Manufacturing Processes Selected

The fuselage was made from molding a fiberglass/foam/honeycomb laminate to make a smooth yet stiff teardrop shaped shell. Honeycomb was used in the load critical areas and blue Styrofoam in the less loaded areas.

Conventional materials were used in constructing the wing and tail surfaces. Blue Styrofoam sheeted with balsa provided a fast, accurate means of making a stiff, lightweight wing section. The tail surfaces were constructed with solid balsa and a 1/32" plywood strip in the leading edge.

The highly loaded components, namely the wing spar and fixed landing gear, were constructed of carbon fiber. The wing spar was made from commercially available .75" I.D., .030" wall carbon tube.

The fixed landing gear used a carbon/fiberglass/Rohacell foam laminate and was used on the first aircraft for flight test purposes. A commercially available retractable landing gear is currently being installed in the "Raptor." The installation plate used on the bottom of the wing is a carbon fiber/Nomex honeycomb laminate with potting compound injected at the attachment locations to serve as hardpoints.

Even though not highly loaded, the tail boom was also made of the carbon tubing because of the ease of construction compared with the other processes investigated.

#### **VI.b Fuselage Manufacturing Processes Investigated**

One of the lessons learned in the 1996/97 competition was that molded composite manufacturing processes required much more time to develop than was originally anticipated. If we waited until the time to begin construction, then these methods would be screened out due to lack of skill/time even though they could produce strong, lightweight, complex shape parts. Therefore, directly after the 1996/97 competition, a decision was made to focus on the development of molded composite fuselage and forego the development of a fuselage using traditional methods, such as Built-up Balsa fuselage.

In the summer of 1997, a fuselage plug was made from foam/fiberglass/filler and lathed into a NACA 0010 airfoil revolved around its chord line. Molds were made to assess the suitability of using epoxy or polyester resin. Despite the higher cost, the epoxy resin was chosen because it was easier to use and because the higher quality of the mold.

To address the fuselage structure itself, an evaluation was made between Monocoque (fiberglass/core/fiberglass) vs. Fairing/Truss construction methods. As can be seen from Table VI.i, the Monocoque method was more complicated but would make a lighter part and offered significant potential of application to other areas.

In the construction of the first aircraft, the fuselage was made with one mold and then two wing fillets molds were made using sculpted modeling clay for the wing fillet plugs. This process was very time consuming and also left unused space inside between the fillets and fuselage.

In the construction of the second aircraft, the mold incorporated the wing fillets and also had a cutout at the location of the main access panel. This cutout allowed enough space so that 1" wide fiberglass tape could be installed to join the two halves of the part while they were still in the mold. Undoubtedly, this complicated the creation of the mold itself but it was felt the overall manufacturing process was simplified and the space available inside the fuselage was increased.

#### **VI.c Wing Manufacturing Processes Investigated**

Three construction methods were considered for the wing - Built-up Balsa/Covering, Solid Laminate (balsa sheeted foam) and the Hollow Laminate (fiberglass/foam/fiberglass). The resulting evaluation shown in Table VI.ii screened out Built-up Balsa and Hollow Laminate

methods. The Built-up Balsa method was discounted because it is believed that a Solid Laminate wing could be faster to build, be more durable, and easier to repair. While the Hollow Laminate method seems promising and is commonly used in the UAV industry, it would not be ready for WVU without more development. Due to time constraints, this development would need to be scheduled in Summer of 1998.

#### **VI.d Tail and Tail Boom Manufacturing Processes Investigated**

Built-up Balsa, Solid Laminate, Hollow Laminate, Solid Balsa processes were evaluated for the impinge surfaces. In Table VI.iii, the Solid Balsa process was selected because despite small weight increases, the tail was durable, and easily manufactured.

In Table VI.iv, a Commercially Wrapped and a Heat Shrink Wrapped carbon tube were evaluated for the tail boom. The Heat Shrink Wrapped process involved laying carbon/epoxy on a mandrel and using heat shrink tape to debulk the laminate. Although lower in cost and lighter in weight, the time required to develop the Heat Shrink Wrapped process was high and the dimensional accuracy still not reliable.

#### **VI.e Analytical Methods**

Analytical methods were used to see how to optimize the Solid Laminate Construction Method for higher strength, lower weight and easier manufacturing. Using ASTM C393-94 "Standard Test Method for Flexural Properties of Sandwich Constructions", several different laminates were tested in Mid-Span and Third Point Bending. See Table VI.v, VI.vi. These laminates tested were approximately the average thickness of the Raptor 5 wing.

The tests showed that although white foam has a lower density, it has a lower shear modulus when compared to blue foam. For a given load, a laminate with white foam will deflect more than a laminate with blue foam and the ultimate load capability of the white foam laminate is therefore lower than the blue foam laminate. This is because the balsa facing is experiencing a non-uniform stress distribution that is in proportion to the amount of curvature. A sample test result is shown in Figure VI.i.

In all specimens, double sided tape (carpet tape) was used to adhere the balsa to the foam. It did not fail before the facings which indicates the shear strength of the tape was sufficient to carry shear across the laminate. Carpet tape was much easier to apply than the epoxy, less time consuming and therefore preferred over the epoxy.

## VI.f Manufacturing Milestones

The scheduled event manufacturing milestones are shown in Table VI.vii.

Table VI.i Fuselage Manufacturing Processes Investigated

FOM	Weighting	Monocoque		Fairing/Truss	
		Raw	Adjusted	Raw	Adjusted
Strength/Weight	0.40	5	2.00	3	1.20
Time	0.30	3	0.90	5	1.50
Cost	0.10	4	0.40	3	0.30
Strategic Benefit	0.10	5	0.50	1	0.50
Accuracy	0.05	4	0.20	3	0.15
Durability/Repair	0.05	2	0.10	4	0.20
Total	1.00		4.10		3.85

Table VI.ii Wing Manufacturing Processes Investigated

FOM	Weight	Built-up		Solid Laminate		Hollow Laminate	
		Raw	Adjusted	Raw	Adjusted	Raw	Adjusted
Strength/Weight	0.40	5	2.00	3	1.20	5	2.00
Time	0.30	3	0.90	5	1.50	1	0.30
Cost	0.10	3	0.30	2	0.20	1	0.10
Strategic Benefit	0.10	1	0.10	2	0.20	5	0.50
Accuracy	0.05	1	0.05	5	0.25	5	0.25
Durability/Repair	0.05	1	0.05	3	0.15	5	0.25
Total	1.00		3.40		3.50		3.40

Table VI.iii Tail Manufacturing Processes Investigated

FOM	Weighting	Built-up		Solid Laminate		Hollow Laminate		Solid Balsa	
		Raw	Adjusted	Raw	Adjusted	Raw	Adjusted	Raw	Adjusted
Strength/Weight	0.40	5	2.00	3	1.20	5	2.00	3	1.20
Time	0.30	3	0.90	5	1.50	1	0.30	5	1.50
Cost	0.10	3	0.30	2	0.20	1	0.10	5	0.50
Strategic Benefit	0.10	1	0.10	2	0.20	5	0.50	1	0.10
Accuracy	0.05	1	0.05	5	0.25	5	0.25	5	0.25
Durability/Repair	0.05	1	0.05	3	0.15	5	0.25	5	0.25
Total	1.00		3.40		3.50		3.40		3.80

Table VI.iv Tail Boom Manufacturing Processes Investigated

FOM	Weighting	Commercially Wrapped		Heat Shrink Wrapped	
		Raw	Adjusted	Raw	Adjusted
Strength/Weight	0.40	3	1.20	5	2.00
Time	0.30	5	1.50	1	0.30
Cost	0.10	2	0.20	4	0.40
Strategic Benefit	0.10	1	0.10	5	0.50
Accuracy	0.05	5	0.25	1	0.05
Durability/Repair	0.05	4	0.20	3	0.15
Total	1.00		3.45		3.40

Table VI.v Average Properties of Laminates Tested

Core	Ult. Compressive Stress in Balsa Facings [lb/in <sup>2</sup> ]
White Foam 1	342
White Foam 2	402
Blue Foam	521

	Density [lbm/ft <sup>3</sup> ]
White Foam 1	0.914
White Foam 2	1.158
Blue Foam	1.715
Balsa	9.25-9.70



Table VI.vi Specimen Geometry

Type of Loading	Span [in]	Width [in]	Core Thickness [in]	Facing Thickness [in]	No. of Specimens
Mid-Span	4	2	0.75	1/16	3
Third Point	6	2	0.75	1/16	6

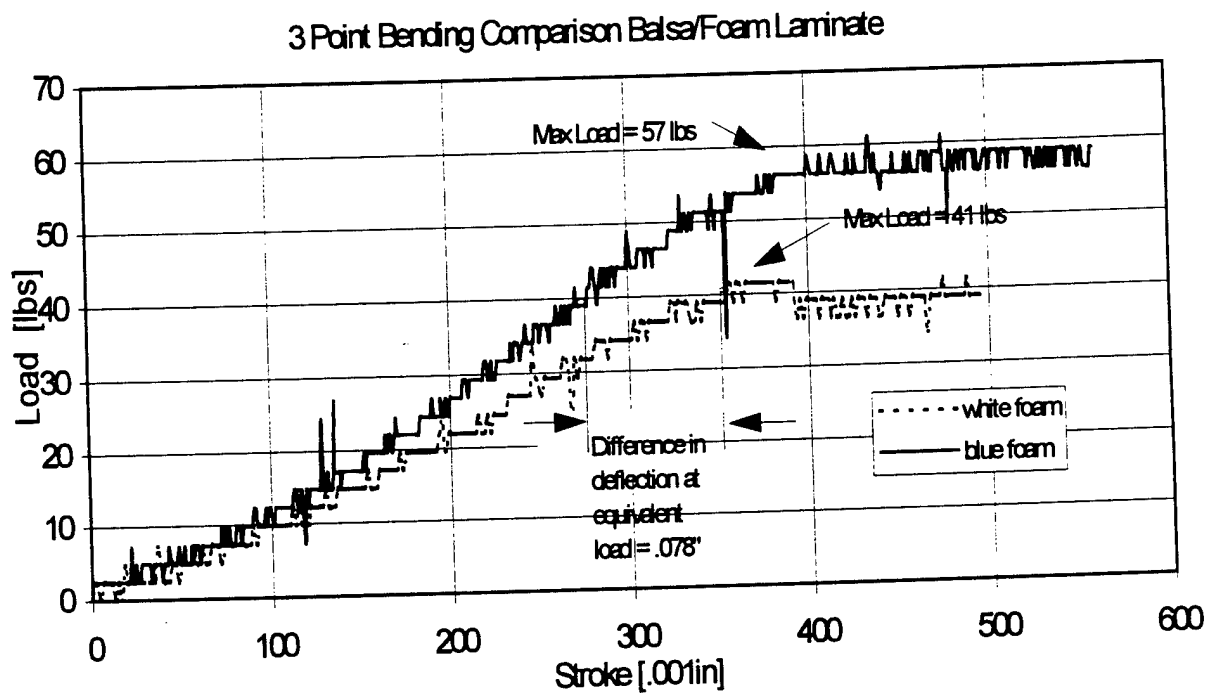



















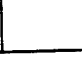




Figure VI.i Sample Test Results

Table VI.vii Manufacturing Milestones Chart

Planned =  Actual = 

Milestone	Jun	Jul	Aug	Sep	Oct	Nov	Dec	Jan	Feb	Mar	Apr
Composite Fuse Dev.											
											
Javelin Fuse Integration											
											
Structural Testing											
											
Javelin Wing/Tail/Gear											
											
Raptor Fuse Dev.											
											
Raptor Fuse Integration											
											
Raptor Wing/Tail/Gear											
											



WEST VIRGINIA UNIVERSITY

ADDENDUM PHASE REPORT

"RAPTOR"

Second Annual AIAA Student  
Design/Build/Fly Competition

Wichita, Kansas

1997-1998 Contest Year

13 April 1998

***Mechanical and Aerospace  
Engineering Department***

College of Engineering and Mineral Resources  
West Virginia University • Morgantown, WV 26506-6106

**WEST VIRGINIA UNIVERSITY FINAL DESIGN REPORT  
"RAPTOR"**

**Second Annual AIAA Student Design/Build/Fly Competition  
Wichita, Kansas  
1997-1998 Contest Year  
13 April 1998**

**Department of Mechanical and Aerospace Engineering  
West Virginia University  
Morgantown, West Virginia**

## TABLE OF CONTENTS (continued)

	<u>Page No.</u>
VII Lessons Learned	36.
VII.a Current Design Alterations	36.
VII.a.i Flap and Aileron Design Alterations	36.
VII.a.ii Landing Gear Design Alterations	36.
VII.b Future Design Improvements	37.
VII.b.i Wing and Fuselage Design Changes	37.
VII.b.ii Tail Size Reduction and Design Changes	37.
VII.b.iii Retractable Landing Gear Developement	38.
VII.c Cost and Weight Breakdown for "Raptor"	38.
VII.d Drawing Package Alterations	38.
References	44.

## **VII. LESSONS LEARNED**

### **VII.a Current Design Alterations**

#### **VII.a.i Flap and Aileron Design Changes**

The original design of the trailing edge of the wing planform was centered around design of the flaps, therefore leaving the aileron design secondary. That is to say the flaps were designed as needed and the ailerons for the most part were fitted to the remaining length of the trailing edge of the wing. This was done for the reason that the aileron size and placement determine the roll rate and the amount of lateral control of the aircraft. These two design parameters were felt to be secondary to the take off performance.

Unfortunately the ailerons were later felt to be undersized for control during landing. Consequently the ailerons and flaps were redesigned. The flaps were reduced to only 50% of the wing span rather than the original 61% of the span. The one inch gap originally left between the ailerons and the flaps was removed and added to the aileron span. Consequently, the aileron size increase was felt to give sufficient control during landing and increased control through the turns at either end of the course.

Changing the span of the flaps changed the takeoff performance, specifically the overall lift coefficient of the wing. This can be compensated by one of two methods. The first method would involve increasing the flap deflection during takeoff. This is undesirable because the flaps were already deflected  $15^{\circ}$ , which is the accepted maximum for takeoff. Increasing the flap deflection any more would cause boundary layer and therefore flow separation during takeoff, resulting most likely in a crash. The second method, which was used, is to deflect the flaps to the original deflection and then use the ailerons as flaps and deflect them to compensate for the loss of the lift coefficient.

#### **VII.a.ii Landing Gear Design Changes**

The "Raptor" was originally designed to have retractable landing gear. Unfortunately, towards the end of the landing gear design, development, and testing it, was found that the retractable gear design was not rigid enough and would possibly buckle under a hard landing. Therefore the landing gear was redesigned as fixed landing gear due to the fact that there was insufficient time remaining to redesign and build the retractable landing gear. The fixed landing gear design was based off of the fixed landing gear of the "Javelin" with the exception of a few

design changes were made. The landing gear of both aircraft were made out of composite materials and towards the end of the "Javelin" flight testing, the landing gear was starting to experience delamination problems. Therefore, the landing gear of the "Raptor" was designed differently to prevent this problem. Additionally, wheel pants were added to the landing gear to help reduce drag.

## **VII.b Future Design Improvements**

### **VII.b.i Wing and Fuselage Design Changes**

The development of the fuselage started during the summer of 1997 and it was originally designed to hold all of the components including the motor, speed controller, radio, servo battery, propulsion battery, payload and tail surface servos. By moving the radio and the servo battery into the wings and by molding the fuselage with the wing fillets rather than separately, a large amount of empty space was generated in the fuselage. Future designs would eliminate this space by making the fuselage smaller.

The wing planform in the future will be made of the same composite molding techniques developed and implemented in the fuselage. It was felt that there was insufficient time to develop and implement composite wing moldings for this years competition. The wing profile may also incorporate geometric and aerodynamic twist in the future to provide a more efficient wing planform and lift to drag ratio.

Depending on the rules for the 1998/1999 contest, a fully integrated fuselage and wing (possibly even a flying wing) made of the composite casting techniques may be constructed. These changes would increase the complexity of the aircraft for both design and construction but would result in lower costs due to the fact that the current method of balsa sheeting is very expensive.

### **VII.b.ii Tail Size Reduction and Design Changes**

The tail of the aircraft in the future would most likely be smaller providing increased maneuverability and decreased drag but coming at a cost of longitudinal stability. This year the static margin was 25% of the mean aerodynamic chord. In the future this may be reduced to 15%

to accomplish the above mentioned objectives while still providing adequate stability. Additionally the tail may not have separate control surfaces but rather the entire stabilizer may be hinged to rotate. These changes would increase the complexity of construction moderately but should have no appreciable cost increase.

### **VII.b.iii Retractable Landing Gear Development**

The landing gear for the future aircraft should be retractable so as to minimize drag of the aircraft. The aircraft this year was designed to have retractable landing gear, unfortunately more development time was needed than was originally thought. Consequently fixed gear was developed for this year. Retractable landing gear would increase cost but the reduction of drag is felt to be more valuable.

### **VII.c Cost and Weight Breakdown for "Raptor"**

In general, the expected costs of the Raptor were very close to the actual costs of the aircraft. This is because most of the construction methods for the Raptor are the same as the previous aircraft, Javelin, and these costs were fairly well understood. In the area where the Raptor varies significantly from the design, namely the landing gear, the costs were also close to expected. As shown in Table VII.v, the landing gear price was roughly \$190, excluding the tail gear portion. The retractable gear (Robart 608 @ \$63.99), retract servo (Airtronics 94734 @ \$61.99) and wheels/accessories (\$21.84) come to a price of \$147.82.

The final cost and weight breakdowns for the "Raptor" can be seen in Tables VII.i through VII.x.

### **VII.d Drawing Package Alterations**

The changes in the drawing package reflect the changes made to the landing gear and can be seen in the drawings following Table VII.x.

Table VII.i Cost Breakdown for Electronics

System Items	Type	Unit Cost	Number	List Price	Actual Price
Radio System	Infinity 600	\$400.00	1	\$400.00	\$0.00
Servos	Airtronics	\$49.99	2	\$99.98	\$0.00
			Sub-total	\$499.98	\$0.00



Table VII.ii Cost Breakdown for Propulsion System

Propulsion Items	Type	Unit Cost	Number	List Price	Actual Price
Motor	MaxNeo-13Y	\$229.95	1	\$229.95	\$160.95
Speed Controller	Maxu35A-25NB	\$249.95	1	\$249.95	\$187.45
Battery	19 cell	\$170.00	1	\$170.00	\$170.00
Propeller	APC 15x8	\$11.99	1	\$11.99	\$11.99
Spinner	60504	\$4.00	1	\$4.00	\$4.00
			Sub-Total	\$665.89	\$534.39

Table VII.iii Cost Breakdown for Wing and Tail

Wing/Tail Items	Size	Unit Cost	Number	Sub-Total	Actual Price
Blue foam	2' x 8'	\$11.25	1	\$11.25	\$11.25
Balsa Sheet	1/16 "x 6" x 36"	\$2.48	16	\$39.68	\$35.71
Balsa Sheet	3/8" x 6" x 24"	\$5.32	1	\$5.32	\$4.79
Monokote	3' x 6'	\$10.99	2	\$21.98	\$21.98
Carbon Tape	.007" x .5" x 48"	\$2.50	2	\$5.00	\$4.25
Carpet Tape	2" x 25'	\$3.95	1	\$3.95	\$3.95
Epoxy/Hardener	10 oz bot.	\$10.99	1	\$10.99	\$10.99
Brass Rod	.25" OD x 12"	\$0.30	1	\$0.30	\$0.30
Carbon Tube	.75" ID x 12"	\$15.84	1	\$15.84	\$13.46
Plywood	1/8" x 12" x 12"	\$5.36	0.75	\$4.02	\$3.62
L.E. Stock	36"	\$1.55	3	\$4.65	\$4.19
			Sub-total	\$122.98	\$114.49

Table VII.iv Cost Breakdown for Fuselage

Fuselage Items	Size	Unit Cost	Number	Sub-Total	Actual Price
Fiberglass	2 oz/sq yard	\$4.00	1.25	\$5.00	\$4.25
Carbon Fabric	5.7 oz/sq yd, 3K	\$35.99	0.5	\$18.00	\$0.00
Carbon Tube	.75" ID x 12"	\$15.84	3.25	\$51.48	\$43.76
Honeycomb	.210" x 36" x 36"	\$44.98	0.5	\$22.49	\$0.00
Alum Tube	.75" OD x 12"	\$3.14	1	\$3.14	\$3.14
Plywood	1/8" x 12" x 12"	\$5.36	0.25	\$1.34	\$1.21
Basswood	1/4" x 3" x 36"	\$2.35	0.25	\$0.59	\$0.53
Epoxy Resin	#88, 35 oz	\$19.95	0.3	\$5.99	\$5.99
Epoxy Hardener	#87, 32 oz	\$17.95	0.06	\$1.08	\$1.08
			Sub-Total	\$109.09	\$59.95

Table VII.v Cost Breakdown for Landing Gear

Landing Gear Items	Size	Unit Cost	Number	Sub-Total	Actual Price
Carbon Fabric	5.7 oz/sq yd, 3K	\$35.99	4.5	\$161.96	\$0.00
Tail wheel	6-8 lbs	\$16.79	1	\$16.79	\$16.79
Wheels	2.25" Dia., pair	\$8.35	1	\$8.35	\$8.35
Wheel Pants	Small	\$9.29	1	\$9.29	\$9.29
Axle Shafts	5/32"	\$2.95	1	\$2.95	\$2.95
Wheel Collars	5/32"	\$1.25	1	\$1.25	\$1.25
Epoxy Resin	#88, 35 oz	\$19.95	0.25	\$4.99	\$4.99
Epoxy Hardener	#87, 32 oz	\$17.95	0.05	\$0.90	\$0.90
Sub-Total				\$206.47	\$44.52

Table VII.vi Cost Breakdown for Miscellaneous Hardware

Misc. Items	Size	Unit Cost	Number	Sub-Total	Actual Price
Push Rods	2-56	\$0.55	2	\$1.10	\$0.99
Push Rod Kit		\$2.99	1	\$2.99	\$2.69
Control Horns	1/2 A	\$0.70	2	\$1.40	\$1.26
Nylon Clevis	Kwik Link	\$0.69	2	\$1.38	\$1.24
Nylon Screws	1/4-20	\$1.00	1	\$1.00	\$0.90
Brass Tubes	3/16	\$0.30	2	\$0.60	\$0.54
Folding Hinges	Robarts	\$3.05	1	\$3.05	\$2.75
Fabric Hinges	3/4" x 1"	\$3.10	1	\$3.10	\$2.79
Sub-Total				\$14.62	\$13.16

Table VII.vii Total Cost Breakdown for Subsystems

	Sub-Total	List Price	Actual Price
Systems	\$499.98		\$0.00
Propulsion	\$665.89		\$534.39
Wing/Tail	\$122.98		\$114.49
Fuselage	\$109.09		\$59.95
Land Gear	\$206.47		\$44.52
Misc.	\$14.62		\$13.16
Total	\$1,619.03		\$766.51

Table VII.viii Weight Breakdown for Fixed Weight Items

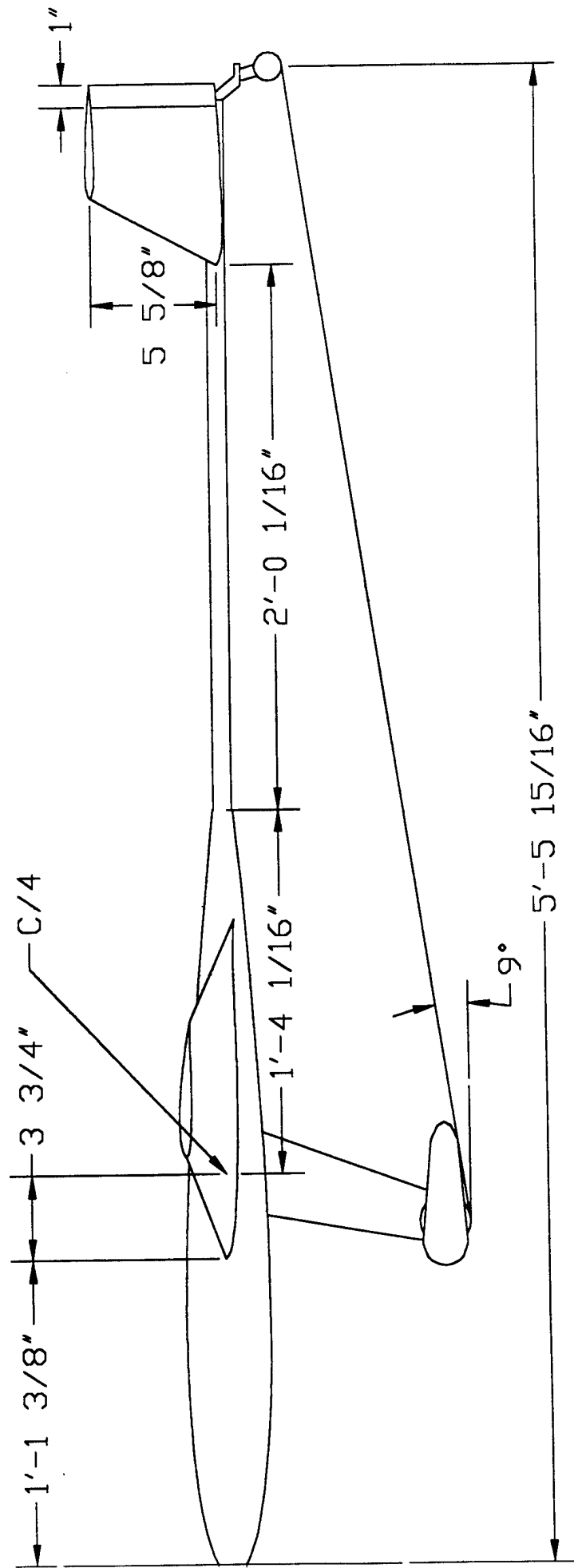
Fixed Wt. Items	#	Unit	Predicted	Actual
		Weight [oz]	Weight [oz]	Weight [oz]
Propeller	1	3.25	3.25	3.25
Motor/Spinner	1	10.00	10.00	10.00
Speed Controller	1	3.50	3.50	3.50
Battery	1	39.50	39.50	39.50
Receiver	1	1.70	1.70	1.70
Rec Battery	1	3.20	3.20	3.20
Servo	6	1.20	7.20	7.20
Payload	1	120.00	120.00	120.00
Sub-Total			188.35	188.35
% of Total			71%	72%

Table VII.ix Weight Breakdown for Variable Weight Items

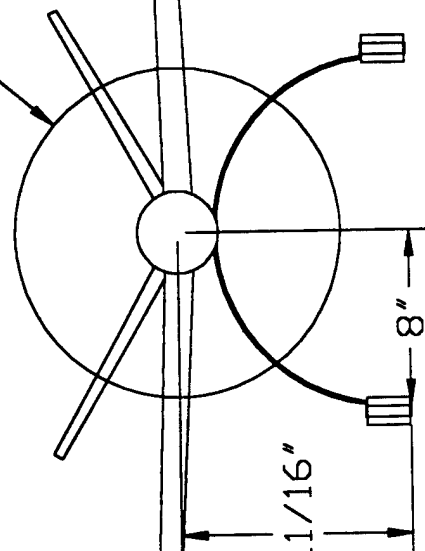
Variable Weight Items	#	Unit	Predicted	Actual	Percent of Variable
		Weight [oz]	Weight [oz]	Weight [oz]	
Left Wing			16	16.70	22.97%
Right Wing			16	16.70	22.97%
Fuselage			12	15.50	21.32%
Main Gear			16	10.50	14.44%
Tail			5	5.60	7.70%
Spar			3	1.40	1.93%
Tail Boom			3	3.60	4.95%
Tail Gear			2	0.70	0.96%
Control Rods/Wires	4	0.75	3.00	2.00	2.75%
Sub-Total			76	72.70	100.00%
% of Total			29%	28%	

Table VII.x Total Weight Breakdown

	Predicted	Actual
Total Weight [oz]	264.35	261.05
Total Weight [lb]	16.52	16.32
Payload Fraction	45%	46%



D 15



$10 \frac{11}{16}"$

$8"$

## REFERENCES

1. Raymer, Daniel P. "Aircraft Design: A Conceptual Approach", AIAA Education Series, Washington D.C., 1992 .
2. Anderson, John D., Jr. "Introduction to Flight, Third Edition", University of Maryland, 1989.
3. Roskam, Jan "Airplane Flight Dynamics and Automatic Flight Controls, Part 1", University of Kansas, Lawrence, 1995.
4. Abbot, Ira H. and Von Doenhoff, Albert E. "Theory of Wing Sections", NASA, 1959
5. Hoerner, S.F. and Borst, H.V. "Fluid Dynamic Lift, Second Edition", 1985
6. Hoerner, S.F. "Fluid Dynamic Drag", 1965
7. <http://amber.aae.uiuc.edu/~m-selig/pd/notes.html>
8. <http://amber.aae.uiuc.edu/~aiaadb/>